



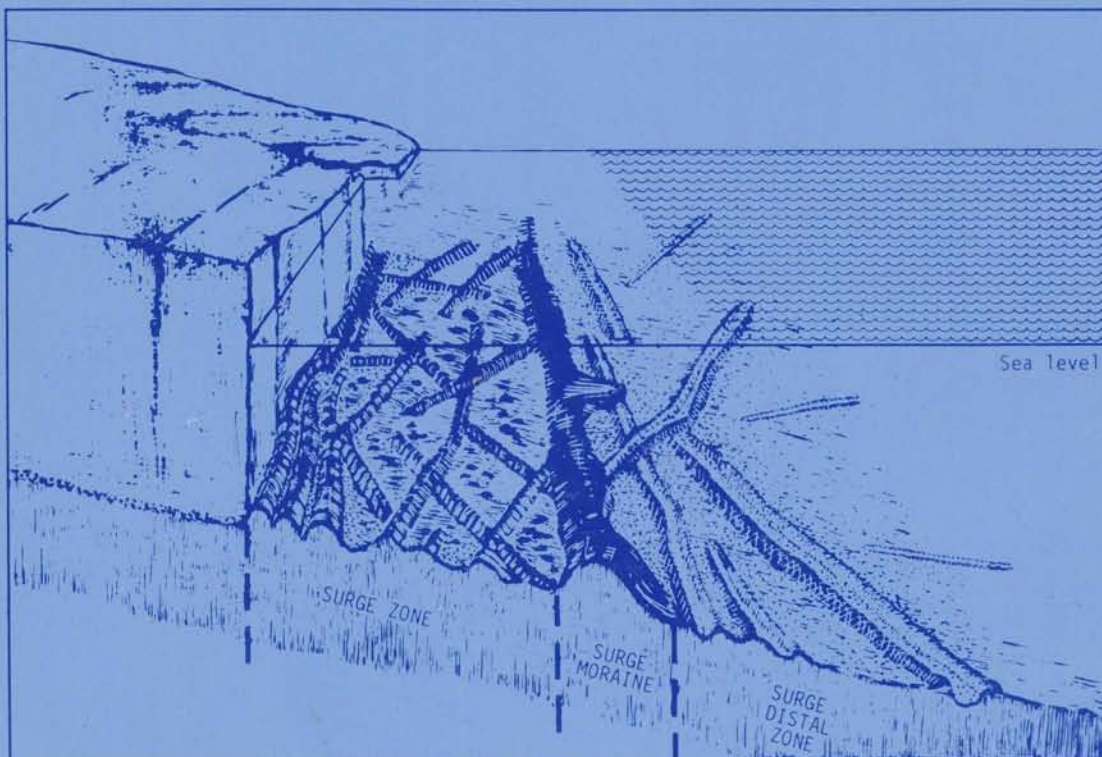
NORSK POLARINSTITUTT

RAPPORTSERIE

NR. 47 - OSLO 1988

ANDERS SOLHEIM:

GLACIAL GEOLOGY OF THE NORTHERN BARENTS SEA, WITH EMPHASIS
ON THE SURGE RELATED, ICE PROXIMAL DEPOSITIONAL ENVIRONMENT



Norsk Polarinstitut
P. O. Box 158
1330 Oslo Lufthavn, Norway

Dr. scient. thesis 1988
Department of Geology
University of Oslo, Norway

CONTENTS

ACKNOWLEDGEMENTS

INTRODUCTION AND MAIN CONCLUSIONS.

Background and objectives

Project progress and the individual papers.

Main conclusions

References

PAPER 1. Solheim, A. & Pfirman, S. L. 1985: Sea-floor morphology outside a grounded, surging glacier, Bråsvellbreen, Svalbard. Marine Geology 65, 127-143.

PAPER 2. Solheim, A. in prep.: The depositional environment of surging sub-polar tidewater glaciers: A case study of the morphology, sedimentation and sediment properties in a surge-affected marine basin outside Nordaustlandet, northern Barents Sea. Submitted to Norsk Polarinstitutt Skrifter.

PAPER 3. Pfirman, S. L. & Solheim, A. in press: Subglacial meltwater discharge in the tidewater glacier environment: Observations from Nordaustlandet, Svalbard archipelago. Marine Geology.

PAPER 4. Elverhøi, A. & Solheim, A. 1983: The Barents Sea ice sheet - a sedimentological discussion. Polar Research, 1 n.s., 23-42.

- PAPER 5. Solheim, A. & Kristoffersen, Y. 1984: The physical environment, Western Barents Sea, 1:1,500,000: Sediments above the upper regional unconformity; thickness, seismic stratigraphy and outline of the glacial history. Norsk Polarinstitutt Skrifter, 179B, 26pp.
- PAPER 6. Solheim, A., Milliman, J. D. & Elverhøi, A., 1988: Sediment distribution and sea floor morphology of Storbanken, implications for the glacial history of the northern Barents Sea. Canadian Journal of Earth Sciences, 25,
- PAPER 7. Elverhøi, A., Pfirman, S. L., Solheim, A. & Larsen, B. B., in press: Glaciomarine sedimentation and processes in high Arctic epicontinental seas, exemplified by the northern Barents Sea. Marine Geology.

ACKNOWLEDGEMENTS

The present Dr. scient. thesis consists of seven papers, written while employed at Norsk Polarinstitutt (NP). Four of the papers are published, two are currently in press and one is submitted for publication. Co-authors on the papers are Anders Elverhøi from NP, Yngve Kristoffersen from the University of Bergen (formerly from NP), John D. Milliman from Woods Hole Oceanographic Institution (WHOI) Stephanie L. Pfirman from Kiel University (formerly WHOI) and Bengt B. Larsen from NP. All of these are greatly acknowledged for their cooperation.

I am grateful to my supervisors, Jørn Thiede (until 1983) and Bjørn G. Andersen (from 1983) and external advisors Tor Løken and Yngve Kristoffersen for their valuable support.

Colleagues at NP are thanked for criticism and discussions throughout the course of the work. In particular I would like to mention Anders Elverhøi and Olav Liestøl, who were responsible for initiating the Bråsvellbreen program, and Jon Ove Hagen for many discussions on the same subject. This part of the project has also greatly benefitted from the cooperation with Stephanie L. Pfirman, in preparing manuscripts (see above) as well as in the field.

The field programmes could not have been as successfully carried out without the positive and cooperative attitude of all crew members of the R/V LANCE. 1984 and 1985 data were acquired during the Norwegian Hydrographic Survey's mapping cruises, with the assistance of Olav T. Egderød and Thomas Martinsen.

During the first four years of this study, funding was provided by the Office of Naval Research, grant N 00014-81-G-0001, to Y. Kristoffersen, who also were partly responsible for some of the data acquisition. The Norwegian Petroleum Directorate has provided a part

of the seismic data base. Economic support for meetings and discussions with J.A.Dowdeswell, at the University College of Wales, Aberystwyth, was given by NATO, grant 0747/87.

A number of other individuals and organizations have been involved in various parts of the project. These are all acknowledged in the individual papers.

INTRODUCTION AND MAIN CONCLUSIONS.

The present study consists of two main parts:

1. Processes, deposits and morphology in the recent, surge affected ice proximal environment of the northernmost Barents Sea (Papers 1, 2,3).
2. Sediment distribution and glacial history of the Barents Sea, with main emphasis on the Late Weichselian (Papers 4,5,6,7).

Background and objectives.

Glaciations of continental shelves and epicontinental seas are well documented in the geological record (Boulton & Denoux 1981, Anderson 1983, Eyles et al. 1985). Up to now, studies of modern shallow glacial marine environments have mainly been carried out along the Antarctic continental shelf or in Arctic and sub-Arctic fjord settings (see for example extensive bibliography by Andrews and Matsch (1983)). None of these may be fully representative for previous marine ice sheets, which covered wide, shallow shelf areas. The Antarctic is dominated by large, floating ice shelves, the meltwater component is essentially lacking, and the continental shelf is anomalously deep and generally slopes towards the continent. Most of the Arctic studies, on the other hand, are carried out in temperate glaciers, often in fjord environments and with a high relief topography in the hinterlands, sometimes undergoing rapid tectonic uplift, supplying large amounts of sediment to the glacial system.

Glacier surges are short-term glacier fluctuations in which a volume of ice is transported rapidly from the accumulation area to the ablation area of a glacier. Most often a surge also involves a frontal advance. Advances can be up to several kilometers and occur in less than 1 - 2 years. Surge-type glaciers surge repeatedly with periods

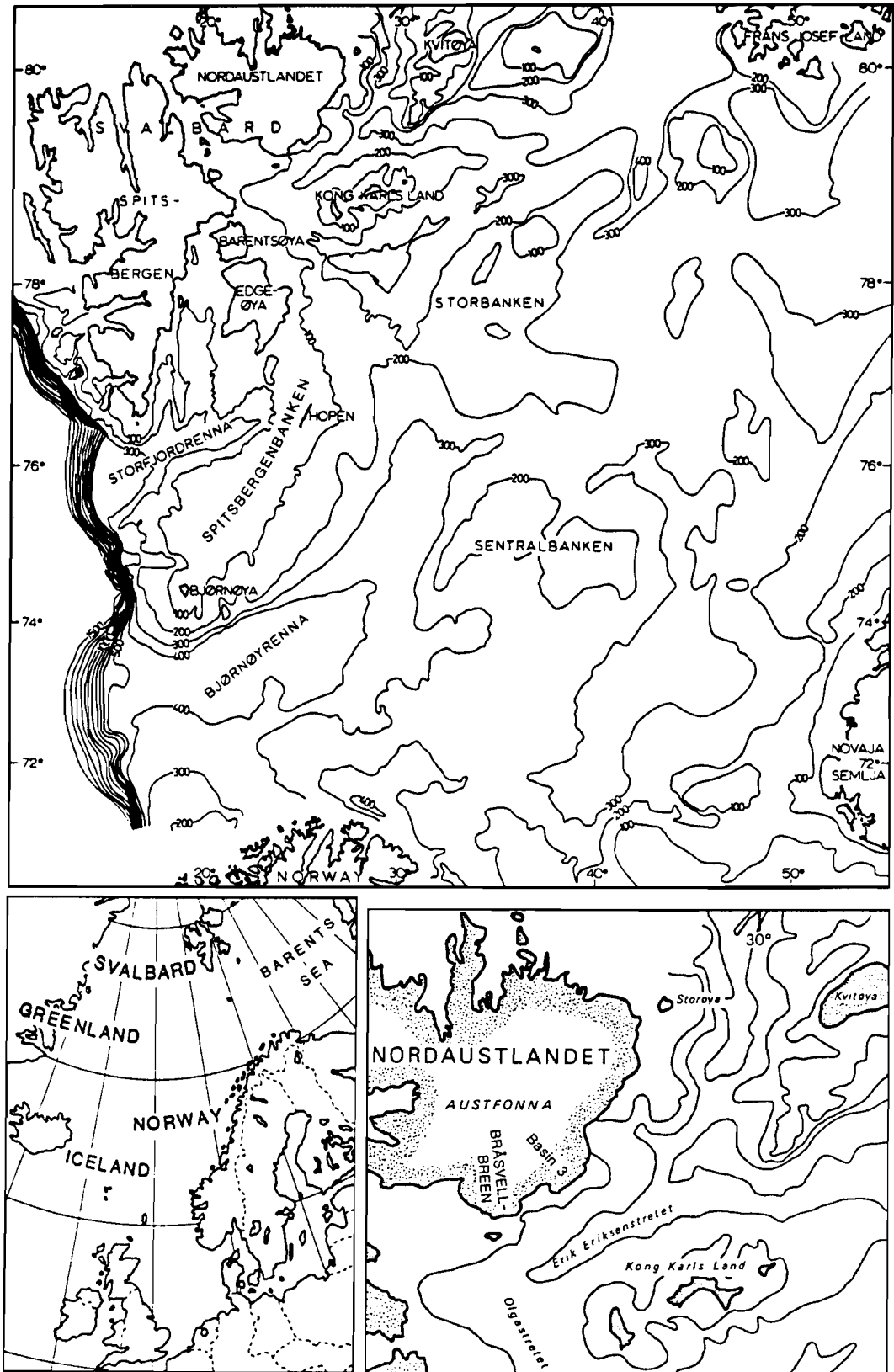


Fig.1. Bathymetry and place names of the study region.

varying from 15 years to greater than 100 years (Meier & Post 1969). Between surges the glaciers are in a quiescent phase. Potential effects of glacier surges on the depositional environment, are essentially neglected in the glaciomarine literature. Recent models for glaciomarine sedimentation (Molnia 1983, Powell 1984) do not include surges as an important mechanism in the tidewater glacier environment.

The Barents Sea shelf and the Svalbard area (Fig.1) present unique regions for studying a number of glacially influenced sedimentary environments and facies distributions, both at present and in the past. The Barents Sea, covering an area of 1.2 mill. km², presently ranges from ice distal, sea ice and current dominated environment to the ice proximal, often surge affected environment along the tidewater glacier peripheries of eastern Svalbard. The present-day ice proximal environment has been extensively studied outside the southern part of the Austfonna ice cap, Nordaustlandet (Fig.1). This ice cap has the longest continuous tidewater ice front on the northern hemisphere (approximately 200 km), and several of the 19 drainage basins of the ice cap (Dowdeswell 1984) show surging behaviour. Characteristic for the two largest drainage basins is surging into an open marine environment, grounded over marine, glacialigenic deformable sediments. This offers a situation which may have been important, or at least occurring in the past.

As the Barents Sea probably has been repeatedly glaciated during the Pleistocene (Solheim & Kristoffersen 1984), the same range of environments as found in the present-day Barents sea, may be recorded downcore. The general stratigraphic succession apparently consists of till, overlain by ice proximal, glaciomarine sediment which again has a thin cover of Holocene ice distal mud. The division between the latter two units is distinct in the south, based on pebble content,

foraminifera fauna, clay mineralogy and amount and type of organic matter (Elverhøi & Solheim 1983, Elverhøi et al. in press.). Towards the northern, presently ice proximal environment, however, the division becomes less distinct, although sediment sections resembling those found in the southern and central Barents Sea may be found locally (Solheim in prep.).

A Late Weichselian Barents Sea glaciation has been disputed by some (Baranowski 1977, Boulton 1979), whereas others have argued for a total cover of ice over the entire Barents Sea during the Late Weichselian (Grosswald 1980, Andersen 1981, Hughes et al. 1981). Several lines of evidence, however, now support the concept of a Late Weichselian Barents Sea ice sheet. They include glacio-isostatic emergence and shoreline displacement gradients for the Svalbard archipelago, the general sediment character and distribution in the northern Barents Sea and morphological features interpreted to be ice marginal, both in the northern and southern Barents Sea (Jonsson 1983, Salvigsen 1981, Salvigsen & Nydal 1981, Solheim & Kristoffersen 1984, Elverhøi & Solheim 1983, Kristoffersen et al. 1983, Vorren & Kristoffersen 1986). However, the maximum extent, exact timing and deglaciation history still remain open for discussion.

This work, which is based on high resolution acoustic data and shallow core samples, acquired during a number of cruises in the period between 1971 and 1985, addresses the following objectives:

1. The recent, surge affected ice proximal environment of the northern Barents Sea.
 - Which processes are active during glacier surges in the marine environment, and how do these affect
 - a) sea floor morphology,

b) sediment types and properties and

c) sedimentation rates

both proximal and distal to the surging glacier.

- Do glacier surges leave diagnostic features that can be applied to other/older sequences to identify surge affected sediments.
- Which processes are important in the present-day ice proximal environments of the northern Barents Sea. What type of sediments are deposited, where and how much.

2. Sediment distribution and glacial history of the Barents Sea.

- What are the sediment distribution, seismic stratigraphy, acoustic character and sedimentological characteristics in the northern Barents Sea in general, and of locally thicker accumulations in particular.
- What are the timing, number and maximum extent of the Plio-Pleistocene glaciations of the Barents Sea.
- What is the temporal and spatial deglaciation pattern of the last Barents Sea glaciation.

Glacial proximal deposition and processes are important subjects for both main parts. Firstly, most of the upper glaciomarine unit in the Barents Sea was probably deposited during relatively short time, close to the retreating Late Weichselian ice sheet. Secondly, present-day northeastern Svalbard offers one of the best existing areas for studying the ice proximal, open marine environment. Although the terms ice proximal and distal have been used differently by various authors, Powell's (1984) definition is essentially used here, stating that the ice proximal environment is directly affected by grounding line processes, whether an ice shelf or a tidewater glacier.

Oscillatory, surging behavior will increase this zone to a width depending on the amount of frontal advance during surge. Furthermore, we include the region where the majority of sediments in turbid meltwater plumes fall out from suspension, which is in the order of 5 km from the glacier front.

Project progress and the individual papers.

The initiation of the surge related part of this project is based on the last surge of the Bråsvellbreen glacier, the second largest drainage basin of the Austfonna ice cap. This occurred between 1936 and 1938, and is the largest surge documented to date (by aerial photography). The terminus advanced in the order of 15 km offshore and has afterwards stagnated and retreated.

Reconnaissance work in 1980 and 1981 revealed overcompacted glacial sediment inside a ridge roughly paralleling the present ice front at a distance of up to 5 km from it. This was taken to indicate that the glacier had advanced over sea floor covered by glaciomarine and glacial sediments. A project termed "consolidation of glacial and glaciomarine sediments by ice loading" was then initiated. High priority was given to the geotechnical and sedimentological aspects of the project to reveal the effects of an ice load on the engineering characteristics of glacial sediments. The Bråsvellbreen situation could be considered a small scale analogue to the Norwegian continental shelf during past glaciations.

However, due to severe sea ice problems during the main coring period and difficulties, caused by the high gravel and pebble content, in both achieving undisturbed samples and to prepare them for geotechnical tests, the sedimentological and geotechnical aspects had to be tuned down. Stronger emphasis was then placed on the acoustic profiling, in particular side scan sonar data. A considerable amount

of cores were recovered from the region, however, and geotechnical and sedimentological studies were carried out, but at a somewhat more simple level than originally planned. The data base collected in front of Bråsvellbreen is considered to give a good overview of a surge affected glaciomarine environment.

The first paper from the region (Paper 1.) was based on the data acquired during the 1982 and 1983 field seasons, and may be considered as a preliminary report on the morphology found proximal to the glacier. During 1984 and 1985, the Norwegian Hydrographic Survey (NSKV) carried out hydrographic mapping along a dense grid of lines outside Bråsvellbreen and adjacent areas. By participating in these cruises, we were able to largely increase the data base of side scan sonar, sparker and 3.5 kHz data, in addition to some cores and sea floor photographs. Furthermore, the new data set was collected with greatly improved navigation, as a Decca Sea Fix system was used, with an accuracy in the order of 10 m, as opposed to the Transit satellite system used on the previous cruises, with accuracy of 2-300 m at the best. Although the main conclusions drawn in Paper 1., for the morphology in the ice proximal area at Bråsvellbreen, were not radically changed, the new data greatly improved our understanding of the spatial distribution of sediments and morphological patterns, now also including the adjacent drainage basin, Basin 3 (Fig.1). As the general understanding of the area improved, some of the interpretations for formation of the morphology have also changed slightly. Hence it was considered necessary to repeat parts of Paper 1. in Paper 2., as the latter is a synthesis of all information from the region, including sedimentological and geotechnical analyses, and it aims towards developing a sedimentary facies model for large, marine surging glaciers.

Paper 3. discusses the post surge depositional environment. Main

emphasis is here placed on deposition from suspension load outside the major meltwater outlet draining this part of the Austfonna ice cap.

Previous to and parallel with the studies off Nordaustlandet, work has been carried out in the northern and central Barents Sea, mainly focused on the glacial history of the region. Papers 4. and 5. are based on data collected up to 1982, and discuss the general distribution of unlithified sediments, their sedimentological characteristics and seismic stratigraphy, and relates this to Plio - Pleistocene glaciations. Special emphasis is given to the Late Weichselian glaciation (Paper 4.).

More geological and geophysical data were obtained in 1983, now also including side scan sonar records, from the northern, central Barents Sea. Characteristic for this region is a generally thin (<10-15 m) cover of unlithified sediments with locally thicker accumulations of till or glaciomarine sediment. Morphological pattern, in particular iceberg plough marks, and sediment distribution in the area of a local accumulation on Storbanken (Fig.1) are discussed in relation to deglaciation of the northern Barents Sea (Paper 6.).

Paper 7. synthesize all available information on the recent depositional environment and processes in the northern Barents Sea. This paper draws the link between the present-day change from ice distal to proximal environments along N-S transects and similar variations recorded downcore (Paper 4.)

Ideas on the Late Weichselian glaciation of the Barents Sea have evolved somewhat during the course of this study. In Paper 4., a tentative maximum ice sheet extent was suggested along locally thicker accumulations fringing the bank areas. However, new information may indicate that these are more likely to represent recessional stages of a larger ice sheet (Paper 7.). Strong indications for this are also presented from the southern Barents Sea, where moraine ridges probably

are formed by ice movement from the north (Vorren and Kristoffersen 1986). Furthermore, the thin cover of glaciomarine mud in Bjørnøyrenna (about 1 m), is unlikely to represent a significantly longer time interval than 10 ky. However strong indications, the final answer to the question of connection between the Late Weichselian Barents Sea and Fennoscandian ice sheets remains open.

Main conclusions.

- Marine glacier surges have a major impact on the depositional environment of the basin into which the surges occur. The strongest impact is seen in the sea floor morphology, but also sediments, sedimentation rate and sediment physical properties are affected. Important processes involve direct ice push, increased meltwater output and deposition from meltwater plumes, local slumping, sub glacial squeeze-up of sediment and increased iceberg production.
- The total suite of surge effects, taken together, is diagnostic for glacier surges. However, parts of the most diagnostic features, subglacially formed squeeze-up ridges, are only likely to be preserved in the stratigraphic record if subsequent surges do not occur over the same area.
- Present-day sedimentation in the ice proximal areas of the northern Barents Sea is dominated by mud deposition from sediment plumes in the vicinity of large meltwater outlets. The most conspicuous effect of these is the formation of acoustically transparent sediment lenses within 1 km off the outlets. This contrasts with the ice distal, major parts of the Barents Sea, where current winnowing with subsequent redeposition, and transport of extra-basinal material with sea ice and icebergs are the dominant processes.
- The cover of unlithified sediments is generally less than 25 ms

(two-way reflection time) over the major part of the northern Barents Sea (north of approximately 74°N). Bedrock outcrop may occur locally, but most areas have a thin mud cover. Locally thicker sediment accumulations (up to 60 - 70 ms) fringes the main bank areas. In contrast, the Barents Sea south of approximately 74°N has an unlithified sediment cover generally more than 50 ms thick, increasing to more than 500 ms towards the western continental margin.

- The unlithified sediments generally consist of acoustically transparent mud of Holocene age and pebbly mud interpreted to be ice proximal, Late Weichselian glaciomarine sediments, covering less transparent sediment found to be overconsolidated pebbly mud. The latter is interpreted to represent Late Weichselian till or glaciomarine sediments subjected to an ice load. The locally thicker accumulations is acoustically interpreted to represent moraine complexes or glaciomarine accumulations. The latter is most likely formed in an ice proximal environment, by deposition from turbid meltwater plumes, as found off Nordaustlandet at present (above).
- Seismically mapped regional unconformities in the outer parts of Bjørnøyrenna, indicate at least seven glacial advances of which at least four reached the shelf edge. However, no core information presently exists to verify the seismic interpretation.
- The Late Weichselian ice sheet reached at least further south than Storbanken, but maximum extent and exact timing for the deglaciation remain unknown. The retreat probably took place in a stepwise manner, with locally thicker accumulations formed in ice proximal positions during halts in the retreat.
- ^{14}C datings of cores from Erik Eriksenstredet show that this area was deglaciated approximately 10.4 kA, at the latest. Extrapolation of sedimentation rates of the interpreted glaciomarine sediments

below the dated levels, indicates that onset of glaciomarine sedimentation may have occurred as early as 13 kA.

References

- Andersen, B.G. 1981: Late Weichselian ice sheets in Eurasia and Greenland. In Denton, G.H. & Hughes, T.J. (eds.) The last great ice sheets. John Wiley & sons, 1-65.
- Anderson, J.B., 1983: Ancient glacial-marine deposits: Their spatial and temporal distribution. In Molnia, B.F. (ed.) Glacial-marine sedimentation, Plenum Press, New York, 3-92.
- Andrews, J.T. & Matsch, C.L. 1983: Glacial marine sediments and sedimentation; an annotated bibliography. Geo Abstracts Ltd., London, Bibliography no. II, 227pp.
- Baranowski, S. 1977: The subpolar glaciers of Spitsbergen seen against the climate of this region. Results of investigations of the Polish scientific Spitsbergen expeditions, vol.III, 93pp.
- Boulton, G.S. 1979: Glacial history of the Spitsbergen archipelago and the problem of the Barents Sea ice sheet. Boreas, 8, 31-57.
- Boulton, G.S. & Deynoux, M., 1981: Sedimentation in glacial environments and the identification of tills and tillites in ancient sedimentary sequences. Precambrian Research, 15, 397-422.
- Dowdeswell, J.A. 1984: Remote sensing studies of Svalbard glaciers. Unpubl. Ph.D. thesis, University of Cambridge, 250pp.
- Elverhøi, A. & Solheim, A. 1983: The Barents Sea ice sheet - a sedimentological discussion. Polar Research In.s., 23-42.
- Elverhøi, A., Pfirman, S.L., Solheim, A., & Larsen, B.B. in press: Glaciomarine sedimentation and processes on high Arctic epicontinental seas - exemplified by the northern Barents Sea. Marine Geology.
- Eyles, C.H., Eyles, N. & Miall, A.D., 1985: Models of glaciomarine

- sedimentation and their application to the interpretation of ancient glacial sequences. Palaeogeogr., Palaeoclimatol., Palaeoecol., 51, 15-84.
- Grosswald, M.G. 1980: Late Weichselian ice sheet of northern Eurasia. Quaternary Research 13, 1-32.
- Hughes, T.J., Denton, G.H., Andersen, B.G., Schilling, D.H., Fastook, J.L. & Lingle, C.S. 1981: The last great ice sheets: A global view. In Denton, G.H. & Hughes, T.J. (eds.): The last great ice sheets. John Wiley & Sons.: 263-317.
- Jonsson, S. 1983: On the geomorphology and past glaciation of Storøya, Svalbard. Geografiska Annaler, 65A, 1-17.
- Kristoffersen, Y., Milliman, J.D. & Ellis, J.P. 1984: Unconsolidated sediments and shallow structure of the northern Barents Sea. Norsk Polarinstitutt Skrifter 180, 25-39.
- Meier, M.F. & Post, A. 1969: What are glacier surges? Canadian Journal of Earth Sciences, 6, 807-817.
- Molnia, B.F. 1983: Subarctic glacial-marine sedimentation: a model. In: Molnia, B.F. (ed.) Glacial-marine sedimentation, Plenum Press, New York, 95-114.
- Powell, R.D. 1984: Glacimarine processes and inductive lithofacies modelling of ice shelf and tidewater glacier sediments based on Quaternary samples. Marine Geology, 57, 1-52.
- Salvigsen, O. 1981: Radiocarbon dated raised beaches in Kong Karls Land, Svalbard, and their consequences for the glacial history of the Barents Sea area. Geografiska Annaler, 63A, 283-291.
- Salvigsen, O. & Nydal, R. 1981: The Weichselian glaciation in Svalbard before 15 000 B.P. Boreas, 10, 433-446.
- Solheim, A. in prep.: The depositional environment of surging sub-polar tidewater glaciers: A case study of the

morphology, sedimentation and sediment properties in a surge affected marine basin outside Nordaustlandet, Northern Barents Sea.

Solheim, A. & Kristoffersen, Y. 1984: The physical environment, western Barents Sea, 1:1,500,000, sheet B; Sediments above the upper regional unconformity: thickness, seismic stratigraphy and outline of the glacial history. Norsk Polarinstitutt Skrifter 179 B, 26pp.

Vorren, T.O. & Kristoffersen, Y. 1986: Late Quaternary glaciation in the south-western Barents Sea. Boreas, 15, 51-59.

PAPER 1.

SEA-FLOOR MORPHOLOGY OUTSIDE A GROUNDED, SURGING GLACIER; BRÅSVELLBREEN, SVALBARD

ANDERS SOLHEIM and STEPHANIE LOUISE PFIRMAN

Norwegian Polar Research Institute, P.O. Box 158, N-1330 Oslo Lufthavn (Norway)

*Woods Hole Oceanographic Institution, Department of Geology and Geophysics,
Woods Hole, MA 02543 (U.S.A.)*

(Received December 5, 1983; revised and accepted September 5, 1984)

ABSTRACT

Solheim, A. and Pfirman, S.L., 1985. Sea-floor morphology outside a grounded, surging glacier; Bråsvellbreen, Svalbard. *Mar. Geol.*, 65: 127–143.

Acoustical profiling and bottom photography reveal several different sea-floor morphological features adjacent to the grounded Bråsvellbreen glacier on Svalbard, north-western Barents Sea. Some of the features and their distribution may be closely related to a major glacial surge in 1936–1938, and as such are valuable in identifying former surges in other locations. A continuous, wide ridge with a characteristic asymmetrical cross-section, running subparallel to the glacier, is the end moraine defining the maximum extent of the surge. A large part of the material forming this ridge is most likely rapidly deposited from meltwater during the surge. A rhombohedral pattern of smaller mounds inside the ridge is probably an expression of relief in the glacier sole during the surge. Discontinuous arcuate ridges define local, minor oscillations during retreat of the ice at a later stage. Iceberg plough marks are most frequent seaward of the end moraine, their orientation is controlled by the combination of a coastal current, offshore katabatic winds and topography. Superimposed on plough marks are secondary features such as a “washboard pattern” and striae, most likely caused by push-up of overconsolidated material during gouging and multi-keel icebergs, respectively. Bottom sediments, observed in photographs and cores, are loose, pebbly muds with high variability in clast content, resting on overconsolidated material, probably basal till. Mud deposition presently prevails close to the glacier.

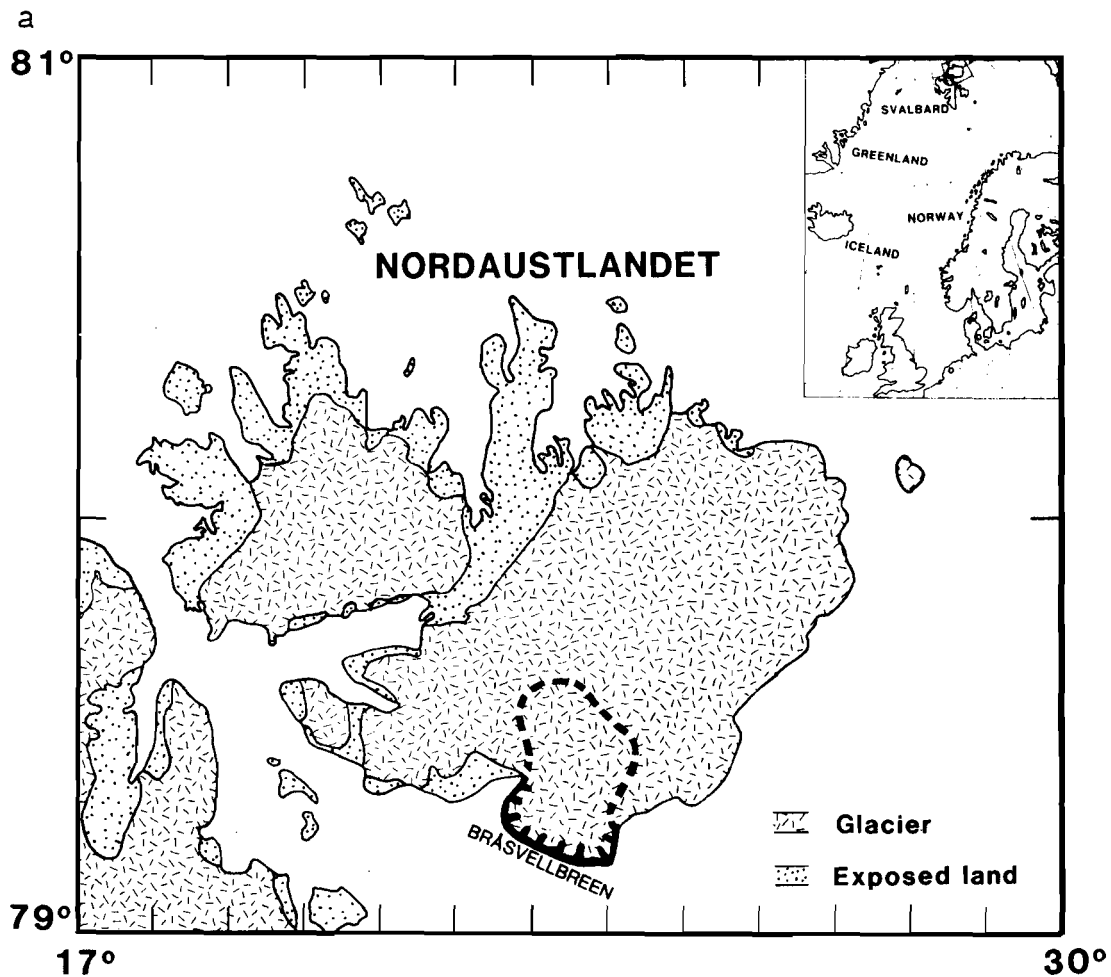
INTRODUCTION

Glacial readvances during a general deglaciation are usually interpreted as expressions of climatic fluctuations. However, glacial surges are important in many areas today, and were probably also common in the past. Glacier surges occur independently of climatic variations, although they do imply sufficiently high precipitation over a period of time to build up an unstable mass distribution. Thus attempts to correlate ice-marginal features to regional or global climatic shifts may have little relevance. Prest (1969) considered, for example, the possibility that several of the Laurentide readvances were due to surging on a local scale with no climatological significance. Similarly,

Holdsworth (1977), suggests that surge activity on Baffin Island may have been important during the decay of the last ice sheet. Glacier thinning through surges, according to Holdsworth (1977), may also help to explain the apparent difficulties of accounting for the rapid decay rates of large ice sheets in terms of the energy requirements for melting ice (Hare, 1976).

Bråsvellbreen glacier (Fig.1a, b) is situated in the Svalbard archipelago, northwestern Barents Sea, adjacent to the Arctic Ocean in the north and the Norwegian Greenland Sea in the west. The Barents Sea is the largest recent epicontinental sea (Bjørlykke et al., 1978). The glacier (1110 km²) is part of an ice cap (8130 km²) which covers most of Nordaustlandet, the second largest island in the archipelago. The glacier front is grounded in water depths ranging from 30 to 100 m, and forms a vertical wall 25–35 m above sea level. The terminus appears stable, and fracturing is presently limited to a few parallel fractures (Fig.2a). According to satellite images, large-scale features of the ice front, like embayments and protrusions, have persisted at least since 1976.

Glacial surges tend to occur sporadically at intervals of 30–100 years (Meier and Post, 1969). A surge usually lasts 1–2 years (Paterson, 1981),



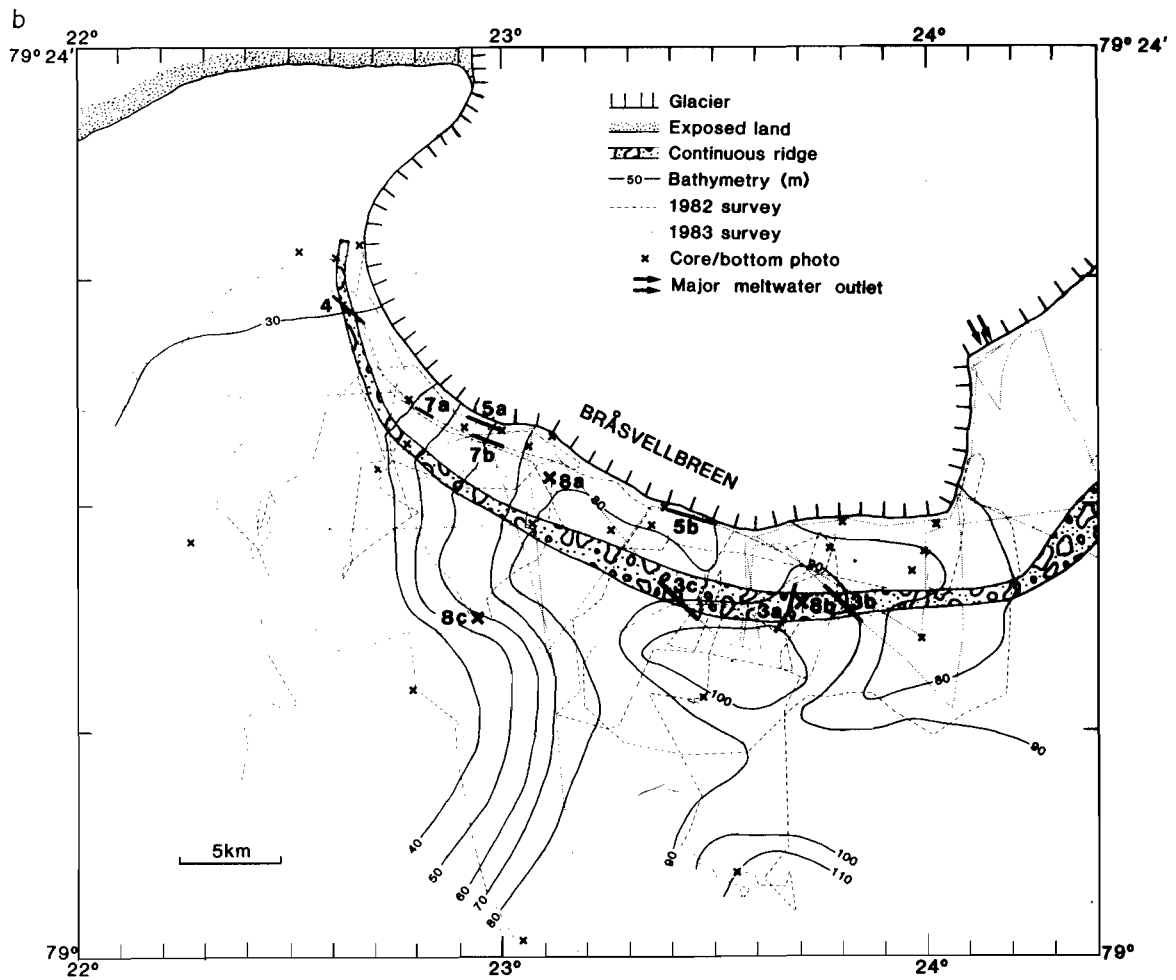
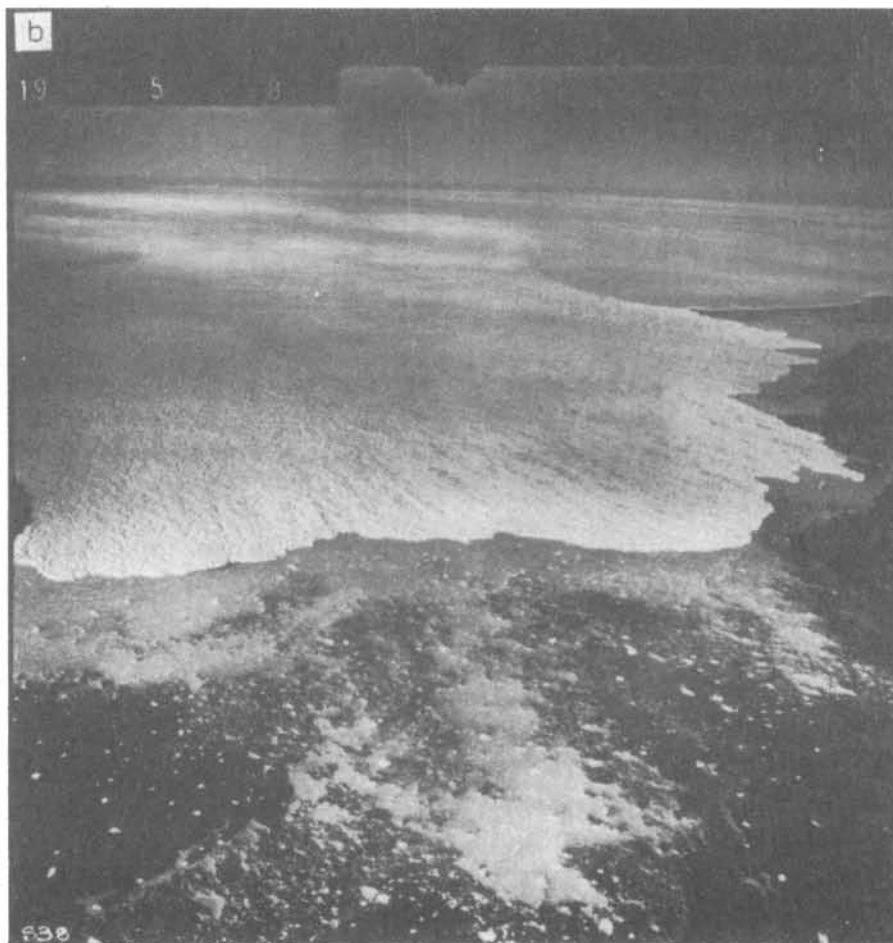


Fig.1. *a.* Distribution of glaciated areas and exposed land on the island of Nordaustlandet. Map area is shown by hatching in the location map. Outline of Bråsvellbreen (heavy line) after O. Liestøl, pers. commun., 1984. *b.* The survey area outside Bråsvellbreen glacier. Numbers on heavy lines and crosses refer to later figures.

during which time the glacier front advances rapidly. Surges constitute a common form of glacier advance on Svalbard (Liestøl, 1969). On Spitsbergen, the largest island in the archipelago, advances of up to 12 km in less than one year have been measured (Liestøl, 1969). The forward movement of the glacier ceases at the end of the surge, and, in the case of tidewater glaciers, calving causes retreat of the ice front.

Between 1936 and 1938, Bråsvellbreen surged up to 20 km (Schytt, 1969), and has retreated several kilometers since that time. Extensive crevassing during the surge is documented from aerial photography (Fig.2b, c). Surge boundaries probably were controlled by underlying bedrock topography in central parts of the Nordaustlandet ice cap (Schytt, 1964; O. Liestøl, pers. commun., 1983).

This situation presents a unique opportunity to study the effects of glacier advances on different sea-floor parameters, such as morphology,



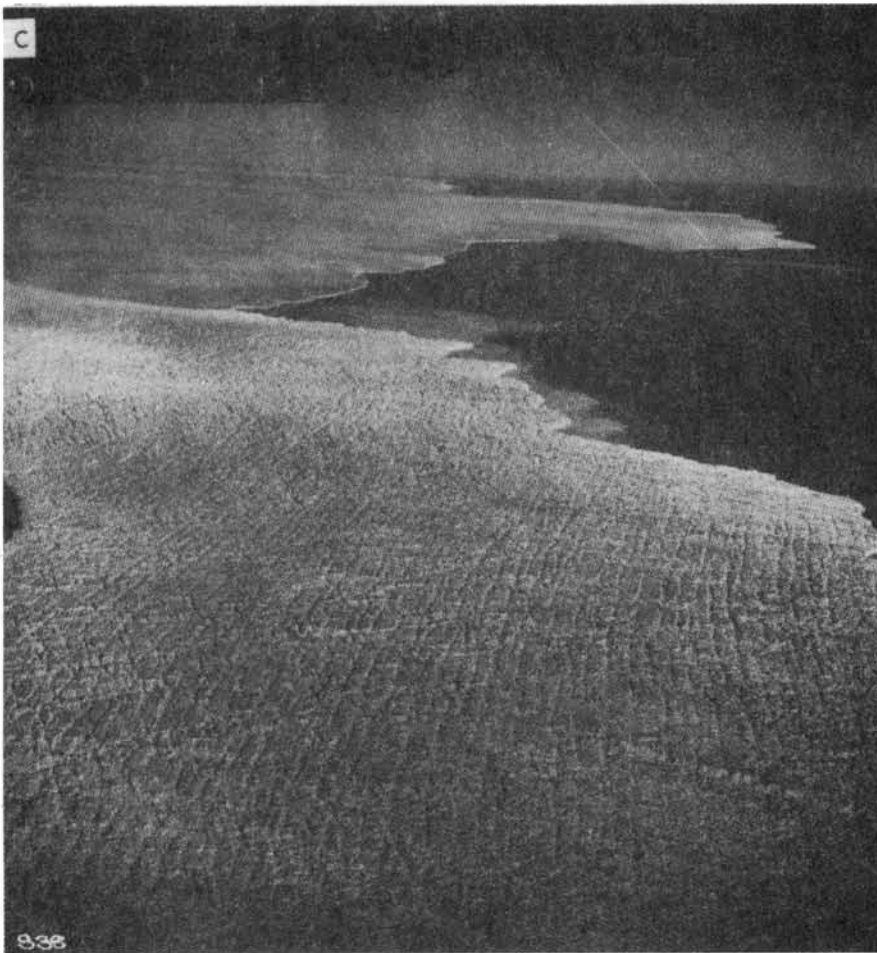


Fig.2. Aerial photos. *a.* Photo taken from helicopter in 1982, showing the present-day Bråsvellbreen. Exact location and flight height is unknown, camera lens 28 mm. *b.* Photo taken in 1938 of the eastern part of Bråsvellbreen. Note how the extensively crevassed glacier surface contrasts with the present-day situation as shown in *a.* Also note the "old" ice-front in the right-hand part of the photo, and the boundary between crevassed and uncrevassed glacier towards central parts of the ice cap. Flight height is approximately 2200 m, camera lens 210 mm (Norsk Polarinstitut photo S-38, 1958). *c.* Photo taken in 1938, showing pattern of crevassing on the eastern flank of Bråsvellbreen. Also note the boundary to the "old" glacier front and surface. Flight height is approximately 1800 m, camera lens 210 mm (Norsk Polarinstitut photo S-38, 1921).

sediment distribution and composition and geotechnical properties. A program of acoustical profiling, core sampling and bottom photography has been carried out proximal to the glacier front. In this paper, emphasis will be placed on the morphological features mapped seaward of the glacier.

DATA ACQUISITION

The main data base was collected during two cruises in August 1982 and August 1983 (Fig.1b) aboard the R/V "Lance". Acoustic instrumentation consisted of a hull-mounted 3.5 kHz echo-sounder (O.R.E. traneiver with

an EPC 3200 analogue graphic recorder), a Klein side-scan sonar system, operating with 50 kHz transducers and an E.G. & G. sparker system (only in 1983) with analogue recording via a single-channel streamer in the pass band 100–600 Hz. Bottom photographs were taken with a Benthos deep-sea camera, and cores with 110 mm diameter gravity-corer and 90 mm diameter vibro-corer.

Due to severe sea-ice conditions, the side-scan survey of 1982 was limited to a narrow region of open water along the western part of the glacier front. Extensive coverage was, however, obtained with the 3.5 kHz echo-sounder, which has been run continuously while being in the area. In 1983, the area was almost ice-free, and additional profiling was done to obtain better coverage with side-scan sonar and sparker. Altogether, the data include 150 km of sparker and side-scan sonar profiles, 400 km of 3.5 kHz echo-sounder profiles, 14 bottom photograph stations and 27 core sampling locations.

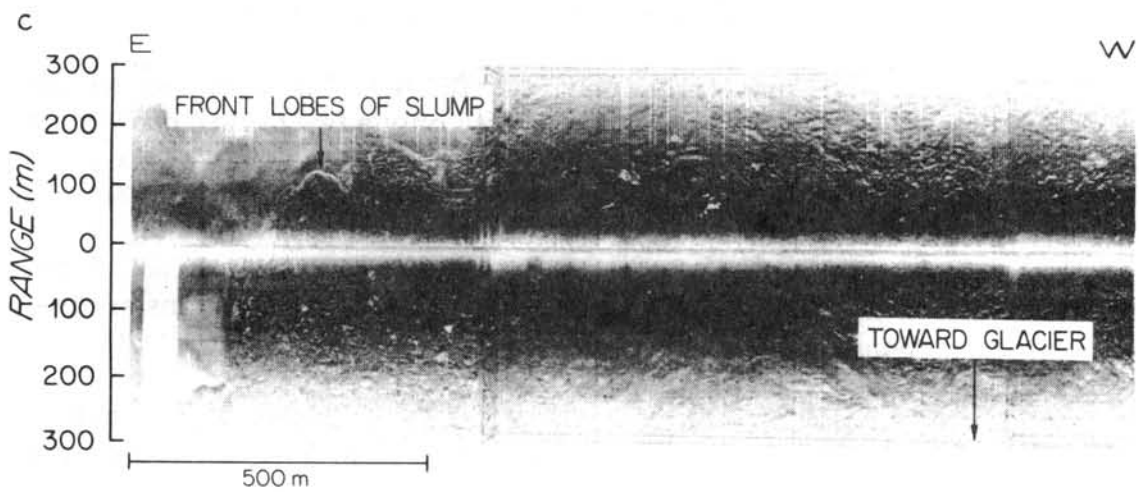
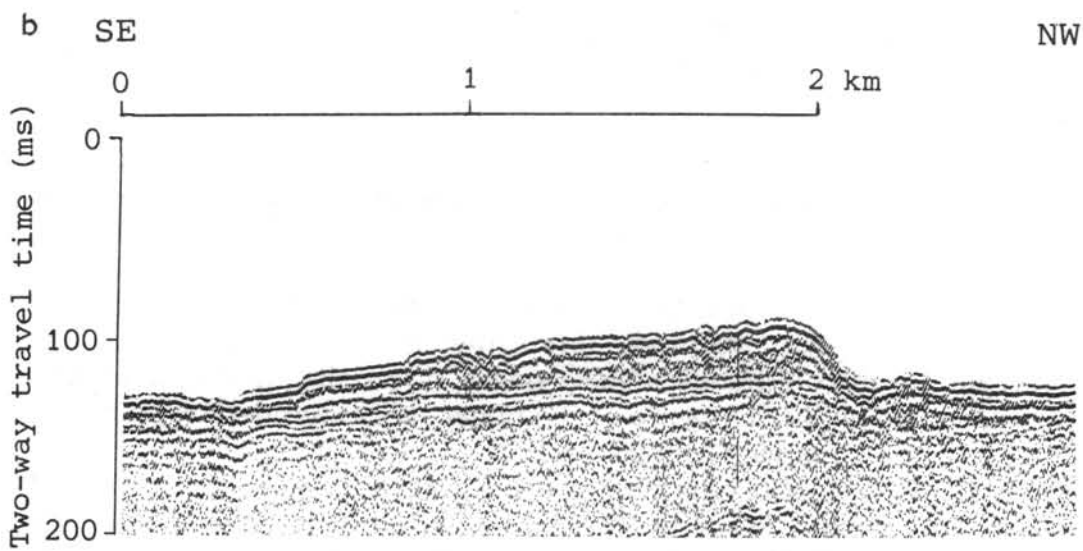
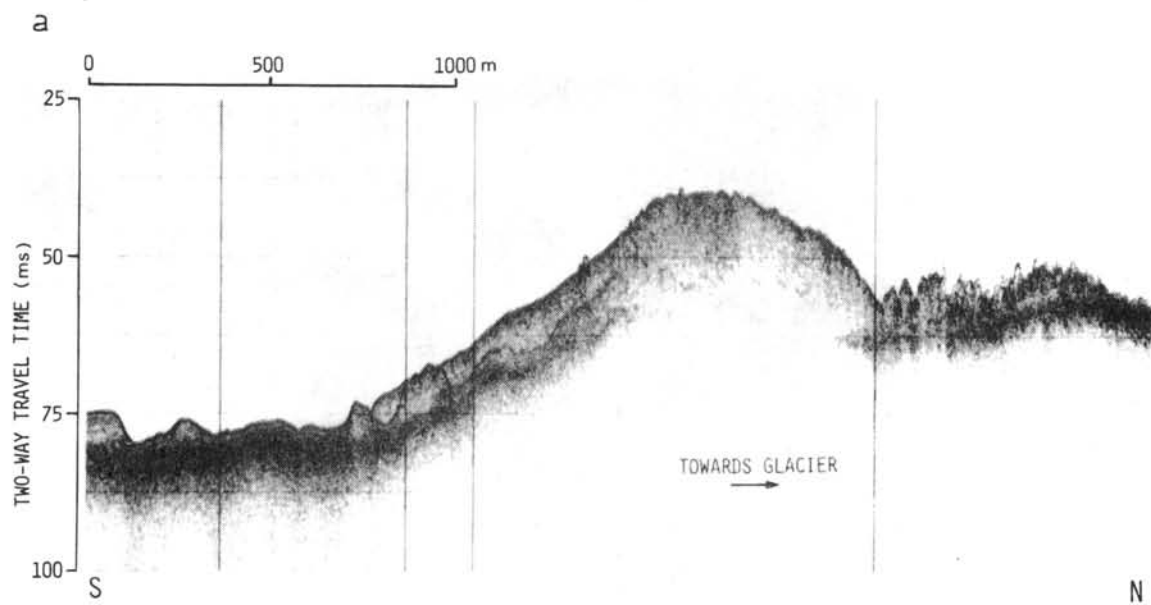
MORPHOLOGICAL FEATURES

Bråsvellbreen glacier thins to the west, exposing bare land and forming the southwestern boundary of the Nordaustlandet ice cap (Fig.1a). The front of the ice cap continues northeastward from the study area for another 120 km. Water depth increases to the east in the study area from less than 30 to 100 m, with the steepest bathymetric slope being midway along the front, where a broad depression runs perpendicular to the glacier (Fig.1b).

Several distinct bottom morphological patterns are present in the survey area. The most prominent feature is a continuous ridge, subparallel to the glacier front. The distance from the ridge crest to the glacier front varies from 500 m in the western sector to >5 km in the eastern, deeper regions. Ridge relief varies from 8 to 20 m, and width ranges from 500 to 1700 m; the highest and widest region (Fig.3a) is located in the central depression. True slopes are 2–3° on the side facing away from the glacier, distal side, and 4–6° (locally steeper) on the proximal side. Slumps are observed on the distal flank (Fig.3c), with locally rougher surface morphology and lobate margins. The distal flank is acoustically more transparent than central and proximal portions of the ridge, and a distinct contact with the underlying surface is visible on 3.5 kHz records, although this may be somewhat obscured under the crest and inner slope (Fig.3a). On sparker records, a seismic reflector can be followed under the deposit (Fig.3b).

Sea-floor morphology inside the continuous ridge is quite different from that outside, with respect to both relief and type of features. In general, the sea floor has a more disturbed appearance inside than the more regular, ice-ploughed surface outside the ridge (Figs.3a and 4). Distinguishable features proximal to the glacier are: (1) rhombohedral pattern, formed by linear,

Fig.3. *a.* 3.5 kHz echo-sounding across the continuous outer ridge. For location, see Fig.1. *b.* 1 kJ sparker record across the ridge. For location, see Fig.1. *c.* Side-scan sonograph showing slumps on the distal flank of the ridge. For location see Fig.1.



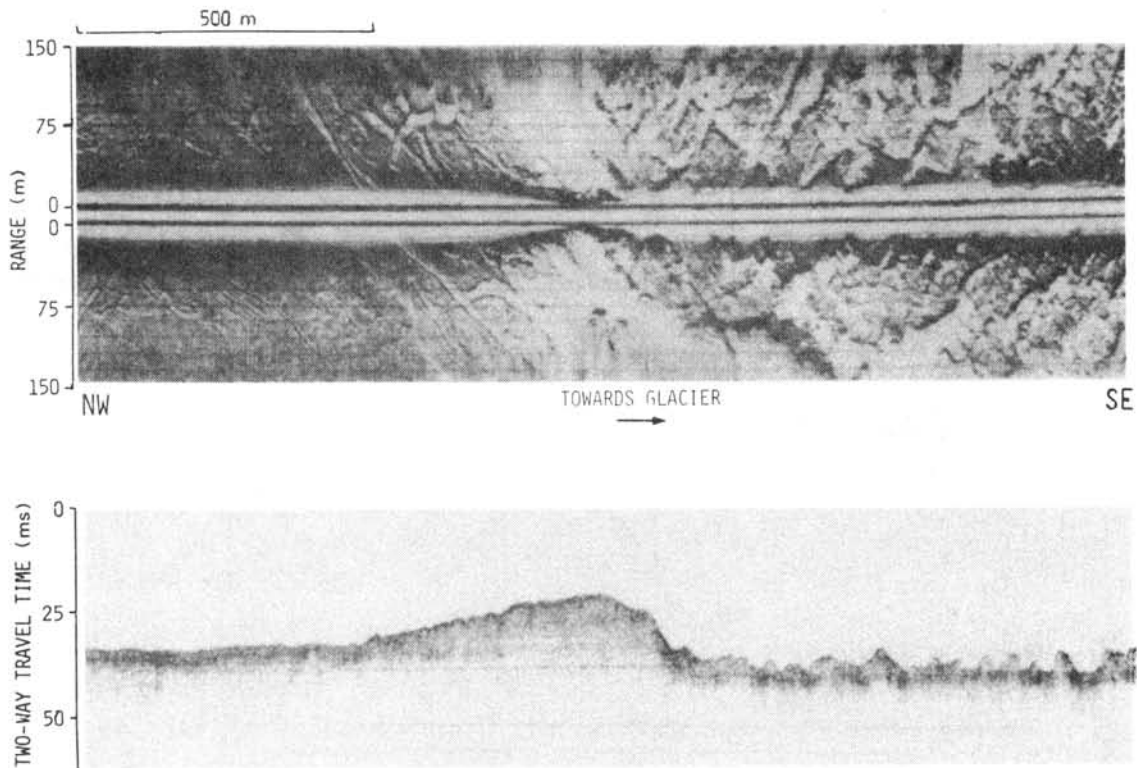


Fig.4. Side-scan sonograph and 3.5 kHz echo-sounding trending obliquely across the continuous outer ridge. For location see Fig.1.

discontinuous ridges with a relief of about 5 m and spacing in the order of 20–50 m (Fig.5a); (2) irregularly distributed mounds up to 10 m high (Fig.5a); and (3) discontinuous, arcuate ridges, subparalleling the glacier over short distances (Fig.5b). The scale of the ridges varies considerably, but they tend to be within 25 m wide and 2–5 m high.

In general, the rhombohedral pattern and irregular mounds cover most of the area while arcuate ridges are found in a narrow belt along the present-day glacier front (Fig.6). In the westernmost and shallowest part of the area, however, the rhombohedral pattern is observed at the glacier front (Fig.5a).

Iceberg gouges are most prominent and frequent on the smoother sea floor on the distal side of the major ridge, with only a few occurrences closer to the glacier. The furrow widths range from 10 to 30 m, and vertical relief is 2–5 m. These dimensions have also been found in relict plough marks on the North Sea shelf (Belderson and Wilson, 1973), although most relict plough marks along the Norwegian coast are larger (Rokoengen, 1980; Lien, 1983). Most of the gouges show distinct levees. Plough directions are predominantly sub-parallel to the glacier front, but some at high angles are also observed, especially inside the ridge.

Secondary features are included within some of the ice gouges proximal to the glacier. A distinct “washboard pattern” (Lien, 1982) is observed at

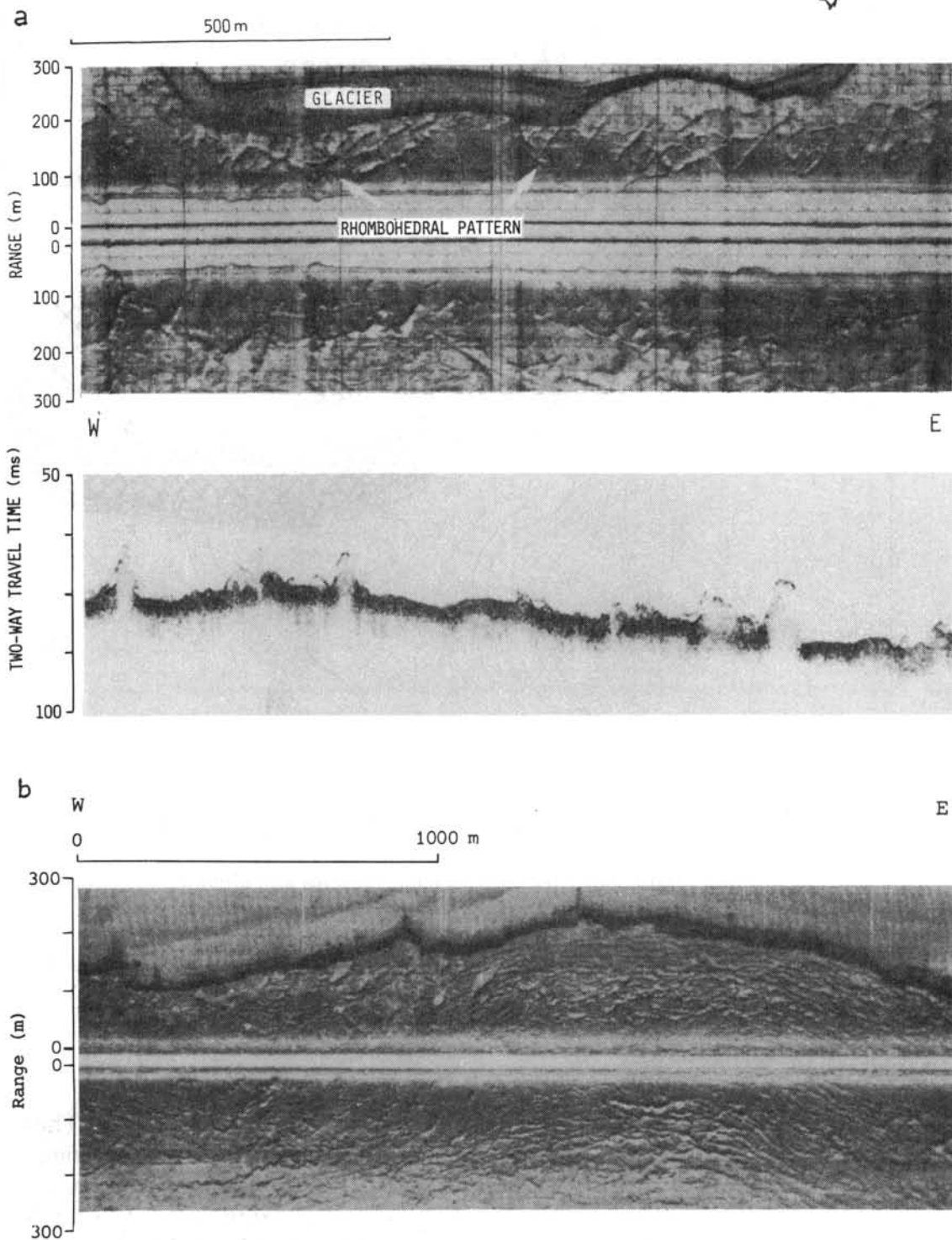


Fig.5. *a.* Side-scan sonograph and 3.5 kHz sounding along the glacier front, showing rhombohedral ridge pattern and irregular mounds. For location, see Fig.1. *b.* Side-scan sonograph along the glacier front, showing arcuate discontinuous ridges paralleling the ice front. For location see Fig.1.

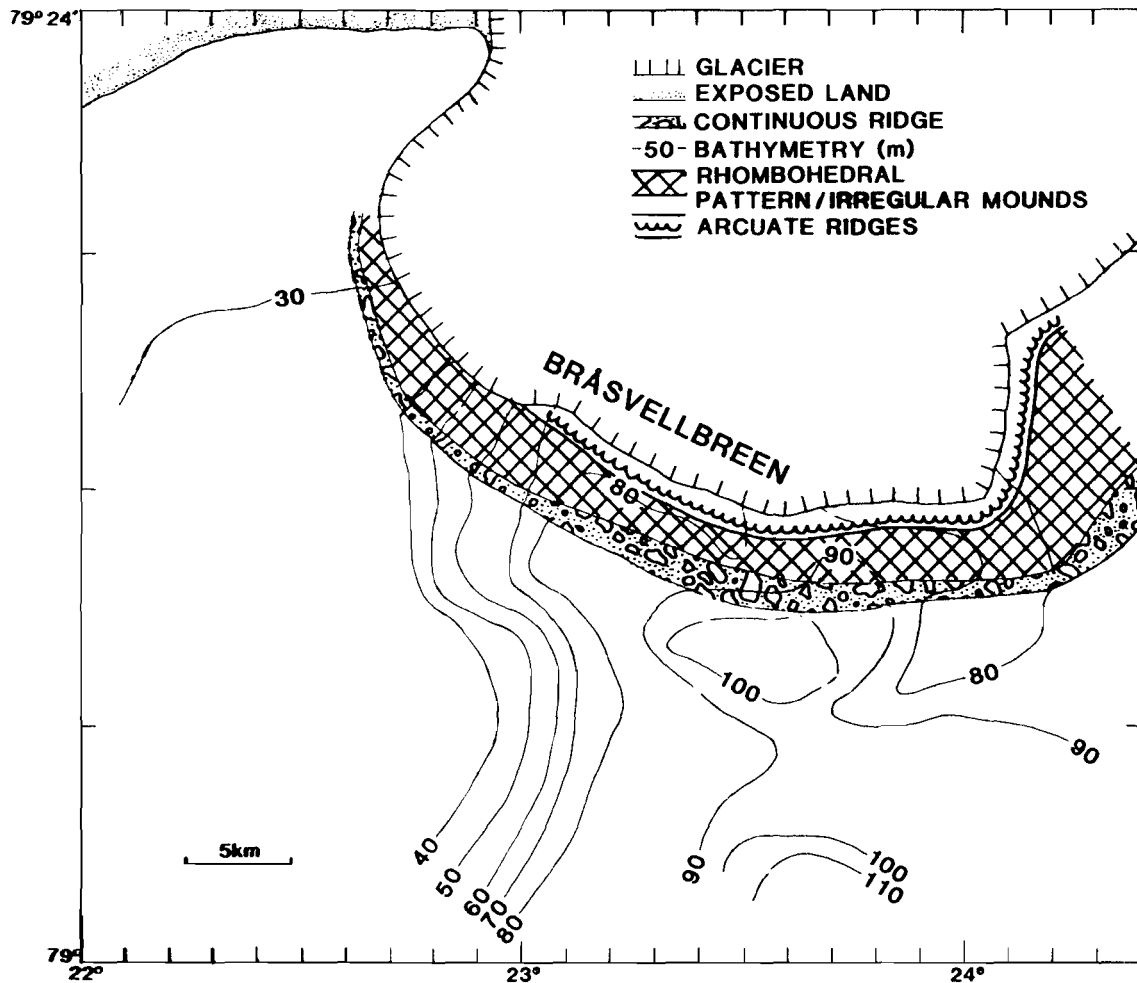


Fig.6. Distribution of rhombohedral pattern/irregular mounds and arcuate, discontinuous ridges outside the Bråsvellbreen glacier.

the outer edges of a wide plough mark proximal to the glacier (Fig.7a), while other plough marks are striated parallel to the gouge direction (Fig.7b).

SEDIMENT DISTRIBUTION

The surface sediments have high lateral variability in the study area. They are generally pebbly muds, but the pebble content shows considerable range both in cores and bottom photographs (Fig.8). Photographs from four stations taken within 200 m of the glacier front have turbid water obscuring most of the picture; however the bottom in this area appears muddy with few cobbles. Turbid bottom water was not observed at greater distances from the glacier. Bands of clean cobble pavement (Fig.8c) are observed outside the continuous ridge. Except for this pavement, no signs of current activity (i.e. ripples or scour marks) are seen at any of the bottom photographic stations.

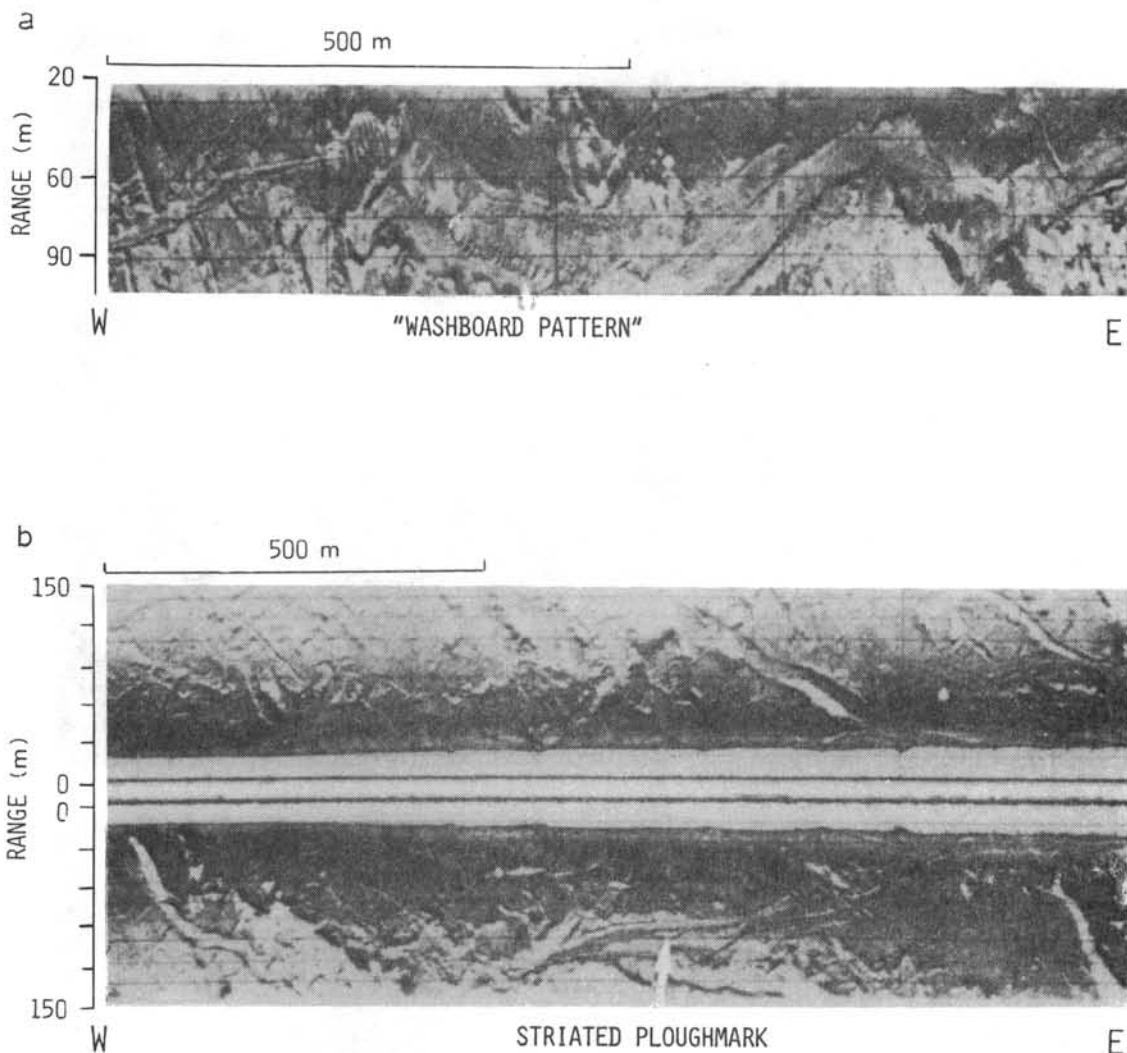
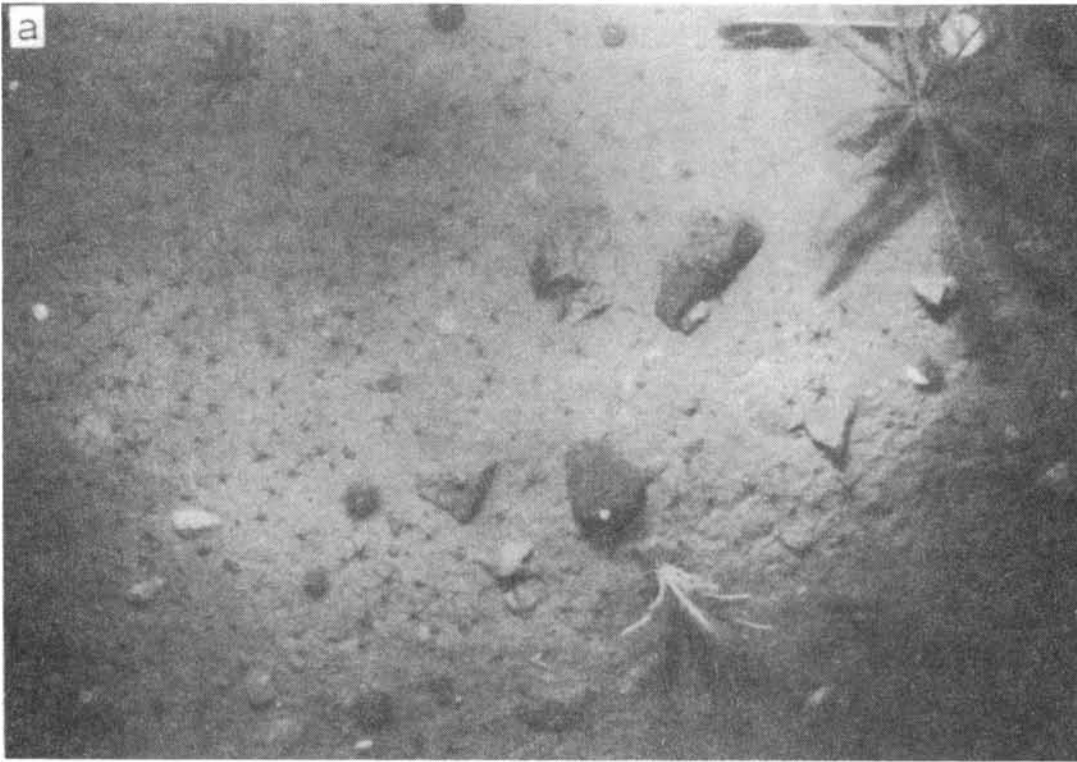


Fig.7. Side-scan sonographs showing iceberg plough marks with secondary features. *a.* "Washboard pattern" along edge of plough mark. *b.* Striated plough mark. For location see Fig.1.

Apart from variable pebble content, the main downcore change is in degree of consolidation. The top layer is usually a loose (s_u less than 10 kPa, measured with pocket penetrometer and falling cone apparatus), pebbly mud and is seen from the 3.5 kHz records to form a major part of the local topography. A thin and patchy layer of somewhat overconsolidated material ($s_u = 30\text{--}50$ kPa) exists below the top layer inside the continuous ridge. In a few cores, very stiff material (s_u in excess of 100 kPa) was recovered. This lowermost layer forms an even reflector on 3.5 kHz records and is interpreted to represent older basal till, probably of Late Weichselian (Late Wisconsin) age as is also inferred for similar material further out in the Barents Sea (Elverhøi and Solheim, 1983). The intermediate material could, on the other hand, owe its overconsolidation to the surge (Solheim, in prep.). This material is probably too patchy and has too small an acoustic



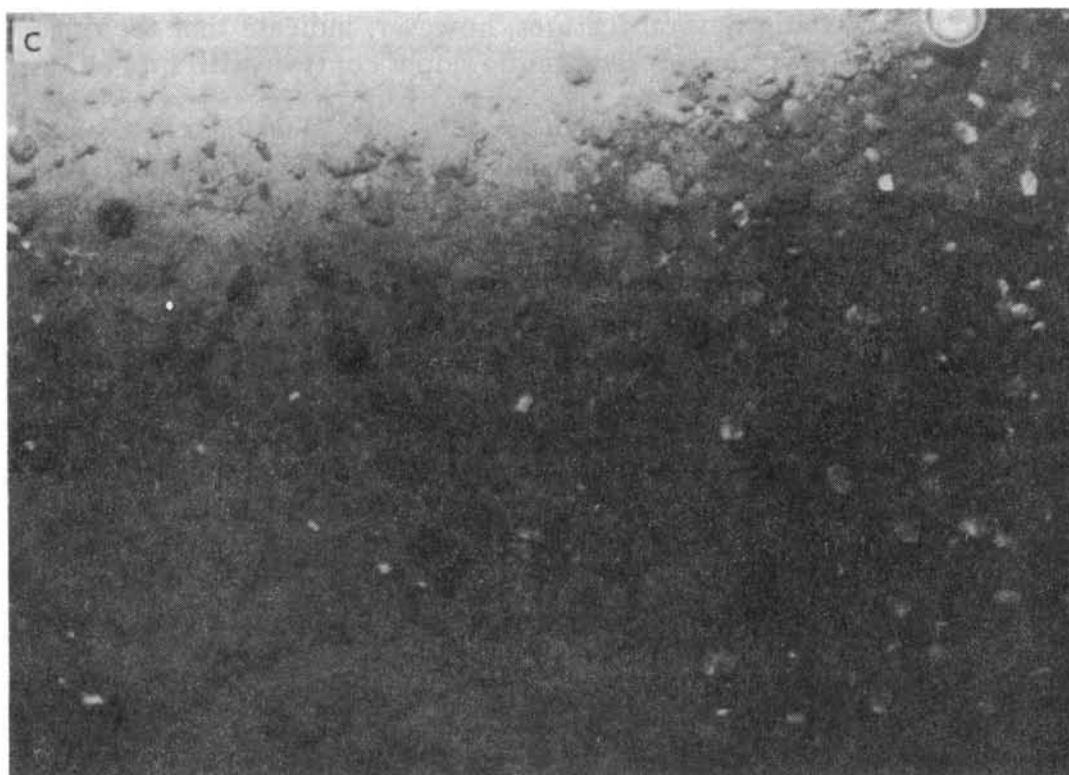


Fig.8. Bottom photos. *a.* Inside the continuous ridge, showing muddy surface with drop-stones. *b.* On the ridge, showing mud with high content of cobbles. *c.* Outside the ridge, showing rapid variation between mud-dominated surface and clean cobble pavement. For location see Fig.1.

impedance contrast to be resolved with the seismic equipment used. The reflector followed underneath the continuous outer ridge (Fig.3b) represents the assumed Late Weichselian till.

FORMATION OF THE MORPHOLOGICAL FEATURES

The continuous ridge is interpreted, from several lines of evidence, as being the end moraine expressing the maximum extent of the glacier during the surge in 1936–1938, although effects from former surges cannot be excluded: (1) the ridge is continuous and subparallel to the recent glacier front; (2) the cross-sectional shape (Fig.3a, b) is characteristic of formation in close contact with an ice front, with the steepest slope toward the glacier (Elverhøi et al., 1983); (3) a marked change in bottom morphology occurs across the ridge, as shown by all acoustic profiles; and (4) frequency of plough marks dramatically decreases inside the ridge, indicating a shorter period of exposure to gouging.

Two mechanisms may be important for formation of the end moraine; ice push and rapid deposition from meltwater. A portion of the material may have been pushed up in front of the advancing glacier; “bulldozer effect”

(Sugden and John, 1976). Several features, however, indicate that the ridge is not entirely an ice-push feature. The gentle slopes contrast with submarine push-up ridges in Arctic Canada, where slopes of up to 45° occur on both proximal and distal sides (Lewis et al., 1977). Upper and distal parts of the ridge have draped acoustically semitransparent sediments, suggesting deposition from meltwater during the period of maximum glacier extension. Meltwater discharge thus seems to have occurred along the entire surging ice front. This contrasts with the present situation, in which only two major meltwater outlets, one of which is situated just east of Bråsvellbreen (Fig.1b), drain the entire Nordaustlandet ice cap. Both theory and field evidence of high rates of meltwater output during surges, indicate high material transport capacity during a surge (Weertman, 1969; Robin and Weertman, 1973; Thorarinson, 1976; Sugden and John, 1976). The observed slumps on the distal side (Fig.3c) also indicate rapid deposition, causing an unstable sediment configuration. The slumping process has probably also modified parts of the original shape of the end moraine, causing the abrupt termination on the distal side (Fig.3a). The ridge contains approximately 0.5 km^3 of sediment. Since aerial photos taken during the surge (Fig.2b) show highly turbid water outside the glacier front, it appears likely that large amounts of fine material (silt, clay) have been transported further out. Under the assumption that all material in the ridge is derived from erosion by Bråsvellbreen proper, this corresponds to an average lowering of about 45 cm of the substratum.

The rhombohedral ridge pattern and the irregularly distributed mounds are interpreted to be an expression of relief in the glacier sole during the surge. Similar features observed on land are inferred to be crevasse fills, formed by squeeze-up of underlying material (Gravenor and Kupsch, 1959; Flint, 1971). To preserve features caused by such a process, the glacier, at least the snout, must have become stagnant. This is consistent with experience from other surging glaciers (Meier and Post, 1969). In this particular case, the retreat after stagnation has taken place through calving.

The small arcuate, discontinuous ridges (Fig.5b) paralleling the glacier are probably caused by minor movements (Andrews and Matsch, 1983, pp.15), possibly annual oscillations, of the modern Bråsvellbreen glacier. The pattern indicates that at least part of the glacier regained its normal mode of movement at some stage between 1938 and the present. This is consistent with the crevassing indicating slight movement in the present-day Bråsvellbreen.

Icebergs may disturb the sea floor in the calving process, even if they are too small to touch the bottom after they have come to rest. Thus it cannot be excluded that some features may arise from redistribution of sediment through calving activity.

The two dominant directions for iceberg gouging are parallel and normal to the ice front. These directions are probably determined by currents, wind and bathymetry. A strong westerly surface coastal current is observed along the ice front (Novitskiy, 1961; Pfirman, in prep.), while katabatic winds from the ice cap dominate the local wind field. The bathymetric slope in the western part of the study area also modifies the local iceberg movement.

The most prominent aspect of iceberg gouging, however, is the marked decrease in frequency inside the end moraine. Since the ridge crest has variable water depth, it cannot represent a barrier to icebergs in general. Therefore the most likely explanation for the decrease in gouge frequency is a shorter period of exposure to drifting icebergs inside the moraine, the surge zone. Also, the abundance of icebergs was probably higher during and shortly after the surge.

The striated gouge patterns (Fig. 7b) are most likely caused by multi-keel icebergs. Similar features are described from Arctic Canada by Lewis et al. (1968). Figure 7a shows a "washboard pattern" along one side of a 30 m wide plough mark. Washboard patterns, described from the Antarctic continental shelf by Lien (1982), are attributed to wobbling movement of grounded icebergs. The features described from Antarctica, however, are an order of magnitude larger, and are caused by tabular icebergs. Wobbling movements of icebergs (in this case due to swell, as tides are only 0.5 m) may be a possible cause of the washboard pattern outside Bråsvellbreen. Another possibility is that the pattern results from blocks of overconsolidated material that are pushed up during gouging (Lien, 1983). The latter cause is considered the most likely. Since the pattern is not observed outside the surge zone, it is probably formed by material from the thin, intermediate layer, interpreted to owe its overconsolidation from surge activity.

CONCLUSIONS

The different sea-floor morphological features mapped outside the Bråsvellbreen glacier may be summarized as follows:

- A continuous ridge, subparalleling the glacier front at a distance of 500 m to >5 km, is considered to be the end moraine defining the maximum extent of the major glacier surge in 1936–1938. A part of the moraine may have been pushed up as the glacier advanced. However, the cross-sectional shape seen on 3.5 kHz echosoundings, as well as results from sediment coring, imply that a large part was deposited from meltwater at the time of maximum extension. Deposition took place all along the surging ice front. This contrasts with the present configuration, which exhibits two major meltwater outlets for the entire Nordaustlandet ice cap. The original end moraine shape is partly modified by slumping on the distal flank. The 0.5 km^3 of sediment in the end moraine alone is approximately equivalent to the annual sediment discharge of the Amazon River, which has the third largest sediment discharge of all the world rivers (Milliman and Meade, 1983). Although this sediment represents material eroded beneath the glacier during many years prior to the surge, it was deposited during only a few years. Judging from the amount of material moved during this latest Bråsvellbreen surge, glacier surges may prove to be important mechanisms in the long-term transport history of glacial sediments.

- A rhombohedral pattern of linear discontinuous ridges between the end moraine and the glacier may represent relief in the glacier sole during the surge, which has been preserved through stagnation of the glacier.

— Small, discontinuous arcuate ridges, subparallel to the glacier front, are most likely caused by minor, local readvances of the glacier, possibly annual oscillations.

— The relative distribution of rhombohedral pattern and discontinuous, arcuate ridges (Fig.6) indicates that the eastern, thicker part of the glacier disintegrated more than 3 km through calving before again becoming active. In the westernmost part, however, the glacier is probably still stagnant.

— Iceberg plough marks show two prevailing directions, most likely controlled by a combination of a westerly coastal current, offshore katabatic winds and sea floor topography. Plough mark frequency decreases markedly inside of the end moraine, indicating shorter time of exposure to drifting icebergs.

— Striated plough marks are caused by multi-keel icebergs.

— Washboard pattern along plough marks is most likely caused by push-up of blocks of overconsolidated material during ploughing.

The end moraine and the general distribution of sea floor morphological features are related to surge activity. The scale of these features may seem small when discussing larger ice sheets, but structures like these may be important aids in interpreting former glacier surges. Orientation and distribution of such structures yield information on the direction and distance of movement, and retreat history of the glacier.

ACKNOWLEDGEMENTS

We thank Robert Oldale, Reidar Lien, Tore O. Vorren and colleagues at the Norwegian Polar Research Institute and Woods Hole Oceanographic Institution for their critical comments on the manuscript. Yngve Kristoffersen is acknowledged for valuable help during data acquisition. The work could not have been carried out without the valuable cooperation of Captain Terje Langvik and his crew aboard the R/V "Lance". This research was partly supported by the Norwegian Marshall Fund for Scientific Research. ARCO Norway, Inc., is acknowledged for financial support to data analysis. NPRI contribution no.229, WHOI contribution no.5743.

REFERENCES

- Andrews, J.T. and Matsch, C.L., 1983. *Glacial Marine Sediments and Sedimentation; an Annotated Bibliography*. Geo Abstracts, London, Bibliography No.II, 227 pp.
- Belderson, R.H. and Wilson, J.B., 1973. Iceberg plough marks in the vicinity of the Norwegian Trough. *Nor. Geol. Tidsskr.*, 53: 323—328.
- Bjørlykke, K., Bue, B. and Elverhøi, A., 1978. Quaternary sediments in the northwestern part of the Barents Sea and their relation to the underlying Mesozoic bedrock. *Sedimentology*, 25: 227—246.
- Elverhøi, A. and Solheim, A., 1983. The Barents Sea ice sheet — a sedimentological discussion. *Polar Res.*, n.s., 1: 23—42.
- Elverhøi, A., Lønne, O. and Seland, R., 1983. Glaciomarine sedimentation in a modern fjord environment, Spitsbergen. *Polar Res.*, n.s., 1: 127—149.
- Flint, R.F., 1971. *Glacial and Quaternary Geology*. Wiley, New York, N.Y., 892 pp.

- Gravenor, C.P. and Kupsch, W.O., 1959. Ice-disintegration features in western Canada. *J. Geol.*, 67: 48–64.
- Hare, F.F., 1976. Late Pleistocene and Holocene climates: some persistent problems. *Quat. Res.*, 6: 507–517.
- Holdsworth, G., 1977. Surge activity on the Barnes Ice Cap. *Nature*, 269: 588–590.
- Lewis, C.F.M., MacLean, B. and Falconer, R.K.H., 1968. Iceberg scour abundance in Labrador Sea and Baffin Bay; a reconnaissance of regional variability. Proc. 1st Can. Conf. on Marine Geotechnical Engineering, Calgary, Alta., pp.79–94.
- Lewis, C.F.M., Blasco, S.M., Bornhold, B.D., Hunter, J.A.M., Judge, A.S., Kerr, J.W., McLaren, P. and Pelletier, B.R., 1977. Marine geological and geophysical activities in Lancaster Sound and adjacent fjords. *Geol. Surv. Can.*, Pap. 77-1A: 495–506.
- Lien, R., 1982. Sea bed features in the Blaaenga area, Weddell Sea, Antarctica. Proc. 6th Int. Conf. on Port and Ocean Engineering under Arctic Conditions, Quebec, pp.706–716.
- Lien, R., 1983. Iceberg scouring on the Norwegian continental shelf. Continental Shelf Institute, Norway, 109, 147 pp.
- Liestøl, O., 1969. Glacier surges in West Spitsbergen. *Can. J. Earth Sci.*, 6: 895–897.
- Meier, M.F. and Post, H., 1969. What are glacier surges? *Can. J. Earth Sci.*, 6: 807–816.
- Milliman, J.D. and Meade, R.H., 1983. World-wide delivery of river sediment to the oceans. *J. Geol.*, 91: 1–21.
- Novitskiy, V.P., 1961. Permanent currents of the northern Barents Sea. *Tr. Gosudarstvennogo Okeanogr. Inst., Leningrad*, 64: 1–32 (U.S.N.O. translation 1967).
- Paterson, W.S.B., 1981. *The Physics of Glaciers*. Pergamon Press, Oxford, 380 pp.
- Pfirman, S., in prep. Water mass distribution of the northwestern Barents Sea.
- Prest, V.K., 1969. Retreat of Wisconsin and recent ice in North America. *Geol. Surv. Can.*, Map 1257 A.
- Robin, G. de Q. and Weertman, J., 1973. Cyclic surging of glaciers. *J. Glaciol.*, 12: 3–18.
- Rokoengen, K., 1980. Shallow geology on the continental shelf off Møre and Romsdal. Description of 1:250,000 Quaternary Geology Map 6203. Continental Shelf Institute, Publ. No.105, 49 pp.
- Schytt, V., 1964. Scientific results of the Swedish glaciological expedition to Nordaustlandet, Spitsbergen, 1957 and 1958. Part I and part II. *Geogr. Annal.*, 46: 243–281.
- Schytt, V., 1969. Some comments on glacier surges in eastern Svalbard. *Can. J. Earth Sci.*, 6: 867–871.
- Solheim, A., in prep. Sediment distribution and characteristics outside a grounded, surging glacier, Bråsvellbreen, Svalbard.
- Sugden, D.E. and John, B.S., 1976. *Glaciers and Landscape. A Geomorphological Approach*. Edward Arnold, London, 376 pp.
- Thorarinsson, S., 1969. Glacier surges in Iceland, with special reference to the surges of Bruarjökull. *Can. J. Earth Sci.*, 6: 875–882.
- Weertman, J., 1969. Water lubrication mechanism of glacier surges. *Can. J. Earth Sci.*, 6: 929–939.

PAPER 2.

Submitted to Norsk Polarinstitutt Skrifter.

THE DEPOSITIONAL ENVIRONMENT OF SURGING SUB-POLAR TIDEWATER GLACIERS:

A case study of the morphology, sedimentation and sediment properties in a surge affected marine basin outside Nordaustlandet, northern Barents Sea.

Anders Solheim

Norwegian Polar Research Institute

P.O.Box 158

N-1330 Oslo Lufthavn

NORWAY

ABSTRACT.

The present study addresses the importance of glacier surges in the marine environment. Glacier surges are common in Svalbard, as well as in other Arctic and sub-Arctic regions, and surging of tidewater glaciers may have been an important process during past glaciations, when extensive continental shelf areas were covered by grounded ice.

An area outside Austfonna ice cap, Nordaustlandet, Svalbard, has been extensively studied by means of shallow seismic profiling, side scan sonar and core sampling over a period of several years. Austfonna has several well defined drainage basins, some of which are known to surge. Bråsvellbreen, the second largest drainage basin, had the largest surge ever documented when it advanced 12-15 km along a 30 km wide front, between 1936 and 1938. The glacier has, since then, retreated by up to 5 km. Most of the data base is located outside Bråsvellbreen, but results from this glacier is also applied to show that an adjacent drainage basin also has experienced a surge of comparable size. Using present-day climatic parameters and volumetric estimates from the study area, the surge interval of Bråsvellbreen may be as much as 500 years, whereas the adjacent, larger basin has at least three times shorter period, due to difference in the ratio of accumulation area to ablation area, which is greater for the latter basin.

Important aspects of the shallow geology discussed include; sea floor morphology, sediment distribution and sediment types, sediment physical properties and sedimentation processes and rates. One objective is to find whether surges leave diagnostic features that can be used to identify surges in other areas or in older sequences. A suite of sea floor morphological patterns, including a terminal moraine (here termed surge moraine) and patterns of sub-glacial squeeze-up ridges in the zone previously covered by surging ice (here

termed the surge zone), is the most characteristic feature. This zone contrasts strongly to the area outside the surge moraine (here termed the surge-distal zone), which is characterized by normal marine processes and iceberg ploughing. Sediments are mainly gravel -and pebble-rich diamictons, but patches of pre-surge, more fine grained glaciomarine mud are preserved, embedded in the diamicton, and compacted by loading of the surging glacier. Sediment physical properties vary greatly as a function of variable lithology and differences in compaction. Although the greatest amount of directly surge-related deposition takes place within few kilometers from the ice front, with emplacement of the surge moraine being the most important event, surges apparently affect depositional rates also some tens of kilometers out into the surge-distal zone through increased output of suspended material. Chronostratigraphic control is sparse, but there seem to be large variations in depositional rates, reflecting surges or periods of increased surge frequency.

Surging glaciers are not found to produce sediments that are unique to this environment, but, taken together, the combination and variations in sediment types, physical properties, sedimentation rates and morphology can be diagnostic and used in the interpretation of older sequences and areas where surges are not documented.

INTRODUCTION

Glacier surges are an important aspect of the dynamics of many Svalbard glaciers (Liestøl 1969), and are relatively common in other Arctic and sub-Arctic regions, for example Alaska, Iceland and the Soviet Union (Horvath & Field 1969, Thorarinsson 1969, Dolgushin & Osipova 1974, Clarke et al. 1986). Surges have been quite extensively studied from a glaciological viewpoint (e.g. *Can.J.Earth Sci.*, vol.6, 1969: various refs., Hagen 1987) and surge mechanisms have been much debated (Robin & Weertman 1973, Budd 1975, Clarke 1976). Recent glaciological work on surging glaciers has greatly improved the understanding of the surge process (Clarke et al. 1984, Kamb et al. 1985, Kamb 1987, Raymond 1987). However, the majority of studied surges are from on-shore areas, whereas surges of marine based glaciers have been much ignored. Furthermore, reports on possible effects of surges on sediments and sedimentation are essentially lacking, in particular from the marine environment.

Surges have been proposed as a mechanism for thinning and disintegration of large ice sheets. Hence, ice marginal features may result from past surges, as, for example, is suggested for several readvances during the retreat of the Laurentide ice sheet (Prest 1969, Dyke & Prest 1987), rather than being of climatic significance. Major surges of ice streams have likewise been suggested as a probable mechanism for disintegration of particularly marine ice domes (Budd 1975, Stuiver et al. 1981, Denton & Hughes 1981). These surges are somewhat different from presently observed surges. The disappearance of buttressing ice shelves leads to surging of marine based ice streams. The ice stream surges proceed from the margin to the centre of marine ice domes (Hughes 1974), whereas "traditional" ice sheet surges proceed from central parts towards the margin (Budd 1975, Weertman 1976). Large ice stream surges

would lead to downdraw and finally collapse of marine ice domes. Denton & Hughes (1981) claim that disintegration of large parts of the northern hemisphere Late Weichselian/Wisconsin ice sheets can be accounted for by this mechanism. Paleontological and stable isotope data which indicate an early phase of rapid deglaciation from 16 to 13 kA give further support to the marine downdraw mechanism (Ruddiman & McIntyre 1981, Ruddiman & Duplessy 1985). Likewise it is also proposed as a possible mechanism for the West Antarctic ice sheet (Stuiver et al. 1981). Downdraw through ice stream surges would also partly resolve the problem of derivation of sufficient energy to waste major ice sheets, as put forward by Andrews (1973) and Hare (1976).

Although the above theories may be disputed and involve different mechanisms and scales, the discussion shows that glacier surge is important and may have had immense geologic and climatic consequences.

In 1936-38 Bråsvellbreen, a well defined drainage basin of the Austfonna ice cap, Nordaustlandet, Svalbard (Fig.1) had the largest surge documented in historical times on the northern hemisphere, when an approximately 30 km wide front advanced possibly as much as 15-20 km into the Barents Sea in less than two years (Schytt 1969). The glacier has retreated up to 4-5 km since the surge and the present situation is that of a grounded, apparently quite stationary ice front with a subaerial cliff of around 20 m height and a submarine draft varying from 20 to 110 m. This situation offers an unique opportunity to study the effects of a glacier surge on the ice proximal glaciomarine environment. Important aspects of this type of event are:

1. What happens to the substratum over which the surging glacier advances, in terms of morphology, erosion/deposition and changes in the physical properties of the sediments?
2. How does a surge affect sedimentation and sedimentary processes at

- various distances from the surging glacier?
3. Are former glacier surges identifiable and, if so, what are the diagnostic features?
 4. Can the sedimentary features give any indications of surge mechanisms and mode of advance and retreat?
 5. Can surge frequency and timing be predicted?

The Antarctic is widely used as a model for description of glaciomarine sedimentation and interpretation of ancient glaciomarine deposits (Molnia 1983). However, the Antarctic is atypical compared with northern hemisphere glaciated areas, both present and past, for several reasons: the apparent lack of meltwater outflows; the generally very deep continental shelf with a gradient towards the continent; the importance of extensive ice shelves. Studies of glaciomarine sediments and sedimentation in the northern hemisphere have, on the other hand, mostly been carried out off temperate glaciers in fjord settings. This may likewise be an inadequate model for past glaciations, as extensive marine based ice sheets probably covered several continental shelf areas.

A more applicable model for northern hemisphere glaciomarine sedimentation is probably presented by the modern Austfonna ice cap with its dynamically distinctive drainage basins, several of which are known to surge (Liestøl 1969, Schytt 1969, Dowdeswell 1984), and the adjacent parts of the Barents Sea. Austfonna has the most extensive marine, grounded ice front (approximately 200 km long) in the present day northern hemisphere, and the entire front is situated in open, marine conditions. Furthermore, the regional glaciology of the ice cap has recently been mapped using radio-echo

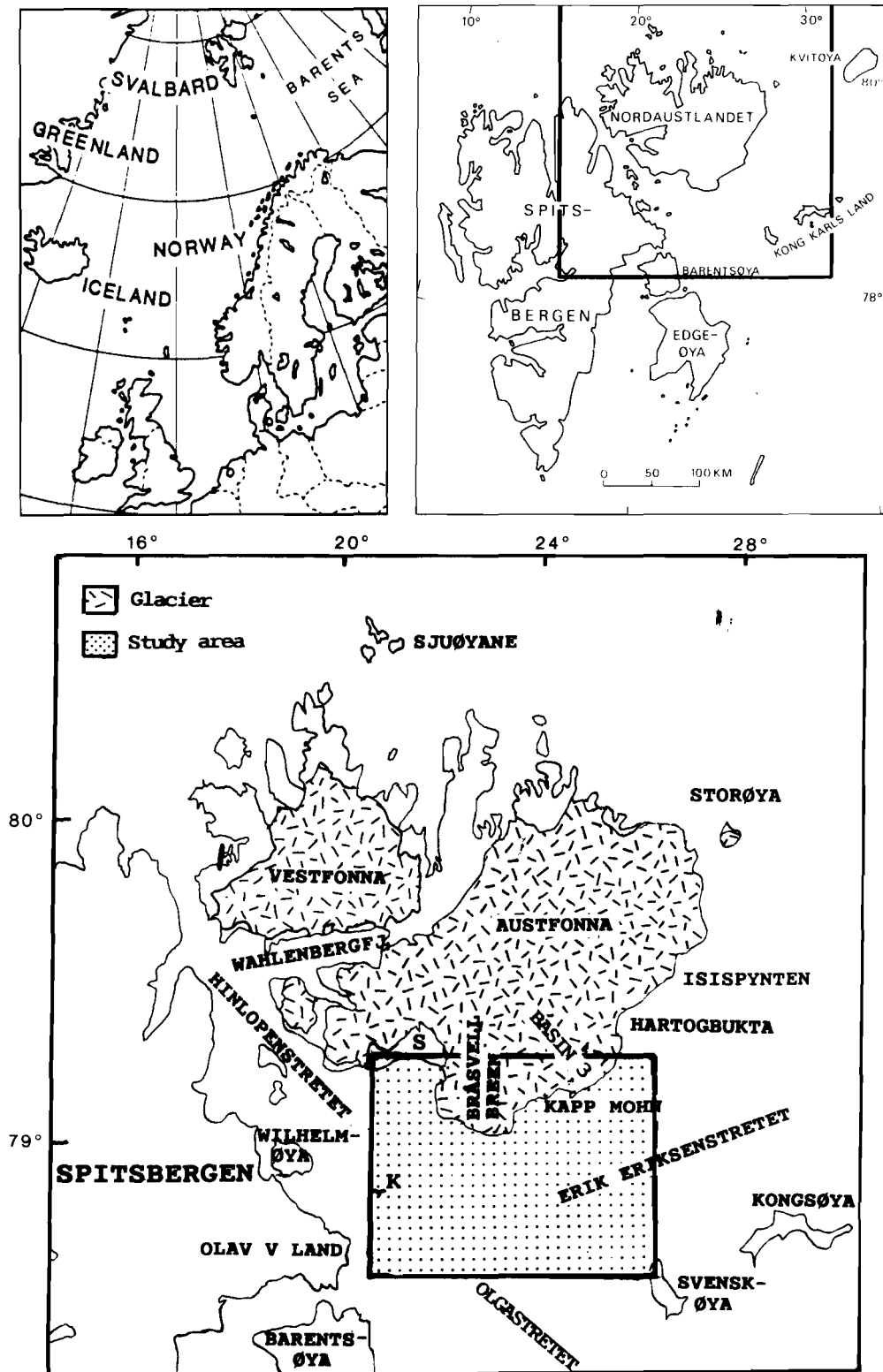


Fig.1. Location of Svalbard, Nordaustlandet and the study area, with place names used in the text. S: Svartknausflya, K: Kiepertøya. Glacial coverage of Nordaustlandet is indicated.

sounding methods (e.g. Dowdeswell 1984, Dowdeswell et al. 1986) providing necessary background information for studies of the sedimentary environment outside the glacier.

In this paper, questions 1-5 (above) are addressed through a study of the region off the southern portion of the Austfonna ice cap, Erik Eriksenstredet (Fig.1). Answers are sought through the interpretation of high frequency acoustic data (side scan sonar, 3.5 kHz echo sounder and sparker) and sedimentological/geotechnical analyses of sediment cores. The data were collected to cover the entire region, from the present ice front of Austfonna to the more distal regions, in order to establish a model for sedimentation and sedimentary processes in a surge affected, open marine environment. A preliminary paper (Solheim & Pfirman 1985) reported on the morphological features in the northern, most glacier proximal part of the study area using some of the acoustic data. This paper presents a synthesis of all the acoustic and sedimentological/geotechnical data.

PHYSICAL SETTING

Quaternary geology

Generally, the Quaternary sediments found on land next to the study area consist of a relatively thin (less than 5 m) cover of till, reworked by wave action below the upper marine limit (Blake 1962). In the outer part of Hinlopenstredet (Salvigsen 1978), Holocene raised beaches indicate, through isostatic depression by ice loading, a considerably wider extension of the ice cover during the Late Weichselian maximum (approximately 18kA), and striae and erratics point towards ice flow from southeast to northwest through Hinlopenstredet (Blake 1962). However, while the Early Weichselian glaciation probably reached Sjuøyane to the north (Fig.1), the Late

Weichselian glaciation most likely did not reach much beyond the northern coast of Nordaustlandet (Salvigsen & Nydal 1981). The pattern of ice movement from the southeast is in accordance with data which show Kong Karls Land to have the highest raised beaches, with a maximum of 110 m, in the Svalbard archipelago (Salvigsen 1981). This again supports the idea of an extensive glaciation of the Barents Sea shelf, which also is strongly indicated by the sediment distribution and seismic stratigraphy of the Barents Sea (Elverhøi & Solheim 1983, Solheim & Kristoffersen 1984, Vorren & Kristoffersen 1986). Hence, the entire study area was covered by grounded ice that probably flowed from southeast towards the northwest during most of the Late Weichselian. It should be mentioned, however, that various views have been presented on the existence and size of a Barents Sea ice sheet. Elverhøi and Solheim (1983) give a review of this discussion.

Deglaciation of Nordaustlandet began sometime before 10 ka (Blake 1962, Østerholm 1978). The emergence curves from Svartknausflya and Kong Karls Land (Fig.1) (Salvigsen 1978,1981), indicate that the water depth was between 80 and 110 m deeper than at present for the first 1000 years after deglaciation, while the shallowing during the last 5000 years has been approximately 20-30 m.

The general Quaternary succession of the northern Barents Sea (Elverhøi & Solheim 1983) consists of an overconsolidated basal till (less than 10 m thick) with a cover of soft, Late Weichselian glaciomarine sediments (usually 1-5 m thick). Mainly in water depths in excess of 300 m and in local depressions this sequence is covered by a thin (< 1 m) layer of Holocene, fine grained mud, which mostly results from reworking in shallower regions (Forsberg 1983) and sediment transport by sea ice (Elverhøi et al. in

press). However, the distinction between the Late Weichselian glaciomarine sediments and the top Holocene mud becomes less apparent northwards in the Barents Sea (Wensaas 1986) towards the heavily glaciated regions of eastern Svalbard. At present, sedimentation in the study area is dominated by deposition from turbid meltwater plumes (Pfirman 1984).

Bedrock geology

Lithology of the glaciogenic sediments may be used to trace different source areas and their relative importance, provided sufficient lateral bedrock variation exists. Based on relatively few exposures, a rough division can be made along an east-west line through Wahlenbergfjorden (Fig.1), between post Caledonian rocks to the south and older rocks mainly of the Hecla Hoek complex (Late Riphean to early Paleozoic sediments (partly metamorphosed), granites, gneisses and gabbroic intrusives) to the north (Lauritzen & Ohta 1984).

The Hecla Hoek complex differ markedly from the overlying younger, sedimentary rocks found in the southern part of the island. The latter rocks range from middle Carboniferous to Lower Jurassic in age. The main part of the area, including the southwestern periphery of Austfonna, consists of Carboniferous and Permian rocks. Although a few sandstone exposures are found, the majority of these rocks are limestones and dolomitic limestones, characterized by a high chert content and silicified sediments, which renders the formation highly resistant to weathering. A few exposures show Triassic to Lower Jurassic siltstones and shales to overly the limestones, and are cut by Late Jurassic to Early Cretaceous dolerites.

To the south of Erik Eriksenstredet, the islands of Kong Karls Land

consist of late Triassic to early Cretaceous sediments (mostly clastics, with some limestones and coal beds) with interbedded lavas. The location of the boundary between these rocks and the upper Paleozoic carbonates on southern Nordaustlandet is tentatively placed along the central part of Erik Eriksenstredet and cannot be mapped more accurately from the present shallow seismic data.

Southwest of the study area, Triassic and Lower Jurassic clastic rocks outcrop in Olav V Land and on Wilhelmøya (Fig.1). Mesozoic doleritic intrusions form small islands and skerries, for example Kiepertøya in the southern part of Hinlopenstredet (Fig.1,).

Bathymetry and hydrography

The study area covers the southwestern, shallowest part of Erik Eriksenstredet, a trough which continues north-northeastwards between Nordaustlandet and Kvitøya (Fig.1), and forms one of the three deep passages from the Barents Sea to the Arctic Ocean. Trough depths in the study area range from 260 m in the eastern part to 180 m in the central part (Fig.2). A sill at 120 m waterdepth separates Erik Eriksenstredet from the Olgastredet trough between Kong Karls Land and Barentsøya.

Below approximately 100 m depth in the north and 150 m in the south, Erik Eriksenstredet has a gentle, rather smooth topography. The north slope is slightly steeper than the south slope and in the northeastern part the upper 30 m is steeper than the lower part of the slope. While the contours of the southern slope appear straight, the north slope forms a major embayment with its apex towards Bråsvellbreen. The rather gentle deep trough contrasts distinctly with both shoulders, where the topography is highly irregular on a 10 m scale, with numerous smaller shoals and troughs. To the west, the sea floor rises to depths less than 50 m on

the sill in the southern part of Hinlopenstredet.

The current pattern in this part of Erik Eriksenstredet is dominated by the approximately 20 km wide Nordaustlandet coastal current flowing in a southwesterly direction. Calculated geostrophic current velocities vary from 4 cm/s in the east to more than 16 cm/sec near the western border of Bråsvellbreen (Pfirman 1985). The water mass is vertically stratified into a 25-30 m thick layer of fresher surface water, a core of cold Arctic water down to 125 m and a bottom layer of warmer Atlantic water (Pfirman 1985). No long-term current measurements exist from this part of Erik Eriksenstredet. Further northeast, between Nordaustlandet and Kvitøya, one-year measurements at 75 and 220 m levels (Aagaard et al. 1983) reveal a dominant tidal component with velocities up to 15cm/s and 5cm/s in the upper and lower levels respectively (tidal range in the area is in the order of 0.5 - 1.0 m (T.Eiken pers. commun. 1987)). Net velocity, however, is less than 2cm/s in a northward direction.

Due to the shallow sill (<60 m) in the southern part of Hinlopenstredet, there is no deep water exchange through this strait. However, a relatively strong tidal current component can be expected in this area and thus also in the western part of Erik Eriksenstredet.

Glaciology

Glaciers are usually classified as polar, temperate or sub-polar (Lagally 1932, Ahlmann 1933). Polar glaciers are entirely below the pressure melting point. Temperate glaciers are at the pressure melting point below the penetration depth of the winter cold wave. Sub-polar glaciers form an intermediate category between the two extremes. The overall glacier coverage of Svalbard is approximately

60%, with a general increase towards north and east (Dowdeswell 1984). More than 75% of Nordaustlandet and 99% of Kvitøya are glacierized. Despite the high latitude, most Svalbard glaciers are of sub-polar type (Baranowski 1977). In general, the glaciers have been slowly retreating for approximately the last 100 years (Baranowski 1977), after a period of advance mainly between the 17th to the late 19th century, known as the Little Ice Age (Lamb 1977).

A number of Svalbard glaciers have short-term fluctuations due to surging behaviour (Fig.3). Glacier surges in general have been extensively discussed, and a detailed discussion of surge theories is beyond the scope of this paper, but it is important to note that most of them involve build-up and activation of large amounts of pressurized water at the bed or in permeable sediments below the glacier (Clarke et al. 1984). Field observations also verify that increased amounts of meltwater are involved in surges (Thorarinsson 1969, Kamb et al. 1985).

Most of Nordaustlandet is covered by the two ice caps Vestfonna (2511km²) and Austfonna (8120km²). The geography and glaciology of Austfonna has been investigated by several expeditions during the last 115 years (Nordenskiöld 1873, Ahlmann 1933, Glen 1937, 1941, Dege 1948, 1949, Hartog 1950, Harland & Hollin 1953, Thompson 1953, Hollin 1956, Palosuo & Schytt 1960, Schytt 1964, Ekman 1971). However, a detailed picture of the entire ice cap was not obtained until the Scott Polar Research Institute (SPRI) and the Norwegian Polar Research Institute (NP) carried out extensive airborne radio-echo sounding operations over Nordaustlandet in 1983 (Dowdeswell 1984, Dowdeswell 1986a,b, Dowdeswell et al.1984a,b, Dowdeswell & Drewry 1985, Drewry & Liestøl 1985). The ice distribution and glaciology is thoroughly described by Dowdeswell (1984), and only a brief review will be given here, with

emphasis on the southeastern part of the ice cap, including Brásvellbreen.

Based on surface topography, the ice cap is divided into 19 drainage basins (Fig.4a) the largest of which are also reflected in the mapped subglacial bedrock topography (Fig.4b). The two largest drainage basins are Brásvellbreen and Basin 3 (1109 km² and 1251 km² respectively). The maximum surface elevation of the ice cap is 790 m (Fig.4a), and the ice thickness reaches almost 600 m (Fig.4c). The southern and eastern limits of Austfonna constitutes the longest tidewater ice front on the northern hemisphere, with its ca. 200 km of grounded glacier terminus. 28 % of the total ice cap is based below sea level, and the major part of this is in the southeastern region, including 57 % of Brásvellbreen. Depths below the sea floor reach 157 m, but no part of the glacier is afloat. Information on the thermal regime in the ice cap is presently sparse, but a few shallow temperature measurements have indicated it is frozen to the bed in its outer parts and at the pressure melting point under its central parts, and hence can be classified as a sub-polar glacier (Schytt 1969).

There are presently two major meltwater outlets draining Austfonna (and numerous smaller ones); one is just to the east of Brásvellbreen, and the other is in Hartogbukta, just to the east of Basin 3. The former of these has a sea floor valley outside the outlet, while little detail is known on the bathymetry of Hartogbukta. Both these areas, however, have bedrock depressions continuing underneath the ice (Fig.4b). This may indicate that meltwater outlets are at the base of the glacier, with a location most likely determined by the bedrock topography. The fact that there appears to be only sparse meltwater activity during the winter, indicates that most of the water results from surface summer melting.

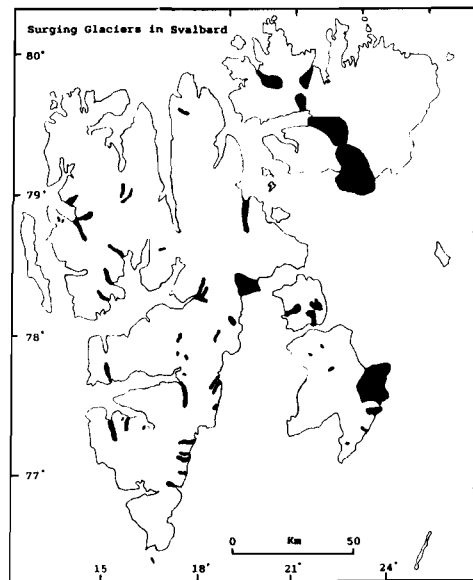


Fig.3. Major Svalbard glaciers that have been observed to surge. A total of more than 80 glaciers are known to show surging behaviour. Map from Dowdeswell (1984), based on data from Liestøl (1985).

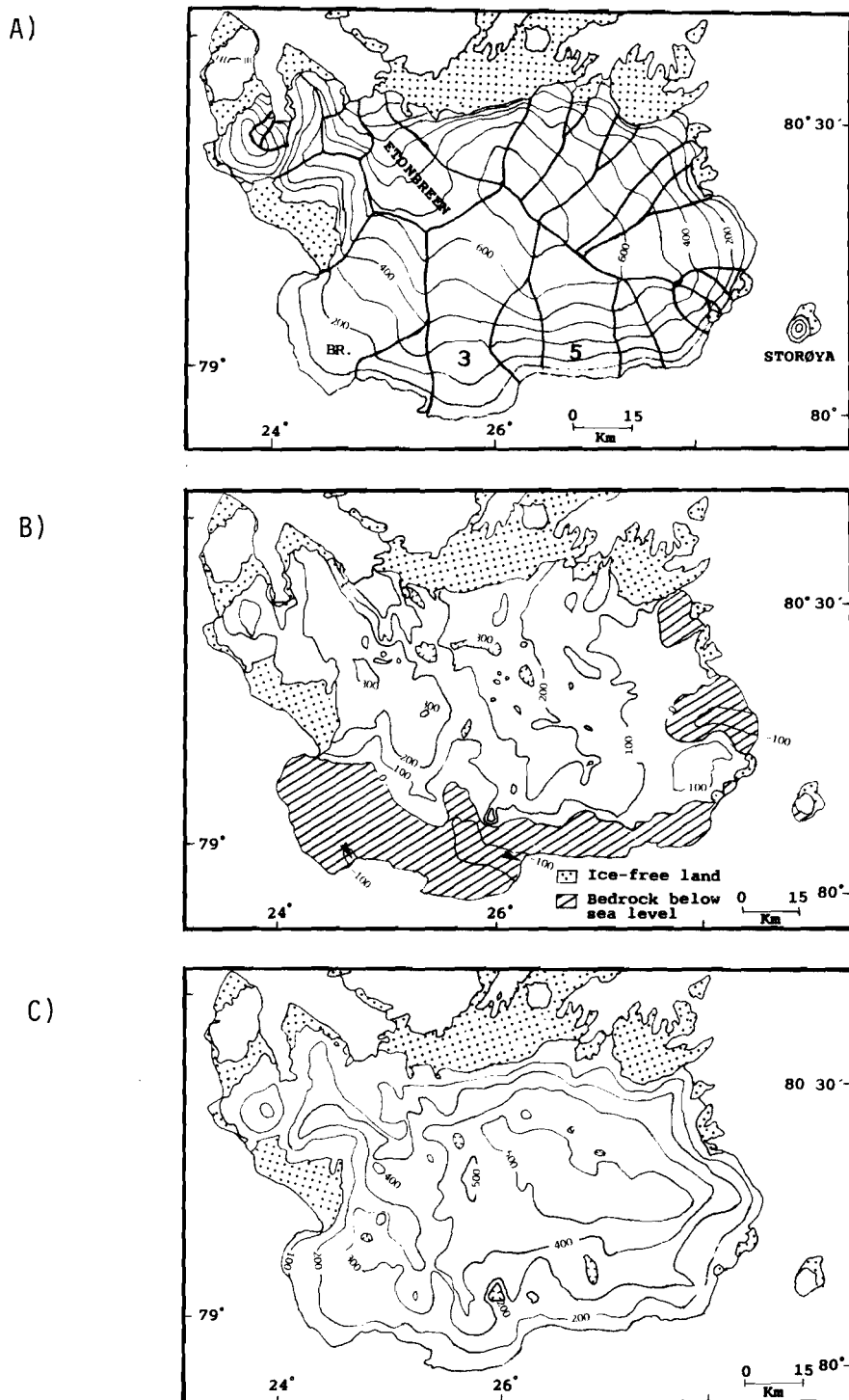
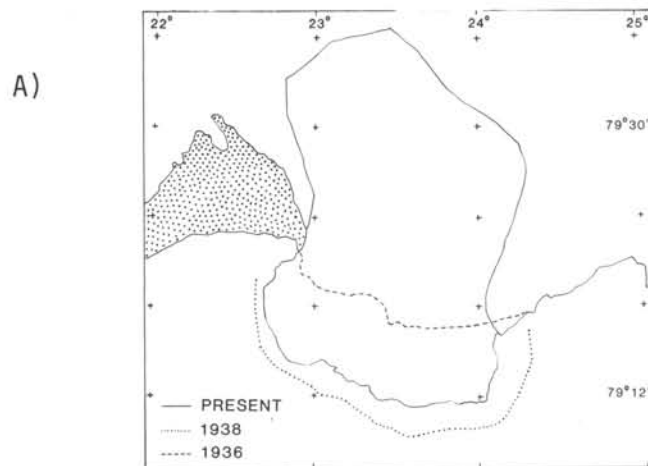


Fig.4. Regional characteristics of Austfonna ice cap (From Dowdeswell et al. 1986). A) Surface elevation (m) and drainage basins. B) Bedrock topography (m) Main meltwater outlets are marked with arrows. C) Ice thickness (m).



B)



Fig.5. A)Map showing the coastline of Bråsvellbreen before 1936 (very approximate, modified after Glen (1937), in 1938 (taken from the morphologically defined maximum surge extent described by Solheim and Pfirman (1985) and later in this paper) and at present. B) Two aerial photographs taken during the surge in 1938 (Norsk Polarinstitutt archive photo). Note high concentrations of icebergs outside the surging glacier.

Bråsvellbreen surge

The Bråsvellbreen surge occurred sometime after 1936 when an undisturbed glacier surface was reported (Glen 1937) and before 1938, when aerial photography revealed a heavily crevassed glacier tongue protruding from the pre-surge coastline (Fig.5). The surging glacier probably advanced up to 15 km along a 30 km long front. 15 km is a somewhat tentative figure as the pre-surge coastline was not precisely mapped. Previous articles have reported up to 20 km advance (e.g.Schytt 1969), but this is most likely based on published maps that suffer from inadequate navigation. A continuous submarine ridge was considered by Solheim and Pfirman (1985) to define the maximum surge extent, but its position differs by several km from the 1938 coast on the published map (Norsk Polarinstitut Chart 507, 1957 edition).

After an advance, the terminal regions of the surging glacier will tend to stagnate (Meier & Post 1969). In the case of a marine ice mass, relatively rapid retreat of the glacier through calving from the heavily crevassed glacier ice most likely takes place (Solheim & Pfirman 1985). Sealers reported the number of icebergs in 1938 to be an order of magnitude higher than during the non-surge situation (Vinje 1985). Solheim and Pfirman (1985) estimated a retreat of up to 5 km from the maximum 1938 position of the Bråsvellbreen front as defined by the terminal ridge. Dege (1948, 1949) reported much calving from the Bråsvellbreen terminus during 1944, while Hartog and Thompson (1959) reported little calving and few open crevasses during 1948. Thus, crevasses on the fractured glacier surface may have closed during the period between 1944 and 1948, and a large part of the retreat from the maximum position may have occurred before 1948. Satellite images since 1976 indicate little ice front movement and modification during the last decade, and

studies of aerial photographs taken between 1969 and 1977 show a retreat of 180 m for the western 5 km of Bråsvellbreen during this period (Dowdeswell 1986b).

Ice surface profiles based on the 1983 radio echo soundings (Dowdeswell 1984) clearly fall below the theoretically calculated surface profile, and calculated basal shear stress is low. This is typical for glaciers in the quiescent phase between surges.

Basin 3

Basin 3 (Fig.4a) is the largest drainage basin on Austfonna. Glaciologically, it shows several similarities with Bråsvellbreen. The coastline between Kapp Mohn and Hartogbukta (Fig.1) protrudes from the rest of the ice cap margin, the basin is well defined by the subglacial bedrock topography and here the surface profile also falls below the theoretical profile and basal shear stress is low (Dowdeswell 1984, 1986a). Furthermore, a Swedish sledge expedition that crossed the ice cap in 1873 reported badly crevassed ice (Nordenskiöld 1875) in a location that matches with the inner parts of Basin 3. Taken together, there are both historical and glaciological indications that Basin 3 also is a surging glacier.

DATA ACQUISITION AND PROCESSING

Reconnaissance work in 1980 and 1981 revealed that a thin layer of soft surface sediments covered overconsolidated material in front of Bråsvellbreen. Furthermore, the assumed surge terminal ridge separated this setting from that beyond it, where a thicker soft glaciomarine cover with no overconsolidated sediments were found within reach of 3 m coring equipment. A more detailed program of acoustic profiling and core sampling was then designed to verify if the 1936-38 surge was the cause of the morphology and sediment distribution. If

verified, this presented a situation where the direct effects of a surging glacier and a subsequent ice load on a marine, glacial sediment could be studied. For sediment distribution and sea floor morphology studies, 3.5 kHz PDR and side scan sonar, respectively, were considered particularly important. The laboratory analysis program were designed to investigate sedimentological and geotechnical differences between different sediment types, affected and unaffected by the surge, and to obtain information about sedimentation rates and their variability in the Erik Eriksenstredet basin. Acoustic profiles and sample locations are shown in Figs. 6a, b & c.

Sea ice and strong surface currents caused problems for work in the area. The ice situation was particularly problematic during the 1982 survey, when the major part of the sampling program was planned. Current velocities in excess of 1 knot were observed, and abundant large drifting ice floes made station work difficult. One aspect of the sampling program during the 1982 and 1983 surveys was to obtain long cores with penetration into the underlying overconsolidated unit. However, the overconsolidation, combined with a high boulder content made coring difficult at a number of localities. The total number of core stations appear high (Fig.6c), but several of the cores were only partly successful. The total number of 3.5 kHz profile kilometres similarly appears high (Fig.6a). This results from the fact that the 3.5 kHz echo sounder was running continuously, also during periods of searching for routes through the ice or suitable sample locations.

Satellite navigation with a Magnavox MX1105 single channel receiver integrated with ship's log and gyro was used during the 1980-83 surveys. The accuracy of the system (approximately 300-500 m) is normally insufficient for detailed work. However, accuracy on a

A)

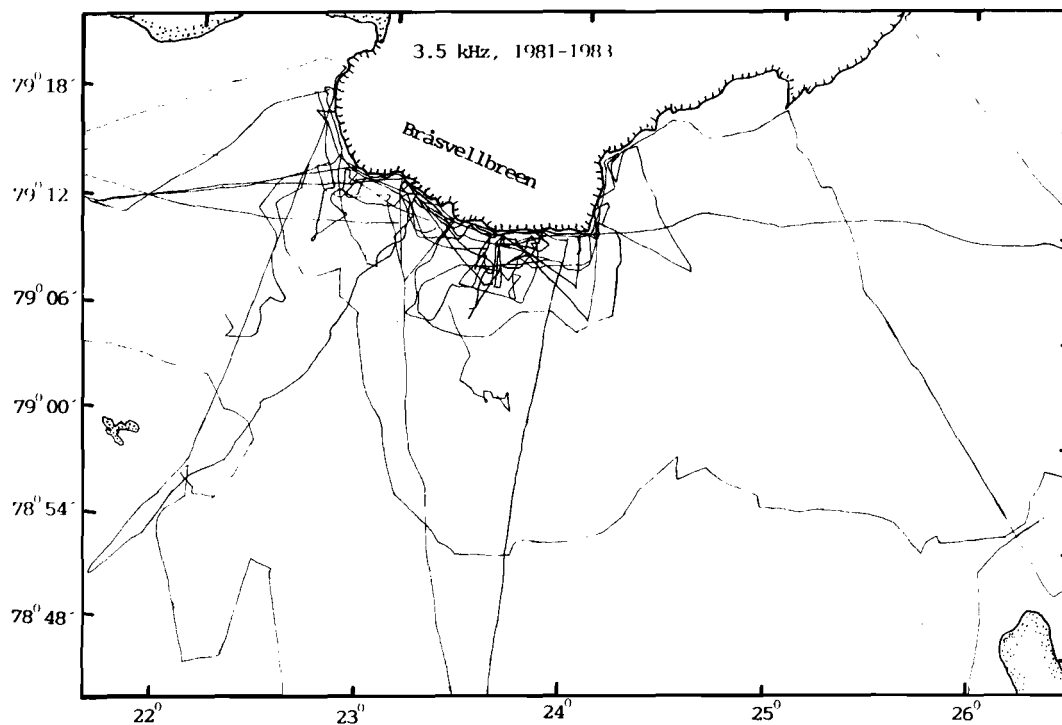
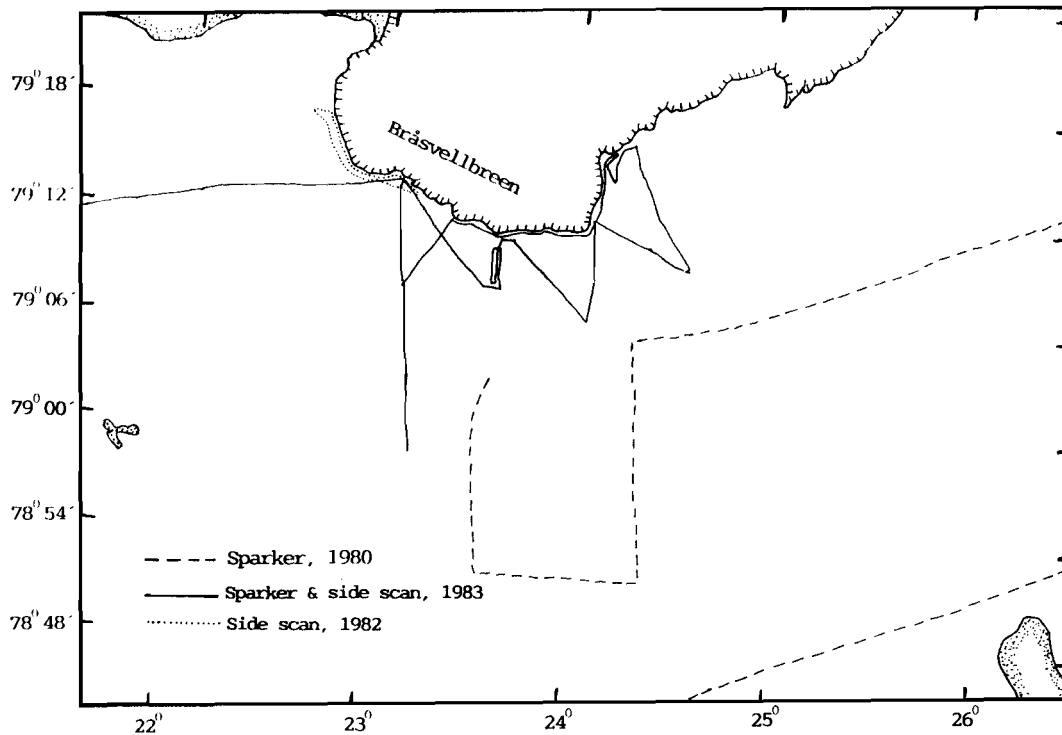


Fig.6. A) Acoustic profiles run by Norsk Polarinstitutt (NP) in 1980-83. Sparker was used in 1980 and 1983. Side scan sonar was used in a small part of the 1982 lines, and along all 1983 sparker lines. All lines after 1980 have 3.5 kHz information. B) Acoustic profiles run by The Hydrographic Survey of Norway (NSKV) in 1984 and 1985. Lines 464500 - 486500 were run in 1984 and the rest in 1985. All lines have 3.5 kHz information. Sparker lines are marked with arrows. Lines with side scan sonar data in 1984 are marked by asterisks. In 1985, essentially all lines were run with side scan. C) Sampling localities from all cruises. In 1984 and 1985, gravity cores were taken at 7 locations, the rest were surface grab samples.

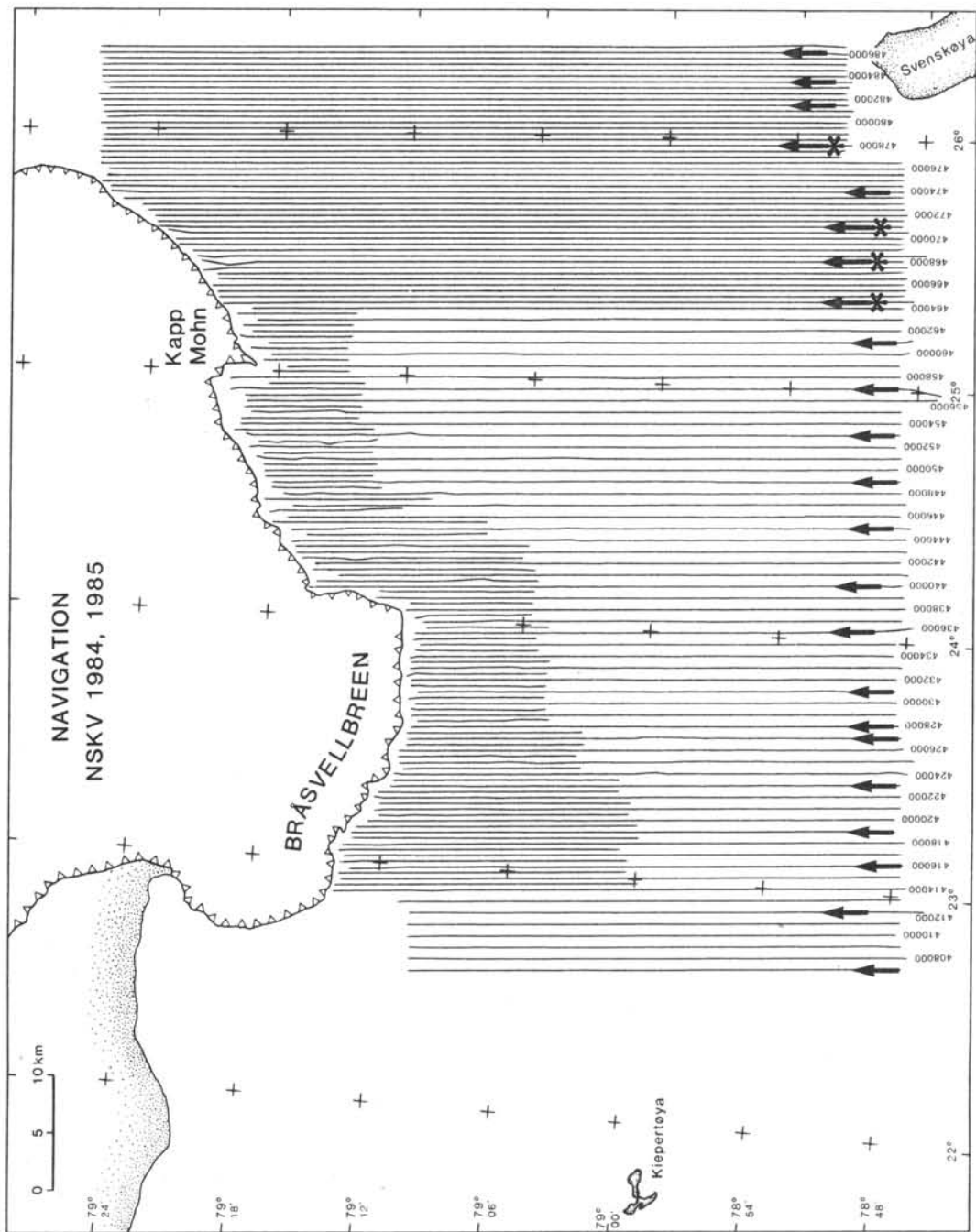


Fig.6B.

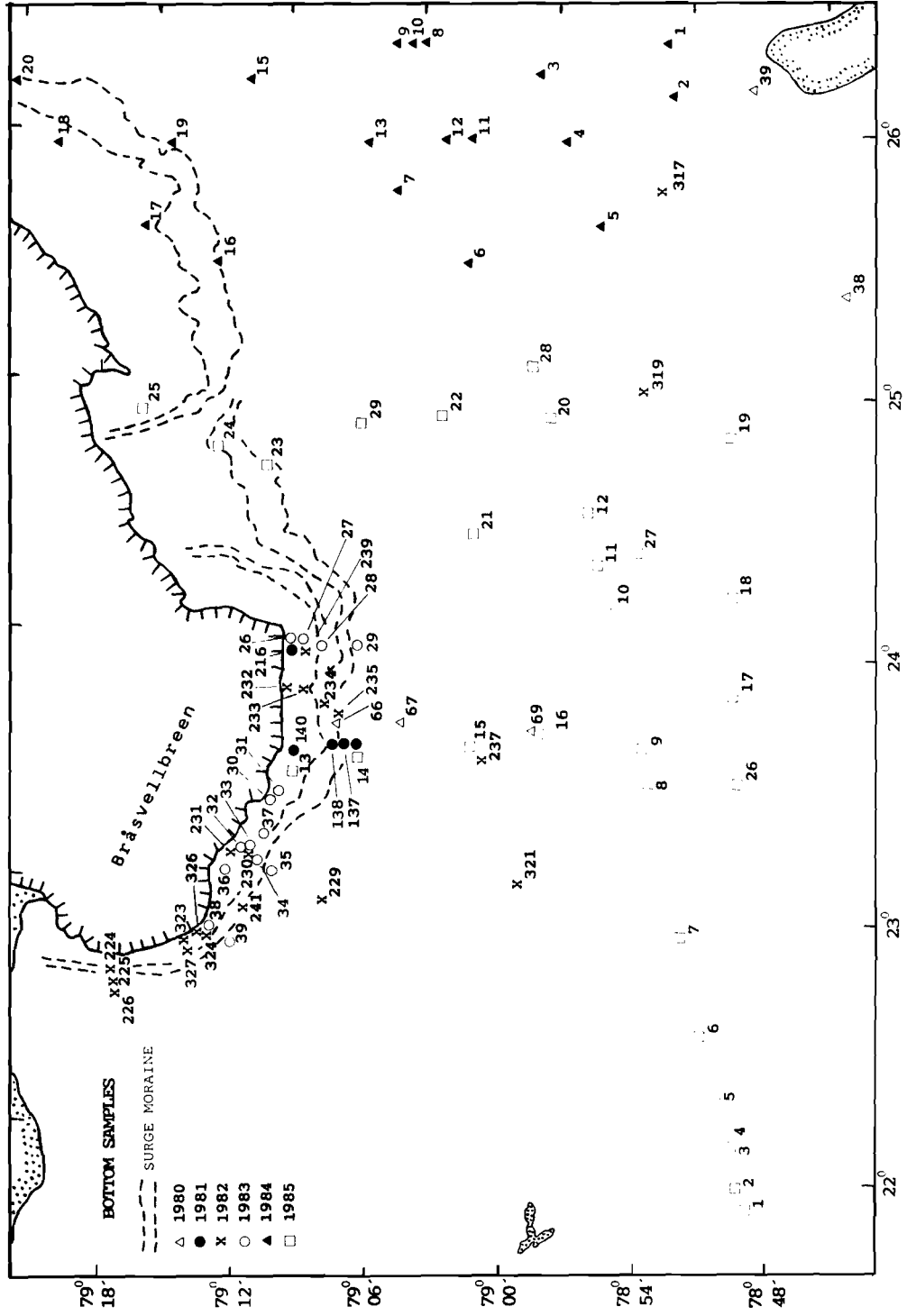


Fig.6C.

relative scale was improved using observed radar distances to the ice front. One or two good satellite fixes pr. hour were usually obtained and all core stations are positioned by at least one satellite fix with an accuracy of 100-150 m.

In addition to the NP cruises of 1980-83, the Norwegian Hydrographic Survey (NSKV) carried out hydrographic mapping in this part of Erik Eriksenstredet during the autumn of 1984 and 1985 and included sparker, 3.5 kHz PDR and side scan sonar in the program (Fig.6b). These surveys were run with lines in a N-S direction and nominal line spacing of 500 m in the eastern part and 1000m in the western part with infill lines of 250 and 500 m spacing, respectively. Part of the sparker data were of generally poor quality due to severe noise problems. In addition to the acoustic profiling, 7 gravity cores and 50 surface grab samples were recovered.

The NSKV surveys were run using a local Decca Sea Fix navigation system, with slave stations positioned on the surrounding islands. Accuracy of the system is on the order of 10 m.

On board analyses of a selection of the sediment cores included:

- Description of core section ends and cutter/catcher material (long cores were cut in 1 m sections).
- Munsell soil color.
- Pocket penetrometer shear strength on core section ends.
- Measurements of compressional wave velocity, by means of a PUNDIT (Portable Ultrasonic Non-destructive Digital Indicating Tester, trade mark of C.N.S. Instr. Ltd., England, ASTM 1983). This instrument measures travel time through the sediment with 1 ms accuracy. Measurements were taken both along and normal to the cores. This was done immediately after retrieval of the plastic

liner to ensure contact between liner and sample. Travel time delay caused by measuring through the plastic liner was corrected for.

- Water content on samples from core section ends (only done on-board in 1982).

Subsequent laboratory work included:

- A selection of the cores were x-radiographed prior to splitting. A few of the 1983 cores were also run through a computer tomograph.
- Core splitting and visual description including Munsell soil color and photography of split cores. Cores with relatively stiff material were split by breaking in two halves, while softer material was cut with knife or wire saw.
- Shear strength on split core halves by pocket penetrometer or fall-cone apparatus. Shear strength values given are usually averaged from several measurements in the same interval where this was possible.
- Compressional wave velocity measurements with the PUNDIT, mostly on smaller sections of the cores, giving interval velocities. The main source of error is exact determination of the distance between the transmitter and receiver transducers, in particular when used in soft material. Velocities were measured both along and perpendicular to the cores, but no significant difference was recorded. To minimize the distance error, long intervals were preferred.
- Consolidation tests (oedometer) were done on two samples to measure pre-consolidation stress of the material.
The intervals chosen for consolidation testing were cut from the cores before splitting, after inspection of x-radiographs. A majority of the sampled material was too gravelly to be tested in standard sized equipment.
- Water content and bulk density were determined on subsamples of 100-200 g wet weight. Volume was measured by submerging the sample

in kerosene. As the material generally had a high but varying content of gravel and pebbles, a correction was applied to obtain water content values that could be compared within the study area. Hence, a set of values is included that are corrected for material greater than 0.5 mm.

- Grain size distribution have been measured on a number of subsamples. Size fractions greater than 0.063 mm were separated by dry sieving, while clay and silt fractions were determined by Falling Drop Analysis (trade mark Geonor A/S, Norway, Moun 1966). This apparatus utilizes the falling time of a drop of sediment suspension through an organic liquid. It is largely temperature dependent, and as this apparatus did not have automatic temperature control, it was calibrated for every 0.5 °C. Some samples were analyzed both with the falling drop method, and in a sedigraph. Within small limits (<5 %), the results were comparable. This was also the case for some samples where all the material was size-fractionated, in addition to falling-drop analyzed. We therefore consider the falling drop method reliable for the present purposes. The majority of the samples analyzed for grain size distribution were greater than 100 g wet sediment.
- XRD on oriented samples of clay and silt fractions.
- Atterberg limits were determined after wet sieving through a 0.063 mm sieve.

SEA FLOOR MORPHOLOGY.

The sea floor morphology outside Bråsvellbreen was initially described by Solheim and Pfirman (1985), based on acoustic data mainly from the 1982 and 1983 cruises. However, the NSKV cruises of 1984 and 1985 have given a more detailed and complete data set,

and also cover a wider area. The total data base is used in this paper.

A range of different morphologic patterns in defined provinces have been mapped (Fig.7). The most dominant morphological pattern is considered to define the signature of each province. However, there may be large variations within a province and changes between patterns may be gradational. Therefore, the location of the boundaries is a matter of interpretation in some areas.

The most striking morphological feature in the study area is the system of ridges that roughly parallels the ice front at a distance of a few kilometres. Solheim and Pfirman (1985) mapped the ridge in front of Bråsvellbreen and argued that it was the end moraine resulting from the 1936-38 surge. The dense grid of new lines confirms the continuity of the feature, and furthermore shows that there is a system of three ridges. A second ridge, similar to the Bråsvellbreen ridge, runs subparallel to the Basin 3 ice front, while a third ridge has an intermediate position. The latter merge with the Bråsvellbreen ridge, but not with the Basin 3 ridge (Fig.7). The following description and discussion will show that the ridges are terminal features. I therefore propose to term them surge moraines and this term will be used below, even before indications have been presented for the Basin 3 and intermediate ridges to be surge-related features.

The study area is divided into 3 zones, each with several characteristic features:

- The surge moraines.
- Inside the surge moraines, the surge zone (Solheim & Pfirman 1985).
- Outside the surge moraines, the surge-distal zone.

The surge moraines.

The most typical cross sectional shape of the Bråsvellbreen surge moraine is that of an asymmetrical ridge with a smooth outer (distal) slope of $1-3^{\circ}$ and a steeper ($3-6^{\circ}$, locally steeper) inner (proximal) slope (Fig.8a,c,d). However, in places the moraine has only a minor topographic expression (Fig.8b). The distal part of the moraine appears on the 3.5 kHz records as a smooth, acoustically transparent sediment lense which is draped over pre-existing topography and with an abrupt termination (Fig.8b) Its relief varies between 5 m and 20 m and the distance from the base of the proximal slope to the present-day glacier front ranges from 500 m to 3.5 km, the widest and most distinct part being in the area where it splits into two ridges. East of this, it is generally narrower and less distinct than further west. The easternmost two kilometres show little relief and are outlined only from its side scan sonar character.

The intermediate surge moraine changes character from being a narrow, low-relief feature in its western part (Fig.8d) to a wide, well expressed feature further east (Fig.8e,). Towards its easternmost extension, it loses its bathymetric expression again. The central part of this ridge is wider (up to 3 km) and has a larger maximum relief (35m) than the Bråsvellbreen ridge, but the overall shape is quite similar.

The Basin 3 surge moraine (Fig.8f,g,h) has a character somewhat different from that outside Bråsvellbreen. The western part is narrow and poorly expressed bathymetrically (Fig.8f), although locally it resembles the Bråsvellbreen ridge (Fig.8g). In its central and widest (up to 4.5 km) part, the moraine has the shape of a wide, low-relief sediment lense, (Fig.8h) and the proximal boundary is difficult to define. The distal part, however, is easily recognized by its draped,

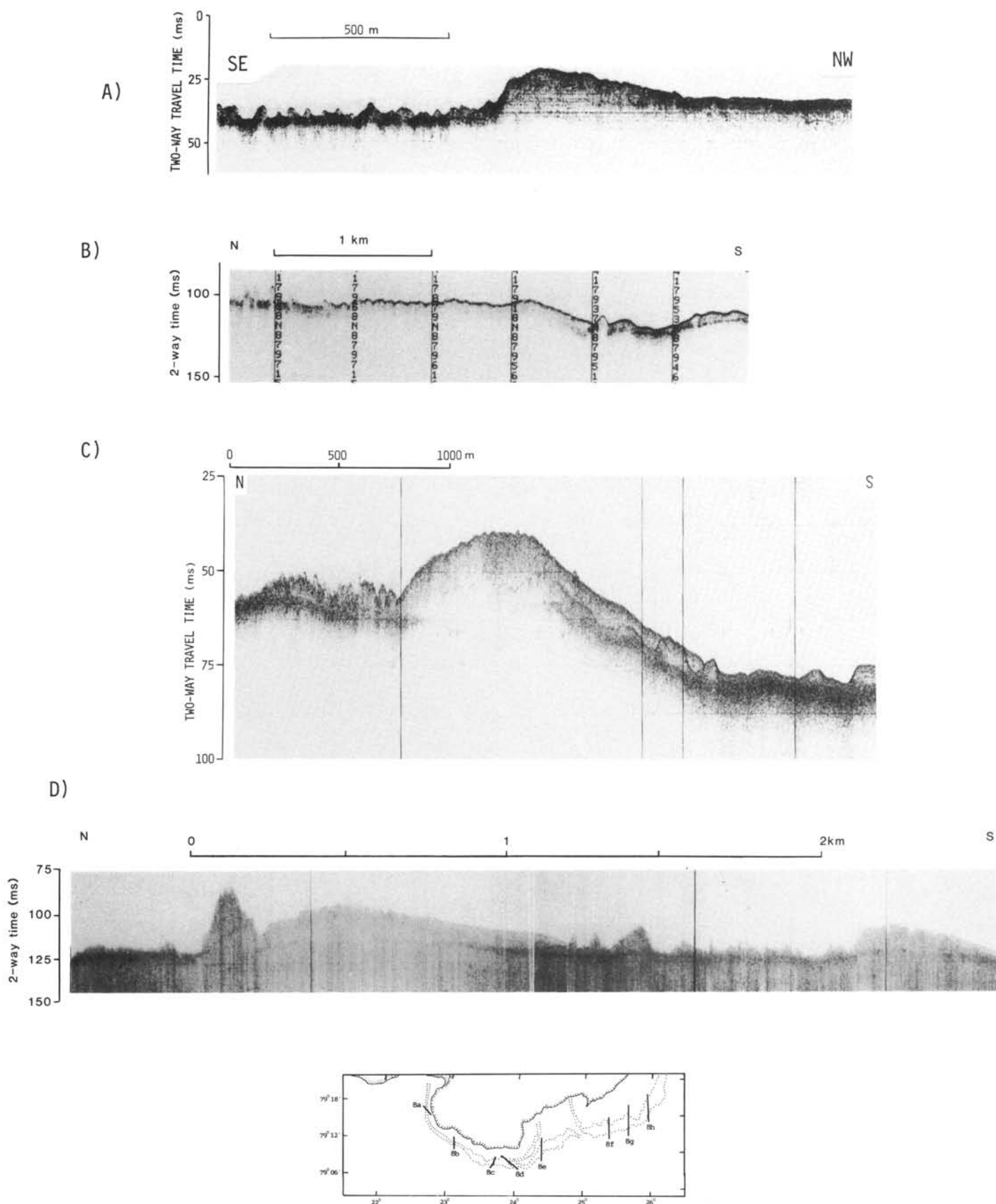
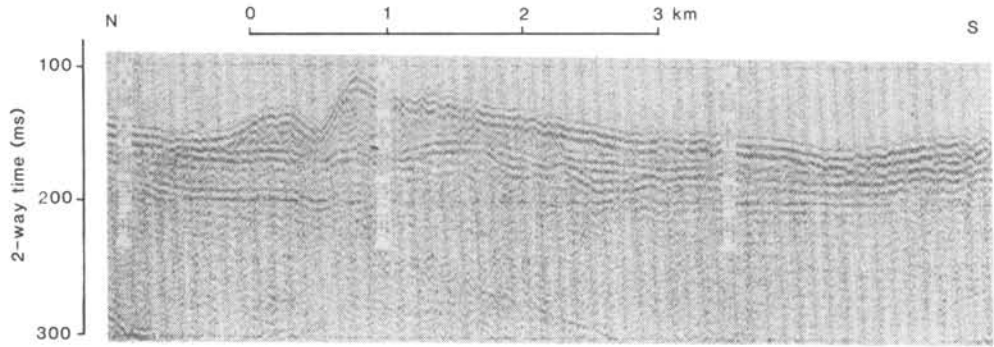
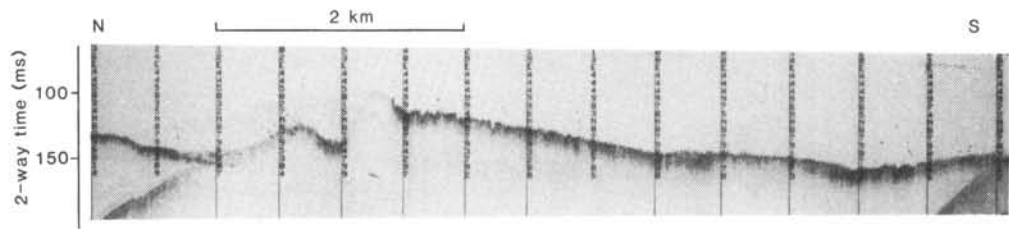
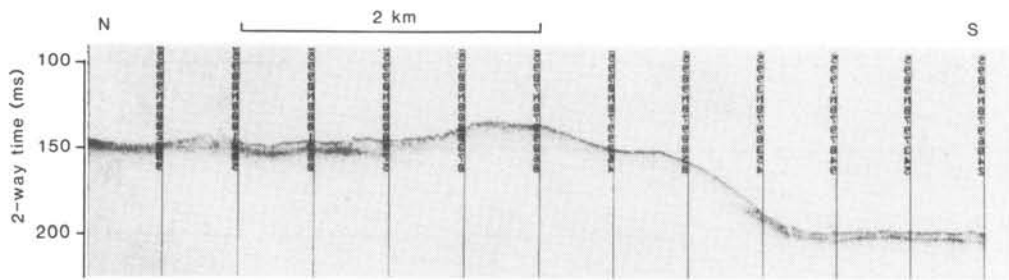


Fig.8. 3.5 kHz and sparker (Fig.8e, lower part) records across the surge moraines.

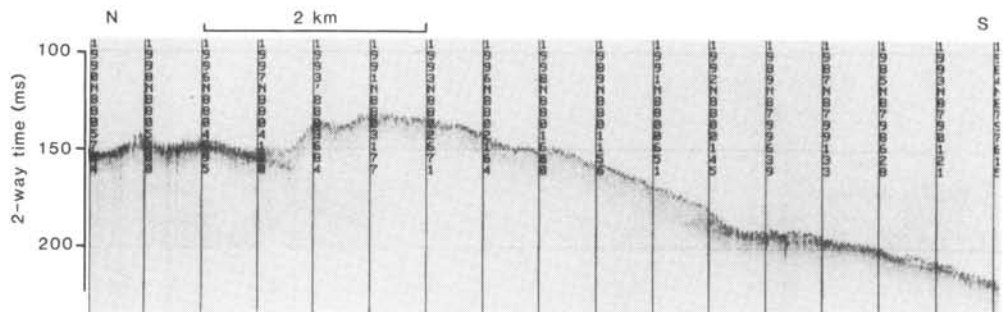
E)



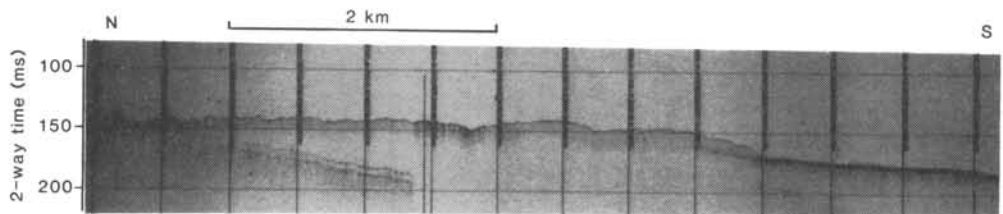
F)



G)



H)



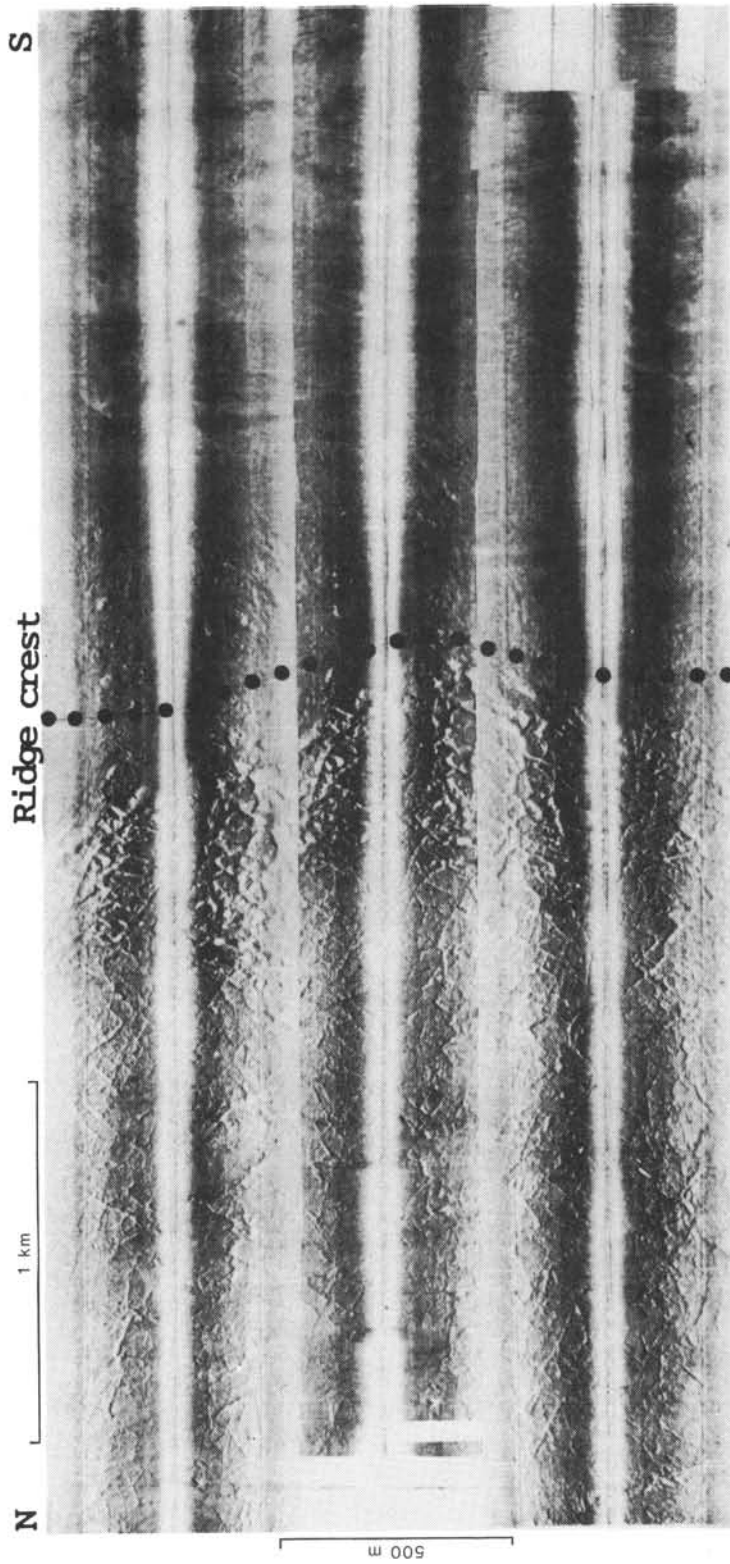


Fig.9. Side scan sonar mosaic across the Bråsvellbreen surge moraine. Notice the marked morphological change across the ridge. For location, see Fig.10.

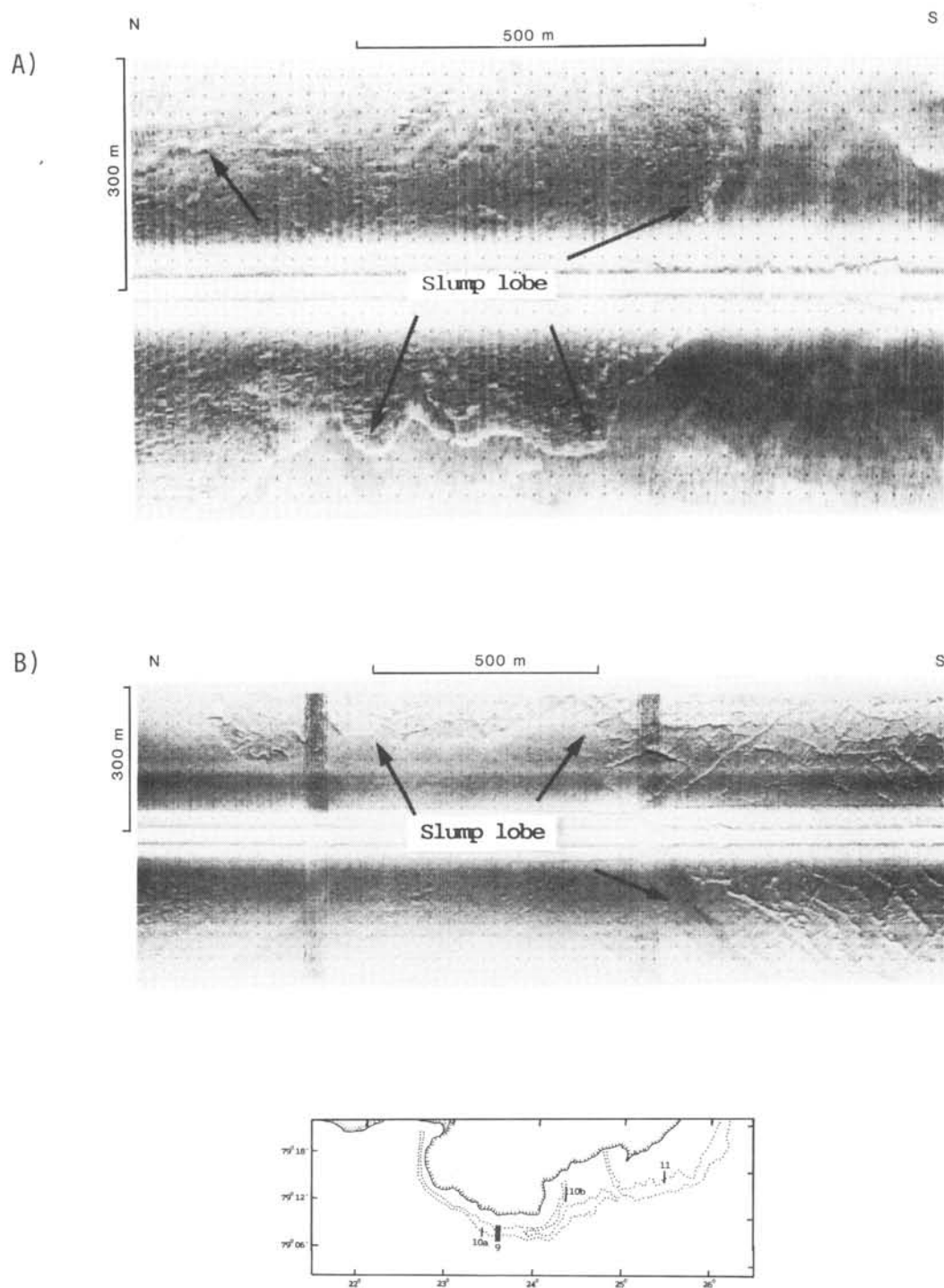


Fig.10. Side scan sonographs showing slump lobes on the distal part of the surge moraines. Note that the slumps cover pre-existing relief. Note also the small disturbances in the smooth slump lobe surface, and the possible detachment scars (arrow) in a).

acoustically transparent character.

Common for the three surge moraines is that they mark a distinct change in the sea floor morphology between the area towards the glacier and the deeper parts of the basin. This is so both on the 10 m scale, as seen from the bathymetric map (Fig.2), and at a smaller scale, as seen from the side scan sonograms (Fig.9).

Although patterns mapped on either side of the ridge may continue on to the ridge proper, the Bråsvellbreen moraine ridge has a generally smooth surface, dissected by occasional iceberg plough marks. The distal part of the moraine ridge shows an abrupt termination (e.g. Fig.8c). Side scan sonograms clearly show this to be the termination of slump lobes covering the pre-existing morphology (Fig.10). Furthermore, the smoothness is disturbed by small irregularities forming a small scale swell and swale morphology (Fig.10). The disturbed areas usually terminate along the slump edge. Most likely these represent creep features in the soft, acoustically transparent sediments. In the northeastern part of Fig.10a, some vague, larger features can be seen that may represent detachment scars caused by the slumping.

Side scan sonographs from the moraines proper show that their small scale surface morphology in general differs between the Bråsvellbreen moraine and the two other moraines (Fig.7). Outside the eastern part of Bråsvellbreen, where the moraine ridge splits, the inner ridge is characterized by a smooth surface, obscured by the small disturbances and occasional iceberg plough marks. The outer, intermediate moraine and its continuation eastwards, however, is dominated by iceberg plough marks. This is also the situation on the moraine outside Basin 3, but here the plough marks are associated with small ridges, mounds and depressions, in both linear and random arrangements (Fig.11). This is defined as a separate morphological

province (Fig.7). At the distal part there is again an area of smooth, slightly disturbed sea floor.

The surge zone.

The area inside the Bråsvellbreen ridge was termed the surge zone by Solheim and Pfirman (1985) because this area was directly affected by grounded surging ice in 1936-38. Two different morphological patterns predominate. The main part of the area, 0.5 - 1 km south of the ice front, has a system of smaller, linear ridges orientated in different directions that together form a rhombohedral cross-pattern (Figs.7,12). The ridges have reliefs on the order of 5 m and spacing of 20-70 m and are larger and more pronounced close to the surge moraine. Ridge directions vary, and 2-3 different directions may be present within a region (Fig.13). Most often, however, there are directions sub-parallel and sub-perpendicular to the present-day ice front. In general the distal limit of the rhombohedral pattern follows the proximal edge of the moraine, but in some locations it may extend on to the topographically defined ridge. In the eastern part, where the moraine ridge splits into an outer and an inner ridge, a clear rhombohedral pattern exists between the two moraine ridges (Figs. 7,12b).

Although the side scan data coverage is more sparse outside Basin 3, a rhombohedral ridge pattern can also be mapped here. It is best expressed in the eastern part, but is generally not as clear as that outside Bråsvellbreen. The distal limit roughly follows the proximal side of the end moraine, but the latter is more difficult to define, due to its lesser topographic expression. The inner limit of the rhombohedral pattern is generally 3-5 km off

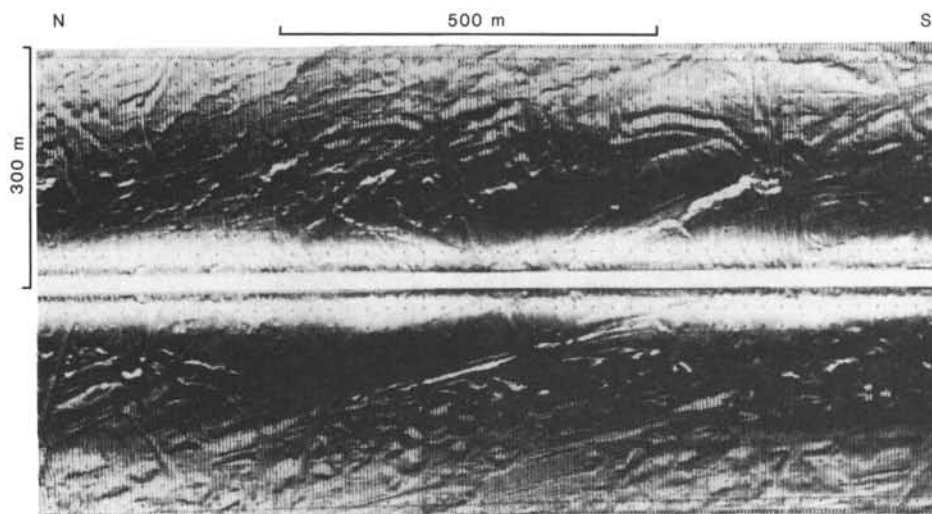


Fig.11. Side scan sonograph showing the mixed morphology of Fig.7. For location, see Fig.10.

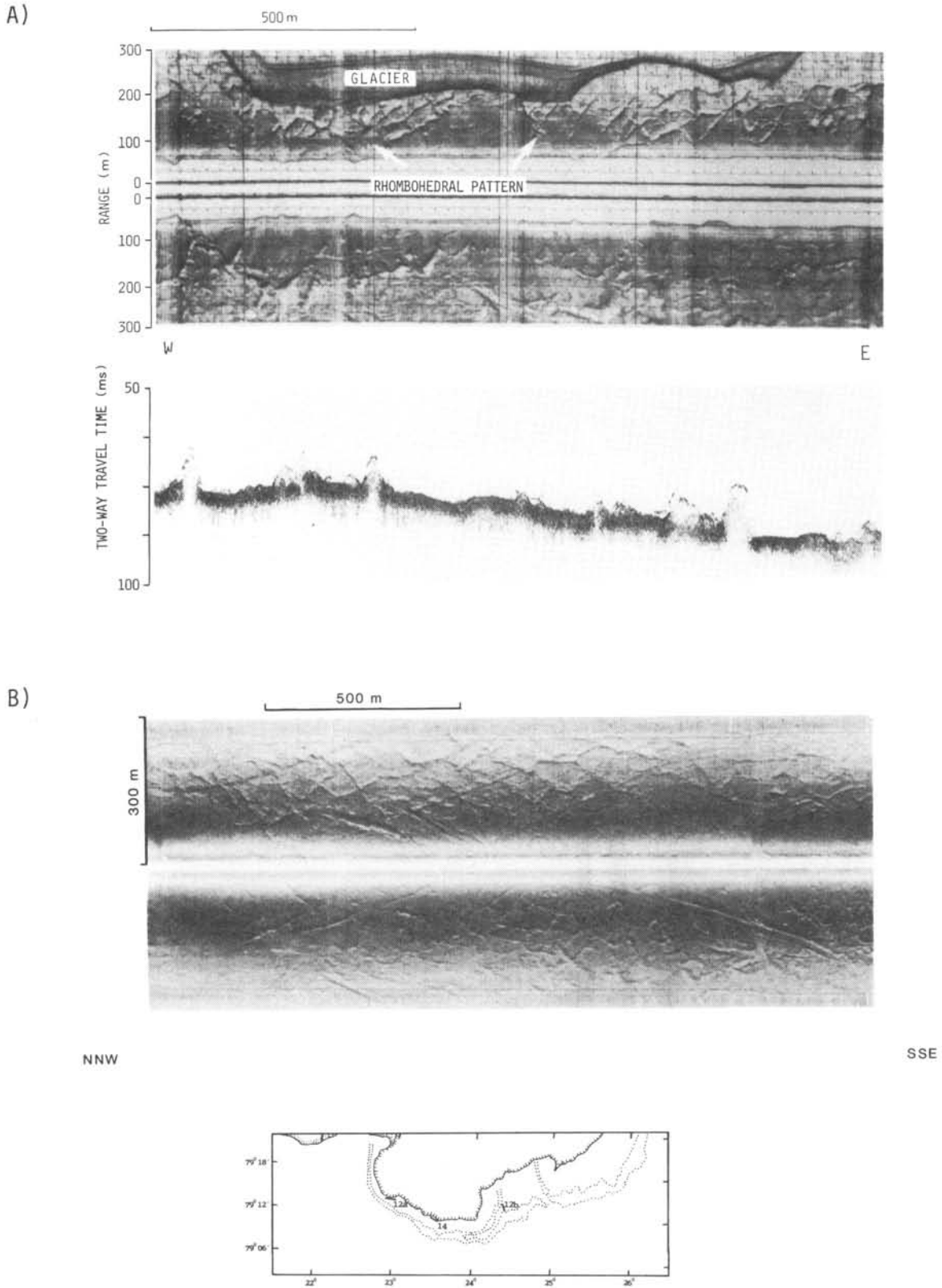


Fig.12. Side scan sonograms and 3.5 kHz echogram from the rhombohedral ridge pattern of the surge zone.

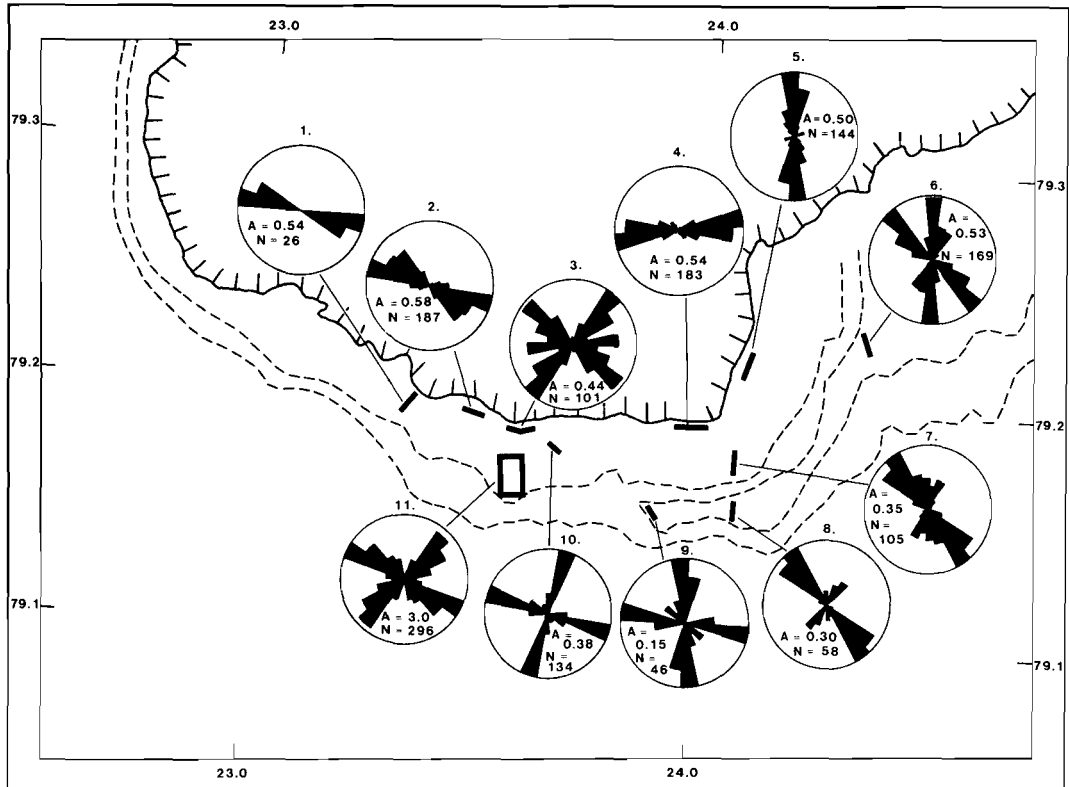


Fig.13. Rose diagrams of directions of ridges in the surge zone. The analyses were done inside a sliding window of 100 x 200m across each area. N is number of counts.

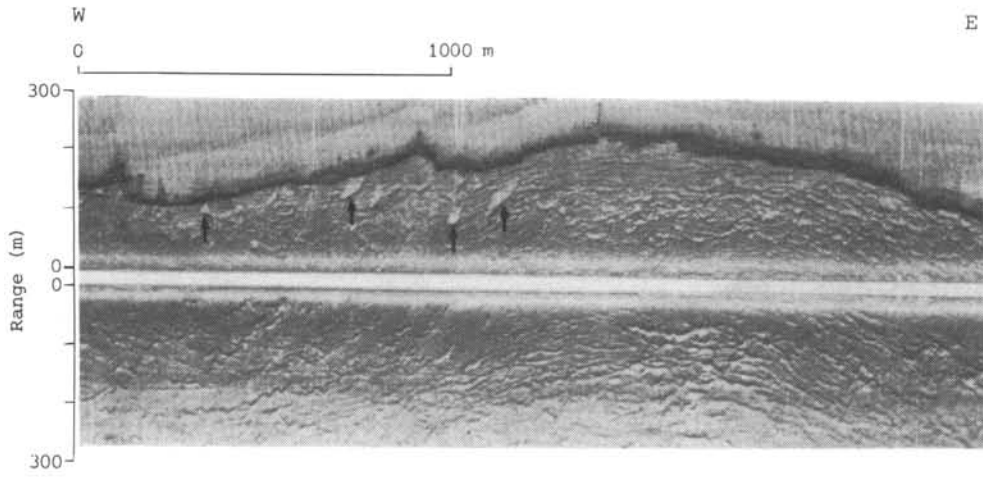


Fig.14. Side scan sonograph of the discontinuous, arcuate ridges subparalleling the ice front. Some possible iceberg calving impact features are marked with arrows. For location, see Fig.12.

the present-day ice front, except close to Kapp Mohn.

Between the two drainage basins, a rhombohedral ridge pattern disturbed by smaller mounds and depressions prevails. The disturbances seem to overprint the rhombohedral pattern in this area.

In the western part of Bråsvellbreen the rhombohedral ridge pattern can be traced to the ice front (Fig.12a), while further east, in a 500 m to 1 km wide zone adjacent to the ice front, a system of discontinuous arcuate ridges trending subparallel to the front, prevails (Figs.7&14). Relief and width of individual ridges are of the same order as the linear ridges forming the rhombohedral pattern. The zone of arcuate ridges widens markedly to the east of Bråsvellbreen, from approximately 1 km to generally 3-5 km in the rest of the area. Both adjacent to Basin 3 and Bråsvellbreen, the ridges are relatively distinct, and the glacier-parallel trend predominates even though other directions do occur.

Also within this morphological province the pattern is most varied and least distinct in the region between Bråsvellbreen and Basin 3. The above mentioned pattern of mounds and depressions obscures the ridges, and directions vary from parallel to subperpendicular to the ice front. In the shallowest region, immediately SW of Kapp Mohn, the ridge system is overprinted by recent iceberg plough marks, which are the dominant morphological features of the region (Fig.7).

The surge-distal zone.

Two broad classes of sea floor morphologic provinces prevail south of the surge moraine system, in the surge-distal zone;

1. Areas where iceberg plough marks predominate.
2. Areas where smooth sea floor predominates, but where a number of other features also exist.

Two classes of iceberg plough marks are defined in the study area:

- a. "Recent" plough marks, formed under the present-day water depth and glacier configuration.
- b. "Fossil" plough marks, mostly found in water depths below the probable reach of present-day icebergs.

The distinction between a. and b. is made only from their appearance on the side scan records. The recent plough marks have a sharp, fresh appearance which contrasts markedly with the weakly pronounced, probably degraded fossil ones (Fig.15). However, the differentiation is not always straightforward, as a range of plough marks intermediate between the two end members exist.

The most recent ploughing is found in the shallower areas on either side of Erik Eriksenstredet, with the exceptions of the intermediate surge moraine, the area southwest of Kapp Mohn and occasional plough marks elsewhere in the regions inside the surge moraines. Typical widths of these plough marks are 10 to 50 m, averaging around 25 m (Fig 15a). Relief (top of berm to bottom of trough) is on the order of 2-5 m. The lower limit for the recent iceberg ploughing varies between 120 and 130 m water depth, corresponding well with a maximum submarine ice cliff height of 125 m for Austfonna (Dowdeswell in prep.). This is well expressed, both along the north slope and in the southwestern and southeastern parts of the survey area (Fig.7). In the northwestern part, the intense ploughing grades into a transitional zone of less intense ploughing at 50 - 100 m water depth which terminates at approximately 120 m water depth. Most often, however, the zone of intense, recent ploughing terminates abruptly and changes into smoother sea floor with older plough marks (Fig.16). Locally this occurs at depths shallower than 120 m (Fig.16b).

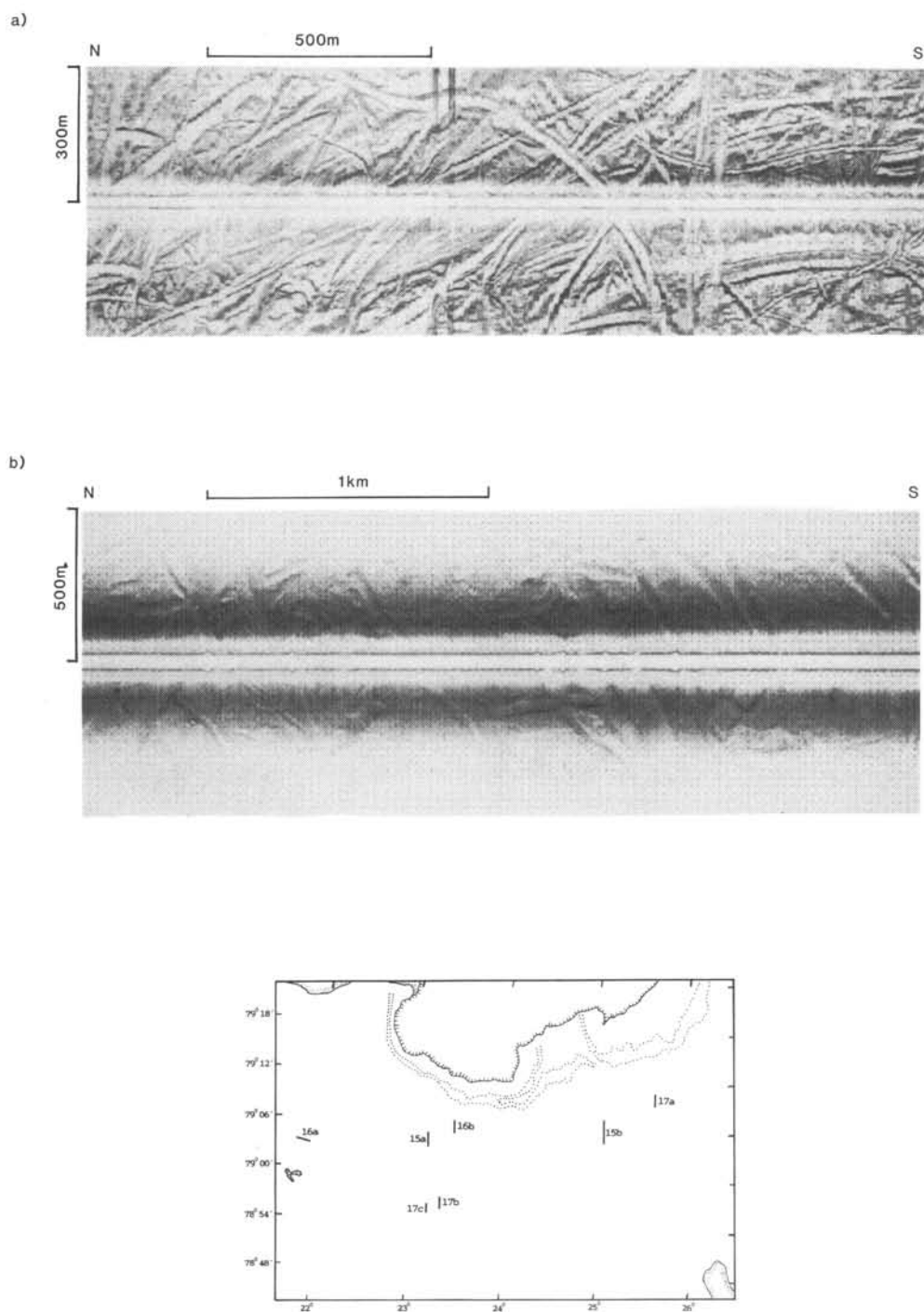


Fig.15. Side scan sonographs of a) recent and b) fossil iceberg plough marks.

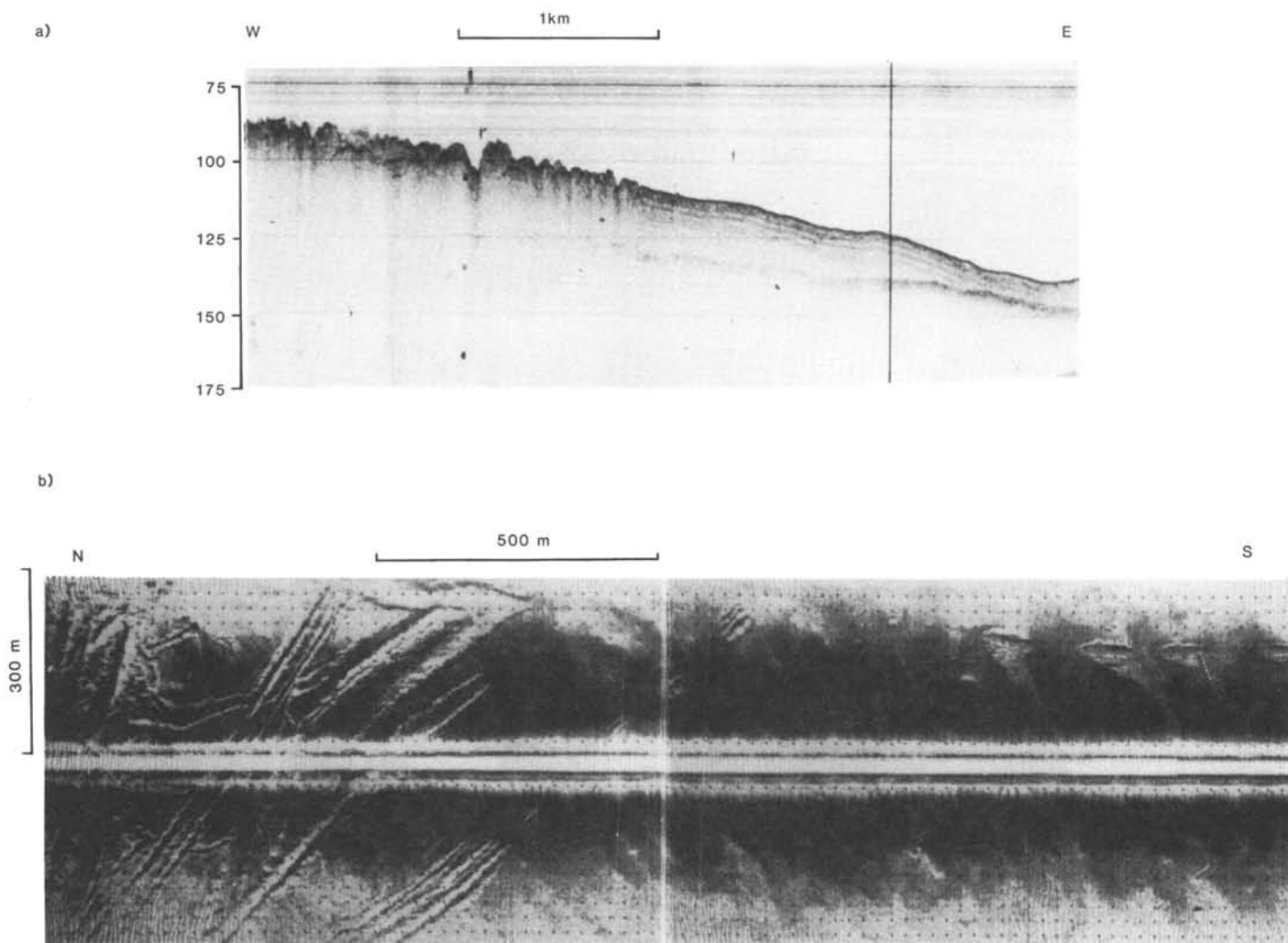


Fig.16. 3.5 kHz record (upper) and side scan sonograph (lower) showing termination of the recent iceberg ploughing. Note that the profiles are from different locations. For location, see Fig.15.

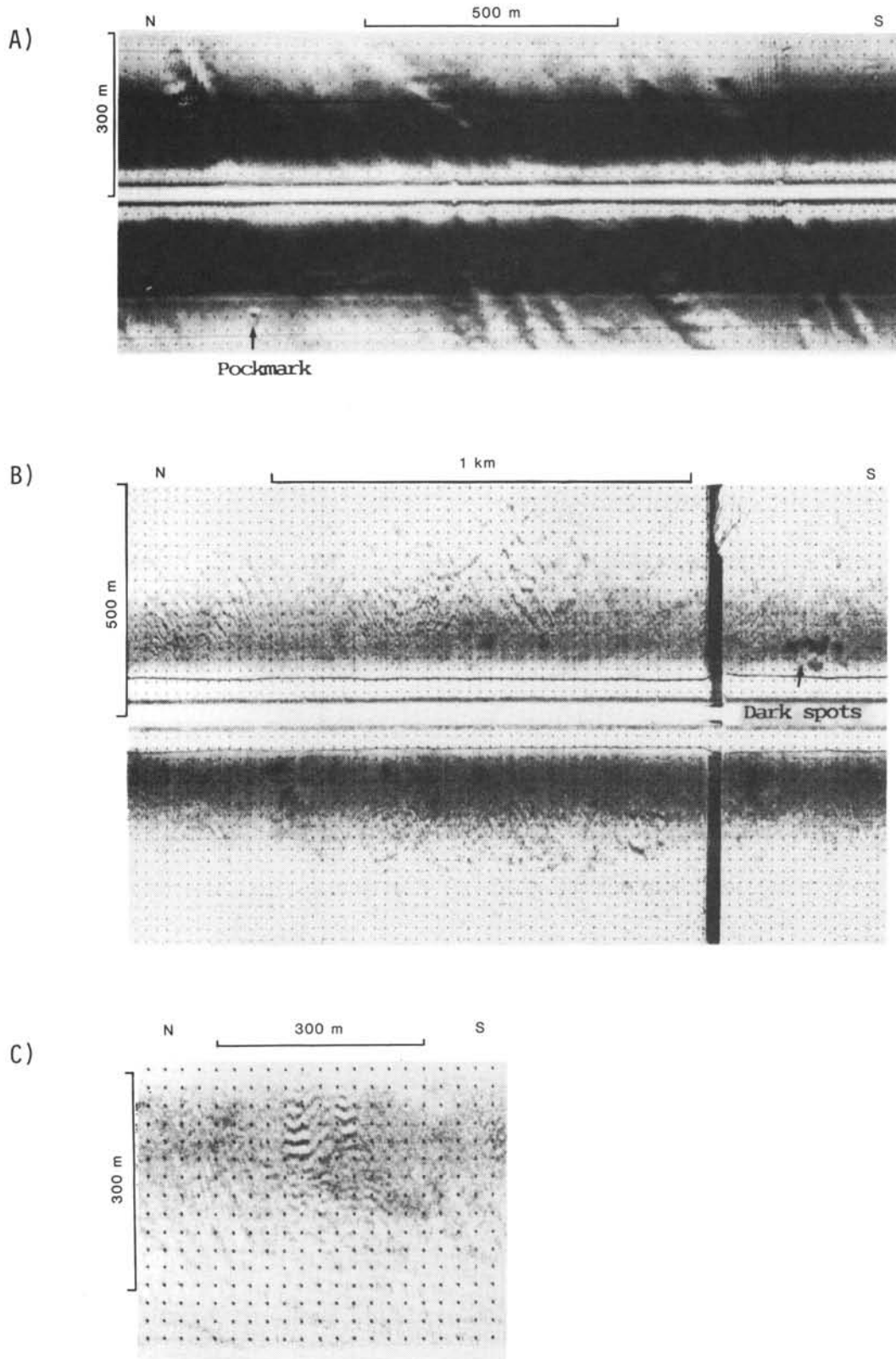


Fig.17. Side scan sonographs showing morphological features found in the "smooth" (Fig.7) deeper region: a) Fossil iceberg plough marks with internal cross-ridges forming a ladder-like pattern. Note pockmark (arrow). b) Dark spots in an area of weakly defined sediment waves. Note cluster of dark spots in southern part of upper channel (arrow). c) Well defined sediment waves (megaripples). For location, see Fig.15.

Dominating directions of the recent plough marks in the northern region generally varies from NW-SE in the western part, through a region of mixed directions in central parts, to more NE-SW'ly directions in the east. In the southern regions, the ploughing directions are generally more variable (Fig.7).

Fossil plough marks are found over the entire basin below 120 - 130 m water depth, including the large region of smooth sea floor. These gouges are degraded to various degrees. They may range from being barely visible on side scan records and having no topographic expression within the resolution of the 3.5 kHz echo sounder, to being well enough pronounced that a recent origin can not be excluded. In general they have less well defined berms than the recent plough marks. Widths range from 20 to 100 m, averaging approximately 50 m. Relief is quite similar to that found for recent plough marks, but smoother. Directional trends are mostly similar to those of the recent plough marks, except for the southeastern region, where the fossil plough marks have a strong NE-SW component, and the small area in the deep, central part of the study area where there is a distinct NE-SW, NW-SE cross-pattern. In the easternmost region, smaller, transverse ridges in the plough marks give a washboard or a ladder-like appearance (Fig.17a).

With the exception of the small areas of more concentrated old ploughing, the areas outside the limit of recent iceberg ploughing are defined as one morphological province. In general this province is defined by a smooth sea floor of low reflectivity to the side scan signals. However, several morphologic features are observed:

- "Old" iceberg plough marks, as described above.
- Pockmarks. These are small (5-15 m diameter) circular depressions in the sea floor (Fig.17a). They are sparse in number, but distributed over the entire area..

- Patches of more reflective sea floor, appearing as dark spots on the side scan sonar records (Fig.17b). These are of similar diameter, but more common than the pockmarks. They may be found in groups covering areas of 100-200 m diameter. Dark spots and pockmarks may also be found grouped together. None of the two can be distinguished in echograms, implying they have reliefs of <1m.
- Sediment waves (megaripples) (Fig.17b,c). In particular in the western half of the region, disturbances resembling megaripples are found. Often they are indistinct (Fig.17b) and only rarely can dimensions and directions be measured. Wavelengths are on the order of 15-20 m and directions mostly vary between NW-SE and NE-SW, although E-W also occurs (Fig.17c).

DISTRIBUTION AND ACOUSTIC STRATIGRAPHY OF UNLITHIFIED SEDIMENTS.

The sediment cover above bedrock in the major part of the study area is generally less than 10 ms (two-way travel time) (Fig.18). Uncertainties in accurately determining the sediment thickness result from the following factors:

- Underlying bedrock is essentially conformable with the sea floor.
- Total sediment thickness is less than the resolution of the sparker system used, over large areas.
- The 3.5 kHz penetration is poor due to overconsolidation and scattering of energy in sediments with high boulder content.

An internally consistent, detailed acoustic stratigraphy is therefore difficult to map.

In the surge zone, the sediment thickness is mostly 2-5 ms, with some areas of 5-10 ms. The latter is most common along the surge moraine outside Basin 3. This is also the region where the proximal boundary of the moraine is difficult to define, and where sediment seems to be "smeared" out over a larger area than the ridge proper.

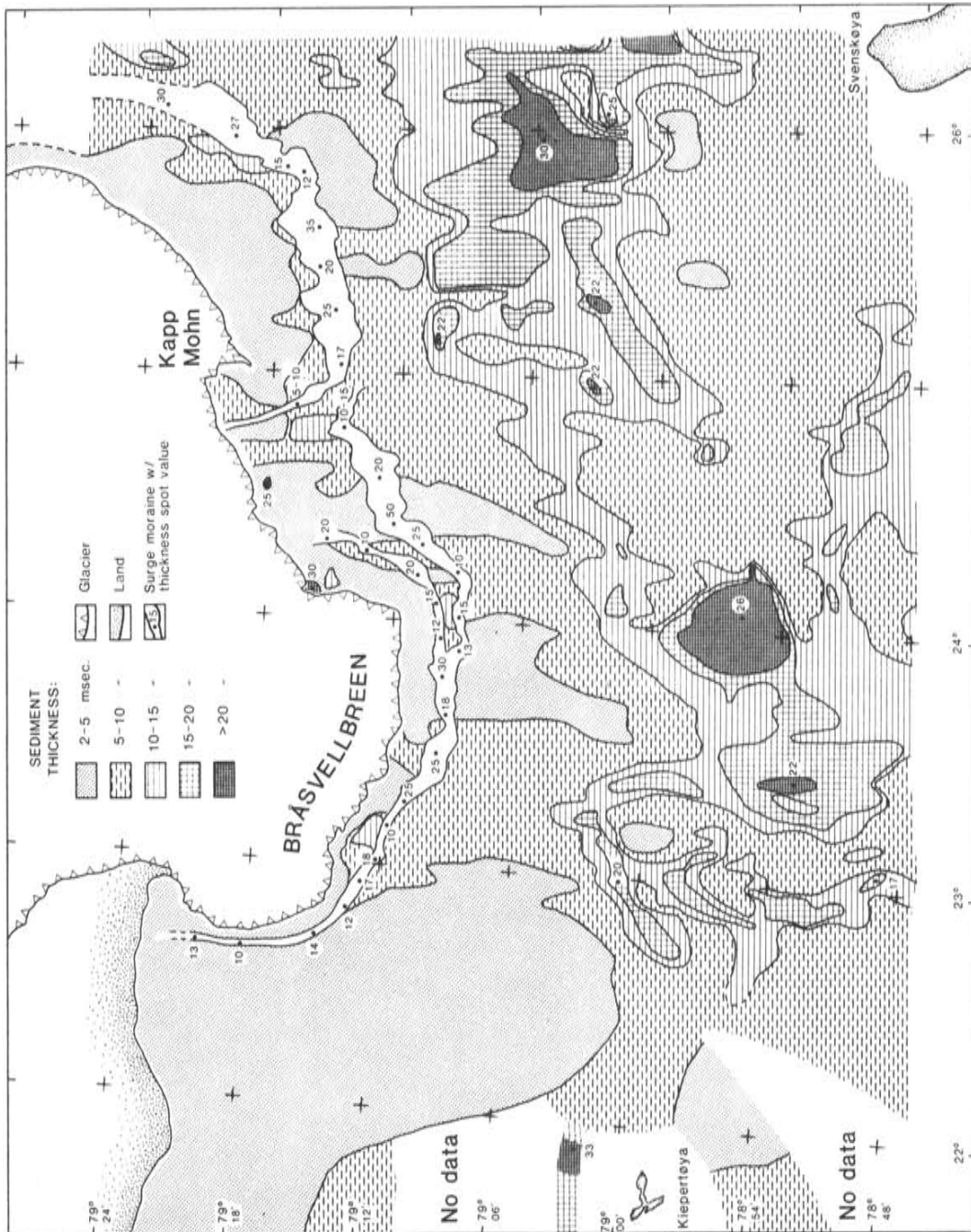


Fig.18. Isopach map of total unlithified sediment cover. Thickness values in two-way reflection time (milliseconds).

Due to the irregular topography, thickness variations are large, and the map (Fig.18) represents average values. Most irregularities are too local to be included in a map of this scale. Deviations from 2-10ms thickness inside the surge moraines include: a small area of 10-15 ms in the western part of Bråsvellbreen (found in the same local bathymetric depression that was also shown to have escaped recent iceberg ploughing outside the surge moraine); two small accumulations which are associated with the meltwater outlet, one of which reaches 30 ms thickness; a local ridge close to the ice front in the intermediate region; an area of 10-15 ms just inside the eastern part of the intermediate surge moraine.

The surge moraine system constitutes the most distinctive sediment accumulation in the region, although its relief and thus sediment thickness vary considerably. The intermediate moraine reaches the largest thickness, of up to 50 ms (Figs.18,8e,f). In the region where this moraine merges with the Bråsvellbreen one, the latter reaches its maximum thickness of 30 ms.

The large region in the western part of the study area, with 2-5 ms sediment, is part of the shallow sill at the mouth of Hinlopenstredet. Water depths in this area are generally less than 50 m. The major part of the deeper basin has 5-10 ms sediment thickness, but locally thicker lenses occur in the deeper part of the strait and thinner ones on the north slope. The trend of the thicker accumulations follows the bathymetric NE-SW trend, with a transition into the more N-S'ly Olgastredet trend in the southwestern part of the map area.

A seismic stratigraphic framework for the Barents Sea glacial sediments was established by Solheim and Kristoffersen (1984) from the thick wedge of glacial sediments on the western Barents Sea margin. Lower resolution in the upper 15-20 ms in this area and lack of tie

lines to the present study area preclude direct correlation, but most likely the entire section above the bedrock in the present study area belongs to the upper of the four seismic sequences defined from the margin, sequence I of Solheim and Kristoffersen (1984). Within this, in the present study area, 5 acoustic stratigraphic units are defined (Fig.19), based on their character in 3.5 kHz records:

Unit 1. Semitransparent top unit in the surge zone.

Unit 2. The surge moraine ridge system.

Unit 3. Transparent top unit in the surge-distal region.

Unit 4. Intermediate, semitransparent unit.

Unit 5. Opaque unit, underlying the transparent sediments over the entire study area.

Some of these units, in particular 1,2 and 3, may be isochronous or at least overlapping in age, but their character and geometry are different enough to justify a separation. The most diagnostic features are acoustic transparency, character of internal reflections and surface roughness. There are no systematic differences between the areas outside the different glacial drainage basins.

Unit 1. is the acoustic unit that forms most of the small scale topography in the surge zone. Due to squeeze-up, ice push and occasional iceberg ploughing, the character of this unit is dominated by its rough surface structure which causes abundant diffraction patterns. The unit rests on a relatively smooth reflector, opaque to the 3.5 kHz signal. Its thickness varies frequently from zero between ridges to several meters in the ridges and other local accumulations. The ridges may be narrow enough to be represented only by a single diffraction hyperbola, and this may contribute to the acoustically transparent character of the sediment. Where Unit 1. is found as a more continuous accumulation, it has a more semi-transparent character, with abundant internal diffraction. Internal reflectors can

be seen, but are local due to the patchiness of the unit.

As the surge moraine ridges are depositional features clearly different from the other stratigraphic units in the region, they have been classified as a separate unit, unit 2. The Bråsvellbreen ridge has the best coverage of good quality data. Most of the ridge, in particular the inner and central (proximal) part, have a relatively homogeneous, semi-transparent character. On some of the 1982 lines, run with high sweep rate under favourable weather conditions, diffraction and discontinuous reflectors can be seen. In distal parts of the ridge, however, dipping layers downlap on a reflector that is continuous with the sea floor outside the ridge (Fig.19). In the profile of Fig.19, the ridge terminates on the berm of a plough mark and some of the ridge material has spilled over and covers the plough mark floor with a 1 ms thick drape. No ridge sediment, resolvable by the 3.5 kHz echo sounder, can be followed further out. The same structure is also seen in other profiles across the Bråsvellbreen ridge. The surge moraine ridges outside Basin 3 and the intermediate area have a more uniform acoustic appearance, but the data in these areas are of lower quality and vertical resolution.

Unit 3. is found as a thin, acoustically transparent layer in central parts of the basin at depths exceeding 140 m. This limit is most distinct along the north slope. Unit 3. reaches its largest thickness of 7 ms in the southwest, between 23° and 24° E, while the thickness generally varies from 1-3ms over most of the region. The existence of a thin drape, below the resolution of the 3.5 kHz system (approx. 1 ms), also in waters shallower than 140 m cannot be excluded.

Unit 4. constitutes most of the sediment thickness in the surge-distal zone. It varies in thickness from zero up to nearly 30

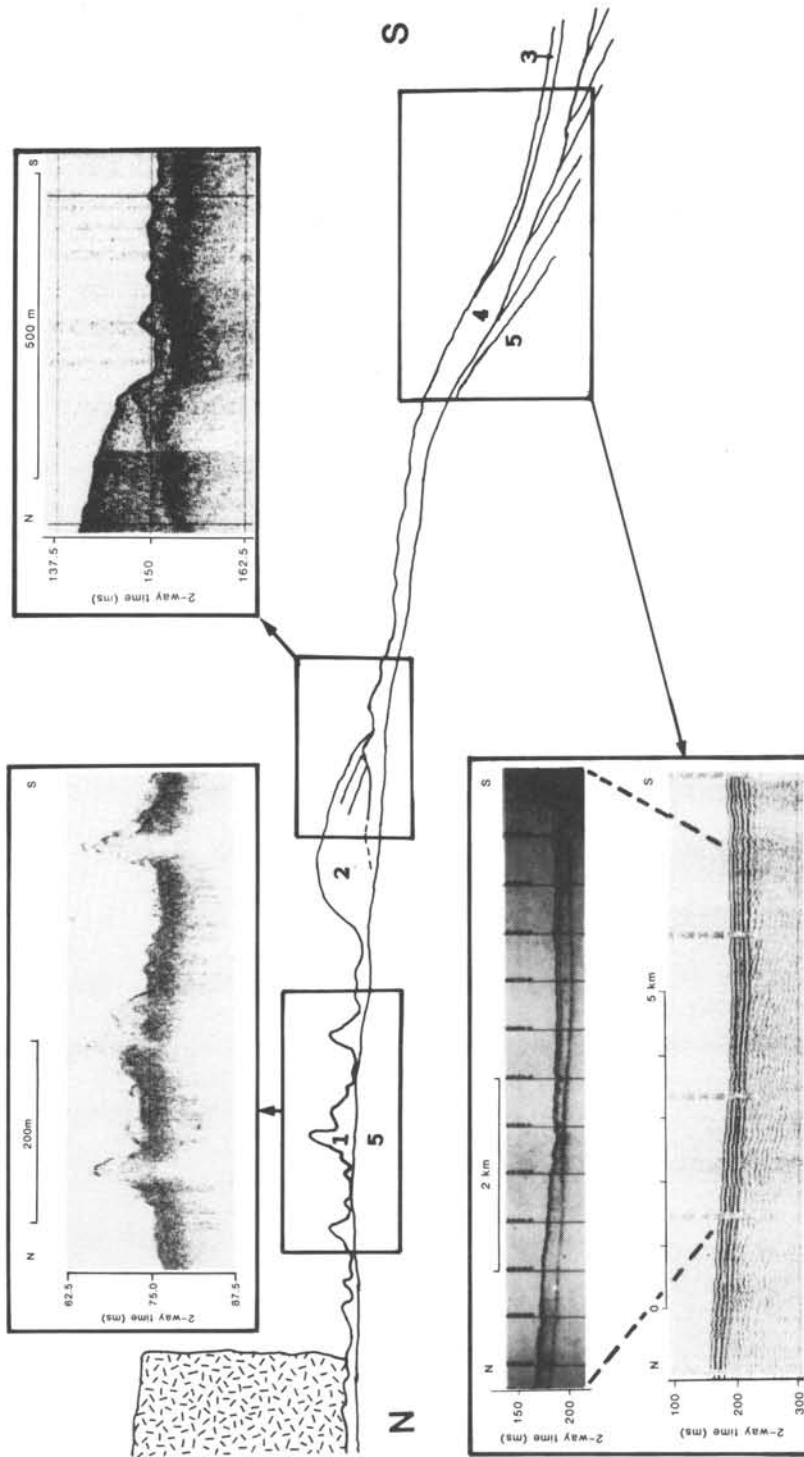


Fig.19. Cross section showing the different acoustic units. Note that the line drawing is only schematic, not drawn to scale.

msec. Its distribution follows the general sediment distribution trend in the basin, with the thickest deposits in the deepest areas. The top surface has a gently undulating character, most likely resulting from old iceberg plough marks. In the central parts of the basin, this undulating surface is draped by Unit 3. sediments (Fig.19). Its lower boundary is a smooth reflector that can be followed regionally over the area, also under the end moraines and in the surge zone. Internally, Unit 4. is mostly homogeneous and slightly less transparent than Unit 3. Occasionally, an undulating, discontinuous reflector can be seen in the lower part of the unit. From its less transparent character the material below this reflector may locally represent thicker till accumulations. Parallel layering, most distinct in the upper half of Unit 4. is observed on the slope towards Barentsøya (Fig.16b). Internal acoustic layering can only be seen below the lower limit of recent iceberg ploughing. Above 120 m waterdepth, Unit 4. sediments are intensively disturbed by recent ploughing in front of the surge moraines. However, in the local deep in front of central Bråsvellbreen (Fig.2) the top surface of Unit 4. is smoothly undulating from old, degraded ploughing, and can be followed under the outer part of the moraine ridge (Fig.19).

Unit 5. is used here as a collective term for all sediments below the smooth, lowermost reflector. It may represent in part the upper bedrock or a highly overconsolidated till, opaque to the 3.5 kHz signal. The sparker resolution is too poor to resolve a thin layer of till. The reflector can be followed under the surge moraine (Fig.19) and seems to outcrop between ridges in the surge zone, where coring has revealed highly overconsolidated, pebble-rich till. Thus, most of unit 5. most likely represents an unresolvably thin and patchy cover of overcompacted till over the sedimentary bedrock.

SEDIMENT COMPOSITION AND PHYSICAL PROPERTIES.

The distribution of cores (Fig.6c) may seem strongly biased towards the surge zone. This results partly from the sea ice conditions during sampling, but also from the fact that many of the stations in the surge zone were considered unsuccessful because the corer failed to penetrate down into the lower, overconsolidated layer (Unit 5). Fig.20 shows the lithostratigraphy of a selection of the cores, arranged along profiles from the present-day ice front and out towards the Erik Eriksenstredet basin. Grain size distribution and physical properties are indicated along the sections to reveal any systematic changes in these parameters either downcore or lateral. Tables 1 and 2 show lithology and physical properties, respectively.

Lithology

In the surge zone, three different lithologies are found. The dominant sediment type, found in most of the cores, is a diamicton with a generally high, but varying content of gravel and larger clasts (Fig.21). There are large and frequent variations in the grain size distribution both downcore and laterally, without any apparent systematic trend.

The second distinct lithology is a clean sand, as seen in the top parts of cores 83-30, 83-31 and 83-26 (Fig.20d,e). These are all well sorted, fining upward sands, with minor content of gravel and mud-sized material. The typical sequence is well exemplified in the uppermost 0.3 m of core 83-26 (Fig.20e) where the silt content decreases while the gravel content increases downcore. As there are only three cores with this lithology, little can be said about the distribution. However, from the generally high number of cores, it is justified to state that the clean sands are relatively restricted in areal extent. Possible mechanisms for formation of the sands include

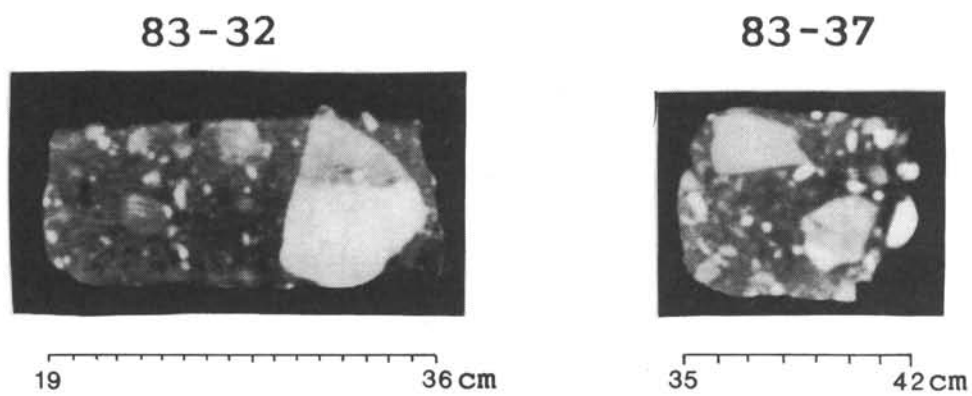


Fig.21. Computer tomographs of two core samples from the surge zone. Note that the highest density have the lightest colour. For location, see Fig.6c.

wave action, currents, iceberg calving -and scouring and glacial meltwater activity. Pfirman (1984) showed that severe storms can disturb and rework sediment down to 150 m water depth in the Barents Sea. However, wave action, as well as currents, would be expected to result in a wider distribution of the sandy sediments (Johnson 1981). Also, during most of the stormy season, the area is covered by sea ice, damping wave action and reducing wind-water coupling. Action of icebergs may stir up sediment and resuspend fines. This may occur during iceberg ploughing, but also from impact of icebergs on the sea floor during the calving process (Powell 1985). The latter would indeed have a local effect. However, it is considered unlikely that such an event could cause 30 cm of well sorted sand within the very short time interval of its duration. This leaves glacial meltwater activity as the most likely mechanism, probably in the form of small, local streams, as also are seen in the area to-day.

The third distinct lithology of the surge zone is even more areally restricted than the clean sand. A greenish fine grained mud is found only in two cores; 83-31 in the interval 0.48 m to 0.85 m, and core 83-32 in the interval 0.58 m to 0.7 m (Fig.20d). The mud is situated between sections of gravel-rich diamictons and is characterized by an olive-gray color (Munsell color 5Y 4/1), only minor amounts of sand-sized and coarser material, abundant foraminifera and a high shear strength. Analyses of the foraminiferal fauna indicates a more ice-distal environment than its present location only 1.5 km from the glacier front (J. Nagy pers. commun. 1985). Based on color, lithology and foraminifera, this material resembles the Holocene muds usually found further out in the Barents Sea (Elverhøi & Solheim 1983), and hence indicates a pre-surge, ice distal origin.

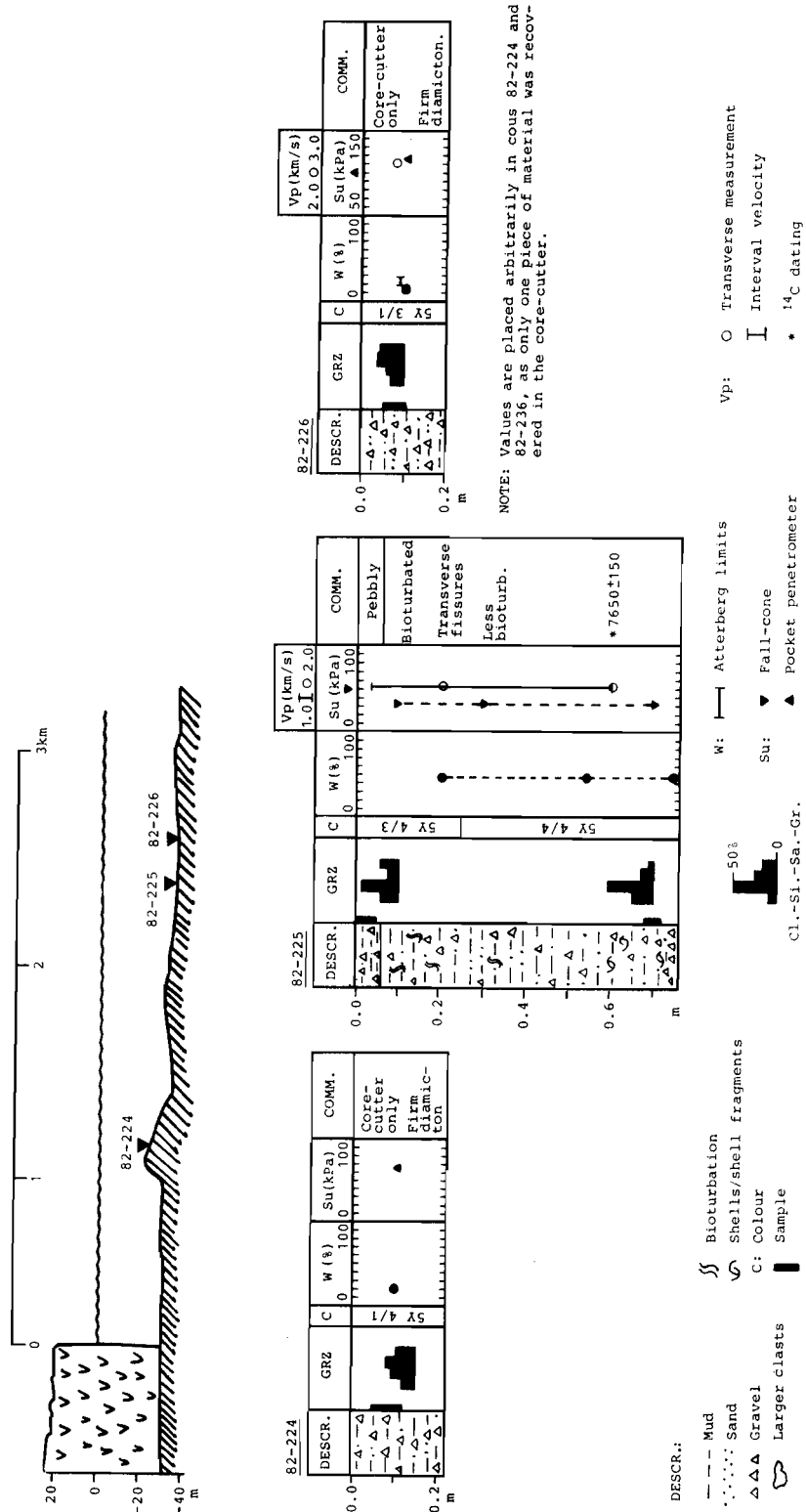
The lithology of the surge moraine (there are only cores from the

Bråsvellbreen moraine) consists essentially of the same relatively homogeneous, gravel-rich diamicton which dominates the surge zone (Fig.21). Although no distinct boundaries exist, there is a tendency for more fine-grained, less gravelly deposits to occur towards the distal parts of the ridge (e.g. cores 82-234 and 82-235 Fig.20d). However, the variation is large, and core 83-29 from the distal part of the outer ridge in the eastern part of the study area, has a gravel content reaching 25-30 %. Intervals of finer grained mud are also found in these deposits (i.e. 82-235, 0.8 m - 0.9 m), but with no corresponding change in other parameters.

In the surge-distal zone, the sediments (acoustic Unit 3) reach a thickness of several meters and consist of a sequence of olive gray mud above darker mud with higher content of dropstones. These sediments most likely represent Holocene mud and Late Weichselian glaciomarine sediment, respectively (Elverhøi & Solheim 1983). The content of coarser material in the Holocene part is relatively high compared to further out in the Barents Sea, as a result of closer proximity to a source area for icebergs throughout the Holocene. The material just outside the Bråsvellbreen surge moraine is clearly more fine grained than the directly surge-affected sediments in the surge zone and the moraine ridge (Fig.20). However, here also the variations are large and frequent. A high content of coarser material is found in the top of some cores (e.g. 82-229, Fig.20c) as well as further downcore (e.g.82-237, Fig.20d). One core (83-39, Fig.20b) 0.5 km outside the end moraine, shows a well sorted, upwards fining sand with lumps of clay in its lower part. According to Powell (1984), this may represent basal debris, most likely released from icebergs.

In summary, the grain size distributions for samples obtained outside the end moraines have stronger tendencies towards the mud fractions than the material in the surge zone and surge moraines

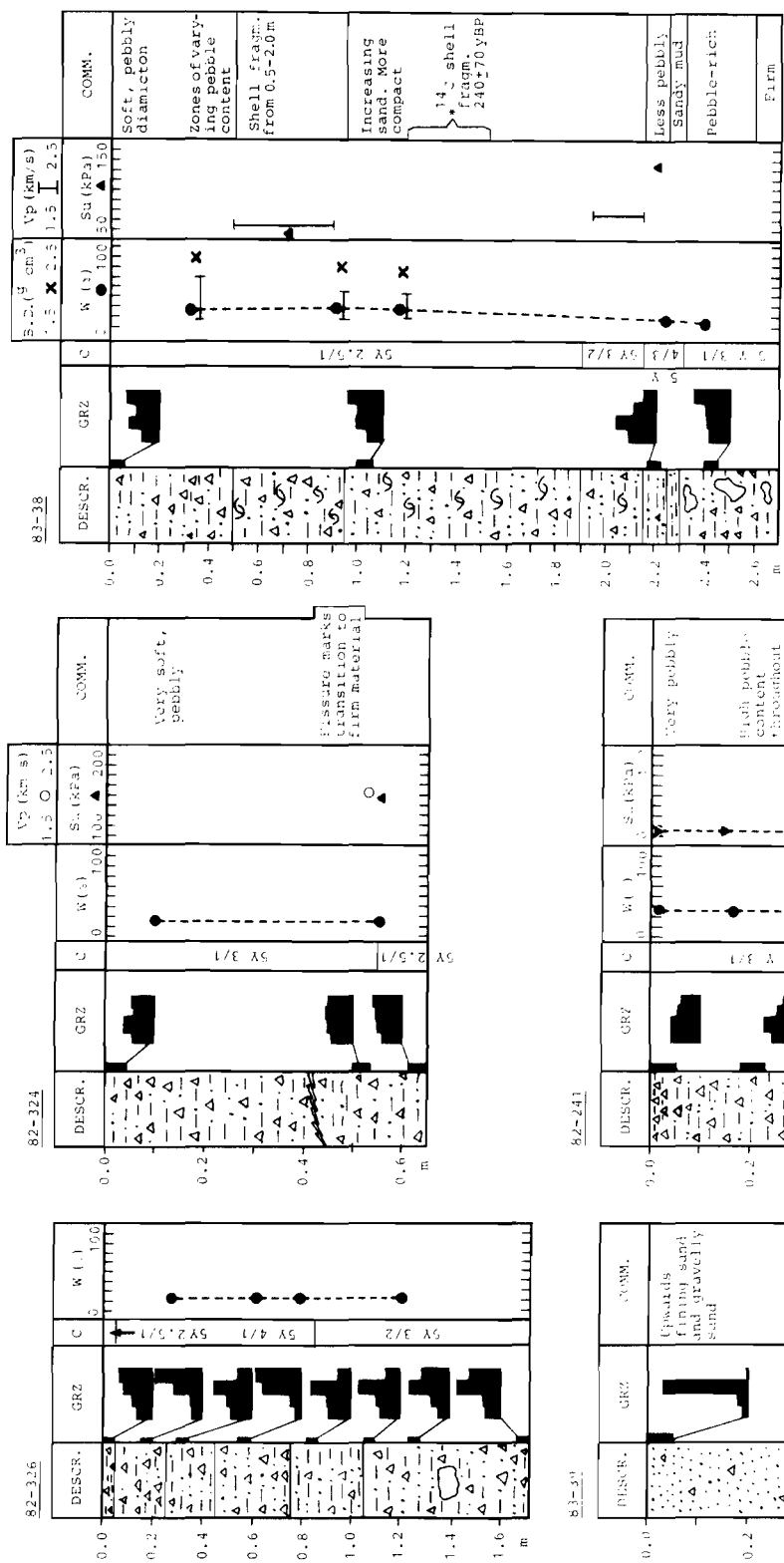
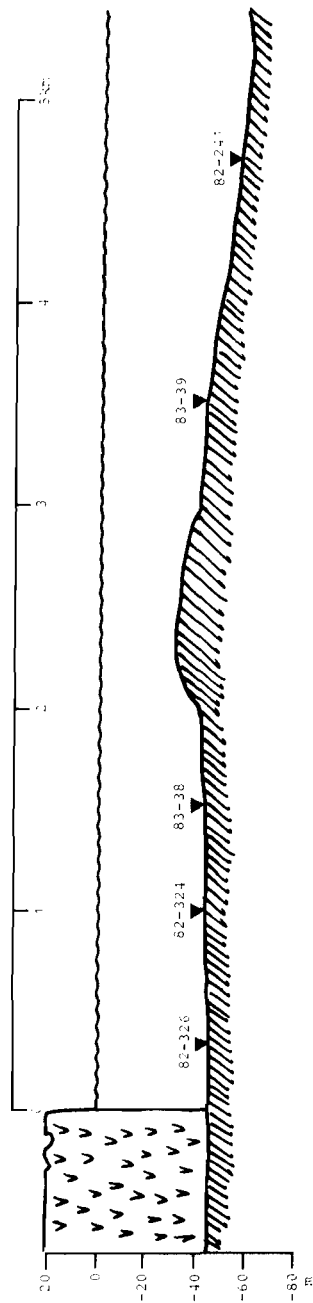
PROFILE P1



NOTE: Values are placed arbitrarily in cores 82-224 and 82-236, as only one piece of material was recovered in the core-cutter.

Fig.20. Sections showing lithology and physical parameters of cores along profiles subperpendicular to the ice front. Note different scales, both down-core and within various parameters. Colour (C) is after Munsell Soil Colour Charts. Water content (W) is in % dry weight. Vp is compressional velocity, Su undrained shear strength and BD wet bulk density. For location of cores, see Fig.6.

PROFILE P2



For legend, see PROFILE P1

Fig.20B.

PROFILE P3

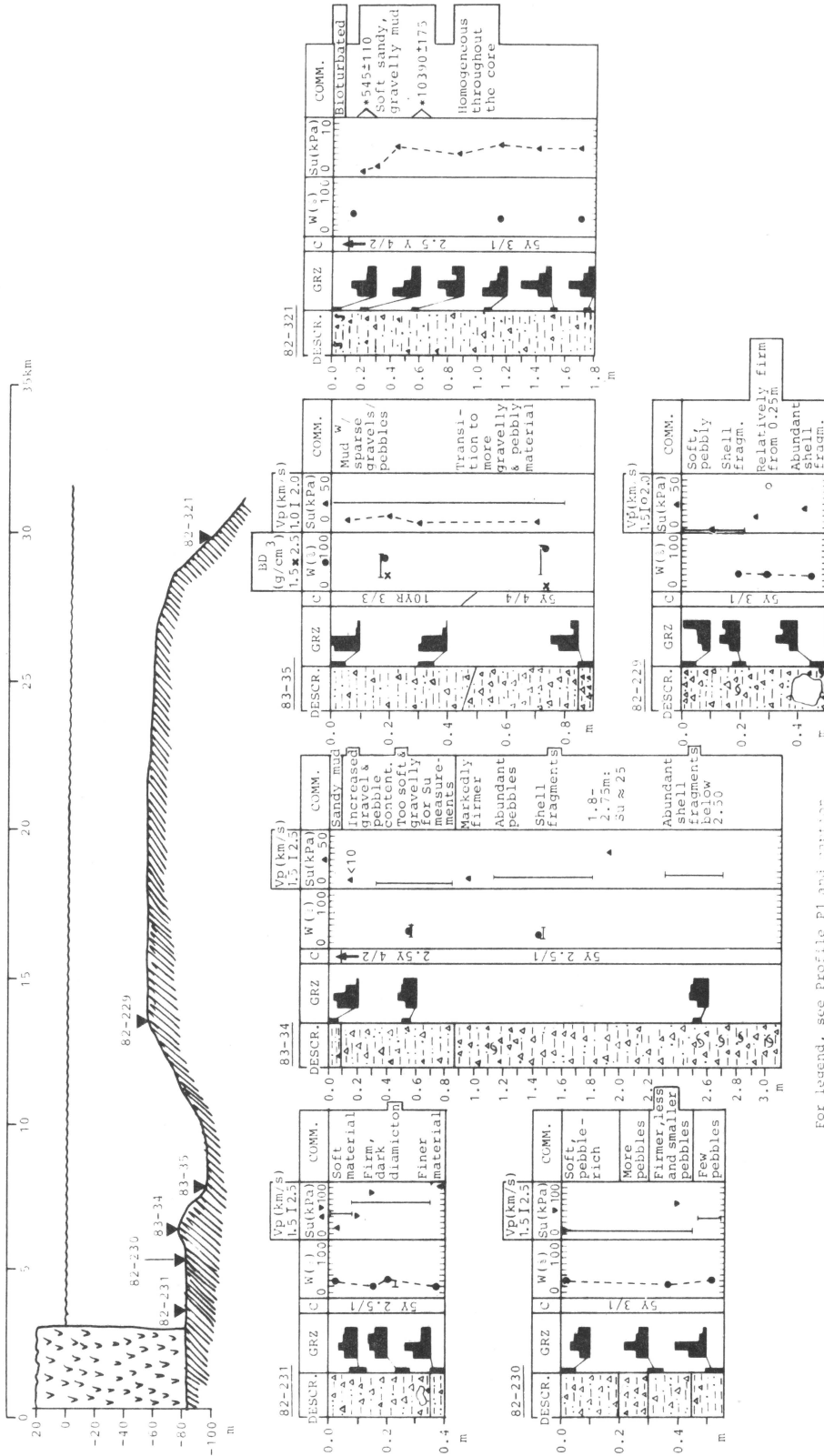
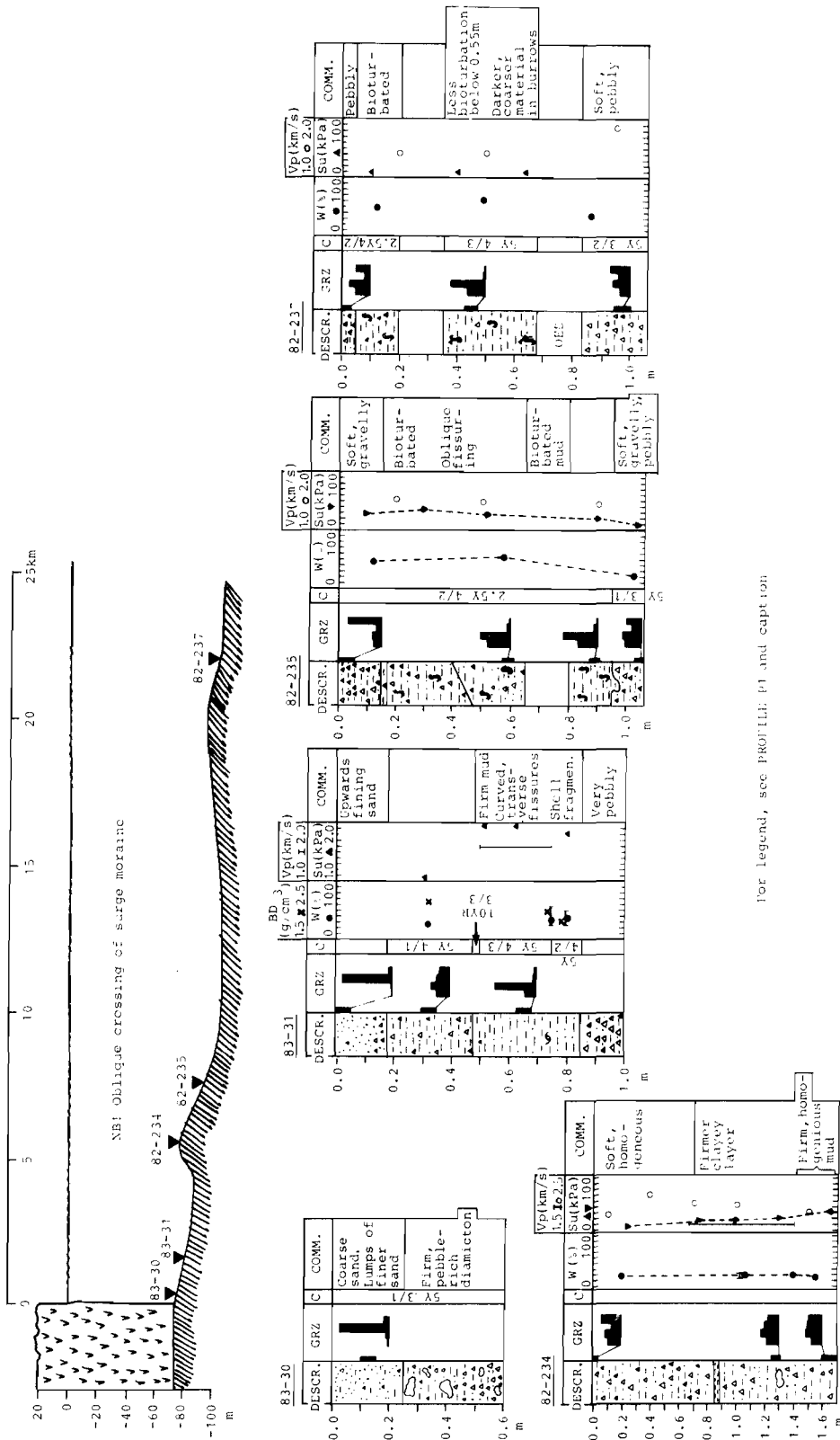


Fig.20C.

For legend, see Profile P1 and caption.

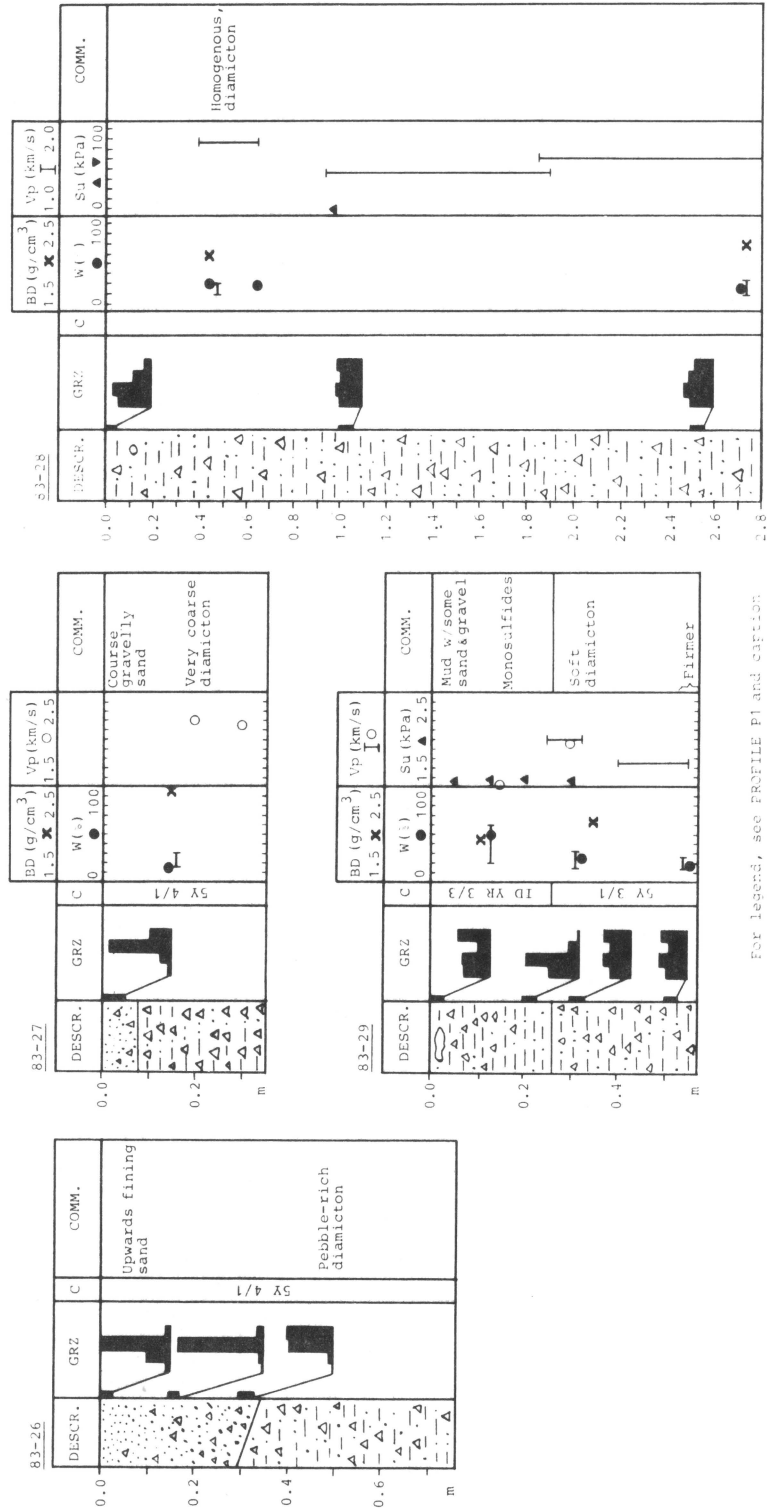
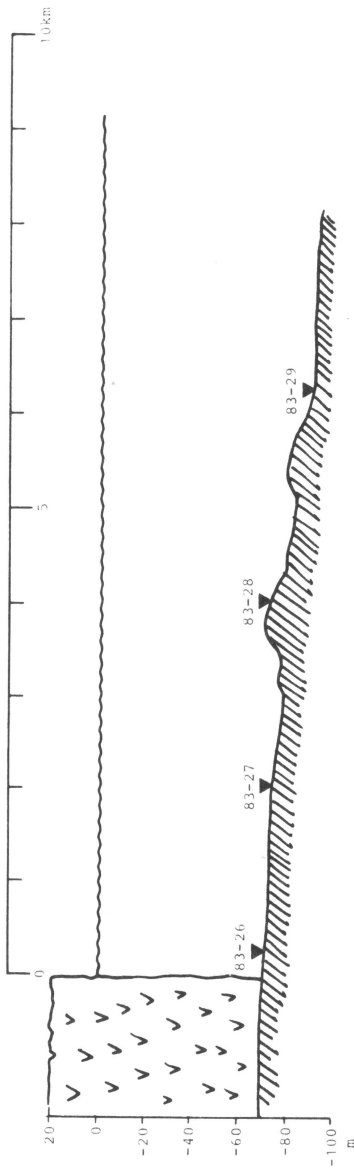
PROFILE P4



For legend, see PROFILE P1 and caption

Fig.20D.

PROFILE P5



For legends, see PROFILE P1 and caption

Fig.20E.

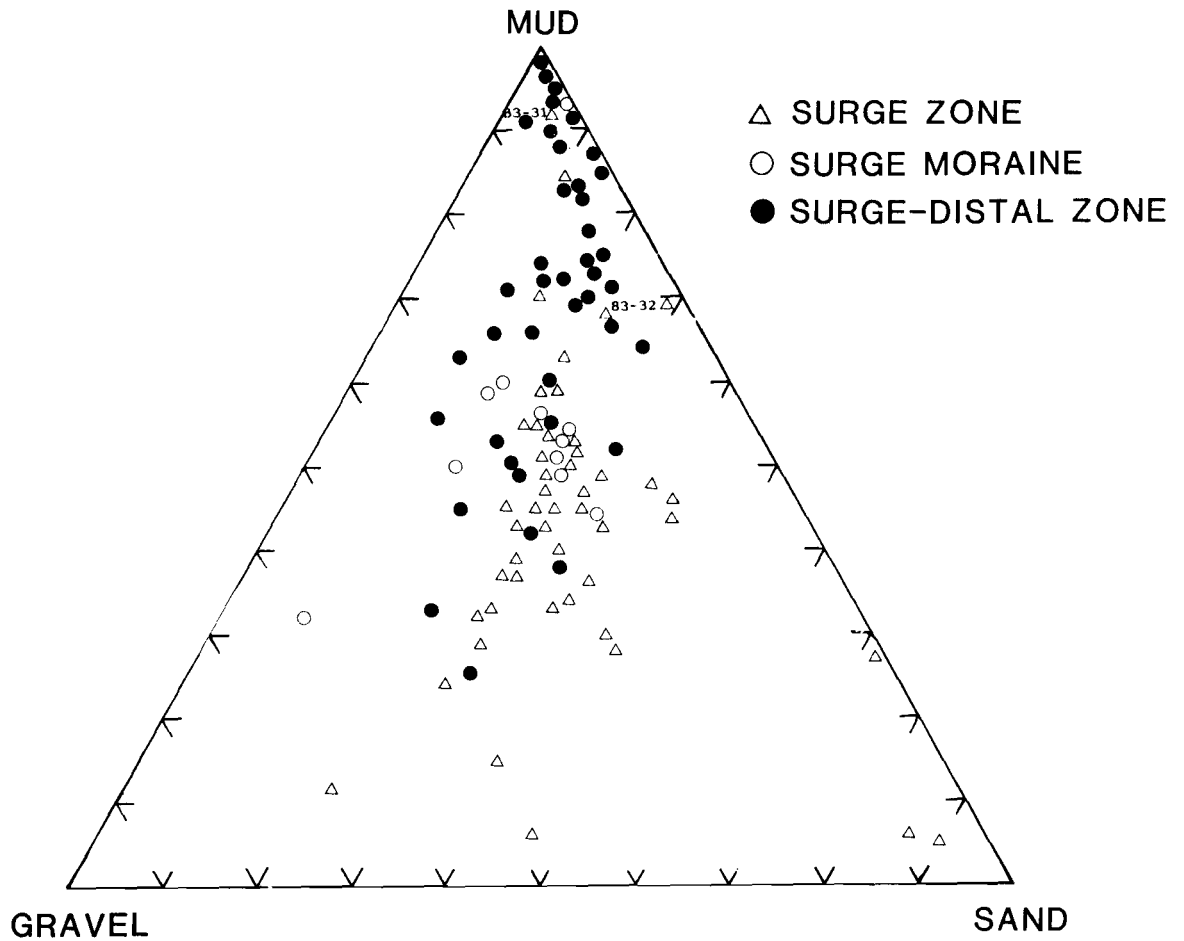


Fig.22. Ternary diagram showing relative amounts of mud, sand and gravel in samples from the surge zone, surge moraine and surge-distal zone off Bråsvellbreen.

Table 1. Grain size distributions.

| STATION | WATER DEPTH (m) | LEVEL (cm) | CLAY | SILT | SAND | GRAVEL | >16mm |
|----------|--------------------|---------------|---------------|------|------|--------|--------|
| | | | ----- % ----- | | | | (g) |
| 81-136,1 | 109 | 0-5 | 21 | 40 | 10 | 27 | 136,7 |
| | | 47-50 | 26 | 67 | 7 | 1 | 0,0 |
| | | 90-93 | 52 | 48 | 1 | 0 | 0,0 |
| 81-137,1 | 112 | 59-62 | 37 | 45 | 13 | 5 | 0,0 |
| | | 70-75 | 18 | 22 | 28 | 30 | 5,25 |
| 81-137,3 | 112 | 42-47 | 34 | 62 | 4 | 1 | 0,0 |
| | | 50-55 | 10 | 14 | 31 | 45 | 38,0 |
| 81-138,1 | 107 | 20-23 | 22 | 36 | 22 | 19 | 0,0 |
| | | 54-57 | 18 | 33 | 26 | 23 | 4,4 |
| | | 82-85 | 19 | 34 | 22 | 22 | 0,0 |
| 81-138,3 | 107 | 95-97 | 18 | 35 | 26 | 21 | 0,0 |
| 81-140,1 | 86 | 16-19 | 21 | 34 | 22 | 23 | 12,0 |
| 81-186 | 320 | 45-50 | 57 | 43 | 1 | 0 | 0,0 |
| | | 107-110 | 2 | 6 | 90 | 0 | 0,0 |
| | | 120-125 | 24 | 31 | 42 | 3 | 0,0 |
| | | 135-140 | 13 | 25 | 60 | 1 | 0,0 |
| | | 150-153 | 24 | 26 | 48 | 3 | 0,0 |
| 81-216,1 | 81 | 0-3 | 10 | 24 | 36 | 30 | 18,1 |
| | | 3-6 | 11 | 25 | 37 | 27 | 13,0 |
| | | 30-33 | 9 | 35 | 35 | 22 | 42,5 |
| | | 37-40 | 16 | 35 | 25 | 24 | 24,85 |
| 82-224 | 26 | 0-20 | 15 | 28 | 34 | 22 | 0,0 |
| 82-225,2 | 36 | 0-5 | 22 | 43 | 12 | 22 | 150,35 |
| | | 68-72 | 25 | 53 | 16 | 6 | 0,0 |
| 82-226 | 36 | 0-20 | 17 | 21 | 33 | 29 | 0,0 |
| 82-229,1 | 56 | 0-5 | 13 | 20 | 22 | 45 | 7,2 |
| | | 18-22 | 16 | 33 | 22 | 28 | 12,9 |
| | | 40-50 | 14 | 36 | 23 | 28 | 29,45 |
| 82-230,2 | 71 | 0-5 | 18 | 34 | 28 | 20 | 0,0 |
| | | 30-35 | 22 | 42 | 21 | 16 | 0,0 |
| | | 50-55 | 30 | 53 | 11 | 5 | 0,0 |
| 82-231 | 83 | 8-13 | 22 | 32 | 24 | 22 | 32,0 |
| | | 23-28 | 20 | 29 | 32 | 19 | 30,44 |
| | | 30-35 | 28 | 43 | 15 | 15 | 0,0 |
| 82-232,2 | 82 | 0-5 | 14 | 25 | 32 | 28 | 0,0 |
| | | 35-40 | 20 | 34 | 27 | 20 | 0,0 |
| 82-233,1 | 97 | 0-3 | 12 | 17 | 29 | 42 | 0,0 |

Table 1. contd.

| STATION | WATER DEPTH (m) | LEVEL (cm) | CLAY | SILT | SAND | GRAVEL | >16mm |
|----------|--------------------|---------------|---------------|------|------|--------|-------|
| | | | ----- % ----- | | | | (g) |
| 82-234.1 | 83 | 0-3 | 23 | 28 | 16 | 34 | 35.43 |
| | | 125-130 | 22 | 32 | 26 | 20 | 15.57 |
| | | 160-168 | 20 | 29 | 27 | 24 | 0.0 |
| 82-234.2 | 83 | 0-5 | 22 | 36 | 16 | 24 | 3.29 |
| | | 100-103 | 21 | 31 | 25 | 24 | 9.95 |
| 82-235.1 | 106 | 0-5 | 15 | 17 | 9 | 59 | 68.0 |
| | | 57-61 | 40 | 53 | 6 | 1 | 0.0 |
| | | 87-90 | 34 | 59 | 6 | 0 | 0.0 |
| | | 103-107 | 27 | 32 | 15 | 26 | 38.09 |
| 82-237 | 106 | 0-3 | 26 | 37 | 10 | 27 | 0.0 |
| | | 43-47 | 32 | 63 | 4 | 1 | 0.0 |
| | | 95-100 | 17 | 30 | 19 | 36 | 28.5 |
| 82-239.1 | 81 | 0-5 | 27 | 32 | 21 | 20 | 0.0 |
| | | 30-35 | 22 | 36 | 22 | 19 | 5.0 |
| 82-239.2 | 81 | 25-30 | 14 | 20 | 35 | 32 | 15.32 |
| 82-241.1 | 56 | 0-5 | 29 | 29 | 21 | 19 | 25.0 |
| | | 18-23 | 28 | 35 | 21 | 16 | 0.0 |
| 82-321 | 99 | 0-5 | 31 | 41 | 14 | 14 | 0.0 |
| | | 20-23 | 45 | 27 | 13 | 13 | 0.0 |
| | | 55-58 | 28 | 44 | 11 | 18 | 0.0 |
| | | 105-108 | 42 | 28 | 16 | 12 | 0.0 |
| | | 150-153 | 22 | 50 | 19 | 8 | 40.18 |
| | | 173-176 | 25 | 44 | 19 | 12 | 35.73 |
| 82-323.1 | 39 | 0-4 | 14 | 18 | 28 | 40 | 8.32 |
| | | 22-26 | 15 | 22 | 28 | 35 | 21.04 |
| | | 63-68 | 20 | 26 | 31 | 22 | 18.22 |
| | | 86-94 | 20 | 25 | 24 | 31 | 0.0 |
| | | 95-100 | 20 | 23 | 29 | 28 | 17.3 |
| 82-323.2 | 39 | 0-5 | 29 | 40 | 29 | 2 | 0.0 |
| | | 58-62 | 20 | 25 | 32 | 23 | 0.0 |
| | | 90-95 | 21 | 24 | 29 | 26 | 0.0 |
| | | 98-103 | 20 | 30 | 27 | 24 | 0.0 |
| 82-324.1 | 43 | 0-4 | 23 | 32 | 21 | 24 | 0.0 |
| | | 50-53 | 22 | 25 | 27 | 26 | 6.73 |
| | | 58-63 | 21 | 24 | 27 | 28 | 19.1 |
| 82-326.1 | 45 | 0-3 | 16 | 21 | 29 | 34 | 0.0 |
| | | 15-18 | 11 | 12 | 28 | 48 | 12.28 |
| | | 30-33 | 22 | 26 | 38 | 14 | 5.65 |
| | | 55-58 | 6 | 10 | 38 | 47 | 9.8 |
| | | 83-86 | 23 | 24 | 41 | 13 | 0.0 |
| | | 105-109 | 20 | 24 | 42 | 14 | 6.3 |
| | | 124-128 | 12 | 18 | 42 | 28 | 0.0 |
| | | 167-172 | 14 | 15 | 44 | 28 | 0.0 |

Table 1. contd.

| STATION | WATER DEPTH(m) | LEVEL (cm) | CLAY ----- | SILT % | SAND ----- | GRAVEL | >16mm (g) |
|----------|-------------------|---------------|---------------|-----------|---------------|--------|--------------|
| 82-327,1 | 44 | 0-5 | 22 | 27 | 28 | 22 | 2,9 |
| | | 31-36 | 18 | 21 | 28 | 33 | 47,3 |
| | | 39-42 | 17 | 26 | 26 | 31 | 0,0 |
| | | 45-48 | 14 | 19 | 28 | 39 | 8,5 |
| 83-26 | 70 | 0-3 | 3 | 24 | 72 | 1 | 0,0 |
| | | 15-17 | 1 | 3 | 90 | 5 | 0,0 |
| | | 30-33 | 1 | 3 | 46 | 48 | 0,0 |
| | | 60-65 | 19 | 24 | 25 | 33 | 35,68 |
| 83-27 | 75 | 0-5 | 2 | 11 | 66 | 22 | 0,0 |
| 83-28 | 73 | 0-5 | 34 | 41 | 19 | 7 | 29,29 |
| | | 100-105 | 23 | 27 | 23 | 26 | 0,0 |
| | | 250-255 | 24 | 31 | 26 | 19 | 5,67 |
| 83-29 | 91 | 0-6 | 28 | 29 | 11 | 33 | 0,0 |
| | | 40-45 | 32 | 56 | 12 | 1 | 0,0 |
| | | 60-65 | 22 | 28 | 22 | 28 | 0,0 |
| | | 100-105 | 23 | 29 | 19 | 28 | 42,45 |
| 83-30 | 76 | 10-15 | 2 | 5 | 86 | 8 | 0,0 |
| 83-31 | 92 | 0-5 | 2 | 3 | 88 | 7 | 0,0 |
| | | 30-35 | 24 | 33 | 24 | 19 | 11,49 |
| | | 50-80 | 20 | 72 | 5 | 3 | 0,0 |
| 83-32 | 54 | 65-70 | 27 | 41 | 23 | 9 | 0,0 |
| 83-34 | 78 | 0-5 | 34 | 42 | 21 | 3 | 0,0 |
| | | 50-55 | 19 | 32 | 26 | 22 | 10,54 |
| | | 250-255 | 17 | 30 | 29 | 24 | 0,0 |
| 83-35 | 96 | 0-5 | 43 | 47 | 6 | 4 | 0,0 |
| | | 22-27 | 48 | 44 | 7 | 2 | 0,0 |
| | | 85-90 | 34 | 46 | 7 | 13 | 9,26 |
| 83-38 | 42 | 0-5 | 17 | 30 | 22 | 32 | 82,92 |
| | | 100-105 | 16 | 25 | 23 | 35 | 0,0 |
| | | 217-222 | 26 | 40 | 22 | 11 | 5,24 |
| | | 240-245 | 19 | 22 | 23 | 37 | 0,0 |
| 83-39 | 43 | 0-5 | 4 | 9 | 86 | 2 | 0,0 |
| | | 60-65 | ----- | | 16 | 84 | 14,67 |
| 84-11 | 225 | 0-5 | 57 | 31 | 8 | 4 | 0,0 |
| | | 20-25 | 51 | 34 | 14 | 1 | 0,0 |
| | | 33-36 | 36 | 39 | 19 | 6 | 0,0 |
| 84-13 | 248 | 0-4 | 59 | 40 | 1 | 0 | 0,0 |
| | | 10-13 | 63 | 34 | 2 | 1 | 0,0 |
| | | 30-33 | 32 | 42 | 18 | 8 | 0,0 |
| | | 45-48 | 60 | 35 | 4 | 1 | 0,0 |
| | | 51-54 | 42 | 31 | 18 | 8 | 0,0 |
| | | 61-64 | 30 | 41 | 22 | 7 | 0,0 |

Table 1. contd.

| STATION | WATER DEPTH(m) | LEVEL (cm) | CLAY | SILT | SAND | GRAVEL | >16mm |
|---------|-------------------|---------------|---------------|------|------|--------|-------|
| | | | ----- % ----- | | | | (g) |
| 85-26 | 153 | 0-4 | 49 | 47 | 3 | 1 | 0.0 |
| | | 10-13 | 55 | 41 | 3 | 1 | 0.0 |
| | | 20-25 | 54 | 36 | 6 | 4 | 0.0 |
| | | 33-36 | 66 | 24 | 3 | 6 | 0.0 |
| | | 46-50 | 54 | 30 | 12 | 5 | 0.0 |
| | | 60-63 | 27 | 40 | 24 | 9 | 0.0 |
| | | 80-85 | 23 | 29 | 32 | 16 | 0.0 |
| | | 120-123 | 29 | 35 | 29 | 7 | 0.0 |
| 85-28 | 218 | 0-4 | 61 | 35 | 4 | 0 | 0.0 |
| | | 15-18 | 51 | 42 | 5 | 2 | 0.0 |
| | | 40-44 | 36 | 34 | 20 | 10 | 0.0 |
| 85-29 | 157 | 0-3 | 51 | 32 | 11 | 6 | 0.0 |
| | | 18-22 | 54 | 41 | 4 | 0 | 0.0 |
| | | 33-37 | 52 | 46 | 1 | 0 | 0.0 |
| | | 60-64 | 53 | 40 | 6 | 1 | 0.0 |
| | | 80-85 | 21 | 34 | 23 | 22 | 0.0 |
| | | 100-105 | 26 | 31 | 16 | 28 | 0.0 |

(Fig.21), but the variation is also larger in the former zone. This most likely results from the wider range of depositional environments spanned by this zone, which include the shallow Hinlopenstredet threshold, where probably no or very little sedimentation took place during the Holocene, and the Erik Erikstenstredet basin with depths of more than 200 m and apparently continuous mud deposition. Furthermore, as the side scan sonar records indicate sediment waves and pockmarks, the Erik Erikstenstredet basin sediments are affected by both bottom currents and gas seepage, both of which may cause depletion of fines. However, lithologies that can be related to these processes were not sampled during this study.

Physical properties

Although large amounts of geotechnical information exist from many high latitude continental shelf areas, relatively little has been done to synthesize the information and to relate variations to different environments. Most work carried out on high latitude surficial sediments covers relatively soft mud and sand (Clukey et al. 1978, Richards et al. 1975, Schwab & Lee 1983). Marine diamictons are still poorly understood geotechnically (Bennett & Nelsen 1983). To the author's knowledge, nothing has been published on geotechnical parameters in modern surge-affected basins. In the following, the different physical characteristics of Erik Erikstenstredet sediments and their variations are discussed, both as a contribution to the general knowledge of diamictons, but also, and more important, to investigate whether any of the measured values or their variations can be related to glacier oscillations.

Undrained shear strength shows large variations in the surge zone diamictons, both laterally and downcore. The soft, acoustically

c. In the surge-distal zone.

| STA | LE | Dw | Su | BD | Vp | TC | TOC | GR | SA | SI | CL | MED | W1 | W2 | Wl | Wp | PI | IMP |
|----------|-----|-----|-------|------|------|-----|------|----|----|----|----|------|----|----|------|------|------|------|
| 81-137.1 | 8 | 112 | 4.0 | | | | | | | | | | | | | | | |
| 81-137.1 | 30 | 112 | 15.0 | | | | | | | | | | 46 | | | | | |
| 81-137.1 | 60 | 112 | | | | | | 5 | 13 | 45 | 37 | 7.3 | | | | | | |
| 81-137.1 | 72 | 112 | | | | | | 30 | 28 | 22 | 18 | 3.0 | 63 | | | | | |
| 81-137.1 | 117 | 112 | | | | | | | | | | | 17 | | | | | |
| 81-137.3 | 10 | 112 | 8.0 | | | | | | | | | | | | | | | |
| 81-137.3 | 30 | 112 | 14.0 | | | | | | | | | | 50 | 52 | | | | |
| 81-137.3 | 45 | 112 | 19.0 | | | | | 1 | 4 | 62 | 34 | 7.1 | | | | | | |
| 81-137.3 | 52 | 112 | | | | | | 45 | 31 | 14 | 10 | -0.6 | | | | | | |
| 81-137.3 | 65 | 112 | | | | | | | | | | | 15 | 28 | | | | |
| 82-225.2 | 20 | 34 | 30.0 | | 1500 | | | | | | | | 46 | | | | | |
| 82-225.2 | 60 | 34 | | | 1506 | 4.7 | 1.70 | | | | | | 42 | | | | | |
| 82-225.2 | 70 | 34 | 31.0 | | | | | 5 | 17 | 53 | 25 | 7.0 | 45 | | | | | |
| 82-226 | 10 | 27 | 110.0 | | 2600 | 6.4 | 0.54 | 28 | 34 | 21 | 17 | 1.8 | 16 | | 26.0 | 17.7 | 8.3 | |
| 82-229.1 | 20 | 51 | 5.0 | | 1500 | 3.3 | 1.01 | 28 | 22 | 33 | 16 | 3.8 | 27 | | | | | |
| 82-229.1 | 30 | 51 | 25.0 | | 2290 | | | | | | | | 23 | 29 | | | | |
| 82-229.1 | 45 | 51 | 38.0 | | | 3.1 | 0.99 | 28 | 23 | 36 | 12 | 3.7 | 24 | 25 | | | | |
| 82-237 | 2 | 101 | | | | 4.6 | 0.89 | 27 | 10 | 37 | 26 | 6.3 | 53 | | | | | |
| 82-237 | 12 | 101 | 7.0 | | | | | | | | | | 47 | 49 | | | | |
| 82-237 | 45 | 101 | 7.0 | | | 4.0 | 2.00 | 1 | 4 | 63 | 32 | 7.2 | 62 | 62 | | | | |
| 82-237 | 95 | 101 | | | 1830 | 2.5 | 0.80 | 36 | 19 | 30 | 17 | 2.0 | 21 | 34 | | | | |
| 82-241.1 | 3 | 53 | 12.0 | | | | | 19 | 21 | 29 | 29 | 5.5 | 35 | | | | | |
| 82-241.1 | 20 | 53 | 15.0 | | | | | 16 | 21 | 35 | 28 | 6.0 | 26 | 34 | 37.4 | 20.7 | 16.7 | |
| 82-241.1 | 45 | 53 | 12.0 | | | | | | | | | | 32 | | | | | |
| 82-317.1 | 14 | 142 | 3.9 | | | | | | | | | | 65 | 65 | | | | |
| 82-317.1 | 33 | 142 | 2.0 | | | | | | | | | | | | | | | |
| 82-317.1 | 55 | 142 | 2.3 | | | | | | | | | | | | | | | |
| 82-217.1 | 63 | 142 | 2.2 | | | | | | | | | | 36 | 39 | | | | |
| 82-317.1 | 98 | 142 | 4.7 | | | | | | | | | | 33 | 33 | | | | |
| 82-317.1 | 103 | 142 | 3.2 | | | | | | | | | | | | | | | |
| 82-317.2 | 10 | 142 | 6.7 | | | | | | | | | | 57 | 57 | | | | |
| 82-317.2 | 27 | 142 | 2.5 | | | | | | | | | | | | | | | |
| 82-317.2 | 63 | 142 | 4.0 | | | | | | | | | | 31 | 32 | | | | |
| 82-317.2 | 100 | 142 | 3.4 | | | | | | | | | | 30 | 30 | | | | |
| 82-319.2 | 12 | 215 | 4.9 | | | | | | | | | | 70 | 70 | | | | |
| 82-319.2 | 40 | 215 | 3.5 | | | | | | | | | | | | | | | |
| 82-319.2 | 50 | 215 | 3.8 | | | | | | | | | | 74 | 74 | | | | |
| 82-319.2 | 60 | 215 | 3.1 | | | | | | | | | | | | | | | |
| 82-319.2 | 76 | 215 | 0.9 | | | | | | | | | | 43 | 50 | | | | |
| 82-319.2 | 100 | 215 | 1.4 | | | | | | | | | | | | | | | |
| 82-319.2 | 133 | 215 | 2.0 | | | | | | | | | | 30 | 35 | | | | |
| 82-319.2 | 158 | 215 | 3.1 | | | | | | | | | | 30 | 35 | | | | |
| 82-321.1 | 16 | 100 | 0.9 | | | | | 13 | 13 | 27 | 45 | 7.9 | 34 | 39 | | | | |
| 82-321.1 | 30 | 100 | 1.6 | | | | | | | | | | | | | | | |
| 82-321.1 | 45 | 100 | 5.1 | | | | | 18 | 11 | 44 | 28 | 6.6 | | | | | | |
| 82-321.1 | 85 | 100 | 3.8 | | | | | | | | | | | | | | | |
| 82-321.1 | 115 | 100 | 5.5 | | | | | 12 | 16 | 28 | 42 | 8.3 | 25 | 30 | | | | |
| 82-321.1 | 140 | 100 | 4.7 | | | | | 8 | 19 | 50 | 22 | 6.2 | | | | | | |
| 82-321.1 | 170 | 100 | 4.7 | | | | | 12 | 19 | 44 | 25 | 6.3 | 24 | 30 | | | | |
| 82-321.2 | 15 | 100 | 6.3 | | | | | | | | | | 50 | 52 | | | | |
| 82-321.2 | 35 | 100 | 6.9 | | 1481 | | | | | | | | 24 | 30 | | | | |
| 83-29 | 10 | 91 | 6.9 | | | | | | | | | | | | | | | |
| 83-29 | 25 | 91 | 7.2 | 1.96 | 1470 | | | | | | | | 49 | 51 | 57.7 | 22.8 | 34.9 | 2.88 |
| 83-29 | 40 | 91 | 7.8 | | | | | 1 | 12 | 56 | 32 | 7.1 | | | | | | |
| 83-29 | 60 | 91 | 4.4 | 2.14 | 2000 | | | 28 | 22 | 28 | 22 | 3.8 | 16 | 26 | 32.0 | 15.1 | 16.9 | 4.28 |

| STA | LE | Dw | Su | BD | Vp | TC | TOC | GR | SA | SI | CL | MED | W1 | W2 | W1 | Wp | PI | IMP |
|-------|-----|----|------|------|------|----|-----|----|----|----|----|-----|----|----|------|------|------|------|
| 83-29 | 110 | 91 | | | 1504 | | | 28 | 19 | 29 | 23 | 4.5 | 12 | 17 | 27.2 | 15.3 | 11.9 | |
| 83-29 | 90 | 91 | | | 1750 | | | | | | | | | | | | | |
| 83-29 | 110 | 91 | | | 2160 | | | | | | | | | | | | | |
| 83-35 | 10 | 96 | 10.0 | 1.74 | | | | | | | | | 53 | 55 | 63.3 | 23.9 | 39.4 | 2.62 |
| 83-35 | 20 | 96 | 12.5 | | | | | | | | | | | | | | | |
| 83-35 | 30 | 96 | 8.0 | | | | | 2 | 7 | 44 | 48 | 8.7 | | | | | | |
| 83-35 | 73 | 96 | 9.0 | | 1504 | | | | | | | | 73 | | 77.0 | 28.2 | 48.8 | 2.41 |

Legend.

STA Station nr.
 LE Level in core
 Dw Water depth (m)
 Su Undrained shear strength (kPa)
 BD Bulk density (g/cm³)
 TC Total carbon (%)
 TOC Total organic carbon (%)
 GR Gravel (%)
 SA Sand (%)
 SI Silt (%)
 CL Clay (%)
 MED Median diameter (phi)
 W1 Water content, uncorrected
 W2 Water content, corrected for fractions >0.5 mm
 W1 Liquid limit (%)
 Wp Plastic limit (%)
 PI Plasticity index (%)
 IMP Acoustic impedance (10⁶ kg/m² s)

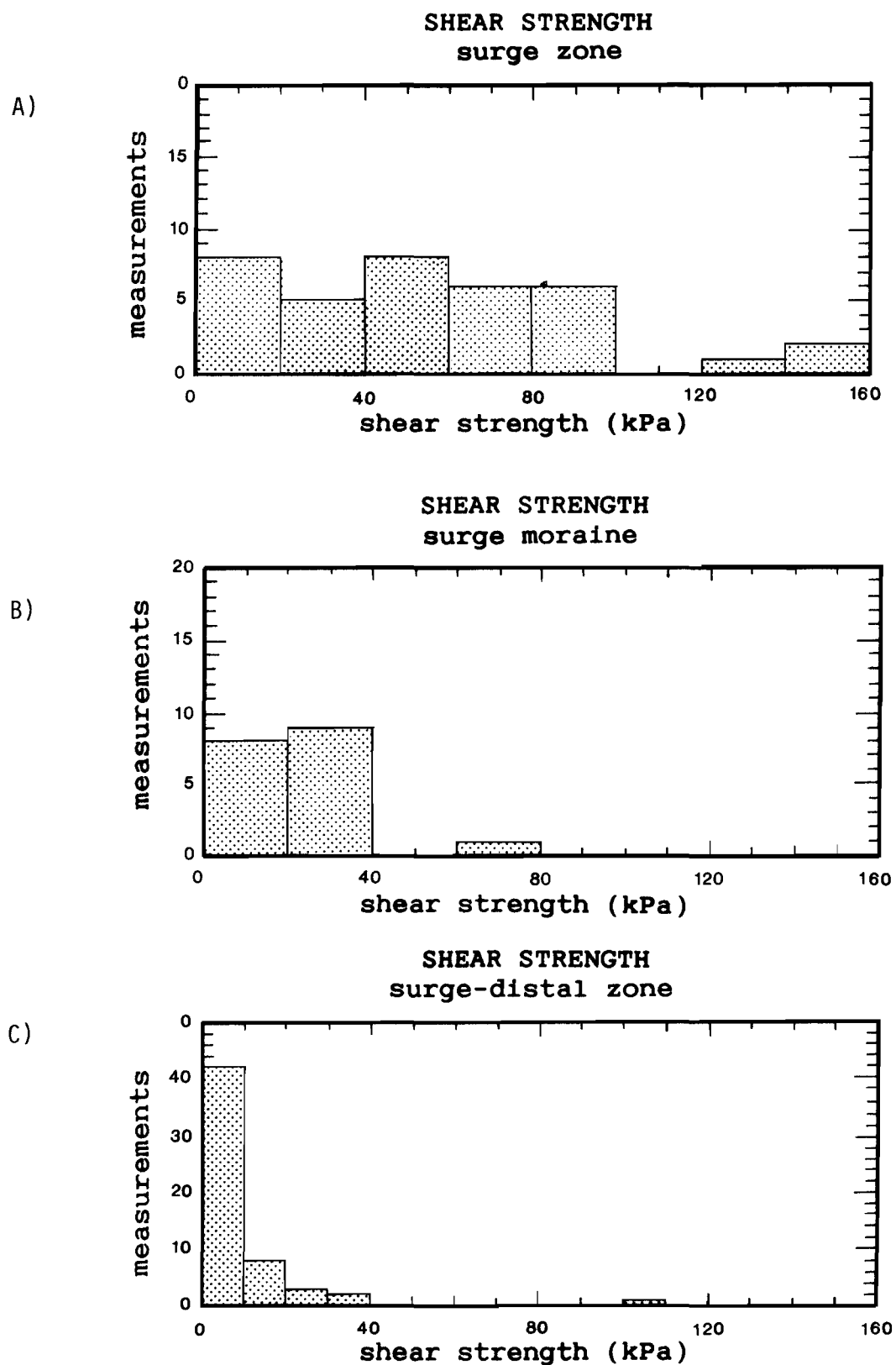


Fig.23. Frequency histograms of undrained shear strength of Bråsvellbreen (pocket penetrometer and fall-cone) a) in the surge zone, b) on the surge moraine and c) outside the surge moraine.

transparent top material usually has an undrained shear strength of less than 30 kPa, but values less than 5 kPa have also been measured. Values are most likely overestimated because of a generally high sand content, but nevertheless, they give an indication of degree of consolidation. In general there is a downcore increase, from the soft top material, through an intermediate zone, and in some cores to a stiff material with values in excess of 100 kPa. The bulk of the material, however plots in the intermediate range, with values between 30 and 100 kPa. A frequency histogram plot (Fig.23a) shows the soft surface material below 20 kPa, the intermediately compacted material between 20 and 100 kPa and the lower, hard till between 120 and 160 kPa. Variations within each level follows no systematic trend, and changes are usually not connected to lithological changes. Exceptions to this are the intervals of fine grained mud in cores 83-31 and 83-32 (Fig.20d and Table 2). In particular 83-31, 50-85 cm, shows a distinct increase in shear strength, from less than 10 kPa in the diamicton above the compacted mud, to 100 kPa at the 55 cm level. The values decrease to 80 kPa near the bottom of the muddy section. The difference is not as distinct in 83-32, where the values increase from 40-60 kPa in the diamictons above, to 80 kPa within the mud (Table 2).

The surge moraine diamictons show less varied and generally lower shear strengths than in the surge zone. All measurements except one fall below 40 kPa (Fig.23b and Table 2), and the majority is below 25 kPa. In one core (82-234,1) (Fig.20d), there is a marked increase downcore, but generally no such trend can be identified. However, due to poor sample quality and the relatively few cores from the surge moraine proper, the number of shear strength measurements from this region is sparse, and cannot be considered statistically significant.

Shear strengths below 10 kPa (Fig.23c & Table 2) reflect the

generally soft, muddy character of the Erik Erikstenstredet sediments outside the surge moraines. One sample (82-226) was strongly overconsolidated, with a shear strength of 110 kPa. This is in the westernmost part of the study area, where the cover of soft sediments above the assumed Late Weichselian till is thin or non-existent. Material was only obtained in the core cutter and catcher and most likely represents the till.

Bulk density was measured only on 1983 samples. The values vary between 1.74 g/cm^3 and 2.47 g/cm^3 (Fig.24 & Table 2). Most of the measurements were done on surge zone samples, with only four and three values for each of the other two zones. However, the values reflect to a great extent the lithology and water content. Much of the variation results from the unsorted character of the diamictons. The highest values were obtained in the compacted surge zone diamictons, while the lowest are found in the soft surge-distal muds. The four values from the surge moraine ridge are relatively high, $2.07 - 2.17 \text{ g/cm}^3$, which result from the generally gravelly lithology of the ridge sediment. Within the surge zone, the lowest bulk densities are found in the compacted fine grained mud sections of cores 83-31 and 83-32, despite the overconsolidated character of these samples.

The water content of the surge zone material generally falls below 30 % (Fig.25). Correcting for fractions $>0.5 \text{ mm}$ shifts the peak by 5-10 %, but values are still low (Table 2). The uncorrected values are used in the subsequent discussions. The low values, also for the soft surge zone diamictons, indicate that compaction rarely reduces water content with more than 10 %. Again, the compacted mud sections of cores 83-31 and 83-32 appear slightly anomalous. The three values measured on this material are the highest in the surge zone (Fig.20d & Table 2), while the sediment obviously is overcompacted.

With the exception of core 82-235 (Fig.20d), the water content of

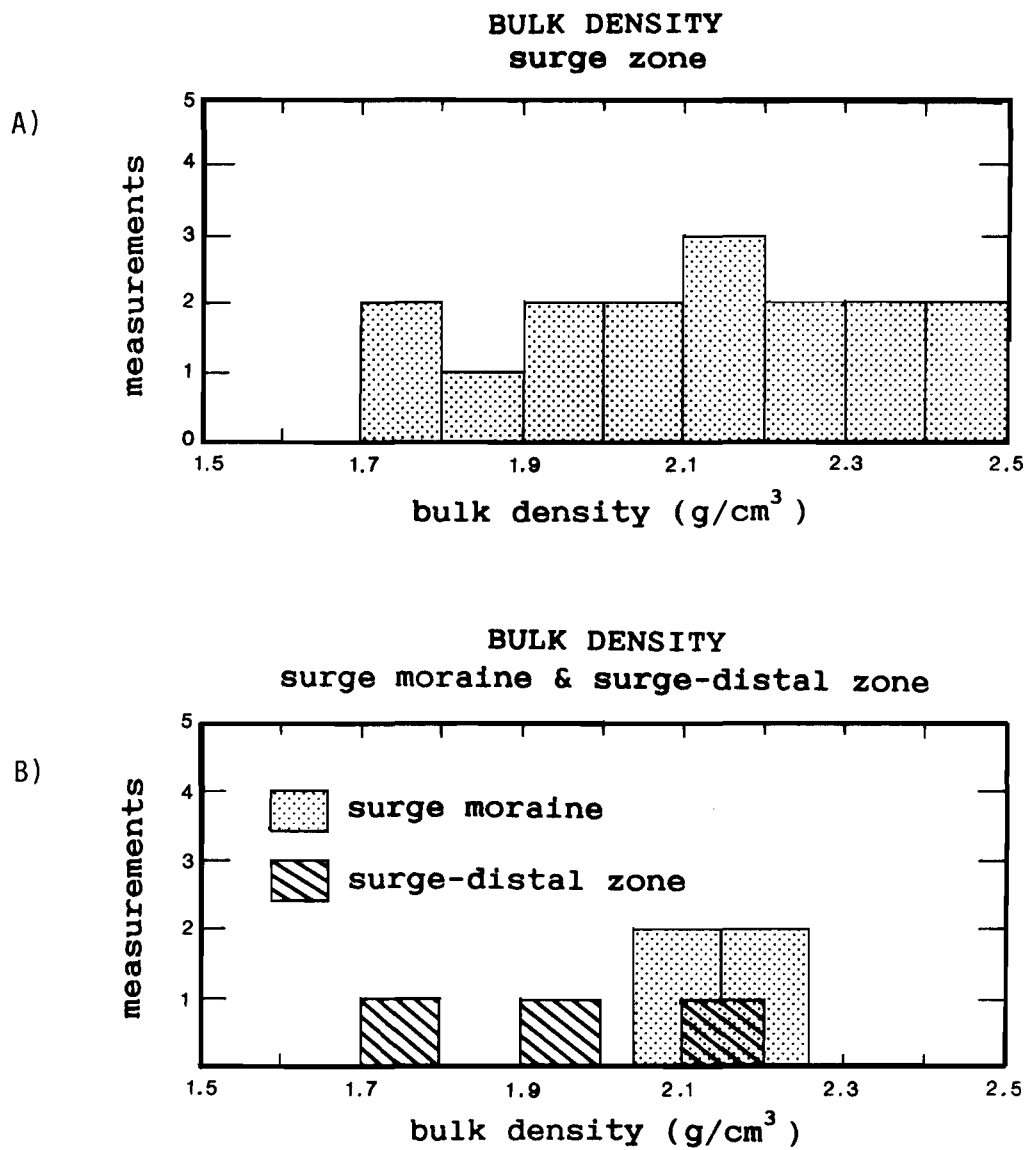


Fig.24. Frequency histograms of bulk density in sediments off Bråsvellbreen.

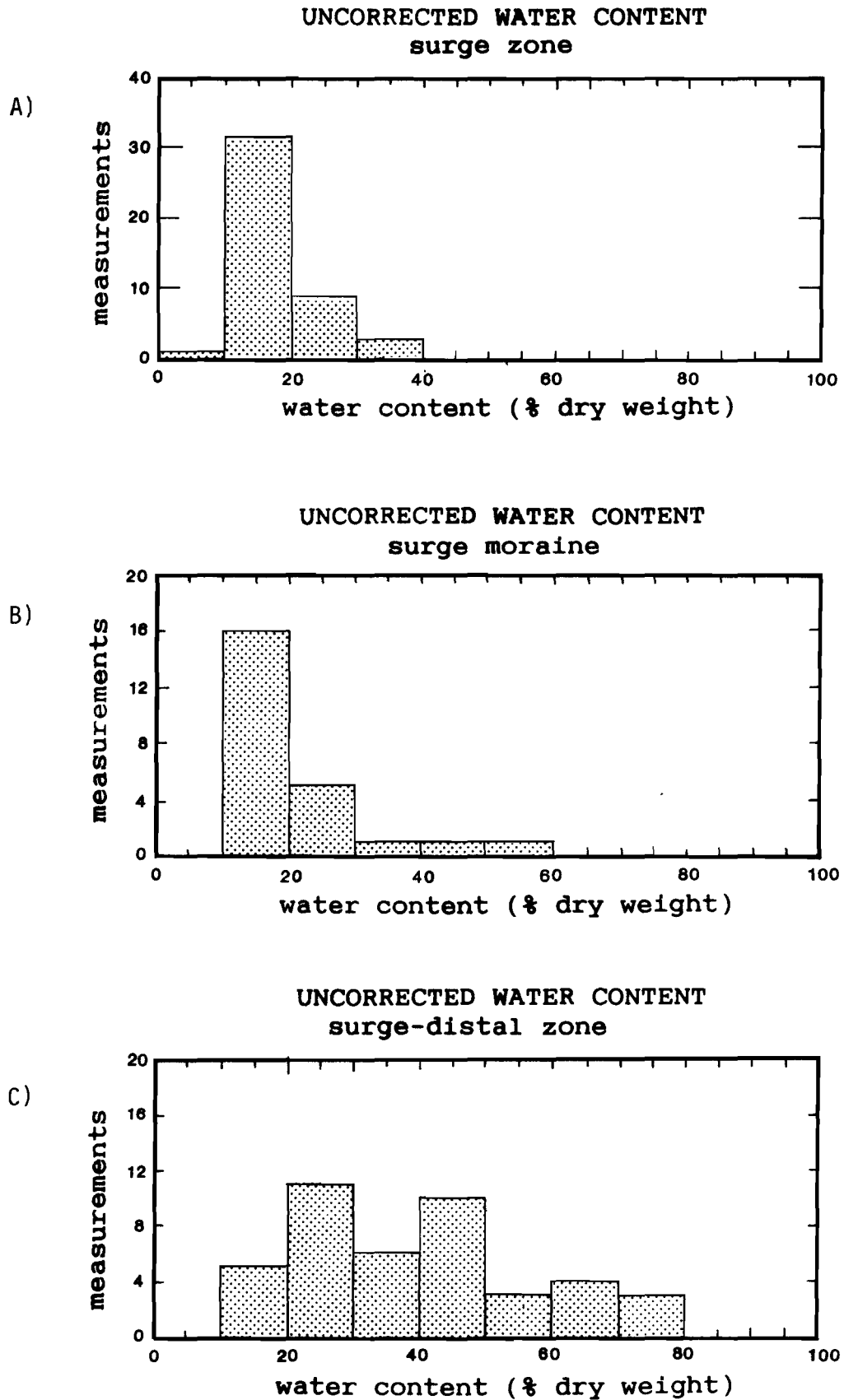


Fig.25. Frequency histograms of water content in sediments off Bråsvellbreen; a) surge zone, b) on the surge moraine, c) outside the surge moraine.

the surge moraine sediments fall in the same range of values as the surge zone diamictons. The surge-distal area sediments, on the other hand, have a larger range of values. Generally they are higher, with a maximum of 73 %, reflecting the more fine grained character of the surge-distal zone sediments.

Compressional wave velocity varies from 1470 m/s to 2600 m/s (Fig.26). Within the surge zone, where there are also most measurements, the bulk of the samples fall between 1800 and 2200 m/s. The velocity distribution generally follows no distinct trend as to what sediment type the different velocities can be ascribed to, but the lowest value in the surge zone, 1573 m/s, is found in the overconsolidated fine grained mud in core 83-31, hence indicating the importance of lithology. On the surge moraine, the majority of the velocity measurements are below 1800 m/s, with only 2 samples of core 82-234 around 2000 m/s. The surge-distal area again shows some variation, but the bulk of the values fall below 1600 m/s. The highest values are mostly found in the more gravelly parts of the surge-distal cores, and in particular in the western part. The highest value of 2600 m/s is measured in overconsolidated, assumed Late Weichselian till (acoustic unit 5) at station 82-226.

Where measured, the Atterberg limits generally embrace the natural water content of the sample, hence showing the weakly to non-overconsolidated character of the bulk of the sediments. In a plot of the plasticity index versus liquid limit (Fig.27) the Erik Erikstredet samples fall above the A-line (Casagrande, 1948) as also has been observed on the shelf off mid-Norway (Rokoengen et al. 1980). The Atterberg limits are essentially a function of the type and amount of clay minerals of a sediment. Boulton and Paul (1976) defined a "T-line" (Fig.27), along which lodgement tills from Iceland and Spitsbergen plot. In general, an increase in clay content will move

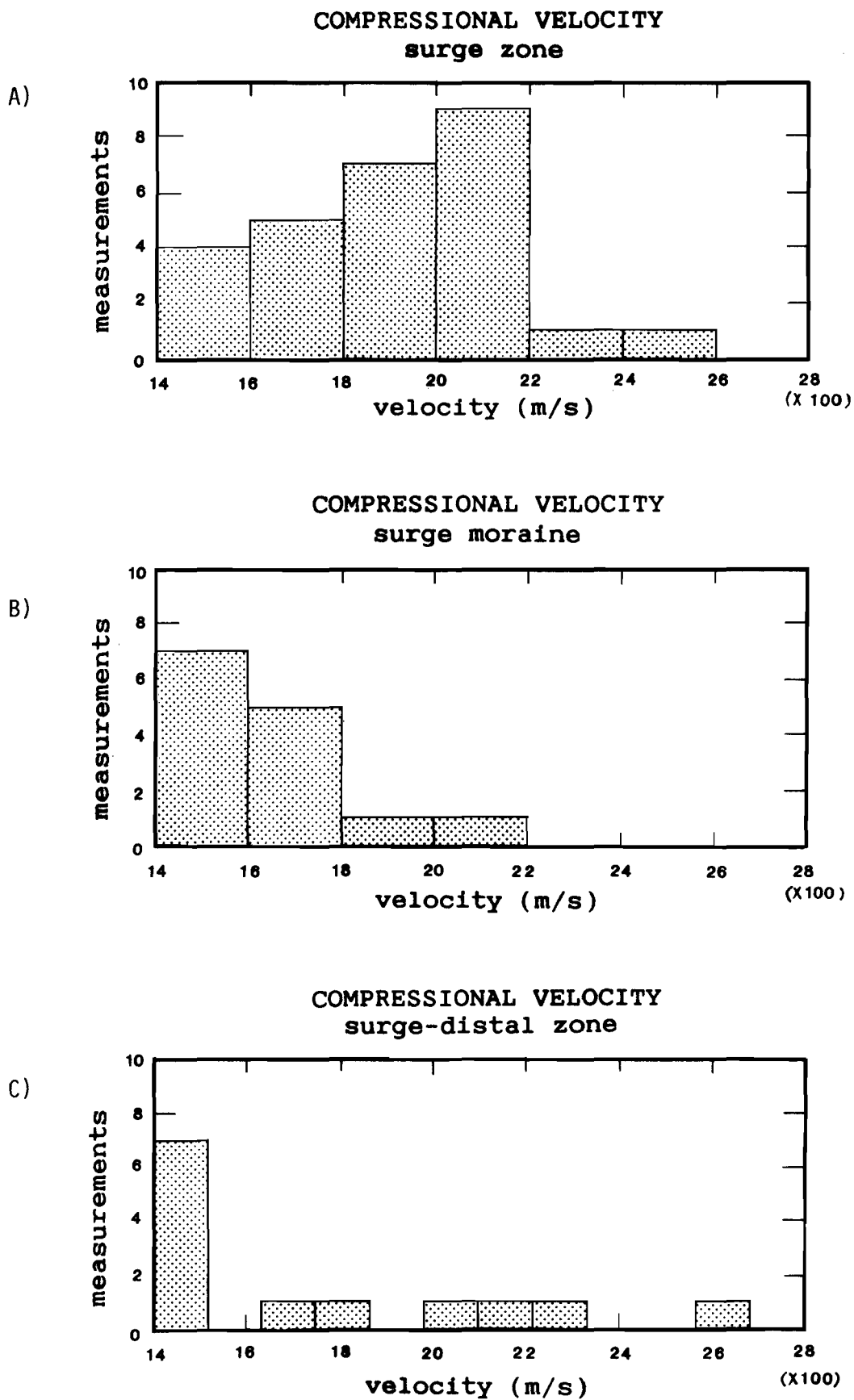


Fig.26. Frequency histograms of compressional wave velocity in Bråsvellbreen sediments; a) surge zone, b) on the surge moraine, c) outside the surge moraine.

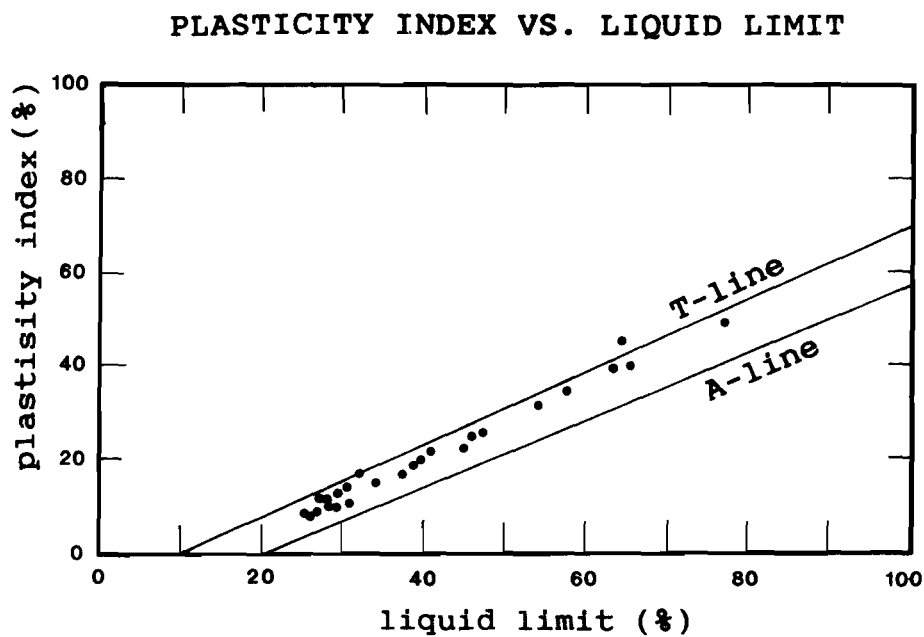


Fig.27. Plot of plasticity versus liquid limit for sediments outside Bråsvellbreen. The A-line (Casagrande 1948) marks the division between sediments of a broadly inorganic nature (above the line) from those with a significant organic content (below the line). The T-line is defined for lodgement tills from Iceland and Spitsbergen (Boulton & Paul 1976).

the sediment towards the right along the T-line, while winnowing of the finest fractions will tend to move the sediment below the line and towards the left. The same effect is found for sediments where the clay fraction to a large degree consists of rock flour (Boulton 1976). The position of the bulk of the samples of this study in the left part of the diagram, most likely reflects a combination of these two causes. The samples are generally characterized by a high proportion of silt relative to clay sized material and the entire mud fraction has a large content of non-clay minerals. However, as the same grain size distributions are found in the soft material of acoustic units 3 and 4, as in unit 5, interpreted to be the Late Weichselian basal till, winnowing is an unlikely cause for the grain size distributions.

Relation to the acoustic stratigraphy.

Most lithologic variations in the surge zone sediments are too local to be resolved by acoustic profiling systems with near surface source and receiver. Furthermore, the division between soft, normally consolidated sediments and sediments in the intermediate shear strength range (20- 100 kPa) is gradational and highly irregular. Therefore, both the soft and the intermediately compacted diamictons, sands and muds are included in acoustic Unit 1. The most distinctive subbottom reflector observed in the 3.5 kHz records is the relatively even, opaque reflector that can be followed under the entire study area. This reflector seems to be exposed locally in troughs in the surge zone, where stiff, highly overconsolidated material has been cored. Acoustic Unit 5 is therefore ascribed to this material, and it is suggested that the top reflector of Unit 5 is the top of the Late Weichselian till. Where the till is absent locally, the reflector represents top bedrock.

The soft mud cored in the deeper parts of the basin belongs to

acoustic Unit 3 (e.g. cores 85-26, 28, 84-11 and 13). None of these cores were long enough to identify a sedimentological change that could correspond to the division between acoustic units 3 and 4, which is usually found at a depth of 2-3 ms in these areas. However, cores from areas where unit 3 is apparently non-existent (e.g. 82-237 and 82-321) should represent Unit 4 material. Although the number of samples is strongly biased towards unit 3, Table 1 shows that both 82-237 and 82-321 generally have a higher gravel content than the unit 3 cores. Thus, from the relatively sparse number of samples, we tentatively relate the difference in acoustic character between unit 3 and 4 to a difference in gravel content. Similar relationships for acoustic character and grain size distribution were reported by Elverhøi et al (1983) from the Kongsfjorden area in Spitsbergen.

Parameter correlation.

By far the majority of published correlations between different acoustic and geotechnical parameters are from deep sea sediments (e.g. Akal 1972, Buchan et al. 1972, Horn et al. 1968, Taylor Smith 1975, Hamilton 1974, 1980 and numerous other papers). This probably results from the more homogeneous conditions found in the deep sea than in the glacially influenced, shallow regime, where large and frequent changes, both laterally and down-core are typical. The establishment of empirical correlations between different parameters is of interest in order to reduce the number of analyses necessary in a geotechnical reconnaissance survey. In particular, relationships between acoustic and geotechnical/sedimentological parameters would be useful, as acoustic measurements often are quick and simple to carry out, and also may be measured in-situ and during acoustic profiling (e.g. Li & Taylor Smith 1969, Taylor-Smith 1975, Bryan 1980).

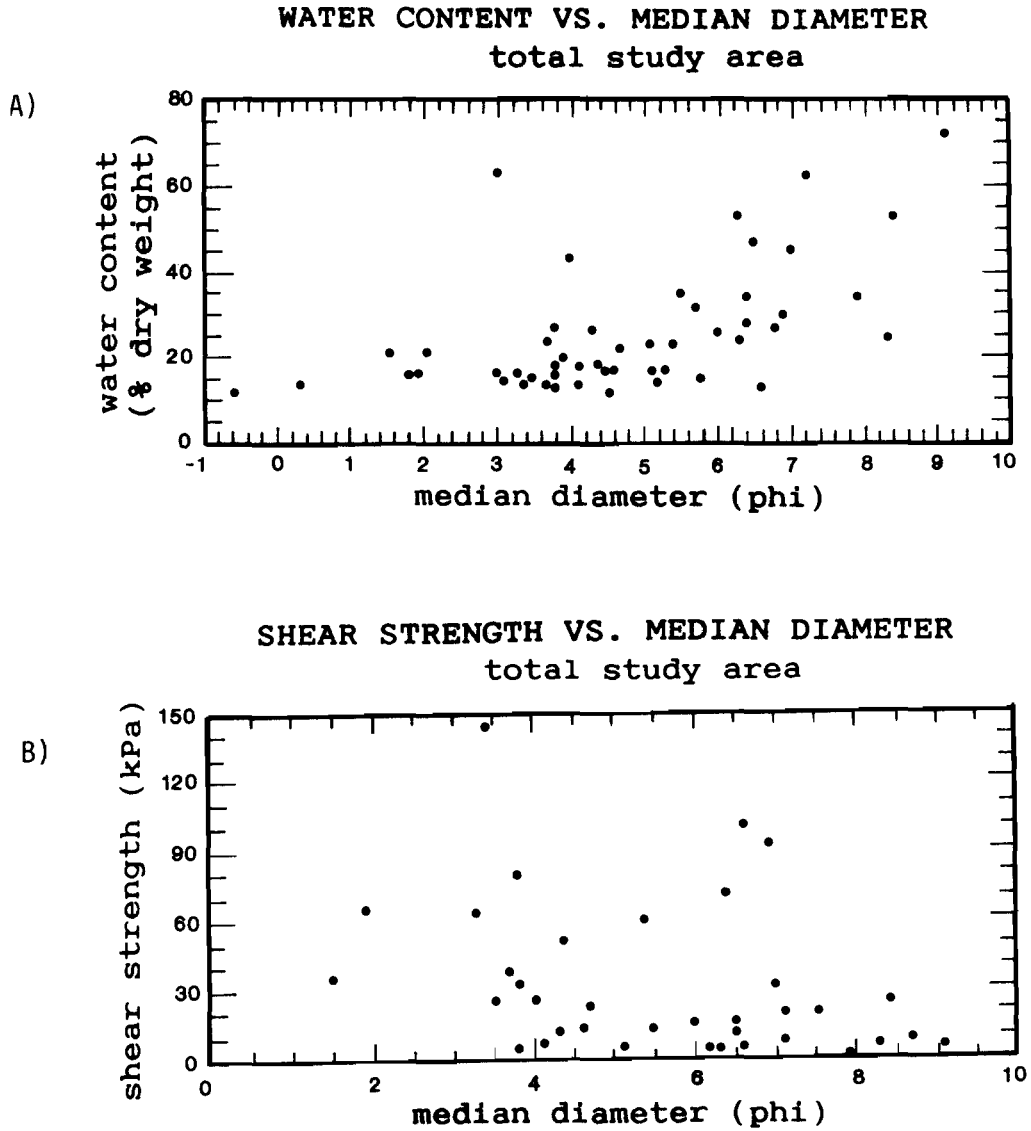
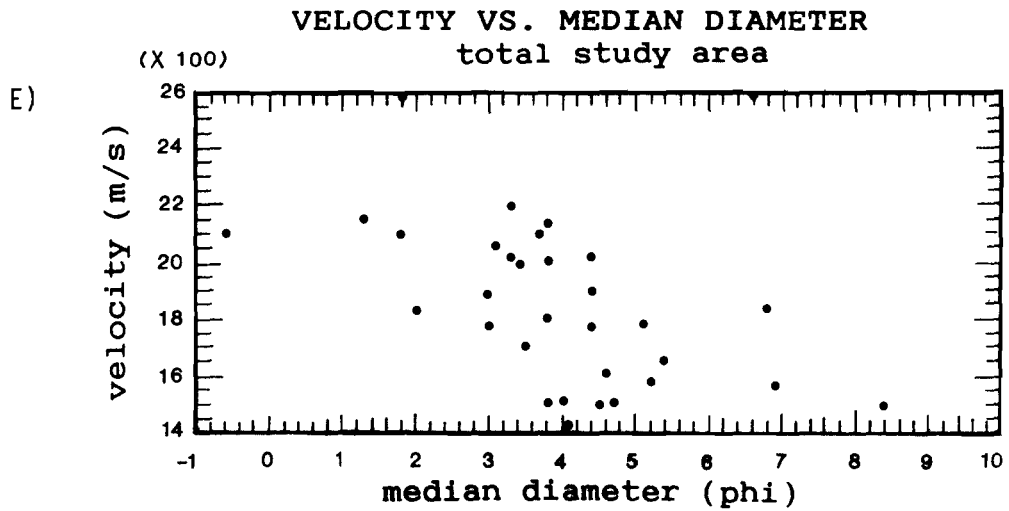
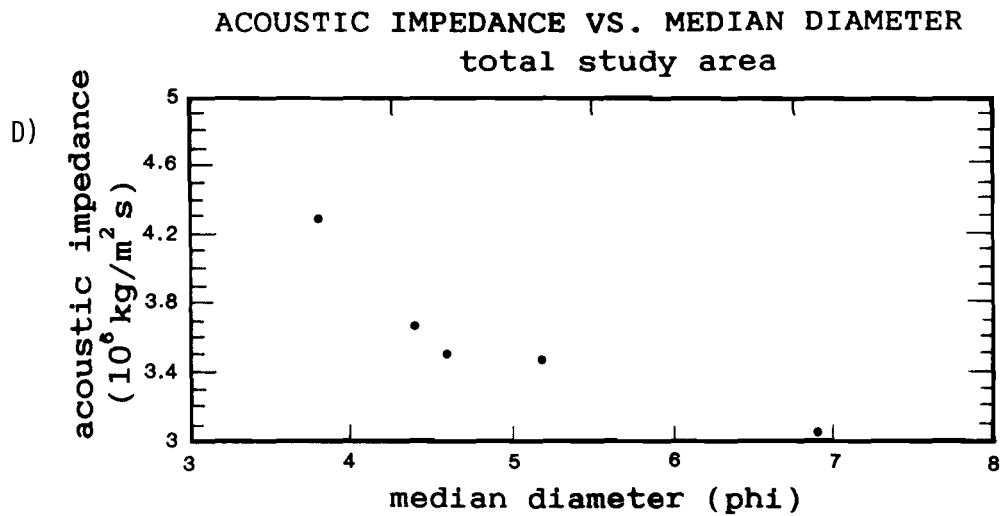
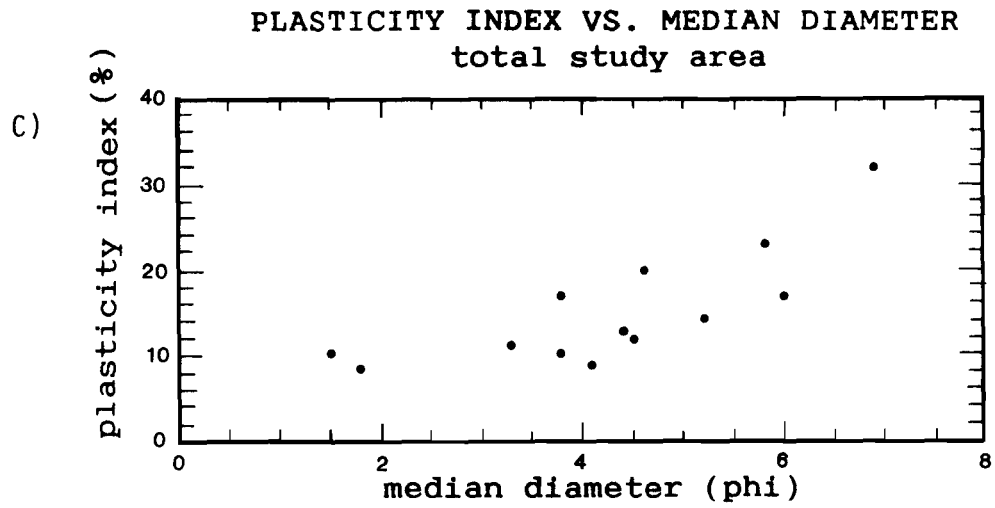


Fig.28. Physical parameters plotted versus median grain diameter; a) uncorrected water content, b) undrained shear strength, c) plasticity index, d) acoustic impedance, e) compressional velocity.



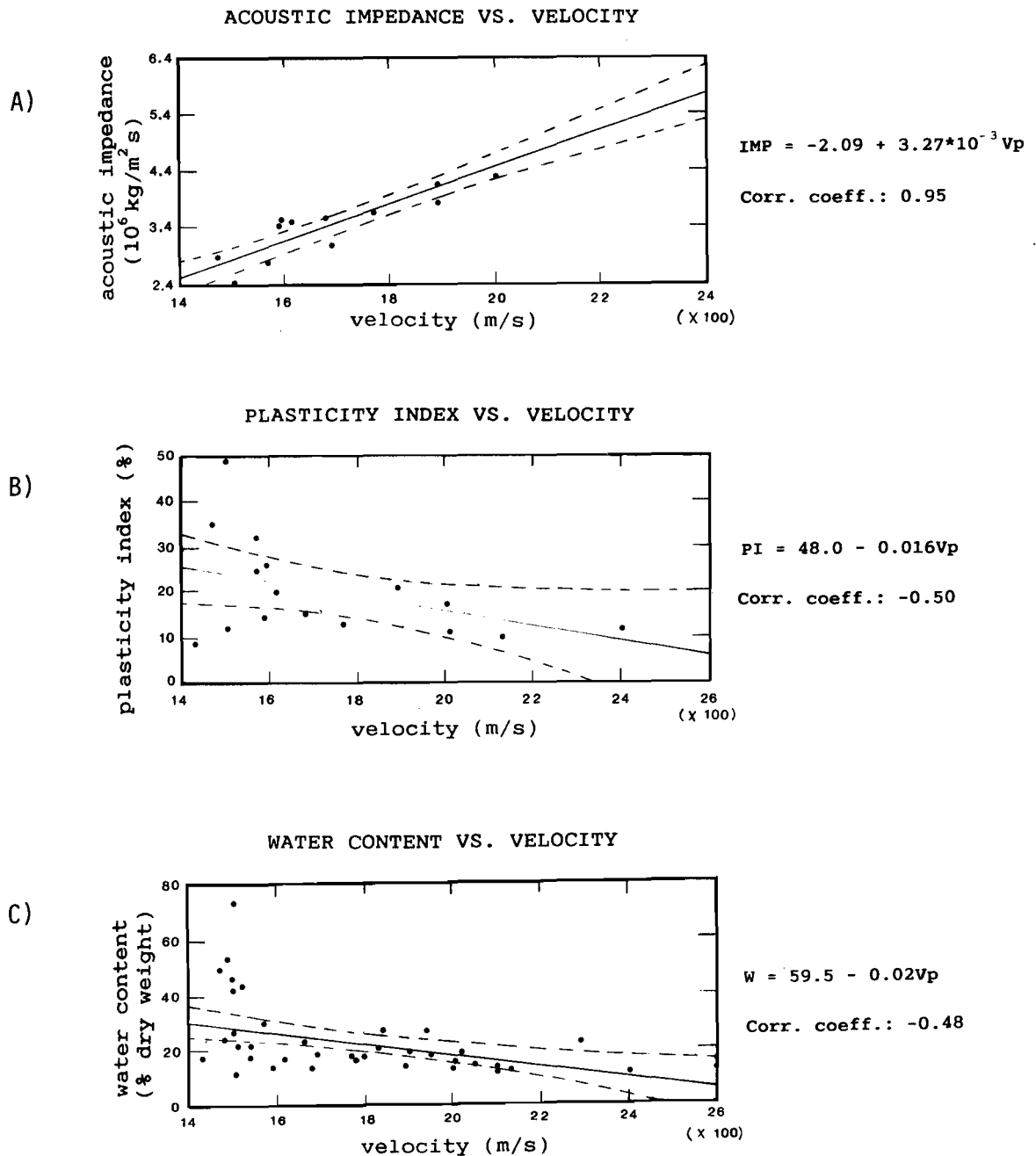
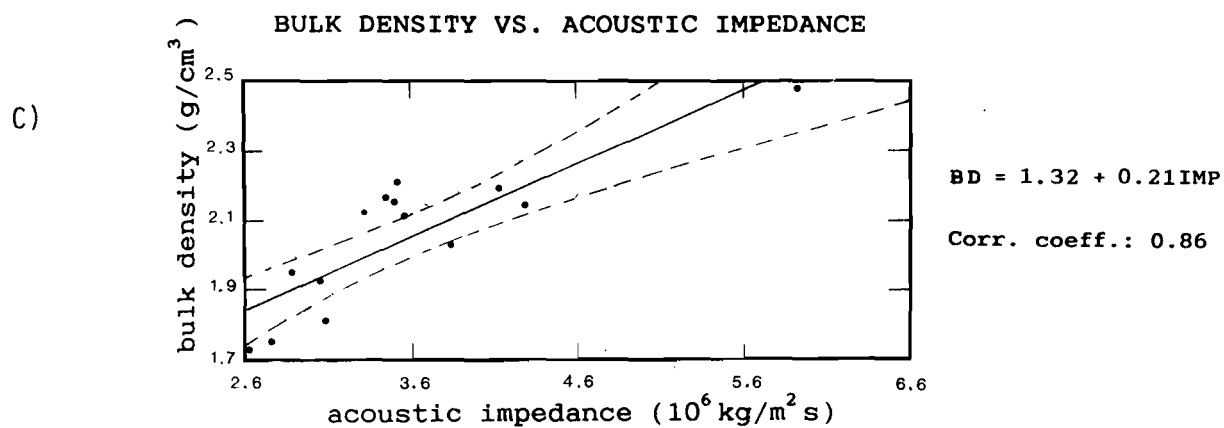
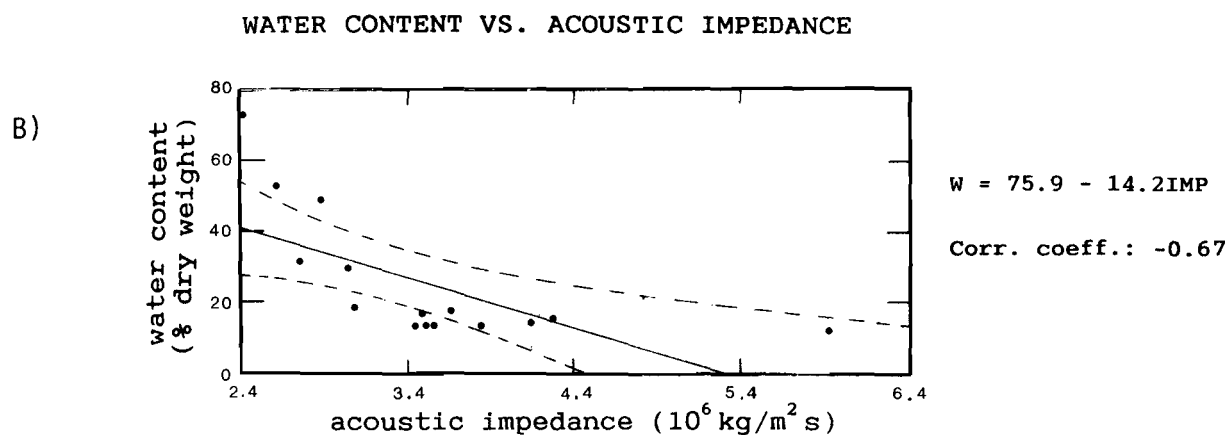
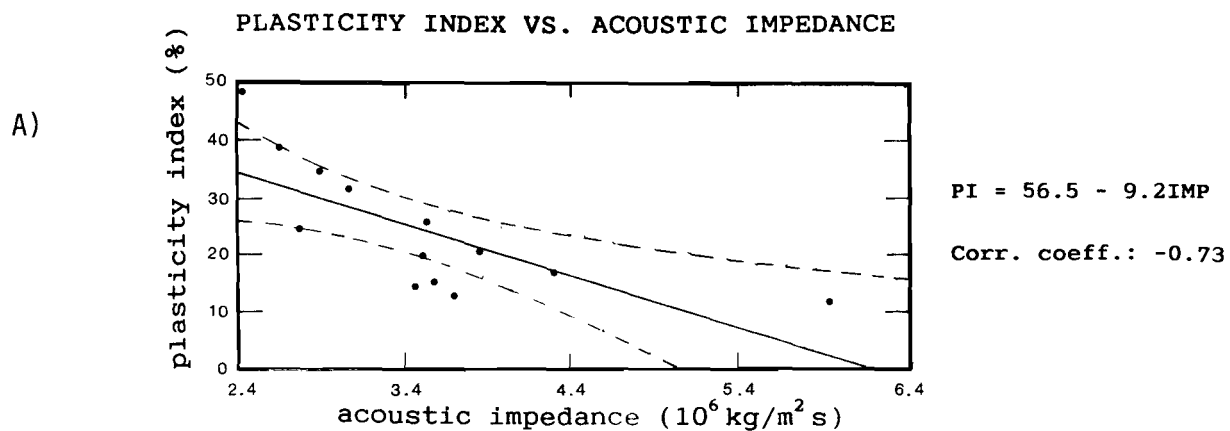


Fig.29. Inter-correlation between acoustical and other physical parameters; a) acoustic impedance versus compressional velocity, b) plasticity index versus velocity, c) uncorrected water content versus velocity, d) plasticity index versus acoustic impedance, e) uncorrected water content versus acoustic impedance, f) bulk density versus acoustic impedance. Correlation is done by simple, linear regression analyses. 95 % confidence and prediction limits shown by stippled lines.



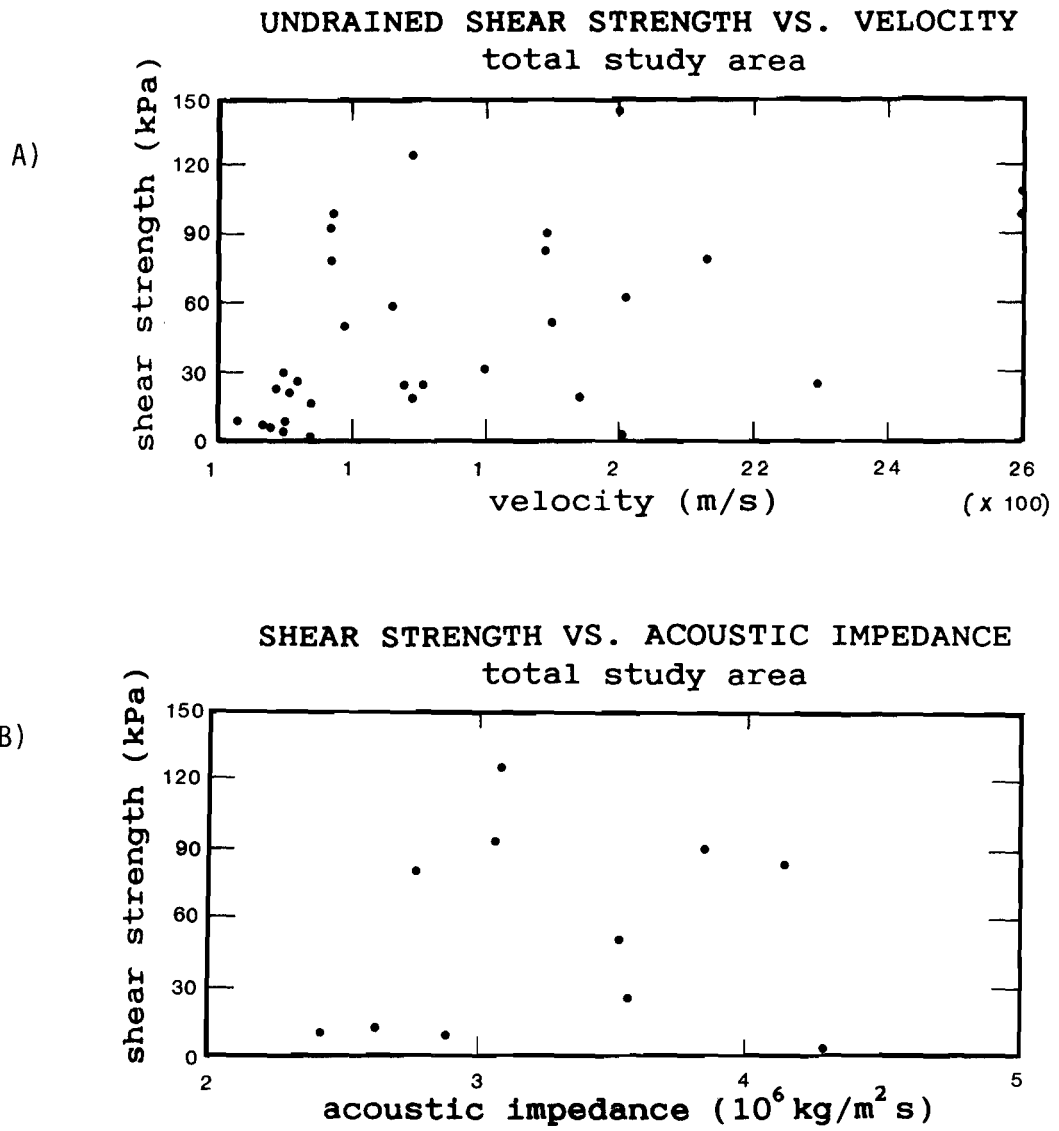


Fig.30. Plots of undrained shear strength versus compressional velocity and acoustic impedance.

The importance of grain size distribution for physical properties is shown by plots of different properties against median diameter (Fig.28). All plots have considerable scatter, clearly showing the inhomogeneous character of the ice proximal environment.

The water content (Fig.28a) is essentially constant for median diameters above 0.016mm (ϕ_6), and then increases markedly. This demonstrates the greater importance of the fine silt - clay fraction in creating large porosity and hence large water contents. Shear strength (Fig.28b) has a large scatter, and the only trend seen is the tendency of high values for coarse grained sizes in the diagram. This reflects firstly the predominance of generally coarser material in the surge zone, where also the bulk of overconsolidated samples were collected, but the plot in general also reflects the source of error that may be involved in shear strength measurements on relatively sandy material. Plasticity (Fig.28c) should be more or less independent of grain size distribution, as the samples picked for Atterberg limits were sieved through 0.063mm and the Atterberg limits are mainly a function of the types of minerals present in the clay fraction. This again reflects the dominance of rock flour in the medium silt and larger fractions, giving rise to a less plastic sediment. The linear increase in acoustic impedance with increasing median diameter (Fig.28d) (only based on 4 datapoints) is a function of the velocity increase with increasing grain sizes (Fig.28e). In the velocity plot, the two anomalously high values of 2600 m/s most likely result from larger stones in the measured interval.

Average values for the above parameters are not significantly different from those found in other polar and subpolar shelf areas (e.g. Josenhans et al. 1986, Bugge 1980, Paul & Jobson 1987, Løken 1976, Rokoengen et al. 1980, Eide 1974), for texturally similar sediments, but the values obtained in this study may show a larger

scatter. This results from the nature of the sediment, both the large variability, and also the fact that this type of material is difficult to analyse due to the high content of gravel and larger stones.

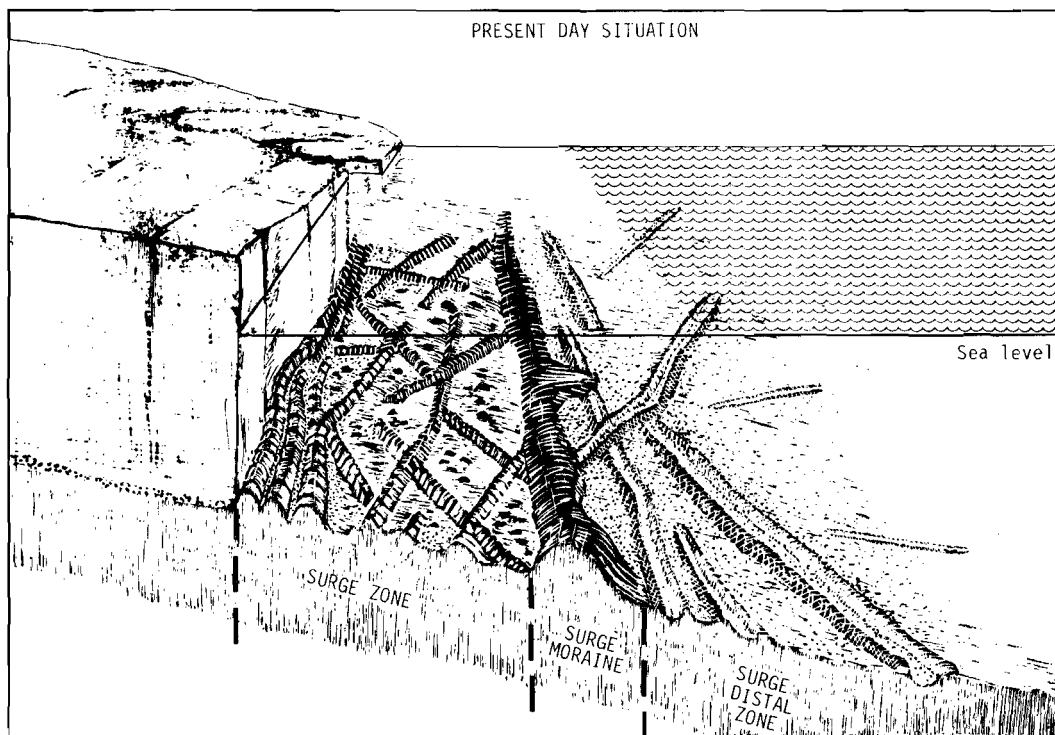
Acoustic velocity and impedance show, despite the variability, a relatively good correlation with other physical properties (Fig.29). The two acoustic properties themselves correlate with a coefficient of 0.95 (Fig.29a), while the correlation between velocity and bulk density is poorer. Hence, obtaining velocity information from this or a similar area gives a relatively good estimate of impedance. This information again would give an indication of the sediment bulk density. Other parameters that correlate reasonably well with the acoustic parameters are the plasticity index and the water content (Fig.29a,c,d,e). Shear strength, on the other hand, shows very poor correlation with the acoustic parameters (Fig.30). This was also noted by Buchan et al. (1972), who, however, found better correlation with acoustic impedance when other parameters (e.g. liquid limit, velocity and grain size parameters) also were included, in a multivariate analysis, showing the more complex nature of shear strength as a property. The present data set is not considered adequate for this type of analysis.

SEDIMENTATION, SEDIMENT DYNAMICS AND FORMATION OF THE SEA FLOOR MORPHOLOGY.

The Bråsvellbreen region.

Several lines of evidence support the surge moraine origin for the continuous ridge outside the Bråsvellbreen glacier; 1) the continuity, which is confirmed by the new, dense grid of acoustic profiles, 2) the

A)



B)

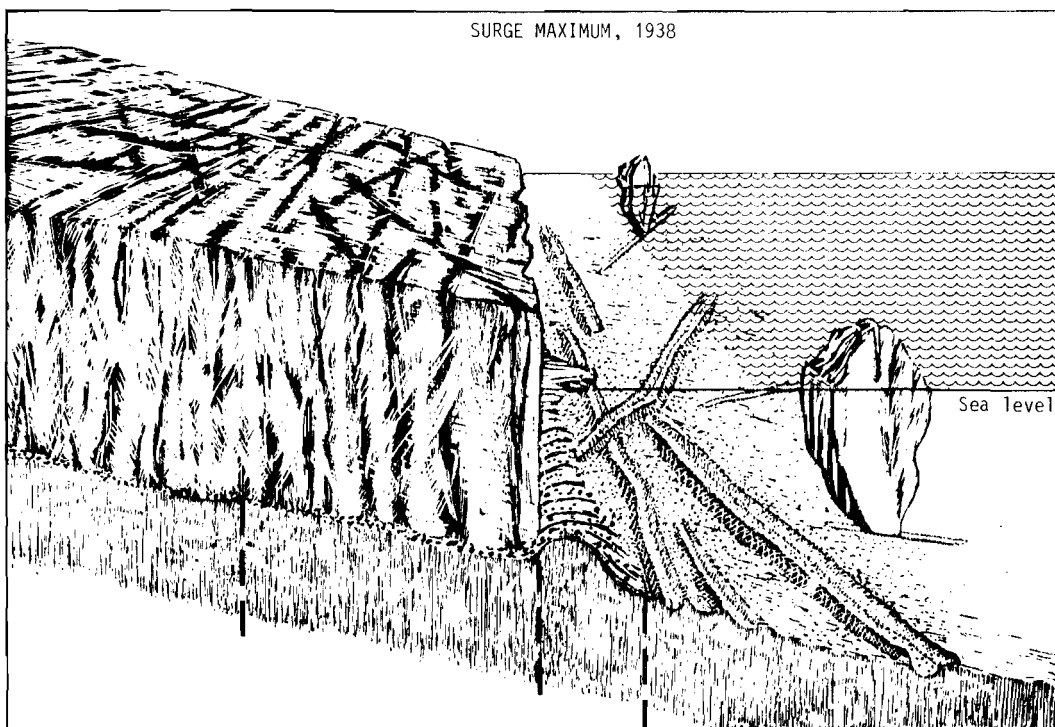


Fig.31. Schematic model showing the evolution of the surge-related morphology in two stages; a) during surge, with the glacier snout in its maximum position and b) the present-day situation.

cross-sectional shape, characteristic of formation in close contact with an ice front, 3) the marked change in sea floor morphology across the ridge, and 4) the decreased frequency of iceberg plough marks inside the ridge, relative to the distal side. However, it now also seems likely that the major part of the ridge is formed through at least two surges. In the eastern part of Bråsvellbreen, the last (1936-38) surge did not reach as far out as the previous one(s), thus giving rise to two surge moraines. Two evolutionary stages in the formation of the morphology in the three zones are shown schematically in Fig.31.

Two mechanisms may be important for formation of the ridge; deposition from meltwater and ice push. Solheim and Pfirman (1985) argued that both mechanisms were important, and that its final shape was partly modified by slumping, which is obvious several places along the distal parts (Fig.10). Before addressing the ridge formational mechanism, the availability of pre-surge sediments and how sediments are supplied to the surge zone during surge should be discussed. Two modes are important; transport of debris embedded in glacier ice (subglacial debris) and transport by meltwater.

Subglacial debris.

As the pattern of surge moraine ridges bear evidence of at least one previous Bråsvellbreen surge, the sediment distribution and characteristics in the surge zone prior to the 1936-38 surge was probably similar to those of to-day. The situation before onset of Holocene surge activity was most likely similar to that of the surrounding areas at the present; a thin veneer of till above the sedimentary bedrock, and with a cover of soft, Late Weichselian ice-proximal sediments and Holocene mud with a thickness depending on the time of onset of Holocene surge activity, which is unknown.

Previous surges reworked the sea floor sediment, brought in sediment carried in the glacier sole and sediment transported by meltwater. The glacier oscillations formed a pattern of soft and intermediately compacted, topographically irregular sediments similar to that observed in the area to-day, and what was encountered by the 1936-38 surge. As supraglacial input of debris is insignificant on Austfonna, the only source of englacial debris is subglacial sediments, which form a debris-rich zone of basal ice, and may, according to Boulton (1970) be brought up through shearing and thrusting, or by repeated folding (M. Hambrey, pers. commun. 1988). The most important factor in supplying allochthonous material to the surge zone is probably transport of subglacial material along and close to the glacier base. Thickness and concentrations of subglacial debris layers may vary considerably (Drewry 1986). Important factors are temperature regime and character of the substratum, both of which are largely unknown for Austfonna. Boulton (1972) stated that the debris layer of temperate glaciers usually was thinner than 0.1 m and only exceptionally reached 1 m. Hagen et al. (1986) observed sediment to 4 m above the bed in the temperate Bondhusbreen in Norway, but concentrations in excess of 10 % were found only in the lowermost meter. Cold glaciers, on the other hand, have thicker debris zones, and 17 m thickness was observed at Camp Century in Greenland (Herron & Langway 1979), while the cold based Foxfonna (Liestøl 1974) in Svalbard had up to 20 m of debris-rich basal ice over large parts (O.Liestøl, pers. comm. 1987). The debris concentrations also show large variations. Based on literature studies, Pessl and Frederick (1981) suggest an average value of 25 % for basal debris bands in temperate glaciers, reaching as high as 30-90 % in marginal zones. Clapperton (1975) found that the debris content in surging glaciers on Iceland and Svalbard was higher than

in non-surging glaciers, and explained this by enhanced regelation because of increased amounts of subglacial water in which increased heat transfer took place. Glaciers that surge over outwash and/or fjord bottom sediments become particularly rich in debris (Clapperton 1975).

The considerations above show that the amount of subglacial debris may vary considerably between glaciers. There is also a marked lack of information in the literature on sub-polar glaciers. Any estimate of the amount of subglacial debris brought to the surge zone will be speculative, but assuming a 1m thick layer of 25 % debris concentration may be reasonable. How much of this sediment contributes to the total sediment volume of the surge zone -and moraine is uncertain. The amount deposited in the surge zone depends on the rate of basal melting. Frictional heating during the surge and the fact that the surge covered unfrozen sea floor will enhance the rate of basal melting. Lodgement processes (Boulton 1975) are here considered to be of minor importance, given the short time active ice covered the surge zone. Lodgement till would also tend to be more dense and compacted (Lawson 1979) than most of the sediments seen in the area. On the other hand, calving is the most important mode of retreat in this environment, and a significant amount of the subglacial material may also be carried away with icebergs, and hence not deposited in the surge zone.

Meltwater.

Both theory and field observations indicate high rates of meltwater output during surges (Weertman 1969, Thorarinnsson 1969, Humphrey et al. 1986). A significant difference from non-surging glaciers is that in the case of a surge, large amounts of meltwater will also be generated during winters (Kamb et al. 1985). Meltwater has been shown

to be a more efficient agent for transport of subglacial material than englacial transport. In a temperate glacier in Norway, a nine-to-one ratio between the two modes of transport was found (Hagen et al. 1986). Any pre-surge subglacial drainage system or newly formed conduits will constantly be disrupted and changed during a surge (in fact, Kamb (1987) proposes such changes to be a cause of surges). Meltwater will probably be discharged along the entire frontal zone, as opposed to the present-day situation of Bråsvellbreen, where there is only one large meltwater outlet, which is located at the very eastern margin of the basin. Disruption and frequent shift of channels lead to increased release of material from the glacier, as well as erosion of the substratum. The sediments in the surge zone -and moraine show no widespread sorting indicative of meltwater action, with the exception of three cores (83-26, 83-30 and 83-31, Fig.20d,e) that had well sorted sand in the upper part. Hence, from the sediment cores, the only effect of meltwater activity in the surge zone proper during the surge may be to enhance subglacial meltout and to redistribute bulk sediment volumes without leading to sorting effects significant enough to be detected by the level of sediment sampling during this study. The significance of increased subglacial meltwater activity for the total sediment volume in the surge zone, is difficult to evaluate given no diagnostic criteria.

Thorarinsson (1969) noted an increase in meltwater discharge from a surging glacier on Iceland before the frontal advance proper. The most significant increase, however, occurred when the surge had propagated to the snout and the advance of the ice front started. Syn-surge meltwater activity most likely will transport and deposit relatively high loads of soft, unstable sediments at the front, making more material available for reworking, mixing with the pre-existing soft

sediments and push by the advancing glacier. Pushed material probably forms the major part of the surge moraines. When the advance of the glacier front stops, however, high discharge of meltwater and thus sediment probably still continue for some time. A pulse of very turbid meltwater appears to coincide with the end of surge (Kamb et al. 1985). The acoustically transparent sediment drape of the distal slope of the surge moraine ridge result from this material in addition to parts of the pushed sediment, which also may be soft, unstable and easily modified by slumping. This gives rise to the characteristic appearance of the distal part of the surge moraine ridge system (Fig.8). Although the number of cores from the ridge proper is inadequate for a detailed textural picture of the ridge sediments, the importance of slumping is shown by the unsorted character of all parts of the ridge. The most distal parts may have a somewhat finer grain size distribution, but the material still encompass a considerable amount of gravel and larger clasts. Some of this may be dropped from floating icebergs, but this is unlikely to be the main source considering the relatively large thicknesses involved.

Slump lobes are only observed on the distal side of the surge moraines. As the proximal side is steeper, this indicates that the major part of the mass movement took place during a relatively short period of time, when the glacier front was in its maximum position and stabilized the proximal slope. The relatively low slope of the proximal side, compared to slopes of up to 45 degrees of marine push-up ridges in Canada (Lewis et al. 1977), may point toward some slope modification after ice retreat, but direct evidence for this is not observed. Locally steeper slopes may represent true ice contact slopes.

The whole system of sea floor morphologies, including a continuous,

terminal ridge, in front of Basin 3 clearly resembles that found in front of Bråsvellbreen. As there are several indications of a Basin 3 surge, it is therefore considered most likely that the patterns found also here results directly from surge and post-surge activity. This was also argued by Solheim (1986), but only from the few 1984 side scan lines. The more expanded data set strongly supports this.

The main difference between the surge moraines in the two regions is the relatively less marked bathymetric expression of the Basin 3 moraine. The proximal boundary is difficult to define, while the distal part shows the same type of acoustically transparent lense character. As it was argued that the Bråsvellbreen moraine mostly resulted from push, but with meltwater supplying sediments to the front, the difference in character may be explained by less efficient push in the Basin 3 region. This explanation is supported by differences in water depths between the two regions. While the Bråsvellbreen moraine is mostly situated shallower than 90 m, the major part of the Basin 3 moraine is between 100 and 110 m waterdepth. As the size of the drainage basins and amount of advance are comparable in the two regions, buoyancy would have decreased the bulldozing capacity of the Basin 3 surge front to a larger degree than for Bråsvellbreen. Pushed material in shallower water closer to the present-day ice front may have been overridden and partly redistributed by the surging glacier when water depth came below a critical value. The low relief character of parts of the Basin 3 surge moraine can be explained this way.

The rhombohedral pattern.

Several lines of evidence point towards the rhombohedral ridge pattern being formed through squeeze-up of sediment into subglacial fractures during and immediately after the surge, as also suggested by

Solheim and Pfirman (1985):

- The ridges show directional trends that match within $10-20^{\circ}$ with the crevasse pattern seen from aerial photos of the surface of the surging glacier (Fig.5b). The surface crevasses show three distinct directions, one roughly parallel to the glacier flowlines and two directions with an angle to the flow lines. All these directions are recognized in the present-day sea floor topography (Fig.13).
- The pattern is only found proximal to surge moraines.
- As the ridges forming the pattern have directions at various angles, up to perpendicular, with the ice front, they can not have been formed by push from the grounded glacier. For the same reason, the ridges are not likely to have been formed by deposition from meltwater or direct melt-out along the ice front during its retreat.
- The material forming the ridges is soft and hence not likely to represent a pre-existing till topography.

Terrestrial landforms, also interpreted to result from crevasse fillings, have been described from several regions. Bjørklund (1985) ascribed parallel ridges in Sweden to a process of infill from supra- and englacial debris during a phase of glacier stagnation. This ablation type crevasse filling was also discussed by Gravenor and Kupsch (1959) and by Johnson (1975). However, infill from above seems unlikely in the case of Bråsvellbreen, due to reasons discussed in the introduction. Both the glacier surface and the exposed part of the front appear clean at present.

Gravenor and Kupsch (1959) also discuss Hoppe's (1952) model of sub-glacial squeeze-up. Ridge systems in Canada show similar dimensions and patterns as those of Bråsvellbreen. According to Hoppe (1952), squeeze-up requires that most of the debris is under the ice (little englacial material), and that the subglacial debris is unfrozen,

susceptible to plastic deformation. Both these requirements seem to hold for Brásvellbreen, as the surge moved over Quaternary glacial and glacial marine sea floor sediments.

Sharp (1985) describes ridges that most likely result from crevasse fillings, in front of a surging glacier on Iceland. These ridges have directions oblique to the local ice flow directions. They can be followed into the present-day glacier front where they are continuous with the subglacial lodgement till, and also where ice structures similar to those interpreted to be crevasse traces by Hambrey & Muller (1978) in a non-surge cold glacier, are found. The ridges are thought to be formed during the very early part of the quiescent phase of the surge cycle, when the heavily crevassed glacier stagnated and sank into its bed, causing subglacial till to flow from areas of ice overburden into crevasses at atmospheric pressure (Sharp 1985). A similar process has been suggested by Boulton (1972) for flowage of sediments into cavities on the lee side of large boulders under Svalbard glaciers.

Ordinarily, crevasse depths rarely exceed 30 m in temperate and subpolar glaciers. In cold glaciers they may reach greater depths (Hambrey & Muller 1978). However, Smith (1976) calculated that crevasses filled with water to a level equal to or greater than 94.6% of its depth can penetrate the bottom of the glacier. Weertman (1973) found a similar value of 97.4%. Water-filled crevasses would most likely be the situation for Brásvellbreen, surging out in up to 100 m waterdepth.

From the above discussion, a crevasse-fill origin through squeeze-up during the early phase of post surge stagnation seems likely for the rhombohedral ridge pattern, similar to that found terrestrially by Sharp (1985) on Iceland.

Post surge preservation of the morphology.

A major problem with the sub-glacial squeeze-up formation theory is the post surge preservation of the ridges. An absolute requirement is that there is insignificant later movement in the glacier sole, or that the glacier moves completely detached from the substratum. The latter is unlikely as the glacier rests on a deformable till bed. Boulton and Jones (1979) proposed models for glacier flow on this type of substratum, where a large part of the glacier movement was contributed by deformation of the bed rather than the glacier. Two preservation modes may be considered if the squeeze-up mechanism is viable;

- Freezing to the bed.
- Post-surge stagnation of the snout.

Schytt (1969) suggested a "cold ring" structure for the Nordaustlandet ice caps in which a core of temperate ice was held in by a ring of cold ice. This is consistent with Clarke's (1976) numerical modelling experiments indicating that the glacier snout soon refreezes to the bed after a surge of a cold glacier, thereby leading to the quiescent phase.

However, the glacier surged out over unfrozen sea floor, it was severely crevassed and thus possibly allowing penetration of sea water, at least in the outermost parts, and, as will be showed in the next chapter, the front probably withdrew from the zone of the rhombohedral pattern in a maximum of approximately 30 years. It is here considered unlikely that the glacier would freeze to its bed in this situation within the time frame presented. Furthermore, the cores and the seismic data show that the glacier rests on deformable sediment, most likely till, of at least 3 m thickness. In the case of a frozen bed, the detachment surface for calving of basal ice probably would be somewhat down in the sediment, or at the sediment -

bedrock interface. Hence, the frozen bed would have been included in the calving of basal ice, causing significant distortion of the morphological pattern.

From the above discussion, post-surge stagnation, caused by mass deficiency in the accumulation area, and not involving freezing to the bed, is considered the most likely mechanism for preservation of the subglacial morphology found in the major part of the surge zone. Retreat mostly took place by calving. The temperature regime during the last part of the post-surge period and at present is uncertain, but will be briefly discussed below.

The discontinuous, arcuate ridges.

These features, sub-parallelizing the glacier in the innermost part of the surge zone (Fig.7) may result from push, probably on an annual basis, squeeze-up similar to the mechanism proposed for the rhombohedral ridge pattern, deposition of englacial debris directly from the ice front or basal debris from meltwater, or impact by calving icebergs (Powell 1985). The latter is considered an unlikely mechanism to produce such a regular pattern, although structures that could be ascribed to impact do occur. These, however, seem to be superimposed on the arcuate ridges (Fig.14). Deposition directly from the glacier does not seem capable to produce ridges of this size, and the action of meltwater most likely would result in more localized accumulations. Squeeze-up is also excluded as a likely mechanism. The aerial photographs from the Bråsvellbreen surge indicate a consistent crevasse pattern normal to the flow lines, but the surface fractures appear straight for relatively long distances and do not show the discontinuous, arcuate character seen on the present-day sea floor.

This leaves annual push moraines as the most likely explanation for these features. Annual push moraines typically have relatively low

relief and occur in swarms of numerous ridges with short inter-ridge spacing (B. Andersen, pers. comm. 1987). Both this and the fact that the ridges can be seen to reflect the overall shape of the ice-front support a push moraine origin. Boulton (1986) has described in much detail similar features from Svalbard, Iceland and Canada, both in marine and terrestrial environments. Annual moraines of comparable size are described from Late Weichselian deposits in northern Norway by Sollid and Carlsson (1984). The size of the ridges, however, will most likely vary with glacier dynamics and amount of available material. Andersen and Sollid (1971) reported presently forming annual moraines with a width of 2-3 m and relief of <1 m from southern Norway. Price (1970) describes series of short, arcuate ridges that are joined together, forming a similar pattern as that found off Brásvellbreen, on Iceland. These are interpreted as annual features, but Price (1970) explains their formation by squeezing out of water-soaked till from beneath the glacier front, rather than simple push. Hence, this involves processes similar to that envisaged here for formation of the rhombohedral ridge pattern. Pebble fabric and a distal slope that is steeper than the proximal, are the main arguments for the squeeze-out theory. In the Brásvellbreen area there are no pebble orientation studies (no oriented cores were taken), but cross sectional shape shows no significant trend in ridge asymmetry, and no other indications of a squeeze-out origin can be found.

A consequence of the annual push moraine explanation of the ridges is that the Brásvellbreen front is no longer totally stagnant. Sharp (1984) interpreted similar ridges on Iceland to be annual moraines and used this pattern as a possible diagnostic feature to indicate that a glacier was not a surge-type glacier. If the Brásvellbreen pattern is taken as annual moraines, this shows that also surging glaciers have a

period of slight activity producing small push ridges during the quiescent stage. Although no velocity measurements are available from Bråsvellbreen, a set of crevasses parallel to the present-day ice front indicates slight movement of the glacier. Information from other surge-type glaciers on Svalbard during their quiescent phase, further supports this. Nathorstbreen on Spitsbergen, another surging glacier, has been measured to have an average velocity of 10 cm/day at the front, and ridges seen on echograms from Van Keulenfjorden in front of Nathorstbreen, were interpreted as annual moraines (Liestøl 1976). Pushed sea ice in front of Negribreen, east Spitsbergen, shows that this glacier also advances during winter (O. Liestøl, pers. comm. 1986). Negribreen is probably the most comparable surging glacier, relative to Bråsvellbreen, on Svalbard, both in size and surface profile.

The size of individual ridges is dependant on both amount of readvance of the glacier and amount of material available to be involved in the ridge formation. Boulton (1986) points at the association between the ice marginal fan complexes and push moraines. Outside Bråsvellbreen, the largest of the push-moraines are found just off the main meltwater outlet, where also most recent sediment is expected to be found.

The discontinuity of the push moraines is probably due to differential movement of the glacier and varying amounts of material available to form ridges. In the case of large readvances, annual ridges may be destroyed in favour of the formation of larger ones. Side scan lines from 1982 and 1983 that run along the glacier, cover only the innermost 500 m, while the 1984 and 1985 lines normal to the glacier do not run close enough to record the innermost area. The 1982 and 1983 navigation is not good enough to merge the two data sets in detail. Thus, we do not have a continuous coverage

between the ice front and the proximal boundary of the rhombohedral pattern. However, counting ridges thought to be annual push-moraines along 4 profiles from the ice front and 500 m seawards, give 16-17 ridges. Hence, with a maximum width of the arcuate pattern of 1000 m in the frontal zone of Bråsvellbreen, the major part of the glacier has been active for the last 17-34 years, leaving a completely stagnant period to have lasted for 16-33 years. The criterion for picking ridges to count was a minimum length of 100 m. Including all smaller ridges, numbers varied between 24 and 29 over the 500 m distance. In the western, thinnest part of the glacier, however, stagnant conditions still prevail, shown by the fact that crevasse-fill pattern can be followed up to the glacier proper (Fig.12).

The formation of annual moraines confirms the conclusion that preservation of the rhombohedral ridge pattern requires stagnant ice. When the glacier again resumes normal activity, this pattern is reshaped into push ridges. This may also give some indications about temperature regime. Formation of the push-ridges implies sliding of the glacier, which is inconsistent with a frozen bed. Furthermore, sediment cores obtained within 100 m from the present-day glacier front (Solheim & Pfirman 1985, and below) did not bear evidence of permafrost conditions.

However, extrapolation of temperature gradients measured in shallow boreholes point towards frozen bed conditions (J.A.Dowdeswell, pers. commun. 1988). An explanation may be that Austfonna is a true subpolar ice cap, as proposed by Schytt (1969), but that there is an outer zone of unknown width where non-frozen conditions exist, in the contact zone between glacier ice, sediment and sea water. Ice movement is then mainly taking place through deformation in the frozen part, but is transferred to a component of basal sliding in the outer, non-frozen

part.

The intermediate region.

As the same suite of morphologic features; terminal moraine, rhombohedral and arcuate ridge patterns are also recognized in the intermediate region, the above discussion leads to the conclusion that this region also have been covered by surging ice. This conclusion is also supported by the fact that the end moraine in the region merges with the Bråsvellbreen moraine. Clearly it has been formed by an advance that also included Bråsvellbreen. A merge with the Basin 3 moraine is not observed from the present data, but from the appearance of the ridges it seems likely that formation of at least the eastern part of the intermediate moraine also involved a Basin 3 advance. From this we can infer that both Bråsvellbreen and Basin 3 had previous surges that were somewhat more laterally extensive than their last surges. Changes in surge directions of previous advances to cover the intermediate region with surging ice seem unlikely for Basin 3, which is situated in a well defined bedrock depression (Dowdeswell et al. 1986), but may not be excluded for Bråsvellbreen (Fig.4b). These questions can not be conclusively answered from the present data base, but the directional trends of the rhombohedral and parallel ridges, although rather inconsistent, seems to indicate both advance and retreat directions sub-parallel to the present-day glacier front also in this region.

Both the intermediate moraine ridge and the Basin 3 ridge have more frequent iceberg plough marks than the Bråsvellbreen ridge. The susceptibility to grounding of icebergs results from the topographic expression of the ridge system, but the relative differences in plough mark abundance clearly reflect the age differences. The intermediate ridge, which is dominated by plough marks, is older than the other

ridges, and it has also experienced the large production of icebergs during the latest Basin 3 and Bråsvellbreen surges. The Basin 3 moraine also has more abundant plough marks than the moraine off Bråsvellbreen, due to its longer exposure to drifting icebergs. However, most of the surface area of this ridge has been classified as a "mixed morphology", characterized by iceberg plough marks and numerous smaller mounds and depressions (Figs.7,11). Sometimes these disturbances appear as 25-50 m wide craters with a circular berm. This pattern is found mostly on the proximal part of the end moraine and immediately inside it, but also in a small area outside the ridge, inside the easternmost part of the intermediate moraine (Fig.7). Due to the location of this pattern in the area of an assumed heavily crevassed surge front, it is likely that the disturbed sea floor result from iceberg impact during calving. Powell (1985) has described this effect from the Antarctic, and has found that calving icebergs may have a great effect on the sea floor also without direct contact, because of the preceding pressure wave. On sloping sea floor, these processes would lead to small scale slumps and gravity flows.

The surge-distal regions (non surge-related features).

The major part of the study area, outside the surge moraine systems, is characterized by two main classes of sea floor morphology; smooth sea floor with other features and iceberg ploughing, both recent and relict. Iceberg plough mark distribution is governed by iceberg production, currents, local and regional bathymetry and time of exposure of the area to drifting icebergs. The lower depth limit of recent plough marks is approximately 120-130 m. However, outside the Bråsvellbreen surge moraine there is a region with smooth sea floor, i.e. lack of plough marks, despite being shallower than 120 m (Fig.7). Comparison with the bathymetry (Fig.2) shows that this

area matches with a local deep in front of the surge moraine. The bank south of the gouge-free area has most likely acted as an efficient trap for icebergs drifting in from other areas than Bråsvellbreen. Icebergs entering from deeper waters would have had to adjust their drafts to cross the shallow area and would thus no longer ground in the local trough. Likewise, bergs from Bråsvellbreen would have to cross the surge moraine, and would then float in the deeper trough. Occasional plough marks are also seen on the ridge crest.

In the surge zone outside Bråsvellbreen, as well as outside Basin 3 and the intermediate region, there are generally only few plough marks, least outside Bråsvellbreen. There are two reasons for this: Firstly, the glacier is grounded, has sparse activity and thus only limited iceberg production. Secondly and more important, however, is the fact that this area has only been exposed to drifting icebergs during a relatively short time interval since the last surge. This time interval is shortest for Bråsvellbreen and longest for the intermediate region. In the latter, as well as in the western part of the Basin 3 surge zone, there is a small region of more extensive gouging (Fig.7). This again is strongly influenced by bathymetry. The area is shallow, and the surge moraine ridges are not well expressed topographically and do not efficiently prevent icebergs from entering the area from outside. Furthermore, the shape of the glacier front at Kapp Mohn (Fig.2) is not a stable one, and indicates extensive calving.

The plough mark directions (Fig.7) are functions of the prevailing current regimes in the region. Close to the mouth of Hinlopenstredet, tidal currents will move bergs both NW and SE. Although there are large calving glaciers further north in Hinlopenstredet, bergs from these glaciers probably do not reach the study area until their

size is greatly reduced, due to the shallow sill at the southern end of the strait. The southwesterly flowing current through Erik Eriksenstredet dominates the iceberg transport in the eastern part of the basin, while the combined effect of this current system and the Hinlopen tidal component cause the unsystematically varying directions in the central part of the study area. The tidewater terminus of the Austfonna ice cap is the main iceberg producer, and in particular its surging drainage basins. During main phases of iceberg production, i.e. at the end of, and shortly after surges, when the glacier front is in an extended position, strong katabatic winds may also reach the area and influence the ploughmark direction pattern, at least locally.

As the fossil plough marks are found over the entire study area, down to depths of at least 270 m, these result from a period with considerably larger icebergs. Since this entire region was glaciated during the Late Weichselian (Elverhøi & Solheim 1983), the fossil plough marks may date back to the period immediately after retreat of the Late Weichselian ice sheet. Blake (1961, 1981) found raised beaches with an age of 11 kA in northwestern Nordaustlandet, while Salvigsen (1981) recorded 10 kA old beaches at 100 m.a.s.l. at Kong Karls land. This implies that icebergs with drafts in the order of 370 m have existed in the region, which is also the reason why abundance variations in the fossil plough marks is not only a simple function of modern bathymetry.

Other features than the fossil, degraded plough marks that appear in the areas of smooth sea floor are pockmarks, "dark spots" and sediment waves. It is now largely accepted that pockmarks are formed by gas ascending through the sea floor, removing fines and preventing deposition, thereby creating a semicircular crater (King & MacLean 1970, Hovland 1983, Solheim & Elverhøi 1985). Because of the close

association found between pockmarks and dark spots, a possible explanation for the latter is that they are pockmarks in an early stage of evolution. No crater large enough to cause an acoustic shadow has been formed, but the fine sediment fractions have been brought into suspension and removed, thereby causing patches of more reflective sea floor. Currents capable of transporting sediment are indicated by the fact that sediment waves (megaripples) (Fig.17c) exist over a large part of the study area. Due to the fact that Erik Eriksenstredet terminates in sills dividing it from Hinlopenstredet and Olgastredet, the currents forming these features are most likely tidal. Oscillatory movement set up by storm generated waves could be another explanation for sediment waves at these water depths (Pfirman 1985), but as the area is ice covered through most of the stormy season, this is considered a less likely mechanism.

DOWN-CORE MINERALOGICAL VARIATIONS RELATED TO SURGING OF AUSTFONNA DRAINAGE BASINS.

As the Permian calcareous bedrock of the Bråsvellbreen drainage basin most likely differs from the basins further north, XRD analyses were carried out on a number of samples to investigate if there is a carbonate signal diagnostic of variations in sediment output from Bråsvellbreen.

The main mineral assemblage consists of 14, 10 and 7 Å minerals, Quartz, Feldspars, Dolomite and Calcite (Fig.32). To focus on variations in carbonate content, clay minerals, Quartz and Feldspar percentages are combined and termed "non-carbonates" (Table 3). Analyses were performed on three different fractions; <63 µm, <4 µm and <2 µm. In one sample, 82-229, 40-49 cm, all the silt fractions

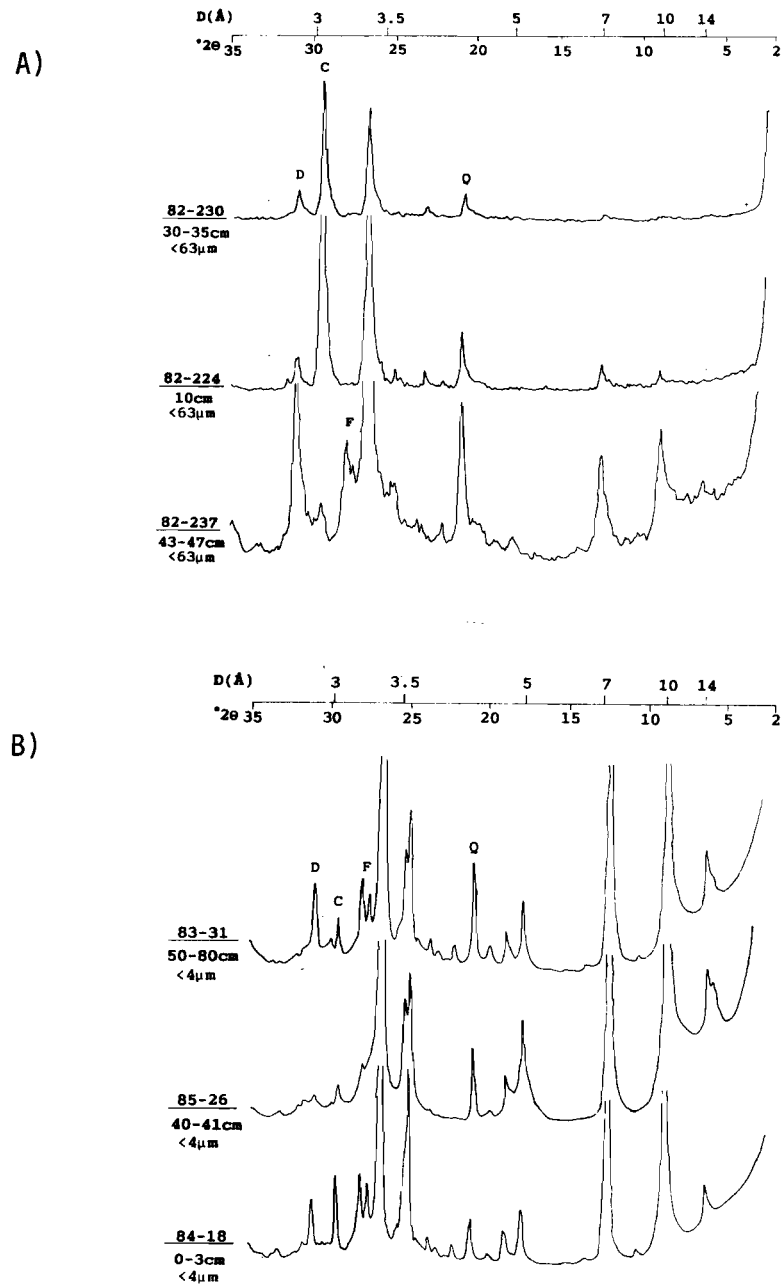


Fig.32. Xray diffractograms of some selected samples. a) <63μm samples from the surge zone (82-230), the surge moraine (82-224) and the surge-distal area (82-237). b) <4μm samples. 83-31 is the overcompacted, fine grained mud found in the surge zone. 85-26 is from the central Erik Eriksonstredet basin and 84-18 is from the surge zone of Basin 3. Note the marked difference to the Bråsvellbreen surge zone sample in a), in spite of the different fractions used in the analysis. For location, see Fig.6c.

Table 3. Mineralogy from XRD.

CA: Calcite

DO: Dolomite

RE: 14, 10 & 7 Å minerals + quartz and feldspar (non-carbonates)

| STATION | LEVEL | Fraction:<63µm | | | Fraction:<2µm | | | Fraction:<4µm | | | COMMENTS |
|---------|---------|----------------|-----|----|---------------|----|----|---------------|----|------|----------|
| | | CA | DO | RE | CA | DO | RE | CA | DO | RE | |
| 81-216 | 0-3 | 64 | 17 | 19 | | | | | | | |
| | 50-55 | 74 | 6 | 20 | | | | | | | |
| 82-230 | 0-5 | 51 | 27 | 22 | | | | | | | |
| | 30-35 | 68 | 17 | 15 | | | | | | | |
| 82-231 | 50-55 | 52 | 23 | 25 | 38 | 10 | 52 | | | | |
| | 0-5 | | | | 32 | 8 | 60 | | | | |
| 82-232 | 35-40 | 62 | 21 | 17 | | | | | | | |
| | 0-5 | 59 | 18 | 23 | | | | | | | |
| 82-233 | 46-51 | 51 | 19 | 30 | 50 | 7 | 43 | | | | |
| | 0-3 | 70 | 16 | 14 | | | | | | | |
| 82-239 | 0-5 | 51 | 25 | 24 | | | | | | | |
| | 30-35 | 60 | 21 | 19 | 45 | 8 | 47 | | | | |
| 82-323 | 0-5 | 73 | 11 | 16 | | | | | | | |
| | 58-62 | 86 | 4 | 10 | | | | | | | |
| | 90-95 | 49 | 22 | 29 | | | | | | | |
| | 100-105 | 38 | 19 | 43 | | | | | | | |
| 82-327 | 0-5 | 71 | 8 | 21 | | | | | | | |
| | 46-51 | 57 | 12 | 31 | | | | | | | |
| 83-31 | 50-80 | | | | | | | 2 | 6 | 92 | |
| 83-32 | 65-70 | | | | | | | 8 | 5 | 87 | |
| 84-17 | 0-5 | | | | | | | 3 | 5 | 92 | |
| 84-18 | 0-5 | | | | | | | 5 | 5 | 90 | |
| 82-224 | 0-20 | 66 | 12 | 22 | 58 | 2 | 40 | | | | |
| 82-234 | 0-3 | 55 | 20 | 25 | | | | | | | |
| 80-37 | 0-2 | | | | | | | 0 | 5 | 95 | |
| | 15-17 | | | | | | | 0 | 6 | 94 | |
| | 55-56 | | | | | | | 0 | 4 | 96 | |
| | 87-88 | | | | | | | 0 | 3 | 97 | |
| 81-136 | 47-50 | 0 | 18 | 82 | | | | | | | |
| 82-225 | 0-5 | 66 | 14 | 20 | | | | | | | |
| | 68-72 | 42 | 22 | 36 | | | | | | | |
| 82-226 | 0-20 | 76 | 10 | 14 | | | | | | | |
| 82-229 | 0-5 | 38 | 23 | 39 | 29 | 8 | 63 | | | | |
| | 18-22 | 20 | 23 | 57 | 7 | 6 | 87 | | | | |
| | 40-49 | 9 | 53 | 38 | | | | | | | 32-63µm |
| | | 5 | 39 | 56 | | | | | | | 16-32µm |
| | | 4 | 28 | 68 | | | | | | | 8-16µm |
| | | 0 | 21 | 79 | | | | | | | 4-8µm |
| | | 8 | 15 | 77 | | | | | | | 2-4µm |
| | 0 | 0 | 100 | | | | | | | <2µm | |
| 82-237 | 0-3 | 35 | 19 | 46 | | | | | | | |
| | 43-47 | 5 | 22 | 73 | 0 | 5 | 95 | | | | |
| | 95-100 | 9 | 19 | 72 | 9 | 0 | 91 | | | | |

| Table 3. contd. | | Fraction: <63 μ m | | | Fraction: <2 μ m | | | Fraction: <4 μ m | | | COMMENTS | |
|-----------------|---------|-----------------------|----|----|----------------------|----|----|----------------------|----|-----|----------|--|
| STATION | LEVEL | CA | DO | RE | CA | DO | RE | CA | DO | RE | | |
| 82-321 | 0-2 | | | | | | | 17 | 8 | 75 | | |
| | 6-7 | | | | | | | 9 | 7 | 84 | | |
| | 8-9 | | | | | | | 7 | 7 | 86 | | |
| | 10-11 | | | | | | | 5 | 6 | 89 | | |
| | 12-13 | | | | | | | 4 | 3 | 93 | | |
| | 14-15 | | | | | | | 3 | 3 | 94 | | |
| | 16-17 | | | | | | | 2 | 2 | 96 | | |
| | 20-21 | | | | | | | 2 | 2 | 96 | | |
| | 23-24 | | | | | | | 2 | 2 | 96 | | |
| | 26-27 | | | | | | | 2 | 2 | 96 | | |
| | 29-30 | | | | | | | 3 | 2 | 95 | | |
| | 32-33 | | | | | | | 4 | 3 | 93 | | |
| | 36-37 | | | | | | | 6 | 4 | 90 | | |
| | 39-40 | | | | | | | 4 | 3 | 93 | | |
| 83-29 | 0-6 | | | | | | | 34 | 8 | 58 | | |
| | 40-45 | | | | | | | 4 | 7 | 89 | | |
| | 60-65 | | | | | | | 34 | 5 | 61 | | |
| | 100-105 | | | | | | | 73 | 4 | 23 | | |
| 84-11 | 0-5 | | | | | | | 0 | 3 | 97 | | |
| | 20-25 | | | | | | | 0 | 0 | 100 | | |
| | 33-36 | | | | | | | 2 | 0 | 98 | | |
| 84-13 | 0-4 | | | | | | | 0 | 0 | 100 | | |
| | 10-13 | | | | | | | 0 | 0 | 100 | | |
| | 30-33 | | | | | | | 3 | 0 | 97 | | |
| | 45-48 | | | | | | | 6 | 2 | 92 | | |
| | 51-54 | | | | | | | 0 | 0 | 100 | | |
| 84-16 | 61-64 | | | | | | | 3 | 0 | 97 | | |
| 85-26 | 0-5 | | | | | | | 4 | 5 | 91 | | |
| | 0-4 | | | | | | | 0 | 4 | 96 | | |
| | 7-8 | | | | | | | 0 | 3 | 97 | | |
| | 10-13 | | | | | | | 0 | 3 | 97 | | |
| | 17-18 | | | | | | | 2 | 2 | 96 | | |
| | 20-21 | | | | | | | 0 | 0 | 100 | | |
| | 23-24 | | | | | | | 3 | 3 | 94 | | |
| | 27-28 | | | | | | | 1 | 2 | 97 | | |
| | 33-36 | | | | | | | 3 | 3 | 94 | | |
| | 40-41 | | | | | | | 2 | 2 | 96 | | |
| | 46-50 | | | | | | | 3 | 0 | 97 | | |
| | 60-63 | | | | | | | 6 | 0 | 94 | | |
| | 80-85 | | | | | | | 12 | 0 | 88 | | |
| | 120-123 | | | | | | | 12 | 0 | 88 | | |
| | 85-28 | 0-4 | | | | | | | 0 | 5 | 95 | |
| | | 15-18 | | | | | | | 0 | 0 | 100 | |
| | | 40-44 | | | | | | | 3 | 0 | 97 | |
| 85-29 | 0-3 | | | | | | | 5 | 6 | 89 | | |
| | 18-22 | | | | | | | 0 | 5 | 95 | | |
| | 33-37 | | | | | | | 0 | 3 | 97 | | |
| | 60-64 | | | | | | | 0 | 2 | 98 | | |
| | 100-105 | | | | | | | 9 | 2 | 89 | | |

were also analyzed. Quantification of the diffractograms was done by multiplying the top height with the width at the 50 % intensity level (Norish & Taylor 1962). Analyses were first performed on the <63 mm fraction and subsequently on selected samples of the <2 mm fraction. This procedure showed that the calcite and dolomite contents decreased significantly relative to the non-carbonate group of minerals in moving from the coarse silt to the clay fraction (Fig.33). The high dolomite sample 82-229, 40-49 cm, shows that the proportion of dolomite decreases more rapidly than calcite with the reduction in grain size. This test showed that carbonates should be present at least in the finer silt fractions, which also could be transported into the deeper basin. The remaining analyses were performed on the <4 μm fraction.

The general trend (Fig.34) in the surge zone sediments outside Bråsvellbreen is a dominance of calcite, with values as high as 86 % in the <63 mm fraction. Dolomite content is lower, with an average of 15-20 %. These percentages decrease in the clay fraction, but still calcite content ranges between 32 and 50 %. Although the number of measurements is small in each core, there seems to be no systematic down-core change. Considering the unsorted, homogeneous character of the surge zone diamictons, this is also to be expected.

Two surface samples from the surge zone of Basin 3 show only 3-5 % calcite and dolomite in the <4 mm fraction, thereby demonstrating that Basin 3 drains non-carbonate rocks and that calcite is an adequate tracer for sediments delivered from Bråsvellbreen.

The most anomalous mineralogy found in the surge zone samples is that of the overconsolidated mud sections of cores 83-31 and 83-32 (Table 3, Fig.34). 92 and 87 % non-carbonates in the <4 mm fraction show that this material has larger input from other sediment sources than the surrounding diamictons.

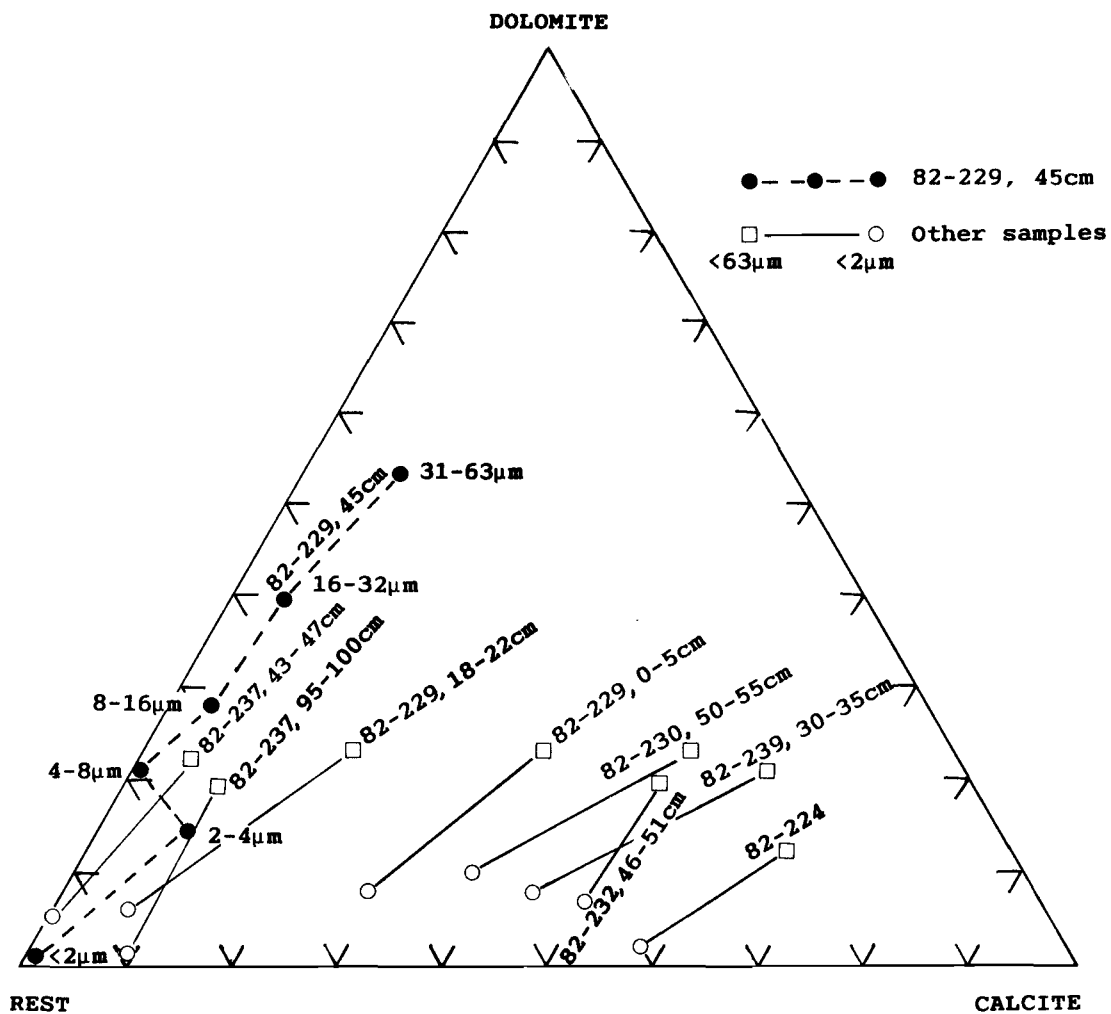


Fig.33. Ternary diagram showing the variations in Calcite, Dolomite and "non-carbonates" with changing grain size in the <63μm fraction.

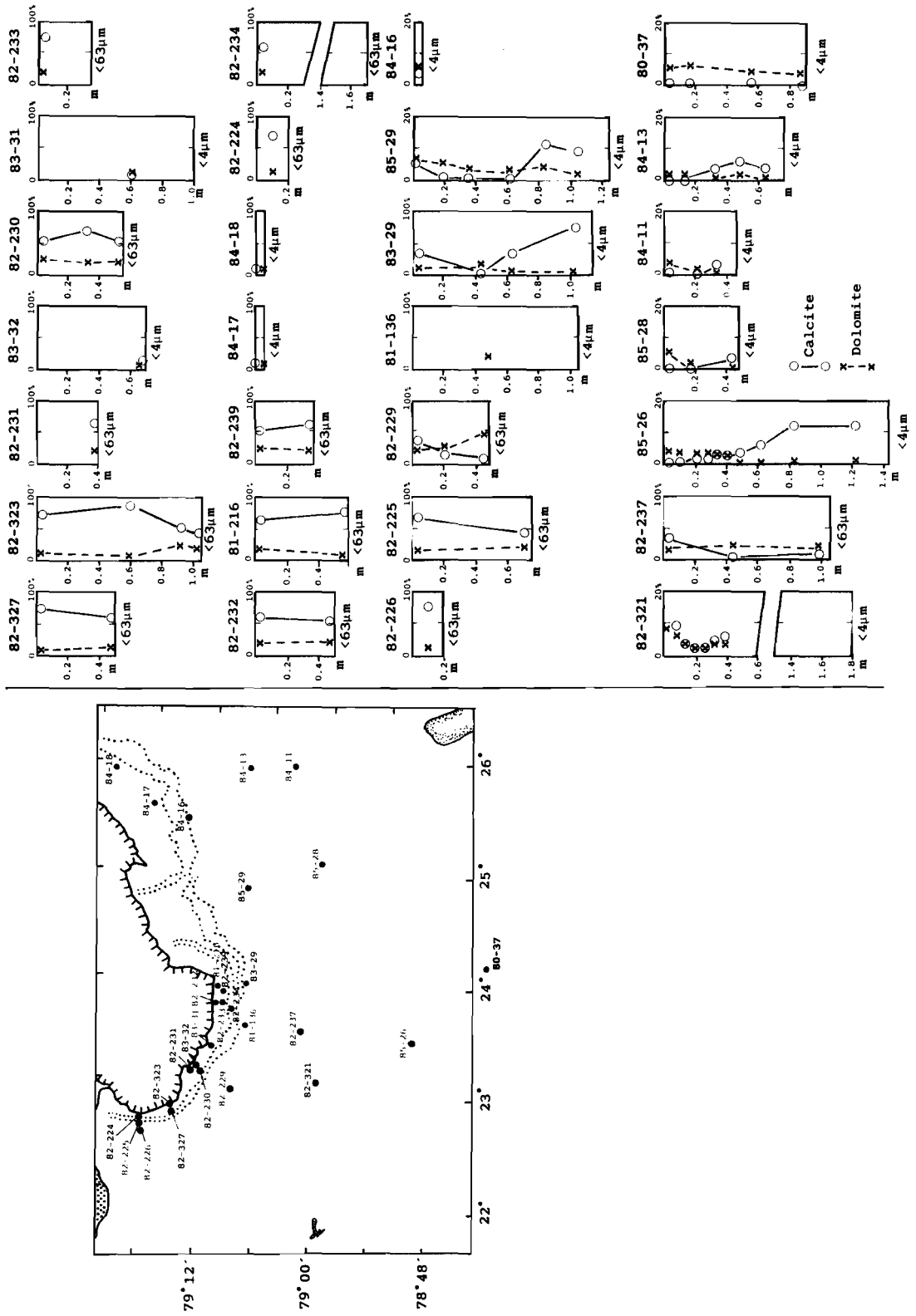


Fig.34. Calcite and Dolomite content in all analysed samples. Note variable horizontal (%) scale in the lower two rows of cores.

Only two samples from the surge moraine ridge are analyzed. These show carbonate contents of the same magnitude as the surge zone diamictons. From the homogeneous character of the surge moraine cores (Fig.20), the two samples are considered representative.

The surge-distal regions show more variation in mineralogy than the surge zone and the moraine. This might be expected since the sediments in the latter regions are deposited from and in direct contact with the Bråsvellbreen glacier, while further out the Bråsvellbreen sediments will be diluted with material brought in with currents, icebergs and sea ice from other source regions.

In the northwestern part of the area outside the surge moraines, cores 82-225 and 82-226 show carbonate contents similar to those of the surge zone in overconsolidated diamictons, apparently similar to the surge zone sediment. Core 82-229, somewhat further east (Fig.34) shows high calcite content in the top sediment, decreasing downcore, while the dolomite content is considerably higher in the bottom of the core than in the top. This also corresponds with an increase in shear strength in the bottom of the core (Fig.21). Thus it seems that the upper and lower halves of this core have experienced different deposition and loading history. Core 83-29, which also is outside the surge moraine ridge in the Bråsvellbreen area, similarly has a high calcite content in the <4 mm fraction of the surface sample (34 %) and in the lower half (34-73 %). The 40-45 cm level, which also corresponds to less sandy and gravelly grain size distributions, has only 4 % calcite.

There is a general tendency of decreasing carbonate content away from Bråsvellbreen, both southwards (82-237 & 82-321 > 85-26 > 80-37) and eastwards (82-237 > 85-29 > 84-11 & 84-13). The most significant change is probably in the calcite content (e.g. 80-37, with no calcite throughout the core). Two cores, 82-321 and 85-26, were analyzed in

greater detail (Fig.34). 82-321 shows a decrease in both calcite and dolomite from the surface to approximately 20 cm, and then a slight increase again down to 40 cm, the largest changes being in the calcite content. Calcite content is zero in the upper 13 cm of 85-26. However, the surface sediment was lost for this core during retrieval of the liner (Martinsen 1985). It then varies in the 1-3 % range before steadily increasing to 12 % in the lower part of the core. Dolomite is 4 % in the top and decreases to zero at 46 cm. Core 85-29, which is the core east of Bråsvellbreen that is closest to the end moraine, shows a calcite minimum in the interval 20-60 cm, increasing to around 10 % in the lower part of the core. The remaining of the eastern cores, 85-28, 84-11 84-13 seem to have a small calcite increase below 20 cm.

To summarize, the above discussion shows that carbonate content, in particular calcite, can be used as a qualitative indicator of sediment input from the Bråsvellbreen drainage basin. While the generally homogeneous surge zone -and surge moraine cores show little systematic variation in mineralogy, several cores in more distal locations show similar trends of variation that may be ascribed to variations in Bråsvellbreen sediment yield. This signal, although possibly filtered due to undersampling and bioturbational mixing, may hence give indications of previous surges or periods with varying surge frequency, and possible effects of these on sedimentation rates, if used additionally to dating.

Carbon content.

The total carbon content (TC) of the surge zone and surge moraine material is generally high, around 6 % (Fig.35a and Table 2). Except for the assumed Late Weichselian till in core 82-226, the values are lower in the surge-distal zone, 2.5-4.7 %. For the total organic

TOTAL CARBON VS. TOTAL ORGANIC CARBON

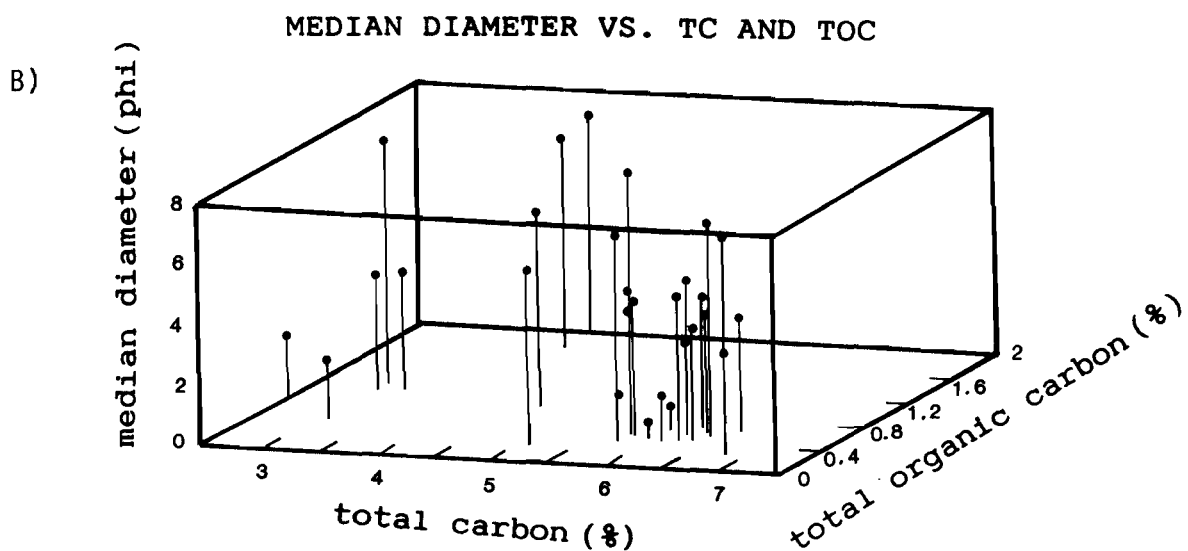
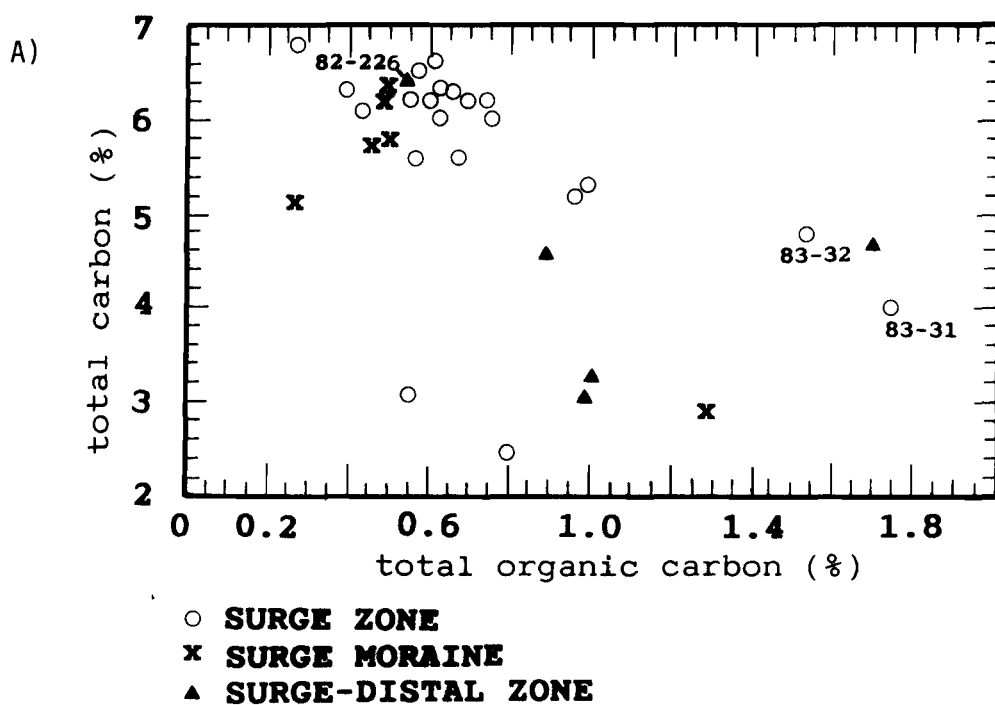


Fig.35. a) plot of total carbon (TC) versus total organic carbon (TOC). b) TC and TOC plotted versus median grain diameter.

carbon (TOC), the values are generally small in the surge zone and the surge moraine samples, with the majority between 0.4 and 0.8 %. In the surge-distal zone, on the other hand, values are between 0.9% and 2.0%. The above numbers show that in the surge zone and surge moraine the majority of the carbon results from carbonate minerals transported from the Permo-Carboniferous bedrock of the adjacent parts of Nordaustlandet, and that this amount is reduced relative to the organic carbon in the more distal parts of the basin. As most of the carbon is found in the silt fraction, the difference is a function of transport distance, in addition to increased dilution by sediments from other sources than the Bråsvellbreen drainage basin, in the distal areas. This is further demonstrated by plotting TOC and TC versus median grain diameter (Fig.35b). The TC value drops off in the fine end of the plot, while the opposite is true for TOC. Both changes in slope occur at approximately ϕ_6 , which demonstrate the importance of this grain size boundary. Most of the carbonate rock fragments occur mainly in the fractions $>0.016\text{mm}$. The organic carbon is found mainly in the fine silt -and -clay fractions, although the increase at this grain size may also partly result from lack of dilution by the rock fragments.

The organic carbon may be either primary or redeposited. TOC values for Late Weichselian sediments in the Barents Sea are mainly found to consist of reworked, Mesozoic coal and dark shale fragments, while Holocene sediments may contain significant amounts of recent carbon (Forsberg 1983). Primary production decreases considerably northwards in the Barents Sea, and is an order of magnitude less at 80°N than in the area of the oceanic polar front at approximately 74°N (Rey et al. 1987). However, the variation should not be significant within the study area. Hence, whereas the TOC values in the more proximal regions may represent mostly primary carbon, the

increased values in the surge-distal zone probably reflect increased influx of recycled carbon, for instance from Mesozoic coal beds in Kong Karls Land.

The most distinct deviation from the trend described above is again the compacted mud sections of cores 83-31 and 83-32 (Fig. 34a). These clearly fall within the highest TOC values measured in the surge-distal zone. However, the number of analyses in surge-distal samples is too small to give a representative average for this region, and a better comparison is average values for Barents Sea Holocene muds, which show comparable values, in the range of 1-2 % (Elverhøi et al. in press). Among the surge-distal zone samples, the most comparable in appearance is the muddy mid-section of 82-237 (Fig.20d), which again is similar to northern Barents Sea Holocene muds, both in terms of colour and grain size distribution.

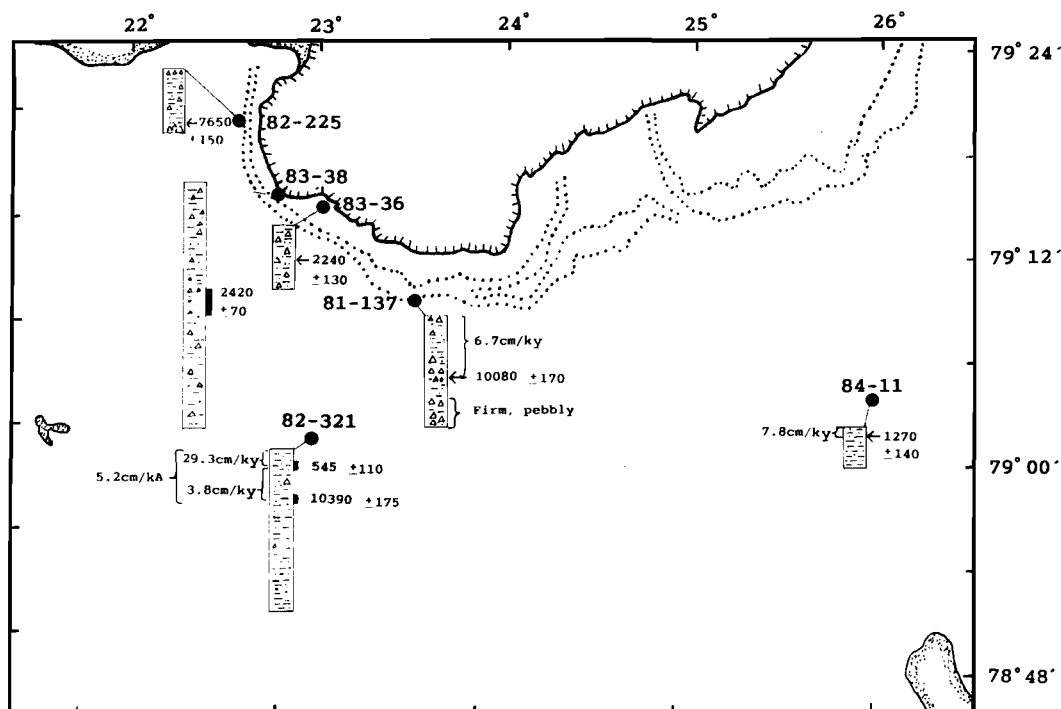
SEDIMENTATION RATES.

Whether the surging behaviour of glaciers has any effect on sedimentation and sedimentary processes outside the region directly influenced by the glacier is an important question in the interpretation of older sequences and formerly glaciated areas. The main problem in Erik Eriksenstredet, and also for the rest of the northern Barents Sea, is to obtain datable material. Seven samples have been dated from the study area (Fig.36). The three samples lab. referenced T have been dated by conventional ^{14}C techniques, while the four Ua samples were dated by accelerator methods. Datable shelly material is rare, and to obtain a sufficiently large sample of foraminifer tests it is necessary to pick all individuals from a relatively large interval (Fig.36). Resolution is therefore limited. For statistical significance a larger number of analyses would be necessary, but some inferences can be extracted from the

obtained dates in terms of sedimentation rates.

The two dates from the surge zone (cores 83-36 and 83-38) are both shell fragments from diamicton in the intermediate shear strength range, previously interpreted to result from reworking and loading by the surging glacier. Due to the reworking, the dates only give a maximum age for the sediment. Thus they confirm that this is not Late Weichselian (or older) till, but results from advance(s) since approximately 2300 y.B.P.

In the two innermost cores in the surge-distal zone (82-225 and 81-137), sedimentation rates of 8.0 and 6.7 cm/ky (Fig.36) calculated down to the dated intervals, are somewhat higher than the average 2-5 cm/ky Holocene rates reported by Elverhøi and Solheim (1983) for the central Barents Sea. As the highest rates, 8 cm/ky in 82-225, only range back to 7650 y.B.P., there could be a trend towards increased rates with decreasing age. The difference is small, however, and could also be due to local variations. It should also be noted that core 82-225 is located in an area which most likely is strongly affected by recent iceberg gouging. 81-137, on the other hand is located in a smooth region, where no, or very little ice gouging has been detected. Core 82-321, which is further away from the glacier, and in a region without recent iceberg ploughing, shows large variations in sedimentation rate with time. Assuming the ages represent the middle of the analysed intervals, the calculated sedimentation rate is 29.3 cm/ky during the last 545 years and only 3.8 cm/ky as an average between 545 and 10390 y.B.P. The total average is 5.2 cm/ky since 10390 y.B.P., which is lower than in the two cores discussed above. Thus considerable variation in sedimentation rates may be undetected due to undersampling. Core 84-11, further east and away from the coast (Fig.36), has a sedimentation rate of 7.8 cm/ky back to 1270 y.B.P. at the



| Core | Level | Lab.ref. | Material. | ¹⁴ C age |
|--------|-----------|----------|--|---------------------|
| 82-225 | 61cm | T-5234 | <i>Mya truncata</i> unruptured | 7650+-150 |
| 83-36 | 36-38cm | T-5830 | Shell fragments | 2240+-130 |
| 83-38 | 120 150cm | T-5829 | Shell fragments | 2420+-70 |
| 81-137 | 68cm | Ua-302 | <i>Portlandia arctica</i> Life position | 10080+-170 |
| 82-321 | 13-20cm | Ua-300 | <i>Astarte sulcata</i> 1 valve | 545+-110 |
| 82-321 | 50-58cm | Ua-301 | Foraminifera | 10390+-175 |
| 84-11 | 10cm | Ua-303 | <i>Portlandia arctica</i> Life position | 1270+-140 |

Fig.36. a) Table of dated samples. b) Map showing cores with C14 dates and calculated linear sedimentation rates. Bulk densities are not taken into consideration.

10 cm level. Variations corresponding to the high rates in the last 545 y.B.P. in core 82-321 is therefore unlikely to have occurred in this region.

Considering the location in the vicinity of a surging glacier, it may be justified to relate variations in sedimentation rate to oscillatory glacier behaviour. Increased input from the Bråsvellbreen drainage area to central parts of the basin, which also receives sediment from other sources, should result in a carbonate increase. The upper 40 cm of 82-321 was analyzed at intervals of 2-3 cm (Fig. 34). Both calcite and dolomite fall from relatively high values in the top to a minimum between 16 and 27 cm, before they rise between 27 and 36 cm and then drop down a little to 40 cm. The high values in the upper part correspond well with the increased sedimentation rate calculated for this interval. The curves are smooth, and no feature indicative of single surge events can be identified. However, considering the previous discussion on present-day deposition outside the meltwater outlets, it seems unlikely that a short-term event like a surge would result in a sediment layer thicker than 2-3 cm 25 km off the glacier front. Mixing through bioturbation will further mask separate signals. It is therefore more likely that intervals of higher carbonate content mark periods of increased surge activity. The increase below 27 cm may then result from another period of relatively frequent surging. Similar down-core distributions of carbonates are also recognized in other cores (Fig.34), although not as distinct for both calcite and dolomite as in 82-321. Most of the other cores, however have a less dense sampling interval.

In summary, surge activity may have a relatively large effect on sedimentation rates over short time intervals. The resulting sediment layers are thin however, due to the short time intervals involved.

Averaging over longer periods, for instance the Holocene, the effect seems restricted in the case of Bråsvellbreen, but could be significant if there were periods of more frequent surging. A situation in which most of the deposition off Bråsvellbreen took place during the surge periods, with significantly lower rates in other periods, cannot be excluded. However, this seems a less likely explanation because a larger difference in the average sedimentation rates between station 81-137, which is located immediately outside the distal part of the surge moraine, and core 82-321, 25 km outside the moraine, would then be expected.

Extrapolating the mean sedimentation rates downwards from the oldest dated interval in core 81-137, gives an age of 13000 y.B.P. for the top of the firm, pebbly material (Fig.36) of acoustic Unit 5, interpreted to be the Late Weichselian till. This implies deglaciation of the region at 13 kA. Core 82-321, on the other hand has at least 1.2 m of soft, pebbly mud below the oldest dated interval of 10390 y.B.P. Possible explanations for this are:

- a) The area was not covered by grounded ice during the Late Weichselian.
- b) Sedimentation rates were higher than in the area of core 81-137.
- c) The thickness of soft, pebbly mud is due to down slope mass movement.
- d) The date in 82-321 is in error, due to mixed ages of the dated foraminifer tests.

Based on previous discussions on the existence of a Late Weichselian Barents Sea ice sheet (e.g. Elverhøi & Solheim 1983), a) seems unlikely. b) appears more likely, and could be caused by winnowing/non-deposition in shallow regions and enhanced deposition in deeper regions. A short time lag in deglaciation of the two locations is also likely due to the differences in water depth. A glacier front

situated on the shallow shoulder in the proximity of 82-321 could supply relatively large sediment volumes in a short time interval, as is reported from other ice-proximal areas (e.g. Elverhøi et al. 1983). However, although no slump indications have been observed in the vicinity of 82-321, neither c) nor d) can be excluded until more dates are obtained from this region.

CONSOLIDATION

The main process taking place in the surge zone during post surge stagnation is that of gravity loading as the ice comes to rest. The two main effects of this are formation of the local topography through redistribution of mobile sediments by subglacial pressure gradients and compaction of the subglacial sediments. Loading by the surged glacier is a likely cause of the wide range of shear strengths measured in the sediments above the assumed Late Weichselian till surface, despite a relatively short time interval. To investigate the consolidation characteristics of the material, oedometer tests were carried out (Fig.37) on two samples; one from the surge zone (station 82-232.1, at the 10 cm level) and one from the area outside the surge moraine (82- 237, 30 cm level).

At station 82-232, overconsolidated material was encountered at the sea floor, and only the core cutter and catcher of the vibrocorer recovered any sample. Sample disturbance can not be excluded, but the firm ($S_u=77$ kPa) and apparently cohesive material did not appear disturbed. Pre-consolidation stress (P_c') was calculated using Casagrande's (1936) method. Due to a weakly defined deflection point on the curve (Fig.37a), P_c' cannot be defined exactly, but falls in the range 300-400 kPa.

The ice thickness over station 82-232 immediately after the surge is uncertain, but based on the present-day glacier surface profile, a

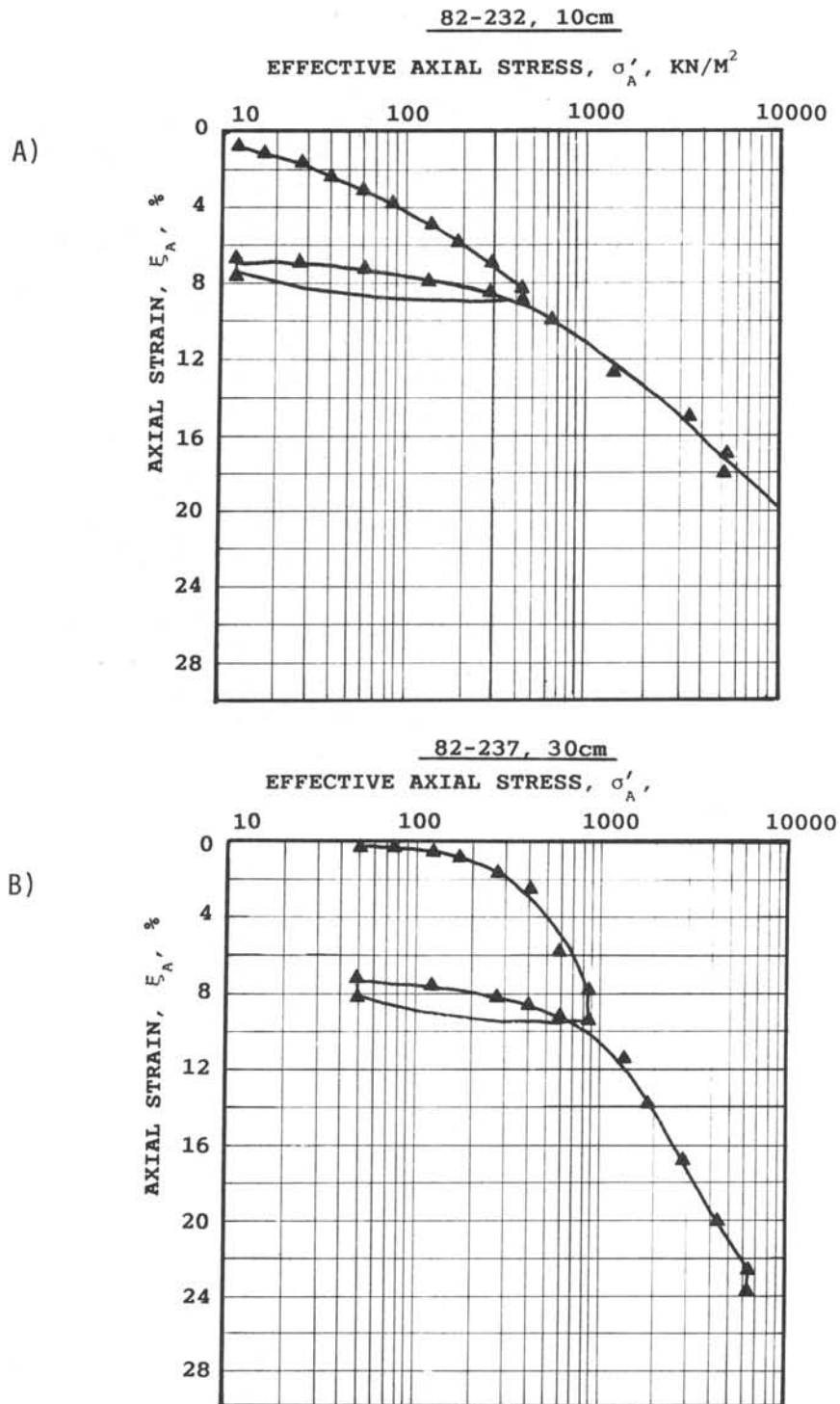


Fig.37. Consolidation curves (Oedometer test) for two samples outside Bråsvellbreen. A) In the surge zone. B) Outside the surge moraine. Note that only the core cutter and catcher recovered sediment in 82-232.

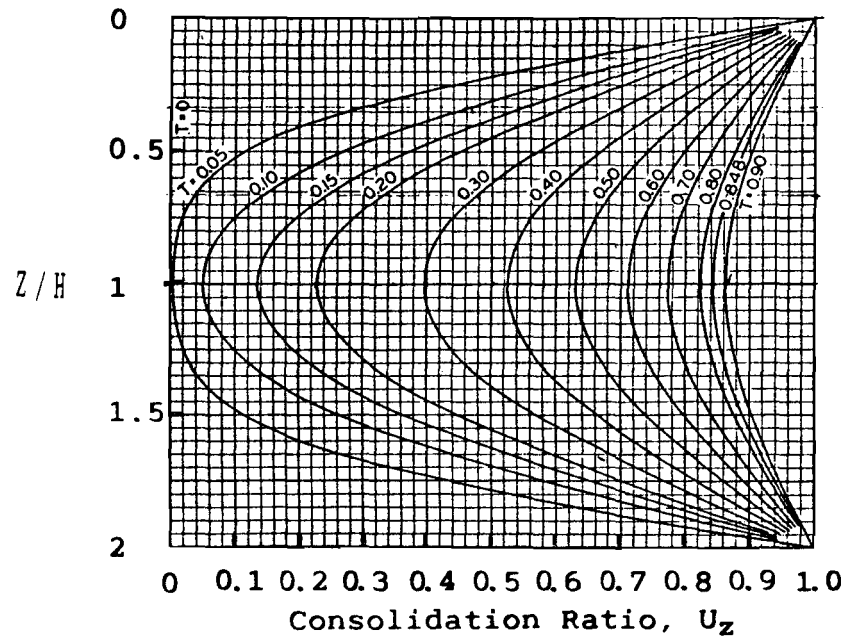


Fig.38. Consolidation as a function of depth and time factor. From Taylor (1942). z = depth to sample, H = total drainage distance.

thickness above sea level in the order of 50-70 m is likely. As the water depth in this region is nearly 100 m, the ice volume exerting a net load on the substratum would have a thickness of 40-60 m. The load exerted would then be 350-530 kPa. When uncertainties both in calculation of P_c' and in estimated ice load are taken into account, the P_c' found from the oedometer test may clearly result from the ice load.

Terzaghi consolidation theory (Taylor 1942) has been used to estimate the time required to obtain the observed consolidation with an ice load of 600 kPa. The consolidation curve (Fig.37 A) shows this to correspond to approximately 10 % deformation. The time t necessary to obtain this deformation, can be found from the following equations (Taylor 1942):

$$T=Cvt/H^2 \quad (1)$$

where C_v is a material constant found from the consolidation test, H is the total drainage distance and T is a "time factor" found from the diagram shown in Fig.38. As the Bråsvellbreen sediments probably rest on essentially impermeable Permian silicified carbonates, we consider only the upper part of the diagram.

In the diagram (Fig.38), z is the depth of the sample, and the consolidation ratio U_z can be found from

$$U_z = \frac{e_1' - e}{e_1' - e_2'} \quad (2)$$

where e_1' and e_2' are the initial and final void ratios, respectively and e is the void ratio of the present, overconsolidated sample. e_1' and e_2' can be found from the consolidation test, while e is found from the general relation between water content (w) and void ratio of

a 100 % saturated sediment;

$$e = w \rho_s / \rho_w \quad (3)$$

where ρ_s and ρ_w are densities of grains and water respectively. Grain density is taken as 2.7 g/cm^3 , and the water content of unloaded sediment is estimated to maximum 40 % by comparison with adjacent samples from similar material (Table 2).

Hence, the following values can be used in the estimation of t : $z=0.1 \text{ m}$, $H=5 \text{ m}$, $C_v=0.4$, $e=0.721$, $e_1'=1.08$, $e_2'=0.55$. Use of these values give a T -value of 0.02 (Fig.38). Now substituting the obtained values in equation (1) results in a required loading time of 1.25 years. This value is not to be taken too literally, it is merely meant to indicate that the time needed to obtain the present consolidation is significantly less than the actual loading time after the 1938 surge. Changing the variables of (1) and (3) within probable limits will not change this fact.

The consolidation test of core 82-237, outside the end moraine is of particular interest because the fine grained mud of this sample apparently corresponds to the overconsolidated mud found in cores 83- 31 and 83-32. Hence, obtaining consolidation characteristics of 82- 237, may provide valuable information that can be applied on the overcompacted samples.

Calculation of a P_c' (Casagrande 1936) of 40-50 kPa shows that the sample has experienced a slight load. A possible cause for this may be the action of icebergs. In any case, the pre-consolidation of 82-237 must result from processes normal to this environment, and it is most likely that the muds in cores 83-31 and 83-32 experienced similar processes prior to loading by the surging glacier. Therefore, considering the glacier loading of the samples in the surge zone, the

mud in core 82-237 may correspond to the initial state of these sediments.

In the following, core 83-31, level 75 cm (Fig.20), will be used. The deformation can be found by:

$$e = e_0 - e / 1 + e_0 \quad (4)$$

where e_0 is the initial void ratio and e the void ratio of the considered sample. This means that

$$e = e_{237} - e_{31} / 1 + e_{237}$$

Using a water content of 30% in equation (3), $e_{31} = 0.81$, and hence $e = 0.24$.

Assumed maximum ice thickness above sea level immediately after the surge is 70 m, resulting in a load of 620 kPa. From the consolidation curve of sample 82-237, this corresponds to a deformation of approximately 0.22. Taking all uncertainties in parameter estimation into account, these values (0.24 and 0.22) are sufficiently similar to state that the assumed ice load is capable of consolidating muds of the type found in core 82-237 to the state found in the overconsolidated samples 82-31 (and also 82-32).

In using the consolidation test of core 82-237 to find the time required to obtain this degree of consolidation, the same approach as for 82-232 can be used. Here $z = 0.3$ m, H is still taken as 5.0 m. This gives $z/H = 0.06$. As the deformation calculated for sample 83-31 is shown to be the maximum deformation achievable by the assumed ice load, e and e_2' in equation (2) become equal and hence $Uz = 1$. Using the values for z/H and Uz in the diagram (Fig.38) gives a $T \approx 0.9$. Now

equation (1) gives the required time, $t=9$ years, which is well within the time the sediment at 83-31 has experienced the ice load.

Andresen et al. (1979) obtained empirical relationships between S_u , P_0' , overconsolidation ratio (OCR) and plasticity index PI. 10 samples from the surge zone with the necessary parameters measured, were tested for P_c' using Andresen et al's (1979) curves. P_c' values estimated with this method range between 300 and 570 kPa, corresponding to ice thickness of 34 to 65 m. This further supports the consolidation effect of the surging glacier. Since maximum consolidation seems to occur relatively rapidly in these sediments, only the first surge cycle will have a consolidating effect. Unless they are larger, any later surges will leave the pre-consolidated sediments unaffected.

POST-SURGE DEPOSITION

The retreat phase will expose subglacial sediment and morphological features and subsequently form new features (push-moraines) as discussed previously. Meltwater discharge will probably rapidly decrease to non-surge values and again be channelized in concentrated outlets. As meltwater activity decreases, deposition through subglacial melt-out also most likely decreases, although some material may still be deposited through this process subglacially or at the front. The most important mode of sediment output and deposition is now through the main meltwater outlets (Pfirman 1984). Both field observations (Larsen 1982) and remote sensing techniques (Dowdeswell 1984) show major sediment plumes in surface waters outside the main outlets. Sea floor morphology and sedimentation outside the major outlet at the east side of Bråsvellbreen have been discussed separately (Pfirman 1984, Pfirman & Solheim in prep.) and only the main conclusions are included here. Water samples obtained in

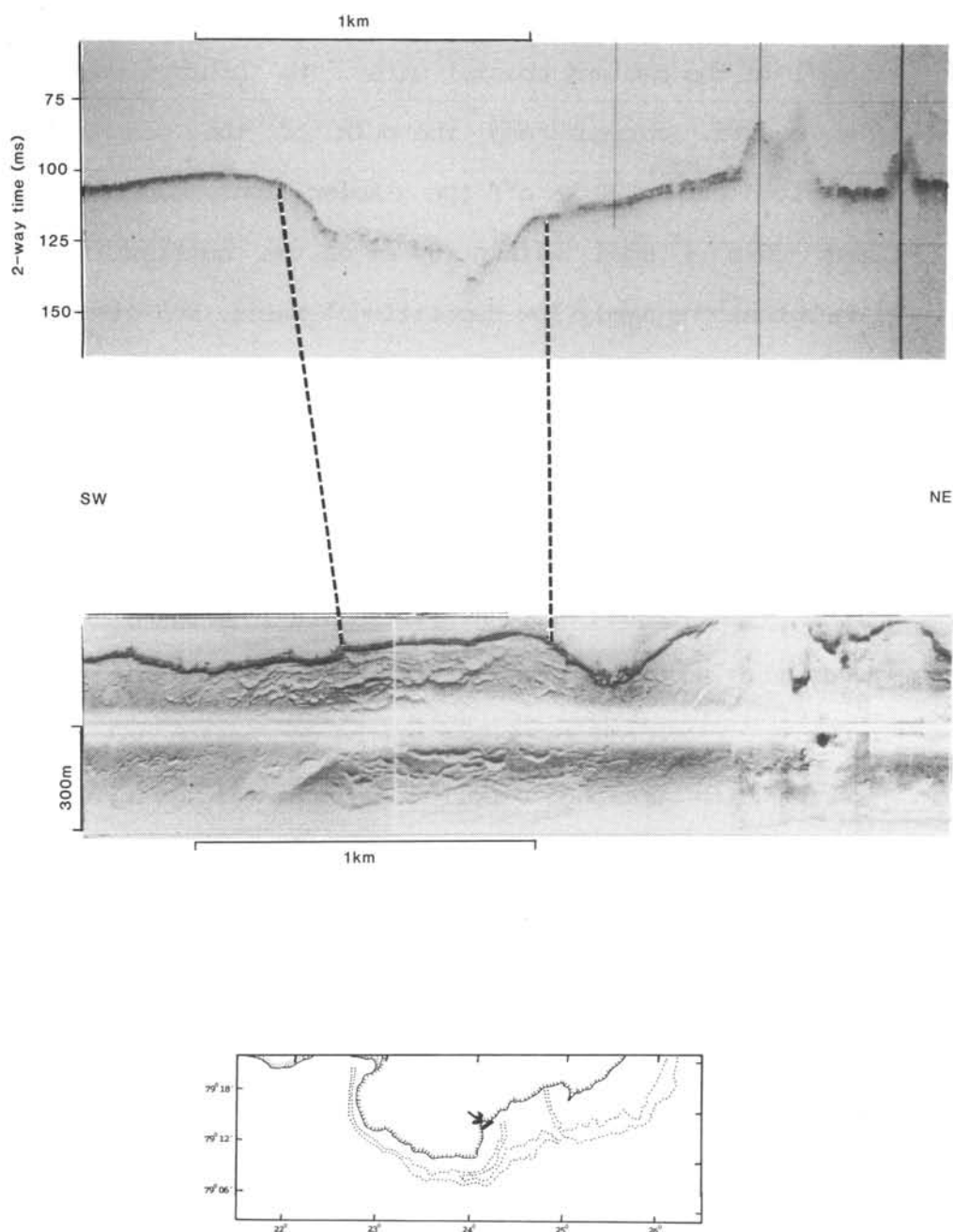


Fig.39. 3.5 kHz record (upper) and side scan sonograph (lower) across the main Bråsvellbreen meltwater outlet (arrow). (Modified from Pfirman & Solheim in prep.).

1981 from the upper 10 m within 300 m of the main meltwater outlets, contained up to 28 mg/l of particulate material, as opposed to 2 mg/l in the ambient coastal water. The turbid plume is entrained in the coastal current and the bulk of the suspended sediment is deposited within 20 km off the glacier front. Concentrations drop to less than 5 mg/l within 5 km of the outflow. The relatively low concentrations imply low depositional rates, and given the short time interval the outlet has been stable after the surge, the deposits are in general not detectable by conventional acoustic means. However, in the vicinity of the main eastern Bråsvellbreen outlet, there are thicker acoustically transparent deposits thought to result from rapid ice proximal deposition from meltwater; an 8-10 ms thick lense in a depression outside the outflow, a 3 msec. drape off the edges of the depression and some (2-4) larger mounds with up to 35 msec. of sediment (Fig.39). The former sediment is formed into annual push moraines similar to other areas close to the ice front, while the latter mounds are interpreted as beaded esker deposits in accordance with the model proposed by Banerjee & McDonald (1973). These are rapidly formed where sediment-laden meltwater encounters sea water, possibly at some distance behind the ice front proper.

Increased iceberg production.

Another important effect of glacier surges is the increased number of icebergs delivered both during the surge (Fig.5b), and during retreat. Sealers reported an order of magnitude more icebergs outside Bråsvellbreen in 1937, than during normal years (Vinje 1985). From the side scan sonar records in the regions of recent iceberg ploughing (Fig.15a) there seems to be almost complete reworking of the uppermost sediments. This usually leads to a depletion of fines,

and Vorren et al. (1983) introduced the term iceberg turbate for this type of sediment. Due to the intense fracturing of the surging ice, the majority of the icebergs are probably of intermediate to small size (Dowdeswell in prep.) causing the largest effect in the shallowest regions, most likely above 100 m water depth off Bråsvellbreen. The enhanced ploughing may contribute to increased redistribution of sediments with redeposition of fine grained material in deeper regions during surge.

EROSION BY THE BRÅSVELLBREEN SURGE.

Glacier surges are short-term, catastrophic events and may not be representative for glacial erosion in general. However, as material obviously is transported and delivered to the surge moraine and as suspension load to the surge distal area, there is a short-term effect.

There is no control on the amount of material brought in from behind the pre-surge position of the ice front. I will, in the following consider a situation where all the material delivered to the surge moraine and the region outside is eroded from the new area covered by the glacier. Since some material most certainly is brought in from other parts of the drainage area, this should give maximum values for erosion. The following figures are important:

- New area covered by the glacier after the surge: 460 km^2 .
- Volume of surge moraine ridge, only the inner ridge in the easternmost part: approximately 0.5 km^3
- Area that received material deposited from suspension, tentatively taken as a zone reaching 35 km from the ice front at maximum extent: 4100 km^2 .
- Average thickness of sediment deposited from suspension in the above area: tentatively 2 cm.
- Volume of material deposited from suspension: approximately 0.08 km^3 .

This probably represents a maximum, as most of the present-day sus-

pended sediment is shown to deposit within 20 km from the glacier. As the surge moraine configuration clearly shows that the western part of the ridge is formed during at least two surges, half the volume of this part of the ridge can be removed, which leaves approximately 0.35 km^3 material in the youngest surge moraine. Based on these values 0.43 km^3 of material has been delivered by the surging glacier. Of this, the suspension load probably plays a minor role compared to the sediment emplaced in the surge moraine. Given a source area of 460 km^2 this implies an maximum average erosion of approximately 1.0 m. As both end members are unlithified sediments, no sediment bulk densities are considered in these calculations. Considering the entire Bråsvellbreen drainage area, including the surge zone, as source area, the total erosion is 0.35 m. With more information on amount of sediment brought in from the entire drainage area, the number for erosion may be further reduced. Furthermore, the possibility that the surge moraine ridge is formed through more than two surges can not be ruled out. Although much reduced, the calculated erosion per time unit will remain considerably greater than what is usually calculated for ice sheets and presently glaciated areas (Larsen & Mangerud 1981, Laine 1980, Elverhøi et al. 1983, Elverhøi 1984). It should be kept in mind, however, that the surging Bråsvellbreen glacier eroded soft sediments with a high frequency small scale topography, similar to that found in the region today.

ICE VOLUMES AND SURGE FREQUENCIES.

The present data, combined with results from recent radio-echo soundings over Austfonna (Dowdeswell 1984, Dowdeswell et al. 1986b), provide a basis for volumetric estimates and hence estimates of surge frequencies for Bråsvellbreen and Basin 3 (Table 4). A very simplified model is used, consisting of two elements; A) The amount

of ice in the "new" part of the glacier, taken as the "surged ice", built out past the pre-surge ice front, and B) total net accumulation. A/B gives an estimate of the surge interval. The most uncertain factors are:

- 1) Position of the pre-surge glacier front (Fig.5). For Bråsvellbreen, the 1936 front published by Glen (1937) is modified to match the present coastline to the sides of the glacier proper, while in the case of Basin 3, the pre-surge ice front was assumed to form a smooth continuation of the coastline on either side of the glacier.
- 2) Mass balance and position of the equilibrium line. A mass balance curve for Midtre Lovenbreen in western Spitsbergen (Liestøl 1984) has been used, but with its position shifted with change in the height of the equilibrium line (Fig.40). Variations in precipitation and mean temperature will result in shifts of the equilibrium line rather than the shape of the curve (O. Liestøl, pers. commun. 1987). Only sparse information exists on the mass balance of Austfonna. Schytt (1964) measured accumulation rates at a number of points near the summit of the inner part of Bråsvellbreen for the 1957-58 season. These values match well with the mass balance curve for Midtre Lovenbreen, shifted to fit an equilibrium line at 300 m a.s.l.. Kristiansen and Sollid (1986) present equilibrium line heights of approximately 350 and 300 m a.s.l. for Bråsvellbreen and Basin 3, respectively. Dowdeswell and Drewry (in press) present recent data from Basin 5, northeast of Basin 3, indicating an equilibrium line at 300 - 350 m a.s.l. for this basin. Based on the above information, the equilibrium line is here placed at 300 m a.s.l. for both Bråsvellbreen and Basin 3, and the shifted mass balance curve for Midtre Lovenbreen (Fig.40) used for estimation of net annual accumulation.

- 3) The boundary between the source and receiving areas during surge is probably situated below the equilibrium line proper. The equilibrium line on Hessbreen, western Spitsbergen is situated at approximately 350 m, whereas the thickening of the snout as the result of a surge in 1973-74, starts at 250 m. A similar effect is demonstrated at Usherbreen, Svalbard (Hagen 1987). However, the surface profile did not change significantly between 250 m and 350 m (Liestøl 1974). At Austfonna, surface profiles immediately after the surge have been estimated by modifying present surface profiles from the equilibrium line to reach the maximum position, with the same height of the ice front above sea level as to-day. Although the exact shape of the glacier snout in maximum position probably was somewhat flatter than to-day, as ablation tends to steepen the profile of a glacier, the error introduced with this simplification is minor compared to 1) and 2).
- 4) Annual loss from the accumulation area. Dowdeswell and Drewry (in press) measured ice velocities of up to 47 m/year near the equilibrium line of Basin 5. Velocities of both Bråsvellbreen and Basin 3 are, however, likely to be much less, probably not more than 10 m/year (J.A.Dowdeswell, pers. commun., 1988). That there must be a difference, is also indicated by the difference in glacier surface shape (Fig.4). The annual push moraines and some fractures along the front indicate that there is a slight movement, but the exact amount is unknown. Calculations of annual surplus accumulation and hence surge interval, have been done with both zero transport and with a velocity of 10 m/year (Table 4), as these values present a reasonable ice velocity bracket for Bråsvellbreen and Basin 3.

Net accumulation averages for 100 m intervals in the

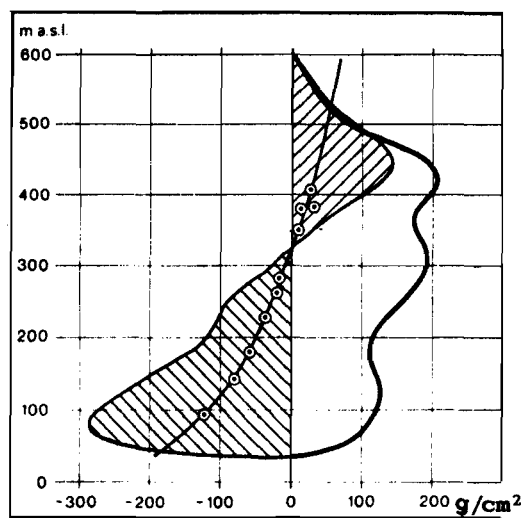


Fig.40. Mass balance curve for Midtre Lovenbreen, western Spitsbergen (from Liestøl 1983). For the Austfonna calculations, the equilibrium line was placed at 300 m a.s.l., and the curve parallel shifted.

accumulation area are summed to give the total net accumulation. All ice volumes are transformed to mass of water in tons, using an ice density of 0.9 g/cm^3 .

Table 4.

| | | Bråsvellbreen | | Basin 3 | |
|--------------------------------------|-----------|------------------------------|-----------------------|------------------------------|-----------------------|
| Total area of glacier | | 1115 km ² | | 1250 km ² | |
| Accumulation area | | 504 km ² | | 878 km ² | |
| Ablation area | | 611 km ² | | 372 km ² | |
| Surged amount of ice | | 96 km ³ | 87*10 ⁹ t | 91 km ³ | 82*10 ⁹ t |
| Net accumulation | | | 238*10 ⁶ t | | 638*10 ⁶ t |
| Annual loss from the acc. area | 0 m/year | 0 | 0 | 0 | 0 |
| | 10 m/year | 0.075 km ³ | 68*10 ⁶ t | 0.063 km ³ | 57*10 ⁶ t |
| Surplus accumulation | | 238 - 170 *10 ⁶ t | | 638 - 581 *10 ⁶ t | |
| Surge interval | | ≈ 370 - 510 years | | ≈ 130 - 140 years | |

The calculated surge interval for Bråsvellbreen confirms Schytt's (1969) estimate of "considerably more than 200 years", based partly on glacier outline from published maps. As present surface profile and

calculated driving stress (Dowdeswell 1984, 1986a) indicate that both Bråsvellbreen and Basin 3 are in a quiescent phase and most likely quite far from a new surge, the calculated surge interval for Basin 3 does not fit with a surge during Nordenskiöld's (1875) expedition in 1873. This may result from a) the observations were not from a surge, b) positioning was inaccurate and they were on a different basin, c) glaciological and climatic changes through time, d) large sources of error in the present calculations, or combinations of these. An unreported surge of these dimensions significantly after 1900 seems unlikely. Therefore, the calculated time interval may be too short. This demonstrates the difficulties in this type of calculations. In that respect c) and d) above are key points. In particular for Bråsvellbreen, variations in ice velocity and position of the equilibrium line will have a large effect on the calculated values. A shift in the equilibrium line to 350 m a.s.l. will increase the calculated surge interval to 620 and 1120 years for the 0 and 10 m/year ice velocity, respectively. When periods of several hundred years are considered, climatic fluctuations may also be important. A possibility that should be kept open, is that surges may partly have been a result of climatic deterioration during the little ice age, and that new surges, for instance of Bråsvellbreen, are unlikely under the present climatic conditions.

Although the calculations are uncertain, some main trends are noticeable:

- Large volumes of ice ($> 90 \text{ km}^3$) are involved in the surges.
- The ratio of accumulation area to ablation area at present is approximately 1:1 for Bråsvellbreen and 2:1 for Basin 3, leading to a correspondingly higher total net accumulation in Basin 3.
- The surge interval of Bråsvellbreen is long, compared to most reported surging glaciers (Meier & Post 1969).

- The calculated surge interval of Basin 3 is significantly shorter than of the somewhat smaller Bråsvellbreen. This demonstrates the effect of the size of accumulation area, although a steeper profile and narrower drainage area also most likely have an effect.

SUMMARY AND CONCLUSIONS; FACIES DISTRIBUTION OFF MARINE, SURGING GLACIERS.

- The Austfonna ice cap has several surging drainage basins. Of these, Bråsvellbreen and Basin 3 are the largest. The last Bråsvellbreen surge was documented by aerial photography in 1938. Basin 3, on the other hand, is interpreted to have surged, based on comparison with results from Bråsvellbreen in combination with glaciological information (Dowdeswell 1984, 1986a,b).
- Calculated surge frequencies show that Bråsvellbreen has a tendency to surge less frequently than Basin 3, demonstrating the importance of size of the accumulation area relative to the ablation area, height of equilibrium line and overall glacier shape.
- Surging tidewater glaciers leave a distinct suite of sea floor morphological features. The most prominent is a terminal ridge, here termed surge moraine, marking the maximum surge extent, and a system of discontinuous ridges in the area inside the moraine, here termed the surge zone. The latter ridges form a rhombohedral cross-pattern. They are related to the topography of the glacier base during surge and is formed through squeeze-up of mobile sediment during and immediately after surge.
- Bråsvellbreen has undergone at least two surges. The fossil trace of a previous surge, either considerably larger than the last surge or with a different direction of motion, is manifested as an outer surge moraine that almost merges with the Basin 3 moraine.
- Sediments in the surge zone and surge moraine are predominantly

acoustically homogeneous gravel -and pebble rich diamictons, formed by reworking of pre-surge sediments mixed with allochthonous material brought in by meltwater or directly carried by the surging ice. In the surge moraine there is a tendency towards finer grades in the distal direction. Patches of pre-surge sediments can be found relatively undisturbed, embedded in the diamictons. These are overcompacted by the glacier, but show a character distinctly different from the surrounding material. Local meltwater activity during retreat forms patches of clean, well sorted sands.

- The most important process for formation of the surge moraine is ice push, but high loads of suspended sediment are also being discharged by meltwater at the glacier front during the surge, The material is then subsequently reworked and pushed by the rapidly advancing glacier.
- Slumping and gravity flow of the rapidly deposited material modifies the surge moraine, particularly the distal slope.
- The squeeze-up ridges in the surge zone are preserved through post-surge stagnation of the ice and retreat through calving. However, after a time period dependant on glacier characteristics, the glacier returns to normal activity. Hence, Bråsvellbreen is presently forming annual push moraines. That surging glaciers are not completely stagnant for all of their quiescent phases is also documented from other Svalbard glaciers (Liestøl 1984).
- An important effect of tidewater glacier surges is a massive increase in the output of icebergs that both carry sediments and cause increased reworking of the sea floor sediments through gouging. Modern iceberg gouging is depth limited to 120 - 130m in the region, but the bulk of the surge-produced bergs were smaller. Local topography may shelter areas shallower than 120m

from scouring. During quiescent periods, the production of icebergs is low.

- With the exception of the modern iceberg ploughmarks, the region outside the surge moraines, here termed the surge-distal zone, is characterized by features "normal" to the high latitude shelf environment; fossil iceberg plough marks, pockmarks and patches of sediment waves, most likely related to tidal currents.
- Surge-distal deposits are mainly glaciomarine muds. Zones of increased pebble content may result from increased iceberg rafting during glacier surges. Increased iceberg gouging will also rework sediment into an iceberg turbate (Vorren et al. 1983), depleted in fines.
- Five acoustic units can be identified if the surge moraine is taken as separate unit (Unit 2). Unit 1 covers all surge zone diamictons above the Late Weichselian till. Changes are too frequent and local within this material to be detected by conventional acoustic surveys using a near surface source and receiver configuration. In the surge-distal zone the upper acoustic Unit 3 is only found in deep water and represents fine grained sediments, while the underlying Unit 4 has a higher coarse component. Unit 5 underlies the entire study area and mostly represents the Late Weichselian till or, locally, upper bedrock if till is absent.
- Physical properties of the sediments are largely dependant upon lithology. A median grain size of 0.016 mm appears to mark an important change in water content, total carbon and total organic carbon contents. The surge zone shows large variation in all parameters due to the unsorted character of the material and various degree of compaction, from the soft top sediment, through different degrees of compaction caused by the surge, to the underlying basal till of presumably Late Weichselian age. The surge moraine has

less sample coverage, but shows values not significantly different from the surge zone sediments, with the exception of the most overconsolidated material in the latter zone. The more muddy deposits in the surge-distal zone in general show properties characteristic for a higher proportion of finer material and lack of overcompaction. However the action of icebergs may have had a compacting effect.

- Compressional velocity and acoustic impedance show good correlation with other physical parameters, in particular with water content and plasticity index. Hence, in the case of impedance, this can be used as a reconnaissance tool for obtaining other properties in this type of environment.
- Down-core variations in mineral assemblage (here also including carbonate content) may be used to define variations in surge frequency, provided sufficiently good control on the different source areas exists. Individual surges may, on the other hand be difficult to detect in the surge-distal zone, due to mixing by bioturbation and only thin sediment layers (in the order of 1-2 cm) being deposited during the short period of a single surge event.
- The most important depositional event is emplacement of the surge moraine. Although of a local character, this feature constitutes an important sediment accumulation in an environment of generally slow deposition. If surges are frequent, the formation of surge moraines may involve large sediment volumes that are moved further offshore. As they constitute relatively significant positive topographic features, these accumulations will also be more susceptible to erosion by other processes, such as waves, currents and icebergs, than their surroundings.
- In the surge-distal region, the increase in sedimentation rate from individual surges may be large, but as the time intervals are short,

the resulting sediment layer is thin. However, if there are periods of more frequent surges, e.g. because of climatic variations, this may have a significant effect on the overall sedimentation rate over a longer time interval, for instance through the Holocene.

- The major increase in sedimentation during a surge appears to be surprisingly local, concentrated to the surge moraine. This is demonstrated by the abrupt distal termination of the surge moraine, and the fact that iceberg plough marks immediately outside it are not filled in with sediment.
- Although of short duration, surging glaciers are capable of consolidating fine grained sea floor sediments. Consolidation, however is laterally variable, probably due to the inhomogeneous and crevassed character of the surging ice proper.

In summary, surging glaciers do not produce sediment characteristics that are unique to this environment. Similar sediments can be found in most ice proximal (term essentially used in accordance with Powell (1984)) environments. However, the combination of lithology, morphology (particularly important), physical properties and sedimentation rates may be diagnostic, and these parameters may therefore be integrated in a facies model (Fig.41), where the area is divided in a proximal zone (including the surge moraine) and a distal zone. When interpreting older sequences and formerly glaciated regions, the whole system of features should be considered, and if possible, both proximal and distal regions should be identified.

ACKNOWLEDGEMENTS.

A large number of individuals and organisations have been involved in various parts of this study; Most of the data could not have been collected without the valuable assistance and enthusiasm of the crew on board the R/V Lance. The Norwegian Hydrographic Survey (NSKV) is acknowledged for giving us the possibility to take part in their hydrographic cruises in 1984 and 1985. Olav T. Egderød and Thomas Martinsen are both thanked for carrying out field operations during these cruises. Anders Elverhøi, Yngve Kristoffersen, Stephanie Pfirmann, Jørn Thiede, Olav Liestøl, Jon O. Hagen, Bjørn Andersen, Julian Dowdeswell, Michael Hambrey, Tor Løken and Toralf Berre all have given valuable, constructive criticism to various parts of the manuscript. Espen Kopperud, Donald Tumasonis and Petter Antonsen did the final drafting of the figures. A part of the study was carried out while the author was funded by the Office of Naval Research (ONR), grant no. N 00014-81-G-0001 to Y. Kristoffersen. ARCO Norway Inc. is acknowledged for providing funds for parts of the geotechnical analyses. The Norwegian Petroleum Directorate (NPD) sponsored and cooperated in the 1980 and 1983 cruises. Funds for meetings with J.A.Dowdeswell and colleagues at the University College of Wales, Aberystwyth, to integrate geological and glaciological data, were provided by NATO grant no. 0747/87.

REFERENCES

- Andrews, J.T. 1973: The Wisconsin Laurentide ice sheet: dispersal centers, problems of rates of retreat, and climatic implications. Arctic and Alpine Research, 5, 185-199.
- Aagaard, K., Foldvik, A., Gammelsrød, T. & Vinje, T. 1983: One-year records of current and bottom pressure in the strait between Nordaustlandet and Kvitøya, Svalbard, 1980-81. Polar Research, 1 n.s., 107-113.
- Ahlmann, H.W. 1933: Scientific results of the Swedish-Norwegian Arctic Expedition in the summer of 1931. Part VIII. Glaciology. Geografiska Annaler, 15, 161-216, 261-295.
- Akal, T. 1972: The relationships between the physical properties of underwater sediments that affect bottom reflection. Marine Geology, 13, 251-266.
- Andersen, J.L. & Sollid, J.L. 1971: Glacial chronology and glacial geomorphology in the marginal zones of the glaciers Midtdalsbreen and Nigardsbreen, South Norway. Norsk geografisk Tidsskrift, 25, 25, 1-38.
- Andresen, A., Berre, T., Kleven, A. & Lunne, T. 1979: Procedures used to obtain soil parameters for foundation engineering in the North Sea. Norwegian Geotechnical Institute, Publication no. 129, 1-18.
- American Society for Testing and Materials (ASTM) 1983: Standard test method for pulse velocity through concrete. Designation: C597-83, 376-379.
- Banerjee, I. & McDonald, B.C. 1973: Nature of esker sedimentation. In: Jopling, A.V. & McDonald, B.C. (eds) Glaciofluvial and glaciolacustrine sedimentation. Soc. Econ. Paleont. Mineral. Spec. Publ. 23, 132-154.
- Baranowski, S. 1977: The subpolar glaciers of Spitsbergen seen against

the climate of this region. Results of investigations of the Polish scientific Spitsbergen expeditions, vol.III, 93pp.

- Bennett,R.H. & Nelsen,T.A. 1983: Seafloor characteristics and dynamics affecting geotechnical properties at shelfbreaks. SEPM Spec. Publ., 33, 333-355
- Bjørklund,G. 1985: Parallel ridges at the former ice-divide zone in Dalarna, Sweden - possible crevasse-fillings. Geografiska Annaler, 67A, 129-131.
- Blake,W.Jr. 1961: Radiocarbon dating of raised beaches in Nordaustlandet, Spitsbergen. In: Raach,G.O. (Ed.): Geology of the Arctic, 133-145, Univ. of Toronto Press.
- Blake,W.Jr. 1962: Geomorphology and glacial geology in Nordaustlandet, Spitsbergen. Unpubl. Ph.D. thesis, The Ohio State University.
- Blake,W.Jr. 1981: Glacial history of Svalbard and the problem of the Barents Shelf ice sheet. Comments, Boreas, 10, 125-128.
- Boulton,G.S. 1970: On the origin and transport of englacial debris in Svalbard glaciers. Journal of Glaciology, 9, 213-229.
- Boulton,G.S. 1972: The role of thermal regime in glacial sedimentation. In Price,R.J. & Sugden,D.E. (eds.) Polar geomorphology, Inst. Br. Geogr. Spec. Publ. 4, 1-19.
- Boulton,G.S. 1975: Processes and patterns of sub-glacial sedimentation: a theoretical approach. In Wright,A.E. and Moseley,F. (eds.) Ice ages: Ancient and modern. Seel House Press, Liverpool, 7-42.
- Boulton,G.S. 1976: The development of geotechnical properties in glacial tills. In Leggat,R.F. (ed.): Glacial till. The Royal Society of Canada, Spec. Publ., 12, 292-303.
- Boulton,G.S. & Paul,M.A. 1976: The influence of genetic processes on some geotechnical properties of glacial tills. Quart.

Journal of Engineering Geologists, 9, 159-194.

- Boulton, G.S. & Jones, A.S. 1979: Stability of temperate ice caps and ice sheets resting on beds of deformable sediment. Journal of Glaciology, 24, 29-43.
- Boulton, G.S. 1986: Push-moraines and glacier-contact fans in marine and terrestrial environments. Sedimentology, 33, 677-698.
- Bryan, G.M. 1980: The hydrophone-pinger experiment. J. Acoust. Soc. Am., 68, 1403-1408.
- Buchan, S., McCann, D.M. & Taylor Smith, D. 1972: Relations between the acoustic and geotechnical properties of marine sediments. Quart. Journ. Eng. Geol., 5, 265-284.
- Budd, W.F. 1975: A first simple model for periodically self-surging glaciers. Journal of Glaciology, 14, 3-21.
- Bugge, T. 1980: Shallow geology on the continental shelf off Møre and Trøndelag, Norway. IKU Publ. no. 104, 44pp.
- Casagrande, A. 1936: The determination of the preconsolidation load and its practical significance. Proc. 1st Int. Conf. Soil Mech. Found. Eng., Cambridge, Mass., p 60.
- Casagrande, A. 1948: Classification and identification of soils. Trans Am. Soc. Civ. Eng., 113, 901-930.
- Clapperton, C.M. 1975: The debris content of surging glaciers in Svalbard and Iceland. Journal of Glaciology, 14, 395-406.
- Clarke, G.K.C. 1976: Thermal regulation of glacier surging. Journal of Glaciology, 16, 231-250.
- Clarke, G.K.C., Collins, S.G. & Thompson, D.E. 1984: Flow, thermal structure and subglacial conditions of a surge-type glacier. Canadian Journal of Earth Sciences, 21, 232-240.
- Clarke, G.K.C., Schmok, J.P., Ommaney, S.L. & Collins, S.G. 1986: Characteristics of surge-type glaciers. J. Geophys. Res., 91, 7165-7180.

- Clukey, E.C., Nelson, H. & Newby, J.E. 1978: Geotechnical properties of northern Bering Sea sediment. U.S. Geological Survey, Open-file report, 78-408, 27pp.
- Dege, W. 1948: Das nordostland von Spitsbergen. Polarforschung, 2, 72-83, 152-163.
- Dege, W. 1949: Meine umsegelung des Nordostlandes von Spitzbergen. Festschrift zum 70. Geburtstag des Ord. Professors der Geographie, Dr. L. Mecking., Bremen-Horn, 79-96
- Denton, G.H. & Hughes, T.J. 1981: The Arctic ice sheet: An outrageous hypothesis. In: Denton, G.H. & Hughes, T.J. (eds.) The last great ice sheets. John Wiley & Sons, 437-467.
- Dolgushin, L.D. & Osipova, G.B. 1974: Surging glaciers. Priroda, 2, 85-99.
- Dowdeswell, J.A. 1984: Remote sensing studies of Svalbard glaciers. Unpubl. Ph.D. thesis, University of Cambridge, 250pp.
- Dowdeswell, J.A. 1986a: Drainage basin characteristics of the Nordaustlandet ice caps, Svalbard. Journal of Glaciology, 32, 31-38.
- Dowdeswell, J.A. 1986b: Remote sensing of ice cap outlet glacier fluctuations on Nordaustlandet, Svalbard. Polar Research, 4 n.s., 25-32.
- Dowdeswell, J.A. in prep.: Svalbard icebergs: Their nature and implications for glaci-marine sedimentation.
- Dowdeswell, J.A., Drewry, D.J., Liestøl, O. & Orheim, O. 1984a: Airborne radio-echo sounding of sub-polar glaciers in Spitsbergen. Norsk Polarinstitutt Skrifter, 182, 41pp.
- Dowdeswell, J.A., Drewry, D.J., Liestøl, O. & Orheim, O. 1984b: Radio-echo sounding of Spitsbergen glaciers: problems in the interpretation of layer and bottom returns. Journal of Glaciology, 30, 16-21.

- Dowdeswell, J.A., Drewry, D.J., Cooper, A.P.R. & Gorman, M.R. 1986: Digital mapping of the Nordaustlandet ice caps from airborne geophysical investigations. Annals of Glaciology, 8, 51-58.
- Dowdeswell, J.A. & Drewry, D.J. 1985: Place names on the Nordaustlandet ice caps, Svalbard. Polar Record, 22, 519-539.
- Dowdeswell, J.A. & Drewry, D.J. in press: The dynamics of Austfonna, Nordaustlandet, Svalbard: Surface velocities, mass balance and subglacial meltwater. Annals of Glaciology, 12.
- Drewry, D.J. 1986: Glacial geologic processes. Edward Arnold Publishers, Ltd., 276pp.
- Drewry, D.J. & Liestøl, O. 1985: Glaciological investigations of surging ice caps in Nordaustlandet, Svalbard, 1983. Polar Record, 22, 357-378.
- Dyke, A.S. & Prest, V.K. 1987: Late Wisconsinan and Holocene history of the Laurentide ice sheet. Abstracts from the 16th Arctic Workshop, Edmonton, Canada, 1987, p18.
- Eide, O. 1974: Marine soil mechanics, applications to North Sea offshore structures. Norwegian geotechnical Institute Publication no. 103, 20pp.
- Elman, S.R. 1971: Seismic investigations on the Nordaustlandet ice caps. Geografiska Annaler, 53A, 1-13.
- Elverhøi, A. 1984: Erosjon og sedimenttransport fra bredekte områder. Norsk Polarinstitutt Rapportserie, 17, 43-82.
- Elverhøi, A., Lønne, Ø. & Seland, R. 1983: Glaciomarine sedimentation in a modern fjord environment, Spitsbergen. Polar Research 1 n.s., 127-149.
- Elverhøi, A. & Solheim, A. 1983: The Barents Sea ice sheet - a sedimentological discussion. Polar Research In.s., 23-42.
- Elverhøi, A., Pfirman, S.L., Solheim, A. & Larsen, B.B. in press: Glaciomarine sedimentation and processes on high Arctic

epicontinental seas - exemplified by the northern Barents sea. Marine geology.

- Forsberg, C.F. 1983: Sedimentation and early diagenesis of Late Quaternary deposits in central parts of the Barents Sea. Unpubl. Cand.scient. thesis, University of Oslo, 120pp.
- Glen, A.R. 1937: The Oxford University Arctic Expedition North east Land, 1935-36. Geographical Journal, 90, 193-222, 289-314.
- Glen, A.R. 1941: A sub-arctic glacier cap: the West Ice of North East Land. Geographical Journal, 98, 65-76, 135-146.
- Gravenor, C.P. & Kupsch, W.O. 1959: Ice-disintegration features in western Canada. Journal of Geology, 67, 48-64.
- Hagen, J.O., Liestøl, O., Sollid, J.L., Wold, B. & Østrem, G., 1986: Subglasiale undersøkelser ved Bodhusbreen, Folgefonna. Meddelelser fra Geografisk Institutt, Universitetet i Oslo, Naturgeografisk serie, Rapport no. 4, 82pp.
- Hagen, J.O. 1987: Glacier surge at Usherbreen, Svalbard. Polar Research, 5 n.s., 239-252.
- Hambrey, M.J. & Muller, F. 1978: Structures and ice deformation in the White Glacier, Axel Heiberg Island, Northwest Territories, Canada. Journal of Glaciology, 20, 41-66.
- Hamilton, E.L. 1974: Prediction of deep-sea sediment properties: state-of-the-art. In: A.L. Inderbitzen (ed.) Deep Sea Sediments, Plenum Publ. Co., 1-44.
- Hamilton, E.L. 1980: Geoacoustic modelling of the sea floor. J. Acoust. Soc., 68, 1313-1340.
- Hare, F.K. 1976: Late Pleistocene and Holocene climates: some persistent problems. Quaternary Research, 6, 507-517.
- Harland, W.B. & Hollin, J.T. 1953: Oxford and Cambridge Spisbergen Expedition 1951. Polar record, 6, 800-803.
- Hartog, J.M. 1950: Oxford University Expedition to Nordaustlandet

- (North East Land) 1949. Polar Record, 5, 613-619.
- Hartog, J.M. & Thompson, H.R. 1950: Oxford University Expedition to North east Land, 1949. Oxford University Exploration Club Bulletin, 3, 5-10.
- Herron, S. & Langway, C.C. Jr. 1979: The debris-laden ice at the bottom of the Greenland ice sheet. Journal of Glaciology, 23, 193-207.
- Hollin, J.T. 1956: Oxford University Expedition to Nordaustlandet, 1955. Polar record, 8, 28.
- Hoppe, G. 1952: Hummocky moraine regions, with special reference to the interior of Norrbotten. Geografiska Annaler, 34, 1-72.
- Horn, D.R., Horn, B.M. & Delach, M.N. 1968: Correlation between acoustical and other physical properties of deep-sea cores. J. Geophys. Res. 73, 1939-1957.
- Horvath, E.V. & Field, W.O. 1969: References to glacier surges in North America. Canadian Journal of Earth Sciences, 6, 845-851.
- Hovland, M. 1983: Elongated depressions associated with pockmarks in the western slope of the Norwegian Trench. Marine Geology, 51, 35-46.
- Hughes, T.J. 1974: Study of unstable Ross Sea glacial episodes. ISCAP Bulletin 3: Orono, Me., Institute for Quaternary Studies, University of Maine, 93pp.
- Humphrey, N., Raymond, C. & Harrison, W. 1986: Discharges of turbid water during mini-surges of Variegated Glacier, Alaska, U.S.A. Journal of Glaciology, 32, 195-207.
- Johnson, H.D. 1981: Shallow siliclastic seas. In: Reading, H.G. (ed.) Sedimentary environments and facies, Blackwell Scientific Publications, 207-258.
- Johnson, P.G. 1975: Recent crevasse fillings at the terminus of the Donjek Glacier, St. Elias Mountains, Yukon Territory.

Quaestiones Geographicae, 2, 53-59.

- Josenhans, H.W., Zevenhuizen, J. & Klassen, R.A. 1986: The Quaternary geology of the Labrador shelf. Canadian Journal of Earth Sciences, 23, 1190-1213.
- Kamb, B. 1987: Glacier surge mechanism based on linked cavity configuration of the basal water conduit system. Journal of Geophysical Research, 92, no.B9, 9083-9100.
- Kamb, B., Raymond, C.F., Harrison, W.D., Engelhardt, H., Echelmeyer, K.A., Humphrey, N., Brugman, M.M. & Pfeffer, T. 1985: Glacier surge mechanism: 1982-1983 surge of Variegated Glacier, Alaska. Science, 227, 469-479.
- King, L.H. & MacLean, B. 1970: Pockmarks on the Scotian shelf. Geol.Soc. Am.Bull., 81, 3141-3148.
- Kristiansen, K.L. & Sollid, J.L. 1986: Svalbard, glacialgeologisk -og geomorfologisk kart, 1: 1000 000. Nasjonalatlas for Norge, Geografisk Institutt, Universitetet i Oslo.
- Lagally, M. 1932: Zur Thermodynamik der Gletscher. Zeitschrift für Gletscherkunde, 20, 199-214.
- Laine, E.P. 1980: New evidence from beneath the western North Atlantic for the depth of glacial erosion in Greenland and North America. Quaternary Research, 14, 69-96.
- Lamb, H.H. 1977: Climate: present, past and future, vol.1, Fundamentals and climate now. Methuen, London, 835pp.
- Larsen, E. & Mangerud, J. 1981: Erosion rate of a Younger Dryas cirque glacier at Kråkenes, western Norway. Annals of Glaciology, 2, 153-158.
- Larsen, T. 1982: Rapport fra Norsk polarinstituttets tokt med 'Lance' til Svalbard 6/8 - 2/9, 1982 (Tokt II). Norsk Polarinstitutt Rapportserie, no. 10, 160pp.
- Lauritzen, Ø. & Ohta, Y. 1984: Geological map, Svalbard, 1:500 000,

- Sheet 4G, Nordaustlandet. Norsk Polarinstitutt Skrifter, no.154D, 14pp.
- Lawson,D.E. 1979: Sedimentological analysis of the western terminus of the Matanuska Glacier, Alaska. U.S.Army, Corps of Engineers, Cold Regions Research and Engineering Laboratory, Report 79-9, 112pp.
- Lewis,C.F.M., Blasco,S.M., Bornhold,B.D., Hunter,J.A.M., Judge,A.S., Kerr,J.W., McLarsen,P. & Pelletier,B.R., 1977: Marine geological and geophysical activities in Lancaster Sound and adjacent fjords. Geological survey of Canada, Paper 77-1A, 495-506.
- Li,W.N. & Taylor Smith,D. 1969: Identification of sea floor sediments using underway acoustics.
- Liestøl,O. 1969: Glacier surges in west Spitsbergen. Canadian Journal of Earth Sciences, 6, 895-897.
- Liestøl,O.1974: Glaciological work in 1972. Norsk Polarinstitutt Årbok 1972, 125-135.
- Liestøl,O. 1976: Årsmørener foran Nathorstbreen? Norsk Polarinstitutt Årbok, 1976, 361-363.
- Liestøl,O. 1984: Glaciological work in 1983. Norsk Polarinstitutt Årbok 1983, 35-45.
- Liestøl,O. 1985: Glaciers of Svalbard, Norway. In: Williams, R.S.Jr. (ed.) Satellite image atlas of glaciers. U.S.Geological Survey Professional Paper, Chapter 5.0 - Europe.
- Løken,T. 1976: Geology of superficial sediments in the northern North Sea. Norwegian Geotechnical Institute, Publ. no. 114, 45-60.
- Martinsen,T. 1985: Rapport for lett-seismiske undersøkelser og geologisk prøvetaking 1985, utført i tilknytning til Norges Sjøkartverks opplodding i Barentshavet. Unpubl. report, Norsk Polarinstitutt,13pp.

- Meier, M.F. & Post, A. 1969: What are glacier surges? Canadian Journal of Earth Sciences, 6, 807-817.
- Molnia, B.F., 1983: Subarctic glacial-marine sedimentation; a model. In Molnia, B.F. (ed.) Glacial marine sedimentation. Plenum Press, New York and London, 95-144
- Moum, J., 1966: Falling drop used for grain-size analysis of fine-grained materials. Norwegian Geotechnical Institute, Publ. no. 70.
- Nordenskiöld, A.E. 1875: Den Svenska Polarexpeditionen, 1872-1873. K.Svenska Vetenskapsakademiets Handlingar, 2, no.18, 132pp.
- Norish, K. & Taylor, R.M. 1962: Quantitative analysis by X-ray diffraction. Clay Mineralogy Bull., 5, 98-104.
- Palosuo, E. & Schytt, V. 1960: Til Nordostlandet med den Svenska glaciologiska expeditionen. Terra, 72, 11-19.
- L. 1984: Modern sedimentation in the Northern Barents Sea:
- Paul, M.A. & Jobson, L.M. 1987: On the acoustic and geotechnical properties of soft sediments from the Witch Ground basin, central North sea. Unpubl. report, Department of Civil Engineering, Heriot-Watt University, Edinburgh, Scotland.
- Pessl, F. & Frederick, J.E., 1981: Sediment source for melt-water deposits. Annals of Glaciology, 2, 92-96.
- Pfirman, S. 1984: Input, dispersal and deposition of suspended sediments from glacial meltwater. Unpubl. Ph.D. thesis, Woods Hole Oceanographic Institution, 284pp.
- Pfirman, S.L. & Solheim, A. in prep.: Subglacial meltwater discharge in the tidewater glacier environment: Observations from Nordaustlandet, Svalbard archipelago.
- Powell, R.D. 1984: Glacimarine processes and inductive lithofacies modelling of ice shelf and tidewater glacier sediments based on Quaternary samples. Marine Geology, 57, 1-52.

- Powell, R. D. 1985: Iceberg calving and its influence on ice-proximal subaqueous glacial lithofacies. 14th Arctic Workshop; Land -Sea interaction, Halifax 1985, Abstract. 101-103.
- Prest, V.K. 1969: Retreat of Wisconsin and recent ice in North America. Geological Survey of Canada, Map 1257 A.
- Price, R.J. 1970: Moraines at Fjallsjökull, Iceland. Arctic and Alpine Research, 2, 27-42.
- Raymond, C.F., 1987: How do glaciers surge? A review. Journal of Geophysical Research, 92, no.B9, 9121-9134.
- Rey, F., Skoldal, H.R. & Slagstad, D. 1987: Primary production in relation to climatic changes in the Barents Sea. In: Loeng, H. (ed.) The effect of oceanographic conditions on the distribution and population dynamics of commercial fish stock in the Barents Sea. Proceedings of the third Soviet-Norwegian symposium, Murmansk 1986, 29-46.
- Richards, A.F., Palmer, H.D. & Perlow, M.Jr., 1975: Review of continental shelf marine geotechnics: Distribution of soils, measurement of properties, and environmental hazards. Marine Geotechnology, 1, 33-67.
- Robin, G. de Q. & Weertman, J. 1973: Cyclic surging of glaciers. Journal of glaciology, 12, 3-18.
- Ruddiman, W.F. & McIntyre, A. 1981: The mode and mechanism of the last deglaciation: Oceanic evidence. Quaternary Research, 16, 125-134.
- Rokoengen, K., Gunleiksrud, T., Lien, R.L., Løfaldli, M., Rise, L., Sindre, E. & Vigran, J.O. 1980: Shallow geology on the continental shelf off Møre and Romsdal. Description of 1:250 000 Quaternary geology map 6203. IKU Publ. no. 105, 49pp.

- Ruddiman, W.F. & Duplessy, J.-C. 1985: Conference on the last deglaciation: Timing and mechanism. Quaternary Research, 23, 1-17.
- Salvigsen, O. 1978: Holocene emergence and finds of pumice, whalebones and driftwood at Svartknausflya, Nordaustlandet. Norsk Polarinstitutt Årbok 1977, 217-228.
- Salvigsen, O. 1981: Radiocarbon dated raised beaches in Kong Karls Land, Svalbard, and their consequences for the glacial history of the Barents Sea area. Geografiska Annaler, 63A, 283-291.
- Salvigsen, O. & Nydal, R. 1981: The Weichselian glaciation in Svalbard before 15 000 B.P. Boreas, 10, 433-446.
- Schwab, W.C. & Lee, H.J., 1983: Geotechnical analyses of submarine landslides in glacial-marine sediment, northeast Gulf of Alaska. In Molnia, B.F. (ed.) Glacial-marine sedimentation, Plenum Press, New York and London, 145-184.
- Schytt, V. 1964: Scientific results of the Swedish glaciological expedition to Nordaustlandet, Spitsbergen, 1957 and 1958. Parts I and II. Geografiska Annaler, 46, 243-281.
- Schytt, V. 1969: Some comments on glacier surges in eastern Svalbard. Canadian Journal of Earth Sciences, 6, 867-873.
- Sharp, M. 1984: Annual moraine ridges at Skalafellsjökull, south east Iceland. Journal of Glaciology, 30, 82-93.
- Sharp, M. 1985: "Crevasse-fill" ridges - a landform type characteristic of surging glaciers? Geografiska Annaler, 67A, 213-220.
- Smith, R.A. 1976: The application of fracture mechanics to the problem of crevasse penetration. Journal of Glaciology, 17, 223-228.
- Solheim, A. & Kristoffersen, Y. 1984: The physical environment, western Barents Sea, 1:1500000, sheet B; Sediments above the upper regional unconformity: thickness, seismic stratigraphy

- and outline of the glacial history. Norsk Polarinstitutt Skrifter 179 B, 26pp.
- Solheim, A. & Elverhøi, A. 1985: A pockmark field in the central Barents Sea; gas from a petrogenic source? Polar research, 3 n.s., 11-19.
- Solheim, A. & Pfirman, S.L. 1985: Sea-floor morphology outside a grounded, surging glacier; Bråsvellbreen, Svalbard. Marine Geology, 65, 127-143.
- Solheim, A. 1986: Submarine evidence of glacier surges. Polar Research, 4n.s., 91-95.
- Sollid, J.L. & Carlson, A.B. 1984: DeGeer moraines and eskers in Pasvik, North Norway. Striae, 20, 55-61.
- Stuiver, M., Denton, G.H., Hughes, T.J. & Fastook, J.L. 1981: History of the marine ice sheet in West Antarctica during the last glaciation: A working hypothesis. In: Denton, G.H. & Hughes, T.J. (eds.) The last great ice sheets. John Wiley & Sons, 319-436.
- Taylor, D.W. 1942: Research on consolidation of clays. MIT Seies no.82, 147pp.
- Taylor Smith, D. 1975: Geophysical assessment of sea-floor properties. Oceanology International, 75, 320-328.
- Thompson, H.R. 1953: Oxford Expeditions to Nordaustlandet (North East land), Spitsbergen. Arctic, 6, 213-222.
- Thorarinsson, S. 1969: Glacier surges in Iceland, with special reference to the surges of Bruarjökull. Canadian Journal of Earth sciences, 6, 875-882.
- Vinje, T. 1985: The physical environment, western Barents Sea: Drift, composition, morphology and distribution of sea ice fields in the Barents Sea. Norsk Polarinstitutt Skrifter, 179C, 26pp.

- Vorren, T., Hald, M., Edvardsen, M. & Lind-Hansen, O.-W., 1983: Glacigenic sediments and sedimentary environments on continental shelves: general principles with a case study from the Norwegian shelf. In Ehlers, J. (ed.) Glacial deposits in north-west Europe. A.A.Balkema, Rotterdam, 61-63.
- Vorren, T. & Kristoffersen, Y. 1986: Late Quaternary glaciation in the south-western Barents sea. Boreas, 15, 51-59.
- Wensaas, L. 1986: En sedimentologisk og mineralogisk undersøkelse av bunnsedimenter (<63mm) fra det nordlige Barentshavet. Unpubl. Cand.scient. thesis, University of Oslo, 178pp.
- Weertman, J. 1969: Water lubrication mechanism of glacier surges. Canadian Journal of Earth Sciences, 6, 929-942.
- Weertman, J. 1973: Can a water-filled crevasse reach the bottom surface of a glacier? Union Geodesique et Geophysique Internationale. Association Internationale d'Hydrologie Scientifique. Commission de neiges et Glaces. Symposium on the hydrology of glaciers, Cambridge, 1969, 139-145.
- Weertman, J. 1976: Milankovitch and solar radiation variations and ice age ice sheet sizes. Science, 261, 17-20.
- Østerholm, H. 1978: The movement of the Weichselian ice sheet over northern Nordaustlandet, Svalbard. Geografiska Annaler, 60A, 189-208.

PAPER 3.

In press, Marine Geology.

Subglacial Meltwater Discharge
in the Open Marine Tidewater Glacier Environment:
Observations from Nordaustlandet, Svalbard Archipelago

Stephanie L. Pfirman

GEOMAR

Research Center for Marine Geosciences

Wischhofstr. 1-4, Geb. 4

D-2300 Kiel 14, F.R. Germany

Anders Solheim

Norsk Polarinstitutt

Postboks 158

N-1330 Oslo Lufthavn, Norway

ABSTRACT

The ice-proximal environment of the Nordaustlandet tidewater ice cap, Svalbard Archipelago, is one of the best existing analogues for understanding glacial geologic processes of northern continental shelves during initial Pleistocene deglaciation. Investigations of the proglacial region in 1980-1983 showed that the sedimentary environment is dominated by numerous meltwater outflows which discharge sediment-laden water from subglacial meltwater streams during the summer. Two large, stable meltwater outflows were observed in embayments along the southern portion of the ice front. Landsat images show that both outflows have been in approximately the same position since at least 1976. They are located at the intersection of glacial drainage basins and centered over depressions in the underlying bedrock. An "outflow valley" extending away from the ice front was observed in front of the western meltwater outflow.

Side-scan sonar profiling along the glacier front showed a 200 m wide gap in acoustic reflection at the base of the western meltwater outflow, probably caused by meltwater effluence. Enhanced sediment accumulations in this region, observed as a ~ 3 msec sediment drape in front of the outflow, and large arcuate ridges in the outflow valley, testify to the transport efficiency of the subglacial meltwater stream. Several mounds, more than 25 m high and up to 200 m wide, are observed on side-scan and 3.5 kHz profiles directly in front of the outflow. Although samples are lacking from these structures, they are most likely composed of sediment and are similar to beaded eskers observed in Pleistocene glacimarine sequences indicating locally very high sedimentation rates.

Fine-grained components of the subglacial discharge incorporated in the buoyant meltwater plume are usually entrained in a westerly coastal current. Elevated suspended particulate material concentrations are observed within the coastal waters in a region extending about 15 km perpendicular to the glacier front and at least 60 km along the ice front extending into the northwestern Barents Sea.

INTRODUCTION

Although open-marine tidewater glacier environments dominated most of the ice perimeter during Cenozoic glacial maxima in the Northern Hemisphere, depositional conditions along this type of ice front are not well known because modern-day analogues are rare. Today, glaciers generally terminate: 1) terrestrially, 2) as floating ice shelves, or 3) in restricted environments at the head of fjords. Austfonna ice cap on Nordaustlandet, the second largest island in the Svalbard Archipelago (Fig.1), has a long (~200 km) open-marine tidewater ice front, and is one of the best existing analogues for understanding depositional processes along Northern Hemisphere continental shelves during deglaciation.

Recently, several models have been proposed which provide a general framework for consideration of glacial marine sediment and sedimentary processes. According to Powell (1984), the most important variables for controlling the type of glacial debris and where and when debris is introduced into the ocean are: (1) type of glacial ice source (ice sheet or valley glacier); (2) thermal condition of a grounded glacier; and (3) type of glacier front (ice shelf or tidewater). Sediment deposits in the

proglacial region of tidewater glaciers will be influenced by currents, substrate relief and proximity to nearby ice margins (Eyles et al., 1985). Glacial ice source (Powell, 1984) and drainage basin relief (Eyles et al., 1985) determine erosion and transport mechanisms (supraglacial, englacial, subglacial) and hence determine the grainsize of erosional products (Boulton, 1975). Glacier thermal regime influences production of basal debris and meltwater which flushes debris to the ice front (Powell, 1984; Eyles et al., 1985). Ice flow dynamics and water depth determine the type of ice front; grounded tidewater or floating ice shelf, and therefore the proglacial environment.

According to the models of Powell (1984) and Eyles et al. (1985), predominately fine-grained sediment should be produced by erosion at the base of the subpolar (Schytt, 1969; Baranowski, 1977) Austfonna ice cap. Low drainage basin relief and no nunataks will result in little or no englacial or supraglacial debris. The models predict that basal erosional products will be flushed out by meltwater and transported through a subglacial drainage network to the stable or slowly retreating (Solheim and Pfirman, 1985; Dowdeswell, 1986) glacier margin. Various morphological features, such as eskers and deltas may be constructed at the outflow locations, and a moraine bank may form along the ice front.

Sedimentation and sea-floor morphology were investigated along the marine terminus of the Austfonna ice cap. Investigation along the ice front was hindered by difficult sea ice conditions which prevented sampling in some key locations. In this paper, an overview of the depositional environment prevailing today in the

vicinity of major meltwater outflows (identified during a previous investigation, Solheim and Pfirman, 1985) is presented. These data are then compared with observations from other modern glaciomarine environments and interpretations of Pleistocene deposits.

PHYSICAL SETTING

Austfonna, 8,105 km² (Dowdeswell and Drewry, 1985), is the largest of the two main ice caps of Nordaustlandet. Its ice thickness reaches a maximum of 530 m near the center of the ice cap and there are no nunataks. While the southwestern and northern extremes of the ice cap terminate subaerially, the southern and eastern margins are grounded in the Barents Sea (Fig. 1). Most of the ~200 km long tidewater glacier front is more than 100 m thick (Dowdeswell et al., 1986), situated in water depths ranging from 30 m to more than 100 m (Fig.2) and with terminal ice cliffs extending 20-35 m above sea level. The glacier base continues below sea level for 5-25 km behind the ice front (Fig.3; Dowdeswell et al., 1986). Similar to many Svalbard glaciers, Austfonna is suggested to be of the subpolar type (Schytt, 1969; Baranowski, 1977). Subpolar glaciers are at the pressure melting point in central parts, while the peripheries are frozen to the bed.

Solheim and Pfirman (1985) noted that two major meltwater outflows, observed as turbid surface plumes on Landsat images due to incorporated glacial erosional products, occur along the southern margin of the Austfonna ice cap. Dowdeswell and Drewry (in press) documented numerous similar plumes along the northeastern margin. The plumes provide direct evidence for melting at

the base of Austfonna, and indicate that this melting extends to the margins, at least in some terminal areas (Dowdeswell and Drewry, in press).

Surges constitute a common form of glacier advance on the Svalbard Archipelago (Liestøl, 1969). Bråsvellbreen, 1,100 km² (drainage basin 1, Dowdeswell and Drewry, 1985), comprises the southern sector of the Austfonna ice cap (Fig.3). The terminus of this basin advanced 15-20 km during a surge between 1936 and 1938 (Glen, 1941; Blake, 1962; Schytt, 1964) depositing a moraine ridge at its maximum extent (Solheim and Pfirman, 1985). Bråsvellbreen is now in a quiescent phase between surges, and has very low driving stresses (< 30 kPa up to 20 km from the glacier terminus) reflecting the importance of in-situ ablation, low surface slopes and low velocity (Dowdeswell, 1986). Since the surge, the ice front has retreated 0.5 - > 5 km to its present position. Sea-floor sediments in the region occupied by the glacier during the surge were extensively reworked by contact with the glacier (Solheim and Pfirman, 1985; Solheim, 1986; Solheim, subm.). In close proximity to the modern ice front, small (2-5 m high and > 25 m wide), discontinuous arcuate ridges, subparallel to the front have been interpreted as annual push moraines showing minor modern activity (Solheim and Pfirman, 1985).

Within the study area to the east, three additional drainage basins are defined (Dowdeswell and Drewry, 1985): drainage basin 2 (217 km²), drainage basin 3 (1,250 km²), and drainage basin 4 (261 km²) (Fig.3). Drainage basin 3 is the largest single basin on Nordaustlandet. Based on Solheim's (1986) observation of sea-

floor morphology indicative of a surge in the proximal marine environment, the low ice-surface profile and the low driving stress, Dowdeswell (1986) concluded that basin 3 is probably now in a stage of post-surge stagnation.

METHODS

Thirteen useful (clear view of part or all of the southern ice front and open water along the front) Landsat MSS images, band 4, from 1979-1981 and 5 images from 1976 were used to locate the turbid meltwater plumes along the Austfonna ice front. MSS band 4 was chosen for this purpose because it has been shown to be appropriate for detecting the presence of suspended sediments in near-surface water (Robinson, 1983).

Suspended particulate matter (SPM) was measured at 72 stations in the proglacial environment (Fig.2) by a combination of light attenuation profiles and scattering profiling (Montedoro Whitney TMU transmissometer/nephelometer, one meter folded path length with a white light source, including temperature, pressure, and conductivity), and water samples. Water samples (1-3 liters) were filtered on 0.45 μm Millipore filters to determine SPM concentration. Thirty sub-samples of filtered suspended matter were analyzed for content of combustible organic material.

In 1981 and 1982, 60 hydrographic stations were obtained with a Neil Brown CTD sonde by the Geophysical Institute of Bergen, Norway. Estimates of geostrophic shear calculated for hydrographic sections perpendicular to the glacier front assumed zero velocity at the deepest station pair on each section (T. Gammelsrød, pers. commun., 1982).

Sea-ice conditions limited acoustic profiling to the western portion of the study area. Data in this region were acquired by means of 3.5 kHz (O.R.E. Mod. 140, hull mounted with EPC 3200 analog graphic recorder), sparker profiling (EG&G with 1 kJ energy and multielectrode array), and side-scan sonar profiling (Klein, operated at 50 kHz) (Fig.2). These profiles are discussed in more detail by Solheim and Pfirman (1985) and Solheim (subm.).

RESULTS

Meltwater Outflows

Landsat images of the northwestern Barents Sea show the region near Nordaustlandet to be covered by sea ice from November to May, with patchy sea-ice during the summer (Vinje, 1985). In all 10 useful Landsat images from July and August, turbid water is observed to discharge from numerous locations along the southeastern Austfonna glacier front. It is also observed in one of the five useful images from September. Turbid meltwater discharge is not seen in the May, nor in the two June images. Along the southern ice front, two major plumes, henceforth called the western and eastern plumes, were observed in the same locations since the first satellite photographs were obtained in 1976 (Fig.3). Because of the low relief of the Austfonna drainage basin and the fact that there are no nunataks, these meltwater outflows are interpreted to be the termini of subglacial meltwater channels, transporting basal erosional products to the glacier margin.

These two major meltwater outflows have several distinguishing characteristics: they are located in embayments in the ice front; the embayments are formed by the intersection of a surged drainage basin and a non-surging section; there is a depression in the subglacial bedrock (mapped as >100m below sea level by Dowdeswell et al., 1986); the ice wall above sea-level is generally higher, forming a dome-like structure over a 50 m wide indentation or tunnel at the sea surface (Fig.4); and turbulent, turbid meltwater discharges from this indentation and sometimes forms boils in the sea-surface and streams away from the ice margin.

Most, but not all, satellite images show western deflection of sediment-laden meltwater as it emanates from the embayments, resulting in along-coast flow parallel to the glacier front. Indistinct regions of high surface water turbidity are often observed to extend some 20 km perpendicular to the ice front in the shape of large eddies. In several clear satellite images (e.g. Fig.3), the main body of the turbid plumes has definite features as follows: within 1 km of the discharge point, turbid surface water spreads to a width of approximately 2 km, and then spreads another 0.5 km until about 4 km downstream where the width of the turbid surface plume becomes more or less constant. At about 10 km downstream of the western outflow, there is a 90° corner in the ice front. In this region the plume often separates from the glacier front and flows offshore forming large eddies (~ 15 km diameter). The western plume is often observed as an indistinct region of high surface water turbidity for some 60 km from the outflow (e.g. Fig.3).

Submarine Morphology and Shallow Geology

In general, the cover of glacial sediments outside the glacier is thin, between 2-5 msec (two-way travel time). Although acoustic penetration was poor, partly due to overconsolidation and high pebble content of the till (Solheim, *subm.*), sparker profiling also indicated that the surface layer is thinner than the sparker resolution of 10 msec.

Several distinct features were observed in the sea-floor and ice front morphology and surface sediment in the vicinity of the outflow. A 200 m gap in acoustic reflection from the ice wall is observed in the side-scan sonar profile, due to an indentation or tunnel in the ice at the base of the surface expression of the meltwater outflow (Fig.5). The large size of the indentation or tunnel indicates substantial modification of the ice front morphology in this region, presumably related to meltwater discharge.

A valley, approximately 40 m deep and up to 1 km wide is located just to the west of the major western outflow and can be followed for a distance of 3.5 km to the east, where it turns south-southeast, losing its bathymetric expression within about 1 km (Fig.2). This valley probably represents the submarine extension of the bedrock depression under the glacier mapped with radio echo sounding by Dowdeswell et al. (1986). The depression, as shown by the 100 m contour, extends west under the glacier for 2.5 km (Fig.3). A similar bedrock depression in the vicinity of the eastern outflow extends some 35 km westward into drainage basin 3 (Fig.3). Dowdeswell et al. (1986) and Dowdeswell and

Drewry (in press) mapped a third major bedrock depression under Leighbreen, in the northeast corner of Austfonna (drainage basin 10, Fig. 3).

Sediment formed into arcuate ridges occurs within the outflow valley on the south slope (right hand side as viewed from the glacier front). The arcuate ridges are similar to those observed to the west, along the Bråsvellbreen snout, by Solheim and Pfirman (1985), but are larger near the outflow. Combined, these arcuate ridges form an 8-10 msec thick sediment lens.

Three large mounds are located in front and slightly to the north of the western meltwater outflow and outflow valley. These structures range up to 200 m wide, are more than 25 m high, have a rough surface topography and are either acoustically transparent or have a weak reflection due to sound scattering. Unfortunately, in this region the 1983 side-scan record (Fig.5) is somewhat disturbed because the towfish had to be raised suddenly to clear the features. A similar structure, 100-150 m wide has been observed about 3 km off the outflow.

Directly in front of the major western outflow, the sea floor is smooth and a thin (~ 3 msec) layer of acoustically transparent material is observed in the 3.5 kHz profile (Fig.5) extending between the mounds and the outflow valley. This type of surface layer was not observed in any other 3.5 kHz records in the region to the west, although an extensive survey was carried out (Solheim, subm.). Several indistinct, wave-like disturbances of the surface sediment observed in the side-scan sonar profile along the northern wall of the outflow valley may be caused by downslope sediment movement.

Coastal Hydrography

Westward deflection of the meltwater plumes in the proglacial environment implies that they are discharged into a westerly coastal current. Hydrographic transects confirm that a coastal water mass exists which is between -1 and 0°C (Fig.6), and has lower salinity and density than the more stratified water to the south. The region influenced by the coastal current is approximately 15 km wide, and parallel to the glacier front (Figs. 3 and 6). Relative current shear appears to increase to the west, from 5 cm/sec on a transect just west of the eastern outflow, to greater than 16 cm/sec near the western border of Bråsvellbreen (T. Gammelsrød, pers. commun., 1982).

Concentration of Suspended Particulate Matter

Concentrations of SPM calculated from filtered water samples generally range between 1-4 mg/l along the glacier front (Figs. 6, 7 and 8). Locally higher concentrations were observed in 1981 in the surface waters (upper 10 m) near the major outflow locations: eastern plume 15 mg/l and western plume 28 mg/l (Fig.7). Within about 5 km westward along the glacier front, concentrations of SPM in the eastern plume decreased to less than 5 mg/l in the surface waters, and SPM appears better mixed through the water column (Fig.7). The downstream extension of the western outflow is not well documented because the next closest samples were obtained 6 km away and the concentration had already decreased to < 2.0 mg/l (Fig.7, Station 143). As observed in satellite images and discussed above, the plume often separates from the glacier when it encounters the 90° corner in the Bråsvellbreen glacier, and suspended sediment discharged from the

western outflow is transported southwards, perpendicular to the along-glacier transect (Fig.3).

General cross-sectional characteristics of the ice proximal region can be seen in two suspended matter profiles perpendicular to the glacier front downstream of the major outflow locations (Fig.8). Maximum concentrations, greater than 2 mg/l, occur close to the glacier (Figs.6, 7 and 8), within the coastal water mass (Fig.6). SPM in coastal water is usually about 75% noncombustible, primarily lithologic material (Fig.8). Concentrations of SPM decrease offshore, and reach normal Barents Sea values in central Erik Eriksenstretet (Fig.1): < 0.2 mg/l, and < 50% noncombustible material (Figs.6 and 8). Suspended sediment supplied from Nordaustlandet appears to be largely contained within the coastal water.

DISCUSSION

Subglacial Stream Discharge

In slowly moving glaciers (Weertman and Birchfield 1982) such as the Austfonna drainage basins (Dowdeswell and Drewry, in press), meltwater at the glacier base tends to form subglacial drainage networks, either eroded down into the bedrock (Nye 1973) or melted upward into basal ice (Rothlisberger 1972). Because the major Austfonna discharge locations have remained the same since at least 1976, it is probable that a stable subglacial drainage system has been established. Bedrock depressions observed at the major outflow locations (Dowdeswell et al., 1986; Dowdeswell and Drewry, in press), indicate that these Austfonna subglacial streams are either following or forming topographic depressions.

Discharge of subglacial streams into the sea produces a situation unique from any other sedimentary environment by discharging and releasing sediments at the base of a sea water column (Fig.9), rather than at sea level (Powell, 1984). Deposits in this environment are strongly controlled by sea water characteristics, position and sediment discharge of meltwater streams, iceberg calving, and the rate of glacier front retreat (Powell, 1981; Syvitski, in press). At the ice front, meltwater streams, which may have high velocity, decelerate when they encounter ocean water and are no longer driven by ice pressure. Their trajectory immediately after discharge into the sea depend on discharge velocity (momentum flux) and buoyancy flux (Fisher et al., 1979; Syvitski, in press). In general, if the discharge velocity is greater than the buoyancy flux, the meltwater stream will continue to flow some distance as a jet before it loses momentum and rises as a buoyant plume. In this region of deceleration at the meltwater-seawater interface, the bed and traction load are deposited forming coarse subaqueous deposits. Syvitski (in press) estimates that in this region, approximately within 500 m of the ice front, 70% of the sediment load will be deposited.

If the glacier front is not extensively fractured or retreating the meltwater-seawater interface will occur at the base of the general ice front, and deposition will occur in the proglacial environment (Fig.9). Elverhøi et al. (1980) proposed that subglacial meltwater may also migrate to sea-level some distance behind the front due to intrusion of saltwater at a vertically fractured glacier terminus. In this case, which could occur at Austfonna, coarse components of a basal meltwater stream would deposit near the meltwater-seawater interface located some

distance behind the general ice front. Deposits forming in such an environment would be laterally constrained to the subglacial meltwater channel.

Upward trajectory of the rising plume and incorporated sediment in the marine environment is governed by density stratification and ocean currents (Powell, 1984). In a density stratified coastal environment, with no ambient velocity, such a plume will have a terminal height of rise dependent on its buoyancy (Fisher et al., 1979). Unless sediment concentrations are very high (greater than about 30 g/l, Bates, 1953; Hoskin and Burrell, 1972; Gilbert, 1979; Powell, 1980; Syvitski, in press) it is considered difficult to form underflows in the marine environment. However, Domack (1984) documented rhythmically bedded sediments deposited in relatively shallow water (< 10 m) interpreted to have formed from underflow currents during peak meltwater discharges with high suspended sediment concentrations. In addition, turbidity currents may be stimulated when pulsing of the meltwater jet erodes previously deposited sediments or causes sediments to become unstable (Aario, 1972; Powell, 1984).

If the plume is buoyant enough to reach the surface, it may be observed as a region of turbulent, turbid surface water ("brown zones" Hartley and Dunbar 1938, although Greismann 1979 considered that this phenomenon could be due to upwelling caused by melting of the ice front itself). Syvitski (in press) has documented that concentrations of suspended matter may be 50 to 60 times greater in the zone of water boiling (when the jet is super-elevated) than in water closer to the ice front. The fact that turbid, turbulent water is observed in satellite images and aerial photographs to discharge from the Austfonna ice front

during summer indicates either that basal meltwater has risen within the glacier to discharge at the sea surface, or that it has risen as a buoyant plume along the glacier front.

In low discharge stages with little momentum, the plume may rise along the ice front causing melting (Syvitski, in press) and tunnel widening (Powell, 1980). The indentation in the ice front observed at sea level at the major meltwater outflows (Figs.4 and 9), may be evidence that this type of ice front melting has occurred.

Limited observations of suspended sediment at the major outflow locations indicate low concentrations (15 and 28 mg/l) compared with tidewater glacier fronts in fjords. For example, Elverhøi et al. (1980) recorded concentrations of 500 mg/l. Because salinities of the turbid water discharging from Austfonna were high, about 33 and 32.5 ppt for the eastern and western plume, respectively, it appears that either discharge was low or that it had mixed extensively with seawater, resulting in dilution and deposition. Sedimentation of fine-grained material in this environment is most likely enhanced by formation of biogenic and inorganic agglomerations (e.g. Syvitski and Murray, 1981; Smith and Syvitski, 1982; Syvitski, in press).

Suspended Sediment Dispersal

The two major meltwater outflows are located in prominent embayments in the ice front (Fig.3). If major meltwater outflows are intrinsically related to embayments in open-marine tidewater glacier margins, it may mean that sediment-laden meltwater plumes will be discharged into a somewhat restricted environment. Within

the embayment the plume will mix with ambient seawater and sediment may settle from suspension. Both in satellite images and in the 1981 transect along the glacier front, suspended sediment concentration in the upper layers appeared to decrease within about 5 km from the discharge location, in the outflow embayments. Although the decrease in concentration could be due to deposition from suspension, it is not required. The observed decrease in concentration could also be accounted for by lateral spreading of the plume, and mixing with the underlying water column.

Dispersal of suspended sediment outside of the outflow embayment depends on the ambient coastal environment. If coastal currents are present, they will sweep fine-grained sediments away from the outflow point, possibly distributing and depositing them over a wide region. Some portion of the turbid meltwater from Nordaustlandet remains at the sea surface and can be followed for up to 60 km (Fig.3), transported by the westerly coastal current. The circulation along the Nordaustlandet ice front is no doubt influenced by the general oceanography and wind fields of the Barents Sea. It may also be related to specific conditions at tidewater glacier fronts and therefore be important for consideration of the regional sedimentologic impact of tidewater glacier margins in the Pleistocene. In general, when water with low density is introduced into higher density water at high northern latitudes, the tendency is for the low density water to turn to the right. Katabatic winds from the glacier could enhance this effect, also turning the surface water to flow to the right. In the case of Nordaustlandet, this would be to the west, along the glacier front, consistent with observations reported in this paper. Both density and wind effects should be stronger in the

summer when most sediment-laden meltwater is discharged, because of the greater volumes of low density water supplied, and because katabatic winds are stronger when the air-ice temperature difference is greater. Because the coastal environment is clearly important in determining transport of SPM along the Austfonna ice front, the possibility that an along-glacier current can be developed by ice front processes should be explored in future studies.

Formation of Sedimentary Features

Arcuate ridges along the glacier front were interpreted by Solheim and Pfirman (1985) to be formed by contact with the glacier, during minor advances within a general ice front retreat; possibly as annual push moraines. Annual moraine ridges with similar characteristics were originally proposed by DeGeer (e.g. 1940), and later by Liestøl (1969 and 1977) for features found outside another surging glacier on Svalbard. In a recent paper, Boulton (1986), described push moraines both on land and offshore in Iceland, Spitsbergen and Alaska. If ridges in the outflow valley are also moraine ridges formed during minor advances, their formation appears to indicate that the glacier was grounded without a basal meltwater tunnel in the valley during deposition. This may indicate either that the meltwater tunnel closes or becomes significantly smaller during winter, or that the meltwater outflow location is displaced from the outflow valley. Increased size of the arcuate ridges, in comparison to similar ridges distant from this region, indicates availability of additional sediment in the vicinity of the outflow. Boulton (1986), proposed that push moraine formation is favored if the ice front position is stable long enough for an ice-contact fan

to develop. In the vicinity of the outflow, this may occur over a period as short as one summer.

The ~ 3 msec transparent drape occurring directly in front of the outflow tunnel observed on the side-scan sonar profile, also testifies to increased sediment supply in this region. The deposit is most likely formed by combined deposition from traction load and from suspension, and does not appear to be reworked by ice contact. Indistinct wavelike-surface sediment disturbances possibly indicative of slumping/mass transport are observed on the outflow valley flank.

Origin of the discrete mounds in front of the meltwater outflow is not clear in the absence of samples. They could be composed of ice or sediment: bedrock is excluded because in this region it forms a smooth, nearly horizontal surface. If the mounds are composed of ice calved from the glacier then they must contain enough englacial material to counteract their buoyancy, or be covered by a thick sediment drape. For example, assuming a cone-shaped piece of ice 150 m wide and 29 m high, with a density of 0.92 g/cm^3 , the bottom 1.5 m must contain pure compacted till (density ~ 2.0 g/cm^3) to prevent the block of ice from floating. Similarly, if the bottom 3 m contained about 50% compacted till the block would not float. These values appear somewhat, but not prohibitively, high when compared with Drewry's (1986, pp. 100-102) review of current literature on debris layer thickness.

The other possibility, and the one we consider more likely, is that the mounds are composed of sediment. If so, they resemble beaded eskers, deposited in the meltwater tunnel during sporadic glacier retreat, as envisioned by DeGeer ("ose centra",

1940, Fig.9) and Bannerjee and McDonald (1975) for Pleistocene deposits. The esker beads discussed by Banerjee and McDonald were similarly interpreted to have been deposited in about 100 m water depth, were 10 - 20 m high, isolated from each other and spaced less than 300 m apart, but were deposited in a glacial lake. Beaded eskers form in an environment characterized by rapid deceleration of flow (Bannerjee and McDonald 1975), but need not necessarily form at the general glacier front. If the meltwater stream migrates to sea level within the glacier, as proposed by Elverhøi et al. (1980), the bed and traction load will deposit at some distance behind the general ice margin, forming an esker bead where meltwater encounters sea water. A similar mechanism is proposed for esker deposits formed in close association with annual moraines in northern Norway (Sollid and Carlson 1984) although these are of smaller dimensions than the mounds off Austfonna. The width of the Austfonna mounds (50-200 m) matches the width of the present-day outflow tunnel seen on the side-scan sonar profile (200 m) (Fig.9). Their height, up to about 30 m, would indicate substantial deposition and upward migration of the meltwater stream. Although esker beads are often interpreted to be annual features in Pleistocene deposits, they could form at the meltwater outflow over a longer period of time and be left behind when the ice front sporadically retreated.

If the ~ 3 msec sediment drape observed directly in front of the outflow, and the 5-8 msec sediment lens in the outflow valley (formed by coalescing arcuate ridges), are the only sediment accumulation produced by the glacier for at least 6 years (between the first satellite picture in 1976 and the survey in 1982), this implies maximum accumulation rates of ~ 4 m/6 yr or 67

cm/yr (average thickness 5 msec, 1500 m/sec sound velocity) within about 1 km of the outflow location. Based on counting "annual" moraines along the Bråsvellbreen margin, Solheim (subm.) proposes that this part of the glacier retreated by passive calving until about 20-25 years ago when it resumed normal motion. If the meltwater outflow was also established at the same time, the deposits could be older, and formed with lower sedimentation rates ~4 m/25 yr or 16 cm/yr. For comparison, Eyles et al. (1985) in their review of accumulation rates in various proglacial environments, show that rates of 1-4 m/yr are common for tidewater glaciers in fjords of Alaska. Elverhøi et al. (1983) reported rates of 10 cm/year at a tidewater glacier front in Kongsfjorden, West Spitsbergen. If the mounds observed in front of the outflow are esker beads deposited either annually or as the glacier retreats sporadically and the deposition location shifts, then total accumulation rates must be revised upward.

CONCLUSIONS

If the observations summarized above for the Austfonna ice cap are representative, the proglacial environment of a large, stable, subpolar ice cap eroding low relief sedimentary rocks may be expected to contain the following features:

- 1) A stable subglacial drainage system which follows or forms bedrock depressions and has a limited number of major, stable meltwater discharge locations along the ice front, together with numerous minor discharge points.
- 2) In glacier systems where the ice front has retreated from its maximum extent, bedrock depressions may extend offshore from the meltwater discharge locations.

- 3) Glacial erosional products transported by this subglacial drainage system to the ice front are deposited at the meltwater - seawater interface. Locally high sedimentation rates in a zone with approximately the same dimension as the meltwater efflux may result in isolated sediment mounds, similar to esker beads described in Pleistocene deposits.
- 4) "Normal" ice front features (such as "annual" moraines) are enlarged over a radius of about 1 km from the meltwater discharge location, due to locally increased sediment supply. A sediment drape may also be deposited in the vicinity of the outflow.
- 5) Fine-grained components suspended in meltwater discharge disperse over a proglacial region governed by coastal circulation. In the case of Austfonna, this region extends approximately 15 km perpendicular to the ice front and at least 60 km along the front.

Reliable estimates of sediment flux, location of depocenters, and deposition rate cannot be made on the basis of this study, but are important to determine, and should be addressed in future investigations. In addition, modelling should be carried out to investigate the possibility that ice-marginal circulation could be driven by katabatic winds and meltwater discharge. This investigation shows that meltwater influence was determined to a large degree by coastal circulation.

ACKNOWLEDGEMENTS

Hydrographic data for 1981 and 1982 was processed and provided by Tor Gammelsrød, Geophysics Institute, University of Bergen. We would like to thank J.P.M. Syvitski and J.A. Dowdes-

well for their helpful suggestions on the manuscript. Much of the work was conducted while one of the authors (S.P.) was at Woods Hole Oceanographic Institute, with support from ONR contract no.: N00014-01-C-009, and from the Norwegian Marshall Fund for Scientific Research. Economic support for meetings and discussions with J.A. Dowdeswell was provided by NATO Grant no: 0747/87. This is Norwegian Polar Research Institute contribution no. 256.

REFERENCES

- Aario, R., 1972. Associations of bed forms and paleocurrent patterns in an esker delta Haapajarvi, Finland. *Ann.Acad.Sci.Fenn. Series A/III*, 55p.
- Bannerjee, I. and McDonald, B.C., 1975. Nature of esker sedimentation. In Jopling, A.V. and McDonald, B.C. *Glaciofluvial and Glaciolacustrine Sedimentation. Soc.Econ.Paleont.Mineral. Spec.Pub.* 23:132-154.
- Baranowski, S. 1977. The subpolar glaciers of Spitsbergen seen against the climate of this region. Results of investigations of the Polish Scientific Investigations, vol. 3, 293 pp.
- Bates, C.C., 1953. Rational theory of delta formation. *Am.Assoc.Pet.Geol.Bull.* 37(9):2119-2162.
- Blake, W., 1962. Geomorphology and glacial geology in Nordaustlandet, Spitsbergen: Vol. I and II. Ohio State Univ.Ph.D. thesis. 470 pp.
- Boulton, G.S., 1975. Processes and patterns of subglacial sedimentation. In: A.E. Wright and F. Mosely (Editors), *Ice ages: Ancient and Modern.* Seel House, Liverpool, pp. 7-42.
- Boulton, G.S. 1986. Push-moraines and glacier-contact fans in marine and terrestrial environments. *Sedimentology*, 33:677-698.
- Charlesworth, J.K., 1957. *The Quaternary Environment: With Special Reference to its glaciation.* Edward Arnold, London, 1700 pp.

- DeGeer, G., 1940. Geochronologia Suecica Principles: Kungl. Svenska Vetenskapsakademiens Handlingar, ser. 3, v. 18, 367 pp.
- Domack, E.W., 1984. Rythmically bedded glaciomarine sediments on Whidbey Island, Washington. J.Sed.Petrol. 54(2):589-602.
- Dowdeswell, J.A., 1986. Drainage-basin characteristics of Nord-austlandet ice caps, Svalbard. J.Glaciol., 32(110):31-38.
- Dowdeswell, J.A. and Drewry, D.J., 1985. Place names on the Nordaustlandet ice caps, Svalbard. Polar Record, 22(140):519-539.
- Dowdeswell, J.A. and Drewry, D.J., in press. The dynamics of Austfonna, Nordaustlandet, Svalbard: Surface velocities, mass balance and subglacial meltwater. Ann.Glaciol. 12.
- Dowdeswell, J.A., Drewry, D.J., Cooper, A.P.R., Gorman, M.R., Liestøl, and Orheim, O., 1986. Digital mapping of the Nordaustlandet ice caps from airborne geophysical investigations. Ann.Glaciol., 8:51-58.
- Drewry, D., 1986. Glacial Geologic Processes. Edward Arnold, London, 276 pp.
- Elverhøi, A., Liestøl, O., and Nagy, J., 1980. Glacial erosion, sedimentation and microfauna in the inner part of Kongsfjorden, Spitsbergen. Nor.Polarinst.Skr., 172:33-61.
- Elverhøi, A., Lønne, Ø., and Seland, R., 1983. Glaciomarine sedimentation in a modern fjord environment, Spitsbergen. Polar Res., 1:127-149.

- Eyles, C.H., Eyles, N., and Miall, A.D., 1985. Models of glaciomarine sedimentation and their application to the interpretation of ancient glacial sequences. *Palaeogeog.Palaeoclimat. Palaeoecolog.*, 51:15-84.
- Fischer, H.B., List, E.J., Koh, R.C.Y., Imberger, J., and Brooks, N.H., 1979. Mixing in inland and coastal waters. Academic Press. 483 pp.
- Gilbert, R., 1979. Observations of the sedimentary environments of fjords on Cumberland Peninsula, Baffin Island. In *Free-land*, H.J., Farmer, D.M., and Levings, C.D. Fjord Oceanography. Plenum Press, New York and London, pp. 633-638.
- Glen, A.R., 1941. A sub-arctic glacier cap: The west ice of North East Land. *Geogr.J.*, 98:135-146.
- Greisman, P. (1979) On upwelling driven by the melt of ice shelves and tidewater glaciers. *Deep-Sea Res.*, 26(9A):1051-1065.
- Hagen, J.O., Wold, B., Liestøl, O., Østrem, G., and Sollid, J.L., 1983. Subglacial processes at Bondhusbreen, Norway: preliminary results. *Ann.Glaciol.*, 4:91-98.
- Hartley, C.H. and Dunbar, M.J., 1938. On the hydrographic mechanism of the so-called brown zones associated with tidal glaciers. *J.Mar.Res.* 1(4):305-311.
- Hoskin, C.M. and Burrell, D.C., 1972. Sediment transport and accumulation in a fjord basin, Glacier Bay, Alaska. *J.Geol.*, 80:539-551.

- Liestøl, O., 1969. Glacier surges in West Spitsbergen. Can.J.Earth Sci., 6:895-897.
- Liestøl, O., 1977. Åsmorener foran Nathorstbreen? Norsk Polarinsitutt Årbok 1976, 361-363.
- Nye, J.F., 1973. Water at the bed of a Glacier. Int.Ass.Sci.Hydrol.Publ. 95:189-194.
- Orvin, A.K., 1969. Outline of the geological history of Spitsbergen. Skr.Svalbard og Ishavet., Oslo, Nr.78, 57 pp.
- Powell, R.D., 1980. Holocene glaciomarine sediment deposition by tidewater glaciers in Glacier Bay, Alaska. Ohio State Univ.Ph.D. thesis. 420 pp.
- Powell, R.D., 1981. A model for sedimentation by tidewater glaciers. Ann.Glaciol., 2:129-134.
- Powell, R.D., 1983. Glacial marine sedimentation processes and lithofacies of temperate tidewater glaciers, Glacier Bay, Alaska. In: B.F. Molnia (Editor), Glacial Marine Sedimentation. Plenum, New York, N.Y., pp. 185-232.
- Powell, R.D., 1984. Glacimarine processes and inductive lithofacies modelling of ice shelf and tidewater glacier sediments based on Quaternary examples. Mar.Geol., 57:1-52.
- Robinson, I.S., 1983. Satellite observations of ocean colour. Philosophical Transactions of the Royal Society, London. Series A, 309:415-432.
- Rothlisberger, H., 1972. Water pressure in intra- and subglacial channels. J.Glaciol. 11(62):177-203.

- Schytt, V., 1964. Scientific results of the Swedish glaciological expedition to Nordaustlandet, Spitsbergen, 1957 and 1958. Part I and II. *Geogr. Annal.*, 46:243-281.
- Schytt, V., 1969. Some comments on glacier surges in eastern Svalbard. *Can. J. Earth Sci.*, 6:867-871.
- Smith, N.D. and Syvitski, J.P.M. 1982. Sedimentation in a glacier-fed lake: the role of pelletization on deposition of fine-grained suspensates. *J. Sediment. Petrol.* 52(2):503-513.
- Solheim, A., 1985. Submarine evidence of glacier surges. *Polar Res.* 4:91-95.
- Solheim, A., subm. The depositional environment of surging subpolar tidewater glaciers.
- Solheim, A. and Pfirman, S.L., 1985. Sea-floor morphology outside a grounded, surging glacier; Bråsvellbreen, Svalbard. *Mar. Geol.* 65:127-143.
- Sollid, J.A. and Carlson, A.B. 1984 De Geer Moraines and eskers in Pasvik, North Norway. In: *Ten Years of Nordic Till Research* C.L.-K. Königsson, ed. *Striae*, vol. 20, pp.56-61, Uppsala.
- Sugden, D.E. and John, B.S., 1976. *Glaciers and Landscape*. Arnold, London. 376 pp.
- Syvitski, J.P.M. (in press) On the deposition of sediment within glacier-influenced fjords: Oceanographic controls. *Marine Geology*.
- Syvitski, J.P.M. and Murray, J.W. 1981. Particle interaction in fjord suspended sediment. *Mar. Geol.* 39:215-242

Vinje, T., 1985. Physical environment western Barents Sea: Drift, composition, morphology, and distribution of the sea ice fields in the Barents Sea. Norsk Polarinstitutt Skr. 179(C), 26 pp.

Weertman, J., 1972. General theory of water flow at the base of a glacier or ice sheet. Rev.Geophys.Space Phys., 10(1):287-333.

Weertman, J. and Birchfield, G.E., 1982. Subglacial water flow under ice streams and West Antarctic ice-sheet stability. Ann.Glaciol., 3:316-320.

Wright., G.F., 1887. The Muir glacier. Am.J.Sci., 33:1-18.

FIGURE CAPTIONS

- Fig.1. Location map of Nordaustlandet, the Svalbard Archipelago.
- Fig.2. Locations of stations discussed in text and shown in Figs.6,7 and 8.
Inset shows location of side scan and 3.5 kHz profiles shown in Fig.5. Location of outflow depression discussed in text shown by cross hatching.
- Fig.3. Landsat image from 23 July 1976 showing major meltwater turbid plumes, and deflection in a westerly coastal current. Sediment is also observed in surface water to the east of the drainage basin 3 due to meltwater discharge along the eastern glacier margin (described in more detail by Dowdeswell and Drewry, in press). Overlay of glacier characteristics and numbering of drainage basins adapted from Dowdeswell et al. (1986) and Dowdeswell and Drewry (1985).
- Fig.4. Photograph of outflow region. Note thickened ice front over an approximately 50 m wide indentation at sea level.
- Fig.5. (a) Side-scan sonar and (B) 3.5 kHz profiles for inner profile, and (C) 3.5 kHz profile for outer profile along the ice front near the major western outflow (for location see inset on Fig.2).
Major subglacial stream discharge location is observed as a lack of acoustic reflection from the glacier front. Outflow depression discussed in text is located

to the west of the outflow. See Fig.9 for schematic representation of this region.

Two discrete mounds can be observed in front and to the east of the meltwater outflow. They are more than 25 m high and up to 200 m wide. The large mound observed on both inner and outer 3.5 kHz profiles is the same feature.

Fig.6. Hydrographic and suspended particulate matter transect obtained perpendicular to the ice front in 1981. See Fig.1 for station locations. Hydrographic data provided by T. Gammelsrød, U. Bergen.

Fig.7. Suspended matter profile obtained parallel to the ice front at a distance of 0.5-1 km (locations shown in Fig.2).

Stations numbers beginning with "1" were obtained in 1981, stations beginning with "2" were obtained in 1982.

Fig.8. Transects of suspended particulate matter obtained in 1980 perpendicular to ice front showing concentration (mg/l) and percent noncombustible material (pie symbols) rounded to the nearest 25%. (locations shown in Fig.2).

Fig.9. Schematic representation of the western meltwater outflow of the Austfonna glacier front. Vertical exaggeration is approximately 5:1.

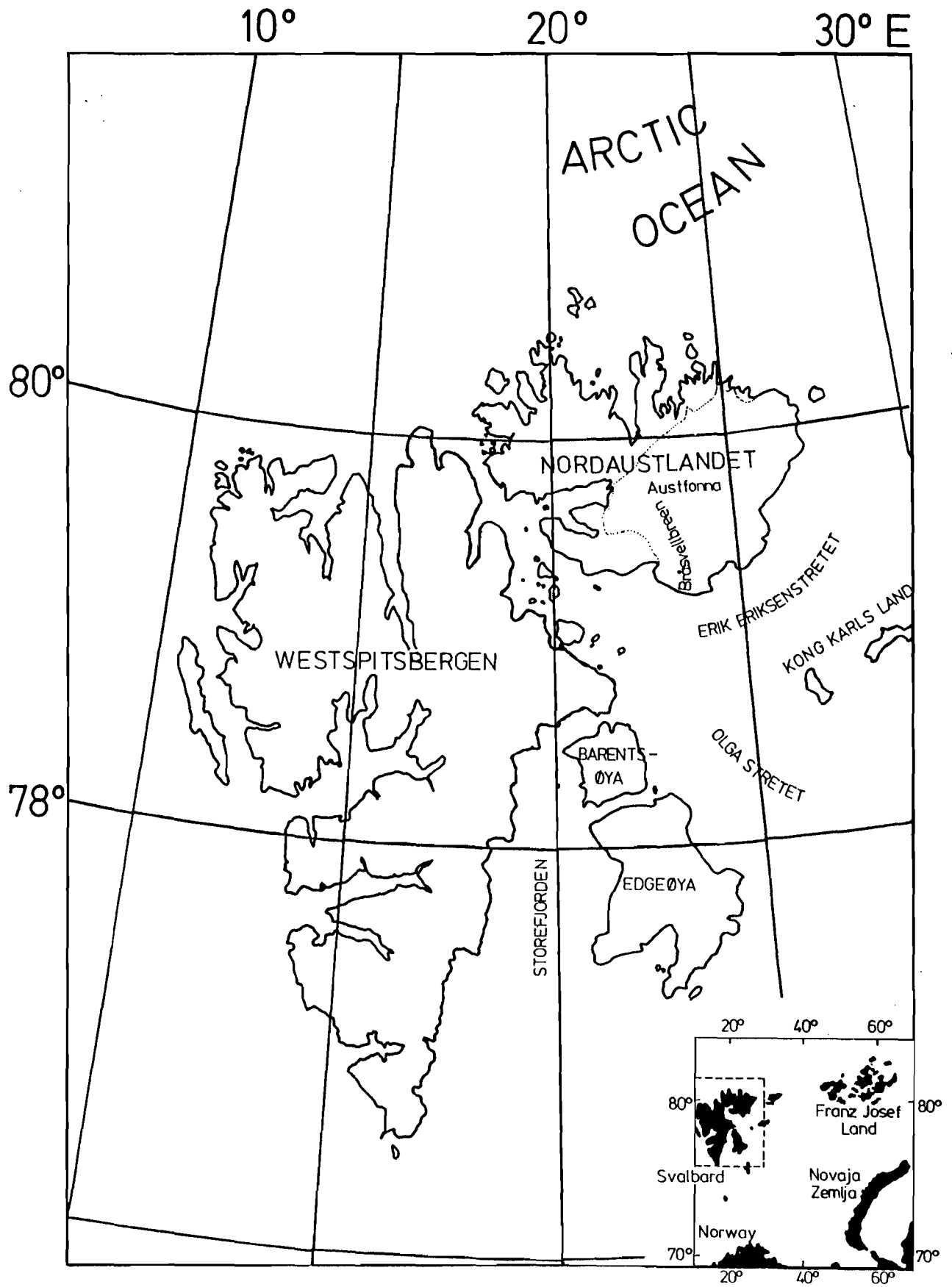


Fig. 1

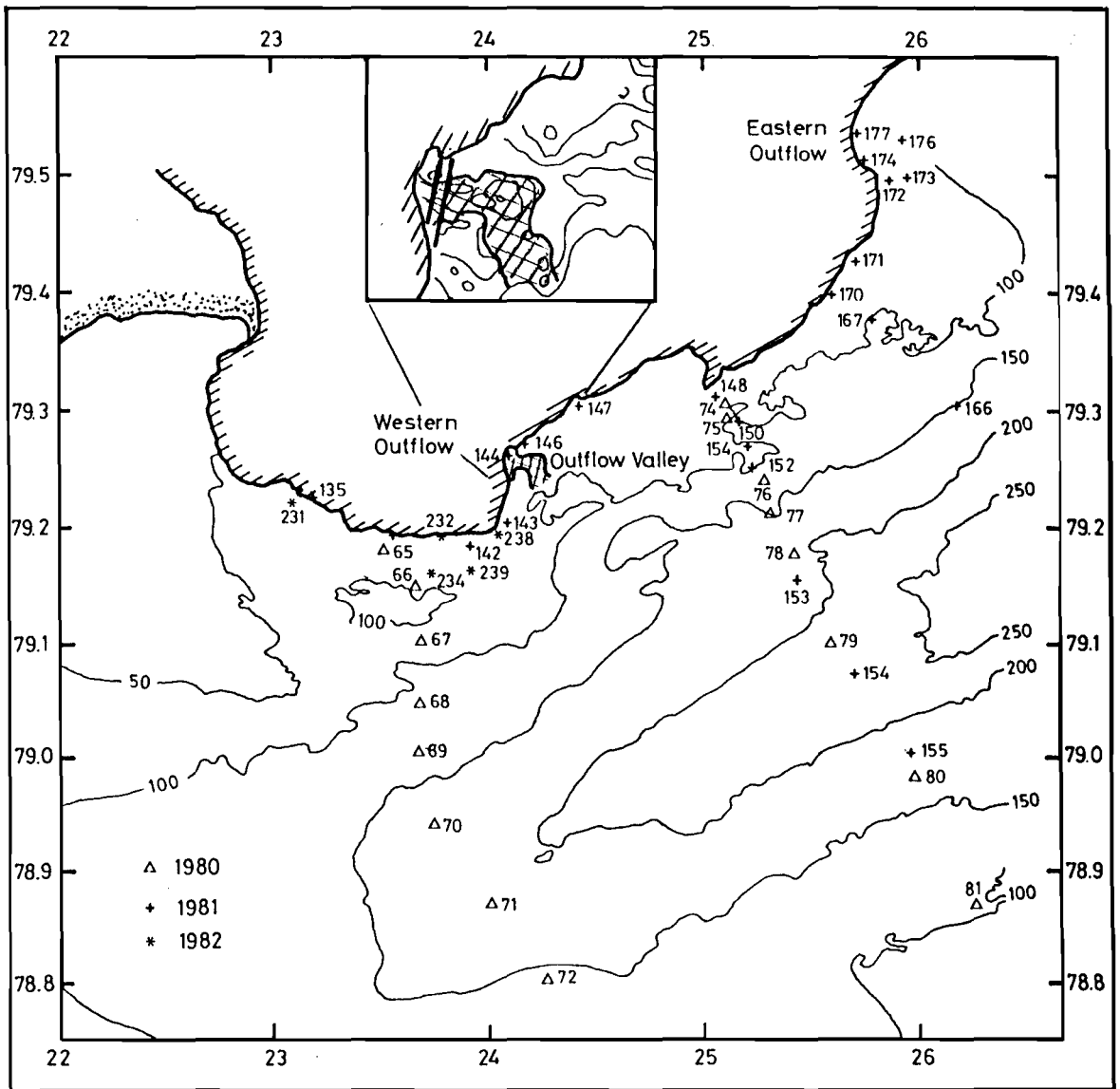
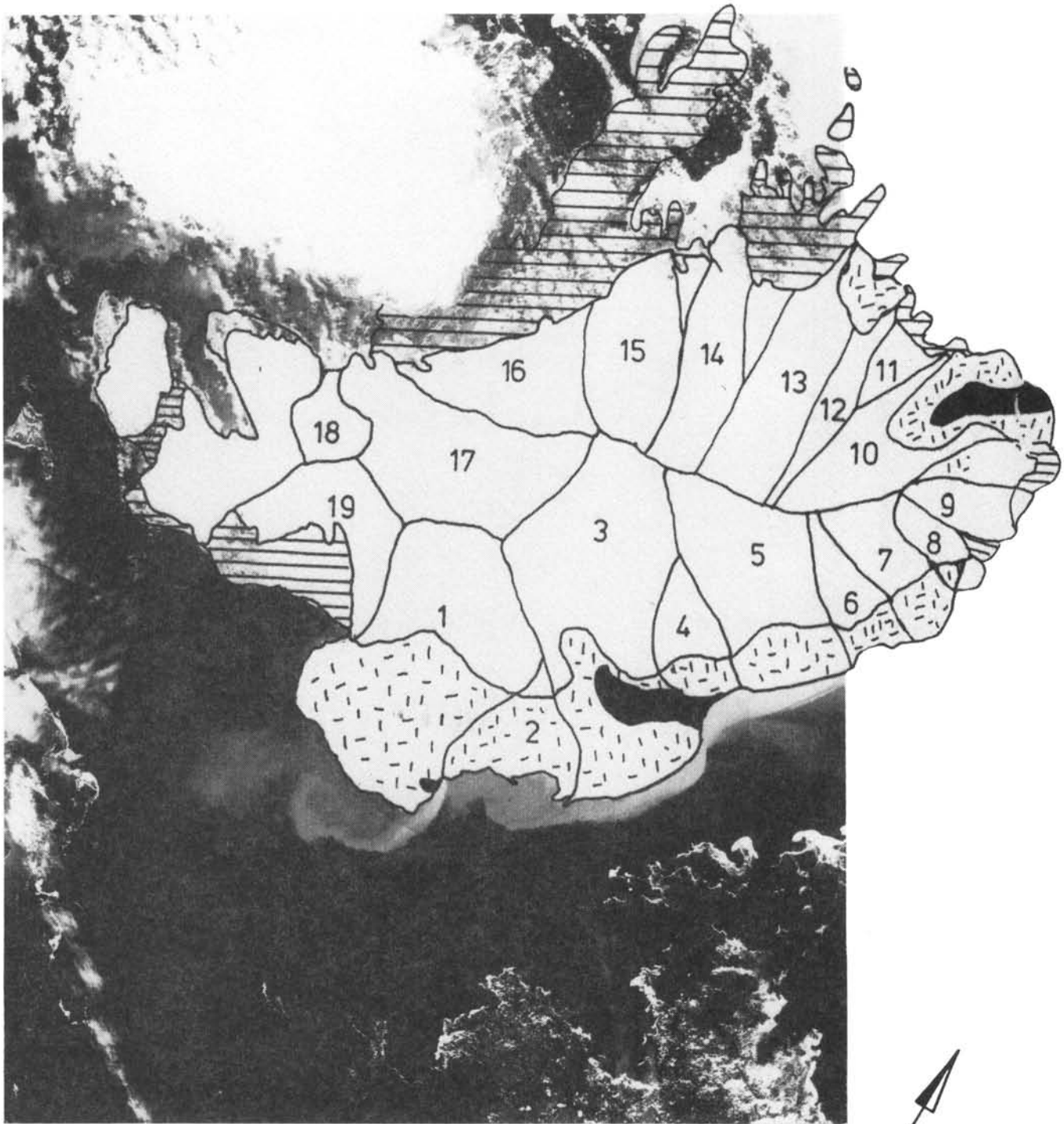
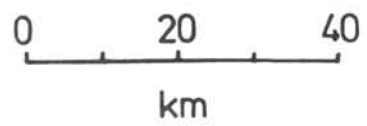


Fig. 2



23. July 1976






-  Exposed land
-  Glaciated regions below sealevel
-  Glaciated regions >100m below sealevel

Fig. 3.



Fig. 4.

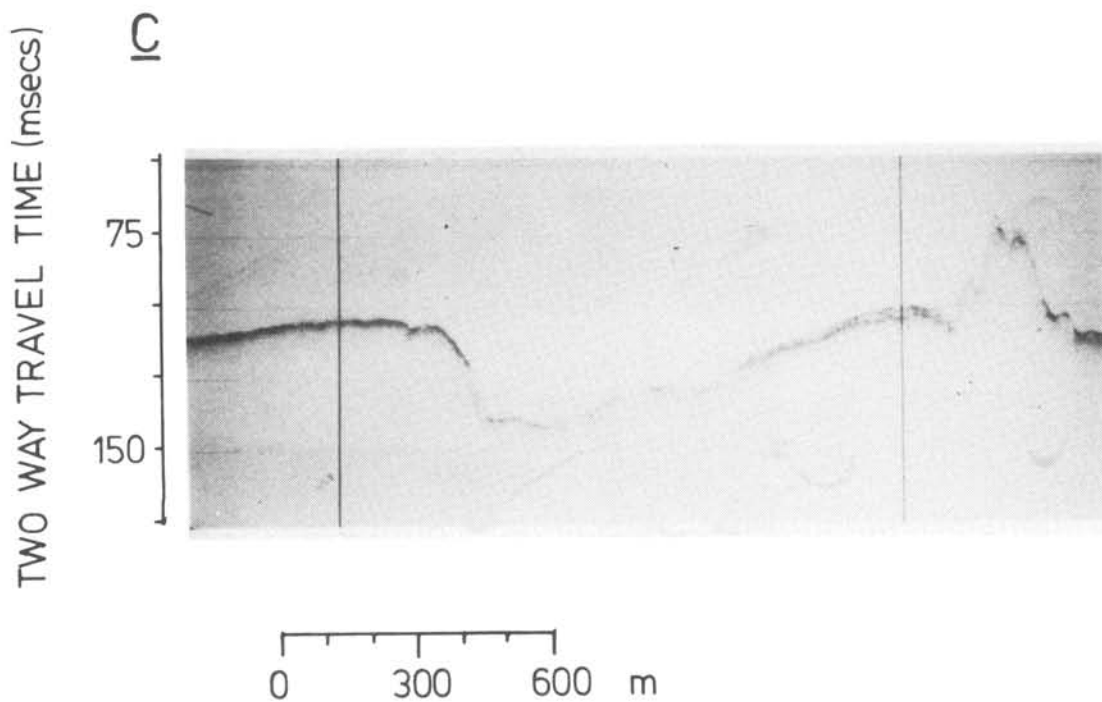
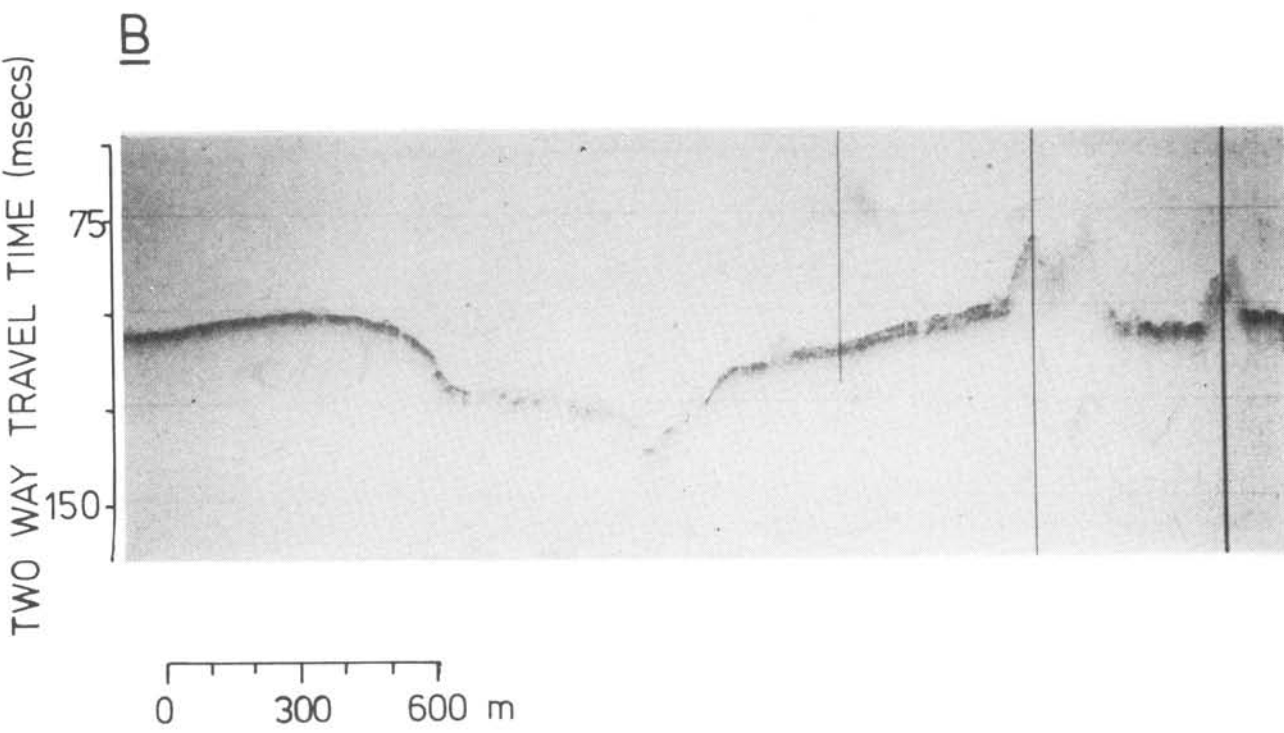
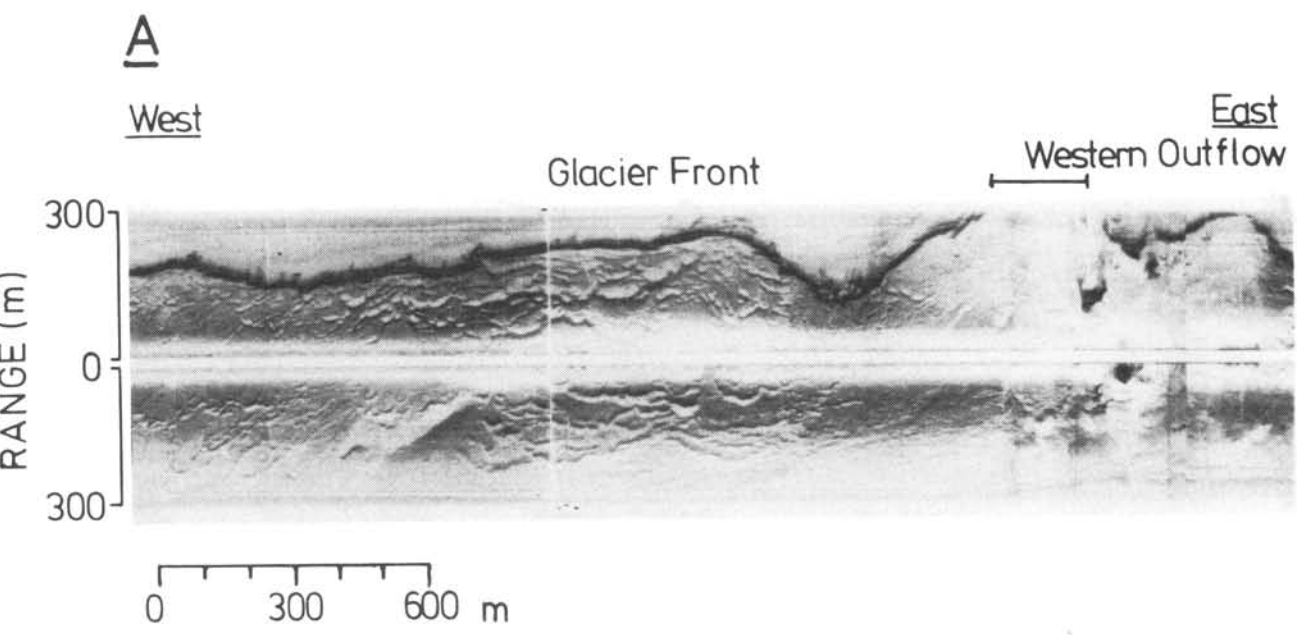


Fig. 5.

Station Number

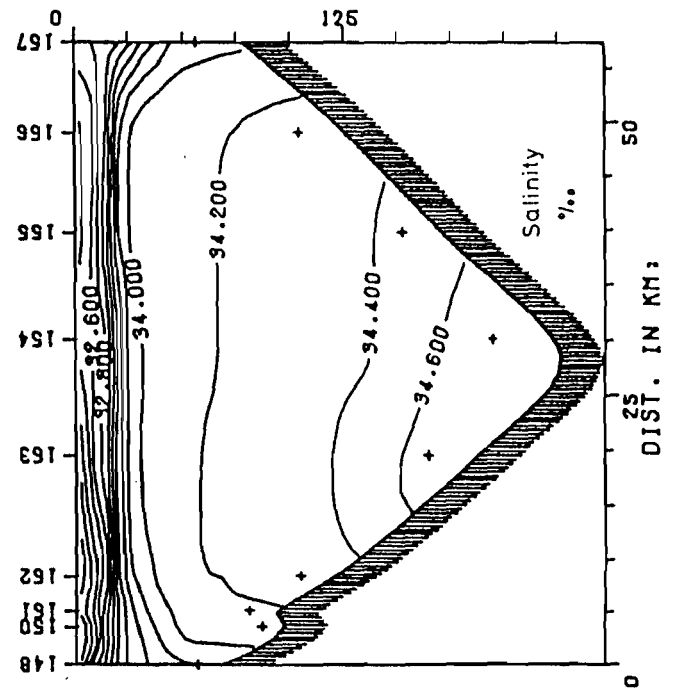
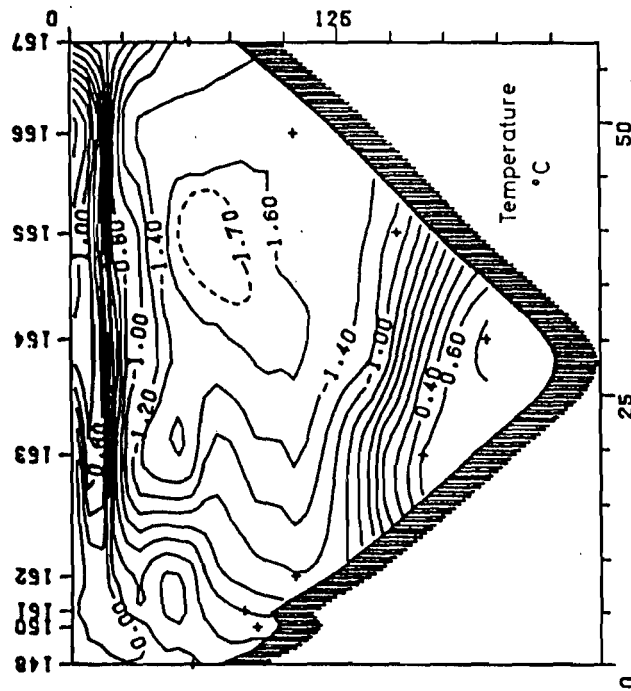
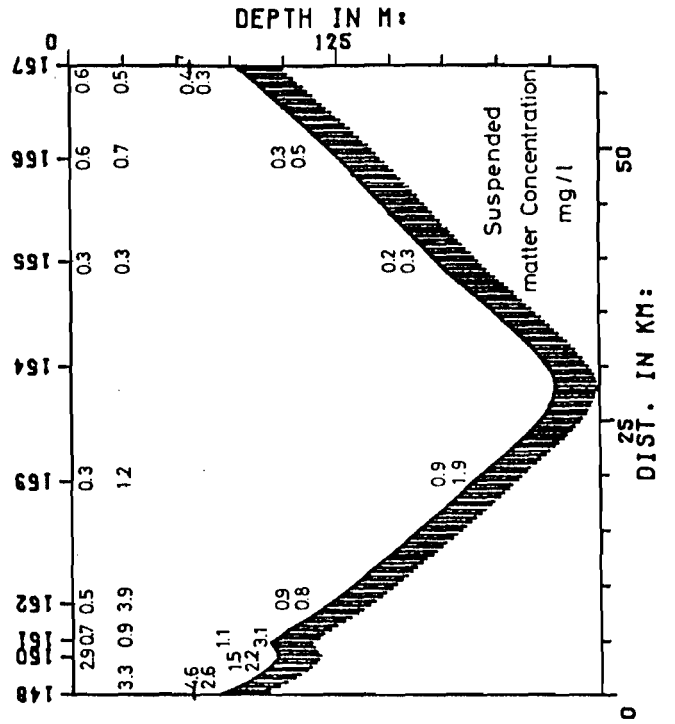
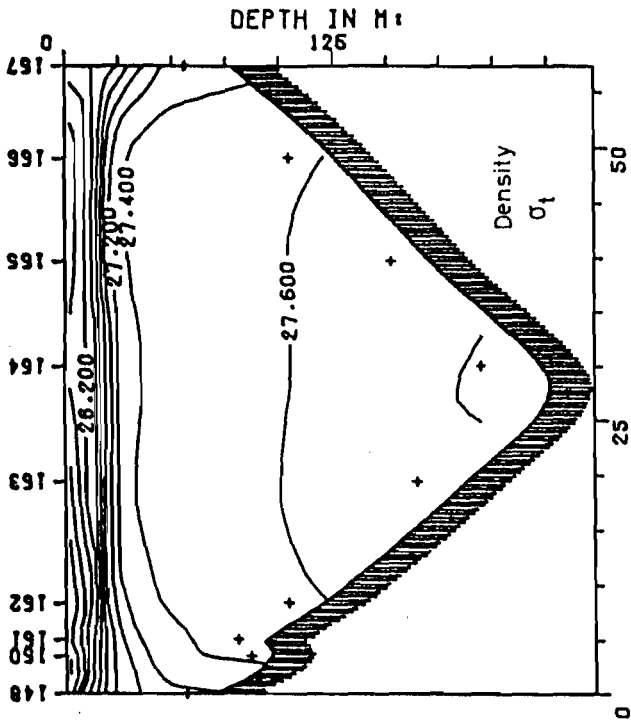
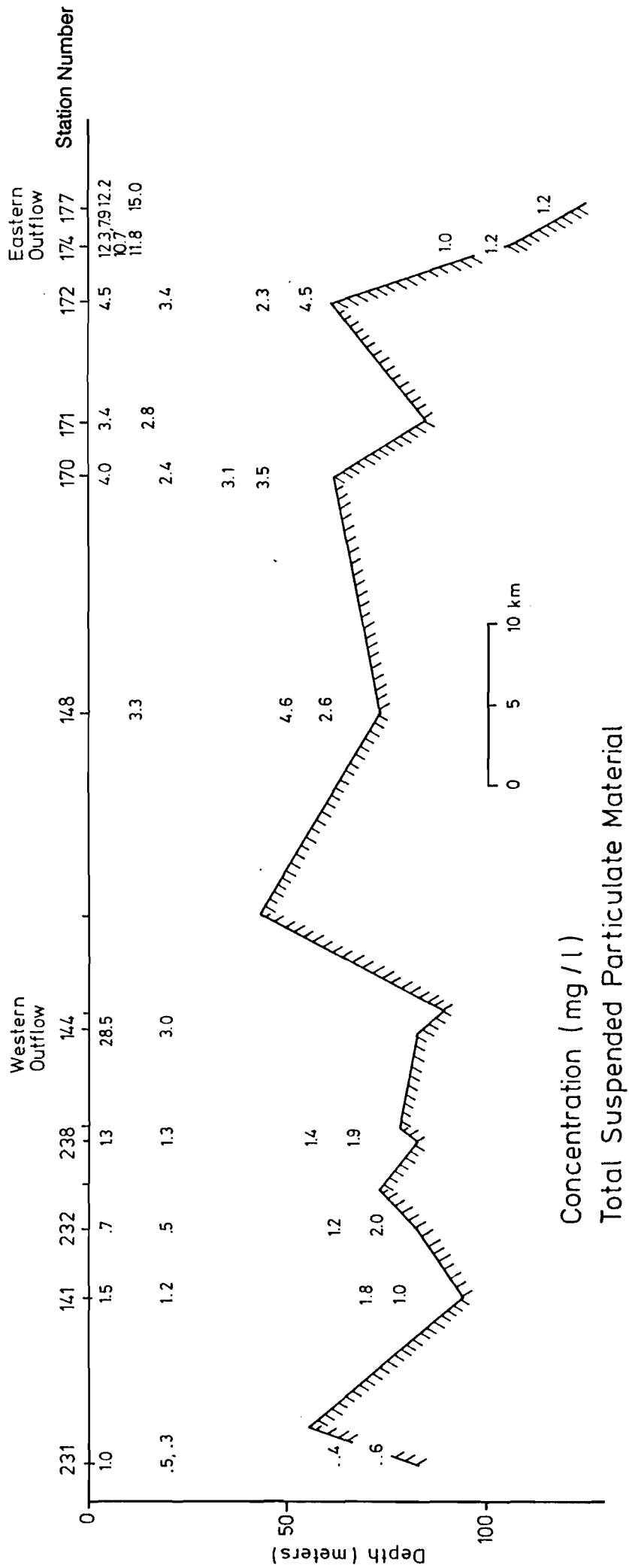


Fig. 6



Concentration (mg/l)
Total Suspended Particulate Material

Fig. 7

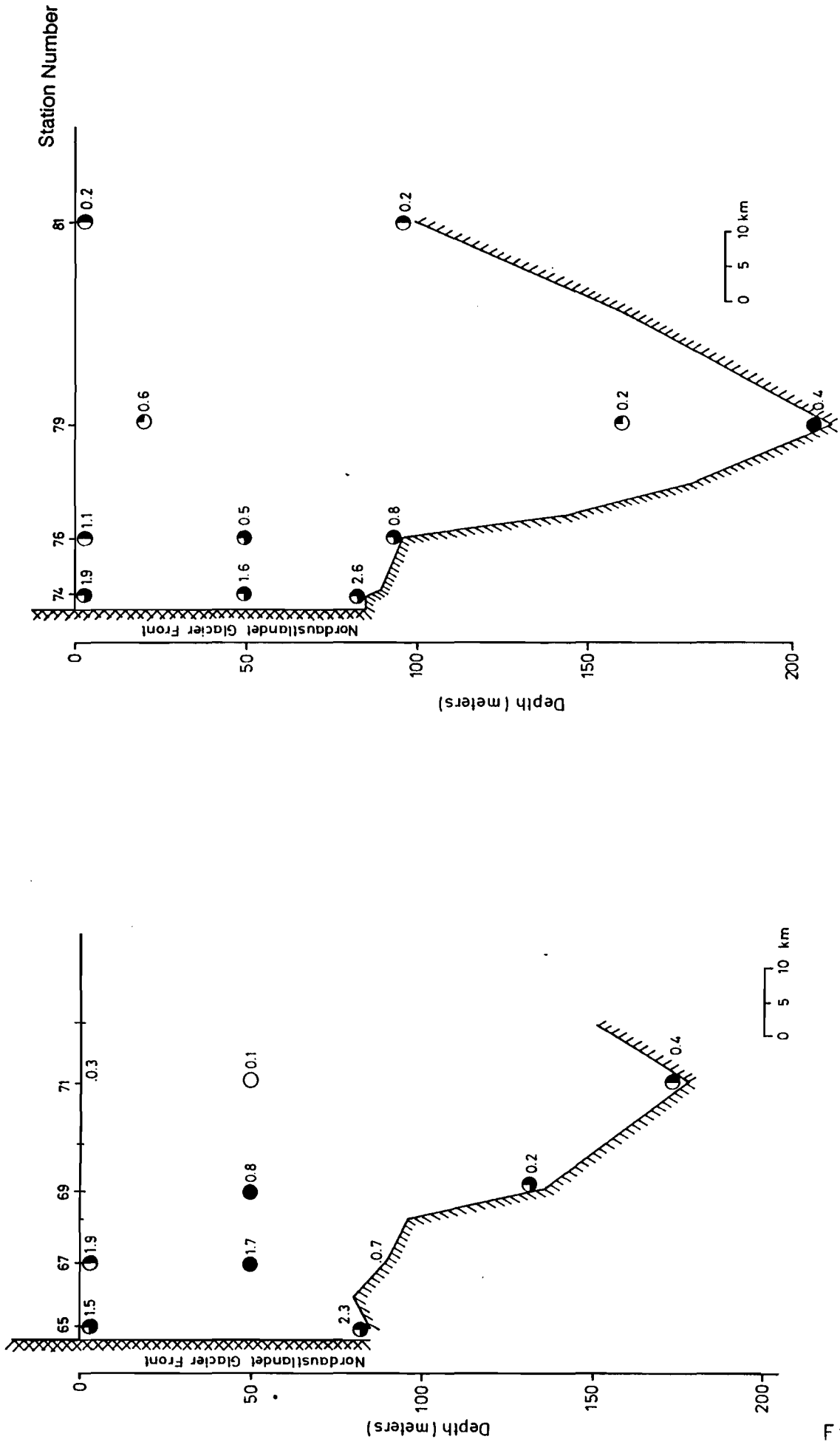


Fig. 8

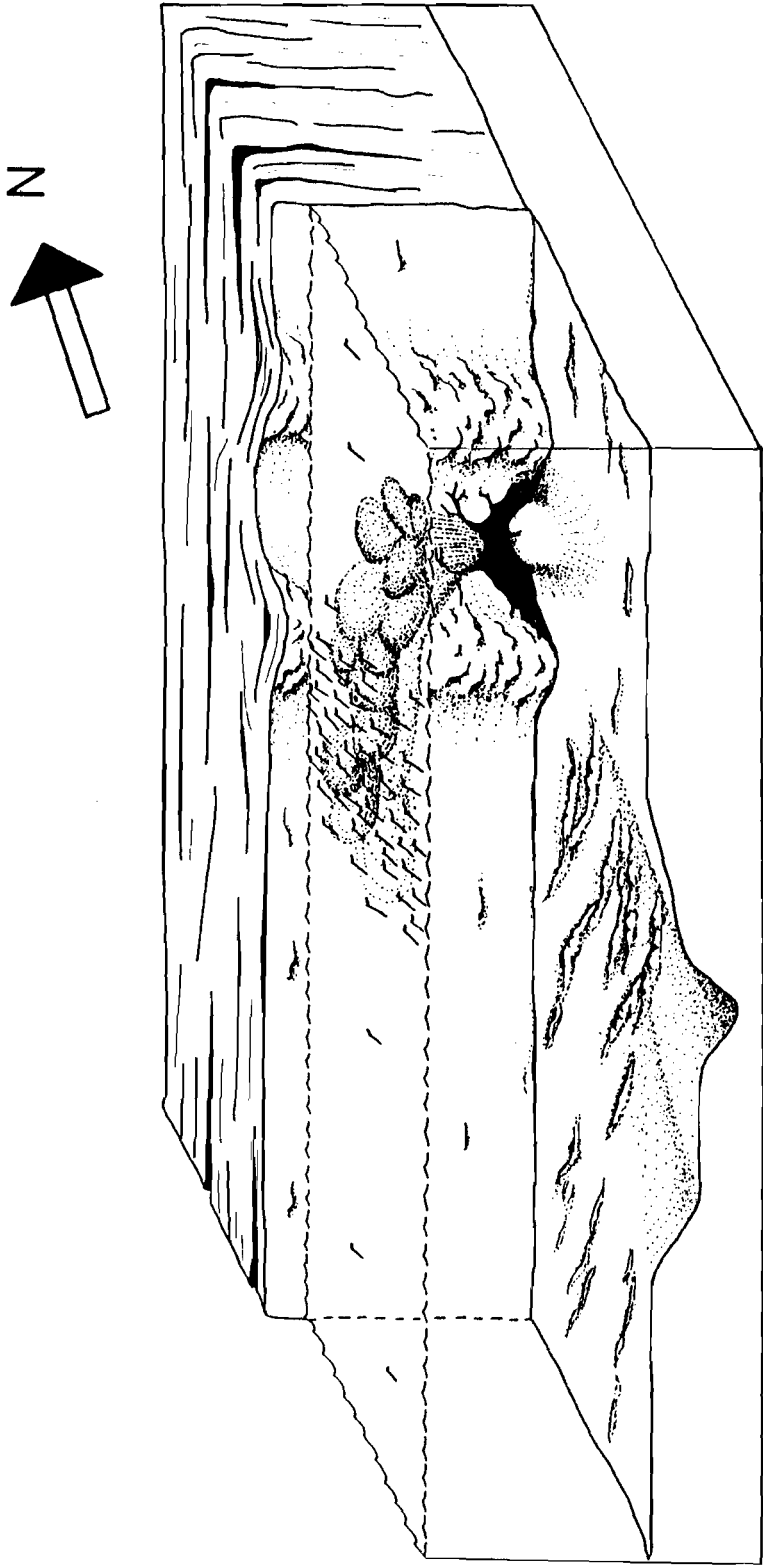


Fig. 9

PAPER 4.

The Barents Sea ice sheet – a sedimentological discussion

A. ELVERHØI AND A. SOLHEIM



Elverhøi, A. & Solheim, A. 1983: The Barents Sea ice sheet – a sedimentological discussion. *Polar Research* 1 n.s., 23–42. Oslo.

Sediment sampling and shallow seismic profiling in the western and northern Barents Sea show that the bedrock in regions with less than 300 m water depth is unconformably overlain by only a thin veneer (< 10 m) of sediments. Bedrock exposures are probably common in these areas. The sediments consist of a Holocene top unit, 0.1–1.5 m in thickness, grading into Late Weichselian glaciomarine sediments. Based on average sedimentation rates (¹⁴C-dating) of the Holocene sediments, the transition between the two units is estimated to 10,000–12,000 B.P. The glaciomarine sediments are commonly 1–3 m in thickness and underlain by stiff pebbly mud, interpreted as till and/or glaciomarine sediments overrun by a glacier. In regions where the water depth is over 300 m the sediment thickness increases, exceeding 500 m near the shelf edge at the mouth of Bjørnøyrenna. In Bjørnøyrenna itself the uppermost 15–20 m seem to consist of soft glaciomarine sediments underlain by a well-defined reflector, probably the surface of the stiff pebbly mud. Local sediment accumulations in the form of moraine ridges and extensive glaciomarine deposits (20–60 m in thickness) are found at 250–300 m water depth, mainly in association with submarine valleys. Topographic highs, probably moraine ridges, are also present at the shelf edge. Based on the submarine morphology and sediment distribution, an ice sheet is believed to have extended to the shelf edge at least once during the Pleistocene. Spitsbergenbanken and the northern Barents Sea have also probably been covered by an ice sheet in the Late Weichselian. Lack of suitable organic material in the glaciogenic deposits has prevented precise dating. Based on the regional geology of eastern Svalbard, a correlation of this younger stage with the Late Weichselian is indicated.

Anders Elverhøi and Anders Solheim, Norsk Polarinstitutt, Rolfstangveien 12, 1330 Oslo Lufthavn, Norway. June 1982 (revised November 1982).

Introduction

The question of a Barents Sea ice sheet represents an outstanding problem in the reconstruction of former glaciations on the northern hemisphere. With regard to the Late Weichselian the views currently held on the glacial history of the region can be summarized:

- (1) Total glaciation of the Barents Sea (Grosswald 1980; Andersen 1981; Hughes *et al.* 1981, maximum model). Extensive glaciation of the Barents Sea is also suggested by Hoppe (1970) and Kvasov (1978).
- (2) Glaciation of the shallower regions with Bjørnøyrenna and Storfjordrenna as calving bays (Matisov 1980).
- (3) No glaciation significantly beyond the coasts of Svalbard (Baranowski 1977; Boulton 1979a, b).

Essential elements in Grosswald's (1980) concept of a total glaciation are:

- (1) A continuation of the 'Egga moraines' (end-moraines on the Norwegian shelf (Andersen

1968)), northwards along the shelf edge west of the Barents Sea (Koteniov *et al.* 1976).

- (2) Presence of stiff pebbly mud in large parts of the Barents Sea implying till deposits (Diebner 1968).
- (3) Moraine ridges in northern Russia formed from a glacial advance from the northwest at the end of the Late Weichselian or in the early Holocene (Grosswald *et al.* 1974).

Matisov (1980 and numerous earlier publications) based his conclusion on a geomorphological study of the sea floor. A main line of argument was ridge complexes near the mouths of submarine valleys, especially those extending out from Spitsbergenbanken.

The main arguments for Boulton's hypothesis of a non-glaciated Barents Sea are:

- (1) The probable presence of extensive glaciomarine sediments in the Barents Sea.
- (2) Earlier observations of till (e.g. Diebner 1968) are doubtful.
- (3) Little apparent evidence of glacial erosion.

Boulton (1979b) argues that the main Barents Sea basin has not been glaciated at all during the Pleistocene.

Essentials for the discussion of a Late Weichselian Barents Sea ice sheet have in general been:

- (1) The presence of undated high beaches on Kong Karls Land.
- (2) The apparent straight-line emergence curves for Kong Karls Land and Hopen published by Hoppe (1970).
- (3) Glacial striae on Hopen (Hoppe *et al.* 1969). These, however, have been reinterpreted as non-glacial (Hoppe 1981).

Boulton (1979a) suggested that the high beaches were probably very old and that the anomalous pattern of the uplift curves on Hopen and Kong Karls Land were the result of one, or a combination of the following three possibilities:

- (1) Uplift of the islands may have been influenced by a substantial glacier regeneration on Svalbard during the late Holocene ('Little Ice Age').
- (2) Uplift could have been restrained during the Holocene by a rapid eustatic sea level rise.
- (3) Uplift may have been influenced by a tectonic component.

A tectonic uplift has also been suggested by Semevsky (1967).

Recent years' detailed glacial geology studies on Kong Karls Land have, however, revealed an early Holocene age for the high beaches 100 m above sea level (Salvigsen 1981). Furthermore, an asymptotic or normal emergence curve has been found. Similar emergence curves have also been published for Nordaustlandet (Salvigsen 1978) and Edgeøya and Barentsøya (Knape 1971), which combined with the observations on Kong Karls Land strongly suggest that a Late Weichselian ice sheet also covered much of the northern Barents Sea (Salvigsen 1981).

In this paper new information on the stratigraphy and facies of the Quaternary sediments in the Barents Sea is related to the question of glaciations.

The investigations have been conducted in the south-western (Bjørnøyrenna), northwestern (Spitsbergenbanken), and the northern (W of 35°E) Barents Sea, and only these areas have been taken into consideration.

Sediment distribution and thickness

The principal findings on sediment type, distribution and composition can be summarized as follows (Figs. 3, 4, & 5):

- (1) Stiff pebbly mud (till and/or glaciomarine sediments overrun by a glacier) covered by soft mud with pebbles (glaciomarine deposits). In areas with <300 m water depth, the thicknesses of the two units are in general <15 m and <3 m, respectively.
- (2) Large sediment accumulations are present in the western part of the major troughs (Bjørnøyrenna and Storfjordrenna) and exceed 500 m in thickness near the shelf edge, decreasing towards the central and inner parts of the troughs.
- (3) In regions with >300 m water depth, the glaciomarine sediments increase in thickness, 15–20 m, and are overlain by fine-grained Holocene mud, rich in foraminifera and organic debris. Thickness of the Holocene mud is commonly <1.5 m. The fine-grained mud is also localized in shallower areas, especially in smaller depressions. The stiff pebbly mud is probably also present underneath the glaciomarine sediments in these areas.
- (4) Transverse moraine ridges are present in the troughs radiating out from Spitsbergenbanken. Ridges are also parallel to the shelf break in Bjørnøyrenna and west of Spitsbergenbanken.
- (5) The boundary between the bedrock and the sediments is seen as a well-defined angular unconformity.
- (6) On Spitsbergenbanken the glacial sediments have been reworked by currents and mixed with Holocene bioclastics. A gravelly lag is also common in shallower (<100 m) parts in the northern and central Barents Sea.

Distribution of the glaciomarine deposits

The soft sediments sampled from Bjørnøyrenna/Storfjordrenna, and the central and northern Barents Sea are characterized by an olive-grey unit, 0.1–1.5 m thick, underlain by blue-grey sediments (Fig. 6a, b).

A similar sequence is found on the northern slope of Spitsbergenbanken, while on the southern slope stiff pebbly mud is frequently exposed

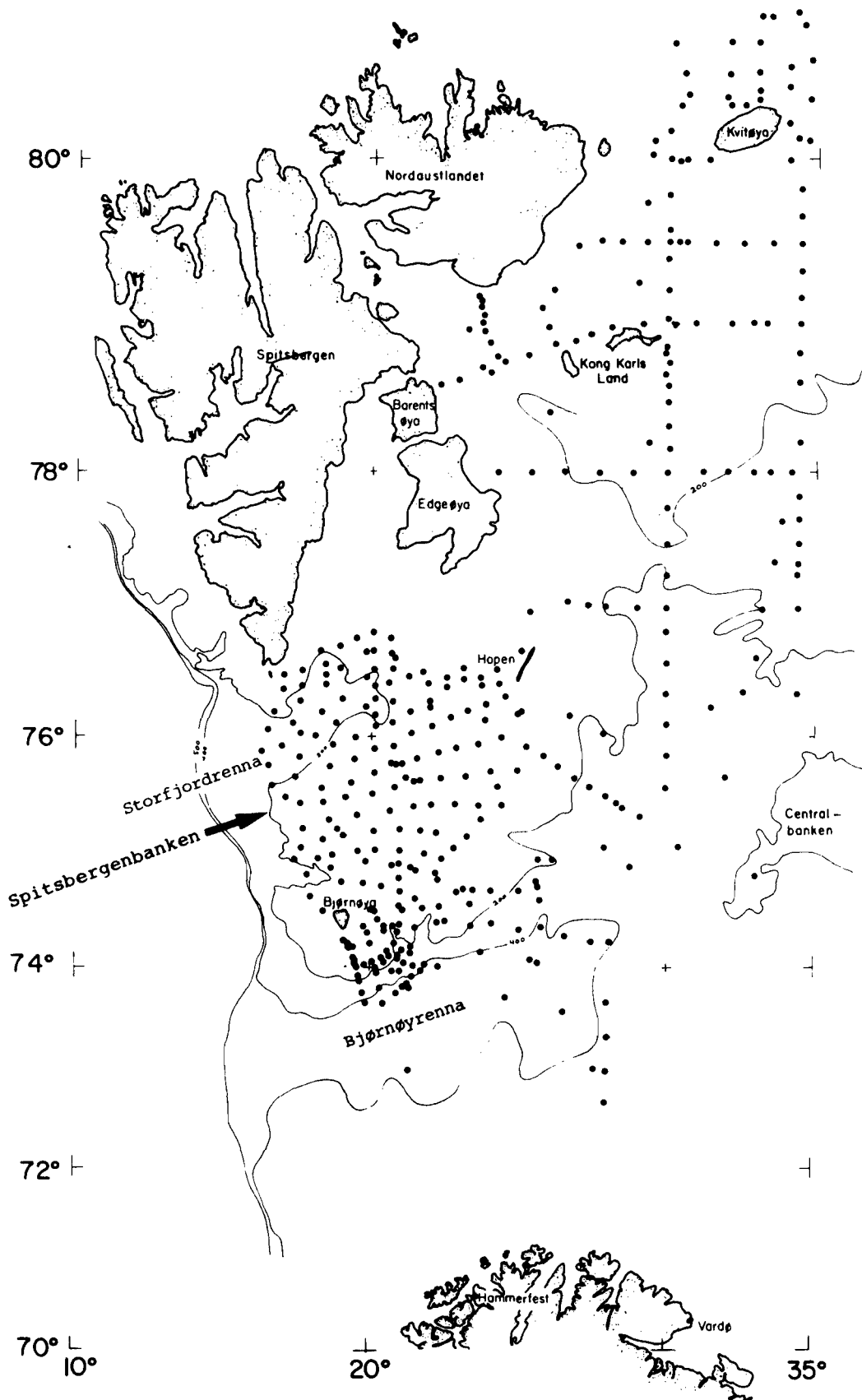


Fig. 1. Sediment samples obtained during geological surveys in the Barents Sea by the Norwegian Polar Research Institute and the Norwegian Petroleum Directorate. In general a 3 m long gravity corer is used, except for Spitsbergenbanken (<75–100 m water depth) where the samples are obtained by grab. Also location map for cores shown in Fig. 6.

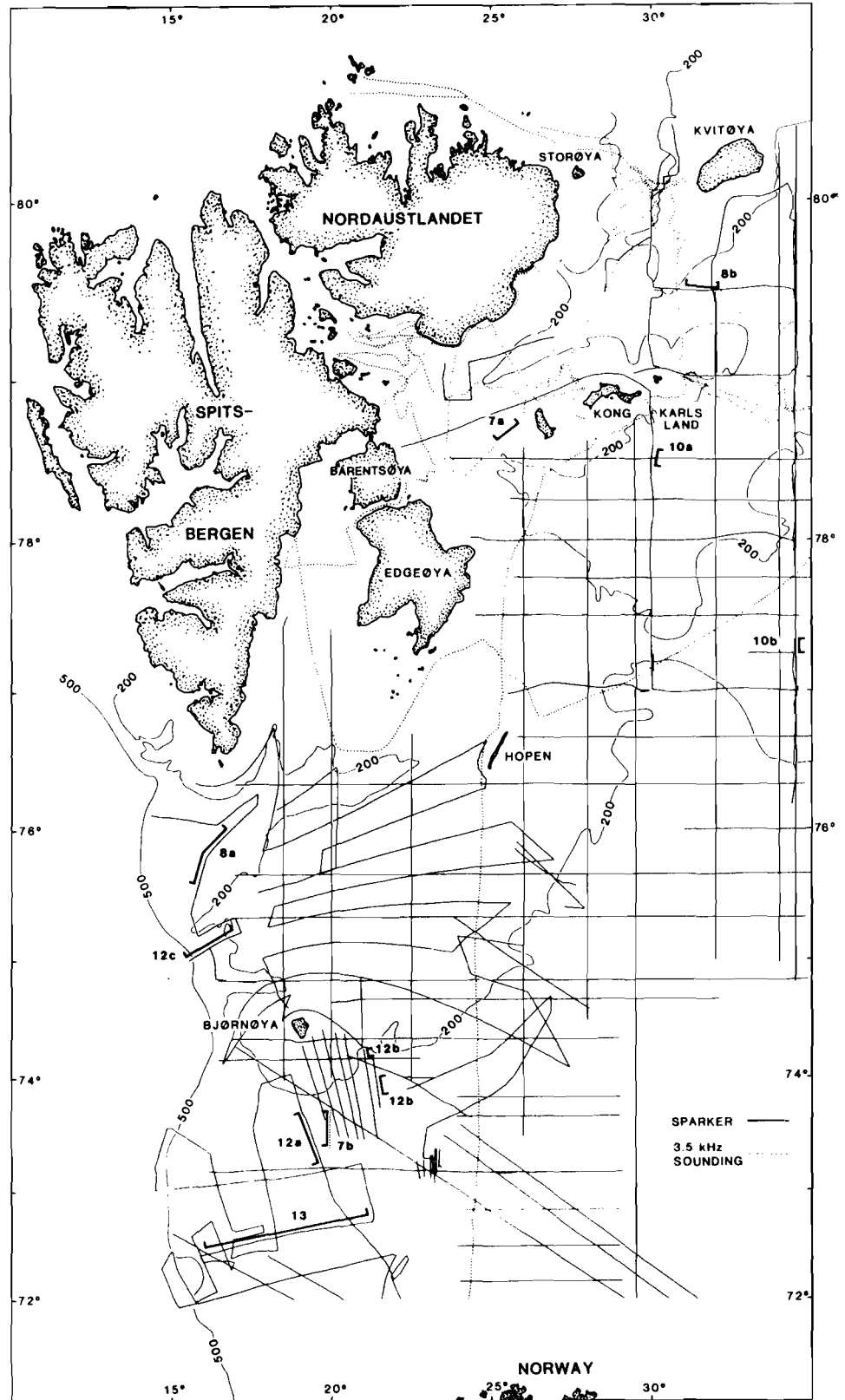


Fig. 2. Shallow seismic profiles in the western and northern Barents Sea obtained by the Norwegian Petroleum Directorate and the Norwegian Polar Research Institute. The numbers refer to seismic profiles presented.

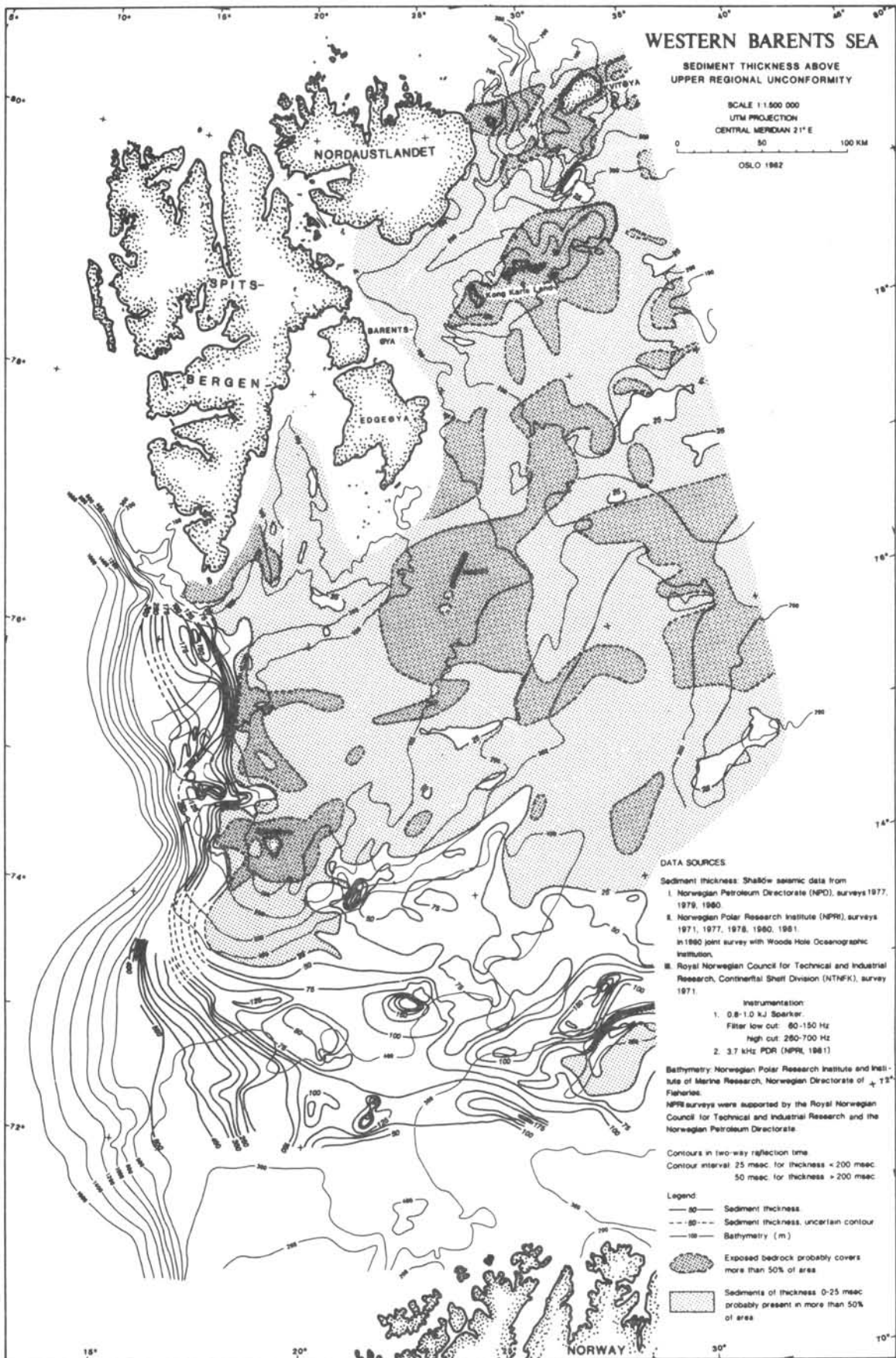


Fig. 3. Sediment distribution map of the northern and western Barents Sea.

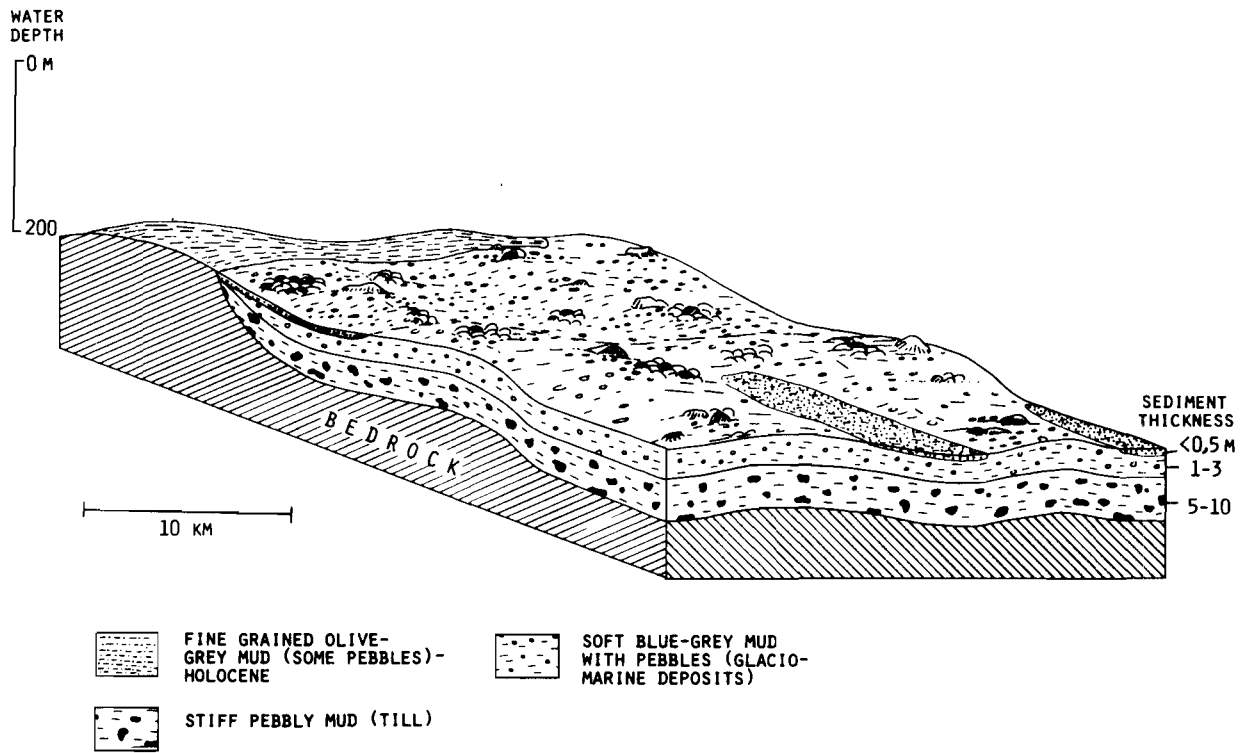


Fig. 4. Generalized block diagram illustrating the sediment distribution in the northern and central Barents Sea.

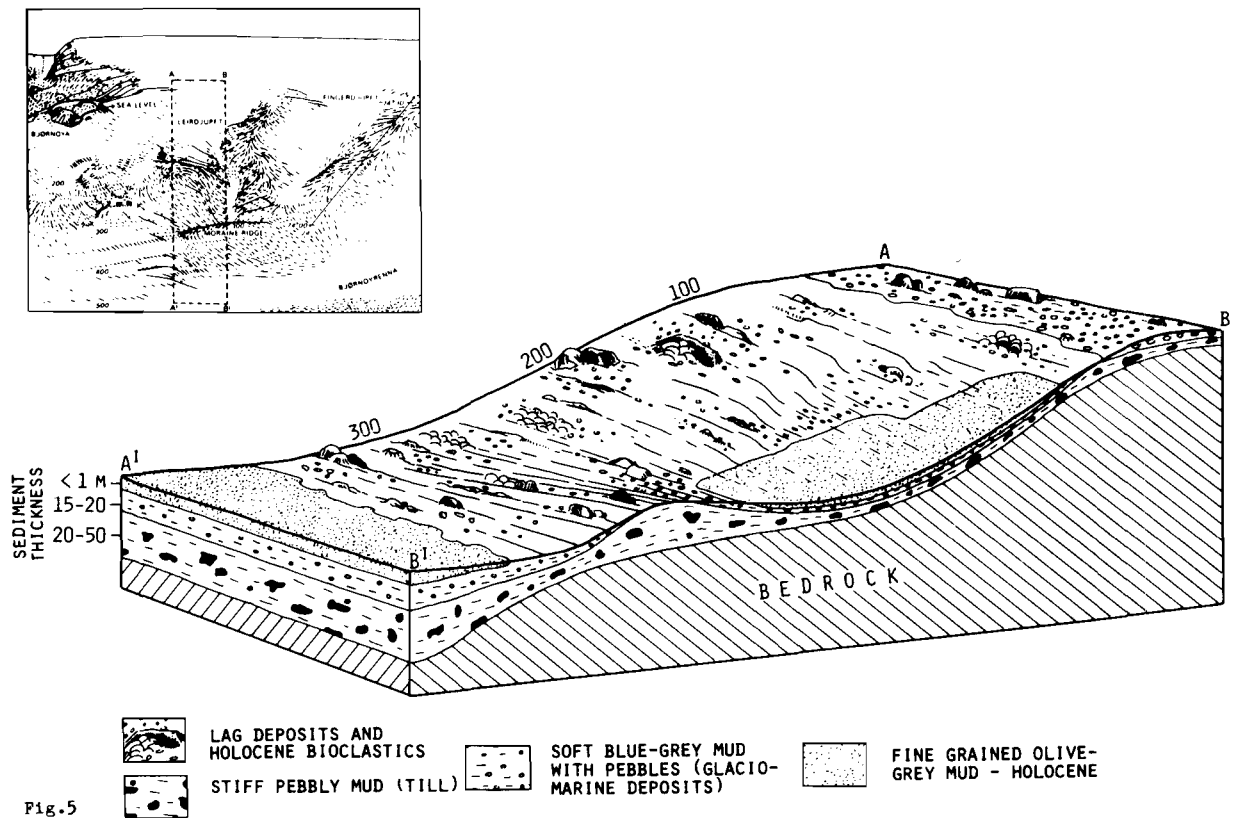


Fig. 5. Generalized block diagram illustrating the sediment distribution on the slope south of Spitsbergenbanken and northern part of Bjørnøyrenna.

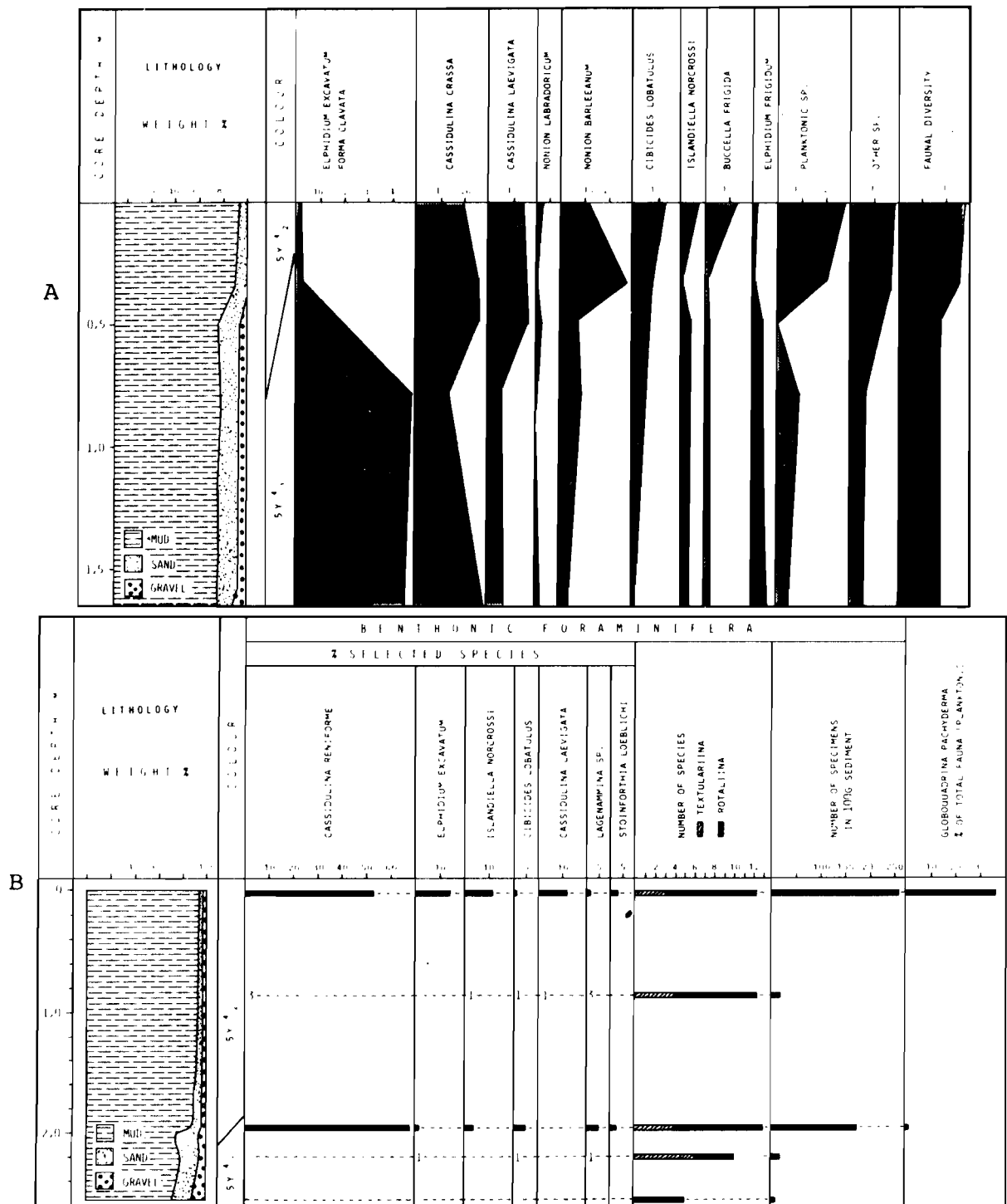


Fig. 6. Characteristic lithology and foraminiferal fauna in sediments from □ A. Bjørnøyrenna (from Elverhøi & Bomstad 1980). □ B. Central/northern Barents Sea. Colour code refers to Munsell Soil Color Charts (5 Y 4/2: olive grey, 5 Y 4/1: dark grey). For location, see Fig. 1.

at the seabed down to 350 m water depth (Bjørlykke *et al.* 1978).

In the northern and central parts of the Barents Sea both units are typical glaciomarine deposits, soft mud with ice-rafted pebbles. The olive-grey

unit is rich in organic debris and foraminifera. The blue-grey unit, however, has a higher content of pebbles and a very low content of foraminifera, all with affinities to cold water (Fig. 6b), showing a more glacially influenced depositional environ-

ment than the overlying olive-grey deposits. In Bjørnøyrenna and Storfjordrenna the olive-grey unit very seldom contains pebbles, but the underlying unit is similar to that found in northern and central regions.

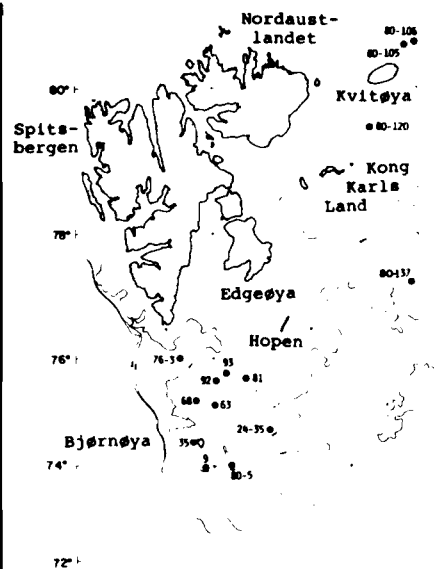
In some cores from the shallower areas (< 200 m water depth) in the central and northern regions, a thin lag of pebbles and shell fragments indicates a minor erosional episode at the transition from the olive-grey unit to the underlying blue-grey one. ^{14}C -dating, core 137, Table 1,

indicates a mid-Holocene age for this event. However, generally, and for all the deeper parts, the boundaries are transitional with regard to colour, texture, as well as foraminifera assemblage (Fig. 6a, b), indicating a continuous sedimentary sequence.

^{14}C -datings of molluscs in the middle and lower parts of the olive-grey unit give an early/mid-Holocene age (Table 1). All datings from cores have been obtained on whole bivalves of *Astarte* sp. in life position. These molluscs live just below

Table 1. ^{14}C -datings of sediments from the western and northern Barents Sea. Datings of surface samples from Spitsbergenbanken are also included (data from Bjørlykke *et al.* 1978).

| SAMPLE NR | WATER DEPTH (M) | MATERIAL | ^{14}C -AGE YEARS BP | DEPTH IN CORE (M) | AVERAGE DEPOSITIONAL RATE (CM/1000 Y) | LAB. REF. NUMBER |
|-----------|-----------------|-----------------------------|-------------------------------|-------------------|---------------------------------------|------------------|
| 80-5 | 275 | Mollusc <i>Astarte</i> Sp. | 8.060 ± 310 | 0.25 | 3.1 | T - 3830 |
| 24-35 | 145 | " | 4.210 ± 330 | 0.10 | 3.4 | T - 3396 |
| 76-3 | 300 | " | 7.230 ± 340 | 0.19 | 2.6 | T - 3333 |
| 80-137 | 125 | " | 4.290 ± 160 | 0.35 | 8.2 | T - 3832 |
| 80-137 | 125 | " | 6.670 ± 120 | 0.50 | 7.5 | T - 3834 |
| 80-120 | 300 | " | 5.780 ± 270 | 0.10 | 1.7 | T - 4171 |
| 80-105 | 149 | " | 8.580 ± 290 | 0.26 | 2.3 | T - 3831 |
| 80-106 | 165 | " | 7.750 ± 200 | 0.30 | 3.9 | T - 3833 |
| 92 | 50 | Mollusc <i>Mya truncata</i> | 4.370 ± 130 | Surface | | T - 1798 |
| 81 | 58 | " | 2.390 ± 110 | " | | T - 1799 |
| 93 | 30 | " | 8.730 ± 110 | " | | T - 1687 |
| 9 | 158 | " | 9.140 ± 100 | " | | T - 2871 |
| 81 | 58 | Mollusc <i>Saxicava</i> | 280 ± 110 | " | | T - 1808 |
| 35 | 60 | Barnacles | 2.250 ± 120 | " | | T - 1800 |
| 68 | 35 | " | 990 ± 110 | " | | T - 1797 |
| 92 | 56 | " | 2.340 ± 120 | " | | T - 1801 |
| 63 | 35 | " | 640 ± 70 | " | | T - 1686 |



the sediment surface and are too big to have been recycled because of bioturbation.

Until now there has been no success in obtaining datable material from the blue-grey unit, but the transition to the overlying Holocene unit can tentatively be dated to the end of the Late Weichselian (10,000–12,000 B.P.):

- (1) There is apparently no sign of a hiatus between the olive-grey and blue-grey deposits.
- (2) An early Holocene to mid-Holocene age was obtained for the lower part of the olive-grey deposits.
- (3) In the few shallower areas with sign of erosion at the transition, the erosional episode is of early/mid-Holocene age.
- (4) A marked lithostratigraphic boundary between glaciomarine and younger non-glacigenic sediments is dated to 10,000 B.P. in the area just south of the Barents Sea (Vorren *et al.* 1978).

A Late Weichselian age for at least the uppermost

part of the blue-grey sediment in Bjørnøyrenna is also seen from data published by Grosswald (1972). In a 'core taken at a sea depth of 370 m between Bear Island and the northern tip of Norway', 12,385 ± 280 B.P. (St.-3341) was obtained on a shell in a depth interval of 37–52 cm. This layer is grey in colour, containing pebbles and a foraminiferal assemblage similar to that found in our blue-grey unit.

The lithology of the blue-grey glaciomarine sediments is homogeneous with no sign of erosional episodes. The recovered foraminiferal fauna is also uniform, consisting of only extremely cold water species, suggesting that the blue-grey deposits form a single depositional unit. However, it should be noted that a complete section through the blue-grey sediments into the underlying stiff pebbly mud has only been obtained in a limited number of cores, confined to the southern slope off Spitsbergenbanken and from the northern Barents Sea. No final conclusion can thus be drawn on whether the blue-grey glacio-

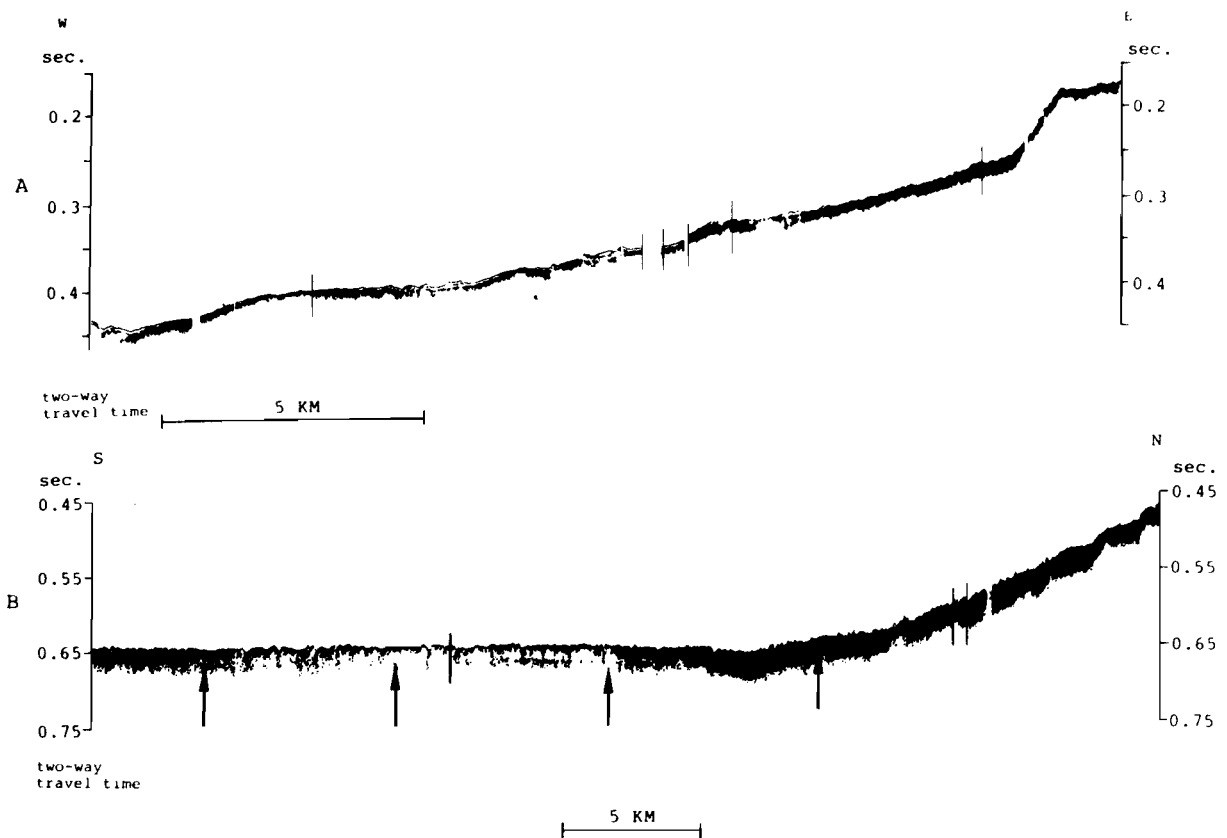


Fig. 7. □ A. Characteristic 3.5 kHz echo sounding profile from the northern Barents Sea, showing 1–3 m of soft sediments above a well defined reflector–till/bedrock. □ B. 3.5 kHz echo sounding profile from Bjørnøyrenna, southeast of Bjørnøya. The lower boundary of the glaciomarine sediments is shown by the arrows. For location of the profiles, see Fig. 2.

marine sediments have been deposited continuously or include periods of erosion/non-deposition.

The thickness of the glaciomarine (blue-grey) sediments has been obtained from sediment coring, and by 3.5 kHz echo sounder records (Figs. 2, 7). A 3.5 kHz echo sounding profile south of Bjørnøya shows the blue-grey glaciomarine deposits apparently increasing to 15–20 m into Bjørnøyrenna (Fig. 7b). These sediments have earlier been interpreted as glacial till or moraine deposits from data mainly based on 3.5 kHz echo sounding (Damuth 1978). On the lower part of the slope from Spitsbergenbanken, the thickness seems to be <2 m, as found by sediment coring.

In Storfjordrenna and also in a trough northeast of Kong Karls Land, thick (40–60 m) deposits have been recorded on sparker profiles (Fig. 8a,

b). Based on their acoustically transparent character and lack of internal reflectors, these deposits probably consist of soft, homogeneous sediments. There are also 3.5 kHz echo sounding profiles across the deposit northeast of Kong Karls Land. Sediment coring, supplemented with ¹⁴C-dating (core 76–3, 80–120, Table 1), revealed the blue-grey glaciomarine sediments below half a metre of Holocene deposits. Because of their homogeneous composition, the blue-grey glaciomarine sediments sampled near the seabed almost certainly make up the entire accumulations. In a depression south of Kong Karls Land, and also at the innermost part of Bjørnøyrenna, similarly acoustically transparent sediments are found below the Holocene sediments. These deposits are also interpreted as consisting of the blue-grey glaciomarine sediments.

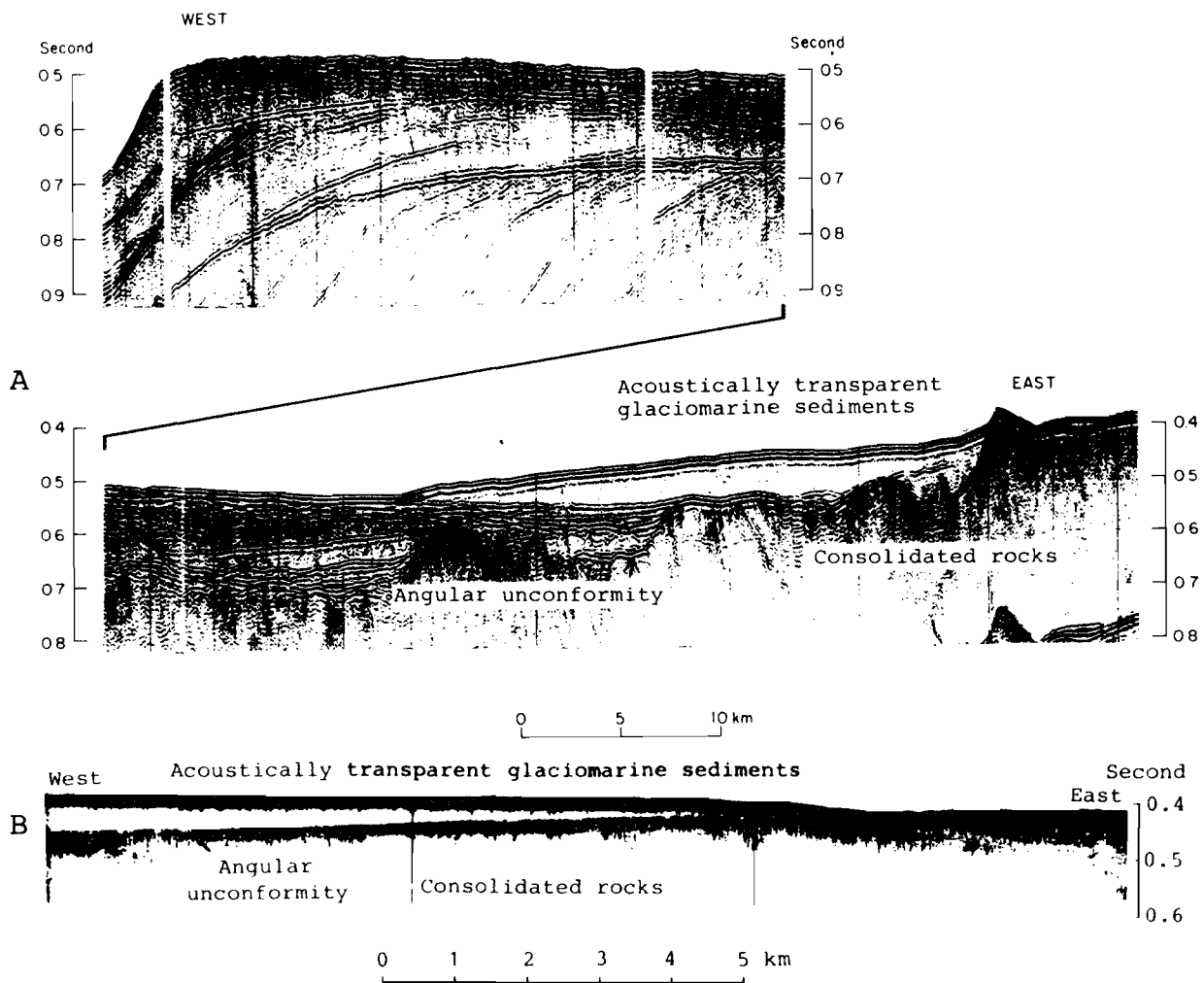


Fig. 8. □ A. Sparker profile from the outer part of Storfjordrenna. The extension of acoustically transparent deposits is confined to the east by a bedrock sill. □ B. Sparker profile across a trough northeast of Kong Karls Land. The acoustically transparent deposits are found at water depths >300 m (from Kristoffersen *et al.* in press). For location of the profiles, see Fig. 2.

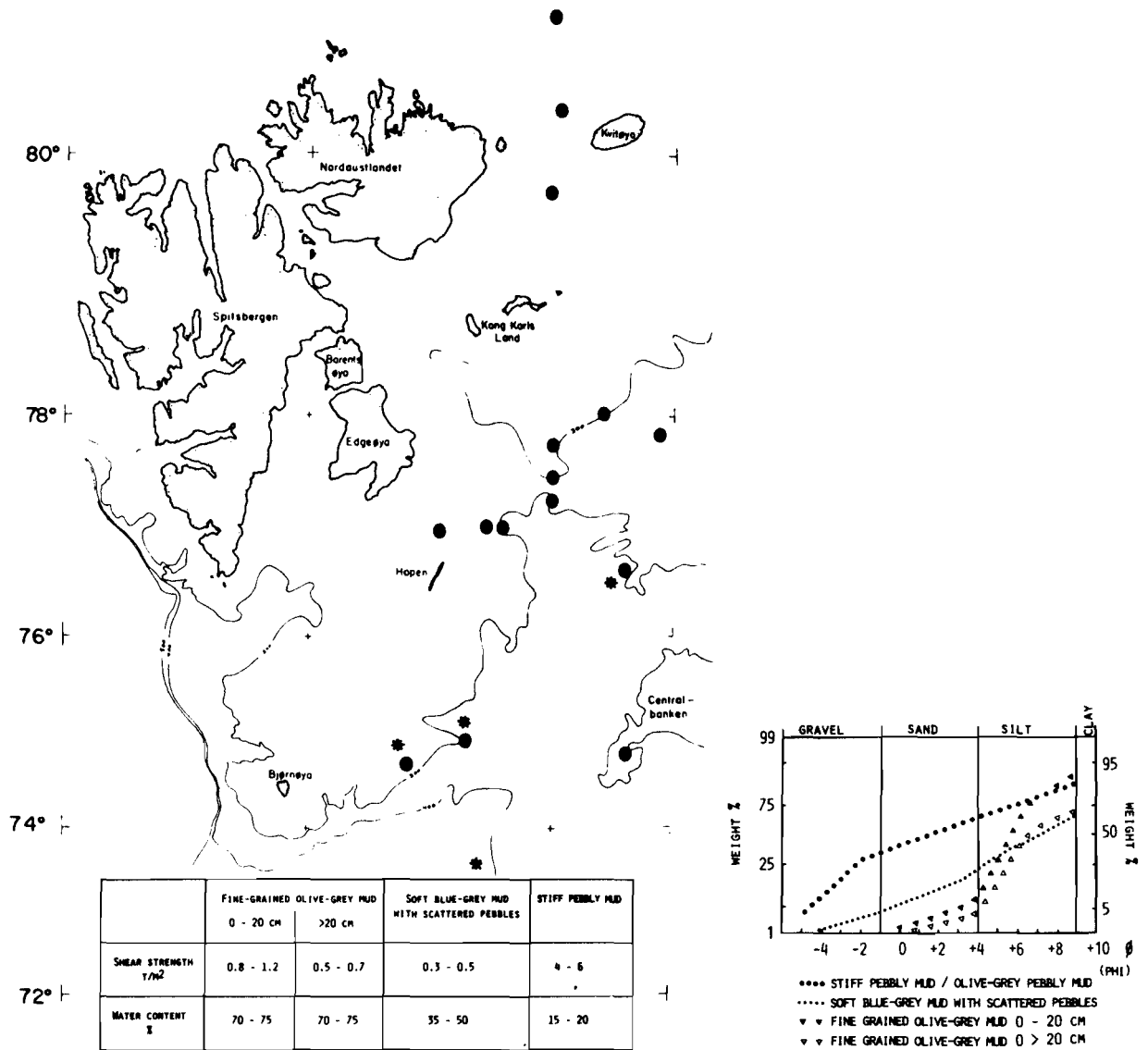


Fig. 9. Map showing localities where stiff pebbly mud has been sampled and investigated. Shear strength and water content determinations from the different lithologies are listed. Grain-size analyses for the samples are shown. *: analysed samples. Analyses: Norwegian Geotechnical Institute.

The stiff pebbly mud

Texture and distribution

In regions shallower than 300 m, the stiff pebbly mud was sampled at ten localities during the surveys in 1978 and 1980 (Fig. 9). Geotechnical tests made on three of the samples show shear strength values in the range of 4–6 t/m² (40–60 kN/m²), which is an order of magnitude higher than that found for normally consolidated surface sediments, e.g. the sample from Bjørnøyrenna (Fig. 9). Because of the stiffness only 20–30 cm of this type of deposit was obtained by gravity coring. Larger samples were collected with the

1 m³ grab. Lumps of the same material were also recovered with a pipe dredge.

These sediments seem to be very thin in regions shallower than 300 m (Fig. 10). From the sparker records the sediment thickness above bedrock is found in general to be <15 m (because of the pulse width, no resolution is obtained in the first 10–15 m below sea bottom). Supported with data from the 3.5 kHz echo sounding and the sediment coring, the sediment thickness is estimated to be <5 m. In some areas the bedrock is exposed, exemplified with a bottom photograph (Fig. 11). There has been no sampling through the stiff pebbly mud into the bedrock.

In areas deeper than 300 m there is a general thickening of sediments above bedrock (Fig. 12a). Based on the 3.5 kHz echo sounding and sediment coring, the upper 15–20 m of the deposit in Bjørnøyrenna probably consists of soft sediments. The reflector seen on the 3.5 kHz profile (Fig. 7) is thinning out to only 1–2 m on the lower part of the slope from Spitsbergenbanken. Sediment coring close to the profile showed exposure of the stiff pebbly mud, to which the reflector is correlated. Consequently the stiff pebbly mud seems to extend into Bjørnøyrenna.

Depositional mechanism

In addition to a basal till origin, stiff pebbly sediments may form from ice-rafted deposits compacted by various factors (a mud flow origin is excluded):

(a) *Sediment loading*. – Removal of overlying sediments due to gravity flow, however, is unlikely because of the low gradient. Alternatively, submarine erosion of glaciomarine sediments would have developed lag deposits, which have not been found.

(b) *Action of permafrost* (Williams 1967). – Sub-sea permafrost has to form out from land (or

beneath a cold glacier). A Late Weichselian drop in sea level of 100–130 m would cause subaerial exposure of parts of the Barents Sea. The stiff pebbly mud, however, is sampled at water depths well below and away from what could have been exposed during that regression. Assuming tectonic stability, the stiff pebbly mud is further sampled below water depths that can have been subaerially exposed during former, larger Pleistocene regressions.

According to the above, the stiff pebbly mud is most likely a till and/or glaciomarine deposits overrun by a grounded ice. At water depths shallower than 300 m, i.e. Spitsbergenbanken and the northern Barents Sea with only a thin sediment cover and frequent exposure of the bedrock, the stiff pebbly mud is tentatively classified as basal till. In areas deeper than 300–400 m, with considerable thickness of sediments above the bedrock, the stiff pebbly mud may, however, have been of glaciomarine origin. According to Dreimanis (1978), these sediments may be classified as deformation till.

Ice marginal features

Ridge complexes and areas of relative topographical highs that are not caused by bedrock have been observed in the following regions:

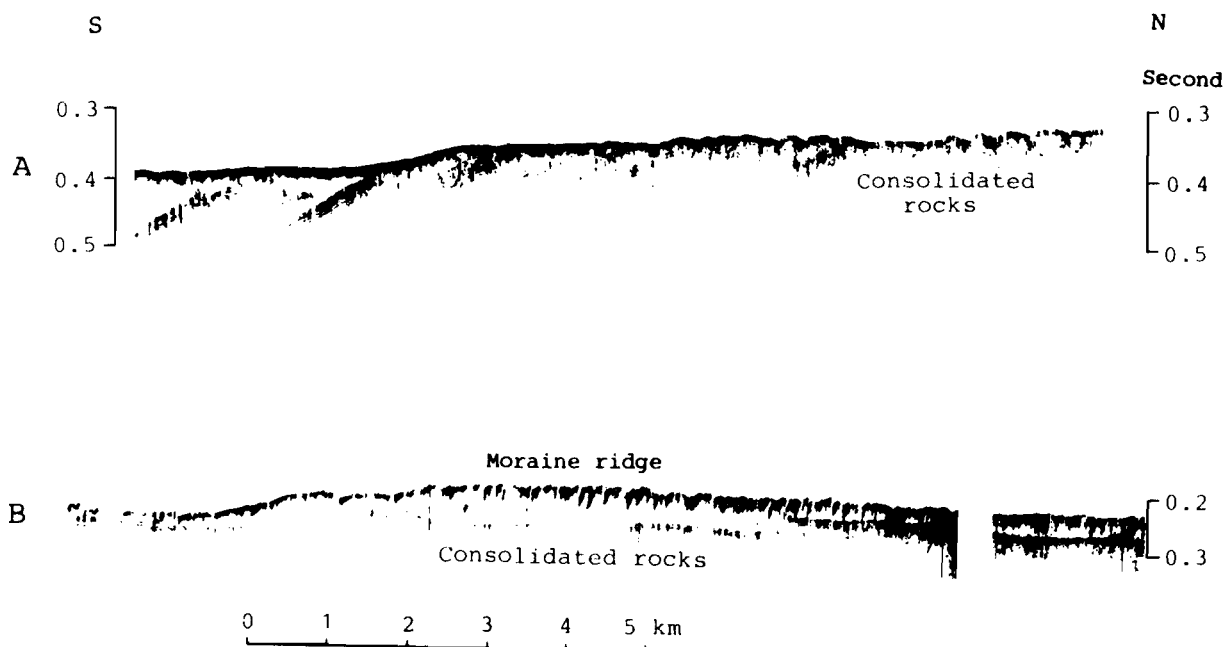


Fig. 10. Sparker profiles from the northern Barents Sea illustrating: □ A. The general existence of only a thin (<15 m) cover of sediments above the bedrock, forming a well-defined angular unconformity with the sea floor. □ B. An up to 50 m thick accumulation of glaciogenic sediments on Storbanken at 150 m water depth. The accumulation is probably a moraine (from Kristoffersen *et al.* in press). For location of the profiles, see Fig. 2.

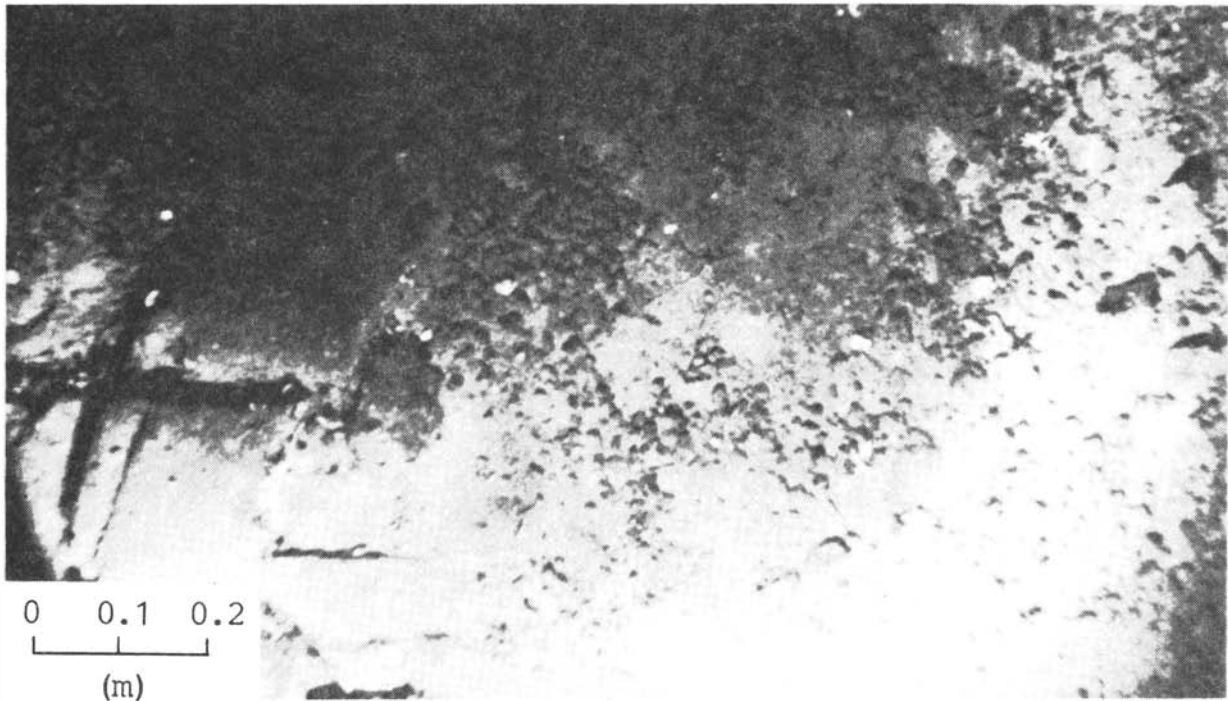


Fig. 11. Bottom photograph from the northern Barents Sea. Bedrock exposed in the left part of the photograph. 80° 24' N, 29° 55' E, 240 metres water depth (published with the permission of C. Craine.)

- (1) In the mouth of troughs radiating from Spitsbergenbanken (Fig. 12b).
- (2) Near the shelf edge at the mouth of Bjørnøyrenna and Storfjordrenna (Fig. 8a and 13).
- (3) On the upper slope/shelf edge west of Spitsbergenbanken (Fig. 12c).
- (4) On Storbanken, central Barents Sea (Fig. 10b).

(1) Both Leirdjupet (SE of Bjørnøya) and Kveithola (NW of Bjørnøya) form overdeepened troughs where the outer high is caused by sediment accumulation. In adjacent areas, only a sparse cover of sediment is present (Fig. 3).

In Leirdjupet the ridge has an asymmetric pattern, with the steepest slope facing southwards (Fig. 12b). The surface, especially the north facing part, is hummocky. Stiff pebbly mud was recovered from the surface. With the exception of a minor reflector in the lower part, no other evidence of internal structures has been obtained so far. From the geometry, the location in front of a valley, and the sediment distribution in adjacent areas, this feature appears to be deposited by a glacier flowing down Leirdjupet.

The thickness (approx. 100 m) and 'width'

(approx. 10 km) of the ridge in Leirdjupet are much larger than commonly found for end moraines on land. On the northern Norwegian shelf, features interpreted as end moraines are also very wide, 5–15 km (Rokoengen *et al.* 1979). Vorren & Elvsborg (1979) suggest that the broad appearance of these shelf deposits reflects a moraine complex rather than a single end moraine. It should be noted that the shelf moraines were deposited by ice influenced by buoyancy. The erosional power of the ice is then strongly reduced in its frontal areas and deposition is likely to start far back from the ice front.

(2) In the central parts of the mouth of Bjørnøyrenna there is a 50 m high sediment accumulation (Fig. 13). The ridge feature, supported with the truncated reflectors, suggests a glacial origin, probably an end moraine. Sparker profiles north of 73°N do not show any northward continuation of the high. Grosswald (1980) and Andersen (1981) suggest a continuation of the 'Egga moraine' to the north. Available bathymetric data from the area, however, are very limited and do not form a reliable data base for detailed contouring. Our seismic profiles also stop southward at 72°N. At the present stage, a con-

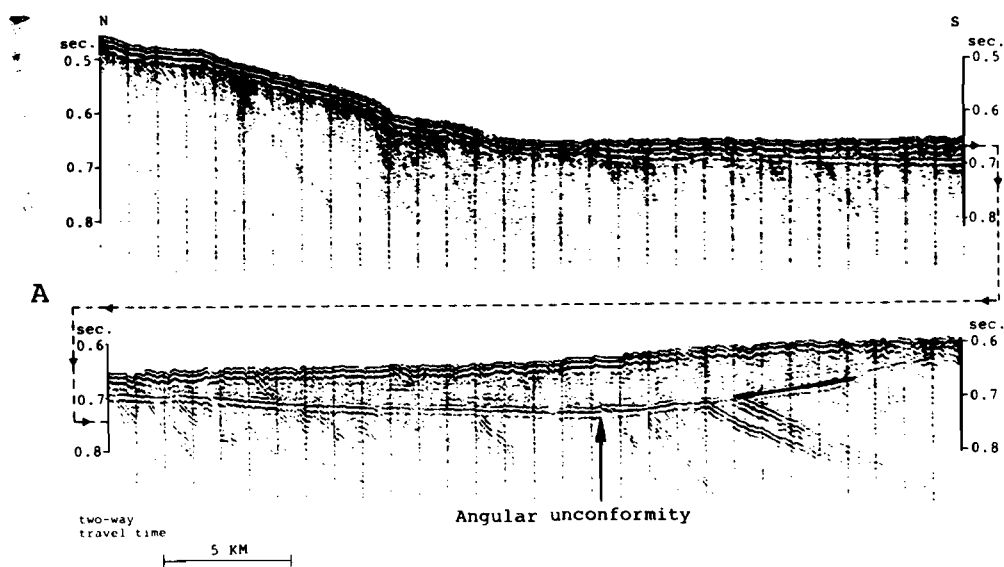
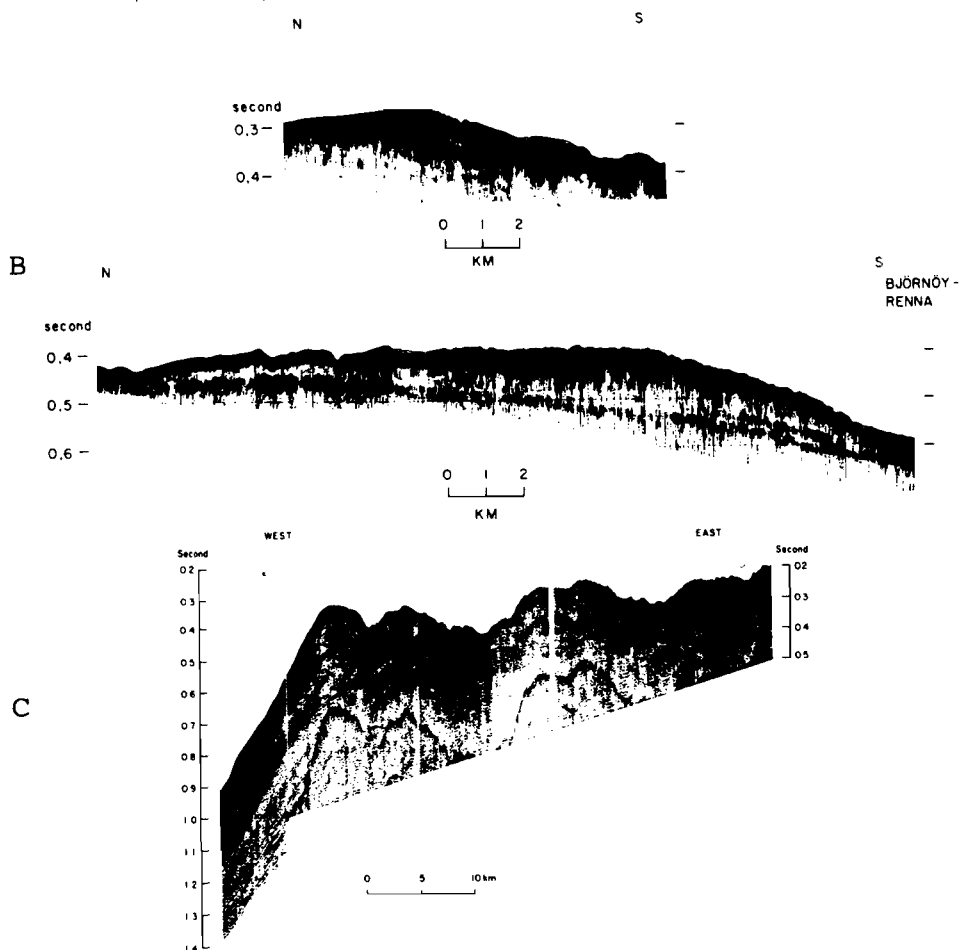


Fig. 12. □ A. Sparker profile from Bjørnøyrenna south of Bjørnøya, illustrating (1) increasing sediment thickness into Bjørnøyrenna, and (2) the well-defined angular unconformity between the bedrock and sediments. □ B. Sparker profile from Leirdjupet showing an up to 150 m thick accumulation of glaciogenic deposits at 300 m water depth. The accumulation is probably deposited in the frontal zone of a southward moving ice sheet. A minor moraine ridge is seen at approximately 200 m water depth (above). (From Elverhøi & Kristoffersen 1977.) □ C. Sparker profile across probable moraine ridges west of Spitsbergenbanken. For location of the profiles, see Fig. 2.



nection between the observed high and the 'Egga moraine' remains an open question.

The mouth of Storfjordrenna (Fig. 8a) also forms a topographical high relative to the inner parts. The reflection pattern on the sparker

records shows truncated reflectors, indicating episodes where glacial advance and erosion were followed by deposition as the ice sheet retreated, instead of a continuous build-up and progradation.

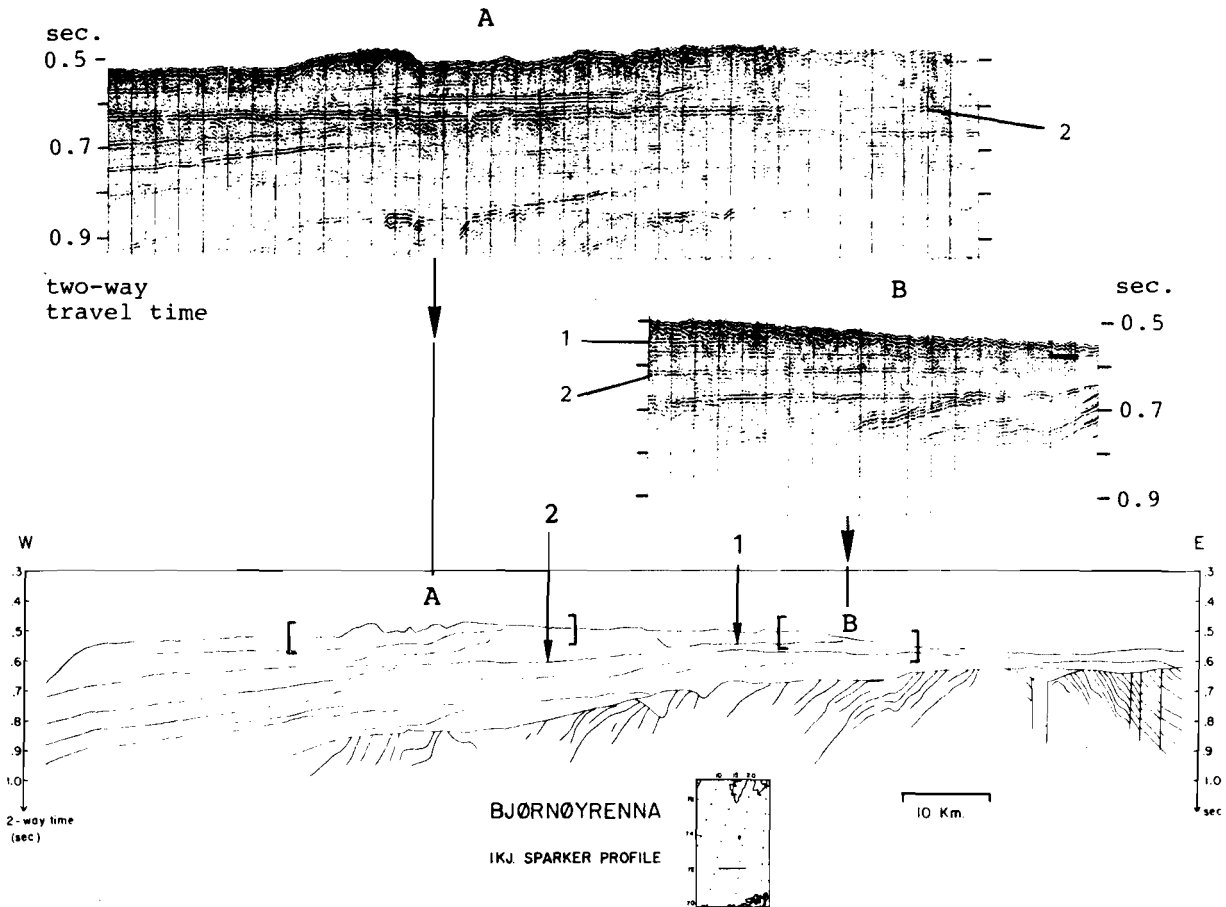


Fig. 13. Interpreted sparker profile from the mouth of Bjørnøyrenna. Note that the outer high is caused by sediment accumulated above reflector 2. For location, see Fig. 2.

(3) On the slope west of Spitsbergenbanken, the bottom is hummocky with a relative scale of 25–50 m (Fig. 12c) forming ridges oriented almost parallel to Spitsbergenbanken. Based on their geometry and orientation, these features are interpreted as end moraines deposited by an ice sheet advancing from Spitsbergenbanken.

(4) The morphology of the ridge strongly suggests a glacial origin, most likely an end moraine.

In addition to these features, local accumulations are found

- (1) at the innermost part of Storfjordrenna,
- (2) at 150–200 m water depth in the troughs extending radially out from Spitsbergenbanken (Fig. 12b),
- (3) on the southern slope off Spitsbergenbanken, and
- (4) at Storbanken and Sentralbanken.

Sediment sampling in the areas of 2, 3, and 4

showed stiff pebbly mud, indicating till (and/or glaciomarine deposits overrun by a glacier).

Erosional features

The sediments are everywhere commonly unconformably overlying the bedrock (e.g. Figs. 8b and 12a). Of special importance are the overdeepened regions in central parts of the Barents Sea (Fig. 14). As these features are formed by excavation into the bedrock (Fig. 3), they are most likely due to glacial erosion.

Discussion

The sediment distribution and stratigraphy (till overlain by glaciomarine sediments grading into postglacial deposits) clearly demonstrate that the Barents Sea has been covered by grounded ice

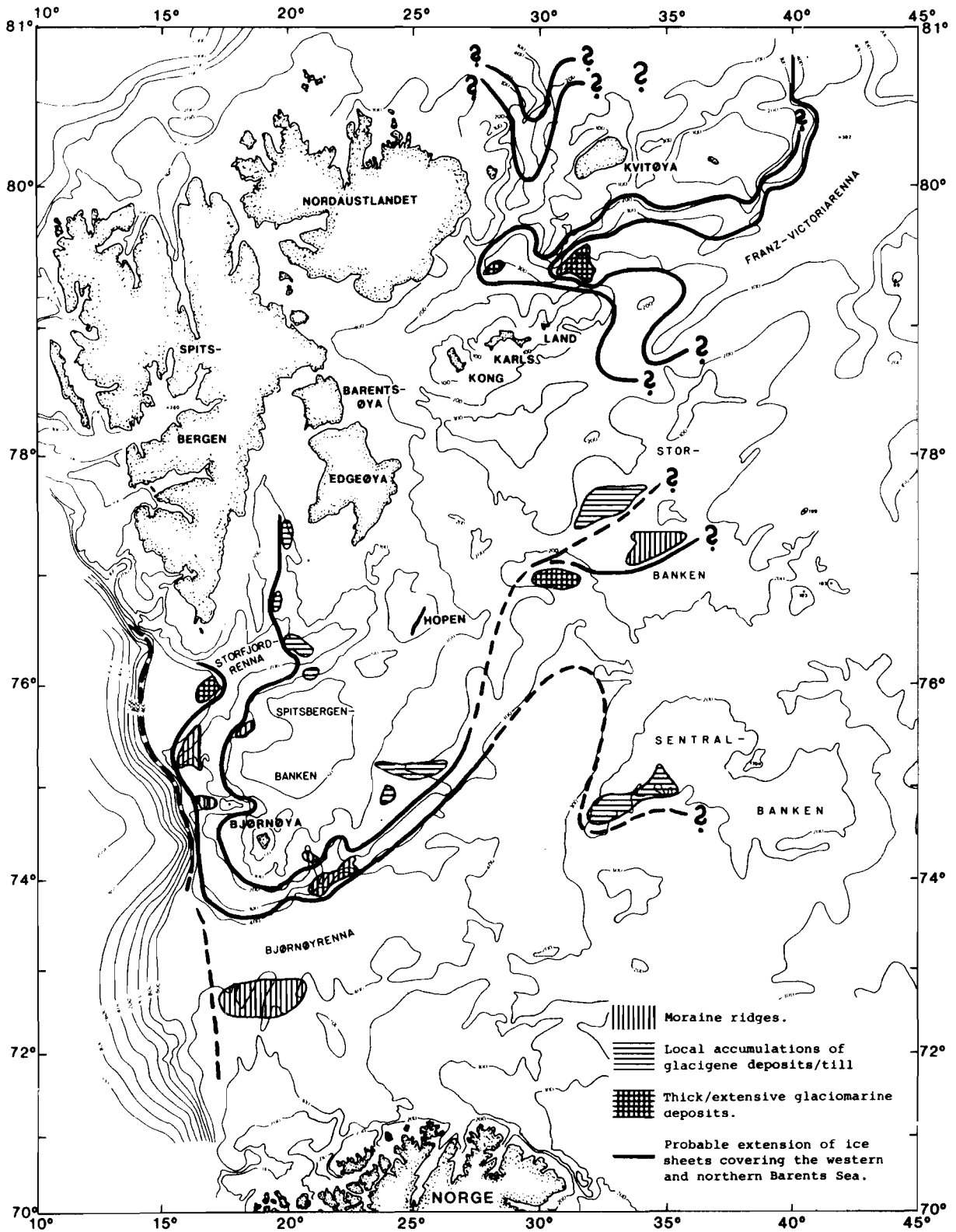


Fig. 14. Bathymetric map showing features related to former ice margins in the western and northern Barents Sea.

at least once. Overdeepened regions south of Kong Karls Land further indicate considerable glacial erosion in the northern Barents Sea. The depositional chronology cannot be established yet because of lack of datable material and inadequate knowledge on the stratigraphy of the glaciomarine deposits. At this stage only a preliminary discussion may be attempted on the extent and age of Barents Sea glaciations.

Sediment distribution in relation to glaciations

The extension of an ice sheet can be reconstructed from the distribution of (1) ice marginal features such as moraine ridges, and (2) areas covered by till or glacially compacted and reworked deposits. In a marine environment the distribution and thickness of glaciomarine deposits have to be included.

As a possible reference for the ice sheets in the northern Barents Sea, at least during their retreat, observations from Austfonna at Nordaustlandet may be applied. This is an ice cap, 100×50 km, terminating in the sea along half its circumference. Considerable parts of the ice cap are believed to be below pressure melting point, while central parts may be at pressure melting point (Schytt 1969). Sediment loaded meltwater discharge into the sea seems to confirm the existence of areas at pressure melting point beneath the ice cap. Preliminary studies of the sedimentation outside the ice cap (Pfirman, pers. comm. 1981; Solheim & Elverhøi 1982) show that the major part of both the suspended matter and the ice-rafted material is deposited relatively close (within 10 to 15 km) to the ice front. With reference to these results, thick glaciomarine sediments with well-defined limits should be regarded as ice marginal features.

The Barents Sea ice sheets were grounded below sea level, i.e. marine ice sheets. The stability and extension of such ice sheets are to a large extent controlled by the sea level (e.g. Thomas 1979). A marine ice sheet covering an area of low relief like the Barents Sea is thus likely to extend down to a common water depth over large regions. This, in turn, makes it possible to reconstruct the margins of such ice sheets into areas lacking well-defined marginal features.

Ice marginal features are situated around Spitsbergenbanken at approximately 250–300 m water depth (Fig. 14). From the fact that these features are observed at the same water depth, we propose

that they define the outline of an ice sheet covering Spitsbergenbanken.

In the northern and central Barents Sea, ice marginal features are found at somewhat shallower water depth, except for the glaciomarine deposit at 300 m water depth northeast of Kong Karls Land (Fig. 14). However, on the western slope off Sentralbanken and in the inner part of Bjørnøyrenna at approximately 300 m water depth, there is a thickening of both the glaciomarine and its underlying deposits. Based on this change in sediment thickness and the glaciomarine accumulations in the northern Barents Sea, we propose a continuous ice sheet covering the central and northern Barents Sea in the Late Weichselian. Furthermore, we also propose that it was connected with the ice sheet on Spitsbergenbanken. To the north a coalescence of the ice on Nordaustlandet/Storøya and Kvitøya is proposed. Due to findings of till on the shelf north of these islands we further propose that the ice extended further north, confined to a water depth corresponding to a present water depth of 250 to 300 m. The extension to the northeast is defined by the Franz-Victoriarenna and the glaciomarine accumulation in its inner part (Fig. 14).

Ice marginal features, somewhat less extensive than the previous ones, are found at about 150–200 m water depth around Spitsbergenbanken, in the inner parts of Storfjordrenna and Bjørnøyrenna and on Storbanken (Fig. 14). Similarly, as for the marginal features and change in sediment thickness at 250 to 300 m water depth, we relate these latter features to an ice sheet somewhat smaller in extent than the former one (Fig. 14). We also propose a similar, smaller ice sheet in the northernmost Barents Sea in the Late Weichselian.

A more extensive—and older—ice sheet is, however, witnessed by findings of till (or glaciomarine sediments overrun by a glacier) in Bjørnøyrenna and a moraine ridge at the mouth of the trough. As illustrated in Fig. 14, this extensive ice cover is believed to have reached to the shelf edge in the west.

Possible age of the Barents Sea glaciations

Pre-Late Weichselian.—On Svalbard an early Weichselian glaciation seems to have been of a larger extent than the Late Weichselian (Salvigsen & Nydal 1981). Such an ice may also have covered considerable parts of the Barents Sea.

Late Weichselian. – The northern extent of the Scandinavian ice sheet is still a subject of controversy. Andersen (1968 and 1981) tentatively placed the maximum limit on the outer continental shelf, defined by the 'Egga moraines'. Based on sediment coring and shallow seismic reflection, Rokoengen *et al.* (1979) also suggested a glacial extension to the outer continental shelf. Vorren *et al.* (1978) demonstrated that the shelf outside Troms was deglaciated 13,000–14,000 B.P. Until now the detailed stratigraphical investigations have been concentrated in the nearshore areas, while information from the outer shelf off northern Norway is limited. Available data do not provide an adequate basis to prove or disprove the existence of a grounded glacier on the outer shelf with a possible extension into Bjørnøyrenna.

On Svalbard, Hoppe (1970) suggested a large continuous ice sheet covering Svalbard with an extension into the northern and northwestern Barents Sea. Investigations by Salvigsen (1977) and Salvigsen & Nydal (1981), however, have shown the existence of more local and limited glaciations of the western part of Spitsbergen, while Salvigsen (1981) suggested that a continuous ice sheet covered eastern Svalbard, including Kong Karls Land.

Recent investigations on Storøya, a small island just east of Nordaustlandet (Fig. 1), show an emergence curve similar to those found elsewhere in eastern Svalbard (Häggblom 1982), indicating an expanded Late Weichselian ice sheet also in that part of the northern Barents Sea. Concerning Hopen, the existence of a Late Weichselian ice sheet in the area has been disputed (e.g. Boulton 1979a). It should be noted, however, that only two levels older than 4,000 years B.P. have been dated so far. Additionally, it seems unreasonable that the displacement on Hopen should have been caused by tectonic movements, in contrast to the rest of eastern Svalbard, since the whole area is on the same basement platform. It seems more likely that the displacement on Hopen is also due to glacial unloading, indicating that Hopen and its adjacent areas were covered by a Late Weichselian ice sheet as proposed by Hoppe (1970).

Bjørnøya, the small island on the western flank of Spitsbergenbanken, was deglaciated 11,500 B.P. according to gytje dates (Hyvärinen 1972). Lack of 'recent' glacial features led Boulton (1979a) to suggest a non-glaciated island. According to Salvigsen and Nydal (1981), Bjørnøya may have escaped glaciation during the Late Wei-

chselian in common with areas in western Spitsbergen. An ice-free Bjørnøya does not, therefore, necessarily contradict the concept of an ice sheet further east on Spitsbergen. Alternatively, as proposed by Hoppe (1970), Bjørnøya may have been covered by only a thin ice sheet due to its position very close to the shelf edge. The general deglaciation may further have been followed by local ice cap formation, partly or completely destroying older traces of glacial movements.

From the above regional geological considerations, it seems likely that the northern Barents Sea and also Spitsbergenbanken seem to have been covered by grounded ice which in turn is compatible with the sediment distribution. From the sediment distribution it cannot, however, be concluded whether this ice sheet extended to the shelf edge, i.e. a total glaciation as proposed by Grosswald (1980) and Hughes *et al.* (1981) (maximum model), or was confined to the Spitsbergenbanken and the central and northern Barents Sea.

Comments on the idea of a non-glaciated Barents Sea

Even though the shoreline displacement in eastern Svalbard strongly indicates the presence of a Late Weichselian ice sheet in the northern Barents Sea, the possibilities of a non-glaciated northern Barents Sea should be taken into consideration. Such a concept implies that the blue-grey glaciomarine sediments in the area have to include deposits from the time when a former ice sheet retreated from the region. However, the sediments show no sign of erosion, reflecting the Late Weichselian regression.

Hiatuses can on the other hand be present as non-depositional episodes. The very low content of foraminifera (10 per 100 g sediment) makes stratigraphical interpretation problematic. The fauna observed in the cores from the northern Barents Sea is composed of species with affinities to cold water, reflecting a High Arctic glacial environment (Fig. 6). This is in contradiction to the finding of pre-Late Weichselian shells, drift wood, and whale bones on Kong Karls Land, which in turn indicate a pre-Late Weichselian climate similar to the present (Salvigsen 1981). A response to such conditions has not been traced in the samples. Theoretically, these sediments could have been removed, but it seems reasonable that such an event should also be recorded in the

underlying sediment. However, the lowermost part of the blue-grey glaciomarine sediments are inadequately sampled and the existence of hiatuses cannot be totally rejected. A more detailed investigation of the stratigraphy of the blue-grey sediments is in progress.

Conclusion

The sediment sequence of till (and/or glaciomarine sediments overrun by a glacier) overlain by glaciomarine deposits which in turn grade into postglacial sediments (Holocene age), demonstrates that the western and northern (West of 35°E) Barents Sea has at least once been covered by grounded ice.

Moraine ridges along the western continental shelf edge, especially at the mouth of Bjørnøyrenna, indicate the occurrence of a large-scale glaciation in the Barents Sea. Moraine ridges and thick glaciomarine accumulations are found radially to Spitsbergenbanken at 150 to 200 m and 250 to 300 m water depth, respectively. At the same water depths, similar ice marginal features are also found in the central and northern Barents Sea. Based on these features and regional geological considerations we propose the existence of a marine ice sheet covering the northern part of the Barents Sea and Spitsbergenbanken during the Late Weichselian. Whether this ice sheet represents a major halt during the retreat of a more extensive ice sheet or the outer limit, is not clear.

It should be noted that such a model is in conflict with:

- (1) the idea of large-scale, catastrophic break-up at the end of the Late Weichselian as suggested by Grosswald (1980) and Denton & Hughes (1981);
- (2) the existence of a Late Weichselian ice shelf covering the Norwegian-Greenland Sea, as proposed by Kellogg (1980); and
- (3) the idea of a non-glaciated Barents Sea, as suggested by Boulton (1979a, b).

Acknowledgements. – Shallow seismic data and sediment samples were collected during the Barents Sea Project funded by the Royal Norwegian Council for Industrial and Scientific Research and the Norwegian Petroleum Directorate (NPD). We thank Yngve Kristoffersen for organizing the 1977, 1978, and 1980 field work providing the data base for this study. Additional shallow seismic data were kindly made available by NPD. Colleagues at the Norwegian Polar Research Institute,

together with Adrian Read and Jan Mangerud, are acknowledged for valuable comments. The authors are indebted to Jens Nagy for foraminiferal analyses.

References

- Andersen, B. G. 1968: Glacial geology of western Troms, north Norway. *Nor. Geol. Unders.* 256, 160 pp.
- Andersen, B. G. 1981: Late Weichselian ice sheets in Eurasia and Greenland. Pp. 1–65 in Denton, G. H. & Hughes, T. J. (eds.), *The Last Great Ice Sheets*, John Wiley & Sons.
- Baranowski, S. 1977: The subpolar glaciers of Spitsbergen seen against the climate of this region. *Wroclaw, Wydawnictwa Uniwersytetu Wrocławskiego. Results of investigation of the Polish scientific Spitsbergen Expeditions 3*, 93 pp.
- Bjørlykke, K., Bue, B. & Elverhøi, A. 1978: Quaternary sediments in the northwestern part of the Barents Sea and their relation to the underlying Mesozoic bedrock. *Sedimentology* 25, 227–246.
- Boulton, G. S. 1979a: Glacial history of the Spitsbergen archipelago and the problem of a Barents shelf ice sheet. *Boreas* 8, 31–57.
- Boulton, G. S. 1979b: A model of Weichselian glacier variation in the North Atlantic region. *Boreas* 8, 373–395.
- Damuth, J. E. 1978: Echo character of the Norwegian-Greenland Sea: Relationship to Quaternary sedimentation. *Marine Geology* 28, 1–36.
- Denton, G. H. & Hughes, T. J. 1981: The Arctic ice sheet: An outrageous hypothesis. Pp. 437–467 in Denton, G. H. & Hughes, T. J. (eds.), *The Last Great Ice Sheets*, John Wiley & Sons.
- Dibner, V. D. 1968: 'Ancient clays' and the relief of the Barents–Kara shelf as direct proof of its sheet glaciation during the Pleistocene. Pp. 124–128 in Belov, M. I. (ed.), *Problems of Polar Geography, Trudy* 285.
- Dreimanis, A. 1978: Till and tillite. Pp. 805–810 in Fairbridge, R. W. & Bourgeois, J. (eds.), *Encyclopedia of Sedimentology Encyclopedice of Earth Sciences Series 6*.
- Elverhøi, A. & Kristoffersen, Y. 1977: Glacial deposits south-east of Bjørnøya, northwestern part of the Barents Sea. *Norsk Polarinstitutt Årbok 1977*, 209–215.
- Elverhøi, A. & Bomstad, K. 1980: Late Weichselian glacial and glaciomarine sedimentation in the western, central Barents Sea. Unpubl. rep., Norsk Polarinstitutt, 1980. 29 pp.
- Grosswald, M. G. 1972: Glacier variations and crustal movements in northern European Russia in late Pleistocene and Holocene times. Pp. 205–221 in Vasari, Y., Hyvärinen, H. & Hicks, S. (eds.), *Climatic Changes in Arctic Areas during the Last Ten-thousand Years. Acta Universitatis Ouluensis, Oulu, Finland 1972*.
- Grosswald, M. G. 1980: Late Weichselian ice sheet of northern Eurasia. *Quaternary Research* 13, 1–32.
- Grosswald, M. G., Lavrov, A. S. & Potapenco, L. M. 1974: The Markhida-Velt ice advance: A twin-surge of the Barents Ice Sheet? *Materialy Glyatsiol. Issled. Khronika Obsuzhdeniya* 24, 173–188. (In Russian with an English summary.)
- Häggbloom, A. 1982: Driftwood in Svalbard as an indicator of sea ice conditions. *Geogr. Ann.* 64A, 81–94.
- Hoppe, G. 1970: The Würm ice sheets of northern and Arctic Europe. *Acta Geographica Lodziensia* 24, 105–115.
- Hoppe, G. 1981: Glacial traces on the island of Hopen, Svalbard: A correction. *Geogr. Ann.* 63A, 67–68.

- Hoppe, G., Shytt, A., Häggblom, A. & Österholm, H. 1969: The glacial history of Hopen. *Geogr. Ann.* 51A, 185–192.
- Hughes, T. J., Denton, G. H., Andersen, B. G., Schilling, D. H., Fastook, J. L. & Lingle, C. S. 1981: The last great ice sheets: A global view. Pp. 263–317 in Denton, G. H. & Hughes, T. J. (eds.), *The Last Great Ice Sheets*, John Wiley & Sons.
- Hyvärinen, H. 1972: Pollen-analytic evidence for Flandrian climatic change in Svalbard. Pp. 225–237 in Vasari, Y., Hyvärinen, H. & Hicks, S. (eds.), *Climatic Changes in Arctic Areas during the Last Ten-thousand Years*. Acta Universitatis Ouluensis, Oulu, Finland 1972.
- Kellogg, T. B. 1980: Palaeoclimatology and paleo-oceanography of the Norwegian and Greenland Seas: glacial-interglacial contrasts. *Boreas* 9, 115–137.
- Knape, P. 1971: *C-14 dateringar av höjda strandlinjer, synkrona pimpstensnivåer och iakttagelser av högsta kustlinjen på Svalbard*. Unpubl. lic. dissert., Stockholm Univ. Naturgeogr. Inst. 142 pp.
- Koteniov, B. N., Matishov, G. G., Belyayev, A. V. & Myslivets, V. I. 1976: Geomorphology of the shelf and continental slope between Spitsbergen and North Norway. *Priroda i Khozyaistvo Severa* 4, 30–38. (In Russian.)
- Kristoffersen, Y., Milliman, J. D. & Ellis, J. P. in press: Unconsolidated sediments and shallow structure of the northern Barents Sea. *Polar Research*.
- Kvasov, D. D. 1978: The Barents Ice Sheet as a Relay Regulator of glacial-interglacial alternation. *Quaternary Research* 9, 288–299.
- Matisov, G. G. 1980: Geomorphological indications of the impact of the Scandinavian, Novaja Zemlja, and the Spitsbergen ice cover upon the surface of the bottom of the Barents Sea. (Geomorfologiceskie priznaki vozdejstvija Skandinavskogo, Novozemel'skogo, Spicbergenskogo lednikovych pokrovov na poverchnost'dna Barenceva morja.) In: *Okeanologija* XX (4) 1980, 669–680. English summary. p. 680. UDC 551.35:551.463 (261). Translated (12 pp.), April 1981.
- Rokoengen, K., Bugge, T. & Løfaldli, M. 1979: Quaternary geology and deglaciation of the continental shelf off Troms, north Norway. *Boreas* 8, 217–227.
- Salvigsen, O. 1977: Radiocarbon datings and the extension of the Weichselian ice-sheet in Svalbard. *Norsk Polarinstitutt Årbok 1976*, 209–224.
- Salvigsen, O. 1978: Holocene emergence and finds of pumice, whalebones, and driftwood at Svartknausflya, Nordaustlandet. *Norsk Polarinstitutt Årbok 1977*, 217–228.
- Salvigsen, O. 1981: Radiocarbon dated raised beaches in Kong Karls Land, Svalbard, and their consequences for the glacial history of the Barents Sea Area. *Geogr. Ann.* 63A, 283–291.
- Salvigsen, O. & Nydal, R. 1981: The Weichselian glaciation in Svalbard before 15,000 B.P. *Boreas* 10, 433–446.
- Schytt, V. 1969: Some comments on glacier surges in eastern Svalbard. *Can J. Earth. Sci.* 6, 867–873.
- Semevsky, D. V. 1967: Neotectonics of the Spitsbergen archipelago. Pp. 225–238 in *Materialy po stratigrafii Spitsbergena*.
- Solheim, A. & Elverhøi, A. 1982: Marin-geologiske og -geofysiske undersøkelser 1981. Toktrappert og foreløpige resultater. *Norsk Polarinstitutt Rapport nr. 7*. 88 pp.
- Thomas, R. H. 1979: The dynamics of marine ice sheets. *Journal of Glaciology* 24, 167–177.
- Vorren, T. O., Strass, I. F. & Lind-Hansen, O. W. 1978: Late Quaternary sediments and stratigraphy on the continental shelf off Troms and west Finnmark, northern Norway. *Quaternary Research* 10, 340–365.
- Vorren, T. O. & Elvsborg, A. 1979: Late Weichselian deglaciation and paleoenvironment of the shelf and coastal areas of Troms, north Norway – a review. *Boreas* 8, 247–253.
- Williams, P. J. 1967: The nature of freezing soil and its field behavior. *Norwegian Geotechnical Institute Publ. No. 72*: 90–119.

PAPER 5.

**PHYSICAL ENVIRONMENT
WESTERN BARENTS SEA, 1 : 1,500,000**

ANDERS SOLHEIM and YNGVE KRISTOFFERSEN:

**SEDIMENTS ABOVE THE UPPER REGIONAL UNCONFORMITY:
THICKNESS, SEISMIC STRATIGRAPHY AND OUTLINE OF
THE GLACIAL HISTORY**

Abstract

Eroded bedrock on the Barents shelf is generally overlain by a thin (< 25 metres) veneer of sediments in the area north of 74°N except for local accumulations (< 70 metres). In the troughs Bjørnøyrenna and Storfjordrenna westward oblique progradational sequences attain a total thickness of > 500 metres near the shelf edge. The seismic character, morphology, and sedimentological evidence suggest that post mid Pliocene glacially influenced sediments comprise a major part of the section. Within the seismic resolution (10 -15 metres) at least four erosional surfaces extend from the inner part of the shelf to the edge, and they are considered to be related to major glacial advances. The last advance reaching the outer part of Bjørnøyrenna is tentatively correlated with a Saalian or early Weichselian glaciation.

Introduction

The first regional description of composition and facies distribution of the sea floor sediments in the Barents Sea was presented by Klenova (1960) based on geologic samples collected from about 1500 localities during four decades by the Polar Scientific Research Institute of Marine Fishery and Oceanography, Murmansk (PINRO). Later, Emelyanov et al. (1971) reviewed the submarine geology and pointed out the dominance of terrigenous sands in the bottom sediments and the widespread occurrence of 'ancient clays' interpreted as glacial deposits.

Estimates of the thickness of sediment overlying bedrock indicated by an upper low velocity layer (< 2 km/s) in sonobuoy refraction measurements were first made by Eldholm & Ewing (1971) and Renard & Malod (1974). Systematic mapping by shallow seismic reflection of the sedimentary sequence above an upper regional unconformity, has been carried out by the NTNF Continental Shelf Division (now IKU) up to 71°N and 22°E (Bugge & Rokoengen 1976). This sequence has been interpreted as Quaternary glacial deposits comprising four major units, i.e. a lower, outer, middle,

Due to technical difficulties the scale of this map is slightly incorrect. It should be 1: 506,000. The projection is UTM, but please note that 21°E is used as central meridian also north of 74°N.

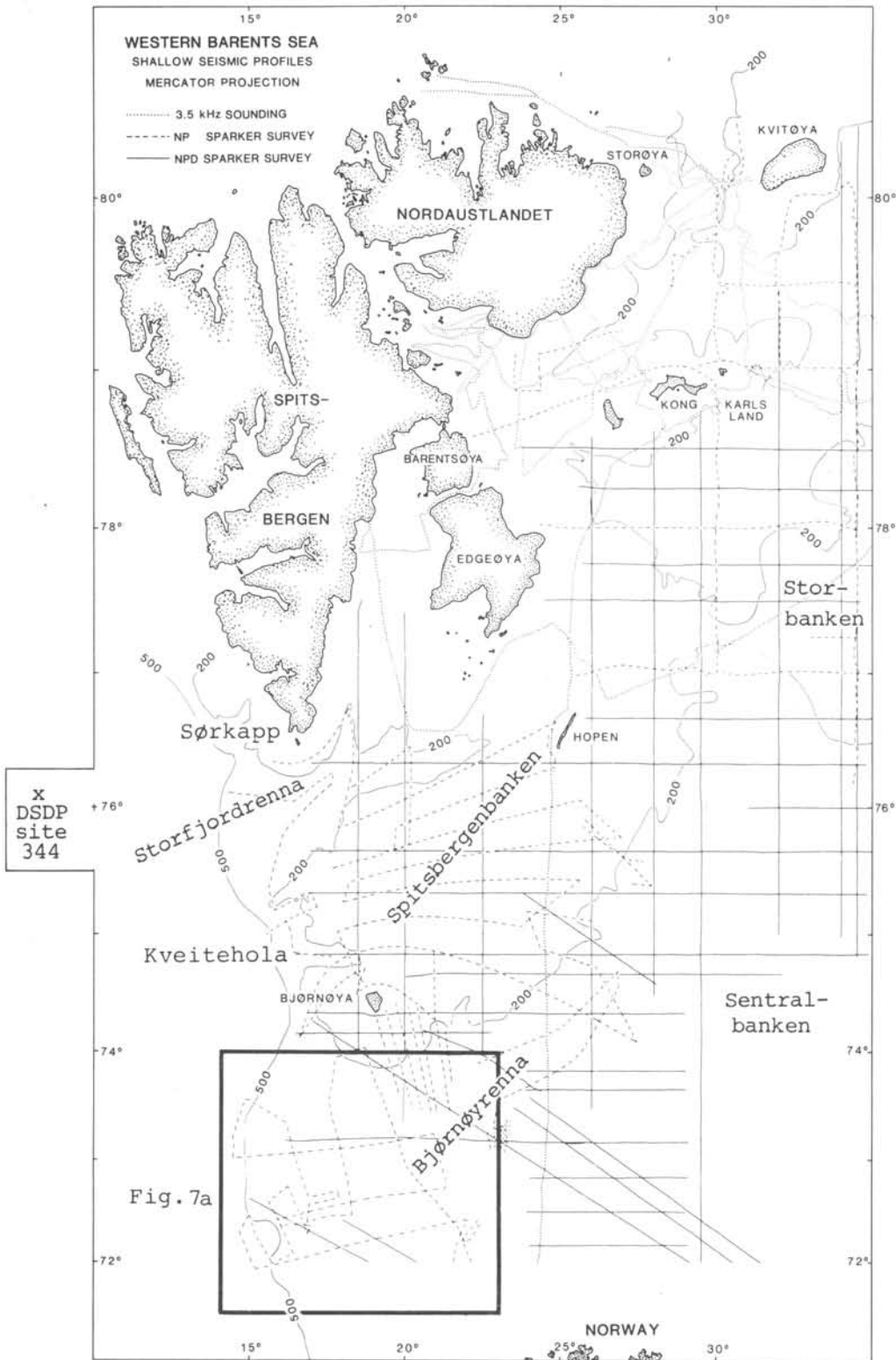


Fig. 1. Bathymetry and coverage of shallow seismic reflection data in the western Barents Sea. NP sparker survey on Spitsbergenbanken was jointly with NTNFK (Table 1). Frame in lower left delineates area shown in Fig. 7A.

and inner glacial unit. The regional unconformity both here and in the North Sea (Sellevoll & Sundvor 1974) has up until recently been interpreted as the base of the Quaternary. However, recent work of Rokoengen & Rønningsland (1983) suggests a mid Pliocene age.

Dibner (1978) compiled a map of bedrock geology inferred from over 1000 dredge hauls from the overlying glacial deposits. Both this and later studies indicate that the upper part of the bedrock is comprised of a Mesozoic sequence over most of the area. Permian and older rocks are found in the northernmost region, while Tertiary rocks probably only exist as a wedge towards the western continental margin (Edwards 1975, Rønnevik & Motland 1979, Elverhøi & Lauritzen 1984, Faleide et al. in press, Spencer et al. in press.)

From the accumulating sedimentological evidence, glaciers seem to have covered at least the shallow bank areas in late Weichselian. This, however, has been subject to discussion, and a number of different views have been presented, ranging from total glaciation of the entire Barents Sea to no glaciation extending significantly beyond the coasts of the Svalbard archipelago (Baranowski 1977, Boulton 1979, Grosswald 1980, Andersen 1981, Hughes et al. 1981, Boulton et al. 1982).

In this paper we present a compilation of all available shallow seismic reflection data in the Barents Sea and outline the major stratigraphic units above the regional unconformity.

TABLE 1

Shallow seismic data used to map the sediment distribution of the western Barents Sea.

| Institution-year | Survey area | Sound source | Energy (kJ) | Filter (Hz) | |
|------------------|-------------------------------|--------------|-------------|-------------|----------|
| | | | | Low | High |
| NP/NTNFK-1971 | Spitsbergen-banken | Sparker | 0.5-8.0 | 150 | 600 |
| NP-1977 | NW&SE of Bjørnøya | - | 1.0 | 50 | 200-500 |
| NPD-1977 | Central Barents Sea | - | 0.8 | 150 | 700 |
| NP-1978 | Western Margin & Bjørnøyrenna | - | 1.0 | 75-100 | 200-400 |
| NPD-1979 | S of 76°30' | - | 1.0 | 60-100 | 260-400 |
| NP/WHOI-1980 | Hopen-Kvitøya area | - | 1.0 | 60-80 | 300-3000 |
| NPD-1980 | All western Barents Sea | - | | 80 | 300 |
| YMER-1980 | 1 line Norway-Kong Karls Land | 3.5 kHz PDR | 10 kW | | |
| NP-1981 | Northern Barents Sea | 3.5 kHz PDR | 10 kW | * | * |
| NP-1982 | Northern Barents Sea | 3.5 kHz PDR | 10 kW | * | * |

* Pulse length: 1 msec. Band width: 2 kHz

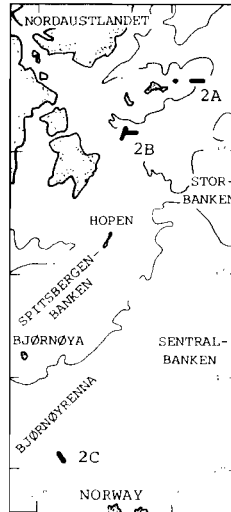
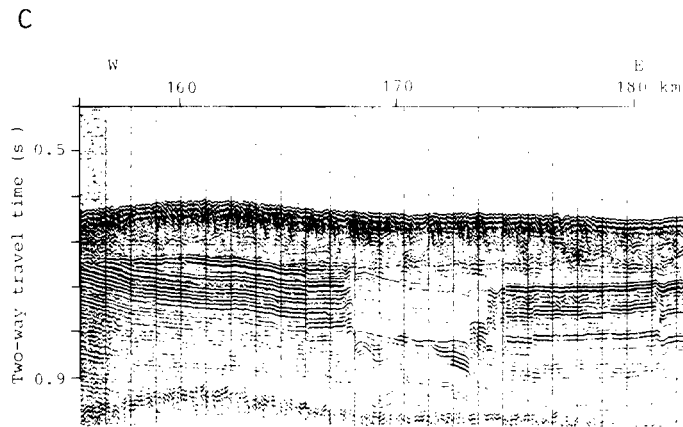
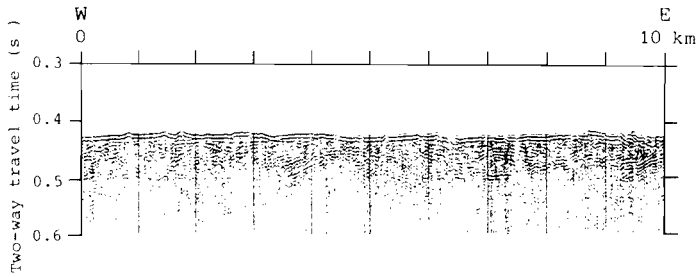
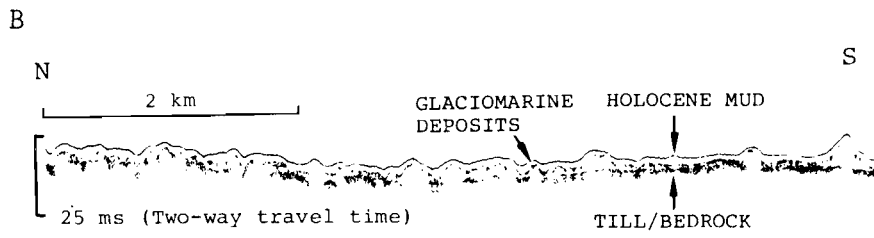
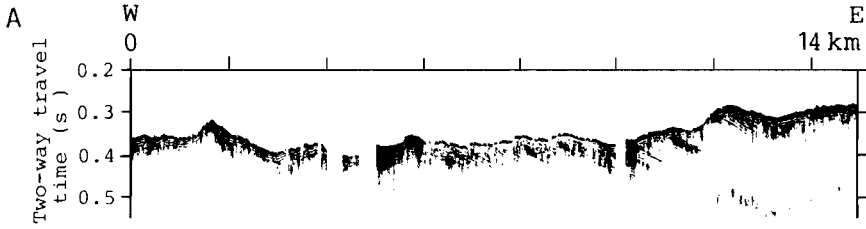
NTNFK = Continental Shelf Division of the Royal Norwegian Council for Scientific and Industrial Research.

NP = Norwegian Polar Research Institute.

NPD = Norwegian Petroleum Directorate.

WHOI = Woods Hole Oceanographic Institution.

YMER = Swedish YMER-80 expedition.



Data acquisition

The data sources and acquisition parameters are listed in Table 1. The principal sound source was 1 kJ sparker with analogue recording via a short, single channel streamer in the pass band 50-700 Hz. The duration of the 3-electrode sparker pulse, ghost reflections and receiver array length limit the resolution to 10-15 milliseconds (ms). Penetration is generally 200 ms or more, with a maximum of 600 ms in the western part of Bjørnøyrenna. The NPD sparker data were obtained concurrently with multichannel seismic surveys.

After 1981, a 3.5 kHz echosounder has been operated on NP cruises in polar waters. A 1 ms pulse length provides a resolution of about one metre, and penetration of 20 metres or more was generally obtainable, depending on sediment type. Although only tracks of NP 1981 3.5 kHz data are indicated on the enclosed map, the 1982 as well as the YMER-80 data have been taken into consideration in compilation of the sediment distribution.

Physiography

The physiography of the western Barents Sea is characterized by broad, gentle depressions extending from the interior to the western (Bjørnøyrenna and Storfjordrenna) and northern continental margins, forming over-deepened troughs in the northern region (Figs. 1 and 3). Storbanken and Sentralbanken form the north-south high ground (water depth 150-200 metres) in the central Barents Sea, whereas the islands of Bjørnøya and Hopen straddle Spitsbergenbanken - the largest and shallowest bank area (water depth 50-100 metres). The shallow part of Spitsbergenbanken has a smooth surface with a more undulating seabed on the slopes and also in the deeper troughs, Bjørnøyrenna and Storfjordrenna, as well as the depressions north and south of Kong Karls Land. Abundant diffraction hyperbolas are associated with major accumulations which fringe Spitsbergenbanken and parallel the shelf edge across the troughs. East and north of Edgeøya - Hopen, depth limited incisions (amplitude: 3-10 metres, and wavelength: 10-40 metres) down to 100 metres are present in the upper soft sediments, probably related to recent iceberg gouging, while relict iceberg ploughmarks cover large parts of the deeper areas (Elverhøi & Solheim 1983a). Areas of apparent resistant crystalline bedrock outcropping at the bottom around Kvitøya have a jagged appearance on the shallow seismic records.

Fig. 2. A. Sample of sparker record across outcrop of stratified bedrock east of Kong Karls Land.
 B. Representative sparker (lower) and 3.5 kHz (upper) records from the northern areas. The uneven surface of the glaciomarine sediments is caused by former iceberg gouging. Note that the two records are from crossing lines (3.5 kHz record from Elverhøi & Solheim 1983a).
 C. Sample of sparker record across graben structure in stratified bedrock at 72°15'N, 22°E.



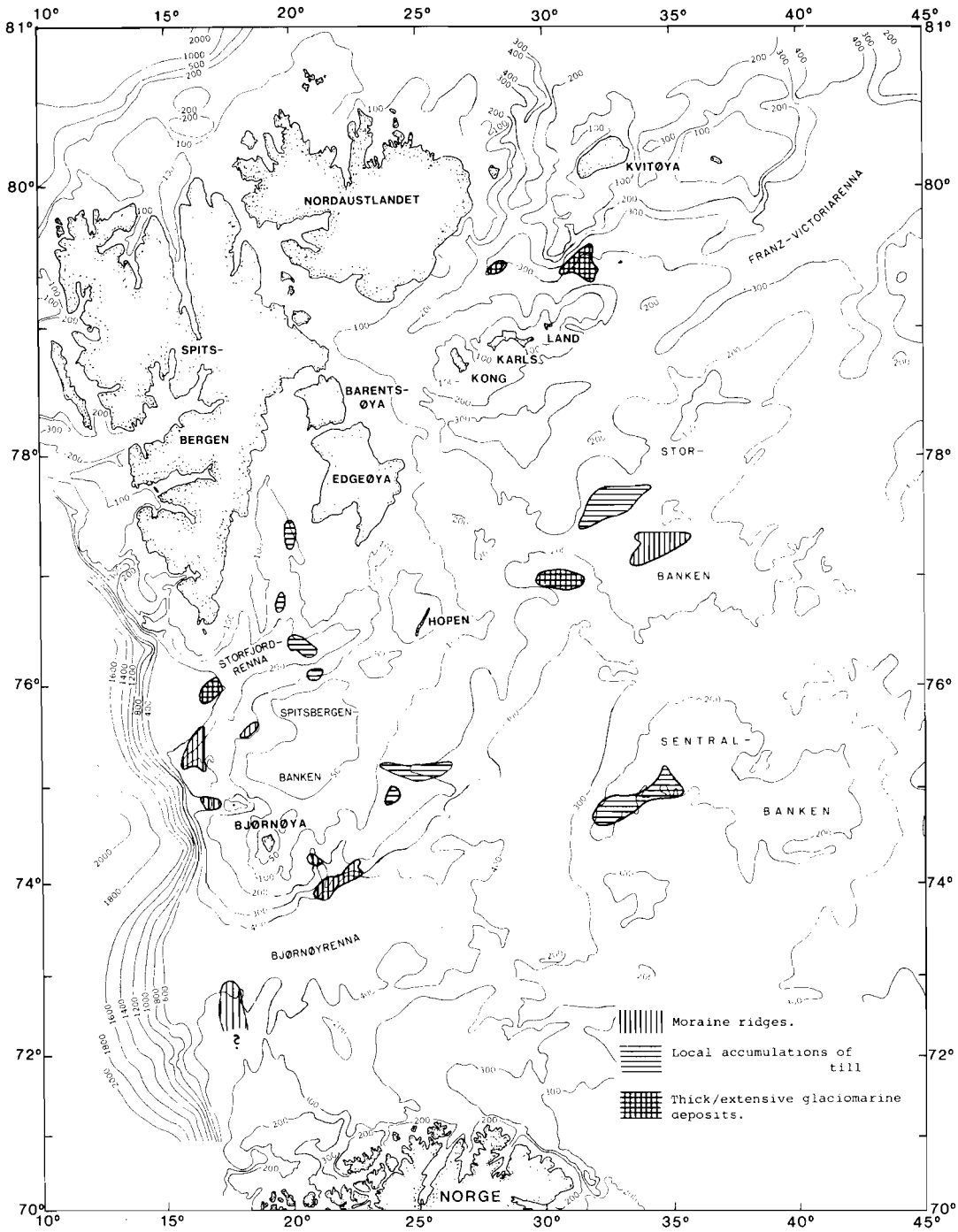


Fig. 3. Distribution of local accumulations of moraine and glaciomarine deposits. Genetic classification is based on seismic character and sediment samples. (Modified after Elverhøi & Solheim 1983a.)

Distribution of sediments above the upper regional unconformity (enclosed map)

A regional angular unconformity between an upper horizontally stratified or transparent section and underlying dipping well bedded strata is clearly distinguishable in most sparker records except on Spitsbergenbanken. Here the units are generally conformable over large areas which makes differentiation difficult.

The western Barents Sea may, apart from the area close to the shelf edge, conveniently be divided into a northern province where the underlying bedrock is generally covered with less than 25 metres of sediments, and a southern province where the thickness is more than 50 metres. The boundary between the two provinces is situated approximately along 74°N, and tends to follow the 300 metre depth contour.

In the northern province, exposed bedrock is interpreted to cover more than 50% of the sea floor over large areas, particularly around the islands of Kvitøya, Kong Karls Land, Hopen and Bjørnøya as well as the north slope of Sentralbanken. Possible outcrops of stratified bedrock have been recognized as distinct cuestas on the bottom coinciding with strong dipping reflectors extending through the bottom pulse (Fig. 2A). Recent investigations with a 3.5 kHz echo sounder (Elverhøi & Solheim 1983b) do, however, indicate a sediment cover of 0.5-3.0 metre thickness for parts of the areas interpreted from sparker records to have bedrock outcrop. Crystalline bedrock is characterized by a rough surface with no internal reflectors.

The major part of the northern province has a cover of less than 25 metres of sediments (generally less than the sparker resolution of 10-15 metres). From 3.5 kHz reflection data and sediment cores (Elverhøi & Solheim 1983a), however, it is possible to resolve three thin units above bedrock: till, glaciomarine sediments and soft Holocene mud (Fig. 2B). The latter is usually found in deeper areas and local depressions.

Local accumulations of sediments (> 25 metres) in the northern province are present as acoustically transparent fill in the depression south of Kvitøya (maximum thickness 70 metres) and as ridge-like features on the southwestern side of Storbanken with a thickness of 40-60 metres (Fig. 3). The former has been interpreted as predominantly glaciomarine deposits trapped in a basin and the ridges to represent moraine complexes (Elverhøi & Solheim 1983a, Kristoffersen et al. 1984).

In the southern province (south of 74°N) the sediment thickness above the regional unconformity increases gradually westward from 25 metres at 30°E to more than 500 metres near the shelf edge in Bjørnøyrenna (Fig. 4). This sediment body has the geometry of a major delta and associated submarine fan complex. Local variations in thickness are related to moraine complexes southeast of Bjørnøya or smoothing of structures in the underlying bedrock, i.e. a rim syncline around a diapir at 73°11'N, 23°E (Kristoffersen & Elverhøi 1978), salt tectonics at 73°N, 28°E (Rønnevik et al. 1982), and block faulting at 72°15'N, 22°E (Fig. 2C).

Along the western continental margin between Sørkapp and Bjørnøya, another major delta/submarine fan complex is built out in front of Stor-

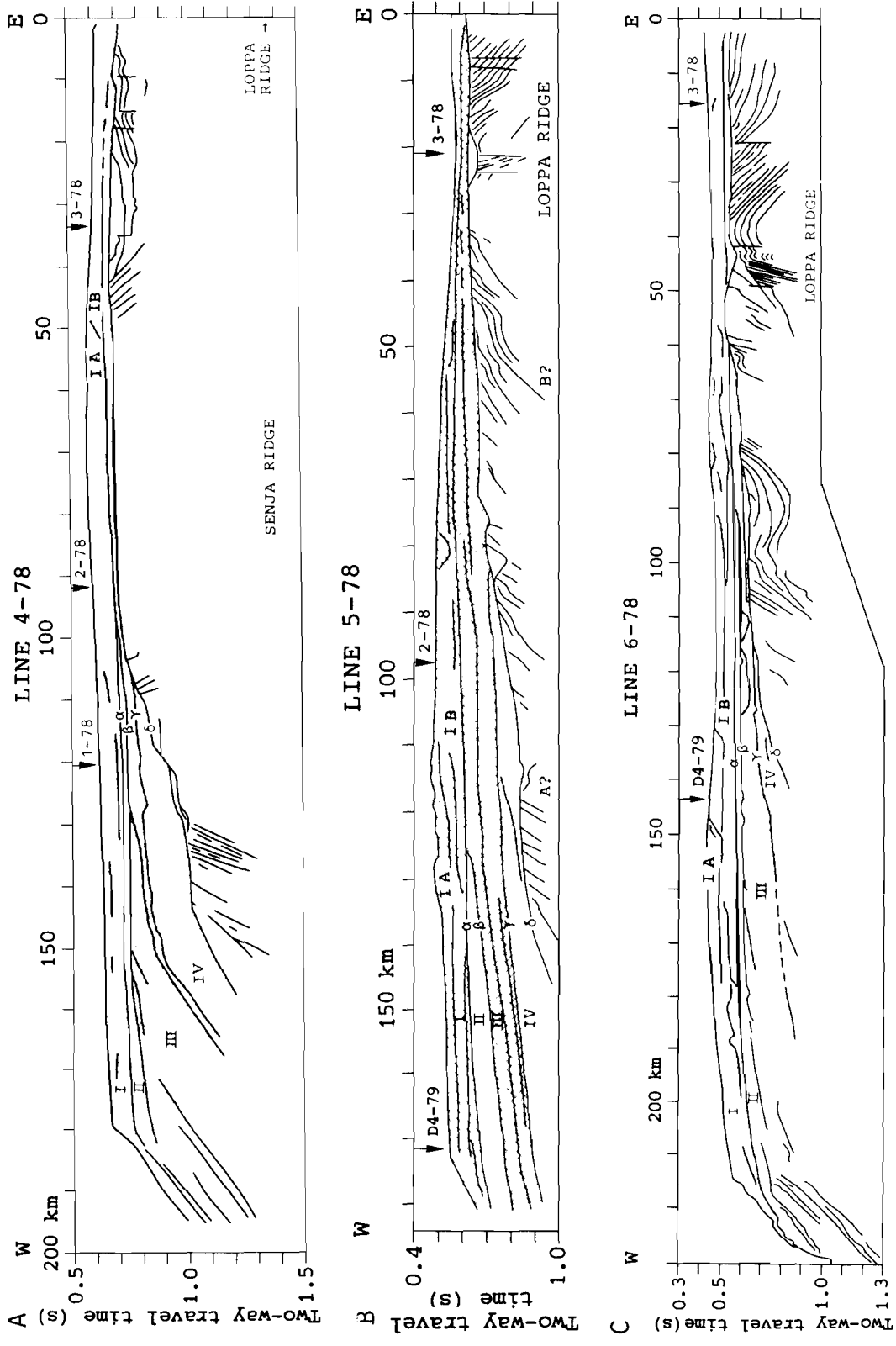


Fig. 4. - Text on page 12.

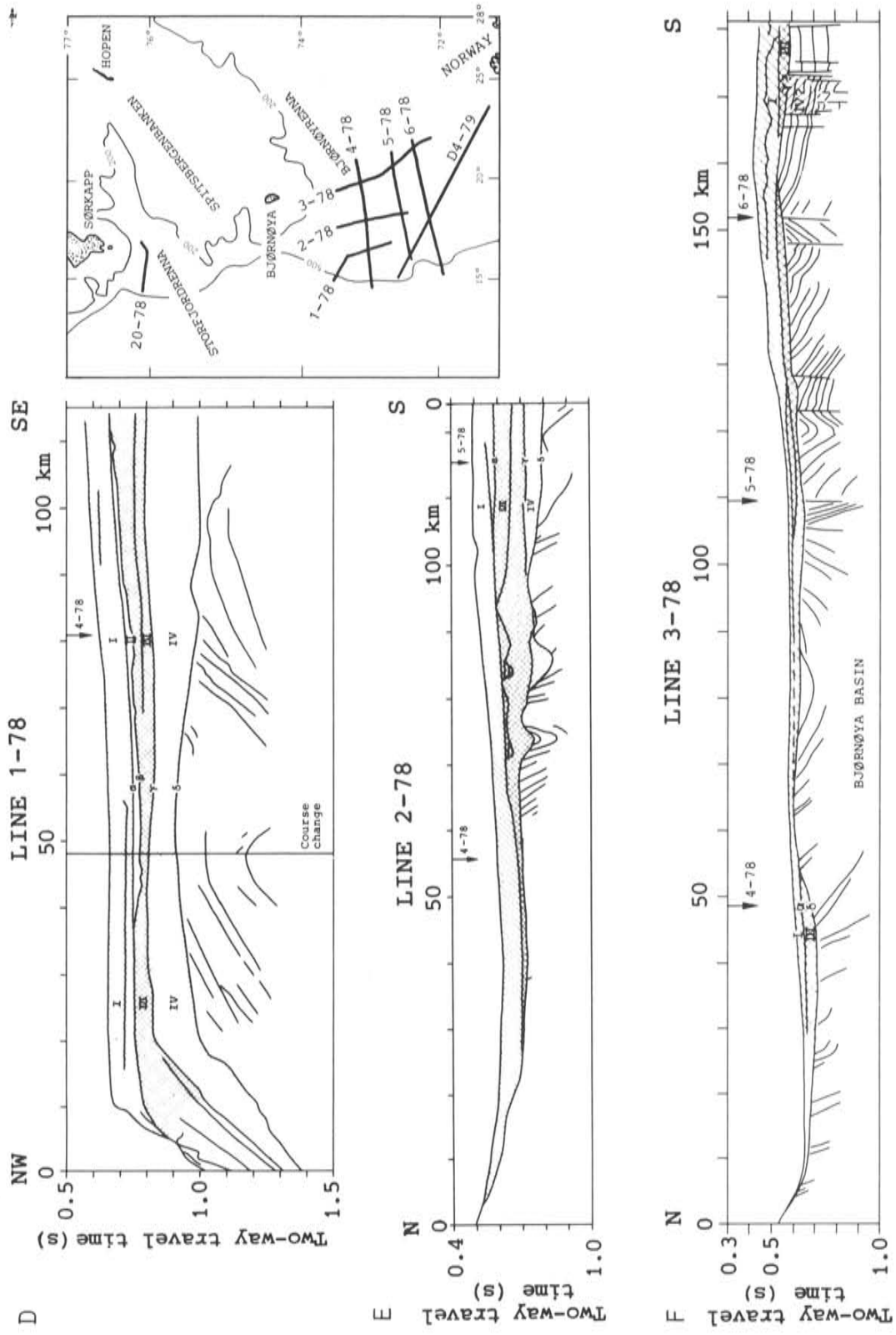


Fig. 4 - continued. Text on page 12.

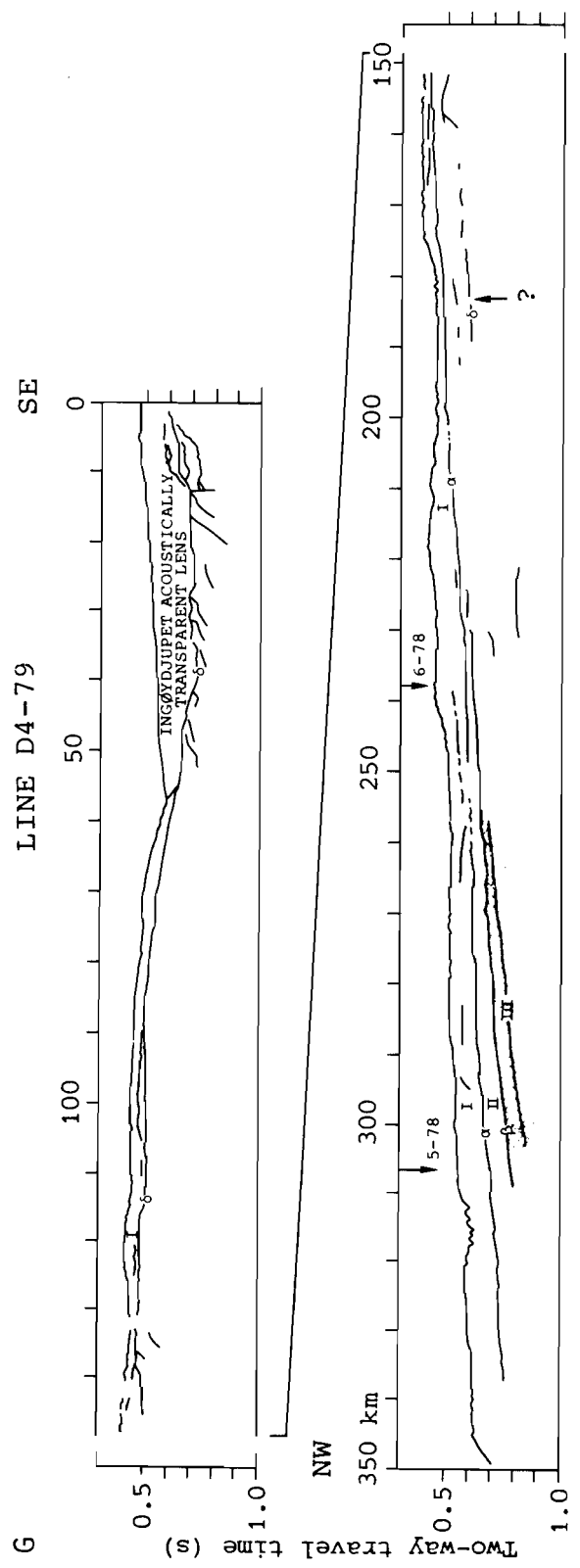


Fig. 4. Interpreted sparker profiles from Bjørnøyrenna. Line D4-79 is kindly provided by NPD. Notations A, B, Senja Ridge and Loppa Ridge, refer to reflectors and structures defined from deep seismic reflection by Rønnevik & Motland (1979).

fjordrenna west of a threshold in the underlying folded bedrock (Fig. 5B). The southwestern side of Storfjordrenna is formed by a southwest-trending sedimentary ridge (Fig. 6B). Between Storfjordrenna and the accumulation in Kveitehola, a series of discontinuous ridges parallels the shelf edge (Fig. 6A).

The seismic stratigraphy

The seismic sections show a series of well defined and regionally correlatable reflectors (α , β , γ , and δ), which define four major seismic sequences (I, II, III, and IV) above the upper regional unconformity (reflector δ) in Bjørnøyrenna and Storfjordrenna (Fig. 4). A seismic sequence is defined as a package of concordant reflections separated by surfaces of discontinuity, i.e. reflection terminations which are interpreted as stratal terminations (Mitchum et al. 1977).

Bjørnøyrenna

Sequence I. - This uppermost sequence, bounded by an erosional unconformity at its base (reflector α), is the most extensive in the southern Barents Sea. The possible presence of any overlying thin units in the eastern and northern part of the Barents Sea cannot be resolved by the available data. Near the mouth of Bjørnøyrenna, Sequence I forms two elongated accumulations (Fig. 7) associated with ridge complexes and regional highs (Fig. 4).

Sequence I is generally characterized by a discontinuous internal reflection pattern. In the western part of Bjørnøyrenna, however, an internal reflector defines two seismic subsequences, IA and IB with IA wedging out eastward oblique to the shelf edge (Fig. 7). Sequence I contains, in its upper part, the till/glaciomarine mud - Holocene mud sequence described for the central and northern areas.

Most of the persistent acoustic diffraction patterns from small-scale sea-floor topography (5-40 metres) is most likely caused by relict iceberg ploughmarks. Smaller depositional ridges as well as larger boulders may also contribute as diffractors.

Mass waste by submarine sliding has removed material at the shelf edge (72°N) to form an indentation in the bathymetric contours (Kristoffersen et al. 1978) (Fig. 8).

Sequence II. - This is a relatively thin sequence, underlying I, and defined by erosional unconformities at its top (reflector α) and base (reflector β). Sequence II is only observed west of 19°E (Fig. 7A), with maximum thickness in the central part of Bjørnøyrenna (Fig. 4). This sequence has no identifiable internal reflectors.

Sequence III. - This sequence, which extends westwards from the inner parts of Bjørnøyrenna, is characterized by generally conformable internal reflectors near the shelf break (Fig. 4). Internal structures of considerable relief are observed (Fig. 4C and E) and the upper and lower boundaries of the sequence are defined by erosional truncations.

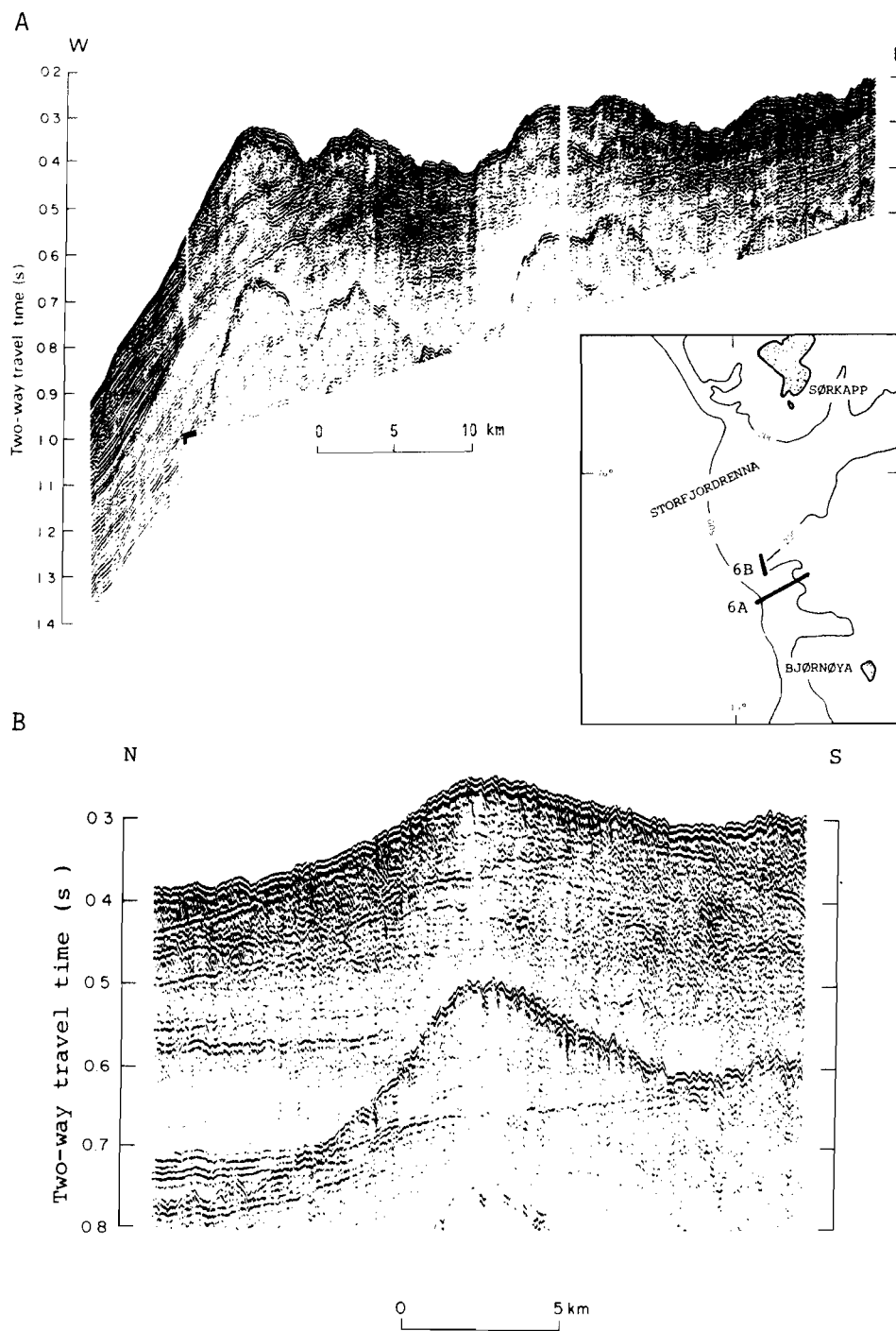


Fig. 6. Sparker records across ridge complexes subparallel to the western flank of Spitsbergenbanken.

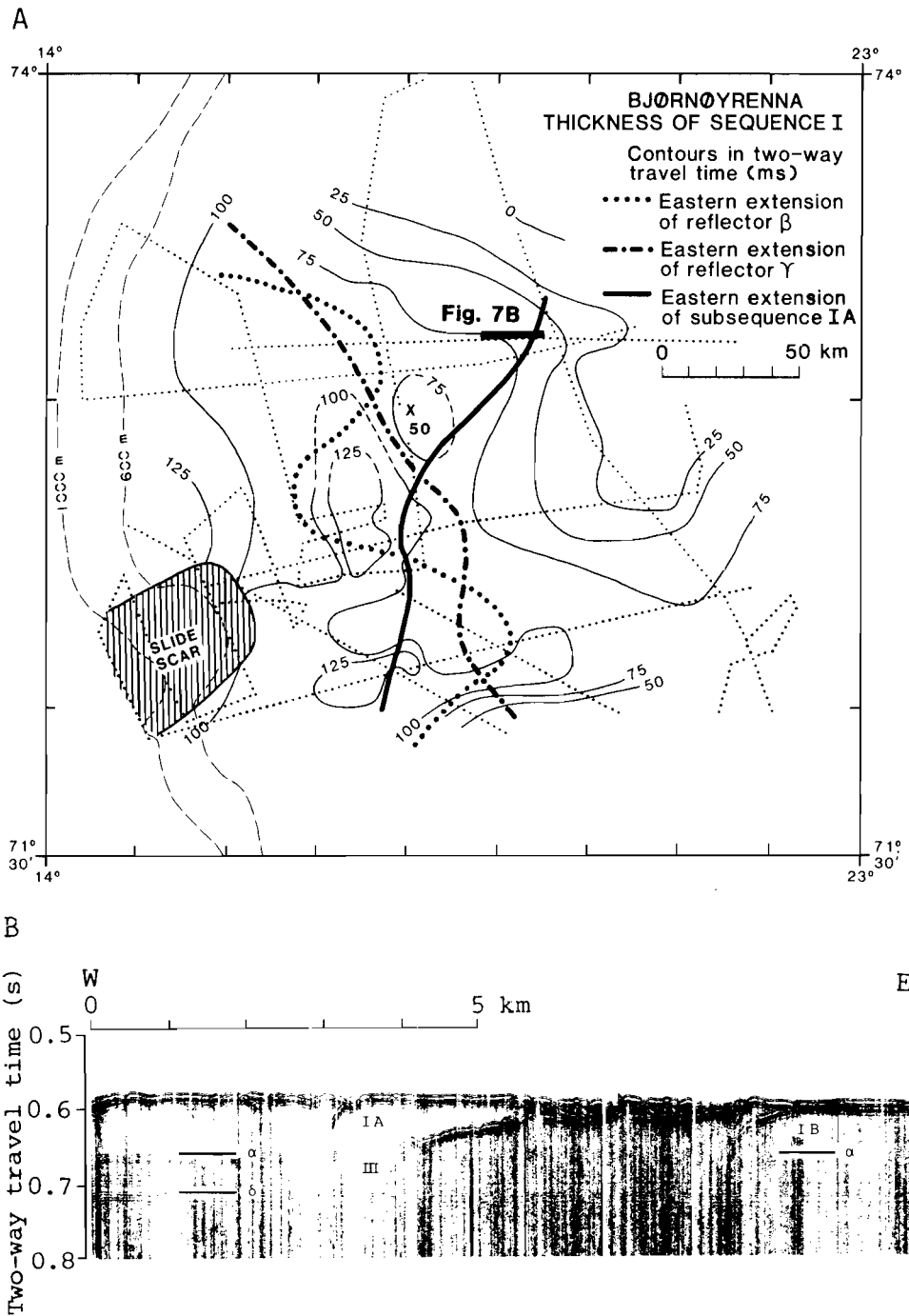


Fig. 7. A. - Isopach map of seismic Sequence I in outer Bjørnøyrenna. Included are also the eastern extensions of reflectors β and γ and Subsequence IA. Thin, dotted lines are track lines. Bathymetric contours 600 and 1000 metres shown by thin, stippled lines.

B. - Sparker record (kindly provided by NPD) across boundary between Subsequences IA and IB. Filter setting (150-700 Hz) is a likely reason why the difference in seismic character between the two subsequences is not seen on the NP-records (200-400 Hz) (Fig. 5A).

Sequence IV. - The lowermost sequence (IV) shows a downflap reflection pattern on the basal regional unconformity (reflector δ) which truncate the underlying folded and well stratified rocks. Sequence IV appears homogenous with few internal reflectors (Figs. 4 and 5). Its eastern boundary is defined by the eastern extension of reflector γ (Fig. 7A).

Bedrock topography in Bjørnøyrenna is smooth and shows a broad east-west depression along its northern side, forking into northeast and southeast trending branches towards the central Barents Sea (Fig. 9).

Storfjordrenna

The outer part of Storfjordrenna is characterized by a relatively short distance (80 km) between a bedrock threshold and the shelf edge (Fig. 5B). Correlation with the seismic stratigraphy in Bjørnøyrenna is based on geometry of the seismic sequences and their individual reflection character. Above the regional unconformity (δ) is the prograding wedge of Sequence IV, overlain by the parallel, continuous internal reflectors which characterize Sequence III. Sequence IA is considered to extend to the shelf edge overlain by an up to 80 ms thick acoustically transparent sediment lense seaward of the bedrock threshold (Fig. 5B).

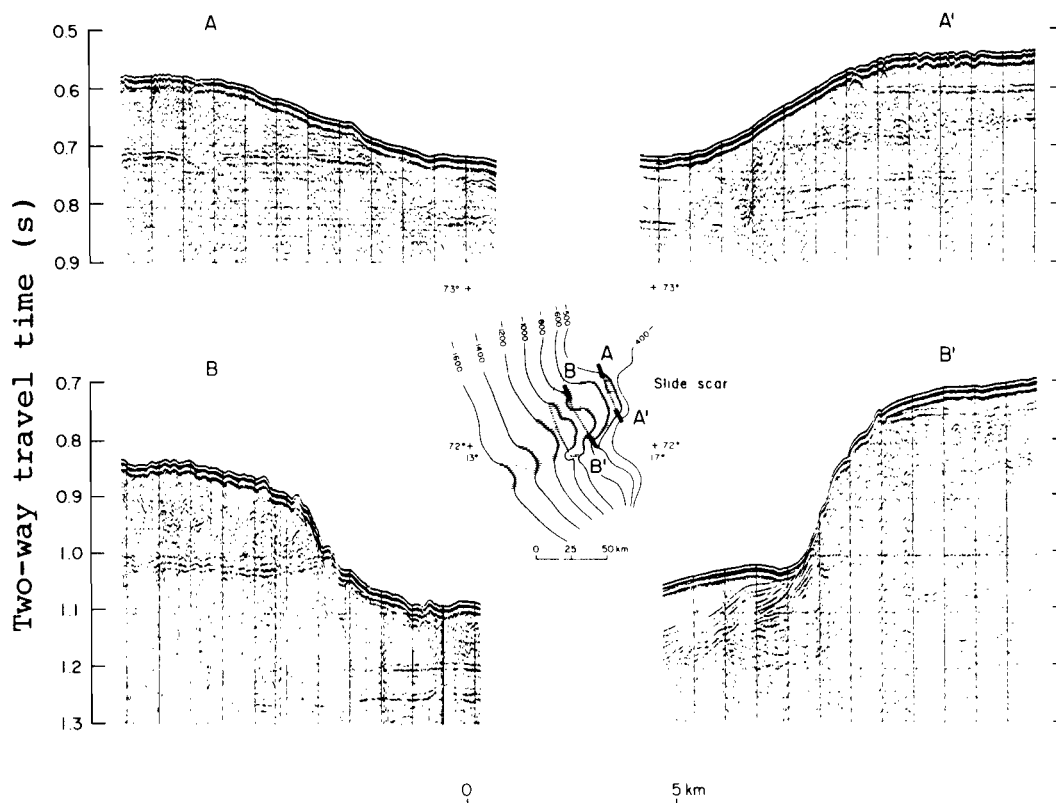


Fig. 8. Sparker records across slide scar on the shelf edge in outer Bjørnøyrenna (From Kristoffersen et al. 1978).

We note that the smooth sea bed on the sediment lense continues also a distance west of the lense proper and covers older and rougher bottom topography seen near the shelf edge and in Bjørnøyrenna. Also the section shows two buried accumulations of relatively transparent material with the appearance of channel fill (Fig. 5B: 22-30 km, 0.6 s and 35-48 km, 0.65 s).

Interpretation of seismic sequences and reflectors

The seismic sequences I-IV are representative of an oblique progradational shelf (Mitchum et al. 1977). The main reflectors form smooth continuous interfaces with erosional truncations of underlying units, whereas the internal reflectors are generally weaker and commonly irregular and discontinuous. The entire section (I-IV) is analogue to the youngest sequence (IV) of Spencer et al. (in press) in their work on the Tertiary development of the western Barents shelf margin.

Several lines of evidence suggest that a major part of the sediments above the upper regional unconformity in the Barents Sea has a glacial origin - i.e. was either deposited directly from a glacier as till, or as glaciomarine sediments in the vicinity of a glacier:

- Contrasting depositional environments are reflected by the lack of fine scale stratification and continuity in seismic sequences above the upper regional unconformity (δ) relative to the well bedded but folded rocks below.
- Overdeepened troughs and generally thin sediment cover over large areas suggest glacial erosion (Fig. 9 and enclosed map).
- A 377 metre thick section of glacially influenced sediments was sampled at DSDP site 344, at a waterdepth of 2156 metres northwest of Storfjordrenna (Fig. 1), and the onset of glaciation tentatively dated to 5 Ma or younger (Talwani, Udintsev et al. 1976).
- Low seismic velocity gradients on the slope west of Bjørnøyrenna suggest rapid deposition of the sedimentary wedge (Hamilton et al. 1977, Houtz & Windisch 1977, Myhre 1984).
- The submarine fans west of Bjørnøyrenna and Storfjordrenna do not show evidence of fan valley and leveed distributary channels which characterize other active submarine fans (Damuth 1978), but rather indicate sediment supply from a broad zone, e.g. boundary of an ice sheet.
- A north-south trending ridge complex parallels the shelf edge in Bjørnøyrenna (Figs. 3 and 4B), and ridge topography is present within Sequence III (Fig. 4C and E).
- Overconsolidated pebbly mud form the bottom sediment on the shallow banks overlain by glaciomarine sediment and Holocene mud in the deeper areas (Elverhøi & Solheim 1983a).
- Till ridges are present on Storbanken (Kristoffersen et al. 1984) and outside depressions on Spitsbergenbanken (Elverhøi & Kristoffersen 1978).

- Bjørnøyrenna and Storfjordrenna show a characteristic shallowing in the vicinity of the shelf edge (Figs. 4A and 5).
- The sea-floor is characterized by abundant linear incisions interpreted as iceberg ploughmarks, indicating proximity to glaciers.
- The pattern of raised shore lines show gradients converging towards the central Barents Sea (Schytt et al. 1968) with more than 100 metre Holocene uplift in Kong Karls Land relative to present sea level (Salvinsen 1981).

Therefore, in view of the above arguments, we find it a reasonable working hypothesis to consider the sequence of erosional and depositional events recorded above the upper regional unconformity, to be related to past Barents Sea ice sheets. The lateral smoothness of erosional surfaces and no clear evidence of cut and fill structures of channelized river courses, suggest erosion by an ice sheet. Some of the erosional surfaces may have been used repeatedly - in particular reflector δ east of approximately 18°E . Local V-shaped incisions in the latter (line 2-78, 70-90 km (Fig. 4E), line 5-78, 70-90 km and 20 km (Fig. 4B)) may, however, also reflect an initial subaerial environment with stream erosion.

The base of a grounded, advancing ice sheet will load the substratum, erode, and deposit material as lodgement till. Thus compaction and expulsion of water from the overridden sediments combined with introduction of new coarser material, generate the laterally persistent impedance contrasts which

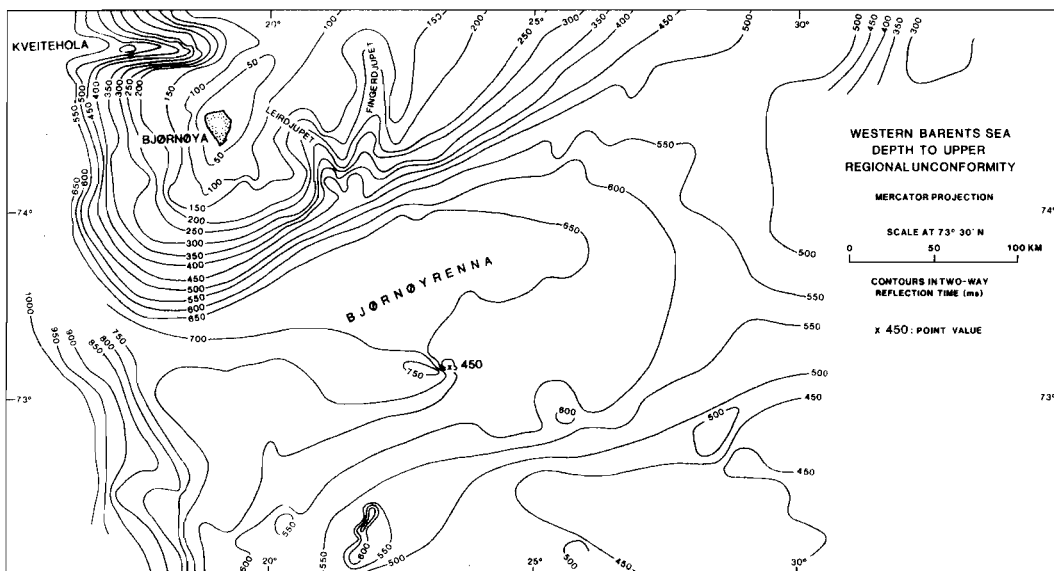


Fig. 9. Minimum depth below sea level in milliseconds to reflector δ in Bjørnøyrenna. In the northern Barents Sea the surface of reflector δ will not differ significantly from the sea-floor topography (enclosed map).

give rise to the continuous seismic reflection pattern. Good reflecting horizons are observed to arise from shear strength contrasts of 50-100 kPa (Solheim & Pfirman in press).

Internal reflecting horizons may arise from differences in material output due to short-term climatic variations. Smaller oscillations are another possible cause, for instance in the form of glacier surges.

The character of the seismic reflection pattern and configuration of internal reflectors give some indications of sedimentary facies and depositional processes. An oblique progradational reflection pattern (Mitchum et al. 1977) is considered to represent a depositional environment proximal to a glacier front (line 5-78, Sequence IV 110-130 km, Subsequence IB 110-130 km, Figs. 4B and 5A). Non-conformable reflectors are generally discontinuous suggesting a complex high-energy environment. A more distal environment is reflected by smooth continuous internal reflectors conformable with the respective lower sequence boundaries (line 5-78, Sequence III 90-170 km, Subsequence IA 140-170 km, Figs. 4B and 5A).

Local deposits which are acoustically transparent in the frequency range 100 Hz - 3.5 kHz (wave lengths 15-0.4 metre) have been interpreted as glaciomarine sediments, trapped in a topographic low as north of Kong Karls Land (Kristoffersen et al. 1984) or deposited outside a bedrock threshold as south of Sørkapp (Kristoffersen et al. 1978, Elverhøi & Solheim 1983 a). From the evidence available to date, these accumulations were probably formed by rapid glaciomarine deposition. An accumulation of similar character is confined to the depression of Ingøydjupet (Fig. 4G), where gravity cores contain firm mud with abundant ice rafted clasts (T. Vorren pers. comm. 1983).

A similar seismic character is observed in Subsequence IA which wedges out eastwards at about 18°E (Fig. 7). A possible explanation is thus that Sequence I east of the dipping internal reflector consists of till material, giving rise to the less transparent character, while Subsequence IA consists of glaciomarine sediments. It is, however, considered likely that consolidation is the same across the boundary, since the entire Sequence I has been compacted by the glacier that formed the ridge complex further out in Bjørnøyrenna (Fig. 4). This glacial advance may also have removed higher parts of Sequence I, and upper parts of Subsequence IA may, consequently, contain material eroded from Sequence I and deposited in front of an advancing glacier. This interpretation also implies that the next latest glaciation recorded in the entire Bjørnøyrenna section probably did not reach further out than the eastern boundary of Subsequence IA.

The ridge complex in outer Bjørnøyrenna (Figs. 4B and 5A, 110-140 km) may be caused by an event (e.g. surge) during retreat of an ice sheet reaching the shelf edge. Another possibility is, however, that the ridge complex marks the maximum extent of an ice sheet. Readvances in the form of local or more regional surges are likely, since surge is a common mode of glacier advance in Svalbard today (Liestøl 1969). A recent surge on Nord-austlandet (Schytt 1969, Solheim & Pfirman in press) is a good example of a large ice cap surging into open marine environment with low relief sea-floor. Surges will also lead to differences in sedimentation, resulting from increased

meltwater and thus also sediment yield (Thorarinsson 1969, Weertman 1969). Several authors have speculated that glacier surges were important movement mechanisms for the vast ice sheets that have existed both in Antarctica and in the northern hemisphere up through the late Cenozoic (Prest 1969, Wilson 1969, Holdsworth 1977, Vorren 1977).

During a glacial cycle, the shelf edge will receive large amounts of sediments, especially during the retreat phase. The high water content of rapidly deposited sediments may lead to instability. A large submarine slide in Bjørnøyrenna (Kristoffersen et al. 1978) (Fig. 8) removed sediments from Sequence I-III over a distance of 35 km along the shelf edge, with a maximum thickness of 500 metres. The slide scar has later been partly infilled with approximately 200 metres of well stratified material. Major submarine slides have occurred several places along the continental slope off Norway, possibly triggered by earthquakes (Bugge 1983). Also increased pore pressures due to migrating free gas or decomposing gas hydrates may trigger slides in unstable sediments (Carpenter 1981, Bugge 1983).

As the shelf edge is the outer limit of a grounded ice sheet, the duration of ice-loading of the sediments is shorter in this area than in more central parts. It may therefore be expected that each sedimentary wedge, interpreted to represent a glacial advance and subsequent retreat, has a decreasing degree of overconsolidation with depth and towards the shelf edge. The sedimentary sequences above the upper regional unconformity may therefore be considered to have varying degrees of overconsolidation with depth.

The general sediment distribution (above reflector δ) in the Barents Sea, seen in relation to theoretical models of deposition associated with ice-caps (White 1974, Sugden & John 1976), strongly support the idea about major ice-caps repeatedly covering the Barents Sea. The central or 'active' zone has a thin and patchy cover of sediments, like what is found in the central and northern regions of the Barents Sea. The outer, or 'wastage' zone may have a thick sedimentary wedge, consisting of individual sub-wedges resulting from repeated occupation of the area by glaciations.

Thus a major part of the section above the upper regional unconformity in the western Barents Sea is considered to be glacially influenced sediments (Fig. 10A). Moreover, the depositional episodes as interpreted from the seismic sequences may be incomplete, due to lack of resolution in the seismic data and obscured or missing sections removed by glacial erosion, or from periods of non-deposition. We stress that in particular Sequence IV, or parts thereof, may be pre-glacial marine sediments derived by fluvial erosion of an emerged Barents shelf later cut to a deeper level by eroding ice.

Dating of the seismic sequences above the upper regional unconformity

Several authors (Laughton, Berggren et al. 1970, Berggren 1972, Berggren & Van Couvering 1974, Shackleton & Opdyke 1977, Poore 1981) define initiation of northern hemisphere glaciations to approximately 3 Ma. Data from site 344, DSDP leg 38 (Talwani, Udintsev et al. 1976) show glacial influence on the sediments, probably back to 5 Ma. Paleomagnetic dating of

central Arctic Ocean sediment cores suggests the oldest ice-rafted pebble to appear at 5.26 Ma (Clark et al. 1980), but one should keep in mind that this chronostratigraphy has recently been questioned (Grantz et al. 1982, Markussen et al. 1984). Later, more or less continuous ice-rafting has occurred, with more intensity in the late Pliocene - Pleistocene than in late Miocene - early Pliocene. Eight intervals of increased Pleistocene glacial ice-rafting and arenaceous sedimentation (also interpreted to be caused by ice-rafting) can be defined (Fig. 10B), and show correlation with periods of continental glaciation. Northern hemisphere glaciation may have started as montane glaciations in the land areas surrounding the Arctic seas (Kennett 1982). Thus glacial influence on marine sedimentation, for example as ice-rafted debris, may have prevailed for a long period before extensive glaciations of the shelf seas occurred.

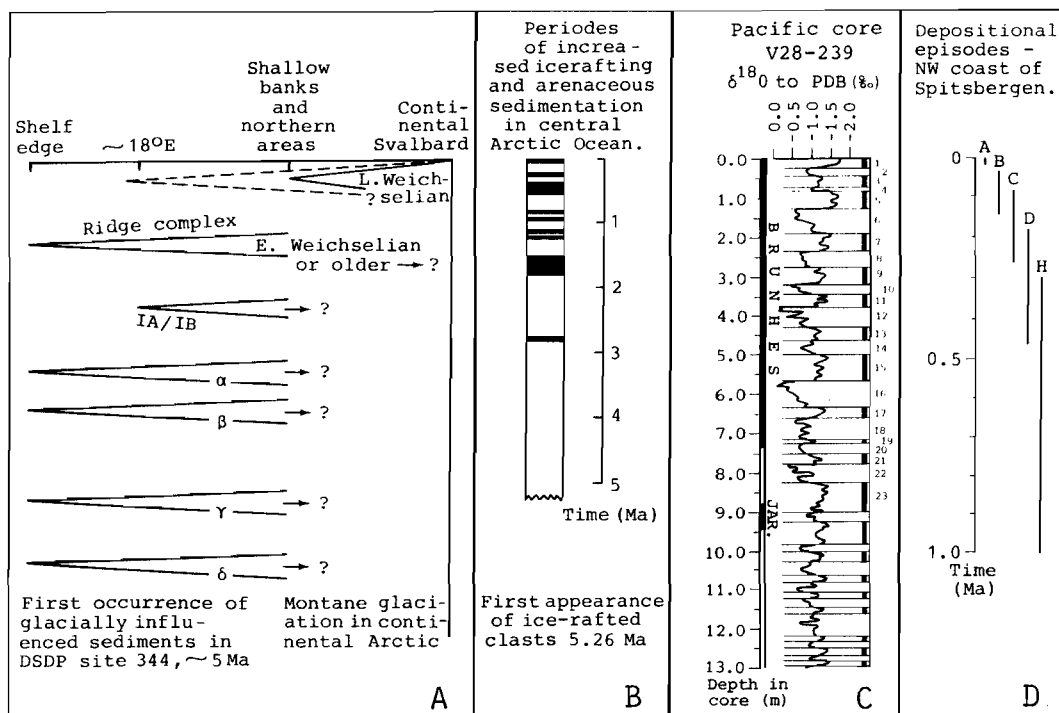


Fig. 10. - A. Glacial episodes in the western Barents Sea as interpreted from the shallow seismic sections in this work.
 B. Results from sediment cores in the Amerasian Basin, Arctic Ocean (After Clark et al. 1980).
 C. Oxygen-isotope record from core V28-239 in the Pacific Ocean. Magnetic record is indicated to the left. Average sedimentation rate is 1 cm/ka, and the total core length is 21.0 metres. Bars to the right indicate warmer periods. (After Shackleton & Opdyke 1976).
 D. Age brackets of depositional episodes from the northwest coast of Spitsbergen, related to sea level variations caused by eustatic, glacioisostatic or possibly tectonic events. Each episode shows indications of local or regional glaciations. (After Miller 1982).

Based on oxygen-isotope analysis, Shackleton & Opdyke (1976) defined eleven glacial stages in a sediment core from the Pacific since approximately 900 ka (Fig. 10C), but climatic shifts also seem to have been abundant prior to this. Results from another Pacific core (Shackleton & Opdyke 1977) suggest initiation of northern hemisphere glaciations at 3.2 Ma, with a major change in character at 2.5 Ma and major glaciations (up to at least two-thirds of the Pleistocene glacial maxima) between 2.5 and 1.8 Ma.

Based on aminostratigraphy of coastal deposits in northwestern Spitsbergen, Miller (1982) is able to resolve several glacial advances within the Pleistocene. The age bracket for the last extensive regional glaciation in the area is 90-260 ka (depositional episode C, Fig. 10D), with another, more restricted regional event prior to the latest Weichselian. This is in agreement with the data from northern Svalbard (Salvigsen & Nydal 1981).

In this work reflectors α , β , γ , and δ are all considered to represent erosion by grounded glaciers reaching the shelf edge, and thus at least four such major glacial advances, as illustrated schematically in Fig. 10A. Durations of the glacials are unknown, but to a first approximation depositional episodes are taken to be proportional to the thickness of the units. Similarly the distance of glacier retreat between each advance is unknown, except for the end of the last episode. Driftwood in the oldest part of the coastal sequence described by Miller (1982), however, indicates periodically open sea conditions at least along the west coast of Spitsbergen since 1 Ma.

The pre-late Weichselian glacial chronology remains completely open at present due to lack of reliable stratigraphic tie points. Relevant information from other oceans and continental areas is compiled in Fig. 10.

At this point we consider the following significant:

1. Glacial sediments in the basal Sequence IV most likely date back to mid Pliocene.
2. A maximum age limit of a few hundred thousand years can be derived for the ridge complex in Bjørnøyrenna (Figs. 4B and 5A) from the apparent absence of any top cover of soft sediments exceeding the sparker resolution (10-15 metres), using Holocene sedimentation rates of 3-5 cm/ka from Elverhøi & Solheim (1983a). Thus the last ice sheet which extended into the deeper western part of Bjørnøyrenna is proposed to be of Saalian or early Weichselian age. It may have been part of the last extensive regional glaciation that covered the entire Svalbard archipelago. Salvigsen & Nydal (1981) interpret this event to be the early Weichselian advance, while Troitsky et al. (1979) and Miller (1982) suggest a Saalian age.
3. In the Barents Sea, the late Weichselian ice sheet was most likely limited to the bank areas and the northern part (Elverhøi & Solheim 1983a), although it cannot be excluded that the ice sheet or an ice stream during this episode could have extended further out into Bjørnøyrenna to form at least part of the ridge complex (Figs. 4B and 5A). In Storfjordrenna, the bedrock threshold may have been the outer limit of the late Weichselian ice. However, an advance to the shelf edge, and a major halt at the threshold during the retreat phase cannot be excluded.

Summary and conclusions

The large as well as small scale physiography of the Barents Sea shelf, with overdeepened troughs and iceberg ploughmarks, indicates action of former glaciers.

The area north of approximately 74°N has a sparse sediment cover above bedrock. Except for local accumulations, the thickness rarely exceeds 25 metres. The sediments are stiff, pebbly mud (till and/or glaciomarine sediments overrun by glacier), draped by glaciomarine sediments and Holocene mud.

In the southern region and along the western margin (division tends to follow the 300 metres depth contour approximately) thickness is generally more than 50 metres, increasing to more than 500 metres in the outer part of Bjørnøyrenna. Local thickness variations are caused by constructional features as till ridges, glaciomarine accumulations and topography in the underlying bedrock, related to salt tectonics and block faulting.

The seismic stratigraphy in Bjørnøyrenna shows four major seismic sequences (I-IV), defined by erosional unconformities (reflectors α , β , γ , and δ). The upper sequence is further divided into two subsequences from the difference in seismic character across a dipping reflector. The sedimentary section above the upper regional unconformity (reflector δ) in both Bjørnøyrenna and Storfjordrenna is considered to consist of glacial/glaciomarine sediments, although it is not excluded that part of the basal sequence may be of preglacial origin. In Storfjordrenna, an accumulation of acoustically transparent deposits in front of a bedrock threshold is interpreted to be glaciomarine sediments deposited in front of a glacier with the front pinned at the threshold. Deposits of similar seismic character are also found as channel fill within the section.

The overall sediment distribution above the upper regional unconformity supports theoretical models of ice-cap associated deposition, with thin and patchy cover in the central zones and thick sedimentary wedges in the outer areas (i.e. near the shelf edge).

Interpretation of a glacial chronology is severely hampered by the lack of stratigraphic tie points and insufficient seismic resolution. However, we infer that:

- At least seven glacial episodes have occurred on the Barents Sea shelf, including the late Weichselian.
- Of these, at least four, possibly five, advances reached the shelf edge.
- The first episode is probably of mid Pliocene age.
- The last glaciation reaching the shelf edge is most likely of Saalian or early Weichselian age.
- The late Weichselian ice sheet covered the northern regions and the bank areas, but an ice stream extending out into Bjørnøyrenna is not excluded.

Acknowledgements

This research was carried out under the Barents Sea Project, at the Norwegian Polar Research Institute, and funded by the Norwegian Council for Scientific and Industrial Research and the Norwegian Petroleum Directorate. Bjørn G. Andersen, Tom Bugge, Anders Elverhøi, Jan Mangerud, and Tore O. Vorren are acknowledged for their critical comments on the manuscript. Espen Kopperud did the final drawing of the map.

References

- Andersen, B. G. 1981: Late Weichselian ice sheets in Eurasia and Greenland. Pp. 1-65 in Denton, G. H. & Hughes, T. J. (eds.): *The last great ice sheets*. John Wiley & Sons.
- Baranowski, S. 1977: The subpolar glaciers of Spitsbergen seen against the climate of this region. *Wroclaw, Wydawnictwa Uniwersytetu Wrochawskeio. Results of investigation of the Polish scientific Spitsbergen Expeditions 3*. 93 pp.
- Berggren, W. A. 1972: Late Pliocene - Pleistocene glaciation. Pp. 953-963 in Laughton, A. S., Berggren, W. A. et al.: *Initial Reports of the Deep Sea Drilling Project 12*. Washington, U.S. Government Printing Office.
- Berggren, W. A. & Van Couvering, J. A. 1974: *The late Neogene: developments in palaeontology and stratigraphy 2*. New York, Elsevier. 216 pp.
- Boulton, G. S. 1979: Glacial history of the Spitsbergen archipelago and the problem of a Barents shelf ice sheet. *Boreas 8*, 31-57.
- Boulton, G. S., Baldwin, C. T., Peacock, J. D., McCabe, A. M., Miller, G., Jarvis, J., Horsefield, B., Worsley, P., Eyles, N., Chroston, P. N., Day, T. E., Gibbard, P., Hare, P. E. & von Brunn, V. 1982: A glaci-isostatic facies model and amino acid stratigraphy for late Quaternary events in Spitsbergen and the Arctic. *Nature 298*, 437-441.
- Bugge, T. 1983: Submarine slides on the Norwegian continental margin, with special emphasis on the Storegga area. *Continental Shelf Institute, Norway, Publ. 110*. 152 pp.
- Bugge, T. & Rokoengen, K. 1976: Geologisk kartlegging av de øvre lag på kontinental-sokkelen utenfor Troms. *Continental Shelf Institute, Norway, Publ. 85*. 51 pp.
- Carpenter, G. 1981: Coincident sediment slump/clathrate complexes on the U.S. Atlantic continental slope. *Geo-Marine Letters 1*, 29-32.
- Clark, D. L., Whitman, R. R., Morgan, K. A. & Scudder, D. M. 1980: Stratigraphy and glacial-marine sediments of the Amerasian Basin, central Arctic Ocean. *Geol. Soc. Am. Spec. Paper 181*, 57 pp.
- Damuth, J. E. 1978: Echo character of the Norwegian-Greenland Sea: Relationship to Quaternary sedimentation. *Marine Geology 28*, 1-36.
- Dibner, V. D. 1978: Morphostructure of the shelf of the Barents Sea. Morfostruktura sel'fa Barenceva morja. *Nedra, Leningrad. NIIGA, Trudy 185* (in russian). 211 pp.
- Edwards, M. B. 1975: Gravel fraction on the Spitsbergen Bank, NW Barents Shelf. *Norges Geol. Unders. 316*, 205-217.
- Eldholm, O. & Ewing, J. 1971: Marine geophysical survey in the southwestern Barents Sea. *J. Geophys. Res. 76*, 3832-3841.
- Elverhøi, A. & Kristoffersen, Y. 1978: Glacial deposits of Bjørnøya, northwestern part of the Barents Sea. *Nor. Polarinst. Årbok 1977*, 209-215.
- Elverhøi, A. and Lauritzen, Ø. 1984: Bedrock geology of the northern Barents Sea (west of 35°E) as inferred from the overlying Quaternary deposits. *Nor. Polarinst. Skr. 180*, 5-16.
- Elverhøi, A. & Solheim, A. 1983a: The Barents Sea ice sheet, a sedimentological discussion. *Polar Research 1 n.s.*, 23-42.
- Elverhøi, A. & Solheim, A. 1983b: Marin-geologiske og -geofysiske undersøkelser i Barentshavet 1983 - Toktrapport. *Nor. Polarinst. Rapportserie 14*. 116 pp.

- Emelyanov, E. M., Litvin, V. M., Levchenko, V. A. & Martynova, G. P. 1971: The geology of the Barents Sea. *Inst. Geol. Sci. Rep. 70(14)*, 1-15.
- Faleide, J. I., Gudlaugsson, S. T. & Jacquart, G. in press: Evolution of the Barents Sea. *Marine and Petroleum Geology*, 1.
- Grantz, A., Johnson, G. L. & Sweeney, J. F. 1982: The Arctic region. Pp. 105-115 in Palmer, A. R. (ed.): Perspectives in regional geological synthesis, planning for the geology of North America. *D-NAG Spec. Publ. 1*.
- Grosswald, M. G. 1980: Late Weichselian ice sheet of northern Eurasia. *Quaternary Research 13*, 1-32.
- Hamilton, E. L., Bachman, R. T., Curray, J. R. & Moore, D. G. 1977: Sediment velocities from sonobuoys: Bengal Fan, Sunda Trench, Andaman Basin, and Nicobar Fan. *J. Geophys. Res. 82*, 3003-3012.
- Holdsworth, G. 1977: Surge activity on the Barnes Ice Cap. *Nature 269*, 588-590.
- Houtz, R. & Windisch, C. 1977: Barents Sea continental margin sonobuoy data. *Geol. Soc. Am. Bull. 88*, 1030-1036.
- Hughes, T. J., Denton, G. H., Andersen, B. G., Schilling, D. H., Fastook, J. L. & Lingle, C. S. 1981: The last great ice sheets: a global view. Pp. 263-317 in Denton, G. H. & Hughes, T. J. (eds.): *The last great ice sheets*. John Wiley & Sons.
- Kennett, J. P. 1982: *Marine Geology*. Englewood Cliffs, N. J., Prentice-Hall Inc. 813 pp.
- Klenova, M. V. 1960: *The geology of the Barents Sea* (in russian). Akad. Nauk, SSSR, Moscow. 367 pp.
- Kristoffersen, Y. & Elverhøi, A. 1978: A diapir structure in Bjørnøyrenna. *Nor. Polarinst. Årbok 1977*, 189-198.
- Kristoffersen, Y., Elverhøi, A. & Vinje, T. 1978: *Barentshavprosjektet, marin geofysikk, geologi og havis*. Unpubl. report, Nor. Polarinst. 81 pp.
- Kristoffersen, Y., Milliman, J. D. & Ellis, J. P. 1984: Unconsolidated sediments and shallow structure of the northern Barents Sea. *Nor. Polarinst. Skr. 180*, 25-39.
- Laughton, A. S., Berggren, A. et al. 1970: Deep Sea Drilling Project, Leg 12. *Geotimes 15(9)*, 10-14.
- Liestøl, O. 1969: Glacier surges in west Spitsbergen. *Can. J. Earth Sci. 6*, 895-897.
- Markussen, B., Zahn, R. & Thiede, J. 1984: Late Quaternary sedimentation in the eastern Arctic basin: stratigraphy and depositional environment. *Nature* (in press).
- Miller, G. H. 1982: Quaternary depositional episodes, western Spitsbergen, Norway: Aminostratigraphy and glacial history. *Arctic and Alpine Research 14*, 321-340.
- Mitchum, R. M. Jr., Vail, P. R. & Sangree, J. B. 1977: Stratigraphic interpretation of seismic reflection patterns in depositional sequences. In Payton, C. E. (ed.): Seismic stratigraphy - applications to hydrocarbon exploration. *Am. Ass. Petr. Geol. Mem. 26*, 117-135.
- Myhre, A. 1984: Compilation of seismic velocity measurements along the margins of the Norwegian-Greenland Sea. *Nor. Polarinst. Skr. 180*, 47-67.
- Poore, R. Z. 1981: Temporal and spatial distribution of ice-rafted mineral grains in Pliocene sediments of the North Atlantic: Implications for late Cenozoic climatic history. In Warne, J. E., Douglas, R. G. & Winterer, E. L. (eds.): The Deep Sea Drilling Project: a decade of progress. *SEPM Spec. Publ. 32*, 505-516.
- Prest, V. K. 1969: Retreat of Wisconsin and recent ice in North America. *Geol. Surv. Can. Map 1257 A*.
- Renard, V. & Malod, J. 1974: Structure of the Barents Sea from seismic refraction. *Earth and Planetary Science Letters 24*, 33-47.
- Rokoengen, K. & Rønningsland, T. M. 1983: Shallow bedrock geology and Quaternary thickness in the Norwegian sector of the North Sea between 60°30'N and 62°N. *Nor. Geol. Tidsskr. 63*, 83-102.
- Rønnevik, H. C. & Motland, K. 1979: Geology of the Barents Sea. *Nor. Petrol. Soc. NSS/15*. 34 pp.
- Rønnevik, H. C., Beskow, B. & Jacobsen, H. P. 1982: Structural and stratigraphical evolution of the Barents Sea. *Norw. Petrol. Soc., Geol. Mem. 8*, 431-440.
- Salvigsen, O. 1981: Radiocarbon dated raised beaches in Kong Karls Land, Svalbard, and their consequences for the glacial history of the Barents Sea area. *Geogr. Ann. 63A*, 283-291.

- Salvigsen, O. & Nydal, R. 1981: The Weichselian glaciation in Svalbard before 15,000 B.P. *Boreas* 10, 433-446.
- Schytt, V., Hoppe, G., Blake, W. Jr. & Grosswald, M. G. 1968: The extent of the Wurm glaciation in the European Arctic. *Int. Ass. Scient. Hydr. General Assembly of Bern 1967*, 79, 207-216.
- Schytt, V. 1969: Some comments on glacier surges in eastern Svalbard. *Can. J. Earth Sci.* 6, 867-871.
- Sellevoll, M. A. & Sundvor, E. 1974: The origin of the Norwegian Channel - a discussion based on seismic measurements. *Can. J. Earth Sci.* 11, 224-231.
- Shackleton, N. J. & Opdyke, N. D. 1976: Oxygen-isotope and paleomagnetic stratigraphy of Pacific core V28-239, late Pliocene to latest Pleistocene. *Geol. Soc. Am. Mem.* 145, 449-464.
- Shackleton, N. J. & Opdyke, N. D. 1977: Oxygen isotope and paleomagnetic evidence for early northern hemisphere glaciation. *Nature* 270, 216-219.
- Solheim, A. & Pfirman S. in press: Sea-floor morphology outside a grounded, surging glacier: Bråsvellbreen, Svalbard. *Marine Geology*.
- Spencer, A. M., Home, P. C. & Berglund, L. T. in press: Tertiary development of the western Barents shelf margin. In Spencer, A. M. (ed.): *Petroleum geology of the North European margin*. Graham and Trotman, London.
- Sugden, D. E. & John, B. S. 1976: *Glaciers and Landscape*. Edward Arnold Publishers Ltd., London. 376 pp.
- Talwani, M., Udintsev, G. et al. 1976: *Initial reports of the Deep Sea Drilling Project, leg. 38*. Washington, U.S. Government Printing Office. 1256 pp.
- Thorarinsson, S. 1969: Glacier surges in Iceland with special reference to the surges of Brúarjökull. *Can. J. Earth Sci.* 6, 875-882.
- Troitsky, L., Punning, J. M., Hutt, G. & Rajamäe, R. 1979: Pleistocene glaciation chronology of Spitsbergen. *Boreas* 8, 401-407.
- Vorren, T. O. 1977: Weichselian ice movement in south Norway and adjacent areas. *Boreas* 6, 247-257.
- Weertman, J. 1969: Water lubrication mechanism of glacier surges. *Can. J. Earth Sci.* 6, 929-939.
- White, G. W. 1974: Buried glacial geomorphology. In Coates, D. R. (ed.): *Glacial geomorphology*, 331-350. State Univ. NY, Binghamton.
- Wilson, A. T. 1969: The climatic effects of large-scale surges of ice-sheets. *Can. J. Earth Sci.* 6, 911-915.

PAPER 6.

Sediment distribution and sea-floor morphology of Storbanken: implications for the glacial history of the northern Barents Sea¹

ANDERS SOLHEIM

Norwegian Polar Research Institute, P.O. Box 158, N-1330 Oslo Lufthavn, Norway

JOHN D. MILLIMAN

Woods Hole Oceanographic Institution, Woods Hole, MA 02543, U.S.A.

AND

ANDERS ELVERHØI

Norwegian Polar Research Institute, P.O. Box 158, N-1330 Oslo Lufthavn, Norway

Received May 14, 1986

Revision accepted June 22, 1987

Acoustical (sparker, 3.5 kHz, and side-scan sonar) and sedimentological data from a local study on Storbanken in the northern Barents Sea support the concept of a late Weichselian ice sheet covering most of the Barents Sea. During a major halt in the retreat of the ice sheet, locally thicker (38 m) accumulations of ice-proximal glaciomarine sediments were deposited, after which rapid retreat took place. Sea-floor morphology indicates that the retreat across Storbanken most likely took place without surging or climatically controlled oscillations.

Intense iceberg ploughing characterizes the sea floor down to water depths of 210–220 m. Most of this is relict, but occasional gouges in the shallower regions may have had a more recent origin. The apparent lower limit of ploughing, interpreted in terms of relative sea level, indicates a rather moderate isostatic depression. This probably resulted from a thin ice sheet, fed from several ice source areas. Depth of the plough marks is largely dependent on thickness of the glaciomarine sediments. A thin and patchy layer of overcompacted till fills local depressions in the sedimentary bedrock surface and forms a flat base for iceberg ploughing.

Les données acoustiques (étinceleur, 3,5 kHz et sonar à balayage latéral) et sédimentologiques d'une étude locale sur les Storbanken dans la mer Barents du nord appuient l'hypothèse de la présence d'une calotte glaciaire recouvrant la majeure partie de la mer Barents au Weichselien tardif. Durant un épisode de stagnation du retrait de la calotte glaciaire, il s'est produit à proximité des glaces des accumulations locales plus épaisses (38 m) de sédiments glaciomarins, par la suite il y a eu accélération du mouvement de retrait des glaces. La morphologie du fond marin indique que le retrait traversant les Storbanken s'est déroulé sans pulsations ou sans oscillations dues à des changements climatiques.

Un labourage intense par les quilles des icebergs caractérise le fond marin jusqu'à des profondeurs de 210–220 m. En général ces phénomènes sont relictuels, cependant des rainures occasionnelles dans les régions d'eau moins profonde peuvent relever d'une origine plus récente. La limite inférieure apparente du labourage, interprétée en termes de niveau relatif de la mer, indique une dépression isostatique plutôt modérée. Ceci résulte probablement d'une mince calotte glaciaire alimentée par plusieurs régions nourricières de glace. La profondeur des marques de labourage dépend largement de l'épaisseur des sédiments glaciolacustres. Une couche mince incluant des poches de till surcompacté remplit les dépressions locales à la surface des assises sédimentaires et offre une surface unie au labourage par les icebergs.

[Traduit par la revue]

Can. J. Earth Sci. 25, 547–556 (1988)

Introduction

The concept of a late Weichselian Barents Sea (Fig. 1) ice sheet, now widely accepted, is supported by the following lines of evidence: (i) The Holocene emergence curves for Kong Karls Land and Storøya (Fig. 1) are exponential, and raised beaches 110 m above sea level at Kong Karls Land have been dated to 10 ka BP (Jonsson 1983; Salvigsen 1981). (ii) The shoreline-displacement gradient for Svalbard (Fig. 1) indicates an ice cap centred east of the archipelago (Salvigsen and Nydal 1981). (iii) A relatively slow emergence between 13 and 10 ka BP on the west coast of Spitsbergen (Fig. 1) may have resulted from deglaciation of the Barents Sea during this interval (Forman *et al.* 1987). (iv) Moraine ridges off the Norwegian coast, at 71°N, indicate ice movement from the north (Vorren and Kristoffersen 1986). (v) A generally thin (< 10–15 m) cover of un lithified sediments above bedrock in central parts of the northern Barents Sea increases towards deeper water in the south and towards the continental margin to

the west (Solheim and Kristoffersen 1984). (vi) The sequence of un lithified sediments seems to consist of overconsolidated till covered by soft glaciomarine sediments and fine-grained Holocene mud (Elverhøi and Solheim 1983a). (vii) Locally thicker accumulations of un lithified sediments, interpreted as ice-marginal features, fringe the shallow banks (Elverhøi and Solheim 1983a; Kristoffersen *et al.* 1984). However, the maximum extent, exact timing, and deglaciation history for the Barents Sea ice sheet are still essentially unknown.

Until now, the sediments above bedrock in the northern Barents Sea have only been mapped through a regional (40–50 km line spacing) grid of single-channel sparker profiles. Higher resolution information has been limited to occasional 3.5 kHz sounding lines. For these reasons, little is known about the nature and geometry of the locally thicker accumulations. Where constituting positive topographic features, they have mostly been considered moraine ridges (Elverhøi and Solheim 1983a; Kristoffersen *et al.* 1984). Furthermore, most sediment cores have only sampled the soft glaciomarine sediments and Holocene mud: no cores have penetrated the entire section. As Holocene sedimentation rates in the Barents Sea

¹Norwegian Polar Research Institute Contribution 248; Woods Hole Oceanographic Institution Contribution 6506.

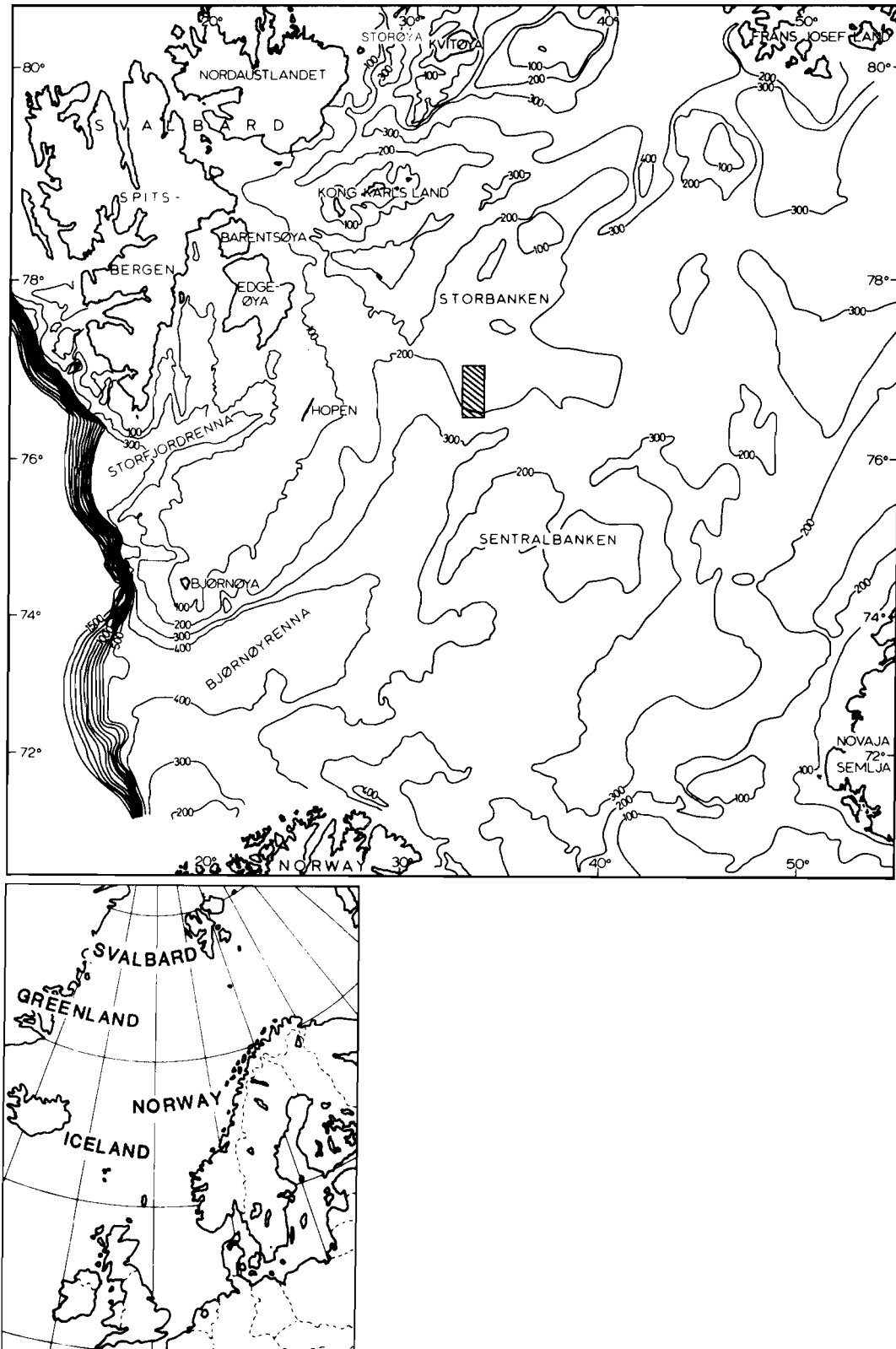


FIG. 1. The Barents Sea, with study area indicated.

are generally less than 5 cm/ka (Elverhøi and Solheim 1983a), sea-floor morphological features, in particular iceberg plough marks, have good preservation potential and can therefore provide information about the deglaciation history. With the exception of a local study off Nordaustlandet (Solheim and

Pfirman 1985), no side-scan sonar data have been reported from the northern Barents Sea. Therefore, studies of iceberg plough marks have essentially been lacking in this region.

In this paper, we present acoustical (sparker, 3.5 kHz precision depth recorder (PDR), and side-scan sonar) and sedimen-

tological data from Storbanken (Fig. 1), a large bank in the north-central Barents Sea and a possible location for a recessional glacier margin. The information is used to interpret the nature of the locally thicker, unlithified sediment accumulations and the character of iceberg ploughing in the region, thereby allowing us to evaluate possible implications for the late Weichselian glacial extent and deglaciation history.

Methods

Acoustic data acquisition and shallow sampling were carried out in local areas in the western Barents Sea during a cruise on the R/V *Lance* in 1983. The seismic profiler was a 1 kJ multi-electrode (144 tips) sparker with analog recording via a single-channel streamer and a band-pass filter of 150–500 Hz. The side-scan sonar was a 50 kHz Klein system. In addition, a 3.5 kHz echo sounder was used continuously. Sampling of unlithified sediments was accomplished using a gravity corer (3 and 6 m barrel) and a vibrocorer (3.5 m barrel). A Magnavox 1105 single-channel receiver utilizing the Transit satellite system was used for navigation throughout the cruise. Although the distance between adjacent north–south lines (2–10 km) is great for many areas, it is a significant improvement over the generally much wider spacing of geophysical data seen in most of the northern Barents Sea (40–50 km).

Sediment cores were split, described, photographed, and subsampled. Grain-size analysis of the coarse fraction was carried out using standard sieving techniques, whereas clay and silt fractions were determined by Falling Drop Analysis (trademark of Geonor A/S (Moum 1966)). Bulk density was determined by weighing the sample submerged in kerosene. Samples for grain-size, water-content, and bulk-density measurements included at least 100 g of sediment. Shear strength was measured by pocket penetrometer, whereas compressional sound velocity was measured by means of a portable ultrasonic nondestructive digital indicating tester (PUNDIT: trademark of C.N.S. Instruments Ltd., England (ASTM 1983)), measuring travel time through the sediment with an accuracy of 1 μ s.

Physiographic and geological setting

The Barents Sea (Fig. 1) is situated between the Arctic Ocean in the north and the Norwegian and Russian mainland in the south. The water depth in the survey area (Figs. 1, 2) ranges from 95 m in the central part to 250 m in the south. Towards the northeast, the main part of Storbanken is defined by the 200 m contour, whereas the western and southwestern slopes border the northern part of Bjørnøyrenna, the major deep trough in the western Barents Sea.

The general Quaternary stratigraphic sequence in the northern Barents Sea, including the study area, as deduced from sediment cores and occasional 3.5 kHz sounding lines (Elverhøi and Solheim 1983a), consists of a lower layer of overconsolidated sediments covered by a veneer of late Weichselian glaciomarine sediment. The glaciomarine character is inferred from the amount of ice-rafted debris (IRD) and a sparse foraminifera fauna consisting of benthonic species having high affinities with cold water. The age of the deposits is extrapolated from Holocene dates. Over large regions, in particular in deep water and local depressions, there is a thin top cover of Holocene mud that differs from the glaciomarine sediment in colour, fauna (warmer), mineralogical assemblage (and therefore source area), and amount of coarse IRD (decreased) (Wensaas 1986). Approaching the presently heavily glaciated areas on eastern Svalbard, the difference becomes less distinct.

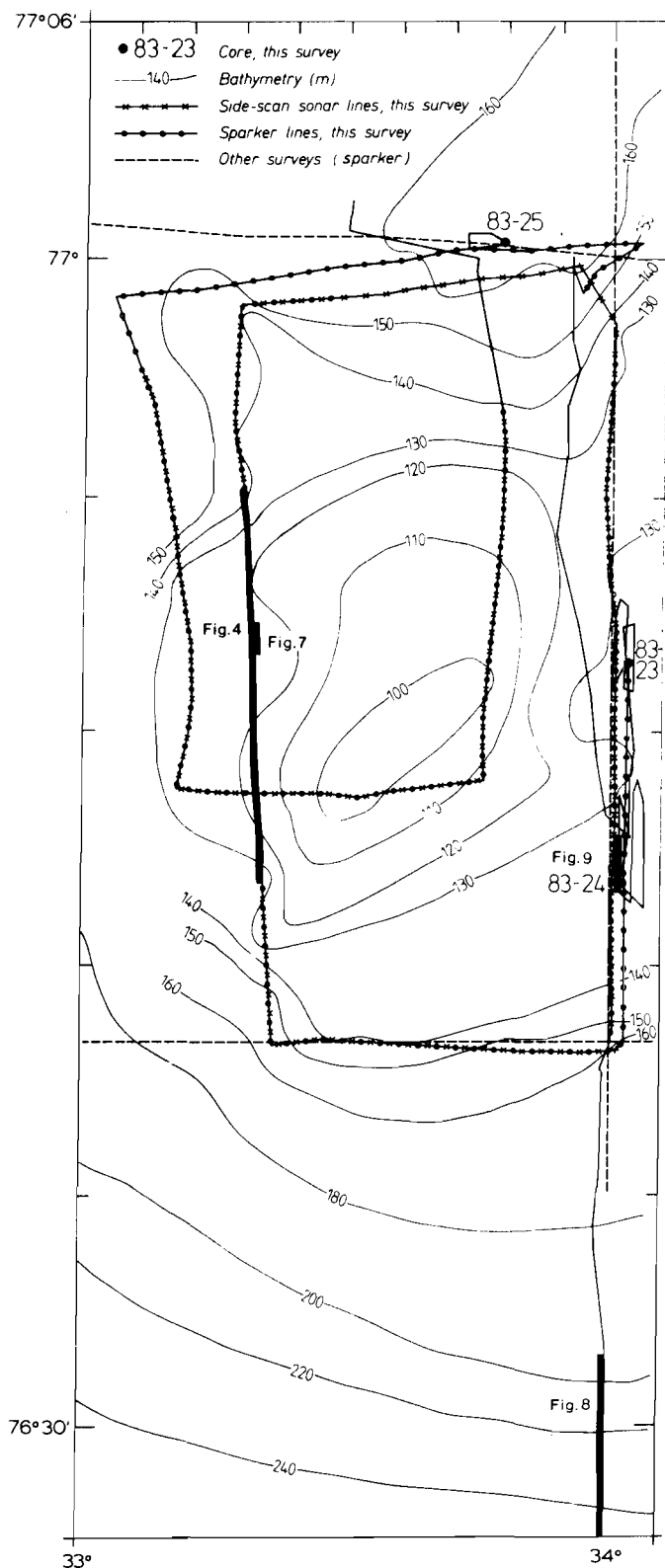


FIG. 2. The Storbanken survey area, with core stations and seismic lines from this and previous surveys. Locations of figures appearing later in the text are indicated by heavy lines.

A regional angular unconformity defines the top of the underlying bedrock. The major part of the northern Barents Sea has less than 25 ms (two-way travel time) of unlithified sediments above the bedrock (Solheim and Kristoffersen 1984).

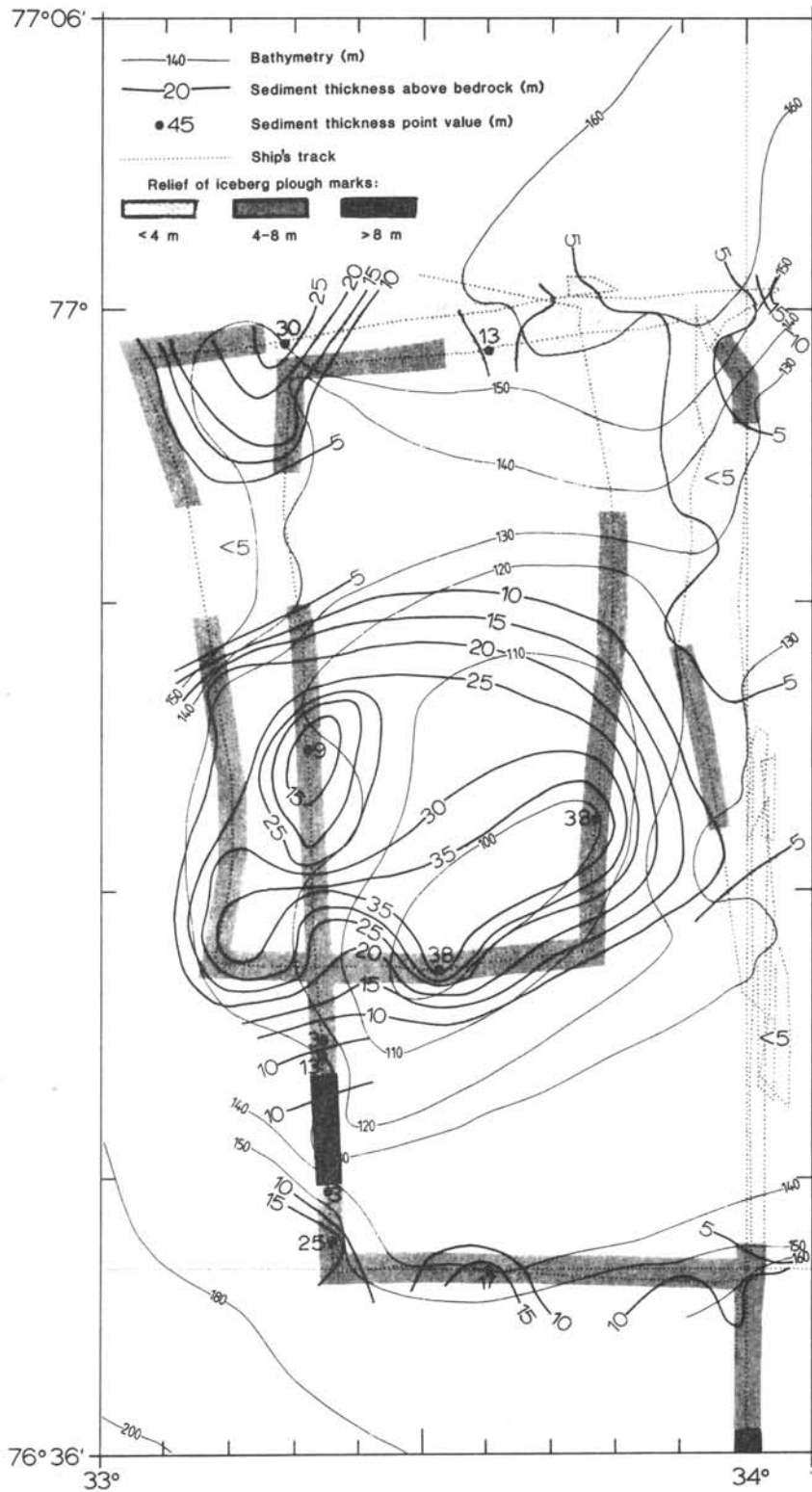


FIG. 3. Thickness of sediments above bedrock in the survey area. Compressional sound velocity of 1700 m/s is used for conversion from travel time to thickness in metres. Relief of iceberg plough marks is indicated by shading.

Sediment distribution and acoustic character

Two thicker accumulations (30 and 38 m) of sediment above bedrock are found in the northwestern and central parts of the survey area (Fig. 3). Thickness estimates from seismic profiles assume a compressional velocity of 1700 m/s, based on values measured in the sediment cores. Both accumulations constitute

positive topographic features and thus have the appearance of low-relief ridge complexes (Fig. 4).

Except for these accumulations, however, the sediment cover is thin, often 5 m or less, although it increases in thickness towards deeper water in the south. The acoustically estimated thickness was confirmed by drilling 4.5 and 5.5 m with

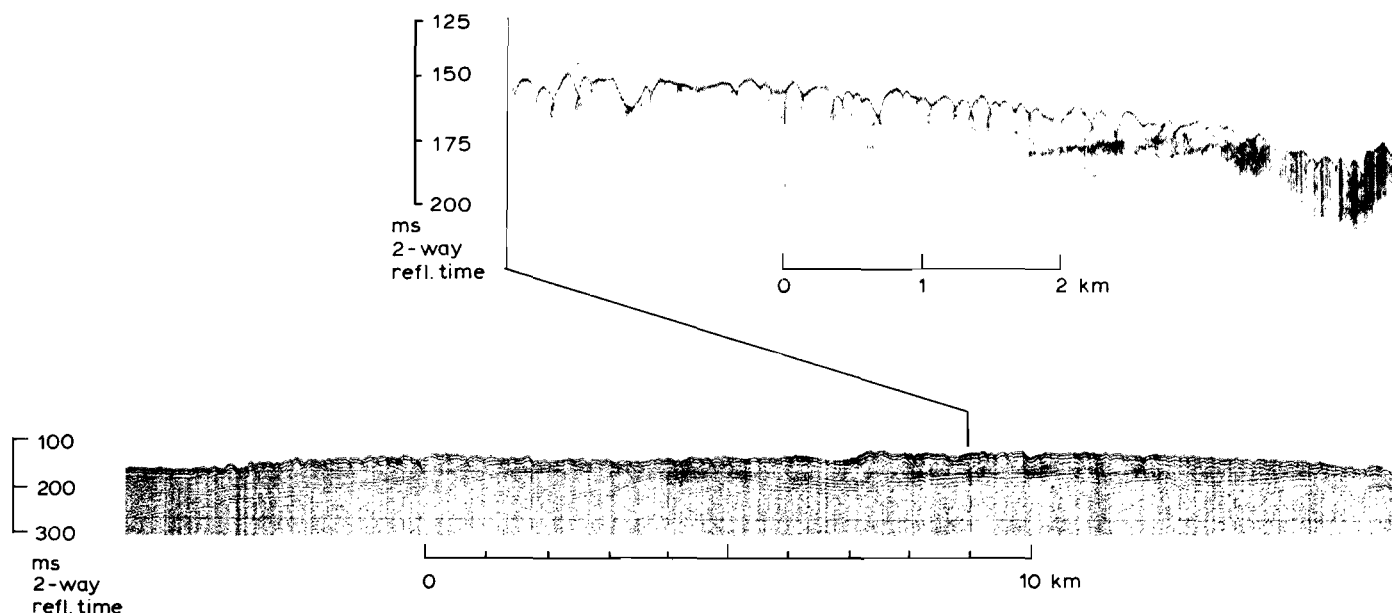


FIG. 4. Sparker (lower) and 3.5 kHz (upper) profiles across the main sediment accumulation. The slightly undulating reflector at approximately 175 ms, followed almost to outcrop on the 3.5 kHz record, marks top of the sedimentary bedrock, possibly modified by a thin layer of till. For location, see Fig. 2.

a rock-core drill prior to reaching bedrock at stations 83-23 and 83-24, respectively.

The general acoustic character (from 3.5 kHz records) throughout the survey area shows a transparent, apparently homogeneous unit above bedrock. In some locations, particularly near station 83-23, this unit can be resolved into an upper, 1–2 m thick layer and a lower, slightly less transparent layer. Resolution, however, is rather badly distorted by the irregular small-scale topography resulting from numerous iceberg plough marks. The transition between the two layers, where seen, appears gradational. Most likely, it represents a downward coarsening of the sediment. A similar relationship between acoustic character and grain size has been reported from other areas (e.g., Damuth 1978; Elverhøi *et al.* 1983). The acoustic character of the thicker accumulations is not significantly different from that of other parts of the study area. The degree of acoustic transparency is indicated by the fact that penetration through 30 ms of sediment cover down to bedrock with the 3.5 kHz echo sounder was frequently achieved.

Sediment composition

Sediment samples (Fig. 5) were obtained by vibrocoreing at two locations (83-23 and 83-24) and gravity coring at one location (83-25) (Fig. 2). Core penetration was generally poor, with a maximum of 0.7 m in a vibration time of 20 min. Most likely, this was caused by high-strength material above bedrock. The rock-core drilling at stations 83-23 and 83-24 confirmed that the vibrocorer only penetrated the upper part of the sequence.

The sections penetrated in stations 83-23 and 83-24 are muddy sands to sandy muds (Elverhøi and Solheim 1983*b*), with no significant lithological changes throughout the sections. The most dominant size fractions are medium silt to fine sand (2–6 ϕ), and station 83-23 has some gravel that apparently disappears down core. There is a clear change to darker colours at approximately the 10 cm level in all four cores at these two stations. The deepest station, 83-25, shows a fining-

upwards sequence from a sand-rich diamicton in the lower part to a sandy mud with no gravel in the upper 20 cm. With the exception of a sand layer in the lower part of the core, there are no distinct lithological or colour changes in the core.

The physical properties (Fig. 5) reflect sample lithology, with the two most sandy locations having higher compressional sound velocities, higher bulk densities, and lower water contents than core 83-25 (except for the interval covering the sand lens). Although determined shear strengths in this sandy material are probably too high, they give some indication of compaction. We interpret the lower 14 cm of 83-23/2, with a measured shear strength of 238 kPa, as clearly overcompacted.

A distinct change in colour from brownish or olive gray (typically 5Y 4/2) to dark gray or black (typically 5Y 3/1–2.5/2) (Munsell soil colour charts), caused by a change in the type and amount of organic matter (Elverhøi and Bomstad 1980; Elverhøi and Solheim 1983*a*; Forsberg 1983), is usually found at the transition between Holocene mud and late Weichselian glaciomarine sediment in the northern Barents Sea. A generally high content of coarse material, also in the Holocene sediments of the bank areas (Wensaas 1986), precludes this from being a diagnostic feature here. This is also indicated at station 83-23 (Fig. 5), which has the coarsest material at the top. With colour taken as a diagnostic feature, the upper 10 cm of the cores at stations 83-23 and 83-24 is considered as representing postglacial Holocene conditions; the rest of the cores, as representing late Weichselian, more ice-proximal conditions. The lower 14 cm of core 83-23/2 is an exception. Based on regional data, this overconsolidated material is till or glaciomarine sediment overrun and compacted by the late Weichselian glacier (Elverhøi and Solheim 1983*a*). As core 83-23/2 was taken in the trough of an iceberg plough mark, the similarity between 83-23/2 and 83-23/1 shows that the entire core 83-23/1 and the upper 31 cm (above the overconsolidated sediment) of core 83-23/2 postdate the ploughing, which therefore must have taken place shortly after the glacier withdrew from the area.

Based on the lack of colour change, the entire core 83-25, on

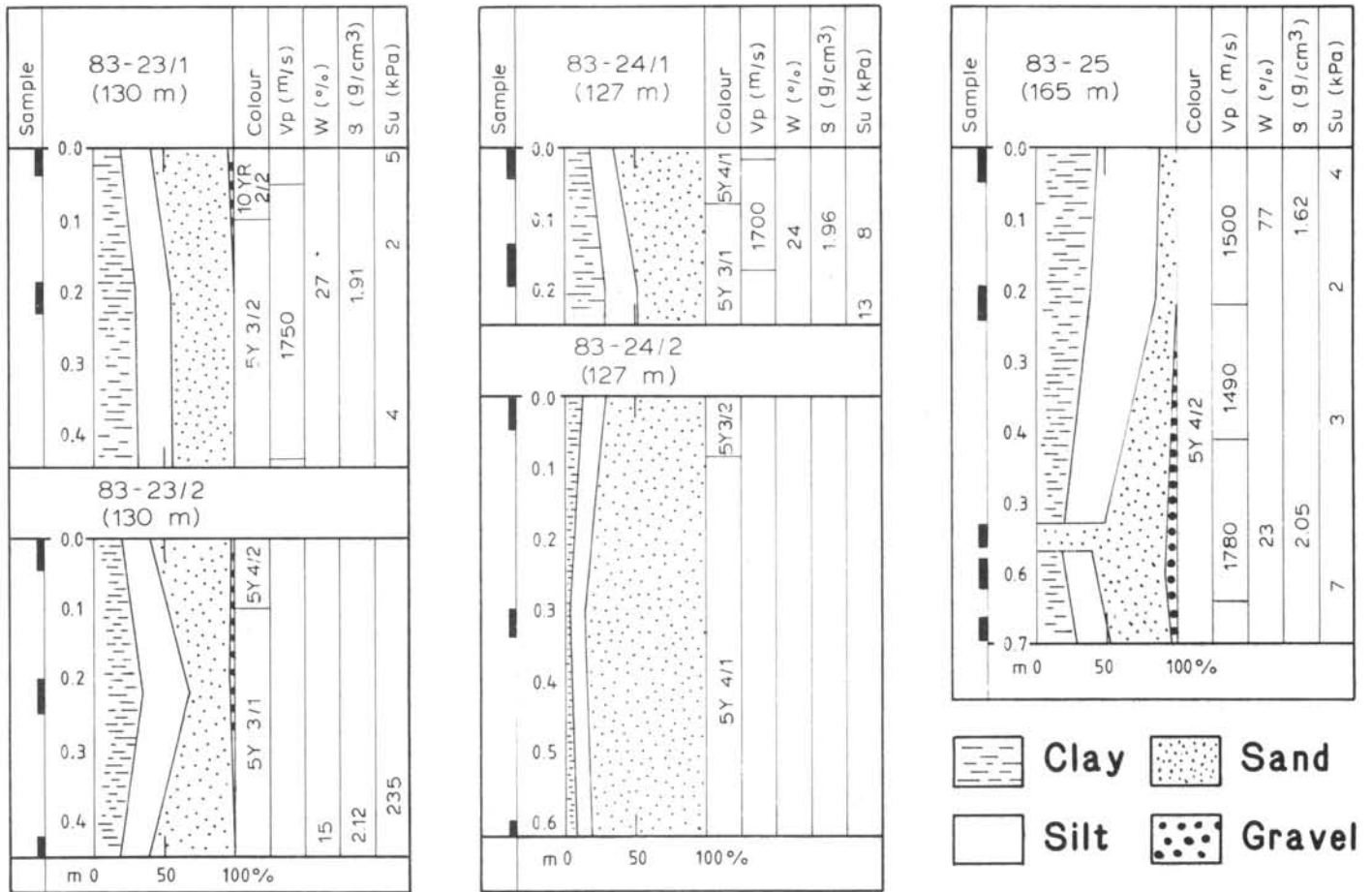


FIG. 5. Gravity cores and vibrocores taken in the study area, with physical properties indicated. All values refer to depth in core where they are placed on the figure. Colour is from Munsell solid colour charts. Compressional sound velocity (V_p) refers to interval between the horizontal lines; water content (W) is in percentage of dry weight; δ is sediment bulk density; shear strength (S_u) is measured with a pocket penetrometer. For location of cores, see Fig. 2.

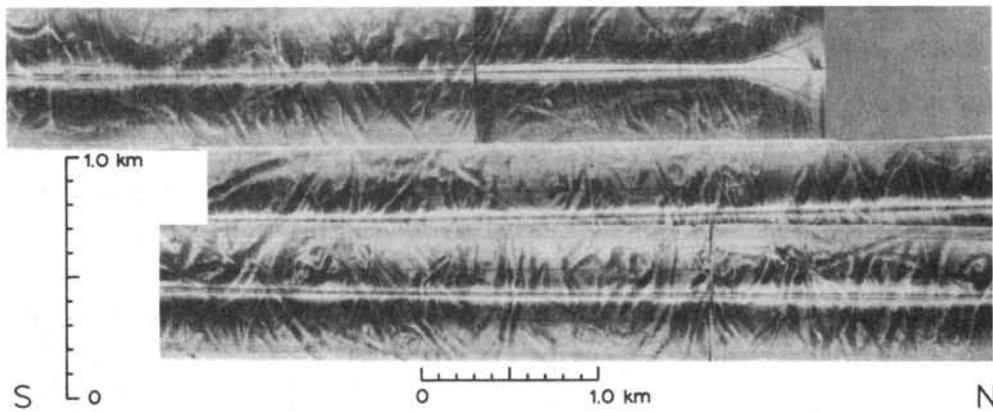


FIG. 6. Side-scan mosaic from the vicinity of station 83-24. For location, see Fig. 2.

the other hand, is considered Holocene in age. Elverhøi and Solheim (1983a) reported Holocene Barents Sea sedimentation rates of 2–5 cm/ka, but this average value may vary locally with topography and proximity to source areas (Wensaas 1986). The most important source of Holocene sediments in the central Barents Sea is winnowing of fine material from the banks and redeposition in deeper areas and local troughs (Elverhøi and Solheim 1983a; Pfirman 1984). This process is

reflected in the lower silt and clay content in core 83-25 (situated in a local trough; Fig. 2), relative to the high Holocene sand content in the other cores (Fig. 5).

Morphological features

Because of the generally sparse cover of un lithified sediments in this part of the Barents Sea (Solheim and Kristoffer-

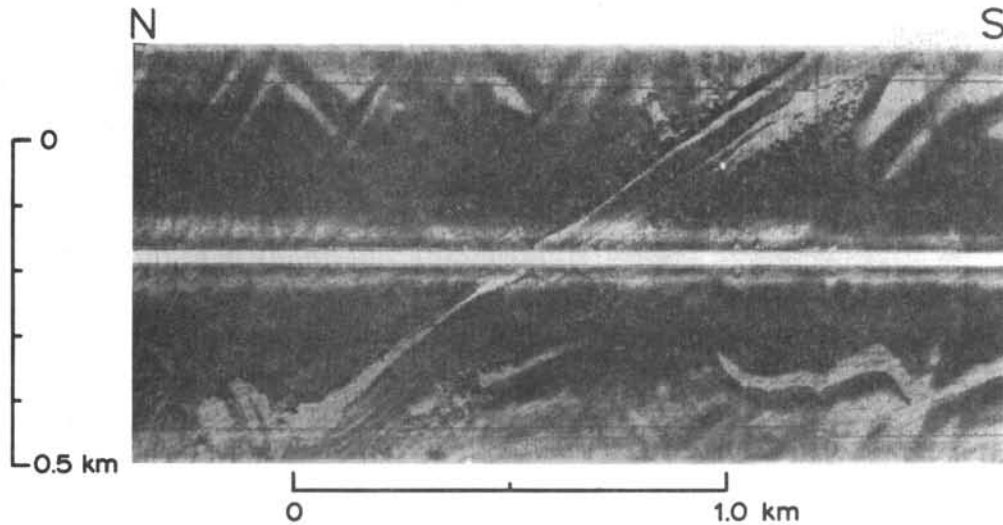


FIG. 7. Iceberg plough mark with "fresh" appearance. Note disturbed sediment along the sides of the gouge proper. For location, see Fig. 2.

sen 1984), the large-scale topography of the study area is mainly determined by the underlying bedrock and by locally thicker accumulations of unlithified sediments (Figs. 2, 3). Small-scale topography, on the other hand, is totally dominated by iceberg plough marks. In some areas, up to 100% of the sea floor is affected by gouging (Fig. 6). Plough marks vary in width from 15–30 m to more than 100 m. The narrowest are straight and up to several hundred metres long, whereas the widest are often winding and can be traced up to 1–2 km. Typical reliefs (top of berms to bottom of trough) are 1–3 m for narrow plough marks and 2–7 m for wider plough marks, but up to 12 m of relief has been recorded for the latter.

No clear-cut age relations can be inferred from the existing data. However, some distinct marks in the western and southwestern parts of the survey area look markedly fresher than the others (Fig. 7), with disturbed sediment more than 50 m from the plough mark itself. The disturbance appears to be sediment blocks formed by the ploughing process (e.g., Lien 1983) and also by small-scale slumping from the ploughed up berms.

The plough marks have a wide range of directions (Fig. 6) but with a strong component subnormal to the local topographic contours. However, the present data appear to be somewhat biased towards directions normal to the ship's tracks, and a more extensive side-scan survey would be needed to map significant changes in plough-mark directions, i.e., with changing water depth. This could give valuable information for reconstruction of paleocurrents.

In the southeastern part of the bank, there is a distinct increase in the frequency of iceberg plough marks between 210 and 220 m water depth, from only occasional plough marks in the deeper areas to a completely gouged seafloor above this depth (Fig. 8). There is also a relatively thick layer of transparent sediment, and the plough marks are up to 7–12 m deep. As this layer thins out, the depth of ploughing clearly decreases, reflecting the change in sediment character and thickness in coming from the flanks onto the bank. Over the entire study area, there is a clear-cut positive correlation between sediment thickness and depth of gouging (Fig. 3), and where seismic penetration is poor, depth of gouging gives a minimum value of sediment thickness.

An extremely flat base to the smaller undulations on the sea floor is a striking feature in the eastern part of the survey area

(Fig. 9). The small-scale undulations are ploughed up ridges, but immediately below them there is an almost level surface, opaque to the 3.5 kHz signal.

Origin of the locally thicker sediment accumulations

No samples exist from the main accumulations, but the 3.5 kHz data show no distinct difference in acoustic character over the survey area. We therefore infer that the accumulations consist of sandy mud or muddy sand similar to that cored at stations 83-23, 83-24, and 83-25 (Fig. 5). The fact that the 3.5 kHz echo sounder penetrated more than 25 m of sediment also indicates relatively soft, fine-grained material as opposed to compacted till (Elverhøi *et al.* 1983). At station 83-23, the 3.5 kHz signal did not penetrate the 4–5 m of overcompacted material, interpreted as till below the glaciomarine section. Furthermore, the acoustic character of the Storbanken sediments is not significantly different from that of Bjørnøyrenna (Fig. 1) to the southwest, except for the transparent section being somewhat thicker and more consistent in the deeper waters. Analyses of cores previously obtained from Bjørnøyrenna (Forsberg 1983) show glaciomarine sediments, although with a higher content of clay and silt than the material in the Storbanken cores.

Thick glaciomarine sediment accumulations may be related to depositional patterns, or they may be erosional remnants. Given the apparent lack of sediment compaction, as inferred from the acoustic character, erosion by a grounded ice sheet, the most likely mode of erosion, does not seem probable. This, combined with its location at the edge of a bank and with thickness decreasing both towards deeper water and towards the central bank area, supports the idea of the accumulations being primary glaciomarine depositional features.

The acoustically homogeneous character of the locally thicker accumulations indicates rapid, continuous sedimentation. Furthermore, relatively sandy material, acoustically extrapolated from the cores, points toward deposition in the proximity of the source, which for this style of glaciomarine sedimentation most likely would be a grounded ice front, with sediment output from meltwater (Powell 1984).

Most calculations of sedimentation rates in tidewater glacier proximal conditions are from fjords, often draining valley

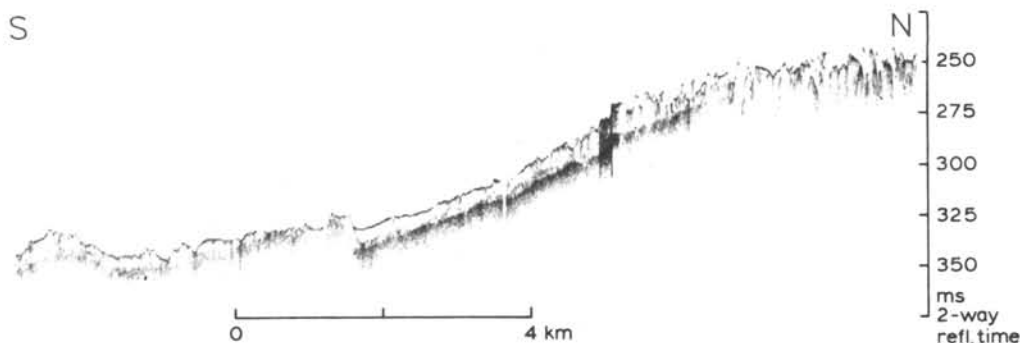


FIG. 8. A 3.5 kHz profile over the flank of Storbanken, southeastern part of the survey area. Note increased gouging of the sea floor above 275–290 ms (approximately 210–220 m). For location, see Fig. 2.

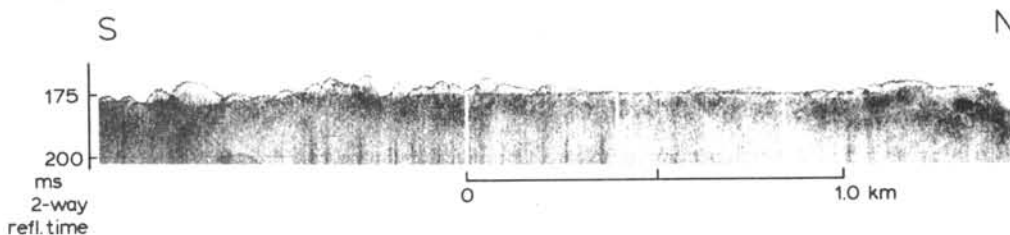


FIG. 9. A 3.5 kHz profile showing flat base of iceberg plough marks. For location, see Fig. 2.

glaciers. Rates are generally high but show large variations. Elverhøi *et al.* (1983) reported recent rates of 5–100 cm/a within 10 km of the Kongsvegen glacier, Spitsbergen, whereas rates from Glacier Bay, Alaska, may vary from 0.2 to 4–8 m/a (Carlson *et al.* 1978; Powell 1980). Although an ice sheet will discharge less sediment than a valley glacier (Powell 1984), the bedrock of the northern Barents Sea is comparable to the unmetamorphic, fine-grained clastic rocks of the Kongsvegen drainage area, and the sedimentation rates off the Kongsvegen glacier may at least be used to obtain a minimum estimate of duration of deposition.

From the above considerations, we propose that the acoustically transparent, locally thicker sediment accumulations on Storbanken were deposited in the proximity of a grounded ice front that was stationary for as much as a few hundred years during its retreat phase. However, higher deposition during a shorter time interval cannot be excluded. Off present-day meltwater outlets at the Austfonna ice cap on Nordaustlandet, Svalbard (Fig. 1), local accumulations up to 30 m thick have been deposited in less than 50 years, but these have an areal extent of less than 1 km (Pfirman 1984). A situation with Storbanken being the maximum extent of the late Weichselian ice sheet, on the other hand, seems unlikely given the relatively sparse total amount of sediments deposited in the region.

Major glacier surges of large ice sheets (Budd and McInnes 1979) have been proposed as a mechanism for enhanced decay, in particular for marine ice sheets that are sensitive to sea-level variations (Denton and Hughes 1981; Stuiver *et al.* 1981). Although the surge mechanisms and timing may be different, the surging of large, marine-based ice sheets should have similar effects on the substratum as surges in smaller present-day glaciers. The best modern analog is probably the one described from Austfonna ice cap, Nordaustlandet, Svalbard, where the outer part of the glacier is marine based and has surged over till-covered seafloor. The surging left a distinct sea-floor morphological pattern, consisting of a continu-

ous end-moraine ridge modified by frequent slumping and of a characteristic system of linear ridges inside the end moraine (Solheim and Pfirman 1985; Solheim 1986). However, there are no sea-floor indications of surges on Storbanken, and we take this as an indication of withdrawal without surging. The low relief and slopes of the accumulations also exclude ice push during climatically controlled glacier advance as a formation mechanism (Lewis *et al.* 1977; Boulton 1986).

Vorren *et al.* (1983) introduced the term "iceberg turbate" for diamictons that were completely reworked by iceberg ploughing. This process results in a depletion of fines that are resuspended. Considering the intense ploughing documented from Storbanken, it is likely that this process also had an effect on the final sediment composition found in the survey area today. However, as the relatively coarse material has been cored below the floor of an iceberg plough mark (station 83-23/2), the iceberg reworking process is most likely not the main reason for the sandy texture of the Storbanken sediments.

Iceberg scouring and deglaciation

The fact that iceberg plough marks are frequent at least down to a water depth of 210 m suggests that most are relict features, as few icebergs presently being calved off from Svalbard glaciers would have drafts significantly deeper than 100 m (Elverhøi and Solheim 1983b). Occasional present-day icebergs may, however, reach deeper, probably because of draft increase through rolling (e.g., Bass and Peters 1984; Lewis and Bennett 1984). Recent work from the Labrador shelf shows high rates of degradation of scours by benthos, current, and wave action (Josenhans *et al.* 1985). Apparently fresh, blocky berms (Fig. 7) will therefore most likely be degraded at a rate dependent on local bathymetric and oceanographic conditions and sediment characteristics, finally reaching the more typical mature form where no distinct sediment disturbance can be seen from side-scan records. Some of the more fresh-

looking plough marks, confined to the shallowest parts of the study area (Fig. 7), thus may have been formed quite recently.

If we assume that most of the icebergs had a local origin, some inferences about paleo-water depth and isostatic depression can be made based on the distinct change in plough-mark frequency at 210–220 m water depth. Tabular icebergs, broken off from the ice front when water depths get too deep for grounding, or from a fringing ice shelf, generally define the largest icebergs of a marine-based ice sheet. Typical drafts of most present-day tabular icebergs, both in the Arctic and in the Antarctic, are 200–250 m (Orheim 1987), although larger drafts do occur. The maximum height of a subaerial ice cliff is limited to approximately 30 m by the plastic properties of ice (Paterson 1981), although larger thicknesses can be reached where the ice is stabilized in narrow embayments.

With the glacier front situated at Storbanken during the late Weichselian maximum and with a eustatic sea-level lowering of the order of 100–120 m (Bloom *et al.* 1974; Bowen 1978), an isostatic depression of up to 130 m would be required to allow icebergs with 200–250 m drafts to float in the area of 220 m present-day water depth. Isostatic depression of this size at the margin of an ice sheet, however, seems improbable based on other past ice margins in Scandinavia and North America (Andrews 1980; Mørner 1980; Bakkelid 1981). This therefore gives further support to a Barents Sea ice sheet extending beyond Storbanken.

As marine ice sheets are likely to disintegrate relatively rapidly (Thomas 1979), eustatic and isostatic adjustments were probably rather small in the study area during the time interval between a maximum glacial extent and that of a Storbanken margin. Therefore, a maximum isostatic depression of significantly more than 130 m is unlikely for the Storbanken region. This is comparable with Salvigsen's (1981) results from Kong Karls Land and points toward a relatively thin ice sheet fed from several ice divides, of which Storbanken and Kong Karls Land were two.

The depth of ice gouging is generally limited by the thickness of glaciomarine sediments. The remarkably flat base of the ice-plough relief, especially in the eastern part of the area (Fig. 9), is suggested to be the top of the overcompacted material that was cored at station 83-23/2 (Fig. 5). The sparker has too poor resolution and the 3.5 kHz echo sounder too poor penetration to show a distinction between the overcompacted sandy sediment and underlying bedrock. However, the dipping sedimentary bedrock layers are unlikely to have a completely flat erosional surface; therefore, the flat surface probably represents till infill in local troughs in the bedrock surface and forms the local base of iceberg ploughing in the area.

Summary and conclusions

(1) Locally thicker (30–38 m), unlithified sediment accumulations on Storbanken consist of sandy glaciomarine material, deposited relatively rapidly, proximal to a recessional glacier margin.

(2) Other than these local accumulations, Storbanken has a generally thin (≈ 1.5 m) layer of sandy glaciomarine sediment overlying an overconsolidated till. The latter fills troughs in the erosional sedimentary bedrock surface and forms a flat base for iceberg plough marks. Deeper waters of northern Bjørnøya have a thicker (≈ 5 m) layer of finer grained mud.

(3) The sea floor is intensively ploughed by icebergs above

210 m water depth. Plough-mark size varies considerably, but relief is largely dependent on the thickness of glaciomarine sediments as well as on iceberg size. The ploughing, most of which probably took place shortly after deglaciation of the region, resuspended fines and further enhanced the sandy character of the glaciomarine sediments.

The sediment distribution and plough-mark characteristics have the following implications for the glacial history of the Barents Sea: (i) During the late Weichselian maximum, the Barents Sea ice sheet had an extension beyond Storbanken. The ice sheet was presumably relatively thin and fed from several ice divides. However, the present data give no information in terms of a possible connection with the Fennoscandian ice sheet. (ii) A major halt in ice retreat occurred when the margin was situated at Storbanken, during which the locally thicker accumulations were deposited from meltwater. The halt most likely did not include any readvances, either as surges or as climatically controlled oscillations. (iii) Further retreat took place relatively rapidly, leaving only the thin cover of glaciomarine sediments.

Acknowledgments

Data acquisition was partly funded by the Norwegian Petroleum Directorate. We thank Captain Terje Langvik and his crew on board the R/V *Lance* for their valuable cooperation in the field. Tore Vorren, Jorge Butenko, Allister Skinner, and Martyn Stoker all provided valuable comments on the manuscript. JDM's support came from funding by the Office of Naval Research, contract N00014-74C-0269.

- ANDREWS, J. T. 1980. Progress in relative sea level and ice sheet reconstructions, Baffin Island, N.W.T., for the last 125,000 years. *In Earth rheology, isostasy and eustasy*. Edited by N. A. Mørner. John Wiley & Sons, New York, NY, pp. 175–200.
- ASTM. 1983. Standard test method for pulse velocity through concrete. American Society for Testing and Materials, Designation C597-83, pp. 376–379.
- BAKKELID, S. 1981. Et foreløpig totalbilde av landhevingen i Norge. Geographical Survey of Norway, Report.
- BASS, D. W., and PETERS, G. R. 1984. Computer simulation of iceberg instability. *Cold Regions Science and Technology*, **9**: 163–169.
- BLOOM, A. L., BROECKER, W. S., CHAPPELL, J. S., MATTHEWS, R. K., and MESOLELLA, K. J. 1974. Quaternary sea-level fluctuations on a tectonic coast: new $\text{Th}^{230}/\text{U}^{234}$ dates from the Huon Peninsula, New Guinea. *Quaternary Research*, **1**: 247–260.
- BOULTON, G. S. 1986. Push-moraines and glacier-contact fans in marine and terrestrial environments. *Sedimentology*, **33**: 677–698.
- BOWEN, D. Q. 1978. Quaternary geology: a stratigraphic framework for multidisciplinary work. Pergamon Press, New York, NY.
- BUDD, W. F., and MCINNES, B. J. 1979. Periodic surging of the Antarctic ice sheet—an assessment by modelling. *Hydrographic Science Bulletin*, **24**: 95–104.
- CARLSON, P. R., WHEELER, M. C., MOLNIA, B. F., and ATWOOD, T. J. 1978. Neoglacial sedimentation in Glacier Bay, Alaska. United States Geological Survey, Circular 804.B, pp. B114–B116.
- DAMUTH, J. E. 1978. Echo character of the Norwegian–Greenland Sea: relationship to Quaternary sedimentation. *Marine Geology*, **28**: 1–36.
- DENTON, G. H., and HUGHES, T. J. 1981. The arctic ice sheet: an outrageous hypothesis. *In The last great ice sheets*. Edited by G. H. Denton and T. J. Hughes. John Wiley & Sons, New York, NY, pp. 440–468.
- ELVERHØI, A., and BOMSTAD, K. 1980. Late Weichselian glacial and

- glaciomarine sedimentation in the western, central Barents Sea. Norsk Polarinstitutt, report.
- ELVERHØI, A., and SOLHEIM, A. 1983a. The Barents Sea ice sheet—a sedimentological discussion. *Polar Research, New Series*, 1: 23–42.
- 1983b. The physical environment, western Barents Sea. Surface sediment distribution. Norsk Polarinstitutt, Skrifter 179 A, Sheet A, scale 1 : 1 500 000.
- ELVERHØI, A., LØNNE, Ø., and SELAND, R. 1983. Glaciomarine sedimentation in a modern fjord environment, Spitsbergen. *Polar Research, New Series*, 1: 127–149.
- FORMAN, S. L., MANN, D. H., and MILLER, G. H. 1987. Late Weichselian and Holocene relative sea-level history of Brøggerhalvøya, Spitsbergen. *Quaternary Research*, 27: 41–50.
- FORSBERG, C. F. 1983. Sedimentation and early diagenesis of late Quaternary deposits in the central Barents Sea. Cand. real. thesis, University of Oslo, Oslo, Norway.
- JONSSON, S. 1983. On the geomorphology and past glaciation of Storøya, Svalbard. *Geografiska annaler*, 65A: 1–17.
- JOSEPHANS, H. W., BARRIE, J. V., WOODWORTH-LYNAS, C. M. T., and PARROTT, D. R. 1985. DIGS-85: Dynamics of iceberg grounding and scouring: observation of iceberg scour by manned submersible. 14th Arctic Workshop: Arctic Land–Sea Interaction, Bedford Institute of Oceanography, Dartmouth, N.S., 6–8 Nov. 1985, Abstract Volume, p. 92.
- KRISTOFFERSEN, Y., MILLIMAN, J. D., and ELLIS, J. P. 1984. Unconsolidated sediments and shallow structure of the northern Barents Sea. Norsk Polarinstitutt, Skrifter 180, pp. 25–39.
- LEWIS, C. F. M., BLASCO, S. M., BORNHOLD, B. D., HUNTER, J. A. M., JUDGE, A. S., KERR, J. W., MCLAREN, P., and PELLETIER, B. R. 1977. Marine geological and geophysical activities in Lancaster Sound and adjacent fjords. In Report of activities, part A. Geological Survey of Canada, Paper 77-1A, pp. 495–506.
- LEWIS, J. C., and BENNETT, G. 1984. Monte Carlo calculations of iceberg draft changes caused by roll. *Cold Regions Science and Technology*, 10: 1–10.
- LIEN, R. 1983. Ployemerker etter isfjell på norsk kontinentalsokkel. Continental Shelf Institute, Norway, Publication 109.
- MØRNER, N. A. 1980. The Fennoscandian uplift: geological data and their geodynamical implication. In *Earth rheology, isostasy and eustasy*. Edited by N. A. Mørner. John Wiley & Sons, New York, NY, pp. 251–283.
- MOUM, J. 1966. Falling drop used for grain-size analysis of fine-grained materials. Norwegian Geotechnical Institute, Publication 70.
- ORHEIM, O. 1987. Icebergs in the southern ocean. *Annals of Glaciology*, 9: 241–242.
- PATERSON, W. S. B. 1981. *The physics of glaciers*. 2nd ed. Pergamon Press, Oxford, UK.
- PFIRMAN, S. L. 1984. Modern sedimentation in the northern Barents Sea: input, dispersal and deposition of suspended sediments from glacial meltwater. Ph.D. thesis, Woods Hole Oceanographic Institution, Woods Hole, MA.
- POWELL, R. D. 1980. Holocene glaciomarine sediment deposition by tidewater glaciers in Glacier Bay, Alaska. Ph.D. thesis, Ohio State University, Columbus, OH.
- 1984. Glaciomarine processes and inductive lithofacies modelling of ice shelf and tidewater glacier sediments based on Quaternary examples. *Marine Geology*, 57: 1–52.
- SALVIGSEN, O. 1981. Radiocarbon dated raised beaches in Kong Karls Land, Svalbard, and their consequences for the glacial history of the Barents Sea area. *Geografiska annaler*, 63A: 283–291.
- SALVIGSEN, O., and NYDAL, R. 1981. The Weichselian glaciation in Svalbard before 15,000 BP. *Boreas*, 10: 433–446.
- SOLHEIM, A. 1986. Sea floor evidence for glacier surges. *Polar Research, New Series*, 4: 91–95.
- SOLHEIM, A., and KRISTOFFERSEN, Y. 1984. The physical environment, western Barents Sea. Sediments above the upper regional unconformity: thickness, seismic stratigraphy and outline of the glacial history. Norsk Polarinstitutt, Skrifter 179 B, Sheet B, scale 1 : 1 500 000.
- SOLHEIM, A., and PFIRMAN, S. L. 1985. Sea-floor morphology outside a grounded, surging glacier, Bråsvellbreen, Svalbard. *Marine Geology*, 65: 127–143.
- STUIVER, M., DENTON, G. H., HUGHES, T. J., and FASTOOK, J. L. 1981. History of the marine ice sheet in west Antarctica during the last glaciation: a working hypothesis. In *The last great ice sheets*. Edited by G. H. Denton and T. J. Hughes. John Wiley & Sons, New York, NY, pp. 319–439.
- THOMAS, R. H. 1979. The dynamics of marine ice sheets. *Journal of Glaciology*, 24: 167–177.
- VORREN, T. O., and KRISTOFFERSEN, Y. 1986. Late Quaternary glaciation in the south-western Barents Sea. *Boreas*, 15: 51–59.
- VORREN, T. O., HALD, M., EDVARDSEN, M., and LIND-HANSEN, O.-W. 1983. Glacigenic sediments and sedimentary environments on continental shelves: general principles with a case study from the Norwegian shelf. In *Glacial deposits in north-west Europe*. Edited by A. A. Balkema, Rotterdam, The Netherlands, pp. 61–73.
- WENSAAS, L. 1986. En sedimentologisk og mineralogisk undersøkelse av bunnsedimenter (<63 µm) fra det nordlige Barentshavet. Cand. scient. thesis, University of Oslo, Oslo, Norway.

PAPER 7.

In press, Marine Geology.

GLACIOMARINE SEDIMENTATION ON EPICONTINENTAL SEAS -
EXEMPLIFIED BY THE NORTHERN BARENTS SEA

Anders Elverhøi*
Stephanie L. Pfirmant+
Anders Solheim*
Bengt B. Larssen*

* Norwegian Polar Research Institute,
Box 158, 1330 Oslo Lufthavn
Norway

+ GEOMAR Research Center for Marine Geosciences
Wischhofstr. 1-3, Bldg. 4
2300 Kiel,
F.R. Germany

ABSTRACT

Sediments on high Arctic shelves result from modern processes and the effect of former glaciations. Based on data from the northern Barents Sea, an area with input from numerous and large surging glaciers, we define two principal zones with different environmental regimes and corresponding sedimentary facies: i) a glacier proximal zone influenced by grounding line processes and the immediately adjacent areas affected by glacial sediment input, and ii) a glacier distal, sea ice and current-controlled zone, which also include a wide sediment-starved region dominated by biogenic carbonate accumulation.

Characteristic for the glacier proximal zone is glacial surges, which effects sedimentation rates and leave a diagnostic pattern of sea floor morphologies. Extensive ice gouging cause a homogeneous sediment texture.

In the glacier distal zone fine grained mud is supplied from sea ice and infrequent coarser material deposited from icebergs is reworked by modern oceanographic processes. On shallow banks, 30-50 m water depth, carbonates accumulate from a prolific bottom fauna formed in response to extensive reworking and nutrient supply.

INTRODUCTION

Glaciation of continental shelves and epicontinental seas are well documented in the geological record (Boulton and Deynoux, 1981; Eyles et al., 1985). During periods of maximum glaciation, grounded ice and/or ice shelf regimes prevailed (e.g. Denton and Hughes, 1981), while sea ice and iceberg dominated regimes characterize the ice recessional stage (Vorren et al., 1983). Until now, studies of modern environments have focused on ice shelf and glaciomarine fjord sedimentation (Drewry and Cooper, 1981; Powell, 1983; Elverhøi et al., 1983; Mackiewicz et al., 1984; Anderson et al., 1984), while studies of ancient sequences are the main base for models of glaciomarine sedimentation of epicontinental seas (Gravenor et al., 1984; Eyles et al 1985).

The Barents Sea, covering an area of 1.2 mill km², is the largest present day epicontinental sea (Fig.1). The shelf is relatively deep (average water depth ~ 230 m) and approximately 2/3 of the area is influenced by sea ice and icebergs. The southern ice limit essentially follows the oceanic Polar Front, i.e. the boundary between the Arctic Water masses and the Atlantic Water masses at approximately 74-75°N. Ice influence increases to the north, where sea ice is present 10 months of the year and icebergs are delivered from the heavily glaciated hinterlands of Svalbard and Franz Josef Land.

The study area covers the northwestern Barents Sea, bounded by approximately 74° N to the south and 35° E to the east. A range of glaciomarine environments are present: glacier proximal conditions prevail along the tidewater glacier peripheries, e.g.

the Austfonna ice cap on Nordaustlandet. (The term glacier proximal here refers to areas affected by grounding line processes). The distal glaciomarine environment comprising the rest of the study area, varies between erosion/nondeposition/redistribution and sea ice-and iceberg-dominated deposition. Biogeneous carbonates accumulate locally on shallow banks in close association with the glacial sediments.

The main objective of this paper is to analyze the present glaciomarine sedimentary environment and the resulting facies in a modern high Arctic epicontinental sea. As accumulation rates in general are low, 2-5 cm/ka, interpretations of surface sediment samples (approximately the upper 5 cm) may include the latest Holocene. According to previous investigations in the western part of the study area, sedimentation is characterized by intrabasinal reworking (Bjørlykke et al., 1978). However, ice rafting becomes increasingly important in the northern regions of the Barents Sea. In this paper, emphasis will be placed on identification on the various sediment sources and analysis of their relative contribution to total flux.

GEOLOGICAL AND GEOPHYSICAL DATA BASE

The study area has been covered by approximately 30,000 km shallow seismic records in a regional grid of ca 20 km line spacing (Elverhøi and Solheim, 1987 a). The principal sound source has been 1 kJ sparker with analog recording via single channel receiver. Higher resolution data have been obtained by 3.5 kHz echosoundings, and in some local areas (south of Nordaustlandet, Storbanken, south of Hopen and in a small area of Bjørnøyrenna) side-scan sonar profiling has been conducted

(Elverhøi and Solheim, 1983a; Solheim and Kristoffersen, 1984; Solheim et al., in press).

Sediment samples (from 400 locations) mainly were obtained by dredges and grabs in shallow, hard bottom areas, while 3 m gravity cores were recovered in deeper areas with soft sediments. Vibrocores and shallow rock cores were used at a few stations (Elverhøi and Solheim, 1983a). Bottom photographs are available from about 100 stations (Elverhøi and Solheim, 1983a; Elverhøi and Solheim, 1983b; Elverhøi and Solheim 1987a).

Water samples were obtained using 5 l Niskin bottles and filtered on board (Forsberg, 1983; Pfirman, 1985) and suspended sediment distribution was mapped in combination with 160 transmissometer (1 m path length) and nephelometer (90° scattering) profiles using a Montedero-Whitney sensor (Pfirman, 1985).

SEDIMENT DISTRIBUTION

General characteristics

In the study area, the thickness of unlithified sediments above the bedrock, seen as a regional unconformity (Solheim and Kristoffersen, 1984), is in general less than 10 metres (Fig. 2). The unlithified sediments consist of till overlain by blue grey ice proximal glaciomarine sediments, deposited during the withdrawal of the Late Weichselian Ice sheet (Elverhøi and Solheim, 1983c). These sediments grade into more fine grained, olive grey, ice distal sediments of mainly Holocene age. The transition between the two latter units is tentatively dated to 10 - 12 ka BP (Elverhøi and Solheim, 1983c; Elverhøi and Solheim, 1987b), reflecting the onset of the present day glaciomarine sedimentary environment.

Surface sediments

Three main sediment types are found in the northern Barents Sea: i) mud (Fig. 3; class ,1 & 2), ii) pebbly mud or diamicton (Fig. 3; class 3,6 & 7) and iii) sand and gravel (Fig. 3; class 8,9,10 & 11). The 200 m contour defines an important environmental boundary with diamicton generally dominating above 200 m and mud being the predominant sediment type below. However, diamicton and sand-and gravel-rich sediments are also found on the southern slope of Spitsbergenbanken down to 300 m water depth, while mud is present in the shallow coastal region outside Edgeøya/Barentsøya.

The largest accumulation of sand and gravel are lag deposits, which occur on Spitsbergenbanken, and on the shallower part (30 - 60 m water depth), carbonates are the main constituents (up to 90 % CaCO_3). Present day hard bottom conditions are evidenced by the high barnacle content. ^{14}C -dating of the *Mya truncata*, which is characteristic of a soft substratum but was obtained from the bank, show that hard bottom conditions have prevailed since early/mid Holocene (Bjørlykke et al., 1978). The change of substratum is probably a response to change in the regional current pattern and shallowing due to the glacio-isostatic rebound (Bjørlykke et al., 1978; Forsberg, 1983). In deeper water (60 - 200 m) along the bank margins, coarse grained clastics prevail. Clastic lag deposits are also found on the shallow platforms surrounding Kvitøya and Kong Karls Land.

In the southern part of the Barents Sea, fine grained clastic sediments generally have an olive grey (5Y 3/2) (Munsell Soil Colour Charts) due to organic debris. To the north, the colour becomes more grey and blue grey. The fine grained sediments are generally homogeneous, and often inten-

sively bioturbated by polychaetes (Elverhøi and Bomstad, 1980). Monosulphides are observed at 15 -20 cm sediment depth, causing a mottled appearance.

Current-related sediment structures have only been observed in bottom photographs or side-scan sonar profiles in three regions in the Barents Sea: on Spitsbergenbanken where ripple marks are observed in carbonate sand; on the southern flank of the Kvitøya platform where sediment waves (5 m scale) are seen on a side-scan profile at 280 m water depth; and in Erik Eriksenstretet where patches of sediment waves occur. In addition, plough marks along the southeastern flank of Spitsbergenbanken appear to be winnowed. Features related to mass wasting are generally not observed except for limited occurrence in glacier proximal environment.

Surface sediment texture

The diamictons have a median diameter in the medium/coarse silt fraction (Figs.4 a,b,c & d), while the mud deposits have a median diameter in the clay fraction. Clay content of the diamictons seems to be depth independent, while it increases with depth in the mud deposits (Wensaas, 1986).

In the glacier proximal regions diamicton is the dominant sediment type. The content of coarser fractions is generally higher than in the diamicton sampled from the distal areas. Coarse grained diamicton of possibly Late Weichselian age is also found on the southern slope of Spitsbergenbanken down to 300 m water depth. These sediments are probably exposed due to erosion and non-deposition during the Holocene (Bjørlykke et al., 1978; Forsberg, 1983).

Mineralogy

The mineral assemblage in the surface sediments is identified from X-ray diffractograms of both the clay fraction (clay minerals only) and the bulk < 63 µm fraction (non-clay minerals). Typical clay minerals are: illite, chlorite, kaolinite, smectite and random mixed-layer smectite - illite (the latter is not included in the semi-quantitative calculations in Fig. 4). A similar assemblage is characteristic for most of the Mesozoic and Tertiary rocks on Svalbard and also for clasts in the Quaternary sediments in the Barents Sea (Bjørke and Dypvik, 1977; Elverhøi and Grønlie, 1981; Elverhøi et al., 1988). However, smectite on Svalbard is restricted to the eastern part of the archipelago and stratigraphically bounded within the Helvetiafjellet Formation (thickness 60 - 70 m, Early Cretaceous) (Edwards, 1980; Elverhøi et al., in 1988).

The mineralogy of the bulk (< 63 µm) fraction shows regional changes, with strong variations in calcite and dolomite (Fig. 4). Carbonate-rich sediments occur mainly in the northernmost regions where calcareous rocks of Carboniferous-Permian age are exposed onshore and are thought to subcrop extensively offshore (Lauritzen and Otha, 1985; Elverhøi et al., 1988). Relatively high dolomite content is also found east of Edgeøya (Fig. 4). However, in this area calcareous rocks are not present below or in adjacent areas (Winsnes and Worsley, 1981; Elverhøi et al., 1988). These carbonate-rich sediments may have been transported to this region from a northern source. In the rest of the northern part of the study area, carbonates occur in trace amounts in the clastic sediments. As the content of foraminifera and other calcareous fossils is low and essentially

confined to the sand fraction, carbonates in the mud fraction most likely have a non-biogenic origin (Wensaas, 1986). An exception is in the region adjacent to Spitsbergenbanken, where fine grained calcite of biogenic origin is deposited from winnowing of the carbonate lag deposit (Bjørlykke et al., 1978).

Sedimentation rate and sediment thickness

From ^{14}C dates (Elverhøi and Solheim, 1987b) and use of the lithological change at 10 - 12 ka BP (extrapolated age, Fig. 2), the average Holocene sedimentation rate in glacier distal areas may be estimated at 3 - 5 cm/ka (Fig. 4). The accumulation rate of carbonates on Spitsbergenbanken is also within the same range (Elverhøi and Solheim, 1983 a/c; Elverhøi and Solheim 1987a). Higher values, 10 - 20 cm/ka, are found outside Nordaustlandet, Barentsøya/Edgeøya and also in deeper regions south of Kong Karls Land.

In the glacier proximal environment of Austfonna on Nordaustlandet, sedimentation rate is highly variable, 0 - 10 cm/year (Solheim, in prep). Locally within this environment, sediment ridges thought to have formed during surge, constitute important sediment accumulations. Outside Austfonna a ridge of 10 - 20 m height and 500 to 1700 m width, ($\sim 0.35 \text{ km}^2$) was most likely deposited during one surge, lasting 1 - 2 years (Solheim and Pfirman, 1985).

BATHYMETRY AND MORPHOLOGY

Due to the thin unlithified sediment cover, the sea floor topography generally follows the underlying bedrock surface, which reflects the main tectonic lineaments and bedrock boundaries (Rønnevik et al., 1982; Solheim and Kristoffersen, 1984; Faleide et al., 1984, Elverhøi et al. 1988). Tertiary uplift and subaerial erosion, followed by Pliocene/Pleistocene glaciations further modified the bedrock surface (Nansen, 1904; Elverhøi and Solheim, 1983c).

Large scale topography of the Barents Sea Shelf is characterized by broad, gentle depressions extending from the interior to the western and northern continental margins (Fig. 1). Bjørnøyrenna, between Spitsbergenbanken and northern Norway is the major deep water connection between the Barents Sea and the Norwegian-Greenland Sea to the west. This trough shoals to the north and east. The major deep water connections to the Arctic Ocean are the strait between Franz Josef Land and Victoria Island where the depth exceeds 300 m and between Franz Josef Land and Novaja Zemlja through the Kara Sea. In addition to the shallow regions around the islands of Kong Karls Land and Kvitøya, the main bank areas are, Spitsbergenbanken (30-100 m), Storbanken (100-150 m) and Sentralbanken (150-200 m).

Accumulations of Late Pleistocene till and glacier proximal glaciomarine sediments may locally form positive bathymetric features (25 - 75 m high and 2 - 20 km long), as observed around Spitsbergenbanken and on Storbanken (Elverhøi and Solheim, 1983c; Solheim and Kristoffersen, 1984; Solheim et al., in press). Late Weichselian glaciomarine sediment accumulated in troughs levels out bedrock topography forming smooth basin floors (Kristoffersen et al., 1984).

Small scale topography of the sediment surface in shallow water depths is dominated by iceberg plough marks although pockmarks may also be abundant observed (Solheim and Elverhøi, 1985). Recent ploughing occurs down to water depths of 120 -130 m south of Nordaustlandet (Solheim, in prep), while ancient gouges have been recorded down to more than 400 m water depth in Bjørnøyrenna (Elverhøi and Solheim, 1987). In some areas, 100 % of the sea floor is affected by iceberg ploughing. Typical relief is 2-5 m, but may reach 12 m, and plough mark widths are in general 30 - 80 m (Solheim et al., in press). The ancient plough marks are usually wider, 30 - 100 m, and have a more degraded appearance. The Barents Sea pockmarks are smaller than similar features recorded along the Norwegian shelf (Hovland, 1983), only 10 - 20 m in diameter and < 1 m deep, but may be locally abundant (Solheim and Elverhøi, 1985). They are most likely formed by gas ascending from a deep petrogenic source. The comparatively small size may be a function of the thin cover of soft sediments, which is needed as a recording medium.

GLACIER REGIME AND PROXIMAL PROCESSES

Glacier coverage of the Svalbard Archipelago is approximately 60 %, composed of mountain/valley glaciers on the main island of West Spitsbergen and ice caps on the islands of Nordaustlandet and Kvitøya. The ice cover increases with descending equilibrium line to the north and the east; 75 % of Nordaustlandet and 99 % of Kvitøya are ice covered (Dowdeswell, 1984). Small (< 100 km²) glaciers are below pressure melting point at their sole, while larger Svalbard glaciers are often at the pressure melting point at the base in their interior regions. Extensive meltwater activity typically occurs in the summer

(July - August). Surge is a common mode of glacier advance on Svalbard (Liestøl, 1969): more than 80 glacier surges have been documented to date (Liestøl, 1985).

Of particular importance for this study is the Austfonna ice cap (8000 km²) which covers most of the island of Nordaustlandet (Fig. 1), although similar conditions are likely to be found for other glaciers along the eastern coast of Svalbard. Austfonna has a marine grounded terminus extending for approximately 200 km (Solheim, in prep.). Several separate drainage basins of Austfonna ice cap have surged, and the 1936-38 surge of Bråsvellbreen (1100 km²) is the largest surge documented on the northern hemisphere. Simple calculations indicate that almost 80 km³ of ice were transported into the new part of the glacier in 1 - 2 years.

The Bråsvellbreen surge, and a former surge of an adjacent drainage basin, have had a large influence on sea floor topography and sediment distribution in this region. In addition to the terminal surge moraine (Fig. 5), soft subglacial material was mobilized and squeezed up into subglacial features when the surge stagnated and the glacier settled into its bed. The surge moraine is suggested to have been formed by a combination of increased meltwater discharge during the surge and direct push by the rapidly advancing ice front (Solheim and Pfirman, 1985; Solheim, in prep). After withdrawal, a rhombohedral pattern of discontinuous, linear ridges were exposed on the sea floor (Fig. 5), most likely deposited within subglacial fractures. During the last 20 - 30 years, the glacier has retained normal activity and is presently forming annual push ridges which are exposed during yearly retreat.

Another important effect of glacier surge in the marine environment is increased production of icebergs, e.g. during the Brásvellbreen surge the numbers of icebergs were increased by an order of magnitude (Vinje, 1985). The increase in iceberg activity is well documented in the occurrence of many relatively small, fresh looking iceberg plough marks on the sea floor in the front of the surge moraine. Hence, surges may also indirectly be important for reworking sediment into an iceberg turbate character (Vorren et al., 1983).

At present, two large and numerous small turbid, sediment laden meltwater outflows are observed along the Austfonna marine ice front (Fig. 6). Evidence of rapid accumulation at or in the vicinity of the meltwater - sea water interface is seen from several large sediment mounds and an acoustically transparent drape in front of the western meltwater outflow (observed on side-scan sonar and 3.5 kHz profiles).

Limited observations of suspended particulate material in this region show that concentrations decrease rapidly from up to 28 mg/l to less than 5 mg/l within about 5 km from the meltwater discharge points (Fig. 7). In satellite images, turbid meltwater plumes emanating from the glacier front often appear to be entrained in a westerly coastal current, transporting the sediment-laden meltwater along the glacier front, and sometimes continuing westward into the southern reaches of Hinlopenstretet (Fig. 6). High concentrations of suspended particulate material are observed both in satellite images and in water samples to extend within a glacier proximal zone approximately 15 km from the glacier front (Fig. 7).

OCEANOGRAPHIC PROCESSES

On high latitude shelves, sea ice and associated dense brine formation, in addition to normal marine processes such as tides, waves and currents, may be important factors for controlling sediment redistribution. Evidence that sediment redistribution by oceanic processes occurs on the northern Barents Shelf includes: 1) the existence of lag deposits; 2) the textural discontinuity in surface sediments at approximately 200 m; and 3) side scan sonar profiles and bottom photographs showing sea floor sediments reworked into sediment waves or ripple marks, and winnowing of iceberg plough marks. Near bottom and detached nepheloid layers, indicating sediments in suspension, occur mostly where the bottom sediments are fine-grained and have the highest rates of deposition: within or along the margins of deep basins, and east of Edgeøya (Fig. 4). Due to limited oceanographic measurements in the Barents Sea, mainly obtained in summer, only general statements can be made about on the direction and rate of sediments transport.

Although many factors need to be taken into account when considering how near bottom currents will affect the sea bed, a critical velocity of 30 cm/sec 1 m above the bed may be used as an average for initiation of transport of very fine sand and silt (Butman, 1987). Clays may be resuspended at velocities of 10 to 20 cm/sec (15 cm above the bed) if they are unconsolidated (Postma, 1967). The strongest mean currents in the Barents Sea are expected to be concentrated along slopes of the banks (Nansen, 1906). Based on limited current meter measurements, mean flow of nearbottom currents appears to be generally less than 10 cm/sec in the study region (Loeng, 1983), except in the

vicinity of the high - velocity Hopen - Bjørnøya Current (Fig.8). Superimposed on the mean circulation is a tidal component which has equal or greater velocities (Loeng, 1983). The combined effects of mean and tidal currents may result in high near - bottom velocity, especially along the basin margins. For example, southwest of Sentralbanken, maximum velocities of 25-30 cm/sec were recorded at 270 m water depth (Loeng, 1983). Sea ice shields much of the northern Barents Sea from the effects of surface waves. However, in shallow regions (generally less than 100 m, Butman 1987) not covered by sea ice, long period surface waves may also be important in causing oscillatory near-bottom flows and sediment resuspension. Sediments resuspended by these processes will be transported with the mean circulation (Fig. 9) mostly as contour currents guided by bank slopes, resulting in complicated transport paths. Deposition will occur where velocities are low enough to allow settling of the fine-grained sediment to the sea floor.

The northern Barents Sea is characterized by a relatively stable overall cyclonic circulation pattern (Fig.8) with seasonal variations (Novitskiy, 1961; Tantsiura, 1973; Midttun and Loeng, 1987). The main hydrographic feature of the Barents Sea is the east - west trending oceanic Polar Front at approximately 74-75 N (Fig.8), following bathymetric zonations (Johannesen and Foster, 1978). Arctic water, occurring north of the Front at 20 to 150 m water depth (Midttun and Loeng 1987), originates from a deep convection layer developed during sea ice formation in the Barents Sea, with input from the Arctic Ocean and the Kara Sea. The cold Arctic and surface waters are transported southwestward through the Barents Sea with the east

Spitsbergen and Persey Currents (Fig. 8, Novitskiy, 1961). To the southwest, these currents contribute to the well - defined, southerly flowing Hopen - Bjørnøya Current, localized along the eastern flank of Spitsbergenbanken and may contribute to winnowing of the bank flank. The general southwestward flow of Arctic and surface water, is important in the transport of sea ice (discussed below) and may also explain the accumulation of muddy, carbonate - rich sediments east of Edgeøya. sediments may be carried in suspension from northern carbonate - rich sources by a southerly current of cold Arctic water along the eastern Svalbard margin (Fig. 8). Generally high sedimentation rate in this region may also reflect sediment input from the adjacent tidewater glaciers on the eastern coasts of Barentsøya and Edgeøya.

South of the oceanic Polar Front, the Barents Sea is dominated by warm saline water from the North Atlantic which generally flows northeastward. Part of the Atlantic water which has been cooled, flows under both the sea ice and cold, relatively fresh Arctic water, and occurs as numerous eastward and northward flowing near-bottom branches north of the Front (Fig. 9). Additionally, Atlantic water enters the Barents Sea from the Arctic basin to the north as a subsurface water mass (Mosby, 1938) (Fig. 9). This near - bottom flow may be important either in redistributing sediments, or in preventing deposition. Near-bottom nepheloid layers are particularly pronounced in two areas in Erik Eriksenstretet which are influenced by Atlantic water (Fig. 10): i) east and south of Nordaustlandet and ii) in the strait and basin south and east of Kvitøya. Sea - floor reworking in these areas is also evident

from observed sediment waves (Fig 11). On the southern flank of the bank south of Kvitøya these features are oriented transverse to the bathymetric contours possibly indicating a westerly contour current.

An additional agent for sediment resuspension and transport on high Arctic epicontinental seas may be the formation of dense brines during sea ice formation. This process of vertical convection occurs over the entire water column over shallow banks (Tantsiura, 1959; Midttun, 1985), and down to at least 150-200 m water depth over deeper regions (Nansen, 1906; Novitskiy, 1961; Tantsiura, 1973), forming the densest water mass in the Barents Sea (Nansen, 1906; Midttun, 1985). The dense water mass has a limited distribution, is observed only in deep basins in the summer, and has large seasonal and annual variations (Nansen, 1906; Midttun pers. comm., 1987). Because dense brines will flow off the banks transverse to bathymetric contours, they may be important agents in transporting resuspended sediment from the banks into deeper basins.

SEA ICE AND ICEBERGS, THEIR EFFECTS ON SEDIMENT FLUX

Ice rafting has commonly been related to icebergs and generally only debris larger than 500 μm has been included. Sea ice is now recognized as an important carrier of mainly fine grained materials (Barnes and Reimnitz, 1982; Barnes et al., 1982), and in the Arctic Basin muddy units are related to sea ice dominated events (Clark et al., 1980; Clark and Hanson, 1983).

In the Barents Sea most of the ice cover is formed locally (Zacharov 1976). Due to the dominance of southwesterly winds,

ice is exported to the Arctic Ocean during the winter (~ 100 km³), while in the summer melt season, flow direction is changed into the Barents Sea, mainly through the strait between Franz Josef Land and Novaja Zemlja (Zacharov, 1976; Vinje, 1985, Vinje pers.comm, 1987). Revised calculation of sea ice transport into the Barents Sea (e.g. Vinje 1985), indicates a volume of 550 km³ of sea ice per year (Vinje, pers.comm. 1987). The maximum southward extension of sea ice is close to the Oceanic Polar Front. The ice edge may retreat rapidly during the melt season of June to August, from approximately 76° N to 82° N (Vinje, 1985, Rey et al., 1987).

Only a few samples of turbid sea ice from the Barents Sea have been obtained. However, information on sediment in sea ice samples obtained from Framstretet (summer only), (Larssen 1987) may also apply to the Barents Sea, as in summer sea ice in both regions may be derived from the Eurasian Shelf / Eastern Arctic Basin (Colony and Thorndike, 1985). Both concentrations (0-3000 mg/l) and distribution of debris in sea ice samples from Framstretet (Figs. 12 & 13) are highly variable. On average, the sampled debris represent a concentration of 55 g/m³ sea ice, but because turbid ice was sampled preferentially, this figure is most likely overestimated. Tentatively, the concentration is reduced by a factor of 2, to 27 g/m³ sea ice (Larssen, 1987).

The material in turbid sea ice from Framstretet was fine grained, generally less than 63 μ m, and mainly inorganic, dominated by clay minerals; smectites, chlorites, kaolinities and illites, in addition to quartz and feldspars. This assemblage closely resembles that found for sea floor surface sediment samples in the Barents Sea (Fig 14).

The annual input of clastic debris by sea ice can be tentatively calculated by using 1) the summer flux of sea ice into the Barents Sea (550 km^3) and 2) the debris concentration in sea ice from the Framstretet (27 g/m^3). Hence, the annual input by sea ice is 15×10^6 tons, a volume which is suggested to essentially melt out north of 74° N . As the study area covers $1/3$ of this region, 5×10^6 tons of mainly fine grained sediments are transported into the study area annually by sea ice. The importance of sea ice as a sediment transport agent has also been documented from the Alaskan shelf, where 3×10^6 tons are supplied from the Prudhoe Bay area (Barnes et al., 1982).

Only occasional icebergs are observed in distal parts of the Barents Sea, with highest concentrations observed over bank areas during the spring (40 - 50 bergs at Hopen in April). The bergs are delivered mainly during late summer, primarily from glaciers on Franz Josef Land and Svalbard (Zubov, 1943). The predominant trajectory is southwesterly, following the main surface water flow at this time of year (Vinje, 1985). Ice bergs calved from Nordaustlandet are found to stay within the coastal current and to ground on shoals in glacier proximal and near coastal areas. Ice bergs are also seen to ground and melt on the shallow parts of Olgastretet and are often efficiently trapped on the shallow Spistbergenbanken (Vinje, 1985).

Due to the fine grained nature of debris generally observed in sea ice, gravel found occasionally over most of the study area is suggested to represent ice berg rafting. Quantitatively, the ice berg rafted material is of minor importance.

CARBON CONTENT AND PRIMARY PRODUCTION

The total organic carbon (TOC) content of the bottom sediments is generally in the range of 1-2 % and concentrated in the mud fraction (Fig.4). The highest values, ca 5 %, are recorded in the southern regions close to the oceanic Polar Front. Total carbon (TC) values are only slightly higher, showing that the carbon is organic in origin. Palynologic investigations demonstrate that to a large degree the organic matter has been reworked from Mesozoic rocks (Thronsen and Bjærke, 1983). This is also confirmed by a high content of dark shale and coal fragments of Mesozoic age within the Holocene sediments.

Part of the organic carbon may, however, be deposited from the spring phytoplankton (mostly diatoms) blooms, which occur along the sea ice edge as the ice melts and retreats northward (Rey and Loeng, 1985). The annual production in the Barents Sea, estimated to average approximately 50 g C/m² (Rey et al., 1987), is only slightly lower than values found for lower latitude shelves. Annual climatic variations influence primary production, and cold-years-conditions have been found favorable for organic carbon sedimentation (Rey et al., 1987). Such years are characterized by ice extension south of the oceanic Polar Front, causing an early ice-edge bloom. However, due to the lower water temperatures, zooplankton development is delayed, and a great portion of the phytoplankton bloom will be left ungrazed and sink to deeper layers or to the bottom (Rey et al., 1987; Skjoldal et al. 1987). This process is expected to be of importance only in the area immediately south of the oceanic Polar Front. an area which interestingly displays highest carbon content (Fig. 4).

Primary production is reduced to the north, and at 80° N, the production is lowered by an order of magnitude compared to further south (Rey et al., 1987). The TC values, however, remain almost constant or increases in some areas, while there is a reduction in TOC values. In these northern regions the high TC values are related to the input of carbonate minerals and the observed TOC values is suggested to mainly reflect reworked organic matter. Insignificant supply of primary organic debris is also indicated from blue grey sediment colour. The typical olive grey colour, indicative of organic debris, is missing in the north.

To more closely analyze the ratio of recent/reworked carbon, rock eval analyses were conducted on samples from the southern parts of the study area (central Barents Sea, between 74 and 76° N (Forsberg, 1983)). The results show that, while the Late Weichselian sediments almost exclusively contain reworked matter, the Holocene deposits also contain recent carbon. There is also a difference in grain size of the carbon. In the Holocene sediments the highest concentration is in the clay fraction, whereas in the Late Weichselian sediments the fine silt fraction has the highest concentration of carbon.

SEDIMENT INPUT AND MAIN SOURCES

In the northern and southeastern regions, except for the areas around Kong Karls Land and Kvitøya, Holocene sediments cap the underlying Late Weichselian deposits, ruling out this sediments as a main source for the overlying surface sediments. A main difference between the Holocene and the Late Weichselian sediments, is the presence of smectite in the former sediments.

The lack of smectite in the underlying Late Weichselian sediments and the restricted exposure of smectite-bearing rocks in eastern Svalbard, suggests a significant contribution from an extrabasinal source. The main smectite source is, however, not identified. Common occurrence of smectite in sea ice samples in Framstretet, and the fact that Arctic sea ice is brought into the Barents Sea during the melt season, point towards an eastern Arctic source for the smectite both in the sea ice (Larssen, 1987). An important source area for sea ice in the Eurasian basin of the Arctic region is the Siberian shelf region, which may ultimately provide the smectite-rich sediments incorporated in the sea ice. Sediments may also be entrained in sea ice locally in the Barents Sea, but generally the water depth appears too deep for resuspension and entrainment.

The total annual (tentative) clastic sediment accumulation in the study area is estimated at $20 \cdot 10^6$ t (Fig. 15, Table I), with an average yield of $80 \text{ t/km}^2/\text{year}$ or 6cm/ka . The depositional rates show however considerable variations. The high values in region 11 and 12 and partly also in area 16 are related to input from the heavily glaciated hinterlands (Fig. 15). The input from land can tentatively be estimated as follows: The typical sedimentation rate in shallow distal areas is 3 cm/ka , and applying this number to region 11 and 12, the annual "excess", or land-derived sediments in these regions is $6 \cdot 10^6$ t.

Previously, the sea-ice transported contribution has been calculated to represent $5 \cdot 10^6$ t. The remaining $9 \cdot 10^6$ t must result from other agents. Former investigations have documented Spitsbergenbanken and its surrounding areas as an important sediment source through winnowing and redeposition (Bjørlykke et

al., 1978; Forsberg, 1983). This area may have contributed to the sediments in region 1 and 13. Similarly, erosion around Kong Karls Land and Kvitøya have influenced the high rates in region 5 and 16. However, the present data is insufficient to estimate this component as part of the total sediment budget, and a total calculation can not be presented. One may, however, also consider larger influence from sea ice and from other land areas.

SEDIMENTARY ENVIRONMENTS/CONCLUSIONS

The sedimentary environment and main lithofacies in the northern Barents Sea can be summarized as follows:

Glacier proximal areas: (Fig. 16)

The heavily glaciated regions of northeastern Svalbard, in particular Nordaustlandet, appears to strongly influence the sedimentary environment of the nearshore areas in the northern Barents Sea. The facies of the glacier proximal region is based on a combination of sedimentary and morphologic characteristics and includes the following elements:

- A surge moraine. Most conspicuous are its asymmetric cross sectional shape and frequent small scale slumps on the distal side. The slumps are evidence of rapid emplacement of soft and unstable sediments.
- A surge zone dominated by discontinuous ridges, formed as syn-surge squeeze-up ridges and annual push-moraines. The relative distribution of the two is dependant on post-surge glacier retreat and present glacier activity. Also typical for the surge zone are few iceberg plough marks, relative to the surge-distal zone.

- The lithology is dominated by unsorted diamictons with a high content of coarser components. Consolidation varies from normal to overconsolidated. Locally, patches of relatively undisturbed pre-surge sediments may be found embedded in the surge diamictons, and clean well sorted sand patches are formed by local meltwater activity.
- Present day sedimentation is dominated by mud deposition in the vicinity of large meltwater outlets, forming acoustically transparent deposits within 1 km off the outflow.

While the above points are based on data in the vicinity of the tidewater glacial front along Nordaustlandet margin, similar facies distributions may be expected off Barentsøya and Edgeøya, influencing region 12 (Fig. 15).

Distal areas (Fig. 17)

Four main lithofacies are identified in the distal zone: 1) mud, 2) diamicton, 3) clastic lag and 4) carbonate lag. Distribution of these lithofacies is a result of water depth, tidal and mean currents, probably also sea ice and brine formation, and rafting by sea ice and to a lesser extent icebergs. The main sedimentary regimes and the resulting facies are:

- On the shallow Spitsbergenbanken (Fig. 17 a) and its adjacent areas, winnowing is most likely caused by strong cold currents, dense brine convection during sea ice formation and erosion by high velocity currents along the oceanic Polar Front. The carbonates accumulate down to a water depth of 60-100m, while diamicton and clastic lag are found down to 350 m water depth. In the carbonate deposits, rafting of coarser material from icebergs is volumetric

insignificant, but diagnostic for the environment.

- In deeper bank areas, 100 - 200 m, resuspension and transport by mean currents with the superimposed effect of tides and dense brine convection, may deplete the sediments of finer components forming a relatively coarse diamicton. The finer grades are redeposited in deeper basins, forming the mud facies. Evidence for bottom current activity is seen in local reworking of sediment surface into sediment waves and winnowing of plough marks (Figs 17 b and c).
- A mud facies is also found at shallower depth, 100 - 200 m, along the eastern coastline of Svalbard, apparently formed by formed by accumulation of redistributed sediments from the north. of sediments from cold, long shore currents transporting glacially derived material.

In conclusion, the sedimentation on the northern Barents Sea, a high arctic epicontinental sea may be characterized as follows.

The main influence of the terrestrial regime is limited to the glacier proximal zone and its immediately adjacent areas. Winnowing and resuspension are the main processes for shallow banks in distal areas, while sea ice and sediments winnowed from bank areas contribute fine grained sediments to the intermediate and deeper areas. Iceberg rafted material is environmentally important, but is volumetrically of minor importance. In the distal zone sediments accumulate at a rate of 3-5 cm/ka or 40 -60 tons per year/km², while in coast near areas input of land derived material increases to 15 - 20 cm/ka.

ACKNOWLEDGEMENTS

This work synthesizes information from various sources, some of which are unpublished theses. Lars Wensaas and Carl Fredrik Forsberg are acknowledged for letting us use results of their work. We thank the Norwegian Petroleum Directorate for providing necessary funding both for parts of the data acquisition and for compilation of this paper. Pfirman's contribution was conducted at Woods Hole Oceanographic Institution under the direction of John D. Milliman (ONR contract N-00014-01-C-009). The transmissometer/nephelometer was kindly provided by the U.S. Geological Survey, Woods Hole, Massachusetts. Hydrographic data courtesy of Institute of Marine Research, Bergen and T. Gammelsrød, University of Bergen. This work is Norsk Polarinstitutt Publication No.249.

The manuscript was carefully reviewed by Dr. S. Haldorsen and Dr. J. Milliman.

REFERENCES

- Anderson, J.B., Brake, C.F. and Myers, N.C., 1984. Sedimentation on the Ross Sea continental shelf, Antarctica. *Marine Geology*, 57: 295-333.
- Barnes, P.W. and Reimnitz, E., 1982. Sediment content of nearshore fast ice-fall 1980, Beaufort Sea, Alaska. Open - file report. US Geological Survey, 716: 18pp. (unpubl.).
- Barnes, P.W., Reimnitz, E. and Fox, D., 1982: Ice rafting of fine grained sediment, a sorting and transport mechanism, Beaufort Sea, Alaska. *Journal of Sedimentary Petrology*, 52: 493-502.
- Bjærke, T. and Dypvik, H., 1977. Sedimentological and palynological studies of Upper Triassic-Lower Jurassic sediments in Sassenfjorden, Spitsbergen. *Norsk Polarinstitutts Årbok*, 1976: 131-150.
- Bjørlykke, K., Bue, B. and Elverhøi, A., 1978. Quaternary sediments in the northwestern part of the Barents Sea and their relation to the underlying, Mesozoic bedrock. *Sedimentology*, 25: 227-246.
- Boulton, G.S. and Deynoux, M., 1981. Sedimentation in glacial environments and the identification of tills and tillites in ancient sedimentary sequences. *Precambrian Research*, 15: 397-422.
- Butman, B., 1987. Physical processes causing surficial-sediment movement. In: A.R.H. Bachus (Editor), MIT Press: 147-162.
- Clark, D.L. and Hanson, A., 1983. Central Arctic Ocean sediment texture: A key to ice transport mechanism. In: B.F. Molnia (Editor) *Glacial-Marine Sedimentation*. Plenum, New York., 844pp.
- Clark, D.L., Whitman, R.R., Morgan, K.A. and Mackey, S.D., 1980. Stratigraphy and glacial-marine sediments of the Amerasian Basin, Central Arctic Ocean. *Geological Society of America, Special Paper* 181: 57pp.
- Colony, R. and Thorndike, S., 1985. Sea ice movement as a drunkard's walk. *Journal of Geophysical Research*, 90 (C1): 965-974.
- Denton, G.H. and Hughes, T.J., 1981. The Arctic Ice Sheet: An outrageous hypothesis. In: G.H. Denton and T.J. Hughes (Editors), *The Last Great Ice Sheets*, John Wiley & Sons: 437-467.
- Dowdeswell, J.A., 1984. Remote sensing studies of Svalbard glaciers. Unpubl. Ph.D. thesis, University of Cambridge, 250pp.
- Drewry, D.J. and Cooper, A.P.R., 1981. Processes and models of Antarctic glaciomarine sedimentation. In: *Annals of Glaciological* 2, Proceedings of the Symposium on Processes of Glacier Erosion and Sedimentation, Geilo - Norway, pp.117-128.
- Edwards, M.B., 1980. Sandstone in Lower Cretaceous Helvetiafjellet Formation, Svalbard: Bearing on reservoir potential of Barents Shelf. *American association of petroleum geologists. Bulletin*, 63, no.12: 2193-2203.

- Elverhøi, A. and Bomstad, K., 1980. Late Weichselian glacial and glaciomarine sedimentation in the western central Barents Sea. Norsk Polarinstitutt Rapportserie, 3, 29pp.
- Elverhøi, A. and Grønli, G., 1981. Diagenetic and sedimentologic explanation for high seismic velocity and low porosity in Mesozoic-Tertiary sediments, Svalbard Regions. American Association of Petroleum Geologists, Bulletin 65 (1): 145-153.
- Elverhøi, A. and Solheim, A., 1983a. Maringeologiske og - geofysiske undersøkelser i Barentshavet 1983, Toktrappport. Norsk Polarinstitutt Rapportserie, 14, 116pp.
- Elverhøi, A. and Solheim, A., 1983b. The physical environment, Western Barents Sea, 1:1500000, sheet A; Surface Sediment Distribution. Norsk Polarinstitutt Skrifter, 179A, 23pp.
- Elverhøi, A. and Solheim, A., 1983c. The Barents Sea ice sheet - a sedimentological discussion. Polar Research, 1: 23-42.
- Elverhøi, A. and Solheim, A., 1987a. Shallow geology and geophysics of the Barents Sea - with special reference to the existence and detection of submarine permafrost. Norsk Polarinstitutt Rapportserie, 37, 51pp.
- Elverhøi, A. and Solheim, A., 1987b. Late Weichselian glaciation of the northern Barents Sea - a discussion. Polar Research, 5:
- Elverhøi, A., Lønne, Ø. and Seland, R., 1983. Glaciomarine sedimentation in a modern fjord environment, Spitsbergen. Polar Research, 1: 127-149.
- Elverhøi, A., Antonsen, P., Flood, S.B., Solheim, A. and Vullstad, A.A., 1988. The physical environment, western Barents Sea, 1:1500000, Shallow Bedrock Geology - Structure, litho - and biostratigraphy. Norsk Polarinstitutt Skrifter, 179D, 40pp.
- Eyles, C.H., Eyles, N. and Miall, A.D., 1985. Models of glaciomarine sedimentation and their application of ancient glacial sequences. Paleogeogr., Palaeoclimatol., Palaeoecol., 51: 15-84.
- Faleide, J.I., Gudlaugson, S.T. and Jacquart, G., 1984. Evolution of the western Barents sea. Marine and petroleum geology, 1: 123-150.
- Forsberg, C.F., 1983. Sedimentation and early diagenesis of Late Quaternary deposits in central parts of the Barents Sea. Unpubl. thesis, University of Oslo, 120pp.
- Gravenor, C.P., Von Brunn, V. and Dreimanis, A., 1984. Nature and classification of waterlain glaciogenic sediments, exemplified by Pleistocene, Late Paleozoic and Late Precambrian deposits. Earth Science Review, 20: 105-166.
- Hovland, M., 1983. Elongated depressions associated with pockmarks in the western slope of the Norwegian Trench. Marine Geology 51: 35-46.
- Johannessen, O.M and Foster, L.A., 1978. A note on the topographically controlled oceanic Polar front in the Barents Sea. Journal of Geophysical Research, 83 (C9): 4567-4571.

- Kristoffersen, Y., Milliman, J.D. and Ellis, J.P., 1984. Unconsolidated sediments and shallow structure of the northern Barents Sea. *Norsk Polarinstitutt Skrifter*, 180: 25-39.
- Larssen, B., 1987. En sedimentologisk undersøkelse av partikulært materiale i havis fra Framstredet, Arctis. Cand. scient. thesis, University of Oslo, 148pp.
- Lauritzen, Ø and Ohta, Y., 1985. Geological map of Svalbard, 1:500000, Sheet 4G, Nordaustlandet. *Norsk Polarinstitutt Skrifter* 154B, 14pp.
- Liestøl, O., 1969. Glaciers syrges in west Spitsbergen. *Canadian Journal of Earth Sciences*, 6.: 895-897.
- Liestøl, O., 1985. Glaciers of Svalbard, Norway. In: R.S. Williams Jr. and J.G. Ferrigno (Editors), *Satellite Image Atlas of Glaciers*. U.S Geological Survey Professional Paper, Chapter 5.0-Europe.
- Loeng, H., 1983. Strømmålinger i tidsrommet 1979-1982 i de sentrale deler av Barentshavet. In: L.I. Eide (Editor), *Environmental conditions in the Barents Sea and near Jan Mayen*, 10pp.
- Mackiewicz, N.E., Powell, R.D., Carlson, P.R. and Molnia B.F., 1984. Interlaminated iceproximal glacialmarine sediments in Muir Inlet, Alaska. *Marine Geology*, 57: 113-147.
- Midttun, L., 1985. Formation of dense bottom water in the Barents Sea. *Deep-Sea Research*, vol.32, 10: 1233-1241.
- Midttun, L. and Loeng, H., 1987. Climatic variations in the Barents Sea. In: H. Loeng (Editor), *Proceedings of the third Soviet-Norwegian Symposium, Murmansk*, pp.13-27.
- Milliman, J.D. and Meade, R.H., 1983. World-wide delivery of river sediment to the oceans. *Journal of Geology*, 91: 1-21.
- Mosby, H., 1938. Svalbard waters. *Geofysiske Publikasjoner*, vol. XII, no. 4, 85pp.
- Nansen, F., 1904. The bathymetrical features of the north polar seas. *Scientific Results of Norway Polar Expeditions* 4, (13): 1-232.
- Nansen, F., 1906. Northern waters: Captain Roald Amundsen's oceanographic observations in the Arctic seas in 1901. *Vitenskaps-Selskabet's Skrifter, I, Matematisk-Naturv. Klasse*, 1906, no.3, 145pp.
- Novitskiy, V.P., 1961. Permanent currents of the Northern Barents sea. *Trudy Gosudarstvennogo Okeanograficheskogo Instituta, Leningrad*. 64: 1-32.
- Pfirman, S.L., 1985. Modern sedimentation in the northern Barents Sea: Input, dispersal and deposition of suspended sediments from glacial meltwater. Woods Hole Oceanographic Inst. Unpubl. Ph.D-thesis, 284pp.
- Postma, H., 1967. Sediment transport and sedimentation in the estuarine environments. In: G.H. Lauff (Editor), *Estuaries*, Publ. 83. Washington D.C., American Association for the Advancement of Science, pp.158-179.

- Powell, R.D., 1983. Glacial-marine sedimentation processes and lithofacies of temperate tidewater glaciers, Glacier Bay, Alaska. In: B.F. Molnia (Editor), *Glacial-Marine Sedimentation*. Plenum, New York, N.Y., pp.185-232.
- Reimnitz, E., Kempema E.W. and Barnes, P.W., 1987. Anchor ice, seabed freezing and sediment dynamics in shallow Arctic seas. *Journal of Geophysical Research*, 92(C13): 14671-14678.
- Rey, F. and Loeng, H., 1985. The influence of ice and hydrographic conditions on the development of phytoplankton in the Barents Sea. In: J.S. Gray and M.E. Christiansen (Editors), *Marine Biology of Polar regions and Effects of Stress on Marine Organisms*, J. Wiley & Sons Ltd., pp.49-63.
- Rey, F., Skjoldal, H.R. and Slagstad, D., 1987. Primary production in relation to climatic changes in the Barents Sea. In: H. Loeng (Editor), *The effect of oceanographic condition on the distribution and population dynamics of commercial fish stock in the Barents Sea*. Proceedings of the third Sovjet-Norwegian symposium, Murmansk 1986, pp.29-46.
- Rønnevik, H.C., Beskow, B. and Jakobsen, H.P., 1982. Structural and stratigraphical evolution of the Barents Sea. *Norwegian Petroleum Society, Geological mem.* 8: 431-440.
- Skjoldal, H.R., Hassel, A., Rey, F. and Loeng, H., 1987. Spring phytoplankton development and zooplankton reproduction in the central Barents Sea, in the period 1979-1984. In: H. Loeng (Editor), *Proceedings of the third Soviet-Norwegian Symposium, Murmansk*.
- Solheim, A. in prep. The depositional environment of surging sub-polar tidewater glaciers: A case study of the morphology, sedimentation and sediment properties in a single affected marine basin outside Nordaustlandet, northern Barents Sea.
- Solheim, A. and Elverhøi, A., 1985. A pockmark field in the central Barents Sea: gas from a petrogenetic source. *Polar Research*, vol. 3 n.s., no. 1: 11-19.
- Solheim, A. and Kristoffersen, Y., 1984. Sediments above the upper regional unconformity: Thickness, seismic stratigraphy and outline of the glacial history. *Norsk Polarinstitutt Skrifter* 179B, 26pp.
- Solheim, A. and Pfirman, S. L., 1985. Sea floor morphology outside a grounded, surging glacier; Bråsvellbreen, Svalbard. *Marine Geology*, 65: 127-143.
- Solheim, A., Milliman, J.D and Elverhøi, A., in press.. Sediment distribution and sea floor morphology of Storbanken, the northern Barents Sea; implications for the glacial history of the region. *Canadian Journal of Earth Science*.
- Tantsiura, A.I., 1959. On the currents of the Barents sea. *Transactins of the Polar Scientific Research institute of Marine Fisheries and Oceanography - N.M. Knipovic (PINRO)* 11, pp.35-53.

- Tantsiura, A.I., 1973. On seasonal changes of currents in the Barents Sea. *Trudy Minist. Ribn. Khoz. SSSR, Poliarn. naucho-issled. Proekt. Inst. Morsk. Ribn. Khoz. Okeanogr. N.M. Knipovich (PINRO)*. 34: 108-112.
- Trondsen, T. and Bjærke, T., 1983. Palynodebris analysis of a shallow core from the Barents sea. *Polar research*. vol. 1 n.s., no.1: 43-47.
- Vinje, T.E., 1985. Drift, composition, morphology and distribution of the sea ice fields in the Barents Sea. *Norsk Polarinstitutt Skrifter*, 179C, 26pp.
- Vorren, T.O. and Kristoffersen, Y., 1986. Late Quaternary glaciation in the south-western Barents Sea. *Boreas*, 15: 51-59.
- Vorren, T.O., Hald, M., Edvardsen, M. and Lind-Hansen, O.W., 1983. Glacigenic sediments and sedimentary environments on continental shelves: general principles with a case study from the Norwegian shelf. In: J. Ehlers (Editor), *Glacial deposits in north-west Europe*. A.A. Balkema, Rotterdam, pp.61-73.
- Wensaas, L., 1986. Sedimentologiske og sedimentpetrografiske studier av kvartære sedimenter i det nordlige Barentshav. Unpubl. Cand. Scient. thesis, University of Oslo, 178pp.
- Winsnes, T.S. and Worsley, D., 1981. Geological map of Svalbard, 1:500000, Sheet 2G, Edgeøya. *Norsk Polarinstitutt Skrifter* 154B.
- Zacharov, V.F., 1976. Cooling of the Arctic and the ice cover of the Arctic seas. *AANII, Trudv*, 37, 96pp.
- Zubov, N.N., 1943. *L'dy Arktiki. (Glavsevmorput)*, Moskva. (Transl. U.S. Navy Electr. Lab.: Arctic Ice.

FIGURE CAPTIONS

- Fig. 1: Bathymetric map of the Barents Sea showing the study area and place names in its northernmost parts.
- Fig. 2: Schematic lithostratigraphic section of the unlithified sediments in the northern Barents Sea. The boundary between the upper mud and the underlying "proximal" glaciomarine sediments is tentatively dated to 10-12 ka BP (From Elverhøi and Solheim, 1987b)
- Fig. 3: Surface sediment composition and distribution in the study area.
Modified from Elverhøi and Solheim (1983b)
- Fig. 4: Transects (a and b) showing grain size distribution, mineralogy, organic carbon and total carbon content and sedimentation rate for selected samples from the northern Barents Sea.
- Fig. 5: Side scan sonographs and 3,5 kHz sounding along the Bråsvellbreen glacier front showing: a) the surge moraine (glacier front to the right), b) rhombohedral pattern and irregular mounds and c) arcuate discontinuous ridges paralleling the ice front. From Solheim and Pfirman (1985).
- Fig. 6: Satellite image (Landsat, 23 July 1976) of Nordaustlandet showing the meltwater plumes and the offshore flow pattern. (For location, see Fig. 1)
- Fig. 7: Suspended matter in two transects south off Bråsvellbreen. Concentration of suspended particulate matter from water samples are noted and the pie diagrams show the percent of noncombustible material rounded to the nearest 25 %.
- Fig. 8. Surface currents of the Barents Sea (after Tantsiura, 1959)
- Fig. 9: Schematic bottom water circulation pattern (modified from Tantsiura (1973)) superimposed on contours of July -September 1981 bottom temperature. Hydrographic data courtesy of Institute of Marine Research, Bergen, Norway and Geophysical Institute, Univ. of Bergen, Norway. On Spitsbergenbanken, near bottom temperatures above 0°C occur only during late summer months (H. Loeng, pers. comm. 1988).
- Fig. 10: Regional distribution of excess near-bottom turbidity and suspended matter. Light shaded regions represent moderate nepheloid layer and dark shaded regions show stronger bottom nepheloid layers. (From Pfirman, 1985)

- Fig. 11: Side scan sonograph showing deep bedforms south of Kvitøya platform near a region with large near-bottom excess turbidity. Wavelength of the sediment waves is approximately 5 m. (From Pfirman, 1985)
- Fig. 12: Vertical section of sea ice from Framstretet showing concentration and grain size of clastic material. (From Larssen, 1987)
- Fig. 13: Schematic cross section of sea ice showing the distribution of the clastic material. (From Larssen, 1987)
- Fig. 14: Clay mineralogy in sea ice from Framstretet and sediments from the Barents Sea. (For identification of transect 1 and 2, see Fig. 4, and for Late Weichselian sediments, see Fig. 2).
- Fig. 15: Bathymetric map showing zones of different depositional rates in the study area. Glacier coverage is shown on Svalbard, the areas show the distribution of glaciers (white areas). For identification of the numbers of the various regions see Table I.
- Fig. 16: Cartoon showing the main ice proximal sedimentary processes and facies.
- Fig. 17: The principal lithofacies and sedimentary processes in the ice distal zone. A) Sediment starved carbonate bank, B) Clastic bank (winter) and C) Clastic bank (summer).

TABLE

Table 1: Sedimentation rate and tentative annual accumulation of clastic sediments in the northern Barents Sea. The accumulation of carbonates on Spitsbergenbanen, zone 14 is also listed, and 17,18 and 19 show non-depositional or erosional areas.

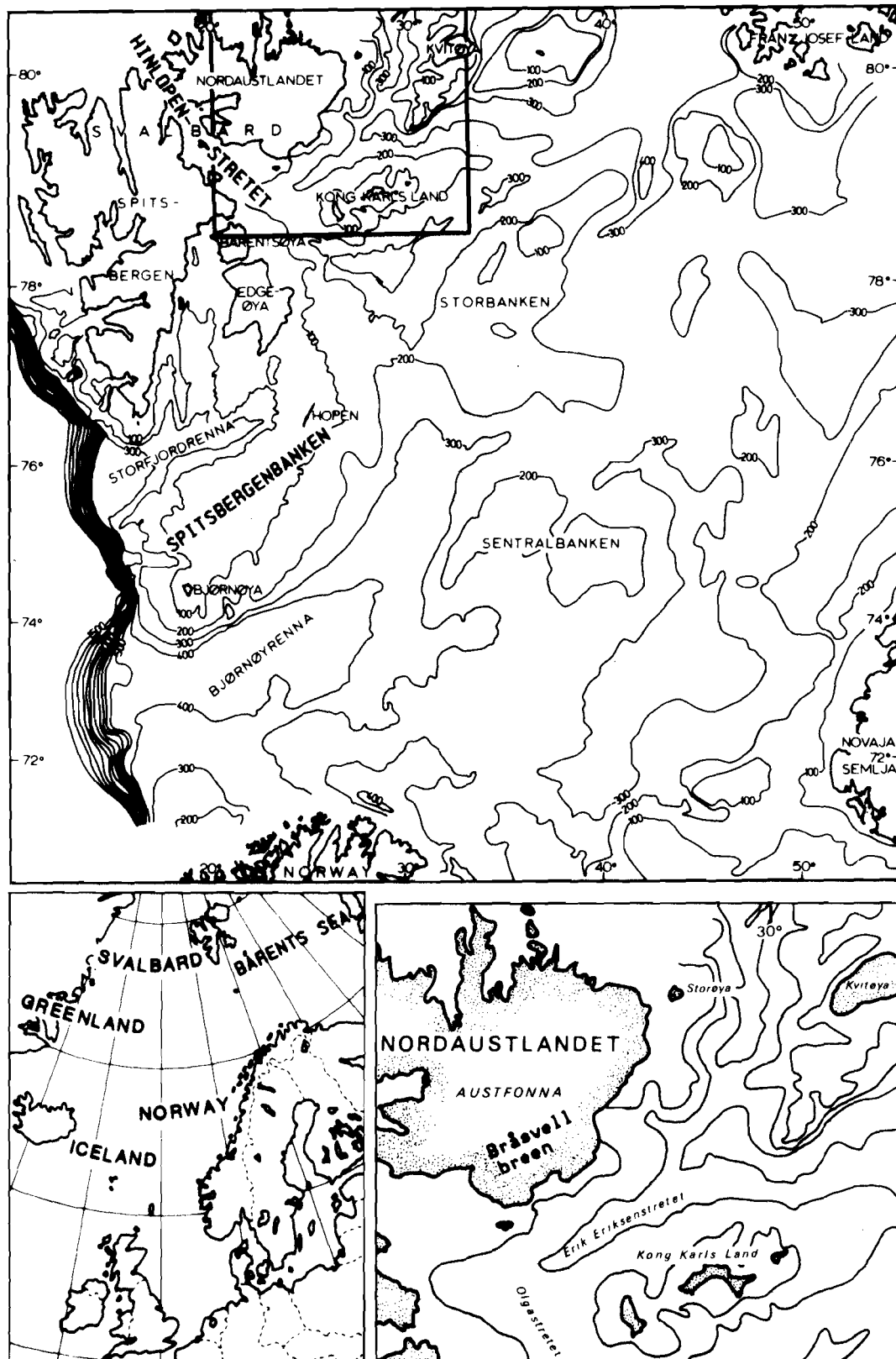


Fig.1.

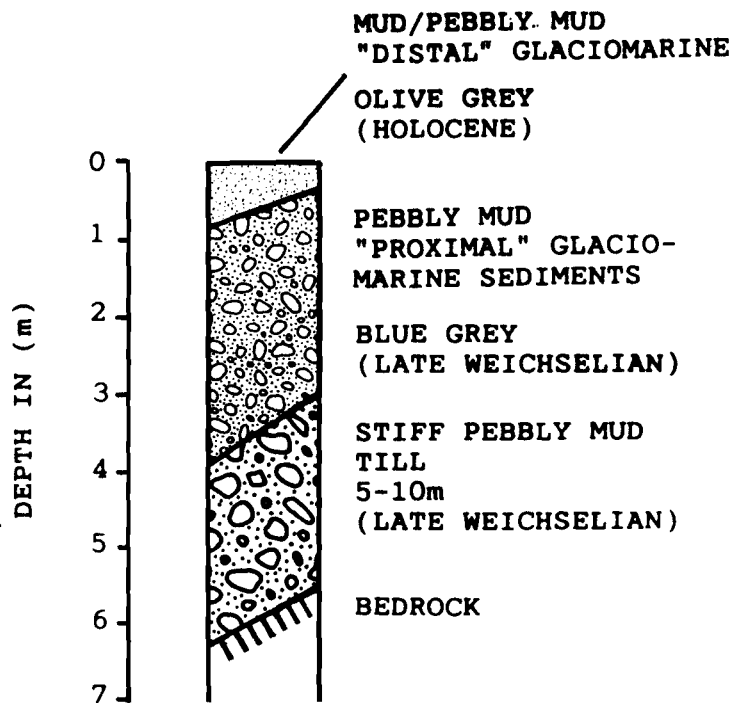
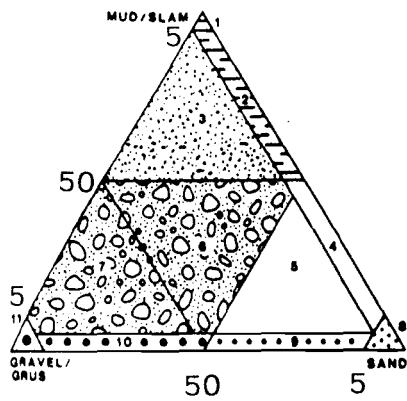
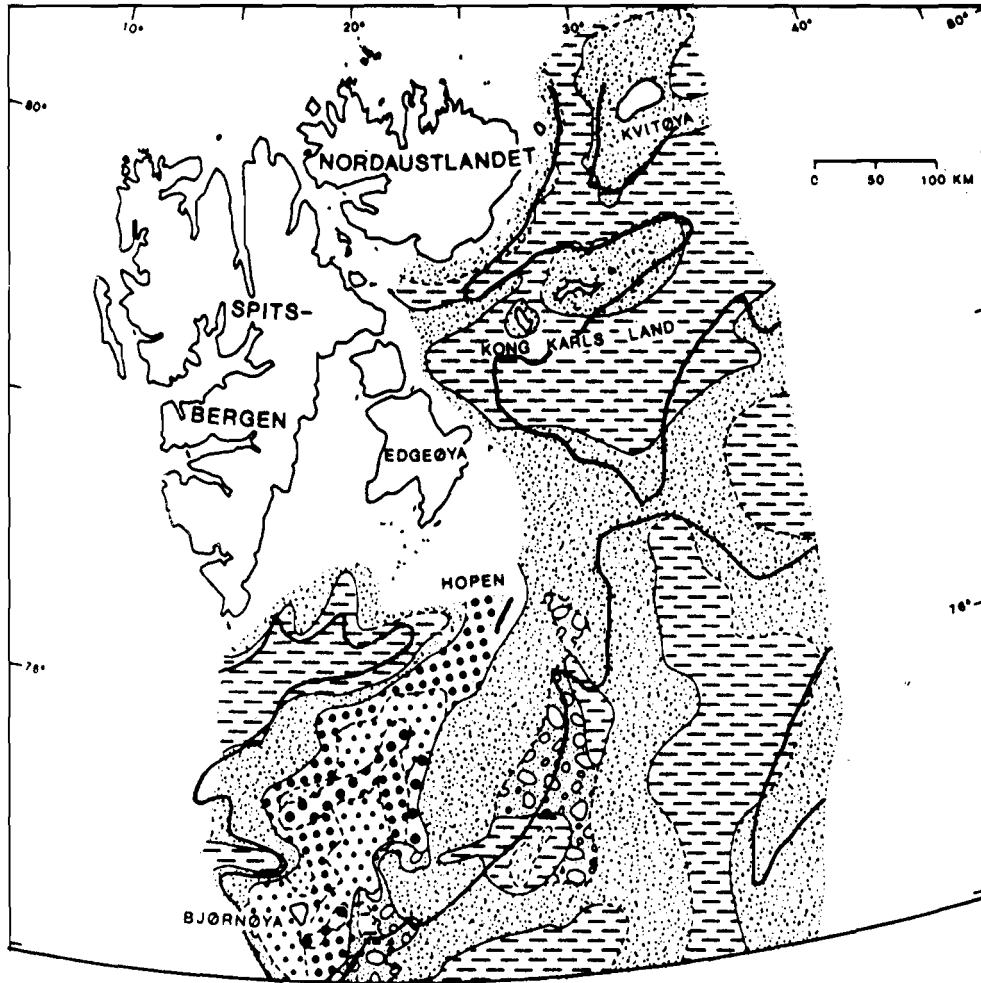


Fig.2.



- 1: Mud. 2: Sandy mud. 3: Sandy gravelly mud.
- 6: Muddy sand and gravel. 7: Sandy muddy gravel.
- 8: Sand. 9: Gravelly sand. 10: Sandy gravel.
- 11: Gravel
- * Mainly carbonate (50-80% CaCO_3)

Fig. 3.

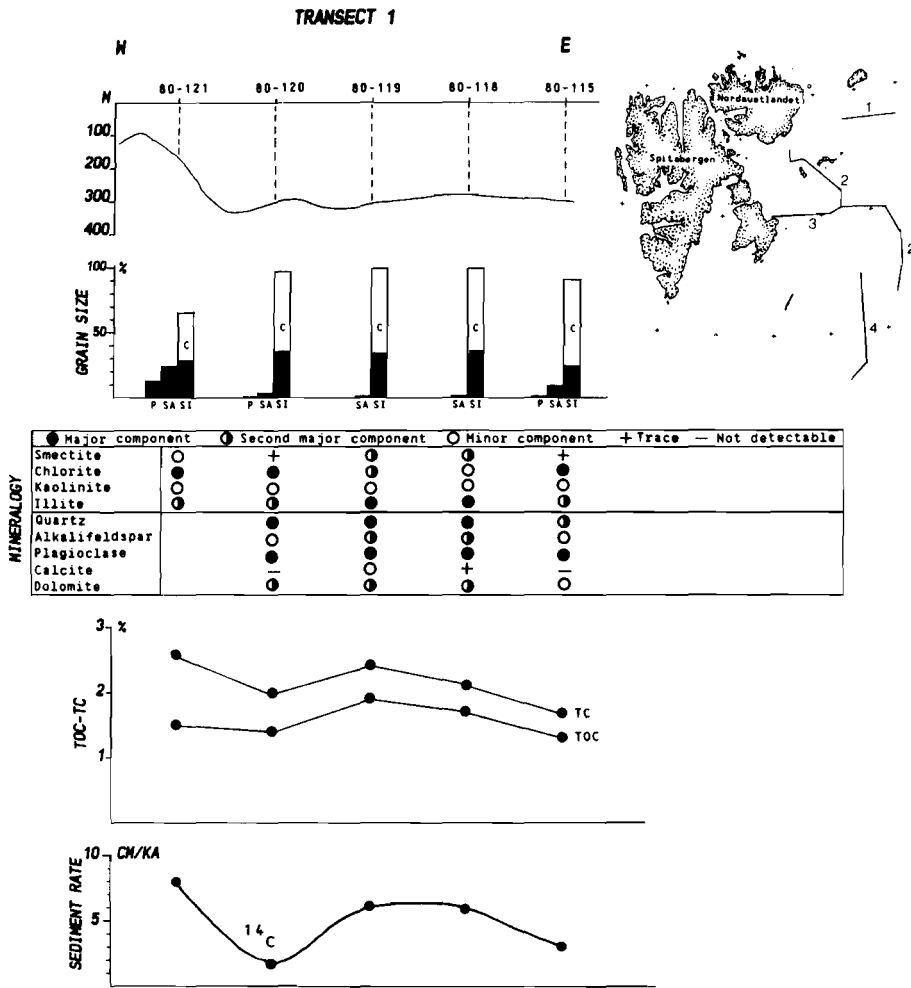


Fig.4a.

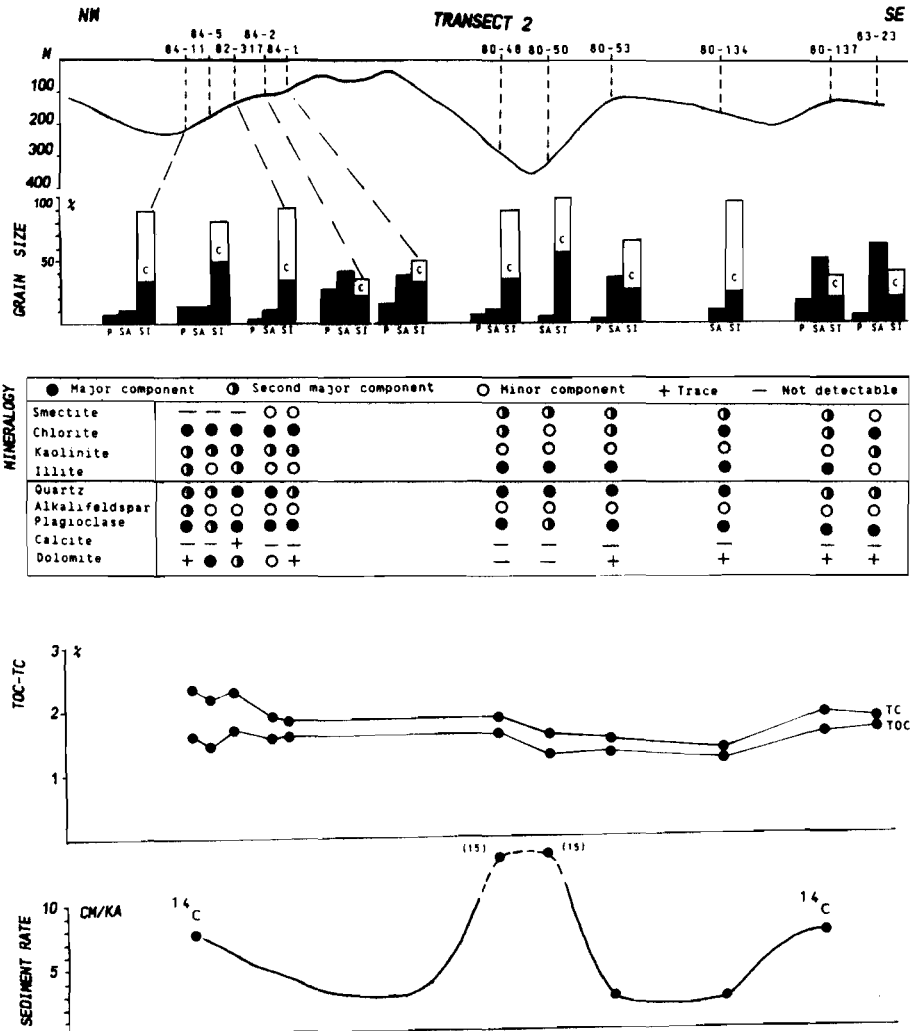


Fig. 4b.

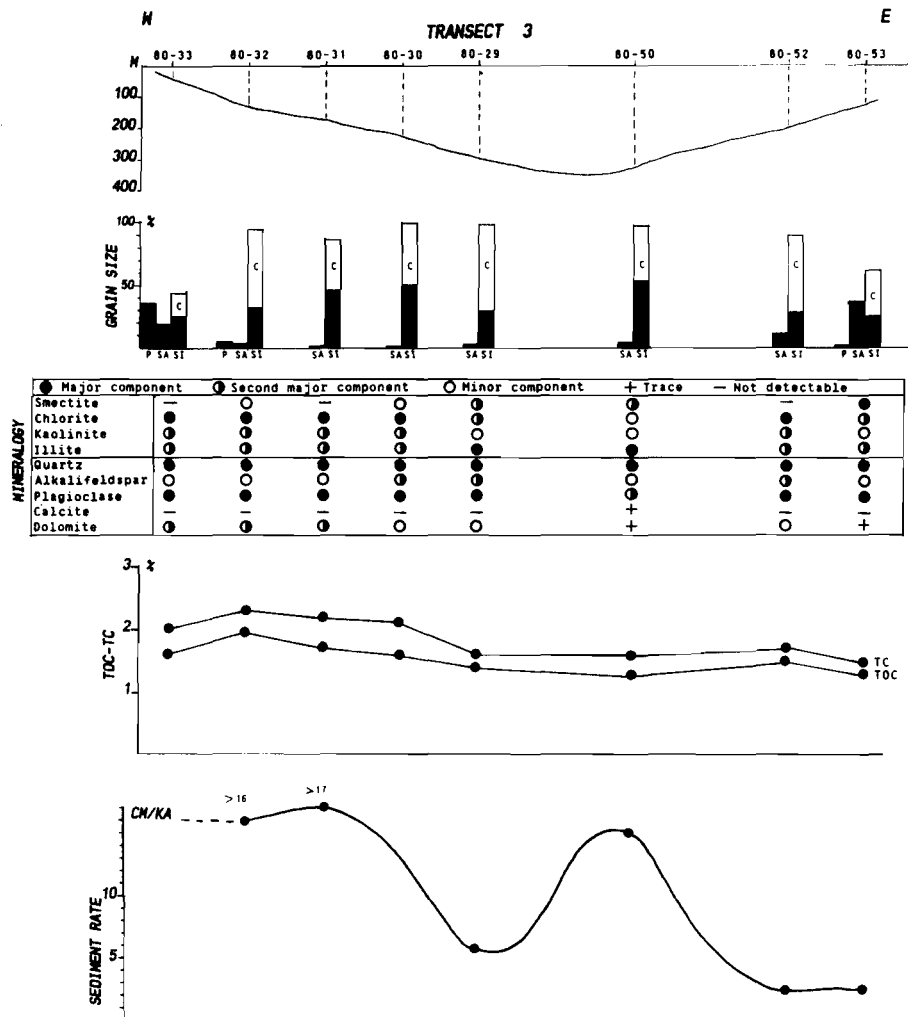


Fig. 4c.

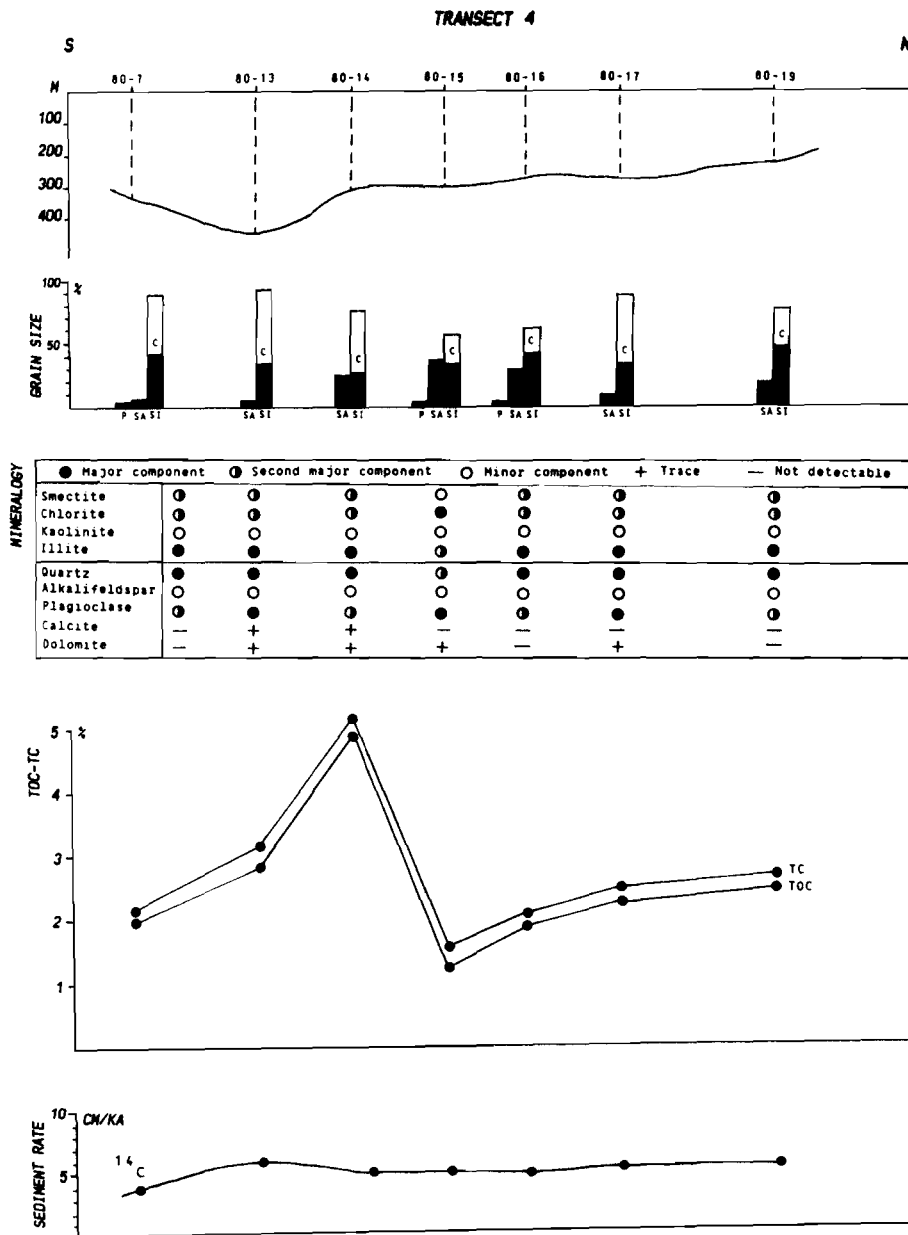


Fig. 4d.

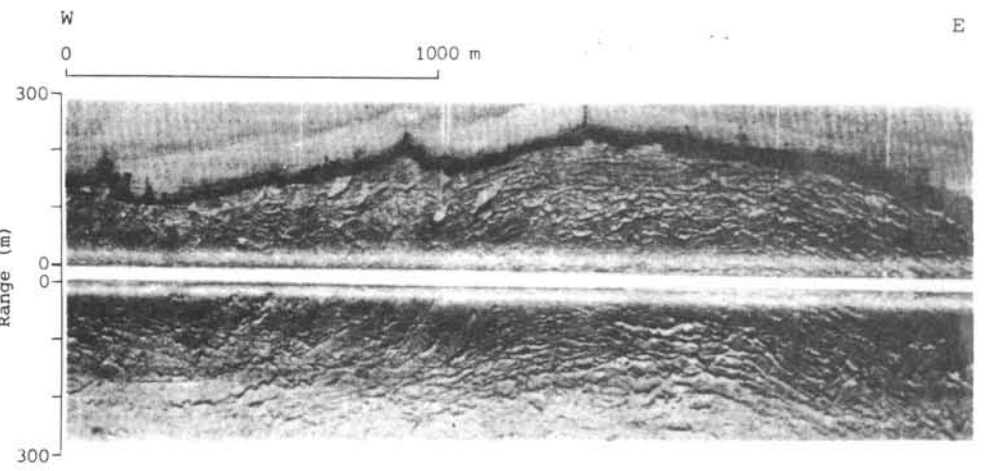
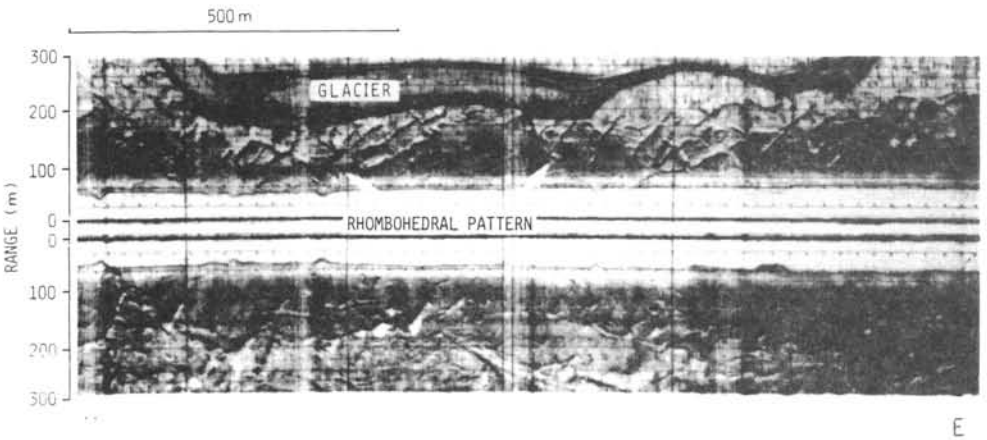


Fig. 5.

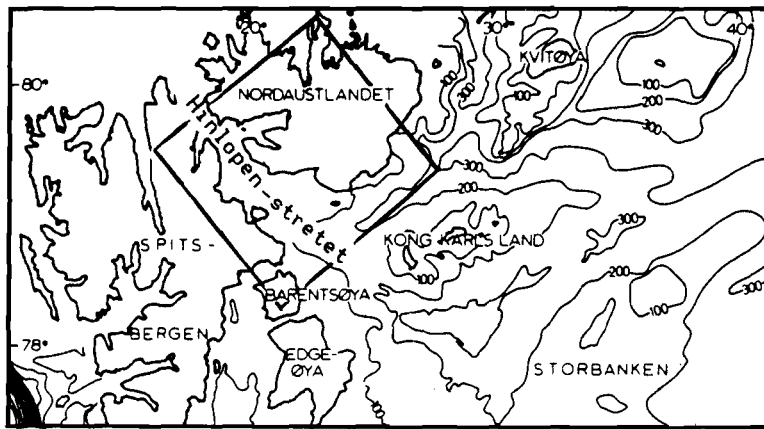


Fig. 6.

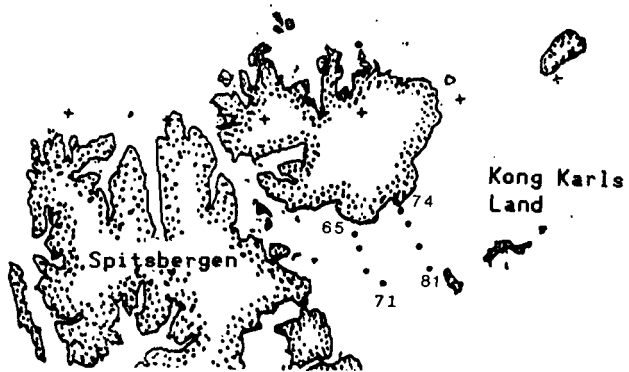
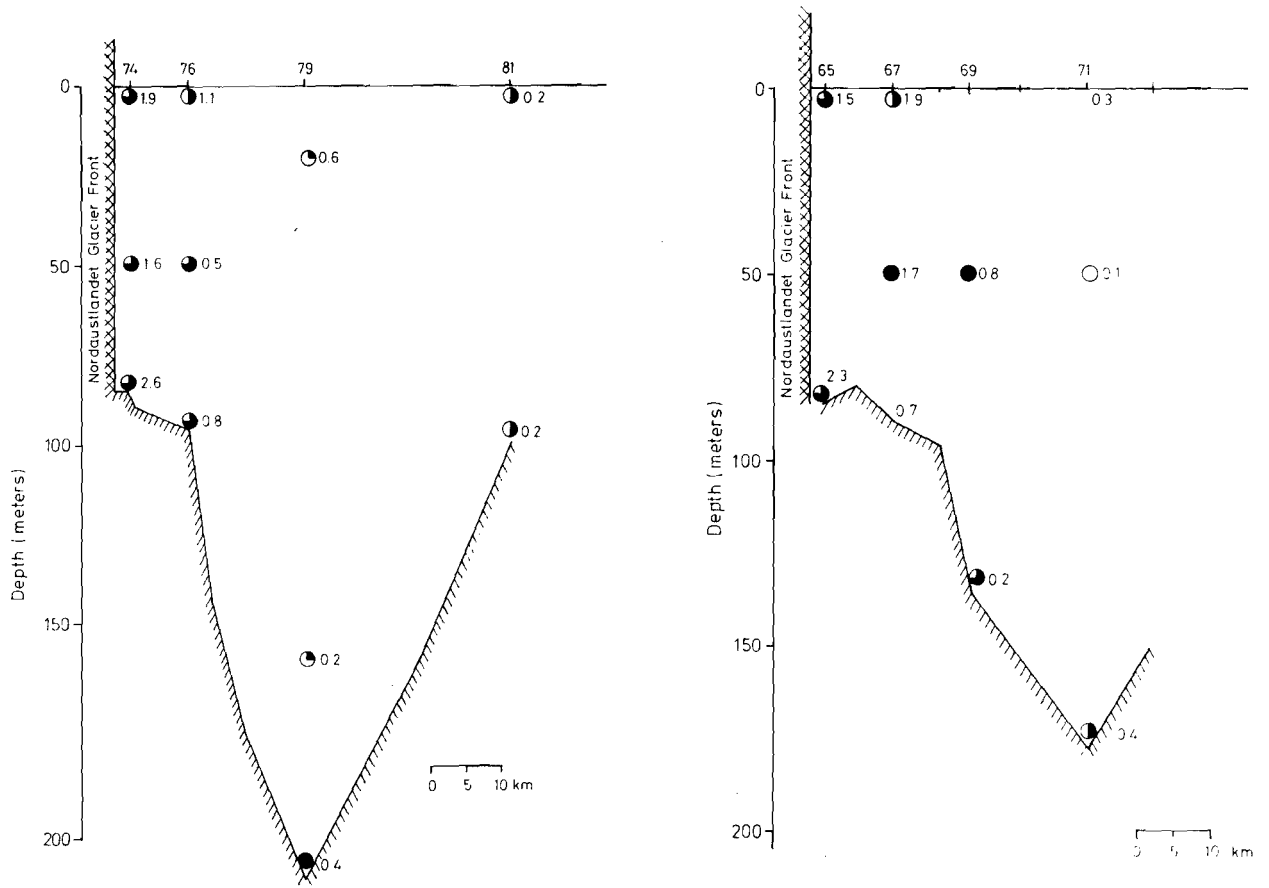


Fig. 7.

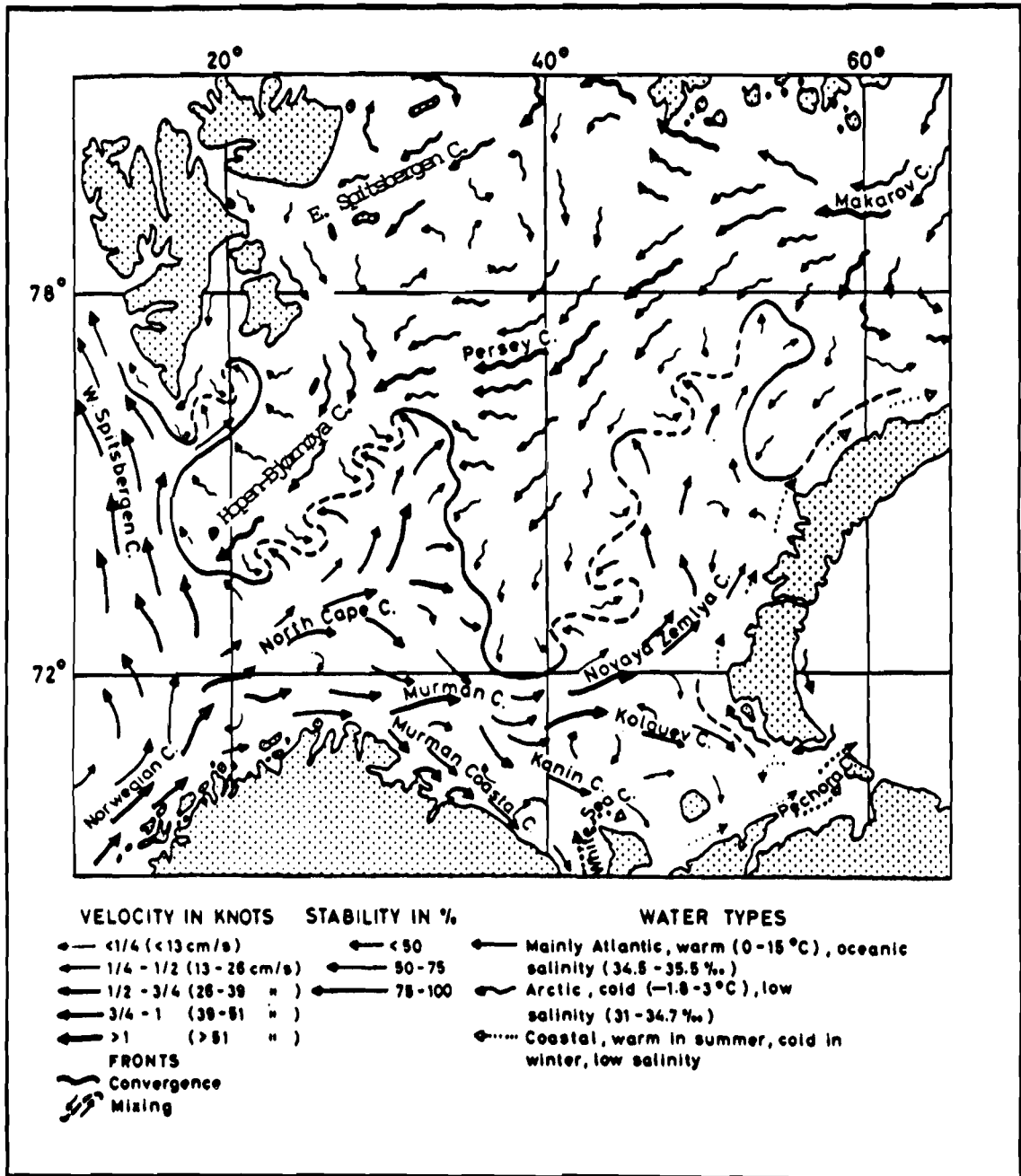


Fig. 8.

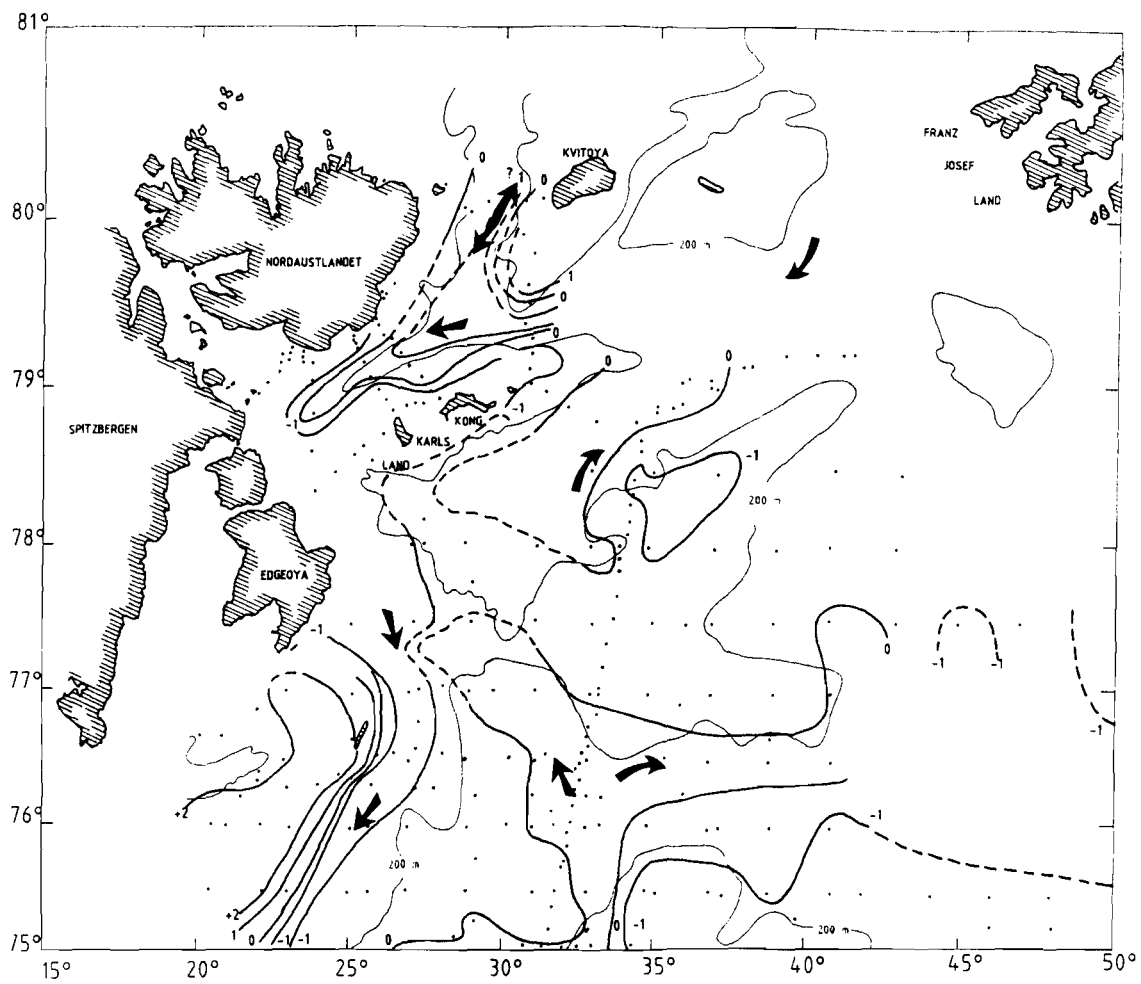


Fig. 9.

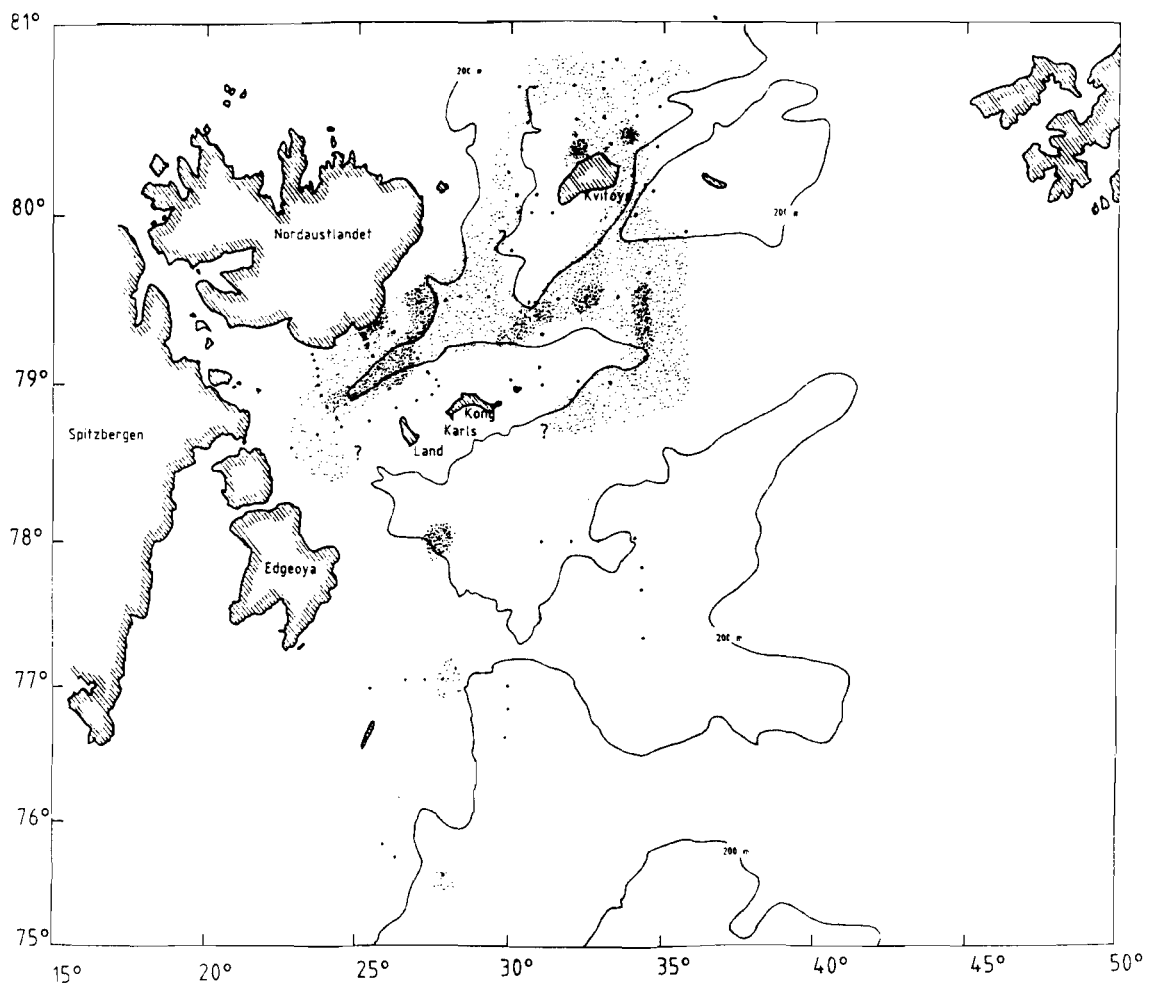


Fig. 10.

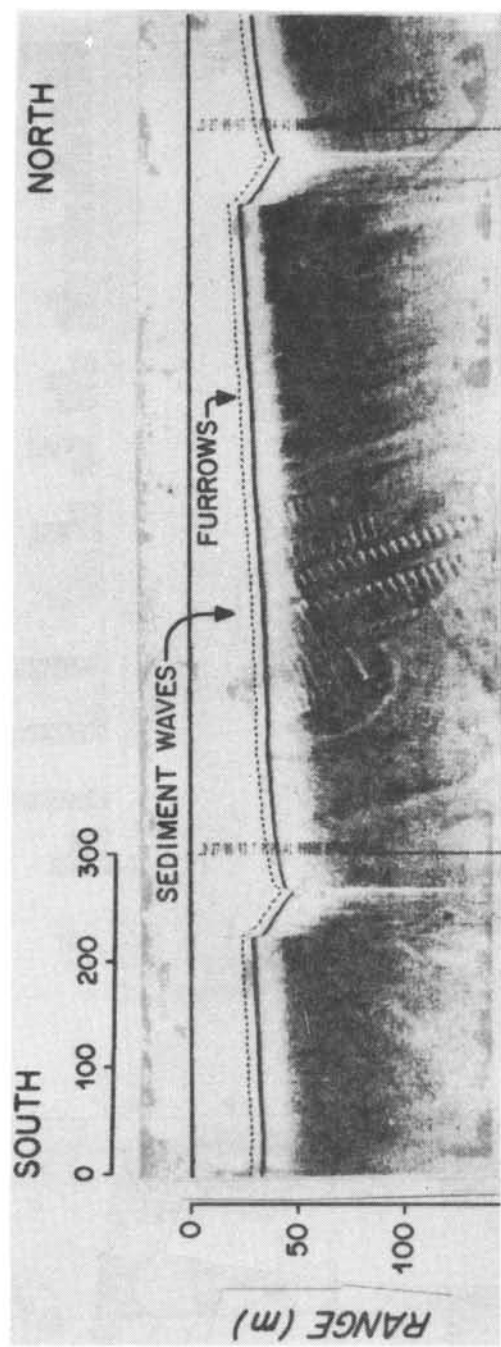


Fig. 11.

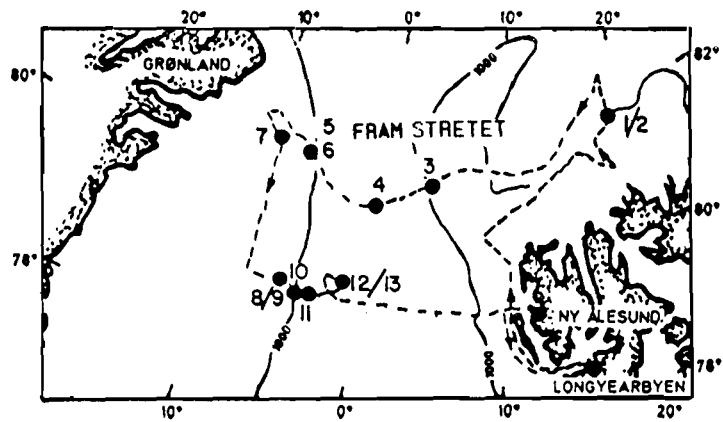
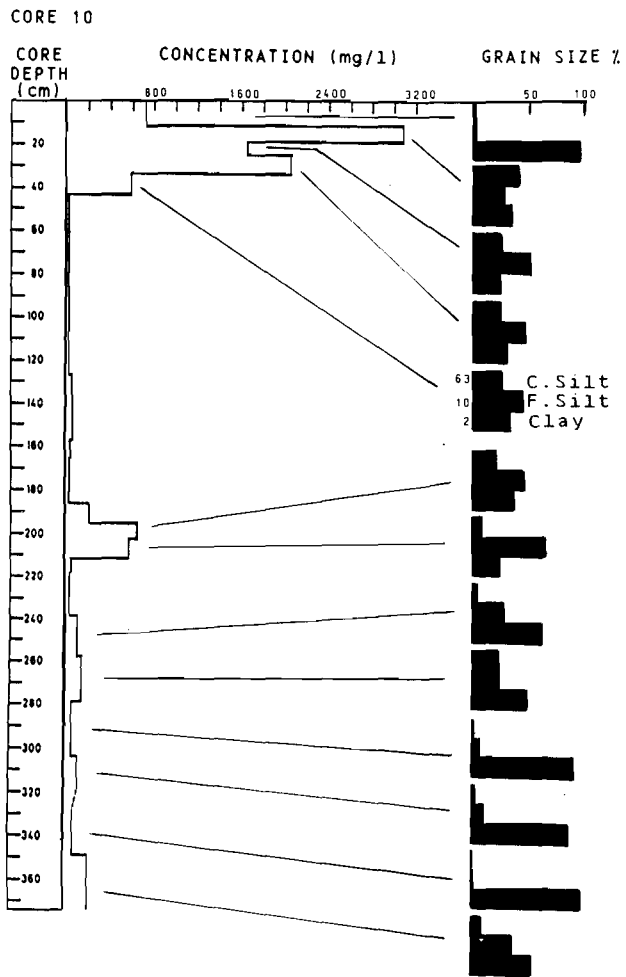


Fig. 12.

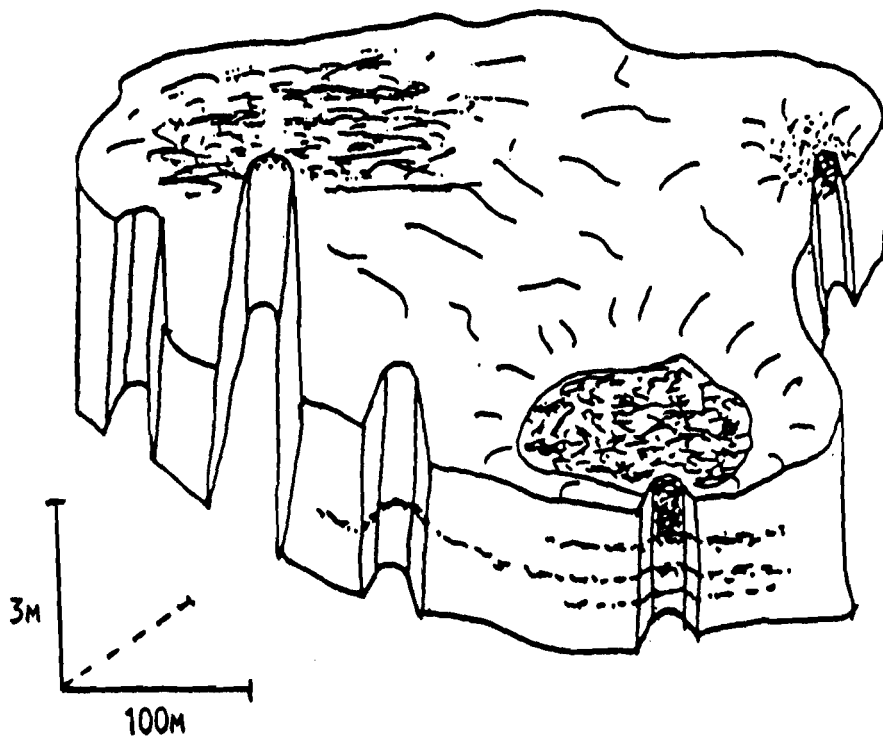
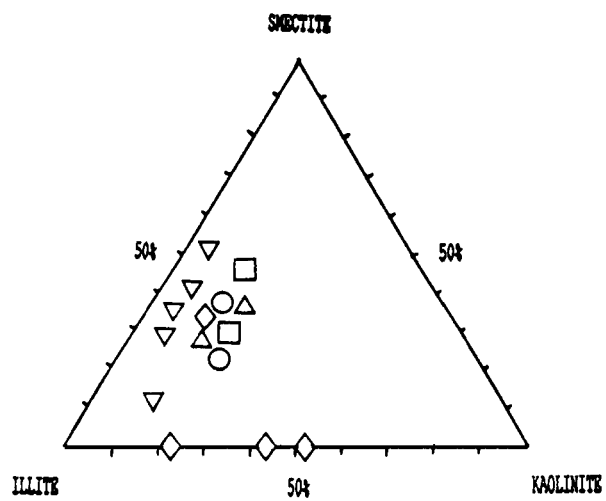


Fig. 13.



- ◇ TRANSECT 1
- △ TRANSECT 2
- TRANSECT 3
- TRANSECT 4
- ▽ SEA ICE-FRAMSTRETET
- ◇ LATE WEICHSELIAN

Fig. 14.

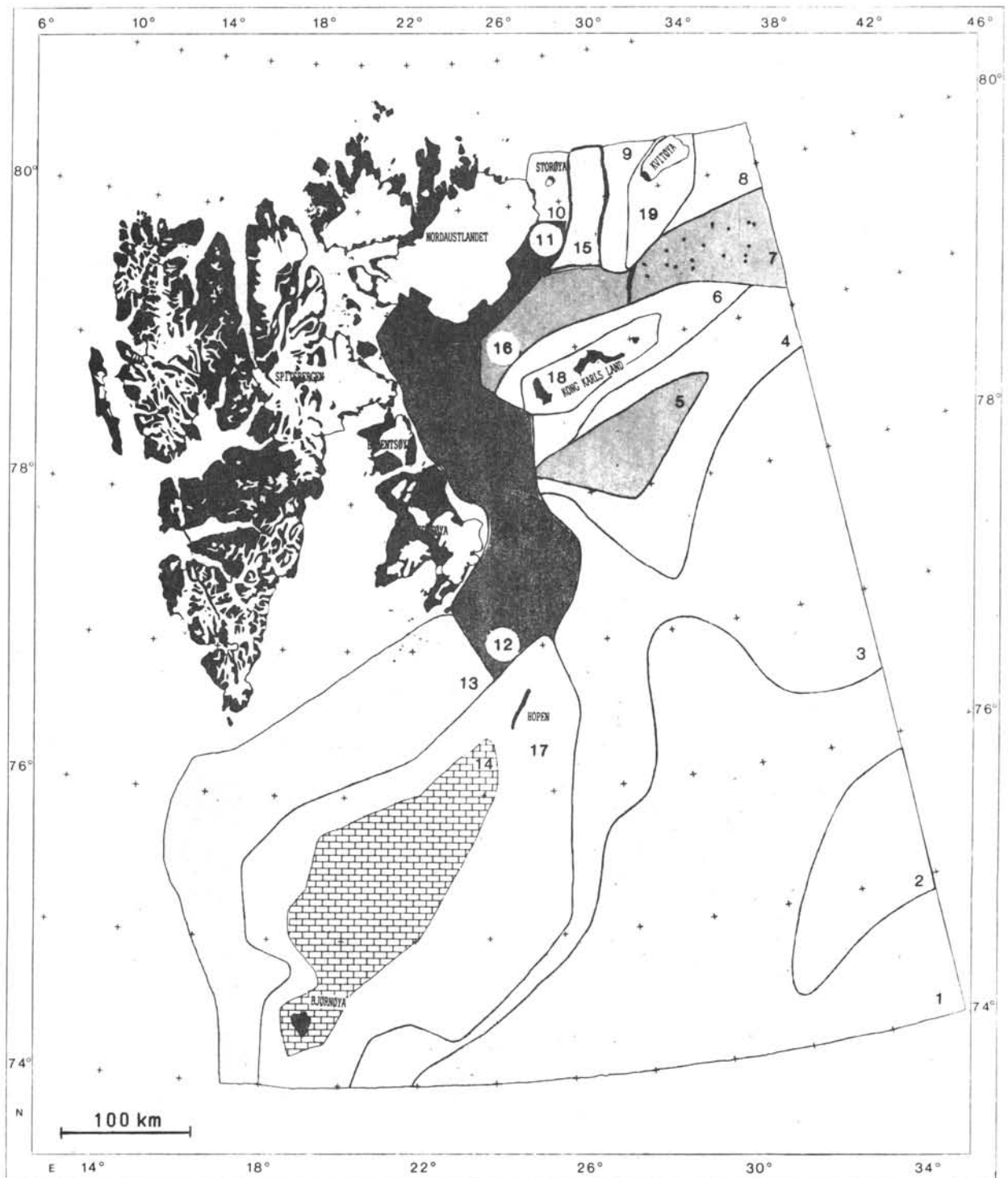


Fig. 15.

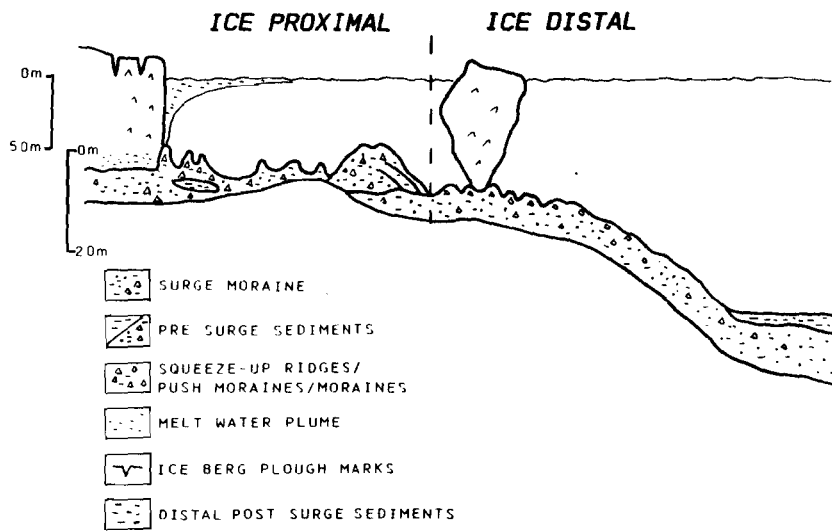


Fig. 16.

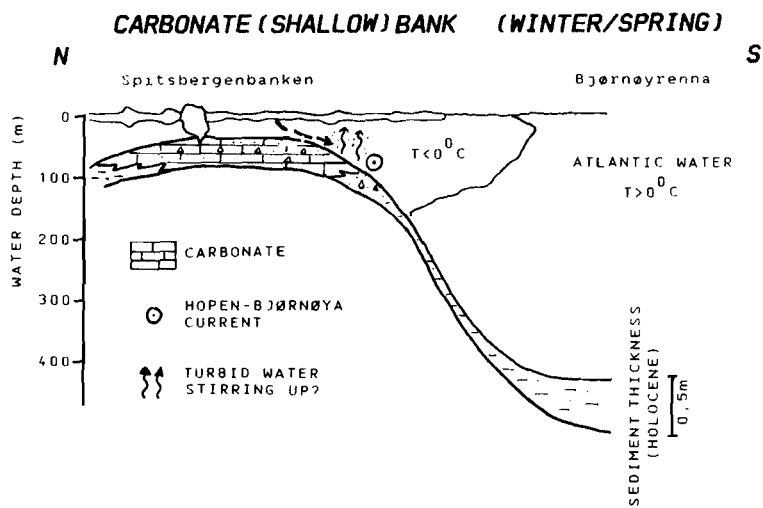


Fig.17a.

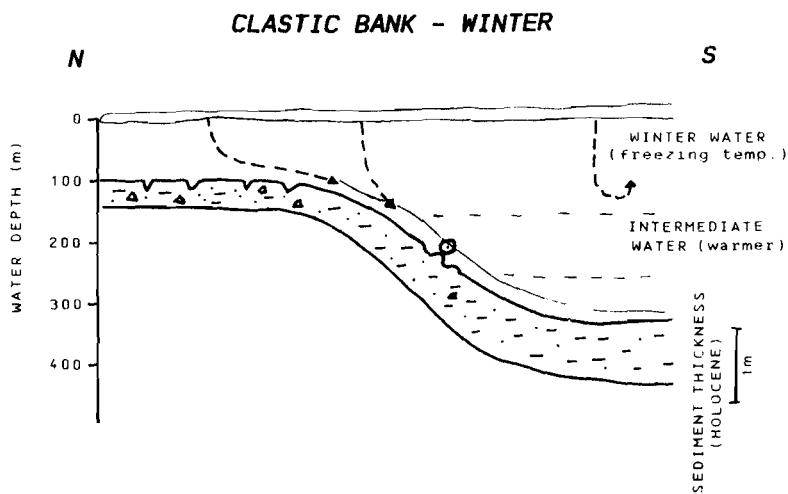


Fig.17b.

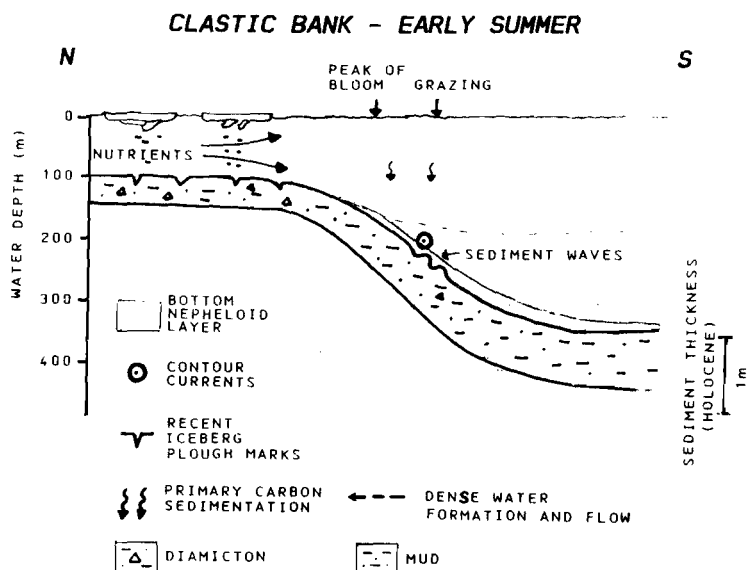


Fig. 17c.

| AREA NO. | SED. RATE (cm/ka) | AREA ⁵ ₂ (10 km ²) | SEDIMENT ACCUMULATION | |
|----------|-------------------|--|-------------------------|------------------------|
| | | | (t/km ² /yr) | (10 ⁵ t/yr) |
| 1 | 5 | .794 | 65 | 51.6 |
| 2 | 3 | .109 | 39 | 4.2 |
| 3 | 3 | .444 | 39 | 17.3 |
| 4 | 5 | .191 | 65 | 12.4 |
| 5 | 15 | .056 | 195 | 10.9 |
| 6 | 3 | .067 | 39 | 2.6 |
| 7 | 4 | .060 | 52 | 3.1 |
| 8 | 3 | .029 | 39 | 1.1 |
| 9 | 3 | .021 | 39 | 0.8 |
| 10 | 3 | .016 | 39 | 0.6 |
| 11 | 30 | .037 | 390 | 14.4 |
| 12 | 20 | .179 | 260 | 46.5 |
| 13 | 5 | .278 | 65 | 18.1 |
| 15 | 5 | .025 | 65 | 1.6 |
| 16 | 15 | <u>.047</u> | 195 | <u>9.2</u> |
| | TOTAL | 2.353 | | 194.4 |
| ----- | | | | |
| 14 | Spitsbergen- | .178 | Carbonate | |
| 17 | banken | .373 | Erosion | |
| 18 | Kong Karls | .036 | Erosion | |
| | Land | | | |
| 19 | Kvitøya | <u>.025</u> | Erosion | |
| | Total | .612 | | |

Table 1

